ANL/RERTR/TM-20
CONF-9409107- --

80
10/7/97

ANL/RERTR/TM-20
CONF-9409107- --

Proceedings of the 1994 International Meeting on REDUCED ENRICHMENT FOR RESEARCH AND TEST REACTORS

Williamsburg, Virginia

September 18-23, 1994

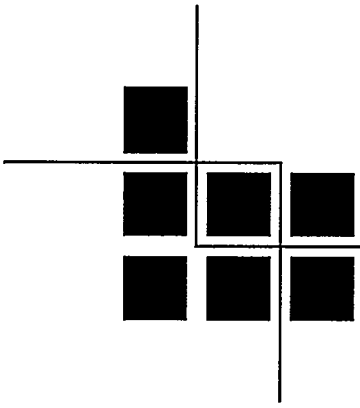

Reduced Enrichment
Research and Test Reactor
Program

ARGONNE NATIONAL LABORATORY, ARGONNE, ILL.
Operated by THE UNIVERSITY OF CHICAGO

Prepared for the U. S. DEPARTMENT OF ENERGY
Office of Intelligence and National Security,
Office of Arms Control and Nonproliferation
under Contract W-31-109-Eng-38

Reproduced from the best available copy.

Available to DOE and DOE contractors from the
Office of Scientific and Technical Information
P.O. Box 62
Oak Ridge, TN 37831
Prices available from (423) 576-8401

Available to the public from the
National Technical Information Service
U.S. Department of Commerce
5285 Port Royal Road
Springfield, VA 22161

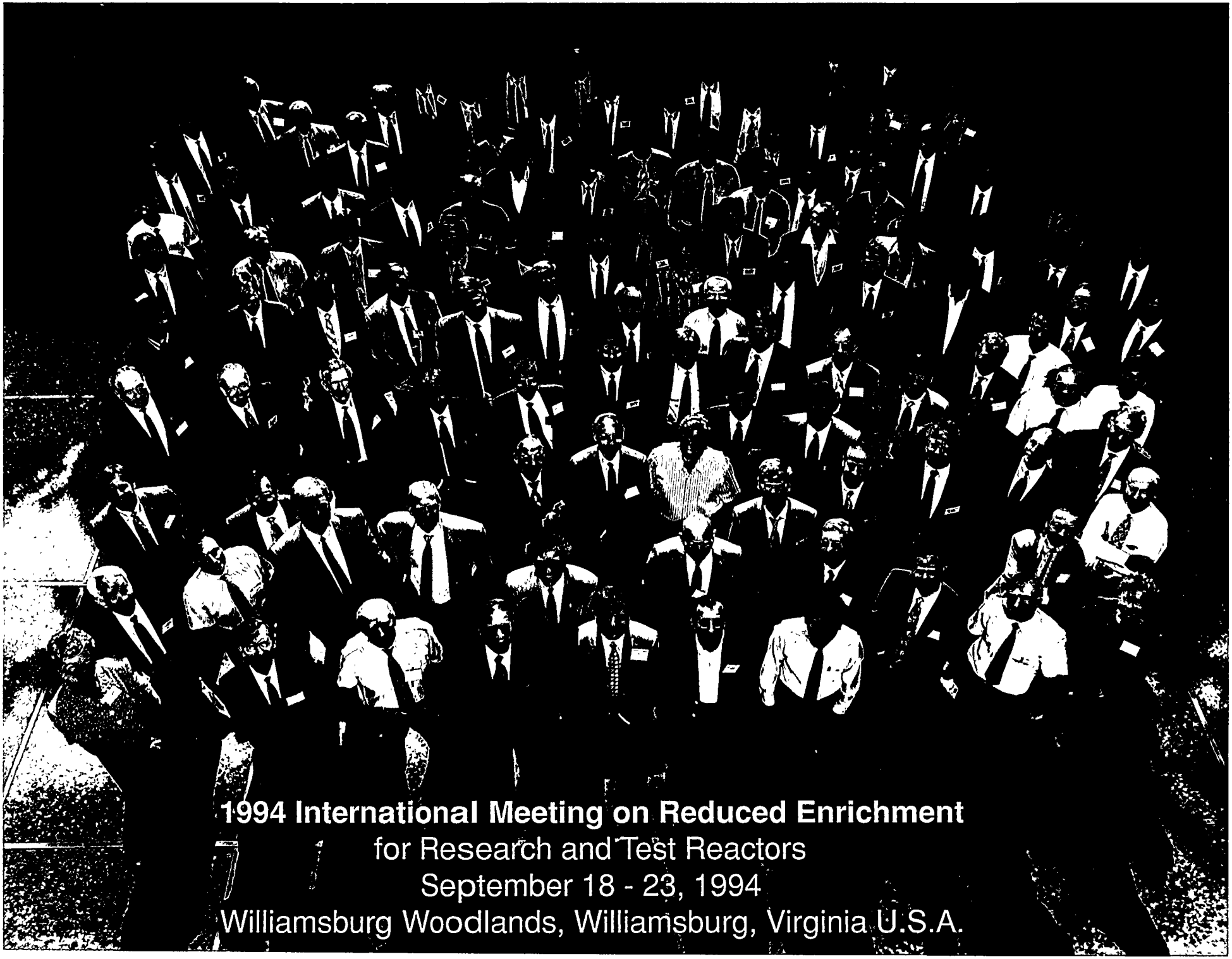

1994 International Meeting on Reduced Enrichment
for Research and Test Reactors
September 18 - 23, 1994
Williamsburg Woodlands, Williamsburg, Virginia U.S.A.

Distribution Category
Nuclear Energy (UC-940)

ANL/RERTR/TM-20
CONF-9409107

ARGONNE NATIONAL LABORATORY
9700 South Cass Avenue
Argonne, Illinois 60439-4841

Proceedings of
the 1994 International Meeting on

REDUCED ENRICHMENT FOR RESEARCH AND TEST REACTORS

Williamsburg, Virginia
September 18-23, 1994

Armando Travelli
Manager, RERTR Program

Administrative Arrangements

Helen Weber
Sharon Richmond

Proceedings Publication

Helen Weber

August 1997

PREFACE

The major participants in the international effort to minimize and eventually eliminate the use of highly enriched uranium in civilian nuclear programs met this year in Williamsburg, VA, a charming New England colonial town deeply rooted in early American history. This was the seventeenth meeting of a series that began in 1978. The previous meetins are listed on the facing page.

The common effort brought together a large number of specialists from many countries. One hundred and forty-eight participants from eighteen countries, including scientists, reactor operators, and personnel from commercial fuel suppliers, fuel shippers, research centers, and government organizations, convened to discuss their results, their activities, and their plans related to the conversion of research reactors to low-enriched fuels.

The University of Virginia, and their recently converted UVAR reactor, provided a welcome addition to the many scientific exchanges. On their way to visit the UVAR, the attendees also had a chance to visit another landmark of American history, Monticello, where Thome of Thomas Jefferson lived.

I would like to thank several members of the RERTR Program who contributed to editing these proceedings and, to organizing the meeting. In particular, James L. Snelgrove and James E. Matos corrected and edited several papers in consultation with the authors. Compilation of the completed papers and assembly of the proceedings in their final form was accomplished by Helen Weber and Sharon Richmond, who also organized the many functions and details without which the meeting could not have taken place. Finally, I thank all the attendees for their contributions and for the cooperative spirit that they brought to the meeting.

Armando Travelli
Manager, RERTR Program

The previous Reduced Enrichment for Research and Test Reactor meeting were held at:

Argonne National Laboratory, Argonne, IL - November 1978

Saclay, France - December 1979

Argonne National Laboratory, Argonne, IL - November 1980

Juelich, Federal Republic of Germany - September 1981

Argonne National Laboratory, Argonne, IL - November 1982

Tokai, Jappan - October 1983

Argonne National Laboratory, Argonne, IL - October 1984

Petten, The Netherlands - October 1985

Gatlinburg, Tennessee - November 1986

Buenos Aires, Argentina - September 1987

San Diego, California - September 1988

Berlin, Federal Republic of Germany - September 1989

Newport, Rhode Island, September 1990

Jakarta, Indonesia - November 1991

Roskilde, Denmark - September 1992

Oarai, Japan - October 1993

Paris, France - September 1995

Seoul, Korea - October 1996

SESSION I

September 19, 1994

NATIONAL PROGRAMS

Chairman: I. Ritchie (IAEA, Austria)

SESSION II

September 19, 1994

FUEL CYCLE

Chairman: F. DiMeglio (University of Rhode Island, USA)

September 20, 1994

SESSION II

FUEL CYCLE (continued)
Chairman: A. Sameh (Mallingkrodt, Netherlands)

September 21

SESSION IV

ANALYSES

Chairman: A. Lee (AECL, Canada)

SESSION V

ADVANCED REACTORS

Chairman: P. Robinson (DOE, USA)

SESSION VI

REACTOR CONVERSIONS
Chairman: K. Kanda (KURRI, Japan)

SESSION I

September 19, 1994

NATIONAL PROGRAMS

Chairman:

I. Ritchie
(IAEA, Austria)

STATUS OF THE U.S. RERTR PROGRAM

A. Travelli
Argonne National Laboratory
Argonne, Illinois, USA

ABSTRACT

The progress of the Reduced Enrichment Research and Test Reactor (RERTR) Program is described. The major events, findings, and activities of 1994 are reviewed after a brief summary of the results which the RERTR Program had achieved by the end of 1993 in collaboration with its many international partners.

The RERTR Program has moved aggressively to support President Clinton's nonproliferation policy and his goal "*to minimize the use of highly-enriched uranium in civil nuclear programs.*".

An Environmental Assessment which addresses the urgent-relief acceptance of 409 spent fuel elements was completed, and the first shipment of spent fuel elements is scheduled for this month. An Environmental Impact Statement addressing the acceptance of spent research reactor fuel containing enriched uranium of U.S. origin is scheduled for completion by the end of June 1995.

The U.S. administration has decided to resume development of high-density LEU research reactor fuels. DOE funding and guidance are expected to begin soon. A preliminary plan for the resumption of fuel development has been prepared and is ready for implementation.

The scope and main technical activities of a plan to develop and demonstrate within the next five years the technical means needed to convert Russian-supplied research reactors to LEU fuels was agreed upon by the RERTR Program and four Russian institutes lead by RDIPE. Both Secretary O'Leary and Minister Michailov have expressed strong support for this initiative.

Joint studies have made significant progress, especially in assessing the technical and economic feasibility of using reduced enrichment fuels in the SAFARI-1 reactor in South Africa and in the Advanced Neutron Source reactor under design at ORNL.

Significant progress was achieved on several aspects of producing ^{99}Mo from fission targets utilizing LEU instead of HEU. Existing fuel data were analyzed and interpreted to derive a better understanding of the behavior of dispersion fuels under irradiation.

The 50 MW Japanese JMTR was converted to LEU silicide fuel, bringing to twelve the number of converted foreign reactors. The University of Virginia Reactor was also converted to LEU, bringing to nine the number of converted U.S. reactors. Approximately 60% of the work required to eliminate the need for further HEU exports has been accomplished.

International friendship and cooperation has been and will continue to be essential to the achievement of the common goal.

INTRODUCTION

During 1994, the U.S. administration has continued to assign high priority to the issue of proliferation of weapons of mass destruction and has acted consistently with President Clinton's announcement, in his speech to the United Nations General Assembly a year ago, that he intended "*to minimize the use of highly-enriched uranium in civil nuclear programs*". This goal has been shared and pursued by our international RERTR program for many years, and is the goal that brings us here today.

The Reduced Enrichment Research and Test Reactor (RERTR) Program was established in 1978 at the Argonne National Laboratory (ANL) by the Department of Energy (DOE), which continues to fund the program and to manage it in coordination with the Department of State (DOS), the Arms Control and Disarmament Agency (ACDA), and the Nuclear Regulatory Commission (NRC). The primary objective of the program is to develop the technology needed to use Low-Enrichment Uranium (LEU) instead of High-Enrichment Uranium (HEU) in research and test reactors, and to do so without significant penalties in experiment performance, economic, or safety aspects of the reactors. Research and test reactors utilize most of the HEU that is used in civil nuclear programs.

Close cooperation with the many international organizations represented at this meeting has been the cornerstone of the RERTR Program since its beginning sixteen years ago. This cooperation and the high quality of the technical contributions which many partners have brought to the overall effort are to be credited for much of the progress which the program has achieved to date.

We have had a long a fruitful collaboration with the University of Virginia, where the 2 MW UVAR is located. As you may already know, the UVAR was completely and successfully converted to LEU silicide fuel during the past year. It is fitting, therefore, that we should meet in Virginia this year, to celebrate the success of our colleagues at the University of Virginia, to enjoy the historic Virginia hospitality, and to have an opportunity to visit the University and its newly converted reactor at the end of the meeting.

OVERVIEW OF THE OCTOBER 1993 PROGRAM STATUS

By October 1993, when the last International RERTR Meeting was held[1], the main results achieved in the fuel development area were:

(a) The qualified uranium densities of the three main fuels which were in operation with HEU in research reactors when the program began (UAl_x-Al with up to 1.7 g U/cm^3; U_3O_8-Al with up to 1.3 g U/cm^3; and $UZrH_x$ with 0.5 g U/cm3) had been increased significantly. The new uranium densities extended up to 2.3 g U/cm^3 for UAl_x-Al, 3.2 g U/cm^3 for U_3O_8-Al, and 3.7 g U/cm^3 for $UZrH_x$. Each fuel had been tested extensively up to these densities and, in some cases, beyond them. All the data needed to qualify these fuel types with LEU and with the higher uranium densities had been collected.

(b) For U_3Si_2-Al, after reviewing the data collected by the program, the U.S. Nuclear Regulatory Commission (NRC) had issued a formal approval[2] of the use of U_3Si_2-Al fuel in research and test reactors, with uranium densities up to 4.8 g/cm^3. A whole-core demonstration using this fuel had been successfully completed in the ORR using a mixed-core approach. Plates with uranium densities of up to 6.0 g/cm^3 had been fabricated by CERCA with a proprietary process, but had not been tested under irradiation.

(c) For U_3Si-Al, miniplates with up to 6.1 g U/cm^3 had been fabricated by ANL and the CNEA, and irradiated to 84-96% in the Oak Ridge Research Reactor (ORR). PIE of these miniplates had given good results, but had shown that some burnup limits might need to be imposed for the higher densities. Four full-size plates fabricated by CERCA with up to 6.0 g U/cm^3 had been successfully irradiated to 53-54% burnup in SILOE, and a full-size U_3Si-Al (6.0 g U/cm^3) element, also fabricated by CERCA, had been successfully irradiated in SILOE to 55% burnup. However, conclusive evidence indicating that U_3Si became amorphous under irradiation had convinced the RERTR Program that this material as then developed could not be used safely in plates beyond the limits established by the SILOE irradiations.

(d) Limited work had been done to develop methods for producing plates with much higher effective uranium loadings.

In other important program areas, reprocessing studies at the Savannah River Laboratory had concluded that the RERTR fuels could be successfully reprocessed at the Savannah River Plant and DOE had defined the terms and conditions under which these fuels would be accepted for reprocessing. These important results had been rendered moot, however, by the closure of the Savannah River Plant. A new DOE policy had been formulated for the return of spent research reactor fuel elements of U.S. origin, but several legal obstacles were still preventing its implementation.

A new analytical/experimental program had begun to determine the feasibility of using LEU instead of HEU in fission targets dedicated to the production of ^{99}Mo for medical applications. A procedure for basic dissolution and processing of LEU silicide targets had been developed and was ready for demonstration on a full-size target with prototypic burnup.

Extensive studies had been conducted, with favorable results, on the performance, safety, and economic characteristics of LEU conversions. These studies included many joint study programs, which were in progress for about 29 reactors from 18 different countries. Coordination of the safety calculations and evaluations was continuing for the U.S. university reactors planning to convert to LEU as required by the 1986 NRC rule. Eight of these reactors had already been converted, three other safety evaluations had been completed, and calculations for five more reactors were in progress. DOE guidance received at the beginning of 1990 had redirected the efforts of the U.S. RERTR Program away from the development of new and better fuels, toward the transfer of already developed fuel technologies, and toward providing assistance to reactors undergoing conversion. The desirability of resuming development of advanced LEU research reactor fuels was being reviewed by the U.S. administration.

PROGRESS OF THE RERTR PROGRAM IN 1994

During the past twelve months the RERTR Program has moved aggressively in the directions which were outlined at last year's meeting in Japan, and which supported the strong nonproliferation policy of the Clinton administration. The main events, findings, and activities are summarized below.

1. An Environmental Assessment addressing the acceptance of 409 urgent-relief elements was completed in April 1994, and a Finding of No Significant Impact was issued on April 22, 1994. The first shipment of spent fuel elements, from Austria, Denmark, Holland, and Sweden, is scheduled for September 1994. A draft Environmental Impact Statement addressing the acceptance spent research reactor fuel containing enriched uranium of U.S. origin is scheduled for completion by the end of December 1994, with a goal of completing the National Environmental Policy Act (NEPA) review process by the end of June 1995[3]. The proposed DOE off-site spent nuclear fuel policy was formulated in response to proliferation concerns and to the needs of foreign research reactor operators, and is intended to allow spent research reactor fuel containing HEU and LEU of U.S. origin to be returned to the U.S. for disposal.

2. The administration has reviewed the desirability of developing LEU fuels with uranium density greater than the 4.8 g/cm^3 which is currently qualified, and has concluded in favor of developing such fuels. Funding is expected to begin in October 1994. A preliminary plan for the resumption of the fuel development effort has been developed and is ready for implementation.

3. The scope and main technical activities of a plan for the equivalent of a Russian RERTR program were agreed upon by the RERTR Program and several major Russian institutes led by the Research and Development Institute for Power Engineering (RDIPE). The objective of this program is to develop and demonstrate within the next five years the technical means needed to convert from HEU to LEU fuels approximately 26 research reactors designed and supplied by institutes of the Russian Federation. The main Russian institutes which will take part in this cooperative undertaking, beside RDIPE, are the All-Russia Research and Development Institute of Inorganic Material (VNIINM), the Novosibirsk Chemical Concentrates Plant (NZChK), and the Yekaterinburg Branch of RDIPE. Both Mrs. Hazel O'Leary, Secretary of the U.S. Department of Energy (DOE), and Mr. Viktor N. Michailov, Minister of Atomic Energy of the Russian Federation (MINATOM), have expressed strong support for this initiative which would expand the scope of the RERTR program and enable it to address the problems created by use of HEU in civil nuclear programs nearly everywhere in the world. Our Russian colleagues will describe their activities and plans in a paper that will be presented at this meeting[4].

4. A joint study to assess the feasibility of using reduced uranium enrichments in the fuel of the Advanced Neutron Source, which is currently under design at Oak Ridge National Laboratory (ORNL), has been in progress for almost a year. The study is being conducted by personnel from Brookhaven National Laboratory, ORNL, the

Idaho National Engineering Laboratory, and ANL. Several papers addressing different aspects of the study of this very important and complex reactor will be presented at this meeting[5, 6, 7].

5. Significant progress was achieved during the past year on several aspects of producing ^{99}Mo from fission targets utilizing LEU instead of HEU [8, 9,10]. This issue is receiving considerable attention by the Clinton administration. The current goal is to develop and demonstrate a viable technology during the next few years, in cooperation with several other laboratories including the University of Illinois, the Indonesian National Atomic Energy Agency (BATAN), and the Argentine National Commission of Atomic Energy (CNEA).

6. Design and safety analyses were performed for reactors undergoing or considering LEU conversions within the joint study agreements which are in effect between the RERTR Program and several international research reactor organizations. In particular, a joint study by the Atomic Energy Corporation of South Africa and the RERTR Program has been in progress for several months to assess the technical and economic feasibility of converting the SAFARI-1 reactor to LEU fuel. The study has yielded several interesting results that will be presented at this meeting [11]. Another contribution of special significance in this area concerns the GRR-1 reactor in Greece[12].

7. Existing fuel data were analyzed and interpreted to derive a better understanding of the behavior of dispersion fuels under irradiation[13, 14].

8. Computer codes have been modified and upgraded to improve our capability to analyze the performance and safety characteristics of research reactors utilizing LEU fuels. In particular, significant progress has been achieved in generating and testing a 69-group cross section library based on ENDF/B-V data for use with the WIMS-D4 code [15,16].

9. The JMTR reactor (50 MW), at Oarai, Japan, was completely and successfully converted to LEU silicide fuel (U_3Si_2-Al) in January 1994. The JMTR is the most powerful research reactor in Japan and is part of a world-class facility. It was converted to 45% enriched uranium fuels in 1987 and now uses LEU silicide fuel. It formerly required HEU containing approximately 35 kg of ^{235}U during an average year.

The list of the fully-converted foreign reactors which used to require HEU supplies of U.S. origin now includes twelve reactors: ASTRA, DR-3, FRG-1, JMTR, NRCRR, NRU, OSIRIS, PARR, PRR-1, RA-3, R-2, and THOR.

I reported last year[1] on the overall progress toward LEU conversion which had been achieved by October 1993 by all the research reactors which required HEU exports when the program began and were still in operation without imminent plans of being shut down. It is of interest to revisit the situation of these reactors today, and to see how much progress has been accomplished during the past year.

The forty-two foreign research reactors with power of at least one megawatt which utilized HEU of Western origin in 1978, when the program began, have been subdivided in seven categories (Unfeasible/ Feasible/ Planning/ Prototypes/ Order/ Begin/ Complete) according to the most advanced conversion step which they have achieved. The two graphs of Fig. 1 illustrate the current distributions of the numbers of the reactors, and of the average number of kilograms of ^{235}U exported yearly for use in their fuels, among the various categories. Both diagrams would be blank if no progress toward reduction of HEU exports had been achieved, and fully shadowed if total success had been achieved and no further HEU exports were to be required. The percentages of accomplished work are now 57.1% for the number of reactors and 63.7% for the yearly ^{235}U exports, while they were respectively 56.3% and 61.2% last year.

Comparable progress has been attained also by the U.S. university reactors, which are considered separately because they do not require HEU exports. The UVAR reactor (2 MW), at the University of Virginia, was completely and successfully converted to LEU silicide fuel (U_3Si_2-Al) on April 20, 1994, bringing to nine the total number of U.S. converted reactors. (FNR, RPI, OSUR, WPIR, ISUR, MCZPR, UMR-R, RINSC, and UVAR). Safety documentation is either complete or nearly complete for four other reactors. Work is in progress on the four TRIGA reactors which use HEU fuel.

PLANNED ACTIVITIES

The major activities which the RERTR Program plans to undertake during the coming year are described below.

1. Resume high-density fuel development as soon as guidance and funding are received from DOE.

2. In collaboration with RDIPE and other Russian organizations, begin to implement the studies, analyses, fuel development, and fuel tests needed to establish the technical and economic feasibility of converting Russian-supplied research and test reactors to the use of LEU fuels. These activities will be conducted according to the general plan agreed upon by the RERTR Program and the four main Russian institutes involved.

3. Continue calculations and evaluations about the technical and economic feasibility of utilizing reduced-enrichment fuels in reactors of special interest, such as SAFARI-1 and ANS.

4. Develop a viable process, based on LEU, for the production of fission ^{99}Mo in research reactors.

5. Complete testing, analysis, and documentation of the LEU fuels which have already been developed, support their implementation, and transfer their fabrication technology to countries and organizations which require such assistance.

SUMMARY AND CONCLUSION

The U.S. administration has acted in full accord with President Clinton's nonproliferation policy, and the RERTR Program has moved aggressively to support his goal "*to minimize the use of highly-enriched uranium in civil nuclear programs.*"

(a) An Environmental Assessment addressing the urgent-relief acceptance of 409 spent research reactor fuel elements was completed. The first shipment of spent fuel elements is scheduled for this month.

(b) The administration has decided to resume development of advanced LEU research reactor fuels. Both guidance and funding are imminent. A plan to resume fuel development is ready for implementation.

(c) The scope and main technical activities of a plan to develop and demonstrate within the next five years the technical means needed to convert Russian-supplied research reactors to LEU fuels were agreed upon.

(d) Joint studies of the feasibility of utilizing reduced enrichment fuels instead of HEU in specific reactors have made solid progress, especially for the SAFARI-1 reactor and for the ANS reactor.

(e) Significant progress was made on several aspects of producing ^{99}Mo from fission targets utilizing LEU instead of HEU. Cooperation agreements are being prepared with several institutes, including the Indonesian BATAN and the Argentine CNEA.

(f) The JMTR was successfully converted to LEU silicide fuel, bringing to twelve the number of converted foreign reactors. The University of Virginia Reactor was also converted, bringing to nine the number of converted domestic reactors. Approximately 60% of the work required to eliminate the need for further HEU exports has been accomplished.

The most important current issues are related to the resumption of fuel development and to finding an acceptable solution for the back end of the fuel cycle. The new fuels can enable conversion of the reactors which cannot be converted today and ensure better efficiency and performance for all research reactors. We are very excited at the prospect of this task and eager to begin. The problems concerning the back end of the fuel cycle are much more complex, but we hope that an acceptable solution will be found. Once more, I ask for the international friendship and cooperation which you have so generously extended to us during the past sixteen years.

REFERENCES

1. A. Travelli, "The RERTR Program: a Status Report," Proceedings of the XV International Meeting on Reduced Enrichment for Research and Test Reactors, Roskilde, Denmark, 27 September-1 October 1992 (to be published).

2. U.S. Nuclear Regulatory Commission: "Safety Evaluation Report Related to the Evaluation of Low-Enriched Uranium Silicide-Aluminum Dispersion Fuel for Use in Non-Power Reactors," U.S. Nuclear Regulatory Commission Report NUREG-1313 (July 1988).

3. Letter from H. O'Leary, U.S. Secretary of Energy, to W. Christopher, U.S. Secretary of State, July 13, 1993.

4. V. G. Aden, E. Kartashov, E. Lukichev, Y. Stetskij, and A. Enin, "Russian Program on Decreasing Fuel Enrichment for Research Reactors," (these proceedings).

5. R. Bari, "Status of the Advanced Neutron Source Reduced Enrichment Study," (these proceedings).

6. C. West, "Studies of the Impact of Fuel Enrichment on ANS Performance and Costs," (these proceedings).

7. M. M. Bretscher, J. R. Deen, N. A. Hanan, J.E Matos, S.C.Mo, R. B. Pond, A. Travelli, and W. L. Woodruff, "Relative Performance Properties of the ORNL Advanced Neutron Source Reactor with Reduced Enrichment Fuels", (these proceedings).

8. J. Hutter, C. Srinivasan, M. Vicek, and G. F. Vandegrift, "Production of Mo-99 Using Low-Enriched Uranium Silicide," (these proceedings).

9. B. Srinivasan, J. C. Hutter, G. Johnson and G. F. Vandegrift, "Development of a Dissolution Process for LEU Metal Foil Targets," (these proceedings).

10. T. C. Wiencek, G. L. Hofman, E. L. Wood, C. T. Wu, and J. L. Snelgrove, "LEU ^{99}Mo Target Fabrication and Testing - Overview, Status and Plans, (these proceedings)."

11. G. Ball, N. Hanan, J. E. Matos, and R. B. Pond, "Neutronic Study on Conversion of SAFARI-1 to LEU Silicide Fuel," (these proceedings).

12. W. Woodruff, J. Deen, and C. Papastergiou, "Transient Analyses and Thermal-hydraulic Safety Margins for the Greek Research Reactor (GRR-1)," (these proceedings).

13. G. L. Hofman, J. Rest, and J. L. Snelgrove, "Comparison of Irradiation Behavior of Different Uranium Silicide Dispersion Fuel Element Designs," (these proceedings).

14. G. L. Hofman and S. Sugondo, "PIE of Indonesian U_3Si_2 Fuel Elements," (these proceedings).

15. J. R. Deen and W. L. Woodruff, "Validation of the WIMS-D4M Cross-Section Generation Code with Benchmark Results," (these proceedings).

16. S. Mo, "Methodology and Application of the WIMS-D4M Fission Product Data," (these proceedings).

Fig.1 PROGRESS TOWARD CONVERSION OF RESEARCH REACTORS REQUIRING HEU EXPORTS

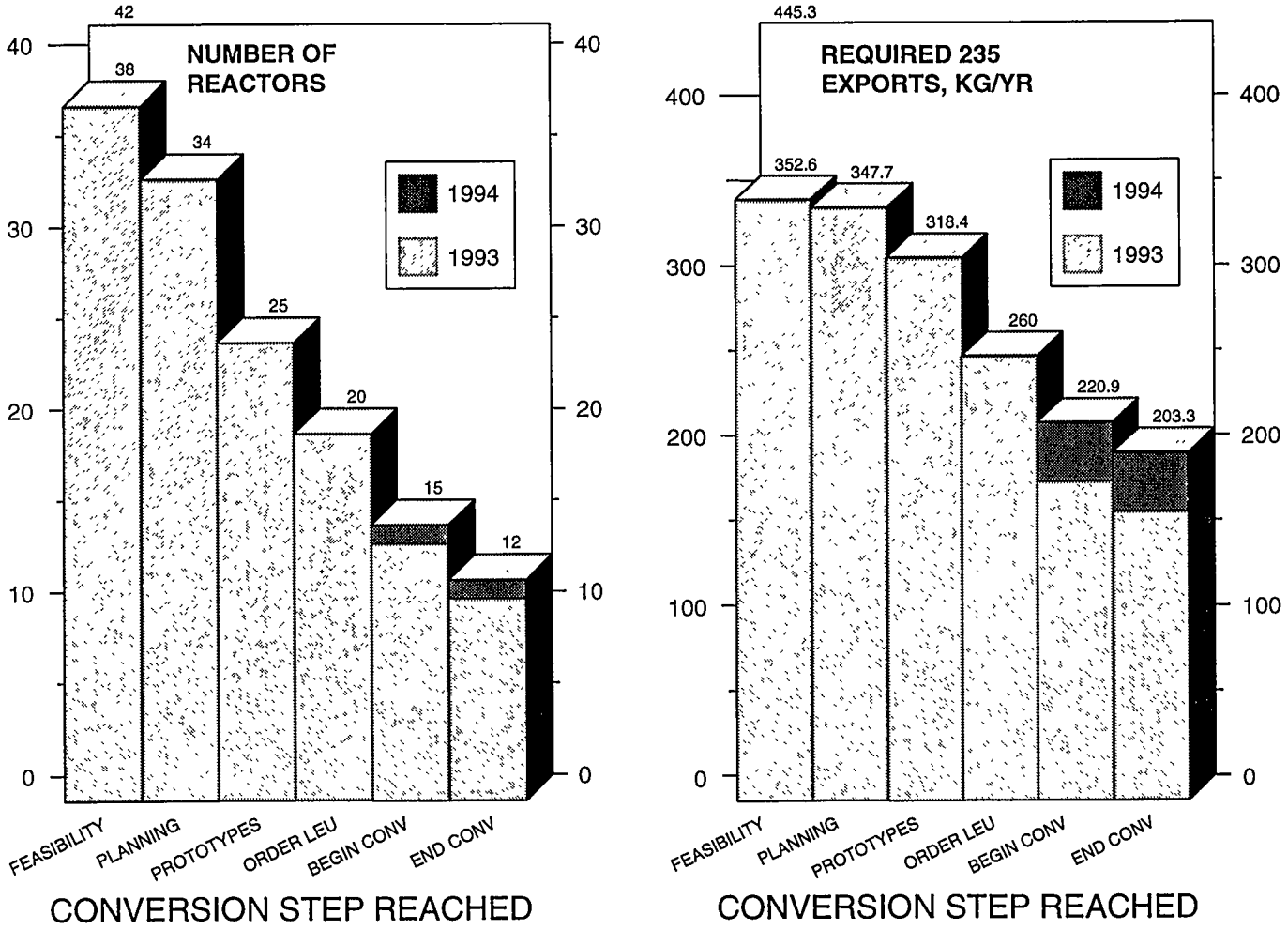

STATUS OF REDUCED ENRICHMENT PROGRAMS FOR RESEARCH REACTORS IN JAPAN

Keiji Kanda, Hideaki Nishihara

Research Reactor Institute, Kyoto University
Kumatori-cho, Sennan-gun, Osaka 590-04, Japan

and

Eiji Shirai, Rokuro Oyamada and Konomo Sanokawa

Japan Atomic Energy Research Institute
Uchisaiwai-cho, Chiyoda-ku, Tokyo 100, Japan

ABSTRACT

The reduced enrichment programs for the JRR-2, JRR-3, JRR-4 and JMTR of Japan Atomic Energy Research Institute (JAERI), and the KUR of Kyoto University Research Reactor Institute (KURRI) have been partially completed and are mostly still in progress under the Joint Study Programs with Argonne National Laboratory (ANL).

The JMTR and JRR-2 have been already converted to use MEU aluminide fuels in 1986 and 1987, respectively. The operation of the upgraded JRR-3(JRR-3M) has started in March 1990 with the LEU aluminide fuels.

Since May 1992, the two elements have been inserted in the KUR. The safety review application for the full core conversion to use LEU silicide in the JMTR was approved in February 1992 and the conversion has been done in January 1994. The Japanese Government approved a cancellation of the KUHFR Project in February 1991, and in April 1994 the U.S. Government gave an approval to utilize HEU in the KUR instead of the KUHFR. Therefore, the KUR will be operated with HEU fuel until 2001.

Since March 1994, Kyoto University is continuing negotiation with UKAEA Dounreay on spent fuel reprocessing and blending down of recovered uranium, in addition to that with USDOE.

INTRODUCTION

Among eighteen research reactors and critical assemblies in Japan (Tables 1 and 2), those which are relevant to the RERTR program are the JRR-2, JRR-3M, JRR-4 and JMTR of JAERI and the KUR of KURRI (Table 3). The RERTR program in Japan has been pursued extensively under the direction of the Five Agency Committee on Highly Enriched Uranium, which consists of the Science and Technology Agency, the Ministry of Education, Science and Culture, the Ministry of Foreign Affairs, JAERI and KURRI, which is held every three months. It has played a remarkable role in deciding policies related to the program, and the 69th Committee was held on August 23, 1994. Recently, reprocessing of spent fuel has been mainly discussed, including the option of reprocessing in UK for the KUR spent fuel.

The program in JAERI for the first step, in which the JRR-2 and JMTR were to be converted to use 45% enriched uranium (MEU) aluminide fuels and the JRR-3 to use 20% enriched uranium (LEU) aluminide fuels, has been completed. The first criticality of the new JRR-3 was achieved in March 1990. After that, the reactor power was increased step by step to high power level and the maximum power to 20 MW was established since August 1990 the JRR-2 have been used 26 times for the irradiation of cancer patients with the boron neutron capture therapy.

Further core conversion of the JMTR for use of LEU silicide fuel with burnable absorber has been studied since 1984 in accordance with the Joint Study with ANL. The safety review application of the conversion was approved in February 1992, and the full core conversion was completed in January 1994.

On the other hand, in KURRI the same efforts as in JAERI to reduce the enrichment of the KUR are in progress. The safety review application for two LEU silicide elements in the KUR was approved in May 1991 and the two elements have been inserted to the core in May 1992. In April, 1994 the U.S. Government gave an approval to utilize HEU in the KUR instead of the KUHFR. Therefore the KUR will be operated with HEU fuel until 2001. In March 1994, Kyoto University started negotiation with UKAEA Dounreay on spent fuel processing and blending down of recovered uranium. Since February 1990, 49 patients were treated in the KUR with the boron neutron capture therapy.

JAERI

JRR-2

After the core conversion to MEU fuel in 1987, the JRR-2 had been operated for sixty one cycles with the total output of approximately 150,000 MWh by the end of March 1994. Since the beginning of April 1994, the reactor operation mode in a cycle has been modified as so-called weekly operation, fifty hours continuous operation with 10 MW for the joint utilization and for the Boron Neutron Capture Therapy (BNCT). Considering the utilization demands, thirty one reactor operation cycles are scheduled in FY 1994 including BNCT for

fourteen patients. Totally 113 MEU fuel elements have served for the reactor operation without troubles up to now. The JRR–2 is planned to terminate the operation in 1996.

JRR–3M

The upgrading work for the JRR–3 was started in August 1985 and the first criticality of the JRR–3M was achieved in March 1990, using LEU aluminum fuels (2.2 gU/cc). The JRR–3M has been operated for capsule irradiation, beam experiments and so on at the reactor power of 20 MW since November 1990. One operational cycle consists of four weeks for operation and one week for shut down work. The equilibrium core was attained in May 1991, and twenty seven operation cycles have been subsequently achieved with the total output of approximately 290,000 MWh as of beginning of June 1994.

Neutron fluxes at horizontal beam tubes in the JRR–3M are quite satisfactory and the cold neutron source has been also operated successfully. Twenty two beam experimental facilities are currently being utilized with quite good performance and six facilities are now under way for installation or preparation.

Modification of the silicon irradiation facility with high performance will be done next year and the core conversion to silicide fuels are expected in future.

JRR–4

It is expected that the reactor operation with HEU fuels will be continued up to the end of 1995, when almost all the HEU fuels will be consumed in the JRR–4. Then, the conversion works of the reactor core to LEU fuels might be followed by using U_3Si_2–Al dispersion type fuels for about two years.

The core design with LEU fuels is now under way. Seismic analyses of the reactor building, reactor accident analyses and so on are carrying out for the safety evaluation. The upgrade of utilization facilities is also under consideration.

JRR–4 is planned to resume its operation in 1998.

JMTR

The LEU fuel for the JMTR LEU core is silicide fuel (U_3Si_2) with 4.8 gU/cc, and burnable absorbers of cadmium wires are placed in each side plate. The use of silicide fuel allows the JMTR to operate consecutively for twenty six days without refueling which had been carried out after twelve days' operation for the MEU fuel core. Major operating characteristics remain unchanged.

The JMTR core conversion was started with the transition core (2 LEU fuel elements and 20 MEU fuel elements) operation from November 24 to December 20, 1993. The two

LEU fuel elements were subjected to visual inspection and sipping test after the operation, and they were verified to perform well. The JMTR was completely and successfully converted to the LEU silicide fuel in January, 1994.

After the first LEU core operation ended in February 1994, LEU equilibrium core was constituted and two operation cycles were carried out from March to July, 1994.

Core characteristics measurements were carried out through the core conversion. Shutdown margin and temperature coefficient of moderator were measured, and safety of the LEU core was confirmed. Excess reactivity change during reactor operation, which agreed well with the predicted value, was significantly reduced by effect of cadmium wires compared with MEU core operation.

Issue on Spent Fuel Management from Research and Test Reactors

As of June, 1994, about 1,100 plate type spent fuels from JRR-2, JRR-3M, JRR-4 and JMTR including HEU, MEU and LEU fuels are stored in their pools due to the suspension of reprocessing business of USDOE since 1988. It is worried that the storage capacity of the pool might be exceeded by the production of spent fuels within a few years. As the most promising solution for such issue, the transportation of these spent fuels to the storage facility in the USA is now planned in accordance with USDOE's renewed acceptance policy of foreign research reactor spent nuclear fuel after the completion of Environmental Impact Statement (EIS).

Pulse Irradiation of Silicide Fuels in the NSRR

To provide a data base for safety assessment of research reactors using silicide fuels, the behavior of silicide fuels during off-normal and postulated accident conditions is being studied in the Nuclear Safety Research Reactor (NSRR). Experiments using pulse irradiation capability of the NSRR have been performed to evaluate the thresholds, modes, and consequences of fuel failure in terms of fuel enthalpy and fuel density.

Thirty five experiments have been performed by the end of FY 1993, with low enriched (20%) and high density (4.8 g/cm^3) fresh plate-type silicide miniplate fuels in the test capsule with stagnant coolant water at room temperature and at atmospheric pressure. Through the experiments, crack generation in the cladding, melting and significant relocation of fueled meat region, uranium/aluminum/silicon interaction, and materials dispersion due to fuel/coolant interaction (FCI) were observed. Recently, the tests with relatively low fuel density (4.0 g/cm^3) silicide fuel and with low density (2.29 g/cm^3) aluminide fuel were also performed.

In addition to these experiments, the experimental program for the silicide fuel to be used in Advanced Neutron Source (ANS) reactor of Oak Ridge National Laboratory (ORNL) was newly initiated from FY 1992 with the collaboration of ORNL. Concerning fuel geometry

and density, the ANS-type fuel has differences with the one which has been tested in the previously stated tests. Seven experiments have been conducted recently, and detailed fuel examination are being performed.

Development of High Uranium Density Fuels

Capsule irradiation tests have been conducted for U-Si and U_6Me (Me = Fe, Ni, Mn) miniplates irradiated in the JMTR.

From the preliminary results of nondestructive examinations, it was confirmed that U_6Me alloys do not show excessive fuel swelling causing the plate failure at the modest burnup level of about 50% ^{235}U and at a relatively high irradiation temperature of about 200 °C.

KURRI

The Kyoto University Research Reactor (KUR, 5MW) has been operated since 1964 using HEU fuel. The KUR has been still utilized for boron neutron capture therapy. Since February 1990, 49 patients of cancer were treated by eight chief medical doctors of five groups.

According to the governmental policy, Kyoto University tried to convert the KUR to use the LEU fuel, and already two LEU silicide fuel elements have been inserted to the core in May 1992.

On the other hand, according to the suggestion of the government, the cancellation of the KUHFR (30MW) Project was applied to the government in December 1990 and approved in February 1991. The handling of HEU received for the KUHFR was discussed with the US Government. In April 1994 the U.S. Government gave an approval to utilize HEU in the KUR instead of the KUHFR. Therefore the KUR will be operated with HEU fuel until 2001.

In addition to the negotiation with USDOE to extend the reprocessing contract, Kyoto University is continuing negotiation of the reprocessing contract with UKAEA Dounreay since March 1994, where the meeting were held in April and August 1994. The draft of contract contains (1) reprocessing and (2) blending down of recovered uranium less than 20% with the full scope inspection by IAEA or EURATOM. If the contract is completed the blended down LEU will be fabricated by either UKAEA or CERCA.

Table 1. Japanese Research Reactors in Operation

Name	Owner	Site	Type and	enrichment		Max. Power	Start-up date
JRR-2	JAERI	Tokai	D_2O(CP-5)	U-Al	93%	10 MW	1960.10
				UAl_x-Al	45%	10 MW	1987.11
UTR-KINKI	Kinki Univ.	Higashi-osaka	H_2O(UTR)	U-Al	90%	1 W	1961.11
TRIGA-II	Rikkyo Univ.	Yokosuka	H_2O(TRIGA)	U-ZrH	20%	100 kW	1961.12
TTR-1	Toshiba	Kawasaki	H_2O(pool)	U-Al	20%	100 kW	1962. 3
JRR-3	JAERI	Tokai	D_2O(tank)	NU		10 MW	1963. 9
				UO_2	1.5%		
			H_2O(pool)	UAl_x-Al	20%	20 MW	1990. 3
MITRR MUSASHI	Musashi Inst. Tech.	Kawasaki	H_2O(TRIGA)	U-ZrH	20%	100 kW	1963. 3
KUR	KURRI	Kumatori	H_2O(tank)	U-Al	93%	5 MW	1964. 6
JRR-4	JAERI	Tokai	H_2O(pool)	U-Al	93%	3.5 MW	1965. 1
JMTR	JAERI	Oarai	H_2O(MTR)	U-Al	93%	50 MW	1968. 3
				UAl_x-Al	45%	50 MW	1986. 7
				U_3Si_2-Al	20%	50 MW	1994. 1
YAYOI	Univ. of Tokyo	Tokai	fast (horizontally movable)	U	93%	2 kW	1971. 4
NSRR	JAERI	Tokai	H_2O(TRIGA)	U-ZrH	20%	300 kW	1975. 6

Table 2. Japanese Critical Assemblies in Operation

Name	Owner	Site	Type and enrichment			Max. power	Start-up date
VHTRC	JAERI	Tokai	Graphite horizontally split	U	20%	10 W	1961. 1
TCA	JAERI	Tokai	H_20(tank)	UO_2 UO_2–PuO_2	2.6% 4.0%	200 W	1962. 8
NCA	Toshiba	Kawasaki	H_20(tank)	UO_2	1–5%	200 W	1963.12
JMTRC	JAERI	Oarai	H_20(pool)	U–Al UAl_x–Al	93% 45%	100 W 100 W	1965.10 1983. 8
FCA	JAERI	Tokai	fast horizontally split	U U Pu	93% 20%	2 kW	1967. 4
DCA	PNC	Oarai	D_20(tank)	UO_2 UO_2–PuO_2	1.2% 1.5%	1 kW	1969.12
KUCA	KURRI	Kumatori	various multi-core	U–Al UAl_x	93% 45%	100 W 1 kW (short time)	1974. 8 1981. 5

Table 3. Research Reactor Relevant to RERTR in Japan

Name	Power (MW)	First Critical	Fuel Enrichment	Conversion
KUR (KURRI)	5	1964	HEU → LEU	2001
KUHFR (KURRI)	30	canceled		
JRR-2 (JAERI)	10	1960	HEU → MEU	1987
JRR-3M (JAERI)	20	1962	LEU → LEU	1990
JRR-4 (JAERI)	3.5	1965	HEU → LEU	1998
JMTR (JAERI)	50	1968	MEU → LEU	1994
Related Critical Assemblies				
KUCA (KURRI)	0.0001	1974	HEU → MEU	1981
JMTRC (JAERI)	0.0001	1965	HEU → MEU	1983

* Some delay might be occurred under the present circumstances.

Table 4. History of Reduced Enrichment Program for Research and Test Reactor in Japan

1977.11.	Japanese Committee on INFCE WC-8 was started.
1977.11.	Joint Study Program was proposed at the time of the application of export license of HEU for the KUHFR.
1978. 5.	ANL-KURRI Joint Study Phase A was Started.
1978. 6.	Five Agency Committee on Highly Enriched Uranium was organized.
1978. 2.	ANL-KURRI Joint Study Phase A was completed.
1979. 5.	Project team for RERTR was formed in JAERI.
1979. 7.	ANL-KURRI Joint Study Phase B was started.
1980. 1.	ANL-JAERI Joint Study Phase A was started.
1980. 8.	ANL-JAERI Joint Study Phase A was completed.
1980. 9.	ANL-JAERI Joint Study Phase B was started.
1981. 5.	MEU UAl_x-Al full core experiment was started in the KUCA.
1983. 3.	ANL-KURRI Phase B was completed.
1983. 8.	MEU UAl_x-Al full core experiment in the JMTRC was started.
1983.11.	ANL-KURRI Phase C was started.
1984. 3.	ANL-JAERI Phase B was complete.
1984. 4.	ANL-JAERI Phase C was started.
1984. 4.	MEU-HEU mixed core experiment in the KUCA was started.
1984. 9.	Irradiation of 2 MEU and 1 LEU UAl_x-Al full size elements in the JRR-2 was started.
1984.10.	Irradiation of LEU UAl_x-Al full size elements in the JRR-4 was started.
1984.11.	Thermal-hydraulic calculations for the KUR core conversion from HEU to LEU was performed.
1985. 1.	Irradiation of MEU UAl_x-Al full size elements in the JMTR was started.
1985. 3.	Irradiation of MEU UAl_x-Al full size elements in the JMTR was completed. Irradiation of LEU U_xSi_y-Al miniplates in the JMTR was started.
1985. 6.	Irradiation of LEU U_xSi_y-Al miniplates in the JMTR was completed.
1985.10.	Neutronics calculations for the KUR core conversion from HEU to LEU was performed.
1986. 1.	Irradiation of MEU UAl_x-Al full size elements in the JRR-2 was started.
1986. 5.	Irradiation of MEU UAl_x-Al full size elements in the JRR-2 was completed.
1986. 8.	The JMTR was fully converted from HEU to MEU fuels.
1987.11.	MEU UAl_x-Al full core in the JRR-2 was started.
1988. 7.	PIE of MEU, LEU UAl_x-Al full size elements in the JRR-2 was completed.
1988.12.	Irradiation of a LEU UAl_x-Al full size elements in the JRR-4 was completed.
1990. 3.	LEU UAl_x-Al full core test in the new JRR-3 (JRR-3M) was started.
1990.11.	Full power operation of 20 MW in the JRR-3M was started.
1992. 5.	Two LEU U_3Si_2 elements were inserted into the KUR core.
1993.11.	Two LEU U_3Si_2 elements were inserted into the JMTR core.
1994. 1.	The JMTR was fully converted from MEU to LEU with U_3Si_2-Al fuel.

REFERENCES

1. K.Kanda, "Reducing Enrichment Program for Research Reactors in Japan", in *Proceedings of the International Meeting of Research and Test Reactor Core Conversion from HEU to LEU Fuels,* Argonne, USA, November 8–10, ANL/RERTR/TM–4 CONF–**821155,** pp.24–32 (September 1983).

2. K. Sato, "Opening Statement to the International Meeting on Reduced Enrichment for Research and Test Reactors", in *Proceeding of the International Meeting on Reduced Enrichment for Research and Test Reactors,* Tokai, Japan, October 24–27, 1983, JAERI–M **84–073,** pp.8–10 (May 1984).

3. K. Kanda, T. Shibata, I. Miyanaga, H. Sakurai and M. Kanbara, "Status of Reduced Enrichment Program for Research Reactor Fuels in Japan", in *Proceeding of International Meeting of Reduced Enrichment of Research Reactor and Test Reactors,* Argonne, USA, October 15–18, 1984, ANL/RERTR/TM–6 CONF–**8410173,** pp.11–20 (July 1985).

4. I. Miyanaga, K. Kamei, K. Kanda and T. Shibata, "Present Status of Reduced Enrichment Program for Research and Test Reactors Fuels in Japan", in *Reduced enrichment for Research and Test Reactors,* Proceedings of an International Meeting, Petten, The Netherlands, October 14–16, 1985, D. Reidel Publishing Company, Dordrecht/Boston/Lancaster/Tokyo, pp.21–32, (March, 1986).

5. K. Kanda, T. Shibata, Y. Iso, H. Sakurai and Y. Okamoto, "Status of Reduced Enrichment for Research and Test Reactor Fuels in Japan", in *Proceedings of the 1986 International Meeting on Reduced Enrichment for Research and Test Reactors,* Gatlinburg, USA, November 3–6, 1986, ANL/RERTR/TM–9 CONF–**861185,** pp. 14–22.

6. Y. Futamura, H. Sakurai, Y. Iso, K. Kanda and I. Kimura, "Status of Reduced Enrichment Program for Research and Test Reactor Fuels in Japan", in *Proceedings of the 10th RERTR Meeting,* Comission National & Energia Atomica, Buenos Aires, Argentina, September 28 – October 1, 1987, pp.22–31.

7. K. Kanda, H. Nishihara, Y. Futamura, H. Sakurai and Y. Iso, "Status of Reduced Enrichment Program for Research Reactors in Japan", in *Proceedings of the 11th RERTR Meeting,* San Diego, USA, September 19–22, 1988, ANL/RERTR/TM–13 CONF–**8809221**, pp.31–38.

8. Y. Futamura, M. Kawasaki, Y. Iso, K. Kanda and M. Utsuro, "Status of Reduced Enrichment Program for Research and Test Reactor Fuels in Japan", in *XIIth International Meeting Reduced Enrichment for Research and Test Reactors,* Berlin, FGR, September 10–14, 1989, KFA Jülich, 1991, pp.21–28.

9. K. Kanda, H. Nishihara, Y. Futamura, M. Kawasaki and T. Asaoka, "Status of Reduced Enrichment Program for Research Reactors in Japan", in *Proceedings of the 1990 International Meeting on Reduced Enrichment for Research and Test Reactors,* Newport, USA, September 23–27, 1990 ANL/RERTR/TM–18 CONF–**9009108,** pp.16–24.

10. Y. Futamura, M. Kawasaki, T. Asaoka, K. Kanda and H. Nishihara, "Status of Reduced Enrichment Program for Research Reactors in Japan", in *Proceedings of 14th RERTR Meeting,* Jakarta, Indonesia, November 4–7, 1991, in press.

11. K. Kanda, H. Nishihara, Y. Futamura, E. Shirai and T. Asaoka, "Status of Reduced Enrichment Program for Research Reactors in Japan", in *Proceedings of 15th RERTR Meeting,* Roskilde, Denmark, September 27 – October 1, 1992, in press.

12. M. Saito, E. Shirai, K. Sanokawa, K. Kanda and H. Nishihara, "Status of Reduced Enrichment Program for Research Reactors in Japan", in *Proceedings of 16th RERTR Meeting,* Oarai, Japan, October 4–7, 1993, JAERI–M 94–042, pp.14–22 (March 1994).

RERTR Program

STATUS OF FRENCH REACTORS

A. BALLAGNY

Commissariat à l'Energie Atomique
Centre d'Etudes de Saclay - France

ABSTRACT

The status of French reactors is reviewed. The ORPHEE and RHF reactors can not be operated with a LEU fuel which would be limited to 4.8 g U/cm^3. The OSIRIS reactor has already been converted to LEU. It will use U_3Si_2 as soon as its present stock of UO_2 fuel is used up, at the end of 1994. The decision to close down the SILOE reactor in the near future is not propitious for the start of a conversion process. The REX 2000 reactor, which is expected to be commissioned in 2005, will use LEU (except if the fast neutrons core option is selected). Concerning the end of the HEU fuel cycle, the best option is reprocessing followed by conversion of the reprocessed uranium to LEU.

INTRODUCTION

To date, CEA operates a large number of irradiation facilities :

- 7 critical assemblies (MASURCA, EOLE, MINERVE...),
- 8 source reactors (HARMONIE...),
- 2 training reactors (ULYSSE, SILOETTE...),
- 3 special reactors for safety studies (CABRI, PHEBUS, SCARRABE),
- 4 research reactors (OSIRIS (+ ISIS), SILOE, ORPHEE, RHF).

The only facilities concerned by the RERTR program are the reactors which regularly, consume a large quantity of fuel, and namely ORPHEE, RHF, OSIRIS and SILOE. All the others have a very specific fuel or use only one core from the beginning until the end of their life.

ORPHEE - RHF

These two reactors are only used for basic research. It has been proved that they can not use a LEU fuel with a uranium content limited to 4.8 g/cm^3. These 2 reactors with the BR2 reactor located in Belgium are considered, at the present time, as an exception in the RERTR program because they will continue to use highly enriched uranium.

OSIRIS (+ ISIS)

In 1980, these reactors, which had used highly enriched uranium since they went into service in 1966, were converted to low enriched uranium (7.5 %). To reach a sufficient U^{235} density with such a low enrichment, the fuel plates were made of a multitude of thin square fuel pellets of UO_2 called "Caramels".

In 1987, it was decided to standardize the manufacturing of fuels of the MTR reactors and thus to abandon, in the end, the manufacturing of UO_2 fuels to devote all development and qualification efforts to the silicide fuels.

To date, more than 200 U_3Si_2 fuel elements (4.8 g/cm^3) have been manufactured, representing three years of operation of the OSIRIS reactor.

To start the progressive change process, CEA is waiting until its entire stock of Caramel fuel elements is used up. The last Caramel elements will be put in during December of 1994, and thus the change will start in January of 1995.

The license to use U_3Si_2 to replace UO_2 was difficult to get. The safety analysis of the reactor had to be completely redone and, on that occasion, the use of computer codes qualified according to the quality assurance rules were a constant requirement of the safety authorities and the source of the main difficulties. To get license it has been necessary to make commitments to carry out rapidly specific irradiation experiments in order to provide additional answers :

- The first question regards the release of fission products in the event of a cladding failure. In the case of a cladding failure on a U_3Si_2 plate, how is it possible to be sure that it can be quickly detected ? How can the cladding failure detection system be calibrated in relation to the former fuel ? How does a cladding failure evolve (reaction with water...) ? To be able to provide precise figures to these questions, an irradiation called EPSILON will begin in

November 1994 in a loop of the SILOE reactor with an on-line measurement of the fission products release. Special miniplates with calibrated defects have been made with both U_3Si_2 and UAl alloys to make comparison.

The miniplates will be irradiated at different power levels.

The activity of the water will be continously measured by on-line gamma spectrometry, delayed neutrons detection, and by water sampling.

After irradiation each miniplate will be examined by various post irradiation examination such as metallographies (surface of the defect) and section gamma scanning (fission products distribution in the defect zone).

- Another question concerns the validation of the computer codes (thermohydraulics) in some incidental situations. A special fuel element with a plate equipped with thermocouples has to be made. Tests will be carried out with this element during one cycle of the reactor.

SILOE - SILOETTE

The principle of the conversion of the SILOE reactor was decided in 1989. But in 1993 it has been decided to shut down the reactor definitively in the near future without knowing exactly which year. The reason for the decision is not related to the age of the reactor, nor to the safety, but there are, in fact, fewer and fewer technological irradiation programs and it is not possible to ensure a sufficient work load for both OSIRIS reactor and SILOE reactor.

In this context, we do not think that we can start the planned process of conversion. We plan to continue until the end in burning old stocks of HEU which are available in France (in the range of 85 % to 90 %).

The closing of this reactor could constitute a serious problem for the R & D program on high density silicide fuels because research and development program has been implemented between CEA and CERCA to increase the quantity of U^{235} per fuel element:

- by increasing the thickness of the fuel meat and by reducing correlatively the thickness of the cladding ;
- by increasing the uranium density from 4.8 to 6 g/cm^3 ;
- by a combination of these two parameters.

Since august 1994 an irradiation experiment has been in progress in the IRIS device to test the behaviour of the increase of the thickness of the fuel meat. The high density fuel plates will be loaded in this device early in 1995.

After closing down SILOE, this program will be probably cancelled because it will not be possible to move the irradiation devices in the OSIRIS reactor.

REX 2000

CEA has decided to build on the site of the Centre d'Etudes in Cadarache a "multipurpose" reactor in the 50-100 MW range to replace the OSIRIS and SILOE reactors in the year 2005.

Three designs have been studied :

- a fast neutron core (plutonium) surrounded by a graphite reflector ;
- a RHF GRENOBLE type core, but using LEU,
- a traditional pool reactor (LEU).

The final choice will be made in 1995 on the basis of the needs of technological experiments, such as they can be anticipated today, over the next 30 years.

FUEL CYCLE

The reprocessing is, in France, the reference process to manage the irradiated fuels. So that, all the irradiated fuels elements coming from OSIRIS reactor (UO_2 Caramels) will be reprocessed by the CEA in its MARCOULE plant (APM) in 1996 and 1997.

Concerning the HEU fuel elements, our intent is to mix the reprocessed uranium with depleted uranium to get LEU fuels. Because of the progress made by CERCA in 1994 to use uranium batches containing small amounts of transuranic elements and fission products, CEA is now very confident in the future. CERCA is in a position to ask license from the french regulatory body to use the LEU reprocessed uranium in the fuel manufacturing plant.

Reactor	Type of fuel		Number or irradiated elements as of 7/10/94	Location of elements as of 7/10/94	Planned end of cycle
OSIRIS	UO_2	7.5 %	813	- Reactor site - PEGASE storage - APM (Marcoule)	To be reprocessed in 1996 and 1997 at APM (CEA reprocessing facility in Marcoule)
	U_3Si_2	20 %	15	- Reactor site	CASCAD dry storage (Cadarache)
SILOE	UAl	93 % (85-90 %)	292	- Reactor site - PEGASE storage	Planned options - Cogema reprocessing, UP_1 Marcoule - AEA reprocessing → LEU - Return US DOE 20 %
ORPHEE	UAl_x	93 %	144	- Reactor site - PEGASE storage	↓ Osiris REX 2000
RHF	UAl_x	93 %	18 cores	- PEGASE storage	
REX 2000	LEU (or Pu)		0		CASCAD dry storage (Cadarache)

THE CURRENT STATE OF THE RUSSIAN REDUCED ENRICHMENT RESEARCH REACTORS PROGRAM

V.G.Aden, E.F.Kartashov, V.A.Lukichev and S.A.Sokolov Research and Development Institute of Power Engineering, Russia

N.V.Arkhangelsky and N.I.Ermakov RF Ministry of Atomic Energy, Russia

Y.A.Stetskiy and G.A.Sarakhova All-Russia Scientific Research Institute of Inorganic Materials, Russia

A.A.Yenin and A.B.Aleksandrov Novosibirsk Plant of Chemical Concentrates, Russia

SUMMARY

The report presents the current state of the Russian reduced enrichment research reactors program.

During the last year after the 16-th International Conference on Reducing Fuel Enrichment in Research Reactors held in October, 1993 in Oarai, Japan, the conclusive stage of the Program on reducing fuel enrichment (to 20% in U-235) in research reactors was finally made up in Russia.

The Program was started late in 70th and the first stage of the Program was completed by 1986 which allowed to reduce fuel enrichment from 80-90% to 36%.

The completion of the Program current stage, which is counted for 5-6 years, will exclude the use of the fuel enriched by more than 20% from RF to other countries such as: Poland, Czeck Republick, Hyngary, Roumania, Bulgaria, Libya, Viet-Nam, North Korea, Egypt, Latvia, Ukraine, Uzbekistan and Kazakhstan.

In 1994 the Program, approved by RF Minatom authorities, has received the status of an inter-branch program since it was admitted by the RF Ministry for Science and Technical Policy.

The Head of RF Minatom central administrative division N.I.Ermakov was nominated as the Head of the Russian Program, V.G.Aden, RDIPE Deputy Director, was nominated as the scientific leader.

The Program was submitted to the Commission for Scientific, Technical and Economical Cooperation between USA and Russia headed by Vice-President A.Gore and Prime Minister V.Chernomyrdin and was given support also.

The Secretary of US Department of Energy Mrs. H.O'Leary has noted in her letter addressed to the Minister for Atomic Energy Mr. V.N.Mikhailov that "A joint effort by the United States and Russia to minimize the use of HEU in civil reactors would help implement one of the key objectives of the January 14, 1994 Summit Joint Statement on Nonprolifiration... We believe this is a promising area for U.S.-Russian cooperation in nonprolifiration".

In his reply Mr. V.N.Mikhailov has expressed his gratitude to Mrs. H.O'Leary for the support rendered to the proposals on developing cooperation between US DOE and Minatom of Russia in the field of reducing fuel enrichment in research reactors.

Working contacts were maintained on the problem of reduced enrichment with Argonne National Laboratory.

A group US specialists visited Russia in November, 1993 aiming at getting familiar with Russian institutes potentialities to implement the Program. The specialists have visited Research and Development Institute of Power Engineering (RDIPE) in Moscow, All-Russia Scientific Research Institute Inorganic Materials (VNIINM) in Moscow, Novosibirsk Plant of Chemical Concentrates (NZHK) in Novosibirsk, RDIPE Ekaterinburg Branch in Zarechny, Sverdlovsk Region, Machinery building Plant (MSZ) in Electrostal, Moscow Region. The Russian and American parties have presented a number of scientific and technical reports which demonstrated the achievements in the development of high density fuel (UO_2, U_3Si, U_3Si_2, U-Zr-Nb, U_6Fe), technology for manufacturing fuel elements and fuel assemblies as well as possibilities of fuel elements and fuel assemblies reactor tests and their post-reactor studies under RDIPE Ekaterinburg Branch conditions.

Sharing opinion between Russian and US specialists enabled to specify some propositions of the Russian Program.

The Program final stage content, which will take place during 5-6 years is briefly presented below.

Having in mind a necessity to switch the research reactors as soon as possible to the fuel with 20% enrichment in U-235 the Program stipulates three principle stages in the work:

- develop fuel elements and assemblies of the VVR-M2, IRT-3M, MR types with fuel based on uranium dioxide but with higher uranium density in comparison with the one reached so far;
- develop high density fuel;
- develop fuel elements and fuel assemblies of the VVR-M5, IRT-3M, IVV-10 types with high density fuel.

Such a structure of the Program is aimed at the first stage at switching the research reactors to 20% enriched fuel with the use of uranium dioxide. Then as the high density fuel is being developed it will be possible to replace in some reactors the fuel based on uranium dioxide with the high density fuel, that will allow to improve experimental possibilities of the reactors in service.

It is substantial that the works under all three stages are being carried out in parallel.

The first stage of the Program envisages implementation of the below basic works.

Development of design:

- develop working design documentation on fuel elements and assemblies models in the first turn for reactor service life time tests and ampule devices to study fuel, as well as for tests on determining design limits for fuel elements damage in emergency modes;
- issue a quality assurance program;
- carry out thermal-hydraulic and neutronics calculations of reactor cores under normal and transient conditions.

Development of technology:

- develop a fabricational steps to manufacture of fuel elements;
- develop and manufacture tools;
- technological experiments using a high density compound with uranium dioxide under factory conditions;
- develop techniques and equipment to ensure fuel elements quality monitoring.

In-pile tests:

- develop a program for in-pile tests, technical justification on tests safety and a program on postirradiation examinations;
- manufacture fuel elements and assemblies models for in-pile tests;
- carry out in-pile tests and postirradiation examinations;
- investigations to determine fuel elements destruction threshold energy;
- study the behavior of exposed and unexposed fuel elements as similating severe accidents.

Development of core technical design:

- justify the taken decisions;
- issue the core technical design materials;
- issue materials on safety analysis and justification.

Organization of production:

- fabricate test samples of fuel elements and assemblies, carry out factory tests and tests for reception, organization of their production;
- fabrication of fuel elements and assemblies for two demonstration-type cores.

Trial operation of two demonstration cores.

The second stage of the Program stipulates implementation of the following general works:

- analyze the results of the own investigations previously fulfilled, foreign information on high density fuel, choose fuel types for further investigation;
- assess fuel swelling and determine alloying additions stabilizing fuel crystal structure;
- fabricate fuel samples and compositions on their basis;
- investigate their physical, mechanical and technological characteristics;
- study interactions in the "fuel-coolant" system under pre-reactor and reactor conditions;
- run in-pile tests and postirradiation examinations;
- analyze test and examinations results, choice of fuel.

The third stage of the Program covers the following key works.

Development of design materials including thermal-hydraulic and neutronics calculations of cores in stationary and emergency modes.

Development of technology:

- issue a quality assurance program;
- work out a technology process to fabricate fuel granules;
- organize a test allotted work to fabricate fuel;
- fabricate fuel granules;
- work out a fabricational steps to manufacture fuel, calculate technological parameters, develop and manufacture tools, carry out technological experiments on fabricating fuel elements under industrial conditions;
- create technology and organize a test allotted work to reprocess fuel production wastes;
- develop techniques and equipment to monitor fuel elements quality.

In-pile tests:

- develop a program on in-pile tests, technical justification of tests safety and a program postirradiation examinations;
- fabricate fuel elements and assemblies models for reactor service lifetime tests and for tests aimed at determining fuel elements design-basis destruction limits in accident modes;
- carry out reactor and post-reactor investigations;
- investigate the behavior of exposed and unexposed fuel elements as imitating severe accidents.

Issue materials on core technical projects.

Organization of production:

- fabricate fuel elements and assemblies test samples, carry out factory and formal acceptance tests, organization of their production.

Develop a program to transport fuel from the countries having reactors built with the ex-USSR assistance.

The following works have already been fulfilled by the present time:

- working design documentation on fuel elements and assemblies models with fuel based on uranium dioxide has been developed;
- a test ampule fuel assemblies design has been worked out;
- preliminary thermohydraulic and neutronics calculations have been made;
- according to the Program, fabrication steps for manufacturing fuel elements have been developed at the first stage, technological conditions have been calculated and tools developed and ordered; the first technological experiments for fabricating fuel elements of the IRT- and MR-types have been carried out;
- there have been made analyses and preliminary selection of high-density fuel type such as U_3Si (x%Al), U_3Si (x%Nb, y%Zr), U_3Si_2, U+x%Zr+y%Nb, U_6Fe.

The preliminary neutronics calculations have shown that to maintain the same extent of the reactor fuel burnup as the one of the fuel with 36% enrichment in uranium-235 when uranium dioxide with 20% enrichment in uranium-235 is used as fuel, some design changes need to be made in the existing fuel elements. These changes mainly concern the thickness of fuel elements cladding and fuel meat.

To reduce the nomenclature of fuel elements produced by the plant-producer (NZHK) there have been decided that fuel assembly of the IRT-2M type should be excluded from the Program and that only fuel assembly of the IRT-3M type should be developed. These fuel assemblies have equal external dimensions, however a fuel assembly of the IRT-3M-type has much more developed surface for heat transfer (by a factor of 1.8), which allows either a higher reactor power or a larger thermal reserve.

To provide for necessary loading of uranium-235 the thickness of fuel elements in the IRT-3M fuel assembly has been increased. The thickness of cladding remains unchanged.

For technological reasons the maximum density for uranium was taken to be up to about 4 g/cm^3. It means that if the density of UO_2 is equal to 10.2 g/cm^3, than the volume fraction of uranium dioxide in fuel element core does not exceed 40%.

The first fuel elements of the MR and IRT types have been fabricated.

It is necessary to mention that this Program may be optimized in the course of its implementation. The full completion of the entire program depends on the amount of funds which may be allocated for the Program.

In conclusion it would be desirable to note that Russian Program has been given support at the governmental level. At present the matters of interaction between RF Minatom and US DOE within the framework of the Program in are under consideration of the Commission on Scientific, Technical and Economical Cooperation.

SESSION II

September 19, 1994

FUEL CYCLE

Chairman:

F. DiMeglio

STATUS OF DOE EFFORTS TO RENEW ACCEPTANCE OF FOREIGN RESEARCH REACTOR SPENT NUCLEAR FUEL

Charles R. Head
Office of Spent Fuel Management
U.S. Department of Energy

19 September 1994

BACKGROUND

- Expiration of "Off-Site Fuels Policy"
- 1992 EA
- Requests for DOE to renew acceptance
- Watkins December 1992 letter to Eagleburger
- O'Leary 13 July 1993 letter to Christopher
  - Reaffirmed commitment to RERTR program
  - Three tiered approach

EA DEVELOPMENT

- Proposed Action
- First draft issued for public review
  18 October 1993
    - 30 day comment period
    - Nature of comments:
        - Questioned need for action
        - Questioned status of reactor's SNF storage
        - Disputed basis for port selection
        - Questioned plans for 150 element contingency for near term proliferation concerns

EA DEVELOPMENT (Cont.)

- DOE response:
  - Decided to send teams to each reactor from which SNF acceptance was being considered
  - Decided to reduce the number of elements proposed to be accepted and mix of reactors
  - Added 5 new ports of entry
  - New draft required, issued 9 February 1994, 30 day comment period extended to 60 days
- Final EA and FONSI released on 22 April 1994:
  - 409 SNF elements
  - 8 reactors in 7 countries
  - Receipt via Sunny Point and shipment via rail

EA IMPLEMENTATION

- DOE task team set up
- Numerous meetings with States
- Weekly telephone conferences
- DOE provided training for States, local municipalities & Army
- Dry run of unloading process at Sunny Point, observed by press
- $500,000 in equipment and funding to South Carolina

SOUTH CAROLINA LAW SUIT

- Filed 9 September 1994
- TRO issued the same day
- Hearings on 12 & 13 September 1994
- Judge's decision was against DOE and preliminary injunction was issued on 13 September 1994

SOUTH CAROLINA LAW SUIT (Cont.)

- DOE filed an appeal on 14 September 1994 to the U.S. Circuit Court in Richmond, VA
- DOE filed a motion on 15 September 1994 asking the Circuit Court to stay the preliminary injunction pending appeal
- DOE hopes for a ruling on its stay motion during the week of 19 September 1994
- DOE is considering options in case the appeal is unsuccessful

EIS PREPARATION

- NOI issued 21 October 1993
- Scoping conducted 21 Oct 1993 thru 8 December 1993
- Preparation of EIS began immediately after scoping
- First task was to develop the Implementation Plan (IP)
  - Preparation and staff review is complete
  - Will be issued shortly
- Work on the EIS has proceeded in parallel with development of the IP

IMPLEMENTATION PLAN CONTENTS

NOTE: Contents could still change
Unlikely to do so

- IP records the results of the scoping process
  - Summarizes the comments received
  - Outlines DOE's responses
- Specifies the proposed action and alternatives to be evaluated
- Includes a preliminary outline of the EIS
- Specifies the schedule for EIS preparation

EIS ALTERNATIVES

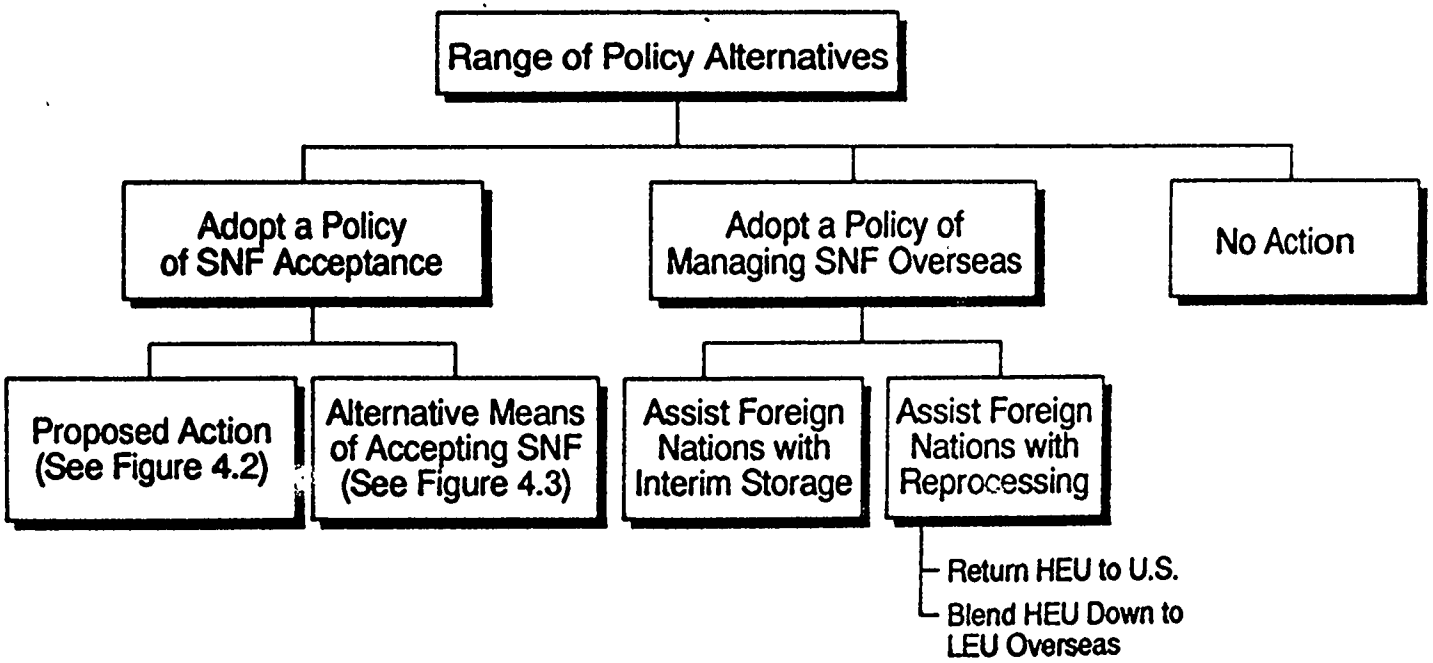

PROPOSED ACTION

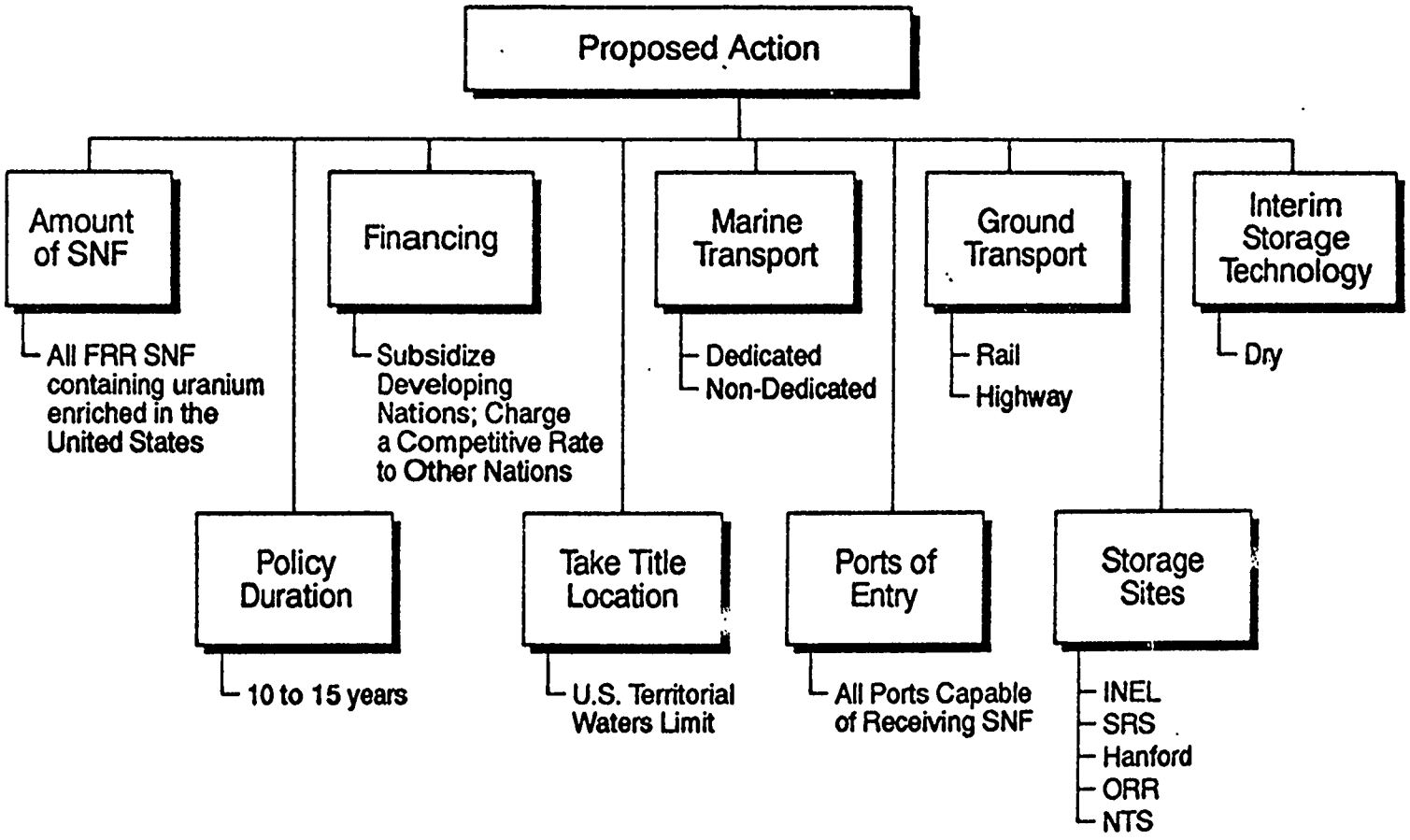

EIS DEVELOPMENT SCHEDULE

- Draft EIS scheduled for release on 10 December 1994
- Public comment period thru 10 February 1995
- Final EIS scheduled for release 30 June 1995
- Record of Decision scheduled no sooner than 30 July 1995, but before 30 December 1995

IMPLEMENTATION ALTERNATIVES

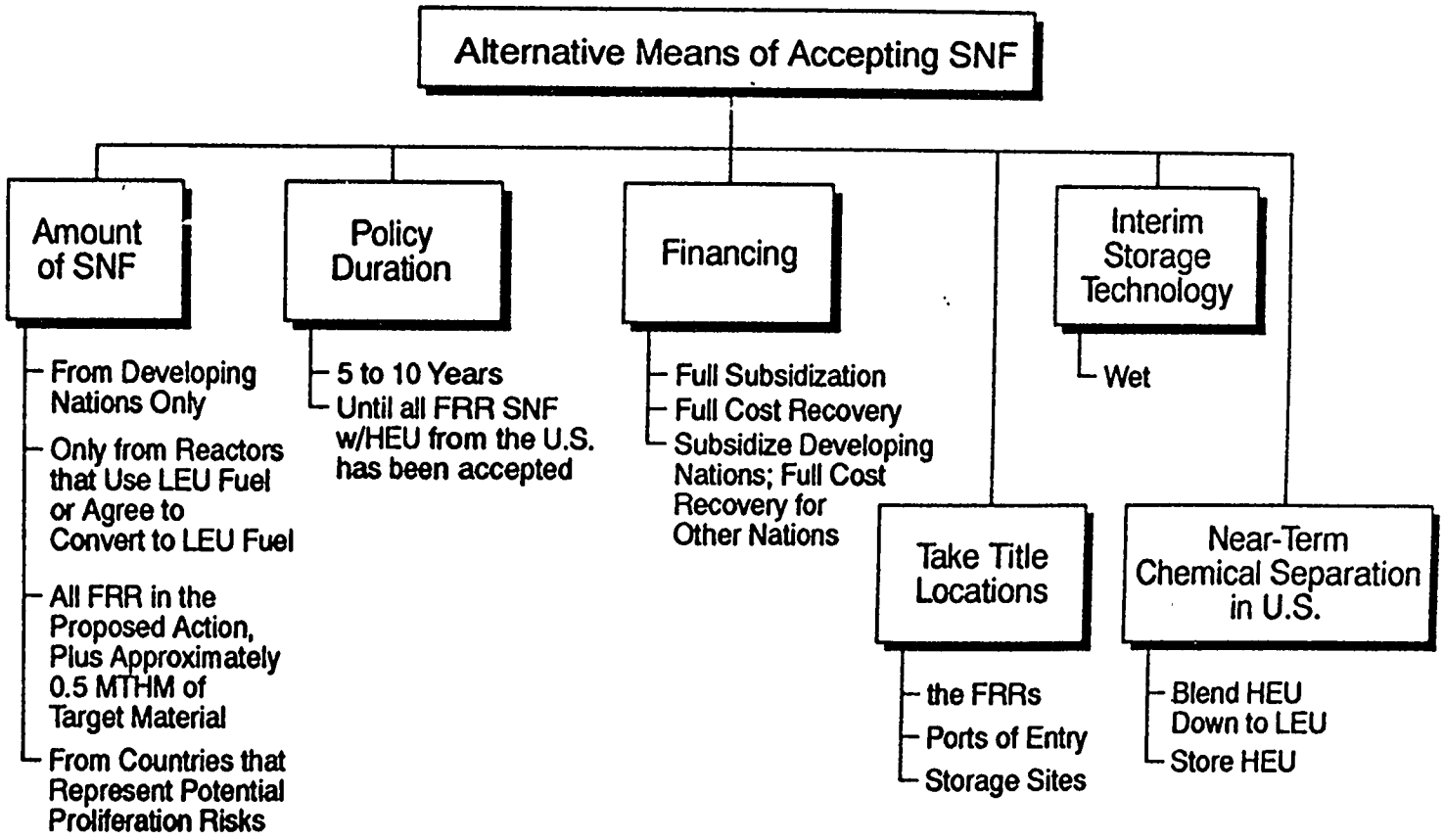

CLOSING

- EA shipments being pursued vigorously
- DOE remains determined to:
  - Support the RERTR program and
  - Complete the EIS on schedule

Foreign Research Reactor Spent Nuclear Fuel Inventories Containing HEU and LEU of US-Origin

J. E. Matos
RERTR Program
Argonne National Laboratory
Argonne, IL 60439

Abstract

This paper provides estimates of the quantities and types of foreign research reactor spent nuclear fuel containing HEU and LEU of US-origin that are anticipated during the period beginning in January 1996 and extending for 10-15 years.

Introduction

The USDOE is currently preparing (Ref. 1) an Environmental Impact Statement for potential acceptance from foreign research reactors of spent nuclear fuel containing highly enriched uranium (HEU, ≥20 wt% U-235) and low enriched uranium (LEU, <20 wt% U-235) of United States origin. This Environmental Impact Statement is scheduled (Ref. 2) to be completed by the end of June 1995. If spent fuel shipments to the United States are eventually authorized, a reasonable starting date to begin the acceptance policy is approximately January 1996. The purpose of this paper is to provide estimates of the quantities and types of foreign research reactor spent fuel containing HEU and LEU of US-origin that are anticipated during the period beginning in January 1996 and extending for 10-15 years.

Data Sources and Assumptions

Information on current spent fuel inventories containing HEU and LEU of US-origin at foreign research reactors and temporary storage facilities were obtained from several sources: (1) questionnaires sent out by DOE and returned by research reactor organizations in 1993 and 1994, (2) data summarized from spent fuel questionnaires sent out by and returned to IAEA in 1993 and 1994, and (3) RERTR Program information on research reactor fuel inventories, operation, and fuel cycles.

Beginning with inventory data available as of June 10, 1994, several assumptions were made, first to normalize the data to a common starting date of January 1996, and then to estimate the quantities of spent fuel that are expected to be generated for the following 10-15 years. These assumptions are:

1. Most reactors will continue operation during the 10-15 year life of the proposed policy. If a permanent shutdown date has been specified by the reactor owner, spent fuel was accumulated to that date only.

2. Known current and planned shutdowns for prolonged periods of maintenance and refurbishment have been incorporated into the estimates.

3. Dates for conversion from HEU to LEU fuel have been estimated, and the enrichment change was incorporated into the inventory data.

4. Estimated spent fuel inventories for reactors that are under construction or plan to begin operation during the life of the proposed policy using enriched uranium of U.S.-origin have been included.

5. Fuel from previously shutdown reactors with fuel in temporary storage has been included.

Fuel Types

Under the Offsite-Fuels Policy that was in effect in 1988 (Ref. 3), the USDOE accepted aluminum-based and Triga research reactor fuels for disposal. The aluminum-based fuels were shipped either to the Savannah River Site in South Carolina or to the Idaho National Engineering Laboratory. All Triga fuels have been shipped to Idaho and stored.

Figure 1 shows cross sections of the main western research reactor fuel assembly geometries: MTR box-type assemblies containing 10-24 fuel plates per assembly (many countries), involute core assemblies containing 280 fuel plates (RHF, France), tubular fuel assemblies with 4-6 fueled tubes per assembly (BR-2, Belgium and DIDO, UK), Triga fuel rod clusters with 1-25 rods per cluster (Triga, South Korea - single rods, and Triga, Romania - 25 rods per cluster), and pin assemblies with 1-12 pins per assembly (Slowpoke, Canada - single pins, and NRU, Canada - 12 pins per assembly). All of these fuel assemblies are roughly 2-3 feet (60-90 cm) in length, except for the NRU assemblies which are ~9 feet (275 cm) long and Slowpoke fuel pins which are ~1 foot (30 cm) long.

All reactor fuel types are shipped in assembly form with two exceptions. Triga fuel rod clusters are disassembled and shipped as individual rods. The Triga reactor core in Romania has ~30 fuel clusters with 25 rods per cluster. A core would be shipped as 750 individual rod units. Slowpoke cores contain approximately 300 fuel pins, which have been shipped in bundles of approximately 150 pins.

Uranium-aluminum alloy fuel pins containing highly-enriched uranium are used as target material in the Canadian NRU reactor to produce nearly all radioisotopes used in nuclear medicine in the United States. After the irradiated fuel pins are de-clad and dissolved in acid, the radioisotope Mo-99 is extracted for use in medical imaging applications. The remaining target material is currently stored in liquid form and could be turned into a powder and shipped in aluminum containers using research reactor spent fuel shipping casks.

In addition to the fuel types discussed above, enriched uranium of US-origin is also used in several fast reactors and other special purpose reactors, in UO_2 rodded assemblies, and in homogeneous liquid and solid fueled reactors. The enrichment of the uranium ranges from 2% to 93%.

Spent Fuel Inventories

Estimated spent fuel inventories of HEU and LEU aluminum-based and Triga fuel from foreign research reactors in January 1996 and January 2006 are summarized in Table 1, based on information available as of June 10, 1994. In January 2006, HEU spent fuel of US-origin is expected to be comprised of ~10,400 aluminum-based fuel assemblies that contained ~4900 kg HEU before irradiation, ~2100 Slowpoke fuel pins that initially contained ~6 kg HEU, and ~1000 Triga fuel rods that initially contained ~66 kg HEU. In January 2006, LEU spent fuel of US-origin is expected to be comprised of ~6800 aluminum-based fuel assemblies that contained ~12,700 kg LEU before irradiation, ~200 Slowpoke fuel pins that initially contained ~6 kg LEU, and ~2000 Triga fuel rods that initially contained ~470 kg LEU.

Table 2 shows the same data as Table 1, but organized into estimated spent fuel of US-origin possessed by developed countries and by developing countries (defined as countries which qualify for IAEA assistance). The developed countries are further broken down into European developed countries and all other developed countires. The vast majority of both HEU and LEU aluminum-based fuels are expected to be generated in the developed countries. Nearly all HEU Triga fuel is expected to be generated in developing countries along with a majority of the LEU Triga fuel.

In addition to the fuels listed in Tables 1 and 2 for a ten year life of the proposed spent fuel acceptance policy, assume that reactors that convert to LEU fuel in the five years between January 1996 and January 2001 would be eligible to return their LEU spent fuel to the United States until January 2011 at the latest. The estimated maximum additional quantities of LEU aluminum-based and Triga fuel that would be eligible for return if all current reactors were to convert to LEU fuel at the end of the fifth year is shown in Table 3.

References

1. C. Head, "Status of DOE Efforts to Renew Acceptance of Foreign Research Reactor Spent Nuclear Fuel", these proceedings.

2. Letter from Hazel R. O'Leary, Secretary of Energy, to Warren Christopher, Secretary of State, July 13, 1993.

3. U.S. Federal Register, Volume 51, No. 32, February 18, 1986 and Volume 52, No. 250, December 31, 1987.

Figure 1. FUEL ASSEMBLY GEOMETRIES

	LIGHT WATER	HEAVY WATER
PLATES	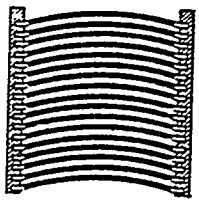	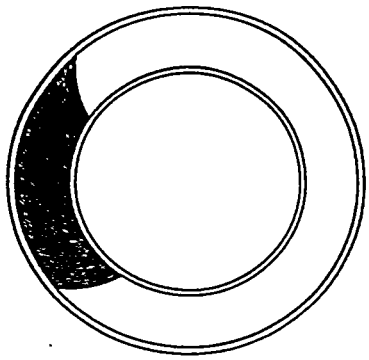
	MTR, 1-50 MW Many Countries	RHF, 57 MW France
TUBES	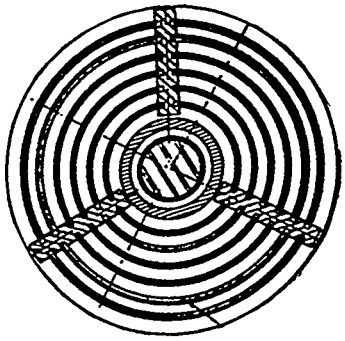	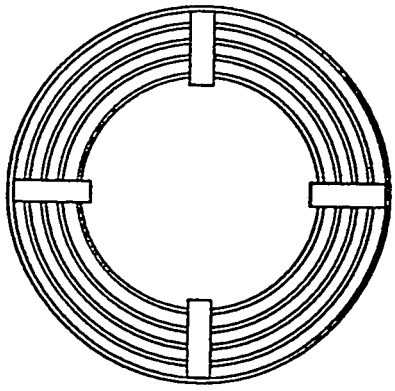
	BR-2, 125 MW Belgium	DIDO, 25 MW UK
PINS	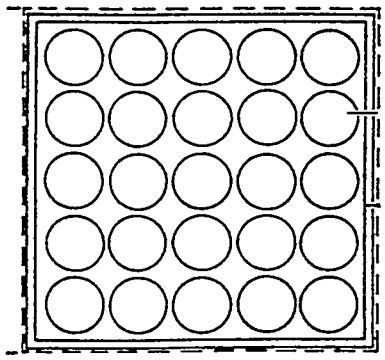	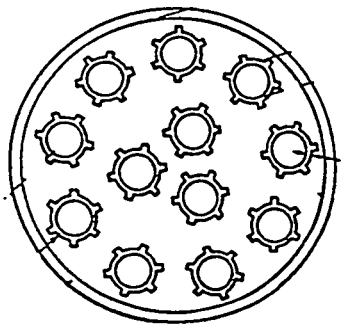
	TRIGA, 14 MW Romania	NRU, 125 MW Canada

Table 1. Summary of Estimated (10 Jun 94) Foreign Research Reactor Aluminum-Based and Triga Spent Nuclear Fuel Containing HEU and LEU of US-Origin

Fuel Type	Enr.	January 1996 Number	January 1996 Kg U*	January 1996 Kg Total Weight	January 2006 Number	January 2006 Kg U*	January 2006 Kg Total Weight
HEU ALUMINUM-BASED FUELS							
MTR Box-Type Fuel Assem.	HEU	4,387	1,574	21,870	5,625	2,039	28,491
Tubular Fuel Assemblies	HEU	2,066	691	7,010	3,551	1,259	11,892
Involute Core Assemblies	HEU	25	228	2,750	110	977	10,503
NRU/NRX Fuel Assemblies	HEU	1,125	591	5,130	1,125	591	5,130
		7,603	3,084	36,760	10,411	4,866	56,016
Slowpoke Fuel Pins	HEU	317	1	5	2,140	6	32
Total HEU Aluminum-Based		7,920	3,085	36,765	12,551	4,872	56,048
HEU TRIGA FUEL							
TRIGA Fuel Rods	HEU	189	21	353	1,019	66	1,030
		8,109	3,106	37,118	13,570	4,938	57,078
LEU ALUMINUM-BASED FUELS							
MTR Box-Type Fuel Assem.	LEU	974	1,427	5,959	4,556	8,186	29,941
Tubular Fuel Assemblies	LEU	195	176	644	671	632	2,302
Involute Core Assemblies	LEU	0	0	0	0	0	0
NRU Fuel Assemblies	LEU	337	838	2,224	1,437	3,572	9,484
MAPLE-X Fuel Assemblies	LEU	0	0	0	180	288	981
		1,506	2,441	8,827	6,844	12,678	42,708
Slowpoke Fuel Pins	LEU	0	0	0	200	6	3
Total LEU Aluminum-Based		1,506	2,441	8,827	7,044	12,684	42,711
LEU TRIGA FUEL RODS							
TRIGA Fuel Rods	LEU	1,062	216	3,614	1,966	468	5,619
		2,568	2,657	12,441	9,010	13,152	48,330

* Inital weight of uranium before irradiation in reactor.

G1 Booster Rods	HEU	16	18	78	16	18	78
Mo-99 Target Material	HEU	(1)	112		(1)	185	
Mo-99 Target Material	LEU	0	0	0	(1)	340	

(1) The number of containers will depend on the container design and on the final form of the material.

In addition to the fuels listed above, enriched uranium of US-origin is currently used in a number of fast reactors and other special purpose reactors, in UO2 rodded assemblies, and in homogeneous liquid and solid fueled reactors. The enrichment of the uranium ranges from 2% to 93%.

Table 2. Summary of Estimated (10 Jun 94) HEU and LEU Aluminum-Based and Triga Spent Fuel of US-Origin Possessed by Foreign Research Reactors (Data in Table 1 Organized by Country Group)

Country Group	January 1996 HEU Fuel No.	Kg HEU*	Kg Total Weight	January 1996 LEU Fuel No.	Kg LEU*	Kg Total Weight	January 2006 HEU Fuel No.	Kg HEU*	Kg Total Weight	January 2006 LEU Fuel No.	Kg LEU*	Kg Total Weight
ALUMINUM-BASED FUELS												
Developing	791	153	3,607	329	251	1,442	1,230	183	4,275	565	521	2,945
Europe	3,542	1,485	18,741	516	836	2,795	5,607	3,070	35,368	3,325	6,113	19,828
Other	3,587	1,447	14,417	661	1,354	4,590	5,714	1,619	16,405	3,154	6,050	19,938
	7,920	3,085	36,765	1,506	2,441	8,827	12,551	4,872	56,048	7,044	12,684	42,711
TRIGA FUEL												
Developing	188	21	349	595	127	1,934	1,017	66	1,023	1,266	335	3,098
Europe	1	0	4	452	86	1,626	2	0	7	675	128	2,431
Other	0	0	0	15	3	54	0	0	0	25	5	90
	189	21	353	1,062	216	3,614	1,019	66	1,030	1,966	468	5,619

* Initial weight of uranium before irradiation in reactor.

Developing Countries

Argentina	Pakistan
Bangladesh	Philippines
Brazil	Portugal
Chile	Romania
Columbia	Slovenia
Greece	South Korea
Indonesia	Taiwan
Iran	Thailand
Israel	Turkey
Jamaica	Uraguay
Malaysia	Venezuela
Mexico	Zaire

Developed Countries

Europe		Other
Belgium	Austria	Australia
Denmark	Finland	Canada
France	Sweden	Japan
Germany	Switzerland	South Africa
Italy		
Netherlands		
Spain		
United Kingdom		

Table 3.

Estimated Maximum Quantities of Aluminum-Based and Triga LEU Spent Fuel of US-Origin That Would be Generated Between January 2006 and January 2011 if All Candidate Reactors Were to Convert from HEU to LEU Fuel in January 2001.

ESTIMATED MAXIMUM ADDITIONAL LEU ALUMINUM-BASED FUEL

January 2006 to January 2011 LEU Fuel			
Country Group*	No.	Kg LEU**	Kg Total Weight
Developing	45	42	229
Europe	1,370	3,840	13,955
Other	275	247	1,013
	1,690	4,129	15,197

* See Table 2 for definition of country groups.

** Initial weight of uranium before irradiation in reactor.

ESTIMATED MAXIMUM ADDITIONAL LEU TRIGA FUEL

An estimated 10 additional TRIGA LEU spent fuel rods would be generated between January 2006 and January 2011 by TRIGA reactors that could convert from HEU to LEU TRIGA fuel by January 2001. These 10 rods would contain about 5 Kg LEU and weigh approximately 36 Kg.

1994 INTERNATIONAL MEETING
ON REDUCED ENRICHMENT FOR RESEARCH AND TEST REACTORS (RERTR)

TRANSPORTATION OF SPENT MTR FUELS

D. Raisonnier - Transnucléaire

This paper gives an overview of the various aspects of MTR spent fuel transportation and provides in particular information about the on-going shipment of 4 spent fuel casks to the United States.

INTRODUCTION

Transnucléaire is a transport and Engineering Company created in 1963 at the request of the French Atomic Energy Commission. The company followed the growth of the world nuclear industry and has now six subsidiaries and affiliated companies established in countries with major nuclear programs.

The expertise of Transnucléaire is specially related to:

- Transport of radioactive material on a worldwide basis, providing each customer with a full "door to door" transport management.

- Design and procurement of appropriate casks and equipment.

MTR SPENT FUEL TRANSPORT

Due to the limited storage capacity of the pools of the MTR reactors, and the availability of reprocessing facilities in several countries (US, UK), numerous MTR spent fuel shipments have been made since 1964.

Up to 1976, the TN group also carries out transports of MTR fuel elements to the European reprocessing plant (Eurochemic) at Mol, Belgium and to Marcoule in France.

Following the closure of these plants, subsequent transports were made to the US DOE reprocessing plants under the «US Off-Site Fuel Policy».

Between 1978 and 1988, the major part of the 365 cask-shipments received by DOE for reprocessing at either the Savannah River Plant or at the Idaho National Engineering Laboratory (INEL) were originating from Western European countries.

During this period all the transports of MTR spent fuel, performed towards the US by the TN Group were carried out without any particular difficulty or incident, using specialized common carriers for overland transport, commercial ports and routine liner services for transatlantic shipments.

ON-GOING TRANSPORT OPERATION

After completion of the Environmental Assessment (EA) of Urgent Relief Acceptance of Foreign Research Reactor Spent Fuel, the Department of Energy has issued a Finding of No Significant Impact (FONSI) and decided to accept a limited number of spent fuel elements (409) coming from European research reactors in Austria, Germany, Greece, the Netherlands, Sweden and Switzerland.

Several specific constraints were imposed by the DOE:

- use of Sunny Point military port
- rail transport in the US
- limitation of the number of shipments.

In addition, and for different reasons, the first shipment should arrive before the end of September at Sunny Point.

MID-JUNE 1994

A meeting conducted by EIC and gathering all the parties involved (reactor operators, cask suppliers, transport companies) was held in Brussels on June 17, 1994.

The aim of this meeting was, regarding transportation aspect, to exchange information/ possibilities and to pool resources to allow completion of the first shipment on time, to the satisfaction of the customers and of the DOE.

Transnucléaire proposed to:

- supply a maximum of 4 IOU4 (Pegase) casks suitable for HFR, DR3, ASTRA, GRR1 and SAPHIR fuels.

- charter a Danish flag vessel, specialized in the transportation of dangerous goods and familiar with the port of Sunny Point.

- Offer safe transport routing including:

    - direct loading in the Nordic ports of the Danish and the Swedish fuel casks
    - routing other fuel casks by rail or by road to a private rail terminal near Cherbourg
    - rail transport from this terminal to Cherbourg port
    - utilization of Cogema port facilities in Cherbourg

Several important points were to be carefully checked, qualified, and approved by a large number of organizations in several countries within a short period time.

- Reactor operators dealt mainly with:

  - cask loadings operations
  - Euratom or IAEA safeguards
  - customs formalities
  - contracts with the DOE
  - transport arrangements with the transport companies

- Transport companies (EIC/NCS/Transnucléaire) dealt with:

  - cask availability according to fuel characteristics and reactor requirements
  - corresponding package design certificates of approval (in the country of origin of the package design, of the shipment, in transit countries and in the United States).
  - transport arrangements with Competent Authorities, customers and subcontractors (trucking companies, railways, shipowners...)
  - insurance analysis (nuclear liability, loss and damage, salvage)

END OF JULY

The following decisions were made:

- Ship material from:

Risoe	DR3/3	- IUO4 cask (supplied by Transnucléaire)
Studsvik	R2	- TN 7-2 cask (supplied by NCS)
Delft	HOR	- GNS 11 cask (supplied by GNS)
Seibersdorf	ASTRA	- IUO4 cask (supplied by Transnucléaire)
Berlin	BER-II	- GNS 11 cask (supplied by GNS)

- Charter the vessel as proposed by Transnucléaire

- Use Cherbourg port with the possibility to bring the DR3 and R2 fuel by sea using the SYGIN (Swedish flag vessel specially built for transporting the Swedish nuclear spent fuel and waste).

- Depart from Cherbourg: early September

MID-AUGUST 1994

We were informed by the Danish Authority of their decision to put immediately in force in Denmark the Code of practice for safe carriage of Irradiated Nuclear Fuel (INF Code) recently adopted by the International Maritime Organization (IMO) but not yet implemented in national laws.

According to this Code the maximum activity for INF 1 class ship is limited to 4,000 Tbq.

The total activity of the 5 casks exceeding 8,000 Tbq, we were unable to load all of them at the same time in our INF 1 ship.

We investigated together several other solutions. Due to the impossibility to have available on time an INF 2 class ship, we decided to charter a second vessel but we were unfortunately unable to include the HMI cask in this shipment in order to remain under 4,000 Tbq per ship.

END OF AUGUST

Sailing of the M/S MARIA from Swedish and Danish ports with two casks on board:
TN7-2 with Swedish fuel
IUO4 with Danish fuel

EARLY SEPTEMBER

Sailing of the M/S MARSUS from Cherbourg, with two casks on board:
IUO4 with Austrian fuel
GNS 11 with Dutch fuel.

THIS WEEK

The two ships are due to arrive together at Sunny point for, hopefully, immediate unloading and subsequent delivery by rail to Savannah River Plant.

NEXT YEAR

Enough casks being available we are studying together the possibility to use an INF 2 ship allowing to load the remaining fuel elements.

We recommend this solution as well as the use of facilities in France (Valognes and Cherbourg) offering handling equipment and an intermediate storage site for road and rail transport.

AFTERWARDS

Spent fuel management is an important issue for the Research Reactors. Interim storage and reprocessing will require transportation services including cask supply for a large number of fuel elements.

Specialized transport companies are in a position to bring appropriate answers to the diversity of technical and regulatory questions by this large scale transportation.

REPROCESSING OF RESEARCH REACTOR FUEL
THE DOUNREAY OPTION

P CARTWRIGHT
UKAEA GOVERNMENT DIVISION
DOUNREAY

ABSTRACT

Reprocessing is a proven process for the treatment of spent U/Al Research Reactor fuel. At Dounreay 12679 elements have been reprocessed during the past 30 years. For reactors converting to LEU fuel the uranium recovered in reprocessing can be blended down to less than 20% U_{235} enrichment and be fabricated into new elements. For reactors already converted to LEU it is technically possible to reprocess spent silicide fuel to reduce the U_{235} burden and present to a repository only stable conditioned waste.

The main waste stream from reprocessing which contains the Fission products is collected in underground storage tanks where it is kept for a period of at least five years before being converted to a stable solid form for return to the country of origin for subsequent storage/disposal.

Discharges to the environment from reprocessing are low and are limited to the radioactive gases contained in the spent fuel and a low level liquid waste steam. Both of these discharges are independently monitored, and controlled within strict discharge limits set by the UK Government's Scottish Office.

Transportation of spent fuel to Dounreay has been undertaken using many routes from mainland Europe and has utilised over the past few years both chartered and scheduled vessel services. Several different transport containers have been handled and are currently licensed in the UK.

This paper provides a short history of MTR reprocessing at Dounreay, and provides information to show reprocessing can satisfy the needs of MTR operators, showing that reprocessing is a valuable asset in non-proliferation terms, offers a complete solution and is environmentally acceptable.

HISTORY OF UKAEA

The United Kingdom Atomic Energy Authority was set up under the Atomic Energy Authority Act (1954) as a government agency committed to research into the peaceful uses of atomic energy. By the late 1960s the UKAEA had grown into a very large and prestigious research and development organisation which also included a Group primarily concerned with engineering and operational aspects of nuclear power. To keep research interests at the forefront of technology, the UKAEA underwent a number of structural changes in the early 1970s, including the removal of the UKAEA Production Group which became British Nuclear Fuels Ltd (BNFL).

The years following 1971 saw the UKAEA expand its nuclear activities by undertaking similar traditional work for other organisations. Funding source changes in the early to mid 1980s resulted in the UKAEA operating on a Trading Fund basis. A Trading Fund is an arrangement under which a Government or quasi-Government organisation develops a `business-like' structure without ultimately changing the status of the organisation. The UKAEA's former Production Group had been a Trading Fund before becoming BNFL. To reflect the changing role of the organisation, the UKAEA adopted the name `AEA Technology' highlighting the new and rather more commercial image.

The launch of AEA Technology in 1989 was followed in 1990 with the formation of Businesses to bring together all the relevant skills and resources that AEA could offer in a given technical field, to serve a specific market, regardless of where the people and resources were located within the network of AEA establishments spanning hundreds of miles.

Further development was undertaken in April 1994 when the staff and facilities merged into three Divisions. The necessity for further change arose from the needs of the expanding non-nuclear activities of AEA Technology which rest uneasily in a quasi-Governmental organisation. To push the limits towards reaching full potential, these activities have been collected within `AEA plc' whose future lies in the private sector of the UK economy. A `Facility Services Division' has been set up for a limited period. These activities will be contractorised unless it is beneficial to absorb them in another Division. `UKAEA Government Division' has been formed to manage the UKAEA's Government decommissioning liabilities, but it will also look toward the management of all UK nuclear liabilities. The major activities of the (former) AEA Fuel Services is placed within `Nuclear Sites Operations' a Division of UKAEA Government Division.

At Dounreay, PFR ceased operation on 31 March 1994, which leaves the Fuel Plants and the Waste Facilities as the only operating nuclear plants. The Fuel Plants are available for commercial work for UK and non-UK customers, subject to the prime customers needs (UK Department of Trade and Industry). The Oxide Fuel Reprocessing Plant will continue operation until 1999 to process the PFR fuel (and reprocessing secured commercial work thereafter) and the remaining Plants, including the MTR reprocessing plant will operate in a commercial mode provided there exists a market for their services, and so long as there is a net benefit to the UK taxpayer.

MTR REPROCESSING HISTORY

In the late 1950's the Research Reactor Reprocessing plant was constructed at Dounreay to service the requirements of the UK uranium aluminium fuelled Research Reactors. The reprocessing plant was sized to not only service the UK reactors, but also to include overseas elements which had been manufactured at Dounreay. When the plant started operating in 1958 and for a number of years following, a complete fuel cycle existed on the Dounreay site, until the Dounreay Material Test Reactor was shutdown due to overcapacity in the UK MTR's.

Reprocessing of overseas fuel commenced in 1962, when elements from Denmark were reprocessed. Further reprocessing campaigns continued until 1973, recovering uranium from MTR fuel from Denmark, Australia, France, India, Germany, South Africa, Greece, Japan and Sweden. A list of the MTR elements reprocessed to date is shown in Table 1.

Table 1 Elements Reprocessed 1958 to 1994

COUNTRY	NO OF ELEMENTS	TOTAL URANIUM (kg)
United Kingdom	9262	1421.9
Belgium	240	59.5
Spain	6	10.8
Denmark	950	105.6
France	289	98.1
Australia	150	16.0
India	83	14.0
Germany	866	129.6
South Africa	216	29.5
Greece	39	29.6
Sweden	168	24.8
Japan	410	82.7
	12679	2022.1

Reprocessing contracts undertaken up to 1973 had no requirement for the return of waste from the UK. Between 1973 and 1989, overseas reactors transferred their elements to the United States of America and received in return uranium credits, for the uranium-235 contained in the spent fuel, which were returned in the form of HEU. During this period MTR reprocessing continued, servicing all of the UK reactors.

Following the cessation of the US spent fuel return policy in 1989, some European reactor operators found themselves to be under increasing pressure to `close' their fuel cycle and in 1990 UKAEA Dounreay started to arrange storage with reprocessing option contracts. These contracts utilised the available pond storage at Dounreay which became available following closure of the Pluto and Dido reactors at Harwell and transfer of their entire fuel inventories to Dounreay. In 1991, the regulatory pressure in Germany and the pressure on some other National Nuclear programmes led to the signature of reprocessing contracts with German and Spanish MTR operators. The terms of these reprocessing contracts differed from the pre-1973 contracts in that they included the return of the radioactive waste products from reprocessing. The return of these waste products is a UK Government requirement and an intergovernmental exchange of letters which states that the reactors host government will not prevent the return of wastes, conditioned to an agreed form within a stipulated period, is essential.

Further contracts for reprocessing were signed with customers for Indian, German and Belgian fuel and between September 1993 and April 1994 approximately 600 overseas elements were reprocessed. This paper focuses on this last reprocessing campaign and details the various stages involved in the reprocessing of MTR fuel.

FUEL TRANSPORT AND STORAGE

The transportation of MTR fuel from the reactor sites to Dounreay has all been accomplished under the IAEA regulations in force at the time. For the last reprocessing campaign fuel elements were received using a variety of transport flasks and transport routes. The flasks used are shown in table 2 and the transport routes shown in table 3.

Table 2 Flasks Received for 1993/94 Campaign

MTR FLASK	ELEMENTS CONTAINED IN EACH FLASK
Goslar	13
GNS 11	33
GNS MTR	33
GNS MTRF	33
TN7	80
Unifetch	24

The flasks normally were transferred in pairs, although in some cases single flask movements were undertaken. In all, twenty flask moves containing MTR fuel occurred between 1992 and 1994.

Table 3 Transport Routes Utilised for 1993/94 Campaign

MAINLAND TRANSPORT	CHANNEL CROSSING	UK TRANSPORT
Road → Rail	Nord Pas de Calais	Rail → Road
Road	Charter	Road
Road	Container Ship	Road

All of the MTR fuel reprocessed in this last campaign was offloaded into an interim storage pond. The interim storage pond is equipped with a 25 tonne capacity crane and is designed to allow the handling of most MTR type flasks. The interim storage pond has capacity to store more than 1000 standard irradiated elements, depending on their type and is equipped with water purification equipment to maintain a high quality of water.

FUEL TRANSFER FOR BREAKDOWN

The route between the interim storage facility and the fuel breakdown pond utilises Dounreay internal transfer flasks. Elements are taken either singly or in groups to a buffer storage matrix, before being presented to the reprocessing plant. The first stage of the reprocessing process occurs when the elements are weighed using an electronic balance. As this weighing operation is carried out underwater a weight correction factor, which relates to the density of the fuel element and water, is used to calculate the actual total weight of fuel for reprocessing. The fuel is then transferred to an underwater hydraulic cropper which cuts the fuel element into short lengths. Some customers for the last campaign benefitted at this stage, where it was possible to remove some of the aluminium components and dispose of them separately. This resulted in a lower fuel weight being prepared for reprocessing and an effective waste management strategy to reduce the amount of waste for future return. With the continuance of reprocessing, this operation may well be undertaken using different equipment in the fuel storage pond.

Underwater fuel breakdown leads to some leaching of fission products from the cut fuel. The use of ion exchange equipment which removes the bulk of the dissolved Cs-137 reduces the effects of this leaching and maintains the pond radiation level within the plant working limits.

FUEL DISSOLUTION AND SOLVENT EXTRACTION

Fuel Dissolution and solvent extraction pose few difficulties due to the experience built up at Dounreay over the past 25 years. Dissolution of all aluminium clad fuels is completed in a nitric acid solution with a mercuric catalyst. However, depending on the uranium/aluminium ratio of the fuel, slightly different dissolution recipes are used. This ensures the feed to the solvent extraction system is within prescribed boundaries for uranium, aluminium concentration and acidity, and the extraction will therefore perform as designed. The solvent extraction system in the MTR reprocessing plant consists of two separate cycles of mixer-settler boxes. Mixing is achieved through the use of motor driven paddles. All the equipment is geometrically safe by shape to permit even low burn-up HEU elements to be reprocessed. For HEU fuels there is very little in-bred plutonium, hence it is not necessary to set the solvent extraction parameters to specifically remove plutonium from the uranium product. For MEU and especially LEU fuels ,the solvent extraction is operated to remove the plutonium in cycle 1 along with the fission products. Whatever solvent extraction regime is selected, the end result is the same. The uranium in the fuel is recovered in a pure form and the other species in the fuel are rejected into the raffinate. The raffinate is routed to active liquor storage tanks, any gaseous fission products are discharged to atmosphere, and a very small amount of activity is discharged in the form of low level liquid waste. Each of these products of reprocessing are considered separately in the next section.

The dissolution and solvent extraction of LEU silicide fuels does require some further consideration. Justification of the reprocessing of such fuels can not focus on the reuse of a valuable product. It is therefore necessary to consider what can be done instead? Aluminium clad fuels are unsuitable for long term storage due to possible cladding corrosion. They could be placed within disposal canisters but the presence of the large amount of uranium may make this prohibitive. Another option is to reprocess, to separate the uranium and to condition the resulting fission product stream for disposal.

Reprocessing of silicide fuels poses several questions. Standard dissolution results in a solution containing substantial amounts of insoluble silicide. In the 1970's this problem was encountered at Dounreay when the high silicon alloy (2% Si) Greek fuel was reprocessed. The problem at this stage was overcome by operating a dilute flowsheet and processing the material at 25% of the normal throughput. This is, of course, unacceptable for a large campaign of silicide reprocessing. At Dounreay in 1990, a large scale recovery programme of unirradiated uranium silicide was undertaken. Different techniques for the removal of the silicide were tried and the process optimised to demonstrate unirradiated silicide recovery.

In 1995 UKAEA intend to reprocess some irradiated MTR silicide fuel. The reprocessing is being undertaken to provide further information on the dissolution parameters and solvent extraction flowsheets. The process equipment necessary to demonstrate routine reprocessing of such fuel will not be installed until after these trials have been completed.

If required, UKAEA can install the necessary solid removal system in the existing plant to permit silicide fuel reprocessing in the future.

RECOVERED URANIUM

Reprocessing results in a pure uranium product with low impurities which can be reused in MTR Fuel at various enrichments. The specification for the uranium produced is shown in Table 4. The reuse of recycled uranium has been the subject of several RERTR papers over the past few years with much emphasis placed on the assumed difficulty of reusing this uranium. At Dounreay we have reprocessed and reused uranium in the form of MTR elements many times, in fact some of the uranium in the final DIDO core had completed four cycles of reprocessing and irradiation. The reuse of the uranium after reprocessing can be achieved in several ways. Uranium as recovered or at a slightly lower enrichment could permit certain reactors to achieve continuity of fuel supply until low enriched fuels of sufficient density are available. For reactors already converted to LEU there should be no difficulty. The blending of recovered uranium with depleted uranium to produce a 19.75% enriched product poses no difficulty and has already been accomplished many times. The uranium isotopic composition of the product also should not pose any manufacturing difficulties and will certainly not affect in-reactor performance. All of the facilities necessary to blend uranium to the required enrichment and produce the required uranium form are available at Dounreay.

Table 4 MTR Uranium Product after Reprocessing

1	Boron equivalence	less than 2.5 ppm
2	Uranium isotopics	as determined
3	Total impurities content	less than 1500 ppm
4	Actinide content	< 10μ Ci/gm

MAIN WASTE STREAM

The reprocessing of MTR fuel produces a main waste stream which contains greater than 99% of the waste products. At Dounreay this waste stream is stored as liquid in underground tanks for at least five years, before it is transferred to the Dounreay Cementation Plant for immobilisation. The Dounreay Intermediate Residue Specification was prepared after detailed consultation with the commercial reprocessors and precisely defines the conditioned waste form that results from MTR fuel reprocessing. As a rule of thumb each 500 litre residue drum will contain the waste products from the reprocessing of 10 kg of MTR fuel. This figure is currently limited by the aluminium content of the cement, not the radio-activity, and research and development to improve the loading is currently underway.

It is UK government policy to return MTR Fuel reprocessing wastes to the country of origin within a period of 25 years. This may not be long enough for some countries to have waste repositories in operation. For this reason the cemented residue drum is also recognised as a form suitable for above ground interim storage.

1993/94 REPROCESSING CAMPAIGN

To permit an assessment of the effect of MTR reprocessing, some data on the last MTR reprocessing campaign is considered in the next sections. The last MTR reprocessing campaign consisted of 596 elements.

ENVIRONMENTAL DISCHARGES

Radioactive discharges to the environment from the reprocessing of irradiated fuel at Dounreay are controlled under an authorisation issued by the UK Government's Scottish Office. In assessment of the permitted discharge from the site, the Scottish office considers the effect of individual radioactive species on the environment and on critical groups of individuals. The limits that are indicated from this study are then reduced to give a site discharge limit which must be adhered to.

The Radioactive discharges from Dounreay fall into two categories: liquid discharges made via a pipeline to the sea, and gaseous discharges made via ventilation stacks to the atmosphere. Liquid discharges are assessed before discharge takes place, and gaseous discharges are subjected to on-line monitoring.

The current site discharge authorisations are shown in Tables 5 and 6.

Table 5 Liquid Discharge Authorisation

COLUMN 1 RADIONUCLIDE(S)	COLUMN 2 ACTIVITY
*Alpha (excluding curium 242)	750 gigabecquerels
*Beta (excluding tritium)	110 terabecquerels
Tritium	130 teraecquerels
Cobalt 60	1 terabecquerel
Strontium 90	12 terabecquerels
Zirconium/Nioium 95	6 terabecquerels
Rutherium 106	12 terabecquerels
Silver 110m	400 gigabecquerels
Caesium 137	50 terabecquerels
Cerium 144	12 terabecquerels
Plutonium 241	15 terabecquerels
Curium 242	1 terabecquerel

*Any reference to "alpha" or "beta" in the above schedule is a reference respectively to the activity of alpha emitting or beta emitting radionuclides.

Table 6 Gaseous Discharge Authorisation

COLUMN 1 RADIONUCLIDE(S)	COLUMN 2 ACTIVITY
*Alpha (excluding curium 242 and 244)	1 gigabecquerels
*Beta (excluding tritium and krypton 85)	45 gigabecquerels
Tritium	40 terabecquerels
Krypton 85	1 petabecquerel
Strontium 90	5 gigabecquerels
Ruthenium 106	7 gigabecquerels
Iodine 129	4 gigabecquerels
Iodine 131	3 gigabecquerels
Caesium 137	1 gigabecquerel
Cerium 144	7 gigabecquerels
Plutonium 241	7 gigabecquerels
Curium 242	1 gigabecquerel
Curium 244	100 megabecquerels

*Any references to "alpha" or "beta" in the above schedule is a reference to the activity of alpha emitting or beta emitting radionuclides associated with particulate matter.

The discharges resulting from the 93/4 reprocessing campaign were

Liquid discharges	Alpha	6.7E9 Bq
	Beta	12.5E11 Bq
Gaseous discharges	Alpha	1.11E4 Bq
	Beta	1.08E7 Bq

These represent a maximum of 1% of the site discharge limits in terms of Alpha and Beta activity. The only individual radionuclide that contributed significantly to the discharge authorisation was Kr^{85}. The 93/94 campaign contributed 5E14 Bq of Kr^{85}, 50% of the overall discharge limit.

WORKFORCE DOSE UPTAKE

The monitoring of the radiation dose uptake of the personnel directly involved in the reprocessing operations is an essential part of the management of fuel reprocessing. During the period of the 93/94 reprocessing campaign a total external body dose of 139.57 mSv was accumulated by the 25 operators employed directly in the reprocessing operations. To this figure must be added an internal body dose figure which is assessed from personnel and environmental monitoring results. The total internal body dose was assessed as 9.82 mSv. Together these figures represent a total operator dose of 149.39 mSv or 0.25 mSv per element reprocessed. In terms of individual dose, the maximum accumulated by an individual operator during the campaign was 8.44 mSv, well below the UKAEA corporate dose restriction of 20 mSv per annum.

SAFEGUARDS AND LICENSING

Operation of the reprocessing plants at Dounreay are subject to constant surveillance by Euratom Inspectors. In fact there is always an Inspector on hand to witness and record material transfers and sampling procedures.

The licensing of the plant and the monitoring of plant safety is undertaken by the Nuclear Installation Inspectorate (NII) on behalf of the UK government. The plant, although constructed in 1958 has undergone continual refurbishment and holds a license for active operation.

SUMMARY

The UK now has no large MTR reactors in operation, however, despite this fact the UK government is supportive of continued operation of the Dounreay MTR reprocessing plant. The technology of MTR reprocessing is well proven, with the waste from reprocessing being conditioned in a single stream to a form suitable for long term storage. Reprocessing operations typically recover 98% of the uranium present in the spent fuel. This recovered uranium can be reused in the manufacture of MTR fuel elements at a reduced enrichment. Radioactive discharges as a result of reprocessing are managed within the discharge authorisation granted by the Scottish Office. Radiation dose to the plant operators during reprocessing is carefully monitored and does not lead to any individual exceeding corporately imposed or internationally accepted limits.

The Dounreay MTR reprocessing plant **is** currently licensed and available for the reprocessing of overseas fuel. Reprocessing offers the only complete solution currently available to MTR operators. The technology is not new, it's safety has been demonstrated for many years, and reprocessing produces an acceptable residue form for long term storage or disposal.

Continued operation of the Dounreay MTR reprocessing plant can meet the reactor operator needs and provide a useful non-proliferation tool where reprocessed uranium is down blended for re-use as LEU.

SUPPLY OF ENRICHED URANIUM FOR RESEARCH REACTORS

Hans Müller

NUKEM GmbH
Fuel Cycle Services Division
Industriestraße 13

D-63754 Alzenau
Federal Republic of Germany

Phone: 49-6023/91-1608
Fax: 49-6023/91-1600

presented at the
17th International Meeting
on
"Reduced Enrichment for Research and Test Reactors (RERTR)"

Williamsburg, Virginia, USA
September 18 - 23, 1994
on September 19, 1994

Abstract

Since the RERTR-meeting in Newport/USA in 1990 I delivered a series of papers in connection with the fuel cycle for research reactors dealing with its front-end. In these papers I underlined the need for unified specifications for enriched uranium metal suitable for the production of fuel elements and I made proposals with regard to the re-use of in Europe reprocessed highly enriched uranium.

With regard to the fuel cycle of research reactors the research reactor community was since 1989 more concentrating on the problems of its back-end since the USA stopped the acceptance of spent research reactor fuel on December 31, 1988.

Now, since it is apparent that these back-end problem have been solved by AEA's ability to reprocess and the preparedness of the USA to again accept physically spent research reactor fuel I am focusing with this paper again on the front-end of the fuel cycle on the question whether there is at all a safe supply of low and high enriched uranium for research reactors in the future.

1. Historic supply of enriched uranium for research reactors

In the Western hemisphere the USA have developed since the late fifties a monopoly on and control over the supply of uranium with higher U-235 enrichments.

In the sphere of influence of the former Soviet Union, Russia had also a monopoly and control over the supply of enriched uranium for research reactors to the former east-block countries and its former satellites.

2. Supply of enriched uranium for research reactors by the U.S. Department of Energy (DOE)

From the late fifties until 1974 DOE's predecessor USAEC provided the research reactor community with enriched uranium on a lease-basis. In 1974 the former USAEC changed its supply policy and research reactor operators had to purchase their enriched uranium from USAEC and later from DOE. Until 1978 there was no major disturbance of supplies of highly enriched uranium (HEU) to research reactors. After 1978, however, with the implementation of the Nuclear Non-Proliferation Act, the USA put on the export of enriched uranium with enrichments of more than 20 % U-235 more stringent export controls, i. e. consequently U. S. export licenses for highly enriched uranium (HEU) can - if at all - only be granted on a case-to-case basis.

Mid of 1993 DOE transferred its enrichment activities for uranium for Power Reactors to the United States Energy Corporation (USEC); under existing contracts, DOE remains in the U.S.A. responsible for the supply of enriched uranium for research reactors. However, future contracts for HEU will be with the USEC.

Already as of the mid-eighties U.S.-exports of both Medium Enriched Uranium (MEU) and later on HEU to the main-consumers Europe and Japan dropped drastically due to large stocks of MEU and certain stocks of HEU in Europe which could be made available to research reactors after termination of several research programs where the uranium was no longer used.

At the end of 1993 DOE has also introduced a changed pricing policy for the supply of MEU and HEU.

Contrary to DOE's previous policy DOE now only accepts natural uranium as feed for the enriched product. The supply of low enriched feed at secondary market conditions is no longer possible. This new policy resulted in a drastic price increase for LEU and HEU.

This is also an additional reason why US-exports of LEU and HEU have been cut drastically and today exports of this material from the USA have to be considered more as sporadic cases.

As test case for the reliability of supply from the USA certainly serves a quantity of 69 kgs of HEU for the RHF reactor at Grenoble. This quantity of HEU is since 1991 stored at DOE and has not yet obtained the U.S. export license. The reason for the hold of the U. S. export license application for the RHF reactor is the change of the reactor vessel and the reactor's temporary shut-down.

3. Supply of LEU and HEU from sources within the European Union (EU)

There are large stocks of U.S. LEU in Europe sufficient to fuel research reactors beyond the year of 2000. Moreover, there are stocks of U.S. uranium having U-235 assays above 20 % stemming from reprocessing of spent fuel from research reactors and fast breeders.

With regard to the supply of HEU having enrichments between 90 and 93 % there are also certain stocks available in the EU.

In addition, the French Cogéma is offering to supply LEU of French origin and has the capability to produce HEU.

The British UKAEA is offering also LEU obtained by mixing HEU from reprocessing.

High attention in the research reactor community has attained the need of HEU for the new Munich research reactor operation of which is scheduled to be in the year of 2000.

The use of HEU for this research reactor has been criticised especially by the USA since in their view it undermines the U.S. efforts to reduce enrichment in research reactors.

In a response to the German opposition party SPD the German Government officially gave the following statement on June 14, 94.

Quote
"The intended construction and operation of the FRM II - also in its planned concept with use of HEU - is in agreement with the terms of the contract for the Non-Proliferation Treaty of nuclear weapons (NPT) and with the international obligations of the Federal Republic with regard to safety measures.

The planned research reactor FRM-II shall exclusively serve for peaceful purposes. In article IV, first paragraph of the NPT there is explicitly stated the inalienable right of all parties to develop the research, production and use of the nuclear energy for peaceful purposes.

In the view of the Government of Germany the use of HEU in research reactors in states with a high standard of non-proliferation and scientific foundation of the use of HEU is in agreement with the results of INFCE. In the recommendations of INFCE it is recognized that despite the desirable reduction of the U-235 assays in research reactors there will be certain uses which can only be obtained by HEU."
Unquote

4. Other suppliers of LEU and HEU

In the former Soviet Union and related satellites research reactors have been fueled with U-235 assays between 36 and 80 %. As was revealed during the 16th RERTR-meeting in Oarai last year the former Soviet Union maintained a reduction program similar to the RERTR-program. The U-235 assay of the reduced fuel is 20 %.

Russia is prepared to offer 19.75 % enriched uranium to research reactors provided adequate governmental assurances about the peaceful use shall be given.

Russia, however, does not offer return-possibilities of the spent fuel of Russian origin.

With regard to the availability of large stocks of weapons-grade uranium stemming mainly from nuclear warheads the USA has concluded two major agreements with Russia with the target to down-grade this material for later use in power reactors. It can, threrefore be anticipated that no HEU of the military arsenal can be inserted into research-reactors.

The following chart provides you with a survey about the involved quantities to be down-graded.

5. Possible future disturbances of the future export of LEU and HEU from the USA to the EU

Basis for the supply of nuclear fuels from the USA to Europe was the U.S. Atomic Energy Act of 1954 which was amended by the Nuclear Non Proliferation Act (NNPA). These acts require among others "prior consent" regulations for co-operation agreements with other states. The European Community refused to adapt the existing agreement for co-operation. The existing agreement for co-operation between the USA and the EU on December 31, 1995.

There exists the possibility that the USA and the EU will not reach a subsequent agreement thereafter.

The following problems might arise on the supply and return of LEU and HEU of U.S. origin.

Without such an agreement no transfers after 31.12.95 of source material, special nuclear material, equipment, production or utilization facilities or sensitive nuclear technology from the USA to the EU would be possible. However, transfers of items which were transferred to the EU before 31.12.95 and obligated to the USA under the existing agreement appear to be capable of retransfer to third countries, without hindrance, as the USA is concerned, but subject to a condition of peaceful use. However, no retransfer could be made from third countries to the EU after December 31, 1985.

HEU and LEU (non U.S. ogigin and U.S. origin) from any country, including Russia, can be imported into the U.S without an Agreement for cooperation. For example even since the U. S. does not have an agreement with Russia but MEU from military arsenals will be imported probably starting next year.

6. Summary and conclusions

Not only the back end of research reactors faces problems, research reactor operators are well advised to focus their attention to the safe procurement of fresh uranium for fuel element production.

NUKEM, being a company active in the external fuel cycle for research and power reactors is ready to assist you in that respect as in the past.

The Research Reactor Community is concentrating since 1989 on the back-end of the Fuel-Cycle (problems with reprocessing or final storage).

What is about the safe supply of fresh uranium?

Suppliers of Uranium for Research Reactors

Supplier	% U-235	Observations
DOE	19.75	not virgin, price increase, problems with acceptance of feed
DOE	90 - 93	dto.
UKAEA	19.75	mixed with uranium from reprocessing
Cogéma	19.75	virgin uranium
Cogema	90 - 93	virgin uranium
NUKEM	19.75	U.S. uranium and from reprocessing
NUKEM	90 - 93	dto.
Russia	19.75	no return of spent fuel
China	19.75	mixed with uranium from reprocessing

LEU Quantities derived from 2150 tonnes of weapon-grade HEU

Military stocks (t)	Country	LEU 4.4% (t)
900	USA	24.400
1250	Russia	38.500
		62.900

HEU blended with 1.5% U-235 enriched LEU

The Research Reactor Community should not only concentrate on the problems of the back-end (reprocessing or final storage),

but also on the front-end (safe supply of fresh uranium).

LEU ^{99}Mo TARGET FABRICATION AND TESTING: OVERVIEW, STATUS, AND PLANS

by

T. C. Wiencek, G. L. Hofman, E. L. Wood,
C. T. Wu, and J. L. Snelgrove

ABSTRACT

As part of the RERTR program, the development of technology to use low-enriched uranium (LEU) for production of the fission product ^{99}Mo has continued. Progress in fabrication development and out-of-pile thermal testing of targets based on uranium metal foils is summarized. Uranium foil of 125 μm (0.005 in.) thickness has been fabricated. Heat treatments have been developed to provide a random crystal structure, which is required for satisfactory irradiation properties. Two target designs, a tapered thermal expansion type and a split-outer-tube type, are presented. After anionic coating and thermal treatment of prototypical targets, no diffusional or dimensional changes were observed. A formal agreement for cooperation between Argonne National Laboratory (ANL) and the Indonesian National Atomic Energy Agency (BATAN) for irradiation testing is in the final stage of negotiation. The first irradiation tests of targets fabricated by ANL are scheduled to begin during the first half of 1995.

INTRODUCTION

As reported last year,[1] the RERTR Program has reactivated its effort to develop use of low-enriched uranium (LEU) to produce the fission product ^{99}Mo. This work comprises both target and chemical processing development and demonstration. Two major target systems are now being used to produce ^{99}Mo with highly enriched uranium (HEU) - one employing research reactor fuel technology (either uranium-aluminum alloy or uranium aluminide-aluminum dispersion) and the other using a thin deposit of UO_2. An LEU replacement for the former is feasible from the target-performance standpoint using a U_3Si_2-aluminum dispersion, whose outstanding irradiation performance properties have already been demonstrated. Considerable work is needed, however, to develop and demonstrate a chemical process for extracting the ^{99}Mo. Progress in this area will be reported in another paper at this meeting.[2] Both a target and its associated chemical processing must be developed to replace the deposited UO_2 target. This paper summarizes progress in fabrication development and in out-of-pile thermal testing of targets based on uranium metal foils. Chemical processing of foil targets will be discussed in a later paper at this meeting.[3]

Before discussing our progress in target development, we will summarize our overall development plans. Today, Indonesia is the only active user of deposited UO_2 targets. For that reason and because the U.S. no longer has suitable irradiation facilities for testing ^{99}Mo targets, we will work with the Indonesian National Atomic Energy Agency (BATAN) to test the uranium metal foil targets and their chemical processing. A formal agreement for cooperation is in the final stage of negotiation. BATAN is already working on

the safety analysis for the irradiation, and we plan to perform the initial irradiation tests during the first half of 1995. The first test targets will be fabricated at ANL, but future targets may be fabricated in Indonesia. Chemical processing studies are under way at ANL and at the University of Illinois. Several tests on irradiated targets are anticipated during the next year in Indonesia. We are in the early stages of negotiating a similar cooperation agreement with the Argentine National Atomic Energy Commission (CNEA) for the testing of U_3Si_2-aluminum dispersion targets. Because target irradiation performance is not an issue here, we will concentrate on chemical processing. Work is also underway in this area at ANL and the University of Illinois-Urbana-Champaign.

EQUIPMENT AND EXPERIMENTAL PROCEDURES

Because all of the proposed irradiation target designs for the production of ^{99}Mo using low-enriched uranium (LEU) are based on use of a clad uranium metal foil, techniques to produce uranium foils were required. A range of 25-125 μm (0.001-0.005 in.) was the goal for the final foil thickness. The decision to produce the foils at ANL was made after an unsuccessful search for a cost-effective commercial source of LEU foil, and also to have in-house control of the processing parameters. After an extensive literature search, a flowchart of current common fabrication methods was produced (Figure 1). Due to safety and time constraints, canning was chosen as the fabrication method to produce foil from cast uranium ingots. Initial rolling experiments were performed with 50 x 50 x 6 mm (2 x 2 x 0.25 in.) depleted uranium plate stock, which was previously cast and hot-worked. This material was canned in plain carbon steel and rolled on a 12 x 20 cm (5 x 8 in.) two-high Stanat mill in the high alpha uranium range (≈625°C). After hot-rolling, the material was cold-rolled on a 15 x 30 cm (6 x 12 in.) four-high Bliss mill.

The as-cold-rolled foils were encapsulated inside Vycor tubes filled with argon gas (99.95%) at 15 in.-Hg partial pressure. Small zirconium chips were sealed inside the tubes to prevent high-temperature oxidation of uranium during the β-treatment. Two Vycor tubes were heated to 690°C at 4°C/min, held for 3 min, and then quenched in water and in air. Another tube was air-cooled after a 10 min hold at 690°C. Texture analysis of the uranium foils before and after the β-treatment was made by X-ray diffraction, using a Philips XRG-3100 X-ray diffractometer with a copper target. Voltage and current used were 40 kV and 15 mA, respectively. The scanning range of 2θ was between 25° and 65°, and the collecting division and time were 0.05° and 2 sec, respectively.

Prototype one-third-scale targets of the tapered plug/thermal expansion design and split-outer-tube design were assembled and thermally tested from 300-500°C for up to one week. Details of these designs were previously presented.[1]

RESULTS AND DISCUSSION

Foil Texture

The first uranium foil produced was 125 μm (0.005 in.) thick. The resulting sheet had a very good surface finish, and no pinholes were observed.

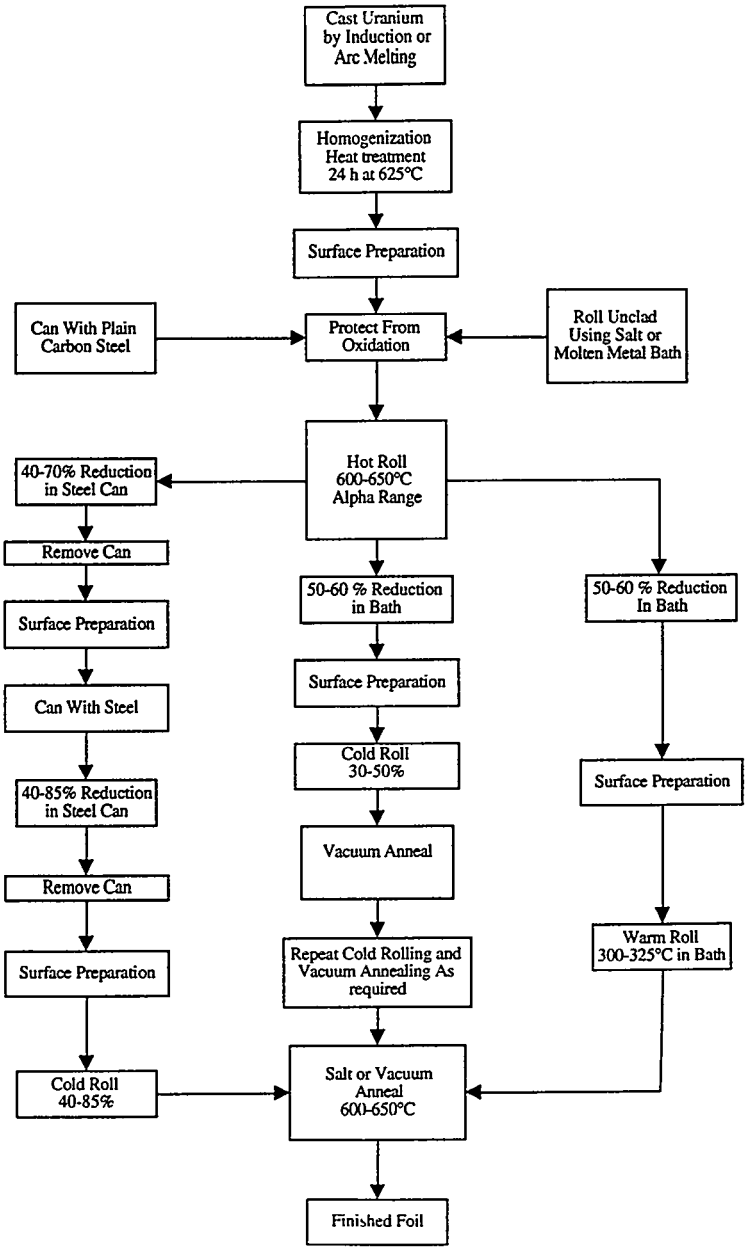

Figure 1. Production of Foil from Cast Uranium

A highly textured structure is inevitably formed after the rolling process,[4] which causes undesirable anisotropic growth that leads to undesirable surface effects such as swelling during irradiation. Paine et al.[5] showed that uranium single crystals elongate in the [010] direction and contract in the [100] direction with no appreciable change along the [001] direction. Buckley[6] explained this phenomenon as mass transport from {110} planes to {010} planes, based on the observation that fission-generated interstitials and vacancies form loops on {010} planes and {100} planes, respectively, as the result of anisotropic thermal expansion induced in uranium by thermal spikes in displacement cascade. In general, randomly oriented and moderately fine-grained uranium is necessary for successful irradiation behavior. β-treatment after rolling is essential to eliminate the foil texture.

Figure 2 shows the relative ratios of the characteristic peaks, (110), (002), (111), (112), and (131), to the (021) peak (the strongest of the random sample) in each sample in the cold-rolled and various β-treatment conditions. Apparently, strong texture was generated after cold-rolling because substantially higher ratios of (110), (111), (112), and (131) peaks than those of the random sample are observed. However, the as-rolled texture was different from that reported by Adam and Stephenson,[7] since most of the (010) planes were perpendicular to the rolling direction after cold-rolling. Relatively high ratios of (111), (112), and (131) peaks were found for the sample that was air-cooled after 10 min at 690°C. This may be attributed to the preferred growth of these planes along the rolling direction due to prolonged exposure at elevated temperature. The sample that was water-quenched after a 3-min hold at 690°C showed higher (110)/(021) and (111)/(021) ratios than those of the random sample. This implies that a certain amount of cold-rolled texture still exists, and that 3 min at 690°C followed by a water quench may not be adequate for completion of the $\alpha-\beta$ transformation. Comparably, the specimen that was air-cooled after 3 min at 690°C exhibited more random microstructural characteristic than the other two specimens. In summary, we suggest that β treatment consist of an isothermal soaking (3 min at ≈690°C) and air-cooling to minimize undesired texture of cold-rolled uranium foils.

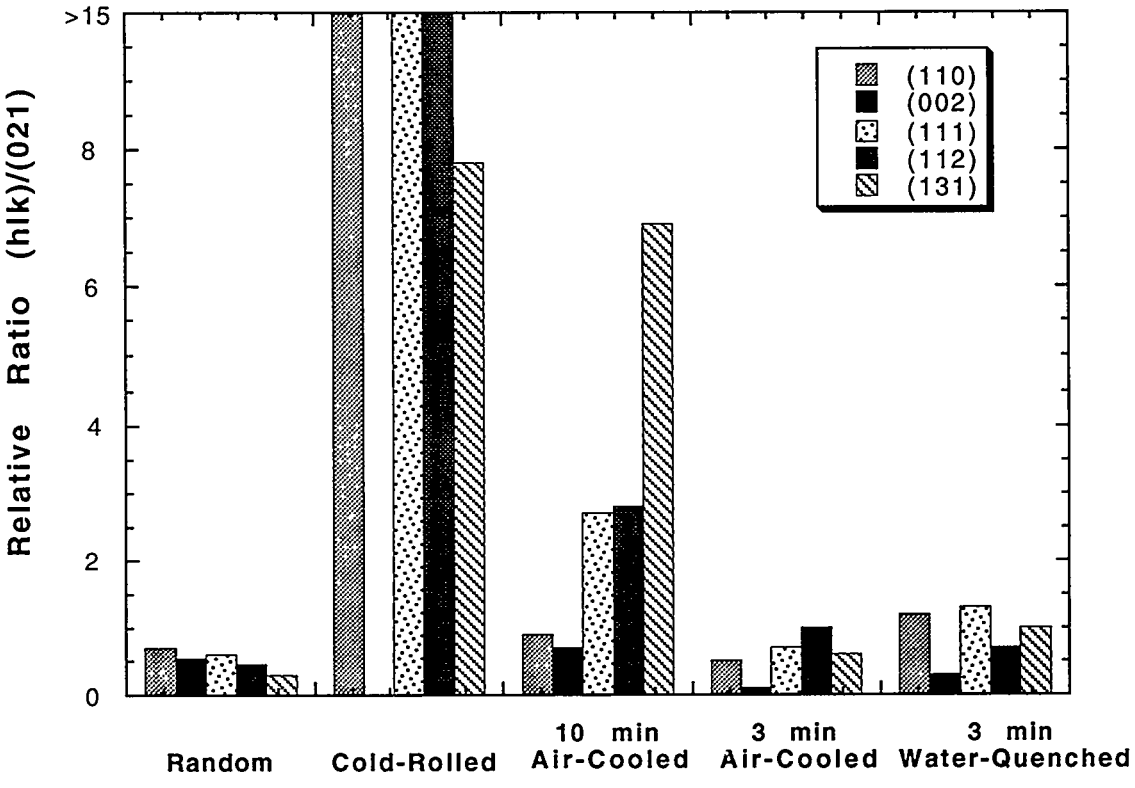

Figure 2. Relative Ratios of (hlk) Peak to (021) Peak for Various Metal-Working and β-Treatment Conditions

Differential Thermal Expansion Target

The Differential Thermal Expansion (DTE) target design is shown in Figure 3. The principal feature of this design is the use of two tubes of materials with different thermal expansion coefficients, between which is situated the U metal target. By installing Zr, which has the lower coefficient of thermal expansion, on the outside, good contact and thus good heat transfer between the U foil and both tubes is ensured when the target temperature is raised during irradiation. The outer tube is Al. Assembly and disassembly of the target is facilitated by machining a fitting taper on both tubes. The outer Zr tube is sealed by welding a blind bottom plug and a top plug equipped with a swagelock fitting to allow removal of fission gas from the target after irradiation. The target is evacuated and filled with He prior to sealing.

To prevent interdiffusion of U with either Al or Zr during irradiation, the Al inner tube was black-anodized and the Zr outer tube was air-oxidized at 300°C to a dark blue color.

Several 15 cm (6 in.) targets were fabricated and heat-treated for approximately one week, after which they were disassembled (the U foil removed) and metallographically examined; test results are summarized in Table 1. The test temperatures were deliberately chosen to be well above the expected irradiation temperature in order to establish whether interdiffusion was likely to occur. Only the non-anodized-oxidized target, which was heat-treated at 400°C, could not be disassembled due to interdiffusion of U and Al (Figure 4). In contrast, no interdiffusion was evident in the other targets (Figure 5). An example of a disassembled target is shown in Figure 6.

The results of the assembly, heat treatment, and disassembly experiments with these DTE targets give us confidence to proceed with the further design and fabrication of in-reactor test targets. Application of oxide diffusion barriers on both the Al and Zr surfaces appear to provide ample protection against diffusion bonding between the U foil and target tubes.

Split-Outer-Tube Target

The latest design of the split-outer-tube target design is shown in Figure 7. A port has been added to allow removal of the irradiation gases before the irradiated target is disassembled. Fittings identical to those of the current production design will be used to facilitate compatibility with existing equipment.

As detailed in the previous section, an anodized coating on the aluminum prevented diffusion during thermal heat treatments. Because it was assumed that the split-outer-tube target would behave in the same manner; no thermal diffusion tests on this design were performed. A single sample of a scaled-up 15 cm (6 in.) version of the initial 7 cm (3 in.) design was assembled and thermal-cycled four times at 400°C over a 168-hr period. No changes in dimensions were detected and destructive examination of the target after the test showed no gap or diffusion.

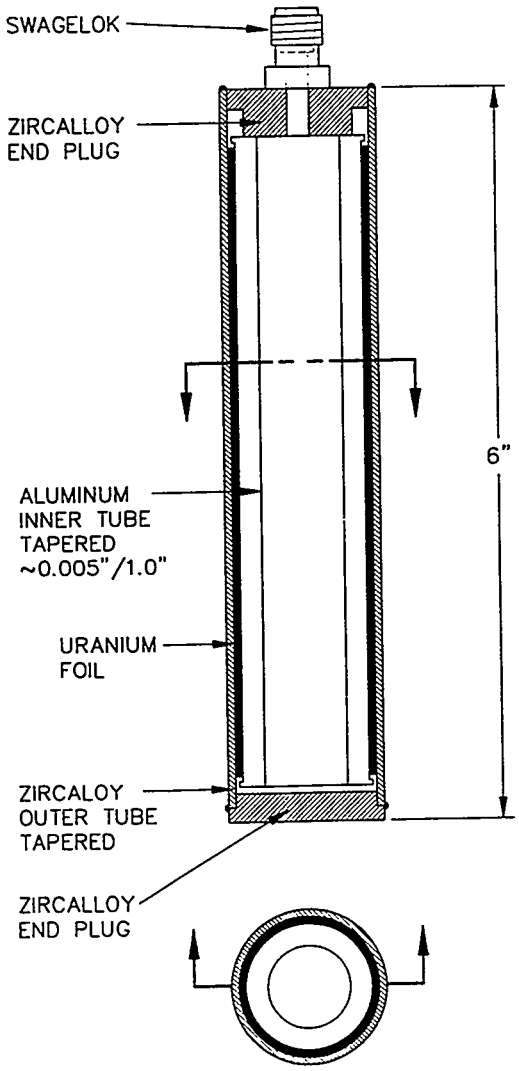

Figure 3. Differential Thermal Expansion (DTE) Target

Other design improvements are being considered. If a tighter fit between the cladding and the foil is required, the outer cladding could be fabricated from an aluminum alloy such as 2219 Al, which has a lower coefficient of thermal expansion than the 6061 Al inner tube. The effect would be similar to that of the DTE target but on a lesser scale. To eliminate the need for a gas-removal fitting and to simplify the production and cost of each target, a device may be designed to seal onto a target, pierce the outer cladding and allow for gas removal.

SUMMARY AND CONCLUSIONS

Two designs of irradiation targets have been developed for the production of ^{99}Mo using LEU. Both concepts, a tapered thermal expansion design and a split-outer-tube target design, are based on cladding over an LEU foil. Out-of-pile testing of LEU targets for the production of ^{99}Mo has progressed to the stage where preparation for irradiation testing has begun. After satisfactory irradiation of the prototypes is demonstrated, scale-up to full-size targets is planned.

Table 1. Testing Conditions of Differential Thermal Expansion (DTE) Targets

Capsule	U Foil	Glovebox Atmosphere	Temperature (°C)	Time (h)	Swelling on Center	Remarks
1	4	Ar-He	Not Heat Treated	-	-	Easily assembled.
2	4	Ar-He	300	144	<1 mil (<0.025 mm)	Foil and Al came out as one piece. Foil removed from Al with a little prying.
3	4	Ar-He	300	156	<1 mil (<0.025 mm)	Consists of 4 cool-down cycles. Cycling did not affect the interface.
4 Anodized	5	He	400	168	4 mil (0.10 mm)	After sectioning ends, foil remained tight around centered Al rod.
5 Anodized	5	He	500	168	1 mil (0.025 mm)	Easy fit. Foil removed very easily.
6	5	He	400	168	12 mil (0.30 mm)	Appeared to have a U-Al reaction.

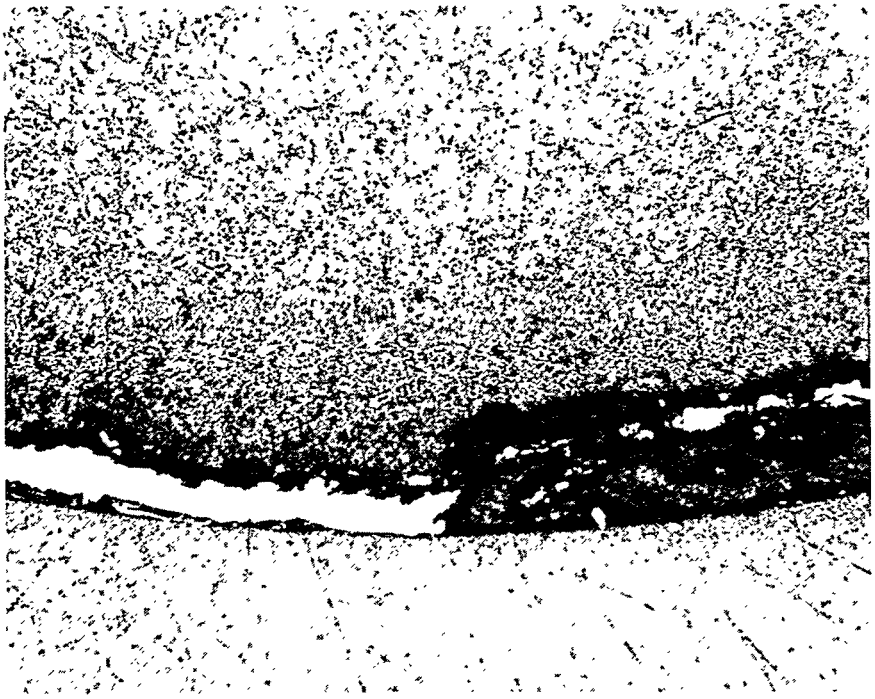

Figure 4. Unanodized Capsule #6 after Heat-Treatment for One Week at 400°C Showing Interaction Between U and Al. ≈25x

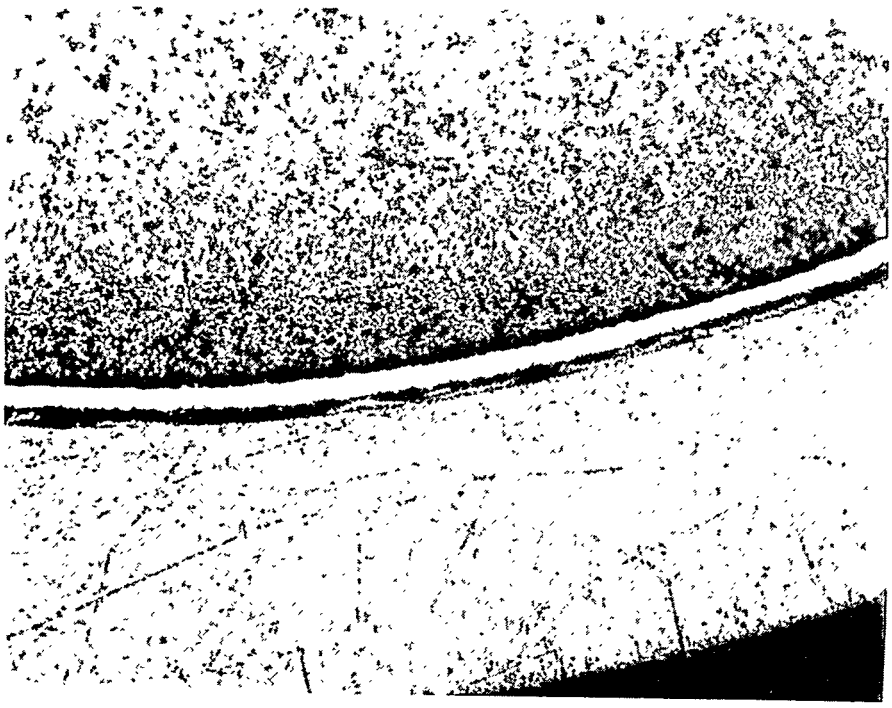

Figure 5. Anodized Capsule #4 after Heat-Treatment for One Week at 400°C Showing No Interaction Between U and Al. ≈25x

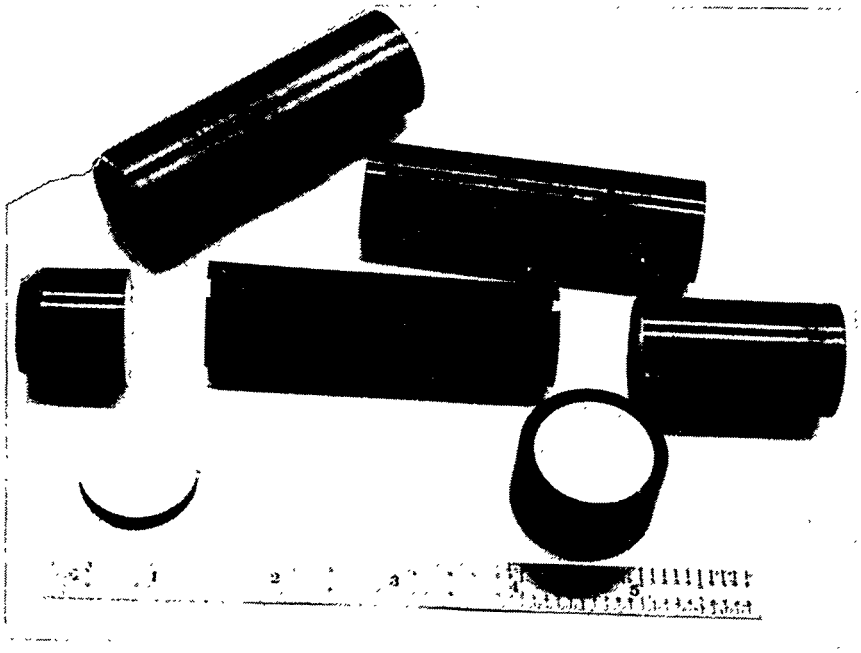

Figure 6. Disassembled DTE Target after Heat-Treating Showing Uranium Foil Removed (center)

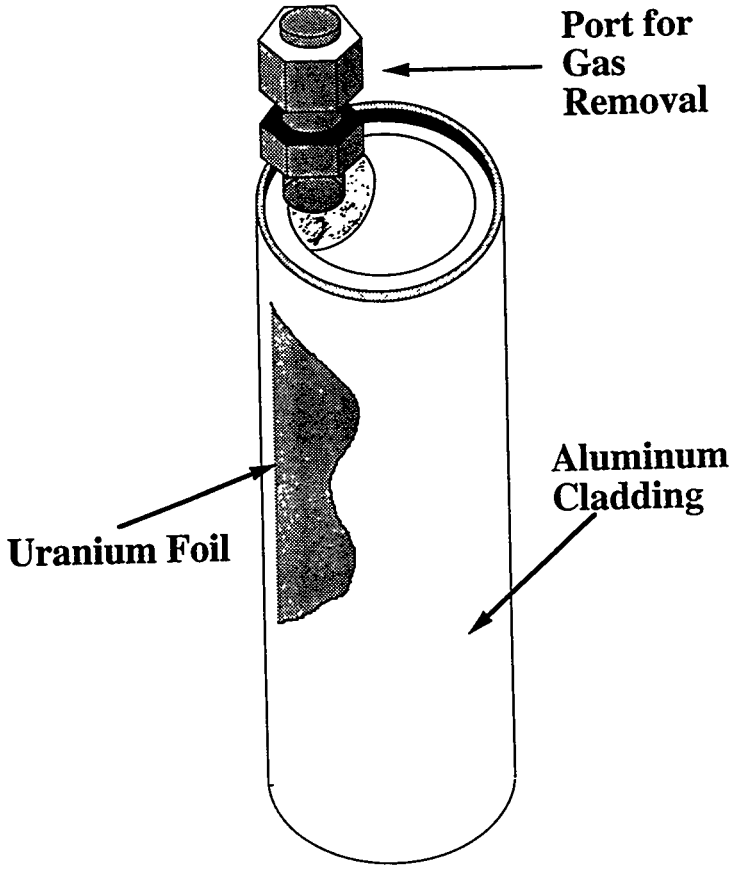

Figure 7. Split-Outer-Tube Target

REFERENCES

1. T. C. Wiencek and G. L. Hofman, "Development of Uranium Metal Targets for ^{99}Mo Production," Proc. 16th International Meeting on Reduced Enrichment for Research and Test Reactors, JAERI-M 94-042, 1994.

2. J. C. Hutter, et al., "Production of ^{99}Mo Using Low Enriched Uranium Silicide." These proceedings.

3. B. Srinivasan, et al., "Production of ^{99}Mo Using Low Enriched Uranium Metal Foils." These proceedings.

4. B. D. Cullity, "Elements of X-Ray Diffraction," 2nd Ed., Addison-Wesley, 1978, p. 295.

5. S. H. Paine and J. H. Kittel (1955) Proc. 1st Intl. Conf.: Peaceful Uses of Atomic Energy, Communication 7, No. 517, Geneva, Switzerland.

6. S. N. Buckley (1961), in: "Properties of Reactor Materials and Effects of Radiation Damage," D. J. Littler, ed., London: Butterworths, p. 143.

7. J. Adam and J. Stephenson, "Preferred Orientation in Rolled Uranium Sheet," J. Inst. Metals. 82: 561-567 (1954).

DEVELOPMENT OF DISSOLUTION PROCESS FOR METAL FOIL TARGET CONTAINING LOW ENRICHED URANIUM

B. Srinivasan, J. C. Hutter, G. K. Johnson, and G. F. Vandegrift
Chemical Technology Division

Argonne National Laboratory
9700 South Cass Avenue
Argonne, Illinois 60439

ABSTRACT

About six times more low enriched uranium (LEU) metal is needed to produce the same quantity of ^{99}Mo as from a high enriched uranium (HEU) oxide target, under similar conditions of neutron irradiation. In view of this, the post-irradiation processing procedures of the LEU target are likely to be different from the Cintichem process procedures now in use for the HEU target. We have begun a systematic study to develop modified procedures for LEU target dissolution and ^{99}Mo separation. The dissolution studies include determination of the dissolution rate, chemical state of uranium in the solution, and the heat evolved in the dissolution reaction. From these results we conclude that a mixture of nitric and sulfuric acid is a suitable dissolver solution, albeit at higher concentration of nitric acid than in use for the HEU targets. Also, the dissolver vessel now in use for HEU targets is inadequate for the LEU target, since higher temperature and higher pressure will be encountered in the dissolution of LEU targets. Our desire is to keep the modifications to the Cintichem process to a minimum, so that the switch from HEU to LEU can be achieved easily.

INTRODUCTION

In October 1992, the United States Congress passed an amendment to the Atomic Energy Act of 1954. This amendment prohibits export of high enriched uranium (HEU) for use as fuel or target in a research or test reactor unless several conditions are met: (1) no alternative low enriched uranium (LEU) fuel or target can be used, (2) the recipient is actively developing an LEU fuel or target for that reactor, and (3) the proposed recipient of the HEU provides assurances that, whenever possible, an LEU fuel or target will be used in that reactor.

In this report, we discuss our continuing research and development (R&D) activities on the substitution of LEU-metal foil target in the place of HEU-UO_2 for the production of ^{99}Mo [1-3]. This isotope is the precursor to ^{99m}Tc, an important nuclide in diagnostic nuclear medicine. Specifically, we report the results of our experiments on the dissolution of uranium metal foil in a mixture of nitric and sulfuric acids, which is the first step in the isolation of ^{99}Mo from

neutron-irradiated targets. The report also contains a comparison of LEU-metal foil targets and HEU-UO_2 targets and summarizes the processing chemistry used to isolate ^{99}Mo from irradiated HEU-UO_2.

PRODUCTION OF ^{99}MO

Molybdenum-99 ($t_{1/2}$ = 66 h) is produced with about 6% yield in the thermal neutron-induced fission of ^{235}U:

$$^{235}U\ (n,f)\ ^{99}Mo \qquad (1)$$

It can also be produced by neutron capture reaction of ^{98}Mo according to:

$$^{98}Mo\ (n,\gamma)\ ^{99}Mo \qquad (2)$$

Molybdenum-99 is commercially produced through the fission reaction rather than by neutron absorption. The specific activity of the nuclide that can be obtained from the former reaction is much higher than the latter. The HEU (~93% ^{235}U) targets used in the production of ^{99}Mo contain either uranium compounds (e.g., UO_2) or uranium alloys (e.g., UAl_x) in the form of fuel plates [4-7], rods [8], or cylinders [9,10]. After irradiation, the cladding is removed either by mechanical or chemical means, and the uranium is dissolved. The ^{99}Mo in the dissolver solution is separated from unconverted uranium, other fission products, and activation products (^{239}Np and ^{239}Pu). The separation procedures are based upon a combination of chromatographic separation, solvent extraction, and/or precipitation methods.

Technetium-99m ($t_{1/2}$ = 6 h) is the daughter product from beta decay of ^{99}Mo. The technetium isomer emits 140 keV gamma-rays to form ^{99}Tc ($t_{1/2} = 2.1 \times 10^5$ y). In diagnostic nuclear medicine, the usual practice is to allow the ^{99m}Tc to grow from the decay of ^{99}Mo contained in a column, and elute the ^{99m}Tc as needed.

In the U.S., until the end of February 1990, ^{99}Mo was produced by thermal neutron irradiation of cylindrical HEU-UO_2 targets in a reactor operated by the Union Carbide Corporation in Sterling Park, New York. The production was stopped at that time because of the closure of the reactor facilities.

At Sterling Park, the separation and purification of the ^{99}Mo generated in the HEU-UO_2 target were done by a procedure known as the "Cintichem process." At the time of closing and decommissioning of the reactor facilities, the proprietary rights governing the process were transferred to the U.S. Department of Energy (DOE). The DOE is considering use of the Cintichem process to produce ^{99}Mo at Sandia National Laboratories. At present, Nordion of Canada is the primary supplier of ^{99}Mo to the U.S. The Cintichem process is also being used by BATAN (Badan Tenaga Atom Nasional) in Indonesia to produce ^{99}Mo from HEU-UO_2 targets. A formal agreement between Indonesia and the U.S. is in the final stages of negotiation to test the replacement of HEU-UO_2 target with the LEU-metal foil target, and also to test the modifications to the Cintichem process to produce ^{99}Mo from LEU targets.

At Argonne National Laboratory (ANL), under the aegis of the Reduced Enrichment for Research and Test Reactors (RERTR) program, we are working toward developing a LEU-metal

foil target to replace the HEU-UO_2 target. The work also includes developing chemical procedures to separate ^{99}Mo from neutron irradiated LEU-metal foil targets. The various steps in the procedure will resemble the steps in the original Cintichem process. In this manner, ^{99}Mo production facilities can make a smooth switch from HEU to LEU targets with minimal process changes.

In the sections to follow, we shall describe the similarities and differences between the HEU-UO_2 and LEU-metal foil targets, outline the Cintichem process, and report progress made by us in developing a dissolution procedure for the LEU-metal foil target.

COMPARISON OF HEU-UO_2 AND LEU-METAL FOIL TARGETS

To develop a satisfactory dissolution and separation process for the LEU-metal foil targets, we must understand the similarities and differences between the HEU-UO_2 and the LEU-metal foil targets. The two targets are compared in Table 1.

Table 1. Properties of HEU-UO_2 and LEU-Metal Foil Targets

	HEU-UO_2	LEU-Metal Foil
Chemical Composition	UO_2	U metal
Total uranium	about 16 g	about 94 g
^{235}U enrichment	~93%	slightly less than 20%
^{235}U	15 g	18.5 g
^{99}Mo	532 Ci (1.11 mg)	545 Ci (1.13 mg)
^{239}Pu	28 μCi (0.44 mg)	722 μCi (11.8 mg)

The HEU and LEU targets produce about the same amount of ^{99}Mo at the end of irradiation, since both targets contain about the same amount of fissionable ^{235}U. However, the activation products (e.g., ^{239}Pu) are about twenty-six times more abundant in the LEU target relative to HEU, because of the higher amount of ^{238}U in the former. The fission products abundance remain about the same in the two targets.

With regard to acid dissolution, six times more LEU will have to be dissolved relative to HEU, 94 g versus 16 g. The HEU dissolution involves oxidizing U(IV) in the target to U(VI) in the solution (two-electron transfer), whereas the LEU dissolution involves a change from the zero oxidation state in the target to the VI state in the solution (six electron transfer). At least three times more oxidant will be needed for the LEU target relative to HEU. Furthermore, the rates of dissolution, the heats of reaction, and the products (especially the gases) from the dissolution of metal foil and UO_2 are likely to be different.

THE CINTICHEM PROCESS

As stated earlier, the U.S. DOE owns the proprietary rights for the Cintichem process and also possesses detailed documentation describing the process. The main features of the Cintichem process are based on a 1974 U.S. Patent [9]. It appears that for the commercial production of ^{99}Mo, modifications and improvements have been made to the procedures described in the patent.

4. Provide guidance to the commercial producers to gain acceptance from the U.S. Federal Drug Administration (FDA) and other government agencies for the ^{99}Mo product from LEU-metal foil targets.

The target design work is being done by our colleagues in the Energy Technology Division of ANL. Their work is reported in a companion paper [11]. Our work on the dissolution of LEU targets and separation procedures for ^{99}Mo is being done in the Chemical Technology Division of ANL and at the University of Illinois in Urbana. The work toward gaining approval from FDA and other government agencies is yet to begin. We have made initial contacts with the FDA to learn about preparing the application for human use of ^{99m}Tc derived from irradiation of LEU targets.

The work on the dissolution of unirradiated samples of uranium metal foil is reported in the following sections. In these preliminary experiments, depleted uranium metal foil samples were used in place of LEU samples. The experiments dealt with the following four aspects:

1. Dissolution rates for uranium metal foil in nitric-sulfuric acid mixtures.
2. Oxidation state of uranium in the dissolved solution.
3. Calorimetry experiments to determine the heat evolved during the dissolution reaction.
4. Gas analysis experiments to determine the nature and abundance of gases evolved during dissolution. These experiments have not been completed yet.

NITRIC-SULFURIC ACID DISSOLUTION OF URANIUM METAL FOIL

We have stated earlier that three times more oxidant is needed for the metal foil dissolution relative to UO_2. Therefore, the nitric acid concentration in the dissolver mixture must be increased for the LEU-metal foil target, relative to the Cintichem process solution, in order to dissolve the foil in a minimum amount of acid. We studied of the dissolution rate of (depleted) uranium metal foil in various nitric-sulfuric acid mixtures and also in pure nitric acid. The nitric acid concentration was 4M to 16M, which is higher than the 0.7M nitric acid used in the Cintichem process.

Samples of depleted uranium metal foil (0.3% ^{235}U) were used in the dissolution experiments; the foil thickness was 127 μm (0.005 in.) and the surface density was 203 mg/cm^2. An unknown amount of surface oxide layer was present on the foil. The oxide layer was not removed prior to dissolution, since in the actual production of ^{99}Mo the oxide layer is expected to be present.

Uranium metal foil samples weighing between 30 and 80 mg were dissolved in about 3 to 6 mL of the acid at temperatures of 25-95°C. The temperature during dissolution was kept nearly constant by immersing the dissolution tubes in a constant temperature bath. During dissolution, gas bubbles evolved from the surface of the foil in a steady stream. The end of dissolution was marked by the cessation of gas evolution. It is certain that NO_2 is one of the gaseous products, as seen by the characteristic brown color of the fumes. Other products are likely to be a mixture of other oxides of nitrogen (NO and N_2O). It is known that in nitric acid dissolution, hydrogen gas is not one of the products [12]. Whether hydrogen gas is evolved in nitric and sulfuric acid mixtures will be a subject of our study in the gas analysis experiments.

The rates of dissolution of uranium metal foil in nitric acid, and in a mixture of nitric and sulfuric acids are shown in Table 2. Note that two surfaces of the thin foil are exposed simultaneously to the acids. For example, a 203 mg foil presents 2 cm^2 surface for dissolution.

We have contacted the U.S. DOE to obtain copies of the Cintichem process documents. We hope to use them in designing post-irradiation chemistry procedures for the LEU-metal foil targets which are similar to the Cintichem process. However, the documents are not yet available, and therefore, we are unable to describe here the exact details of the Cintichem process. In its place, we substitute the information that is available in the patent.

The patent by Arino et al. [9] describes the methods of preparation for the target itself and the various steps involved in the separation of ^{99}Mo from the irradiated HEU-UO_2 target. Here, we are concerned with the dissolution procedure of the irradiated target and subsequent separation of ^{99}Mo from the dissolver solution.

As described in the patent, the HEU-UO_2 target contained 7 g of ^{235}U (~93% enriched) in the form of UO_2, deposited electrolytically on the inner side of a stainless steel cylinder. Note that for commercial production of ^{99}Mo, the target contains about twice the amount of ^{235}U. The procedures described below are for the 7 g ^{235}U target.

The volatile elements (fission product gases) that escaped from the target during irradiation were removed first. The UO_2 was then dissolved in 60 mL of a mixture of 1M sulfuric acid and 0.7M nitric acid. The stainless steel cylinder target served as the dissolver vessel. The pressure during dissolution was a maximum of about 6 atm (70 psi gauge). The dissolution was complete in about 45 min. The concentration of uranium in the dissolver solution was about 0.5M.

The volatile fission products (e.g., iodine, noble gases) released by the dissolution process were then removed to an alumina trap and a cold finger containing suitable absorbents (calcium oxide, calcium sulfate, and zeolite). The acid solution containing molybdenum along with other non-volatile fission and activation products was transferred to another container. The cylinder was washed with dilute sulfuric acid, and the washings also were transferred. After the addition of Na_2SO_3, the molybdenum in the solution was precipitated by the addition of alpha benzoinoxime solution in the presence of hold-back carriers for other fission products. The precipitate was washed with dilute sulfuric acid, and then it was dissolved in alkaline hydrogen peroxide solution. Further purification and additional decontamination were achieved through re-precipitation (again from an acidic solution) using alpha benzoinoxime, followed by dissolution of the precipitate in sodium hydroxide solution. Finally, the alkaline solution containing molybdenum was passed through a silver-coated charcoal column, an inorganic ion exchanger column, and an activated charcoal column. The column purification procedures were repeated to obtain a highly pure product. The specific activity of the final ^{99}Mo product was >1000 mCi/mL. The total of other fission products was less than 1 μCi per curie of ^{99}Mo.

R&D WORK ON LEU-METAL FOIL TARGET AND MOLYBDENUM SEPARATION

At ANL, the R&D work on the LEU-metal foil target is focused on developing suitable targets and post-irradiation chemical procedures for the production of ^{99}Mo. The new chemical procedures are expected to resemble closely the Cintichem process procedures used for HEU targets. Our program goals are as follows:

1. Develop a suitable LEU-metal foil target.
2. Establish acid dissolution procedure for the irradiated target.
3. Establish separation and purification procedure for ^{99}Mo from the acid solution.

In the units of mg/min/cm^2 given in Table 2, this factor of two is taken into account in calculating the surface area from the surface density of the foil given above.

Table 2. Rate of Dissolution of Uranium Metal Foil in Nitric Acid and in Mixture of Nitric and Sulfuric Acids

Acid (mol/L)		Rate (mg/min/cm^2) [a]				
Nitric	Sulfuric	25°C	40°C	59°C	84°C	95°C
4		Very slow [b]				0.76
4	0.56	≥0.03			3.1	
8		0.09	0.15	≥0.42 [c]	1.5	
8	0.56	0.29	0.70	1.7	4.0	
8	1.1	0.52	1.5	4.7		
12		≥0.2 [c]	0.73	1.6	4.0	
12	0.56	1.81	5.64	9.3	21	
12	1.1	5.9	12.6	35		
16		≥0.2 [c]			6.0	
16	0.56				102	

Notes:

[a]The rates of dissolution represent an average value. The samples were not stirred during dissolution. Where determined, the initial rates for dissolution were found to be higher than the average values.

[b]The dissolution rate in 4M nitric acid at 25°C is very low. There is no appreciable change in the mass of the foil even after 164 h.

[c]The ≥ sign means that the exact time for complete dissolution was not known. Several of these experiments were done overnight or over the weekend, and complete dissolution had occurred during this period.

The data in Table 2 are semi-quantitative for the following reasons: First, the foil was not pure uranium metal; a surface oxide layer was present. Therefore, the rates correspond to the dissolution of a mixture of metal and its oxide. Second, the time required for dissolution was determined by visual inspection of the total disappearance of the foil, which invariably coincided with the cessation of gas evolution. Such visual observations yield only approximate values.

In a separate experiment, we studied the rates of dissolution of the metal foil by bubbling air or nitrogen through the dissolver solution (mixture of 12M nitric acid + 0.56M sulfuric acid). The bubbling removed the oxides of nitrogen from the solution as soon as they formed. The dissolution slowed down by a factor of five relative to quiescent conditions. It appears that dissolved NO_2 accelerates the dissolution process, possibly due to reconversion to nitrous and nitric acid according to

$$2\,NO_2 + H_2O \rightarrow HNO_2 + HNO_3 \qquad (3)$$

Additional experiments are necessary to understand the kinetics and mechanism of the dissolution reaction.

Despite the semi-quantitative nature of the data given in Table 2, some general conclusions are possible. For a given nitric acid concentration, the rate of dissolution is higher in nitric-sulfuric acid mixtures than in pure nitric acid alone. An earlier study [13] showed that the rate of dissolution of uranium metal in the mixture is about 30 times higher when the nitric acid contained 3 vol % sulfuric acid (0.56M) as compared with pure nitric acid of the same concentration. However, our study showed that the rate increase is only a factor of two or three higher. Also, the rate of dissolution increases with increasing temperature.

The solution at the end of dissolution is greenish yellow, which upon heating to about 90°C is converted to a yellow solution. Concentration of this solution to a very low volume yielded crystals of uranium compounds. These could be redissolved very easily in a minimum amount of water to yield concentrated solutions of about 200 g of uranium/per Liter. This is comparable to the 0.5M solution that was obtained in the Cintichem process. We have not completed our experiments on the crystallization temperature of the dissolved uranium compounds in the various acid mixtures. These experiments will be done after we decide upon the exact composition of the dissolver solution.

A desirable rate of dissolution for the actual target is about 3 mg/min/cm^2. At this rate, a LEU-metal foil target (see Table 3) will require about 30 min for complete dissolution. Note that the dissolution time is independent of mass, since higher mass of foil has correspondingly higher surface area.

Table 3. Time Required for Complete Dissolution of LEU-Metal Foil Target

Mass of Foil	15.7 g
Dimensions	10.2 cm x 7.6 cm x 0.013 cm (thick)
Surface Area for Dissolution	155 cm^2

Dissolution Rate (mg/min/cm^2)	Dissolution Time (min)
1	101
3	34
10	10

The data shown in Table 2 can be used to define the concentration of the acids and temperature needed to obtain a dissolution rate of 3 mg/min/cm^2. If the dissolution is to take place at 25°C, then the preferred dissolver solution is a mixture of 12M nitric acid and 1.1M sulfuric acid; the dissolution will be complete in about 17 min. If the acid mixture is to resemble the Cintichem dissolver solution, then the mixture of 4M nitric acid and 0.56M sulfuric acid at 84°C may be used. If the mixture is made up from 1.1M sulfuric acid instead of 0.56M , then dissolution can be carried out at <84°C. We plan to carry out dissolution experiments using larger quantities of uranium metal than reported here in order to duplicate commercial processing conditions.

OXIDATION STATE OF URANIUM IN DISSOLVED SOLUTION

Depleted uranium metal foil samples (70 to 130 mg) were dissolved in a mixture of nitric and sulfuric acid (3 to 4 mL), and the visible absorption spectra of these solutions were recorded by a Cary Recording Spectrophotometer. The different experimental conditions for the dissolution are as follows:

a) 8M nitric acid + 0.56M sulfuric acid
b) 12M nitric acid + 0.56M sulfuric acid
c) 12M nitric acid + 0.56M sulfuric acid; nitrogen bubbled during dissolution
d) 12M nitric acid + 0.56M sulfuric acid; air bubbled during dissolution
e) 12M nitric acid + 1.1M sulfuric acid
f) 12M nitric acid + 1.1M sulfuric acid; air bubbled during dissolution.

The absorption spectra in all cases were identical. A typical example is shown in Figure 1. The peak and shoulders in the region of 420 to 470 nm are due to the absorption by the uranyl species (UO_2^{2+}). The absence of U(IV) is indicated by no appreciable absorption in the region around 630 nm. If dissolved NO_2 exists in the solution, then the UO_2^{2+} absorption is masked by the absorption continuum at the short wavelength region (below 450 nm). Bubbling air or nitrogen during dissolution did not change the oxidation state of uranium in the dissolved solution; in both cases, only UO_2^{2+} was present in the solution, with negligible amounts of U(IV). The solution obtained from the dissolution of uranium metal appears to be similar to the solution from UO_2 dissolution; uranyl sulfate is expected to be the major species in both cases. No studies were done to determine the exact nature of the species and their abundance.

CALORIMETRY EXPERIMENTS

The heat evolved during the dissolution of depleted uranium metal foil in a mixture of nitric acid and sulfuric acid was determined at 30, 40 and 50°C by using a LKB 8700 precision calorimetry system. A chemical standard (reference material 724, tris-hydroxymethyl aminomethane or simply tris, from the National Bureau of Standards) was used to verify that the system was working satisfactorily. It also served as a calibration standard for the calorimeter. This material reacts with 0.100N HCl and releases 245.76 J/g of heat at 25°C, at a concentration of 5 g per 1000 cm^3 of solution. In our experiments 500 mg of tris was dissolved in 100 mL of 0.100N HCl, causing a 0.27°C temperature rise in the solution, at 30°C. In the temperature range of 20 to 30°C, the heat of reaction may be corrected for the change in heat capacity with temperature by using the following value: ΔC_p = 1.435 J/(g•°C). But the temperature regime of our experiments was 30 to 50°C. This is outside the limits for which the correction is valid. However, as a first approximation, we have used the above correction factor for all our experiments.

The heat evolved by the dissolution of the depleted uranium metal foil was determined by dissolving 30 to 200 mg of the metal in 100 mL of the 12M nitric acid and 1.1M sulfuric acid mixture at 30, 40, and 50°C. The temperature rise observed in the experiments is given in Table 4. Approximate values for the heat of reaction calculated from the observed temperature rise are also included. The following assumptions were made in calculating the heat of reaction:

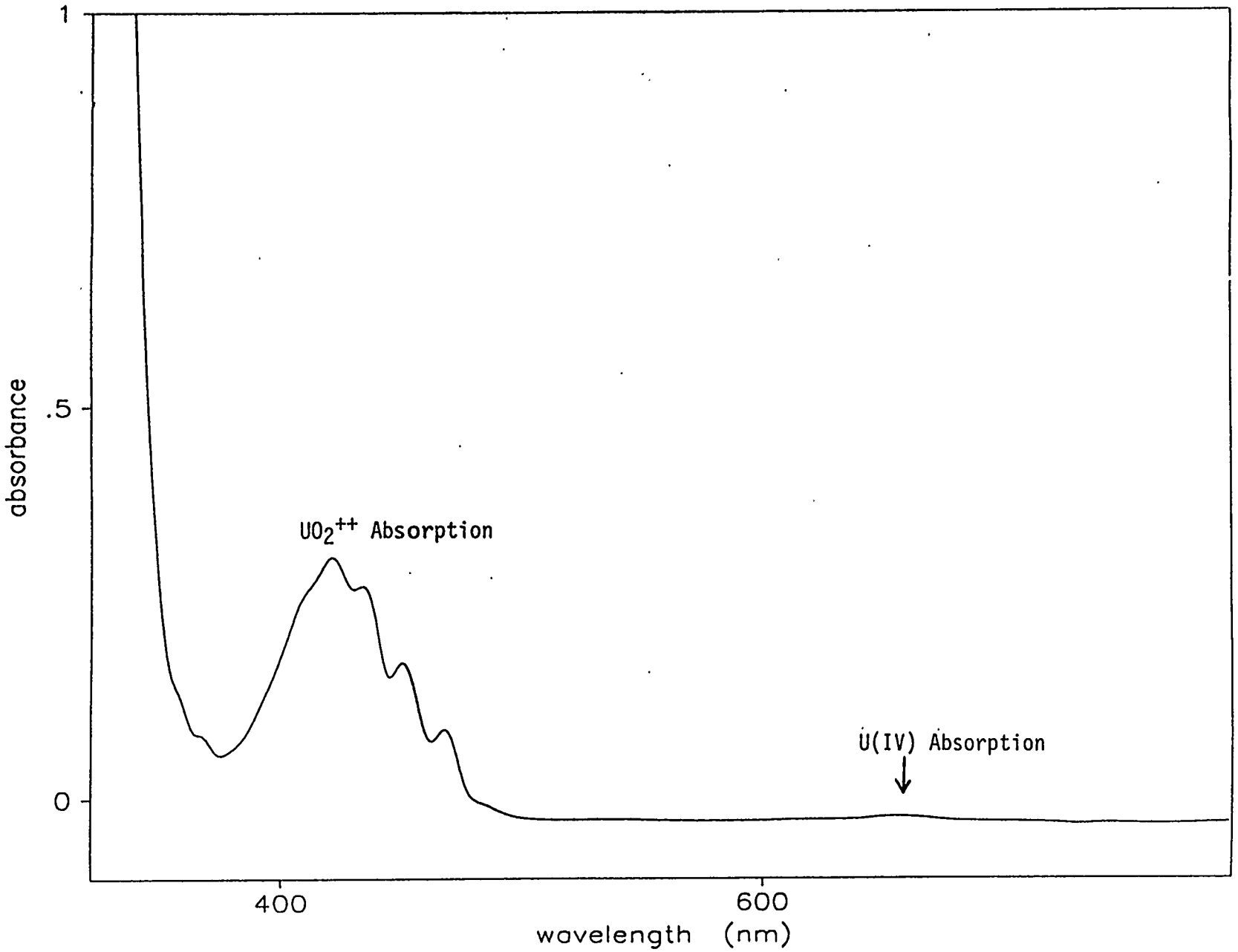

Figure 1. Absorption Spectrum in the Visible Region of Uranium Metal Dissolved in a Mixture of 12M HNO_3 and 1.1M Sulfuric Acid. Uranium concentration is about 0.1M.

1. The results of the tris standard experiment were used to evaluate the quantity of heat that is used up to heat the glass calorimeter and the stirrer to the desired temperature, in addition to the 100 mL HCl present in the calorimeter. The heat capacity of 0.100N HCl was taken to be 4.15 J/(g•°C) at 25°C, as obtained from the National Standard Reference Data Series [14]. No corrections were made for heat capacity variation with temperature.
2. The heat capacity of 12M nitric acid solution was calculated from the data provided by the National Standard Reference Data Series [14]. The calculated value was 2.72 J/(g•°C), at 25°C. The same value was assumed for the nitric and sulfuric acid mixture at all temperatures.

Table 4. Results from Calorimetry Experiments on Dissolution of Depleted Uranium Metal Foil in 100 mL of Mixture of 12M Nitric Acid and 1.1M Sulfuric Acid

Mass of Foil (mg)	Temperature (°C)	Temperature Rise (°C)	Heat of Reaction (kJ/mol)
31.44	30	0.40	1200
30.52	40	0.36	1100
62.47	40	0.74	1100
110.42	40	1.28	1100
204.74	40	2.39	1100
28.32	50	0.34	1100

The heat of reaction appears to be about 1100 kJ/mol (average of the six values in Table 4). The heat of reaction not only includes the dissolution of uranium metal in the acid, but also the heat of dissolution of gases evolved. The dissolved gases may participate in other reactions, such as the production of nitrous and nitric acid from dissolved nitrogen dioxide. No corrections were made for these side reactions or for the heat removed by the escaping gases. Making appropriate corrections for these factors would yield a more precise heat of dissolution of uranium metal. In addition, the heat capacity of the nitric-sulfuric acid mixtures at different temperatures must be obtained. We plan to gather the relevant data in the near future. Nevertheless, the data given in Table 4 are useful in predicting the temperature rise of the reaction mixture in a dissolution vessel that is similar to the one used in the Cintichem process.

The Cintichem process dissolution vessel is a stainless steel cylinder measuring 45.7-cm long, 2.5-cm diameter, and 0.25-cm thick. The volume of the vessel is about 230 cm^3. If such a vessel is used to dissolve the same amount of uranium metal foil (7.5 g) and in the same volume (60 mL) as used in the Cintichem process, the temperature rise is expected to be about 60°C. In this calculation, the heat capacity of the system (vessel and the dissolver solution in a mixture of 12M nitric acid and 1.1M sulfuric acid) is assumed to be 2.76 J/(g•°C).

In the actual production of ^{99}Mo, about six times more LEU-metal foil is needed relative to HEU to obtain the same amount of ^{99}Mo. The dissolution will require a corresponding increase in the amount of the acid, so that the final uranium concentration (0.5M) remains the same in both cases. The Cintichem dissolver is not sufficiently large to hold the higher volume of acid needed

for LEU. A new dissolver is needed. The temperature rise expected in the new dissolver can be calculated from the experimental heats of reaction reported in Table 4. The new dissolver must be designed to accommodate the temperature rise in the dissolution reaction and also safely contain the gases released during dissolution. The results of gas analysis experiments, in progress, will help in calculating the expected pressure inside the new dissolver vessel.

SUMMARY

At ANL, we are developing a LEU-metal foil target to replace the HEU-UO_2 target for the production of ^{99}Mo. About six times more uranium will be needed in the LEU target in order to produce the same amount of ^{99}Mo from the LEU as from the HEU (assuming same duration of irradiation at the same neutron fluence). Our work reported here is confined to studies on the post-irradiation dissolution procedures for the LEU target. Our desire is to design the chemistry procedures along the same lines as the Cintichem process procedures, making minimal changes and modifications. In this manner, the switch from HEU to LEU can be easily accomplished when the latter target becomes available for commercial production of ^{99}Mo.

The dissolution studies show that LEU-uranium metal foil dissolves easily within 30 min in 12M nitric and 1.1M sulfuric acid mixtures at 25°C, in 12M nitric and 0.56M sulfuric acid mixtures at 40°C, or in 4M nitric and 0.56M sulfuric acid mixtures at 84°C. The reaction takes place smoothly with steady evolution of gases from the surface of the foil. Other combinations of acid concentrations and temperature can also be used to achieve a quick dissolution. The final selection of the dissolver solution will be made by taking into account the ease of dissolution, the final concentration of uranium in the dissolver solution, and the similarity between this solution and the corresponding Cintichem process solution. Uranyl ions are primarily present in the dissolver solution with no evidence for U(IV) species.

Calorimetric experiments show that the heat of dissolution of uranium metal is about 1100 kJ/mol. This result can be used to predict the temperature rise that will accompany the dissolution of the LEU-metal foil in the acid mixture.

A new dissolver vessel, which is different from the Cintichem vessel, is needed for the dissolution of LEU-metal foil targets. The new design must take into account the expected temperature rise during dissolution, as well as the pressure increase due to the release of gases. Gas analysis experiments are in progress to determine the nature and abundance of gases released by the dissolution process.

REFERENCES

[1] G. F. Vandegrift, D. J. Chaiko, R. R. Heinrich, E. T. Kucera, K. J. Jensen, D. S. Poa, R. Varma, and D. R. Vissers: Preliminary Investigations for Technology Assessment of ^{99}Mo Production from LEU Targets, 1986 International Meeting on Reduced Enrichment for Research and Test Reactors (RERTR), November 3-6, 1986, Gatlinburg, Tennessee, ANL/RERTR/TM-9, CONF-861185, pp. 64-79.

[2] G. F. Vandegrift, J. D. Kwok, S. L. Marshall, D. R. Vissers, and J. E. Matos: Continuing Investigations for Technology Assessment of ^{99}Mo Production from LEU Targets, presented at the 1987 International Meeting on Reduced Enrichment for Research and Test Reactors (RERTR), September 28-October 2, 1987, Buenos Aires, Argentina.

[3] G. F. Vandegrift, J. C. Hutter, B. Srinivasan, J. E. Matos, and J. L. Snelgrove: Development of LEU Targets for ^{99}Mo Production and Their Chemical Processing,

presented at the 16th Int. Meeting on Reduced Enrichment for Research and Test Reactors (RERTR), October 3-7, 1993, Oarai, Ibaraki, Japan.

[4] J. Konrad: Facilities for the Irradiation of ^{235}U for the Production of ^{99}Mo at the HFR Petten, Irradiation Technology, Proc. of the Int. Topical Meeting, Grenoble, France, pp. 677-683 (1982).

[5] J. Salacz: Production of Fission Mo-99, I-131 and Xe-133, Revue IRE Tijdschrift, Vol. 9, No. 3 (1985).

[6] C. J. Fallais, A. Morel de Westgaver, L. Heeren, J. M. Baugnet, J. M. Gandolfo, and W. Boeykens: Production of Radioisotopes with BR2 Facilities, BR2 Reactor Meeting, Mol, Belgium, INIS_MF_4426, pp. IX-1 to -11 (1978).

[7] A. A. Sameh and H. J. Ache: Production Techniques of Fission Molybdenum-99, Radichimica Acta 41 (1987) 65-72.

[8] R. T. Jones: AEC-2 Experiments in Support of ^{99}Mo Production in NRU, AECL-7335 (1982).

[9] H. Arino, H. H. Kramer, J. J. McGovern, and A. K. Thornton: Production of High Purity Fission Product Molybdenum-99, U.S. Patent 3,799,883 (1974).

[10] H. Arino, F. J. Cosolito, K. D. George, A. K. Thornton: Preparation of a Primary Target for the Production of Fission Products in a Nuclear Reactor, U.S. Patent 3,940,318 (1976).

[11] T. C. Wiencek, G. L. Hofman, E. L. Wood, C. T. Wu, and J. L. Snelgrove: LEU ^{99}Mo Production-Overview, Status and Plans, Proc. of the 17th Int. Meeting on Reduced Enrichment for Research and Test Reactors, September 18-22, 1994, Williamsburg, Virginia, U.S.A.

[12] R. E. Blanco and C. D. Watson: Head-End Processes for Solid Fuels in Reactor Handbook, 2nd edition, eds. S. M. Stoller and R. B. Richards, Interscience Publishers Inc., New York, Vol. II (1961) pp. 60.

[13] B. Elliot: Process Development Quarterly Report MCW-1407, as cited in Nuclear Science Abstracts 14 (1960) 15669.

[14] V. B. Parker: Thermal Properties of Aqueous Uni-univalent Electrolytes, National Standard Reference Data Series, National Bureau of Standards 2, U.S. Government Printing Office, Washington D.C. (1965) pp. 44.

PRODUCTION OF MO-99 USING LOW-ENRICHED URANIUM SILICIDE

J. C. Hutter, B. Srinivasan, M. Vicek, and G. F. Vandegrift
Chemical Technology Division
Argonne National Laboratory
9700 South Cass Avenue
Argonne, IL 60439

ABSTRACT

A process to recover Mo-99 from low-enriched uranium silicide is being developed at Argonne National Laboratory. The uranium silicide is dissolved in alkaline hydrogen peroxide. Experiments performed to determine the optimum dissolution procedure are discussed, and the results of dissolving a portion of a high-burnup (>40%) U_3Si_2 miniplate are presented. Future work related to Mo-99 separation and waste disposal are also discussed.

INTRODUCTION

Molybdenum-99 is a precursor of Tc-99m, which is used in several medical applications. Since Mo-99 is not naturally abundant, it must be produced by one of two types of controlled nuclear reactions. One method produces Mo-99 by neutron bombardment of Mo-98; the Mo-99 is generated by the following nuclear reaction: Mo-98 (n,γ) Mo-99. This method produces Mo-99 with low specific activity and is not widely used [1]. Commercially, Mo-99 is being produced worldwide by the fission of U-235: U-235 (n,f) Mo-99. The Mo-99 is recovered by dissolving the irradiated target and separating the Mo-99 from the uranium and other fission products in the dissolver solution. The world's current supply of Mo-99 is almost exclusively produced from high enriched uranium (HEU).

In October 1992, the U.S. Congress passed an amendment to the Atomic Energy Act of 1954. This amendment prohibits export of HEU for use as a fuel or target in research or test reactors unless several conditions are met: (1) no alternative low-enriched uranium (LEU) fuel or target can be used, (2) the U.S. is actively developing an LEU fuel or target for that reactor, and (3) the proposed recipient of the HEU provides assurances that, whenever possible, an LEU fuel or target will be used in that reactor.

We are investigating the consequences of substituting LEU for HEU on target preparation and processing. The results of substituting LEU U_3Si_2 targets for HEU UAl_x alloys and aluminide targets during basic dissolution for Mo-99 recovery are discussed.

URANIUM SILICIDE TARGETS

Over the last several years, uranium silicide fuels have been under development as LEU targets for Mo-99. The use of LEU silicide is aimed at replacing the UAl_x alloy in the HEU dissolution process practiced by the Institut National des Radioelements (IRE), Fluerus, Belgium

[2]; Comision Nacional de Energia Atomica, Buenos Aires, Argentina [3]; and the Atomic Energy Corporation of South Africa. The difficulty with using uranium silicide targets is that the conditions used to dissolve UAl_x targets are not applicable for the silicide targets. The targets do not readily dissolve in base. In acid, silica is precipitated in the dissolution process, and the Mo-99 cannot be recovered from the solution [4]. In 1987, Argonne workers [5] were able to dissolve uranium silicide in alkaline hydrogen peroxide at 70°C, dissolving 0.3 g U_3Si_2 in 100 mL of liquid. According to the original description, the target was initially placed in 3.0M NaOH to remove the cladding. Once the cladding was dissolved, the cladding solution was removed, and a 1:1 ratio of 3M NaOH and 30 wt % H_2O_2 was used to dissolve the remaining uranium silicide [5].

Two years later, the following optimized procedure was proposed to dissolve uranium silicide targets [6]. A steel dissolver vessel would be loaded with irradiated targets. Initially, the cladding and the aluminum in the fuel matrix were to be dissolved in 3M NaOH. (The addition of $NaNO_3$ was later suggested to keep hydrogen production to a minimum.) A gas sparge during the dissolution was proposed to remove the gaseous fission products and mix the dissolver contents. Once the cladding was dissolved, the flocculent in the solution would be removed from the dissolver, leaving the dense uranium silicide behind. This solution would be filtered, then returned to the dissolver. A 30 wt % solution of hydrogen peroxide would then be added dropwise until the uranium silicide was completely dissolved. Then, the dissolver solution would be heated to destroy the hydrogen peroxide complex and allow the dissolved uranyl hydroxide to precipitate. This solution would be filtered to recover the uranium, and then it would be acidified for subsequent recovery of Mo-99 in the same way as currently done for uranium aluminide targets. This project was discontinued in 1989 due to lack of funding, and no progress was made beyond this point for several years.

In recent work, we have only been able to partially reproduce the earlier procedure. Uranium silicide alone can be dissolved by the procedure described above. However, the cladding dissolution solution cannot be reused since we have not been able to filter or centrifuge it to remove the metal hydroxide alloying elements. Even if a pure aluminum alloy is used, and no flocculent is present in the dissolver solution (so that filtering is not required), we have been unable to dissolve even 0.1 g of silicide by the proposed scheme. This observation remained valid even if up to 500 mL of hydrogen peroxide was used in the attempt. Therefore, our current thinking is that the cladding solution cannot be reused in the subsequent silicide dissolution step; a fresh charge of sodium hydroxide solution must be used. In addition, we have found that stainless steel is unsuitable as a construction material for the dissolver vessel because of its rapid catalytic destruction of hydrogen peroxide.

The first step in recovering Mo-99 from a silicide target is to remove the aluminum cladding. This procedure was developed in the fifties at Oak Ridge National Laboratory (ORNL) [7], and slight variations of it are practiced all over the world. Thus, this well-developed procedure can be easily adapted to the new LEU silicide targets. The problem is that methods to dissolve the silicide itself need to be established. Experiments to optimize the silicide dissolution process are in progress at our laboratory. During the dissolution process, two chemical reactions are occurring, the autodestruction of hydrogen peroxide and the dissolution of uranium silicide. A literature search revealed very little data about the autodestruction of hydrogen peroxide in sodium hydroxide solutions. One source simply identified that the autodestruction reaction is catalyzed in base, but no quantitative data were given [8]. A limited kinetic study of dilute hydrogen peroxide (0.01M) in 0.5-6.0M NaOH at room temperature indicated that hydrogen peroxide was stable in highly basic solutions [9]. This stability was attributed to the following equilibria:

$$H_2O_2 + OH^- \text{ ---> } HO_2^- + H_2O, \quad K = 1.6 \times 10^2 \qquad (1)$$

We have completed experiments to quantify the autodestruction rate in various NaOH solutions over the temperature range 70-100°C. The autodestruction reaction is exothermic, and its kinetics must be understood to optimize the U_3Si_2 dissolution and design a dissolver with the proper heat transfer characteristics so that the dissolution process can be safely controlled.

OPTIMIZED PROCEDURE FOR ALUMINUM CLADDING DISSOLUTION

Aluminum cladding alloys used in the production of Mo-99 in Europe and the USA are shown in Table 1. Both of these types of alloys are easily dissolved in $NaOH$-$NaNO_3$ mixtures. Most of the alloying elements will precipitate, but the sodium aluminate will remain in solution under the optimized dissolution conditions of molar ratios Al:NaOH:$NaNO_3$ of 1.00:1.66:1.47.

Table 1. Composition Range of Common Cladding Alloys (wt %) [10]

Designation	Cr	Cu	Mg	Mn	Si
Al 5052[a]	0.15-0.35	0.1	2.2-2.8	0.1	-
Al 6061[b]	0.04-0.35	0.15-0.4	0.8-1.2	0.15	0.4-0.8

[a]Common use in Europe.
[b]Common use in United States and Argentina.

The ORNL procedure is claimed to minimize hydrogen production and also prevent the precipitation of sodium aluminate [7]. The overall stiochiometry of the dissolution is:

$$Al + 0.85\ NaOH + 1.05\ NaNO_3 \text{ ---> } NaAlO_2 + 0.9\ NaNO_2 + 0.15\ NH_3 + 0.2\ H_2O \quad (2)$$

The published dissolution rate data in boiling NaOH solutions can be correlated with the following equation:

$$Rate = k\ [NaOH]^{1.54} \quad (3)$$

Where,

$k = 5.26$ mg Al/cm^2•min•M$^{1.54}$ at the boiling temperature
Rate = Al dissolution rate, mg Al/cm^2•min

To test this procedure, 3.77 g of Al6061 (60.5 cm^2 surface area exposed) was dissolved in 77.3 mL of 3M NaOH and 3M $NaNO_3$. The dissolver was a 250 mL jacketed glass beaker with a glass sparger. The heat transfer fluid set point was initially 70°C, and the vessel contents were mixed by nitrogen sparging. Within 1 min of introducing the cladding material, the dissolver solution was boiling, 104°C. Within 5 min, no undissolved cladding was visible in the vessel, and the boiling subsided. This dissolution rate is consistent with the published results. A sample of the dissolver liquid was evaluated by inductively coupled plasma-atomic emission spectroscopy (ICP-AES) to determine the concentrations of the dissolved alloying elements and the aluminum (Table 2). As shown in Table 2, the dissolver liquid contains a significant concentration of alloying elements. Care was taken to avoid suspended solids in the liquid sample sent for ICP-AES, even though this sample could not be filtered.

Table 2. Composition of Final Dissolver Solution

Element	Concentration in Dissolver Liquid (mg/L)
Al	55700[a]
Cr	85
Cu	110
Mg	500
Mn	44
Zn	69
Si	b

[a]Equivalent to an Al concentration of 2.06M.
[b]Silicon not determined due to interference from dissolution of the glassware in strong base.

After dissolution, the flocculent of metal hydroxide alloying elements in the cladding solution forms a gelatinous precipitate that cannot be filtered or centrifuged. These flocculent impurities must be removed, since they catalyze the autodestruction of hydrogen peroxide in the subsequent silicide dissolution. Upon acidification, the flocculent particles are easily dissolved and will likely not interfere with the subsequent Mo-99 recovery. Depending on the size of the silicide particle, between 8 and 30% of the Mo-99 produced will be lost to the cladding dissolution solution due to fission recoil. Thus, economic concerns dictate that Mo-99 must be recovered from this solution.

AUTODESTRUCTION OF HYDROGEN PEROXIDE IN SODIUM HYDROXIDE SOLUTIONS

The autodestruction of hydrogen peroxide:

$$2H_2O_2 \text{ ----> } 2H_2O + O_2 \tag{4}$$

was observed to have a first-order dependence on the concentration of hydrogen peroxide:

$$\frac{d[H_2O_2]}{dt} = -k\,[H_2O_2] \tag{5}$$

Where,

$[H_2O_2]$ = concentration of hydrogen peroxide, mol/L
t = time, min
k = first-order rate constant, min^{-1}

Equation 5 can be integrated with the initial condition $[H_2O_2] = [H_2O_2]_0$ at $t=t_0$:

$$\ln \frac{[H_2O_2]}{[H_2O_2]_0} = -k\,(t - t_0) \tag{6}$$

To determine k, we measured the isothermal destruction of a completely mixed batch of hydrogen peroxide in a sodium hydroxide solution over time. The slope determined from ln $[H_2O_2]/[H_2O_2]_o$ vs. time equals to -k. Since this equation has the form y=mx, a least squares fit of the data was used to statistically minimize the errors in the measurements of $[H_2O_2]$.

The hydrogen peroxide autodestruction reaction was carried out in a 1000 mL glass round-bottom flask. Attached to the flask was a 40 cm Allihn condenser to ensure that vaporized water and hydrogen peroxide were returned to the flask. A thermometer was inserted into the liquid to monitor the temperature. A 380 W heating mantle was used to manually control the temperature at various set points. The destruction of hydrogen peroxide is exothermic and is a function of the composition of the peroxide solution [8]. Heats of reaction between 94 and 99 kJ/mol are reported for this reaction in water. The heat of mixing is not included in this number since it is negligibly small compared to the heat of reaction (0.4-1.2 kJ/mol). The autodestruction reaction heats up the reaction mixture during the rate experiments. Temperature control within 1°C was possible during the course of the experiments. A glass shaft and Teflon impeller were used to mix the reactor contents after addition of reagents. During the experiments, the generation of oxygen gas bubbles, caused by the decomposition of hydrogen peroxide, was adequate to mix the flask contents.

Initially, the flask was filled with 30 mL of a sodium hydroxide solution and heated to 10°C less than the required reaction temperature. The experiment was started by adding 40 mL of 30 wt % hydrogen peroxide to the flask. Since the peroxide was stored at 0°C, initially the flask contents cooled slightly, then as the reaction began, the flask contents heated up as high as 95°C. Within a few minutes, the contents cooled to the required temperature of 70, 80, or 90°C. The temperature was then maintained at this temperature by adjusting the heating mantle. Once the set point temperature was reached, a clock was started, and 0.1-0.2 mL grab samples were removed at set time intervals up to 120 min. The grab samples were quickly cooled to 0°C in an ice water bath to slow the reaction before they were introduced into 50 mL of 1M H_2SO_4 and 0.15M KI for titration with 0.1M sodium thiosulfate. This allowed us to determine the hydrogen peroxide concentration [11]. Once the concentration vs. time data were obtained, the rate constant was derived from Eq. 5.

Typical experimental data plot as straight lines on a logarithmic scale; two examples are shown in Figure 1. The straight line indicates that the data fit a first-order dependence well.

The rate constants were calculated and are displayed on an Arrhenius plot in Figure 2. The Arrhenius form for rate constant is:

$$k = A \exp\left(\frac{-E_a}{RT}\right) \tag{7}$$

Where,

k = first-order rate constant, min^{-1}
A= collision frequency, min^{-1}
E_a = activation energy, J/mol
R= universal gas constant, J/(mol•K)
T = temperature, K

This exponential temperature dependence plots as a straight line, as shown in Figure 2. The activation energy for the reaction can be determined by the slope of the line, and the collision frequency by the intercept at 1/T = 0. This equation can be used to predict the temperature dependence of the autodestruction reaction.

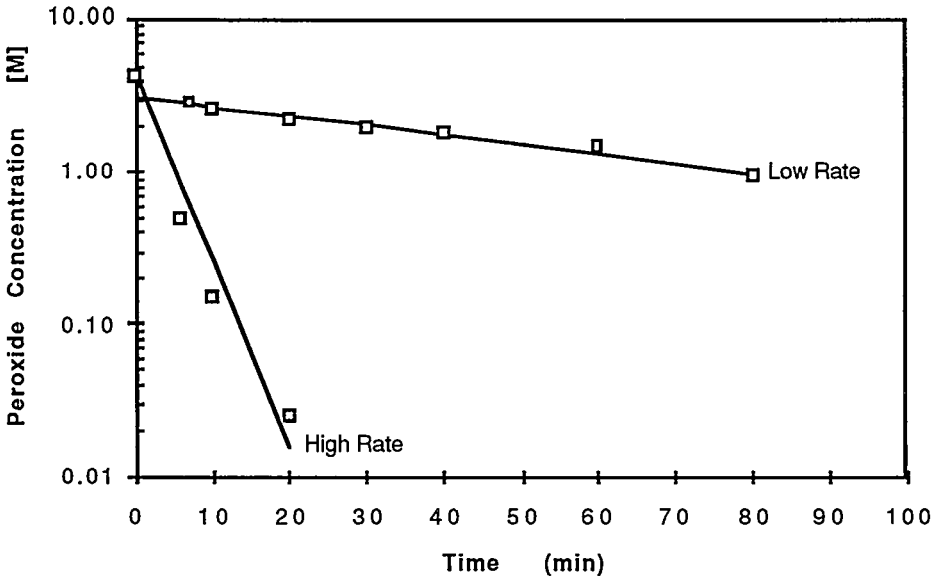

Figure 1. Plot of Typical Concentration vs. Time for Destruction of Hydrogen Peroxide in NaOH Solutions. Shown are the lowest rate in 2.57M NaOH at 70°C, and the highest measured rate in 0.128M NaOH at 90°C.

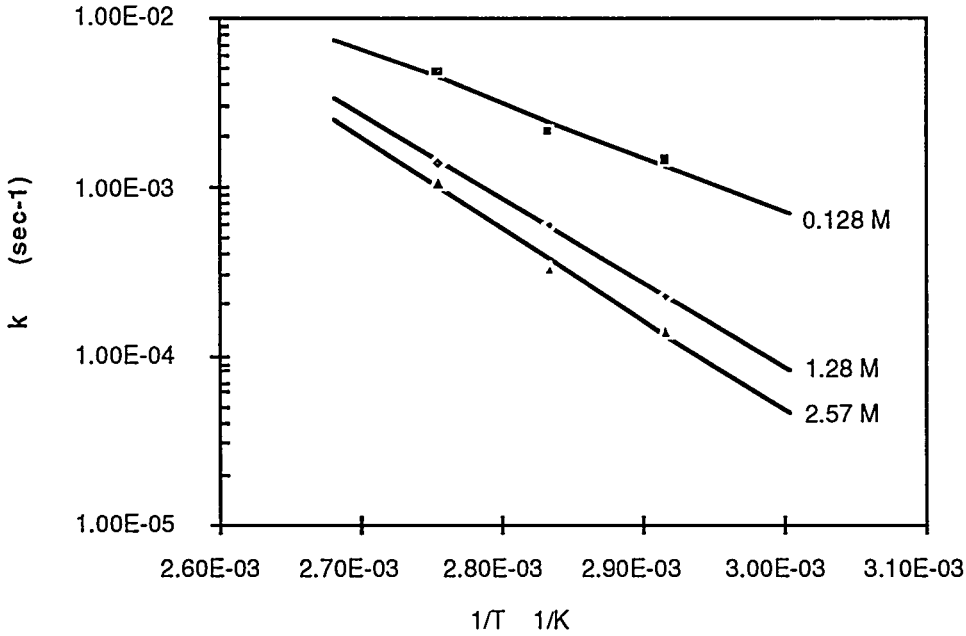

Figure 2. First-Order Rate Constants for Destruction of Hydrogen Peroxide in NaOH Solutions. The three lines are for different NaOH concentrations, as shown.

The activation energies and collision frequencies from the least squares fit to the data are reported in Table 3. The results for water on glass and stainless steel can be found in the literature [12]. In both water and in dilute base, the activation energies are about the same as shown in Table 3. Thus, the rate of increase of these reactions with temperature is about the same in water or dilute base. At higher base concentrations, the activation energy is larger. Thus, the rate of increase of these reactions with temperature is more rapid in higher base. In water, a 30 wt % solution of hydrogen peroxide is slightly acidic (pH of about 4). Thus, the activation energy does not seem to depend on pH over this small range. The difference in the rate constants is due to the large difference in the collision frequencies. For base, the collision frequencies are larger, indicating a much larger destruction rate at these conditions. For the glass vessels reported in the literature, the collision frequency was independent of the surface area of the glass vessel. In stainless steel, the collision frequency depended on the surface area of the exposed steel, indicating a surface catalytic effect.

Table 3. Activation Energies and Collision Frequencies for Hydrogen Peroxide Destruction

Condition	E_a (kJ/mol)	A (min^{-1})
Water on glass[a]	66.9	2.4 E+05
Water on stainless steel[a]	61.9	1.5 E+07
0.128M NaOH	60.5	1 E+08
1.28M NaOH	95.9	6 E+12
2.57M NaOH	104.1	6 E+13

[a]From Ref. [12].

As shown in the table, the activation energy for hydrogen peroxide destruction in aqueous solutions is 61-67 kJ/mol, which is substantially less than the energy to break the O-O bond, 200 kJ/mol. Thus, the rate-controlling step in the reaction probably does not involve the breakage of the O-O bond [12]. The activation energy in 0.128M NaOH was similar to the result in water; however, the activation energy in high NaOH concentrations was substantially larger, which contributes to greater stability of hydrogen peroxide in more concentrated NaOH solutions. If the dissolution had been done in water alone, the destruction rate of hydrogen peroxide would also be lower still in the temperature range studied (70-90°C). The highest destruction rate was found in 0.128M NaOH. When hydrogen peroxide in sodium hydroxide is contacted with stainless steel, the autodestruction rate is about 200 times more rapid than with glass in > 2M NaOH at 70°C. This result eliminates the use of stainless steel as a construction material for the dissolver.

KINETICS OF URANIUM SILICIDE DISSOLUTION

The kinetics of uranium silicide dissolution was determined by the initial rate method [13]. The dissolution was done in a 250 mL jacketed glass beaker. Temperature was controlled by circulating a 50/50 mixture of propylene glycol and water in an external beaker jacket from a Brinkman RMS-6 refrigerator/heater. By this method, temperature of the flask contents was easily controlled within 1°C during the experiments. The temperature of the beaker contents was monitored by a thermometer. The liquid phase was continuously stirred with a magnetic stirrer. The stirring was not adequate to suspend the dense silicide particles, but the liquid phase was completely mixed. During a typical experiment, the hydrogen peroxide and sodium hydroxide

mixture was initially thermally equilibrated in the flask. When the silicide was introduced, the first sample was taken, and the clock was started. Grab samples were taken at predetermined intervals during a 10-min experiment. The grab samples were analyzed for hydrogen peroxide by titration and for dissolved uranium by inductively coupled plasma mass spectroscopy (ICP-MS). During the experiment, the heat generated by the autodestruction of hydrogen peroxide was continuously removed by the circulating heat-transfer fluid. At temperatures higher than 60°C, the heat released by the autodestruction reaction was greater than the capacity of the jacketed beaker to remove the heat; the liquid temperature reached the boiling point, and the dissolution could not be controlled so that accurate initial rate experiments could not be completed.

Typical experimental data are plotted in Figures 3 and 4. These experiments were started in 5M hydrogen peroxide, using 1 g U_3Si_2 with 270-352 mesh particles at 60°C. As shown in Figure 3, the dissolution rate for uranium is higher in 1.28M base than 5.14M base. For longer times than shown in the figure, the hydrogen peroxide is very rapidly consumed, and once the peroxide runs out, the dissolution of the uranium stops. Thus, higher base concentrations allow one to dissolve more uranium due to the longer lifetime of hydrogen peroxide in the dissolver solution. The substantially lower depletion rate of hydrogen peroxide in higher NaOH solutions is illustrated in Figure 4.

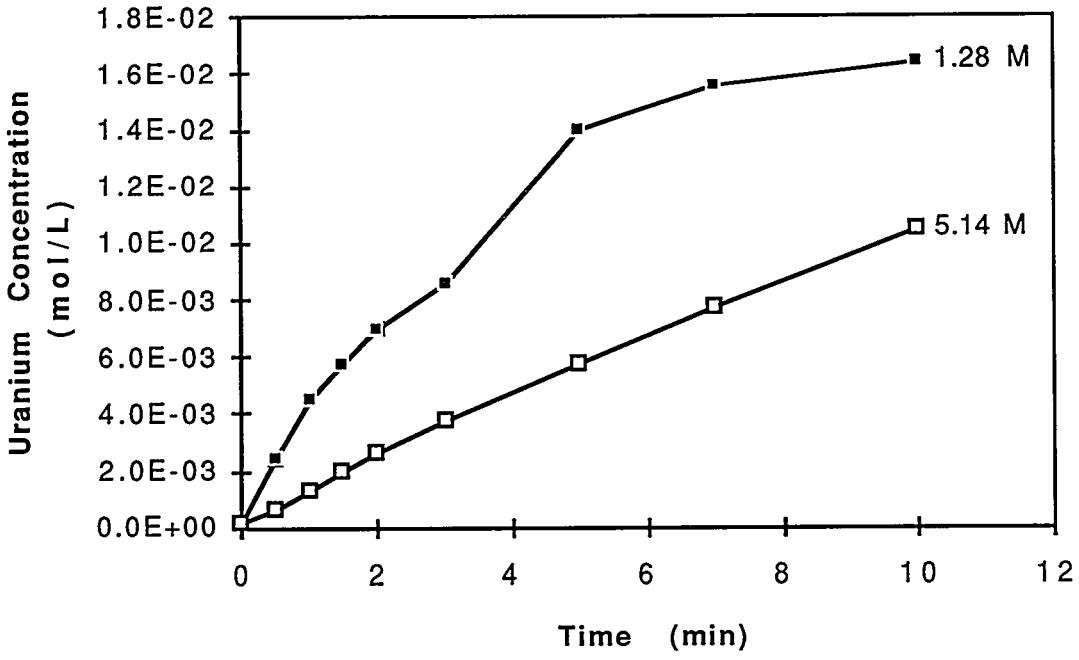

Figure 3. Initial Rate Results for Uranium Silicide Dissolution at 60°C and Two NaOH Concentrations. Uranium silicide in 270-325 mesh particles.

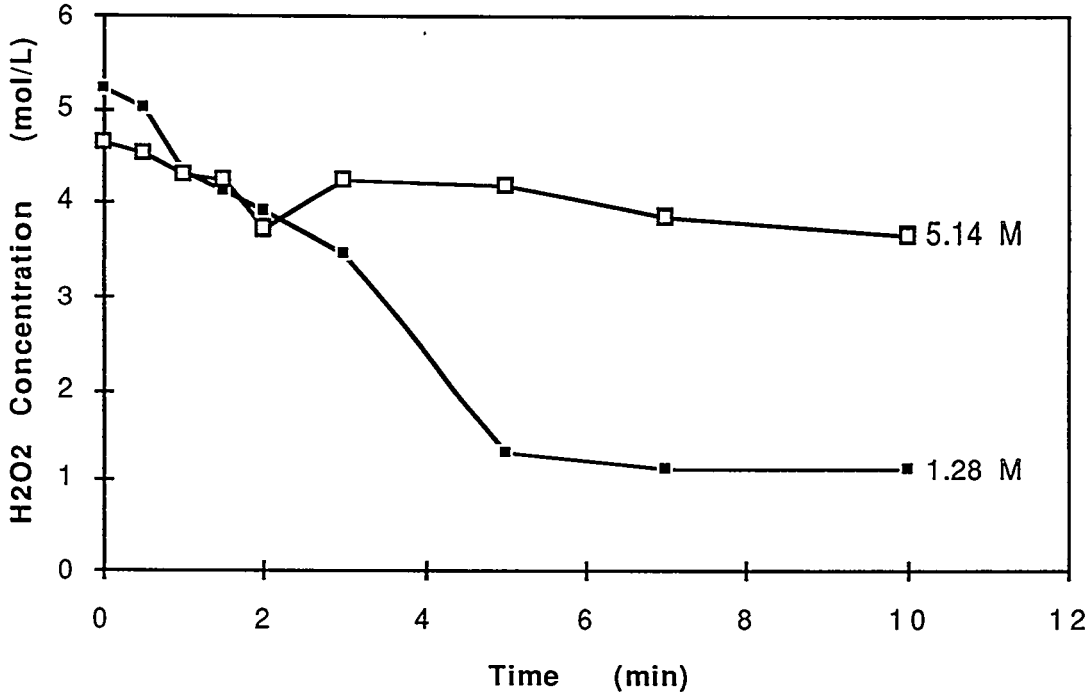

Figure 4. Initial Rate Results for Hydrogen Peroxide Depletion at 60°C and Two NaOH Concentrations. Uranium silicide in 270-325 mesh particles.

The results from the reaction-order experiments with 2.57M NaOH at 50° and 60°C are shown in Figure 5. These results indicate that the reaction order with respect to hydrogen peroxide is two in 2.57M NaOH. Also shown in the figure by the dashed line are the results for 5.14M NaOH at 60°C. At the higher base concentration, the order of the reaction with respect to hydrogen peroxide concentration is 1.3. The effect of the NaOH concentration on the order of the reaction will be investigated further. The present results indicate that the dissolution rate can be correlated by Eq. 8. The dissolution rate constant was determined by dividing the dissolution rate by the hydrogen peroxide concentration to the second power. Thus, the dissolution rate can be correlated by the following expression.

$$\frac{d[U]}{dt} = k_d A\,[H_2O_2]^2 \qquad (8)$$

Where,

[U] = uranium concentration, mg/L
t = time, min
k_dA = dissolution rate constant, mg U/L•min•g U_3Si_2 $[H_2O_2]^2$
$[H_2O_2]$ = concentration of hydrogen peroxide, M

The initial rate experiments also indicated the following trends:

- The silicide dissolution rate is directly proportional to the surface area of the particles. Therefore, as the particle size decreases, the increased surface area will result in an increased dissolution rate. Depending on the base concentration, a 35% decrease in the

particle size will increase the dissolution rate by a 50-75%. This effect is quantified by the variable "A" in Eq. 8.

- The rates of the reactions increase with temperature, as expected. The rate of increase depends on the base concentration being tested. In 5.14M base, a 10°C increase in temperature increases the silicide dissolution rate 300%, and the peroxide depletion rate 150%. Thus, higher temperatures favor the dissolution reaction over the peroxide destruction reaction.

- The order of $[H_2O_2]$ dependency for both the dissolution reaction ($[H_2O_2]^2$) and the peroxide autodestruction ($[H_2O_2]$) did not change with temperature.

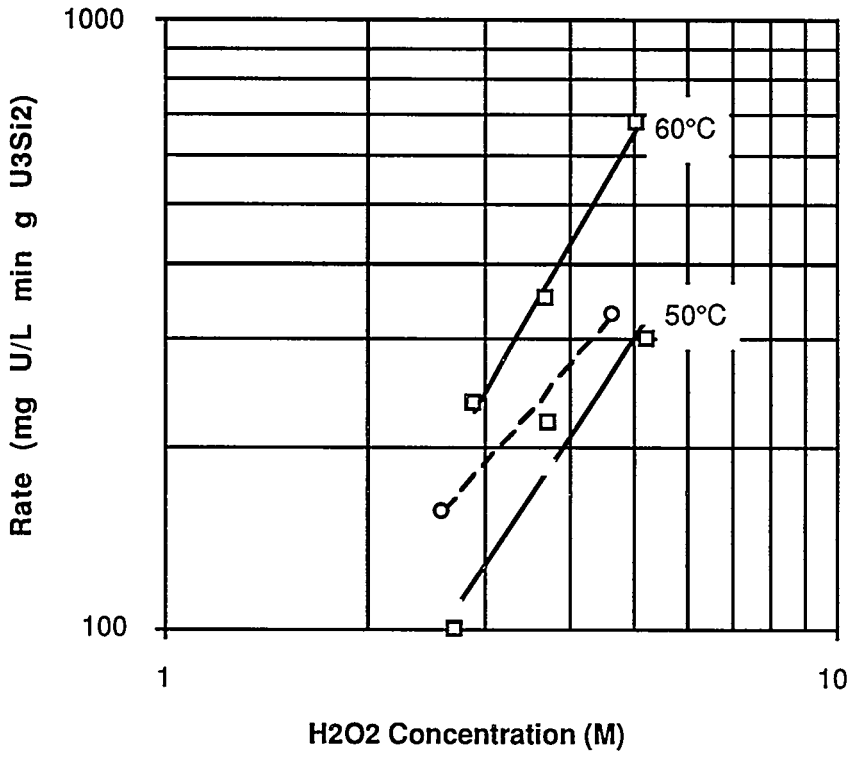

Figure 5. Plot Used for Determining Reaction Order for U_3Si_2 Dissolution. Solid lines, 2.57M NaOH, 50° and 60°C; dashed line, 5.14M NaOH, 60°C.

OPTIMIZED URANIUM SILICIDE DISSOLUTION PROCEDURE

A summary of the initial rate results at 50 and 60°C is given in Table 4. By using an Arrhenius form, these rates can be extrapolated to higher temperatures. Experiments to verify this extrapolation are planned. As shown in the table, the dissolution rate decreases with increasing hydroxide concentration. However, the hydrogen peroxide depletion rate also decreases with increasing base concentration. At low base concentrations, hydrogen peroxide rapidly decomposes, and although the silicide dissolution rate is initially high, it drops to zero as soon as the hydrogen peroxide is consumed; hydrogen peroxide must be present to dissolve the silicide, and these conditions are favored at higher base concentrations. In addition, when the dissolution is

complete, the dissolver solution must be acidified before being fed to an alumina column for Mo-99 removal. Thus, higher base concentrations require more acid to recover Mo-99. The optimum base concentration will be high enough to keep hydrogen peroxide in solution long enough to dissolve the silicide, but low enough to minimize the acid consumption prior to recovering the Mo-99 by ion chromatography. The optimum base concentration to meet these criteria is about 5M NaOH.

Table 4. Summary of Initial Rate Results (5M H_2O_2, 270-325 mesh U_3Si_2 Particles)

NaOH (M)	U Dissolution Rate (mol U/L•min•mol U_3Si_2)		H_2O_2 Depletion Rate (mol H_2O_2/L•min•mol U_3Si_2)	
	50 °C	60 °C	50 °C	60 °C
1.28	1.42	3.68	153	793
2.57	1.23	3.02	-	647
5.14	0.42	1.23	128	185

The effect of temperature is also shown in Table 4. In the 5.14M base case, a 10°C increase in temperature increases the uranium dissolution rate 300%, while the hydrogen peroxide rate increases only 150%. Thus, silicide dissolution is favored over hydrogen peroxide destruction as the temperature increases. Extrapolation of these results indicates at 100°C, near the boiling point, dissolution rates as high as 180 mol U/L•min•mol U_3Si_2 and depletion rates of 270 mol H_2O_2/L•min•mol U_3Si_2. These are about the highest rates obtainable in an atmospheric dissolver. Even higher rates could theoretically be obtained in a pressurized dissolver, but because of the large amount of gas generation caused by peroxide destruction, such a device is impractical.

The dissolver design is limited by the foaming of the dissolution solution at these conditions. If too much hydrogen peroxide (our preliminary work has used up to 5M H_2O_2) is mixed with sodium hydroxide (5M) near the boiling point, the foaming caused by the gas evolution is so great that the contents may be dispersed outside the dissolution vessel. Thus, the problem becomes one of limiting the amount of solution (5M hydrogen peroxide and 5M NaOH) which is added to that batch, so that foam generation can be controlled.

By using the optimized condition described above, quantities of up to 3 g of uranium silicide can be dissolved in less than 1 h. The resulting solution will exceed the uranium concentration required so that the LEU targets will produce a Mo-99 concentration equivalent to current HEU processes. In fact, we have been able to reach concentrations of uranium approaching 0.16M during the dissolution process.

We have found that the following procedure gives the best conditions for dissolving an unirradiated target. After the cladding solution is removed, the jacketed flask is heated to 90-95°C, then for the first 3 g of silicide, 5 mL of 30 wt % hydrogen peroxide (9.56M) and 5 mL of 10M NaOH are added to the dissolver. This combination produces close to the optimum 5M H_2O_2-NaOH. The solution foams, and within about 3 min, the foaming subsides and a dark red uranium solution is produced. Since the dissolution is second order with respect to hydrogen peroxide concentration, high concentrations of peroxide are needed to achieve rapid dissolution. To avoid dilution, the solution is removed from the dissolver and 10 mL of 30 wt % hydrogen peroxide (9.56M) and 10 mL of 10M NaOH are added to the dissolver. More reagents can be added because the foaming is reduced with subsequent reagent additions. As before, the solution foams, and within about 3 min, the foaming subsides and a dark red uranium solution is produced. This solution can be removed from the dissolver and the process repeated until the

entire target is dissolved. We have found that it takes about 150 mL of reagents to dissolve 3 g of U_3Si_2.

These dissolution kinetics are ideal for a plug-flow reactor configuration. We plan to use a jacketed glass filter as a dissolver to test this concept.

DISSOLUTION OF HIGH BURNUP TARGET

Because irradiated uranium silicide targets could behave differently, we tested this process using an irradiated miniplate sample that was stored at Argonne following its post-irradiation examination. The miniplate sample that we used had undergone 42.2% burnup in the 30 MW Oak Ridge Reactor (ORR). This miniplate contained uranium enriched to 19.84% ^{235}U before irradiation. Since the miniplate is nearly 9 years old, the short-lived fission products, including ^{99}Mo, have completely decayed. However, several stable molybdenum isotopes and the long-lived fission products and actinides still remain in the U_3Si_2 miniplates.

The primary benefit to using a sample with a high burnup is to measure the effects on the dissolution step of changes in the fuel caused by the high degree of fissioning. High burnup of the fuel significantly changes its chemical composition. For example, the chemical composition of the target is modified from that of unirradiated or low-burnup fuels by lowering the uranium content of the fuel, producing ^{28}Si from ^{27}Al, producing ^{31}P from ^{30}Si, and causing the formation of fission products and transuranic elements. Such chemical compositional changes coupled to radiation damage to the fuel caused by energy input (about 200 MeV/fission) form new compounds, especially along the contact between the U_3Si_2 fuel particles and the aluminum matrix. The formation of new compounds in highly irradiated fuels was studied earlier by Gerard Hofman and colleagues at Argonne [14] using both optical and electron microscopy techniques on polished metallographic specimens. The salient aspects of their findings are summarized below:

- A new layer caused by the interaction of uranium silicide with aluminum was formed as a result of high levels of irradiation. The thickness of the layer increased with the duration of irradiation. The layer was about 2-μm thick at 40% burnup.

- The new layer can be represented by the chemical formula $U(Al,Si)_3$, where the Al and Si can form a series of solid solutions represented by the end members UAl_3 and USi_3. At 40% burnup, the chemical composition of the layer is about 65 mol% Al, 25 mol% Si, and 10 mol% U.

- A mixture of nitric acid, hydrofluoric acid, and citric acid etched the unaltered U_3Si_2 but did not attack the $U(Al,Si)_3$ layer.

Unlike the unirradiated target, the irradiated miniplate did not dissolve readily by use of our optimized procedure. The decladding procedure did work as expected. But after the cladding was removed, the silicide fuel looked like a monolith, not the particles we obtained during the unirradiated testing. This monolith was resistant to dissolution. Even after the monolith was broken into pieces, the dissolution was very slow. We used 800 mL of 5M NaOH-5M H_2O_2 over a 10 h period (only 150 mL was expected to be used in less than 1 h). A substantial portion of the miniplate did dissolve. Samples from the liquid dissolver solution are being analyzed so that a material balance can be completed. We suspect that the miniplate did not dissolve due to the formation of a surface layer of $U(Al,Si)_3$, and we plan to test this hypothesis by using annealed unirradiated targets later this year.

DEVELOPMENT OF URANIUM SILICIDE PROCESS

During the next year we plan to make considerable progress to evaluating the technical and economic feasibility of an LEU silicide process for Mo-99 production. The highest priority is to develop a dissolution procedure for irradiated targets. In addition, the following issues will be studied.

Acidification of the cladding solution. The cladding solution must be acidified to allow recovery of the Mo-99 by ion chromatography. The HEU processes in use at the IRE acidify the dissolved solution (cladding and fuel are dissolved in one step) to 1M by using concentrated nitric acid. Work at Argonne has shown that Mo-99 is better recovered with 0.5M nitric acid [15]. Experiments to verify this procedure are planned.

Recovery of the uranium. Once the silicide target is dissolved, the uranium can be recovered as sodium diuranate by destroying the peroxide complex. We have finished a limited amount of experimental work to develop this procedure. More experiments are planned to determine the parameters that control this process, including the effect of carbonates on interfering with the uranium precipitation. Processes for recycling the recovered uranium and their cost effectiveness will be investigated.

Acidification of the dissolver solution. Early work at Argonne has shown that the silicon concentration must be less than 0.1M in the acidified dissolver solution [5]; this prevents precipitation of gelatinous silica. Concentrated nitric acid will be used to acidify this solution.

Ion chromatography recovery of Mo-99. This procedure has been used at the IRE on HEU targets for more than 10 years. A detailed description of the process is given elsewhere [2]. Unlike the IRE, the LEU process will produce a slightly different composition solution. Experiments are planned using an irradiated miniplate to determine the material balance for molybdenum, uranium, activation products, and fission products. These experiments will employ the new optimized dissolution procedure and the published ion chromatographic procedure to recover the Mo-99.

Waste disposal. The liquid and solid wastes generated from the process must be characterized and disposed of. A material balance on the optimized process will be done, and the waste streams identified.

CONCLUSIONS

The first roadblock to the use of LEU silicide targets instead of the conventional HEU UAl_x alloys for Mo-99 production is the dissolution of the target. In base, the uranium silicide does not readily dissolve. However, the silicide can be dissolved in alkaline peroxide. The optimum conditions for silicide dissolution appear to be 5M NaOH-5M H_2O_2 at boiling temperatures. The kinetics of the dissolution process favor a plug-flow reactor configuration. Using these optimum conditions we have been able to successfully dissolve significant quantities of unirradiated uranium silicide in less than 1 h. Irradiated targets are not readily dissolved by this procedure. It is suspected that the formation of a $U(Al,Si)_3$ surface layer interferes with the dissolution. This possibility will be studied further during the next year. Downstream of the dissolution, the solutions recovered will produce a Mo-99 yield equivalent to current HEU processes. Work remains to be done on the process downstream of the dissolution, including ion chromatographic recovery of Mo-99 and waste disposal.

REFERENCES

[1] A. A. Sameh, and H. J. Ache, "Production Techniques of Fission Mo-99," *Fission Molybdenum for Medical Use, Proceedings of the Technical Committee*, IAEA, Karlsruhe, Oct. 13-16, 1987, IAEA-TECDOC-515, 35-46.

[2] J. Salacz, "Reprocessing of Irradiated U-235 for the Production of Mo-99, I-131, and Xe-133 Radioisotopes," *Fission Molybdenum for Medical Use, Proceedings of the Technical Committee*, IAEA, Karlsruhe, Oct. 13-16, 1987, IAEA-TECDOC-515, 149-154.

[3] R. O. Marques, P. R. Cristini, H. Fernandez, and D. Marziale, "Operation of the Installation for Fission Mo-99 Production in Argentina," *Fission Molybdenum for Medical Use, Proceedings of the Technical Committee*, IAEA, Karlsruhe, Oct. 13-16, 1987, IAEA-TECDOC-515, 23-33.

[4] K. A. Burrill and R. J. Harrison, "Development of the Mo-99 Process at CRNL," *Fission Molybdenum for Medical Use, Proceedings of the Technical Committee,* IAEA, Karlsruhe, Oct. 13-16, 1987, IAEA-TECDOC-515, 35-46.

[5] G. F. Vandegrift, J. D. Kwok, S. L. Marshall, D. R. Vissers, and J. E. Matos, "Continuing Investigations for Technology Assessment of Mo-99 Production from LEU Targets," *Fission Molybdenum for Medical Use, Proceedings of the Technical Committee*, IAEA, Karlsruhe, Oct. 13-16, 1987, IAEA-TECDOC-515, 115-128.

[6] G. F. Vandegrift, J. D. Kwok, D. B. Chamberlain, J. C. Hoh, E. W. Streets, S. Vogler, H. R. Tresh, R. F. Domagala, T. C. Wiecek, and J. E. Matos, "Development of LEU Targets for Mo-99 Production and Their Chemical Processing Status 1989," *12th International Meeting, Reduced Enrichment for Research and Test Reactors, Proceedings*, Berlin, September 10-14, 1989, 421-433.

[7] S. Stroller and R. Richards, eds., *Reactor Handbook: Fuel Reprocessing*, Interscience Publishers, New York, 1961.

[8] W. C. Schumb, C. N. Satterfield, and R. L. Wentworth, *Hydrogen Peroxide*, Reinhold Publishing Corp., New York, 1955.

[9] D. G. Karraker, "Radiation Effects on the Solubility of Plutonium in Alkaline High Level Waste," Westinghouse Savannah River Center, WSRC-MS-94-0278X, 1994.

[10] R. H. Perry et al., eds., *Perry's Chemical Engineer's Handbook*, 6th Ed., McGraw-Hill Book Co., New York, 1984.

[11] A. I. Vogel, *A Textbook of Quantitative Inorganic Analysis*, Lowe & Brydone, Ltd., London, 1960.

[12] C. C. Lin et al., "Decomposition of Hydrogen Peroxide in Aqueous Solutions at Elevated Temperatures," *Int. J. Chem. Kin.*, 23, 971-987, 1991.

[13] H. S. Fogler, *The Elements of Chemical Kinetics and Reactor Calculations*, Prentice-Hall, Englewood Cliffs, NJ, 1974.

[14] G. L. Hofman, L. A. Neimark, and F. L. Olquin, "The Effect of Fabrication Variables on the Irradiation Performance of Uranium Silicide Dispersion Fuel Plates," Proc. of 1986 Int. Meeting on Reduced Enrichment for Research and Test Reactors (RERTR), November 3-6, 1986, Gatlinburg, Tennessee, ANL/RERTR/TM-9,CONF-861185, p. 201.

[15] J. D. Kwok, G. F. Vandegrift, and J. E. Matos, "Processing of Low Burnup LEU Silicide Targets," Proceedings of the 1988 International Meeting on Reduced Enrichment for Research and Test Reactors, September 18-24, 1988, San Diego, CA.

PRELIMINARY INVESTIGATIONS ON THE USE OF URANIUM SILICIDE TARGETS FOR FISSION Mo-99 PRODUCTION.

Authors: COLS H., CRISTINI P., MARQUES R.

FISSION Mo-99 PROJECT - C.N.E.A. - ARGENTINA

INTRODUCTION

The National Atomic Energy Commission (CNEA) of Argentine Republic owns and operates an installation for production of molybdenum-99 from fission products since 1985 [1-2], and, since 1991, covers the whole national demand of this nuclide, carrying out a program of weekly productions, achieving an average activity of 13 terabecquerel per week. At present we are finishing an enlargement of the production plant that will allow an increase in the volume of production to about one hundred of terabecquerel.
Irradiation targets are uranium/aluminium alloy with 90% enriched uranium with aluminium cladding [1-2]. In view of international trends held at present for replacing high enrichment uranium (HEU) for enrichment values lower than 20 % (LEU), since 1990 we are in contact with the RERTR program, beginning with tests to adapt our separation process to new irradiation target conditions.
Uranium silicide (U_3Si_2) was chosen as the testing material, because it has an uranium mass per volume unit, so that it allows to reduce enrichment to a value of 20 % [3].
CNEA has the technology for manufacturing miniplates of uranium silicide for our purposes.
In this way, equivalent amounts of Molybdenum-99 could be obtained with no substancial changes in target parameters and irradiation conditions established for the current process with Al/U alloy.
This paper shows results achieved on the use of this new target.

EXPERIMENTAL DEVELOPMENT

1) TARGET DISSOLUTION

All tests were carried out with uranium silicide miniplates (natural uranium) with an aluminium cladding. In the dissolving solution, iodide and molybdate (VI) were added as carriers and molybdenum-99, iodine-131, zirconium-95, niobium-95 and ruthenium-103 as tracers, to study their behaviour during purification steps.
As in our production process, sodium hydroxide (NaOH) is used to dissolve the targets, and, in order to mantain this condition, it was evident that it was essential to count with an oxidizing agent for completion of silicide dissolution. Chosen oxidant was hydrogen peroxide (H_2O_2).
The ratio hydroxide/oxidant is very important, because none of them by itself can completely dissolve uranium silicide. The excess of peroxide produces a reaction too violent (so the adding must be gradual) and frees uranium as soluble peruranate, this fact impedes its recovering in only one step (part

of uranium precipitates together with hydrated oxides). Destruction of soluble peruranate by boiling is incomplete,and,although it was not quantified, destruction can be accomplished with manganate (VII) anion (MnO_4^-).
Mean values of needed solvents were 97 ml of 3M NaOH and 5 ml of H_2O_2 100 vol. per gram of target (uranium silicide with aluminium cladding).
In these conditions, silicon is released to the solution, and this doesn't allow separation of molybdenum by means of a strong anionic exchange resin (as DOWEX-I or AG-I) as the one employed in our production process. Molybdenum loaded from this solution shows normal retention, but it is impossible to elute it from the column, probably due to the formation of heteropolyacids of molybdenum and silicon.
Before any purification of molybdenum, it is necesary to filter the resulting solution of target digestion to separate solid uranium and hydrated oxides. This precipitate must be kept for further recovery of uranium.

2) NEUTRALIZATION

Separation of molybdenum, not only from other fission products, but from silicate and uranium that may remain as soluble complex (peruranate not completely destroyed with the treatment described in point 1), is accomplished with an acid aluminium oxide column. For this, pH of silicide dissolution must be adjusted to a value between 2 and 3,to guarantee full molybdate retention [1-2].
During the adjustment of pH, aluminium hydroxide precipitates at first but then it dissolves. To avoid silica precipitation, adding of acid has to be made in stages.It is also essential that silicate concentration be under 0.1 M [3].
Under these conditions, different values of nitric acid concentration were tested. To achieve pH adjustment without precipitation, adding of hydrogen nitrate (V) (HNO_3) must be gradual: first with 4.5 M to neutralize the solution and then with 1 M to adjust pH value. Mean values of resulting volumes were: 900 ml of 4.5 M acid + 300 ml of 1 M acid per litre of solution to be neutralized.

3) ALUMINIUM OXIDE COLUMN

Several tests were carried out, where up to 40 ml of neutralized solution per gram of aluminium oxide were loaded. In this way, a retention for Mo-99 greater than 99% was obtained in every case. Washings of the column were made with 10 ml of HNO_3 10^{-3}M per gram of aluminium oxide, with no molybdenum losses.
It is important to mention that the loading solution, after passing through the aluminium oxide column, gives positive reaction for uranium with 1,3 diphenyl-1,3-propanedione (DBM) and with hexacyanoferrate (II) $[Fe(CN)_6]^{4-}$ and there is no presence of silicon oxide acidifying and boiling the solution with concentrated hydrogen chloride (HCl).
Elution of molybdenum is accomplished with 1 M ammonium hydroxide (NH_4OH) with a yielding greater than 90%.
Several tests were carried out, where up to 40 ml of neutralized solution per gram of aluminium oxide were loaded. In this way, a retention for Mo-99 greater than 99% was obtained in every case. Washings of the column were made with 10 ml of HNO_3 10^{-3}M per gram of aluminium oxide, with no molybdenum losses.

It is important to mention that the loading solution, after passing through the aluminium oxide column, gives positive reaction for uranium with 1,3 diphenyl-1,3-propanedione (DBM) and with hexacyanoferrate (II) $[Fe(CN)_6]^{4-}$ and there is no presence of silicon oxide acidifying and boiling the solution with concentrated HCl.
Elution of molybdenum is accomplished with 1 M NH_3 with a yielding greater than 90%. There is complete absence of uranium and silicon in the elution (the soluble silicate may be adsorbed on the alumina bed). Decontamination factors for I-131 and Ru-103 were only of 20, but those for Zr-95 and Nb-95 showed average values of 1470 and 2300 respectively.

4)SECOND PURIFICATION STEP, EMPLOYING A CHELATING RESIN

Following the scheme of our Mo purification process, it was tested a chelating resin (CHELEX) column, which needs previous formation of a molybdenum / thiocyanate complex.
Loading of this column is carried out with the elution of first aluminium oxide column, where molybdenum / thiocyanate complex has been previously formed.Tests accomplished under these conditions showed a retention greater than 99% for Mo, with non measurable losses of it.
Elution was carried out with NaOH 1 M, with a yield of 99% in every case.
As separation factors for I-131 and Ru-103 were of about 30 in these conditions, it is necessary to repeat the formation of molybdenum / thiocyanate complex and a new passage through another chelating resin column.

5) LAST PURIFICATION STEP

As a last purification step, it was tested a second aluminium oxide column. Volume of this column is one-third of the previous one; loading of this column was accomplished by acidifying with HNO_3 the solution eluted from Chelex column adjusting pH to an adequate value.

6) CONCLUSIONS

Results obtained are considered very promising, because all necessary purification steps can be carried out without changing substantial stages of the current production process.
Next tests will be target irradiation at low neutron flux, to analyse its behaviour, and then to assemble a testing equipment in the new production hot cells. It will allow us to reproduce same tests under real irradiation conditions.

REFERENCES:

[1] - Marques,R.O.; Cristini,P.R.; Fernandez,H.; Marziale,D.

Operation of the installation for fission Mo-99 production in Argentina.

Fission molybdenum for medical use, Proc. of Technical Committee Meeting (I.A.E.A.) Karlsruhe,October 13-16 1987, IAEA-TECDOC 515,1989,p.23.

[2] - Marques,R.; Manzini,A.; Cristini,P.; Mondino,A.; Fernandez,H.; Furnari,E.; Gonzalez,N.

Produccion rutinaria de Mo-99 a partir de productos de fision. Actas de la XIX Reunion Cientifica de la Asociacion Argentina de Tecnologia Nuclear, 1991

[3] - Vandegrift,G.; Kwok,J.D.; Marshall,S.L.; Visser,D.; Matos,J.E.

Continuing investigations for technology assessment of Mo-99 production from L.E.U. targets.

1987 International Meeting on Reduced Enrichment for Research and Test Reactors,September 28 - October 2 1987, Buenos Aires, Argentina.

USE OF LEU IN THE AQUEOUS HOMOGENEOUS MEDICAL ISOTOPE PRODUCTION REACTOR

Russell M. Ball
Nuclear Environmental Services, Inc
Babcock & Wilcox
2220 Langhorne Road
Lynchburg, Virginia 24506-0548
804/948-4728

ABSTRACT

The Medical Isotope Production Reactor (MIPR) is an aqueous solution of uranyl nitrate in water, contained in an aluminum cylinder immersed in a large pool of water which can provide both shielding and a medium for heat exchange. The control rods are inserted at the top through re-entrant thimbles. Provision is made to remove radiolytic gases and recombine emitted hydrogen and oxygen. Small quantities of the solution can be continuously extracted and replaced after passing through selective ion exchange columns, which are used to extract the desired products (fission products), e.g. molybdenum-99. This reactor type is known for its large negative temperature coefficient, the small amount of fuel required for criticality, and the ease of control. Calculation using TWODANT show that a 20% U-235 enriched system, water reflected can be critical with 73 liters of solution.

Introduction

The need in nuclear medicine for the fission product isotope, molybdenum-99, is well known and has been the subject of investigations and presentations at previous RERTR conferences.[1] The concentration of effort has been on creation and processing of LEU targets which are subsequently irradiated in high flux reactors. Other papers in this Session describe further efforts along this line.

The Medical Isotope Production Reactor (MIPR) is a design under development by Babcock & Wilcox (B&W) which eliminates the need for target preparation and dissolution. It is particularly suited for the use of LEU in medical isotope production. The MIPR is an aqueous homogeneous reactor operating at 200 KW thermal power and produces over 2000 curies of Mo-99 per DAY.

Reactor Description

The reactor is composed of a solution of uranyl nitrate ($UO_2(NO_3)_2$) in water. The reactor can be designed to function with U-235 enrichments of 18% to 90%. One variant of the MIPR design, using LEU (uranium enriched to 20% U-235), has been analyzed at Los Alamos National Laboratory by Dr. Robert Kimpland.[2] Using TWODANT with an Sn of 16 to model the core, the uranium concentration is 150 grams/liter and the core volume is 73 liters, giving a critical height of 460 mm. The core would contain about 2.2 kg of U-235 or about 18 kg of salt. The container was assumed to be stainless steel and is fully reflected by water. A second variant used an aluminum container and 100 liters of solution. The critical concentration was 117 gram of uranium/liter, 20% enriched. This means the U-235 content of the whole reactor is 2.34 kg.

In the reference MIPR system, the core container is assumed to be aluminum. The container is cylindrical with cooling fins. On the top cover are stepped aluminum thimbles which permit the insertion of control and safety rods and small tubing for solution addition and removal. The solution is acidic to prevent corrosion of container and thimbles. The entire reactor container is immersed in a pool of water assumed to be 3 by 3 meters and 7 meters high (63 m^3, or 63 metric tons).

The burnup of the fissionable material, U^{235}, is about 1.2 grams per megawatt-day. For a 200 kWt operation, the burnup is less than one quarter gram per full power day. Additions to the reactor core to compensate for burnup can be through the addition of a few grams of solution per month.

The planned power level of the reactor is 200 kWth and the operating temperature of the uranium solution is 80°C (176°F).

The proposed reactor solution container is a cylinder with a volume of 100 liters, approximately 450 mm diameter and 750 mm height. The outer and inner surfaces are finned for enhanced heat transfer. The material is an aluminum alloy chosen for strength and corrosion resistance. The actual size and composition of the container, however, will depend on confirmatory thermal/hydraulic, neutronic, and materials performance evaluations. Figure 1, "MIPR System Design", shows the reactor at the bottom of a pool of ordinary water. The various gas recombiners, filters and traps are under water. The extraction columns are also under water and are fitted with "quick disconnect" fittings for easy replacement. The valving is arranged so that a column can have a small amount of reactor solution pasing through for molybdenum stripping. The valving also permits wash and eluting solutions to pass through the column for the cleaning and removal of the product. Heat removal from the fuel solution container is passive through extended surfaces on the container and is absorbed by the bulk pool water. The pool water is cooled by passing it through a conventional tube-shell heat exchanger. The normal pool water temperature is 22 oC. The water on the secondary side of the heat exchanger is cooled using a forced draft cooling tower.

Figure 1. MIPR System Design

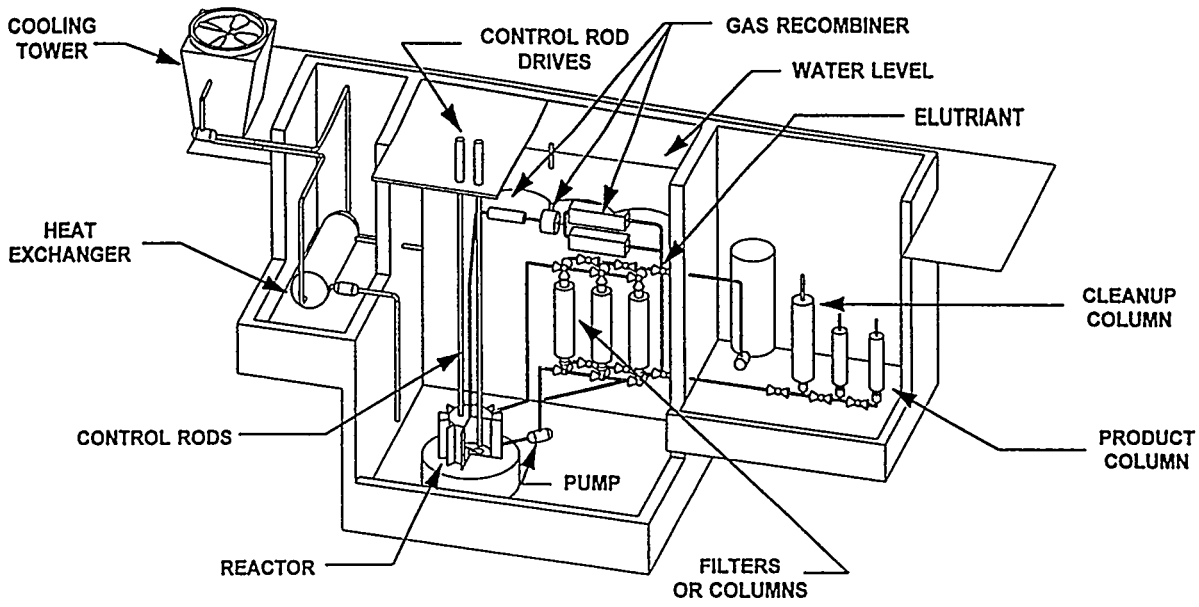

2. Gas Handling

During operation of the MIPR, two types of gas are produced. The radiolytic dissociation of the water results in the production of hydrogen and oxygen. The fission process produces some fission products which are gaseous at standard temperatures and pressures.

Extrapolating from the experience of the SUPO reactor at Los Alamos (RH 13-129), hydrogen gas evolution (and by inference the oxygen evolution, half mole of oxygen for each mole of hydrogen) for a 200 kWt reactor would produce 600 cc/sec of H_2 or 60 milligrams/sec. However, as in the case of pressurized water reactors, it may be possible to operate the reactor with a hydrogen overpressure (about 50 psig) which may obviate the need for a recombiner, or, as in the case of the Homogeneous Reactor Experiment at Oak Ridge, internal recombinaton can be possible with a copper catalyst.

Approximately 60% of the fission products have a xenon or krypton isotope as members of the decay chains. Half of the isotopes, about 15 cc/day for 200 kWt, are stable or have half-lives that permit them to be removed from a fluid fuel before they decay (RH 13-71).

Catalytic recombiners for hydrogen and oxygen have been used industrially for many years. Systems with platinum and palladium catalysts deposited in concentrations of 0.03 to 0.3 weight percent on small (1/8 inch) cylinders of alumina have proven effective for recombining hydrogen and oxygen in non-combustible mixtures. Adsorption of the

krypton and xenon on activated carbon or other adsorbents is a convenient method of storing the gases until most of the radioactivity decays and can be discharged. Most radioactive containers of charcoal can be stored underwater in the pool until essentially all gases except the 10.3-year Krypton-85 have decayed. The production rate of Kr-85 is 110 millicuries per 200 kWt-day.

3. Instrumentation & Control

The excess reactivity of the MIPR is deliberately kept small to reduce the energy of any postulated incident involving reactivity insertion. This excess reactivity and safety shutdown for deep sub-criticality is achieved by the insertion of solid neutron absorbers, such as clad boron carbide, through re-entrant thimbles. Two safety rods are held by electromagnets which are driven from a motor drive. A control rod is similarly placed but without the electro-magnet.

Void and temperature coefficients of this type reactor have been extensively studied and are large and negative. The concentration of U^{235} in the solution is selected such that at operating conditions with movable control and safety rods out of the core, the reactor operates near the design temperature and full power. Fission product poisons and burnup of the U^{235} are periodically compensated for by either control rod movement or the addition of a small amount of U^{235}. The MIPR is configured at maximum reactivity so that geometric changes reduce reactivity and power.

The neutron detectors, source and other radiation detectors can be placed in thimbles which are around the main reactor core tank. Temperature sensors, such as thermocouples or resistance thermometers can be placed in the solution in sheaths or thimbles. Pressures, flows, pump indications, fans, motors, and other parameters which are required to be sensed, conditioned, and displayed or stored are expected to be of conventional design.

4. Heat Removal and Transport

The previous designs of aqueous homogeneous reactors have used internal cooling coils to remove the heat from the reactor solution. The largest power removed was 50 kWt from the ARF reactor in Chicago, Illinois and the KEWB reactor at Atomics International in Canoga Park, California. The KEWB used 90 feet of stainless steel tubing, I/4 inch O.D. with inlet water at 85°F and outlet 109°F. The average fuel temperature was 176°F. The area of the tubing is about 5500 cm^2. The vertical wall area of the MIPR tank is 10,000 cm^2 and the equivalent area can be more than doubled with fins. Avoiding the use of cooling coils will significantly enhance simplicity, reliability, and safety. (KEWB used internal coils rather than external water for cooling because the experimental purpose required a solid shield.)

One shell-and-tube, single-pass heat exchanger is provided to transfer approximately 200 kWt of reactor heat plus 7 kWt from the recombiner. The pool water enters the heat exchanger at 25°C and returns at 22°C. The cooling tower water enters the shell side of the heat exchanger at 16°C and returns to the cooling tower at 18°C. The flow rate for both primary and secondary sides is between 20 and 30 kg/sec. The heat exchanger was designed with 12% excess area for margin. The heat exchanger will be fabricated as an ASME Section III-Class 1 Exchanger using the aluminum alloy 6061.

The secondary cooling system extends from the shell side of the pool heat exchanger to the inlet of the cooling tower and from the cooling tower basin to the heat exchanger inlet. Four-inch aluminum piping connects the heat exchanger to the cooling tower.

A centrifugal pump in the cold leg of the secondary system provides the 28 kg/sec at the 150 meter (500 foot) head to transport the heat from the pool heat exchanger to the cooling tower.

The heat will be rejected to the atmosphere via an induced draft cooling tower. A 15 HP cooling fan draws the air through the tower to remove latent heat from the water. The basin provides 500 ft^2 of area to retain effluent from the cooling tower.

5. Extraction & Purification of Product

The growth of the Mo-99 in the reactor and in the precipitation column is shown in Figure 2. The extraction flow from the reactor is 1 cc/second. Figure A-2 shows the amount of Mo^{99} in the precipitation column considering that after one day of extraction, the column is valved off (another column would be valved in) and the Mo^{99} decays as it moves through the rest of the process and shipping.

At a maximum 200 kWt operating power, the MIPR can produce 10,000 curies of Mo^{99} per five-day week. Allowing 4 days for processing, packaging, and shipping, and some reactor down time for maintenance/contingencies, the customers would receive approximately 2,100 curies per week.

Figure 2. Growth and Decay of Moly-99

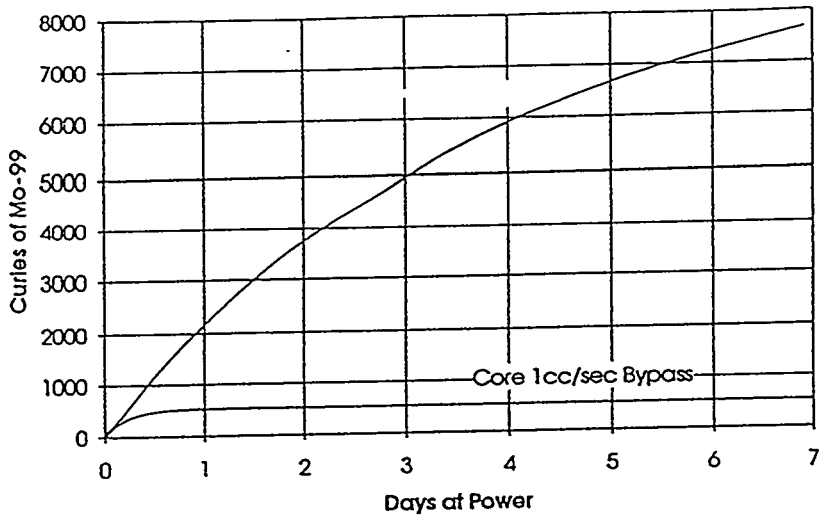

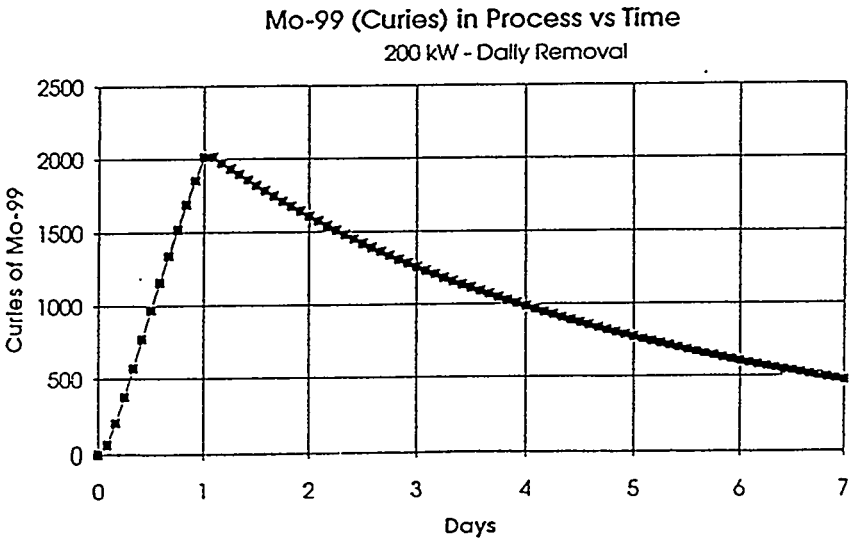

REFERENCES

1. A.A. Sameh, A. Bertram-Berg, Nuclear Research Center Karlsruhe, "HEU and LEU MTR Fuel Elements as Target Materials for the Production of Fission Molybdenum", Meeting on Reduced Enrichment for Research and Test Reactors (RERTR), September 27-October 1, 1992, Roskilde, Denmark

2. Robert Kimpland, Los Alamos National Laboratory, NIS-6, Advanced Nuclear Technology, July 13, 1994, Private Communication

POST-IRRADIATION EXAMINATION OF PROTOTYPE Al-64 wt% U_3Si_2 FUEL RODS FROM NRU

D.F. Sears, M.F. Primeau, C. Buchanan and D. Rose

ABSTRACT

Three prototype fuel rods containing Al-64 wt% U_3Si_2 (3.15 gU/cm^3) have been irradiated to their design burnup in the NRU reactor without incident. The fuel was fabricated using production-scale equipment and processes previously developed for Al-U_3Si fuel fabrication at Chalk River Laboratories, and special equipment developed for U_3Si_2 powder production and handling. The rods were irradiated in NRU up to 87 at% U-235 burnup under typical driver fuel conditions; i.e., nominal coolant inlet temperature 37°C, inlet pressure 654 kPa, mass flow 12.4 L/s, and element linear power ratings up to 73 kW/m. Post-irradiation examinations showed that the fuel elements survived the irradiation without defects. Fuel core diametral increases and volumetric swelling were significantly lower than that of Al-61 wt% U_3Si fuel irradiated under similar conditions. This irradiation demonstrated that the fabrication techniques are adequate for full-scale fuel manufacture, and qualified the fuel for use in AECL's research reactors.

Fuel Materials Branch
Chalk River Laboratories
Chalk River, Ontario K0J 1J0
1994 September

POST-IRRADIATION EXAMINATION OF PROTOTYPE Al-64 wt% U_3Si_2 FUEL RODS FROM NRU

D.F. Sears, M.F. Primeau, C. Buchanan and D. Rose

Fuel Materials Branch
Chalk River Laboratories
Chalk River, Ontario K0J 1J0
Canada

ABSTRACT

Three prototype fuel rods containing Al-64 wt% U_3Si_2 (3.15 gU/cm^3) have been irradiated to their design burnup in the NRU reactor without incident. The fuel was fabricated using production-scale equipment and processes previously developed at Chalk River Laboratories for Al-U_3Si fuel fabrication, and special equipment developed for U_3Si_2 powder production and handling. The rods were irradiated in NRU up to 87 at% U-235 burnup under typical driver fuel conditions; i.e., nominal coolant inlet temperature 37°C, inlet pressure 654 kPa, mass flow 12.4 L/s, and element linear power ratings up to 73 kW/m. Post-irradiation examinations showed that the fuel elements survived the irradiation without defects. Fuel core diametral increases and volumetric swelling were significantly lower than that of Al-61 wt% U_3Si fuel irradiated under similar conditions. This irradiation demonstrated that the fabrication techniques are adequate for full-scale fuel manufacture, and qualified the fuel for use in AECL's research reactors.

INTRODUCTION

Chalk River Laboratories (CRL) has developed and tested low-enrichment uranium (LEU, 19.75% U-235 in U) fuels for use in AECL's research reactors. The LEU fuel core is an extruded metal matrix composite containing high-density uranium silicide particles dispersed in an aluminum matrix. Several uranium silicide compounds have been tested in the LEU fuel development program at CRL. These include the binary U-Si alloys: U-3.96Si (U_3Si) and U-7.3Si (U_3Si_2), and the ternary U-Si-Al alloys: U-3.5Si-1.5Al and U-3.2Si-3.0Al. The results of the U_3Si and U-Si-Al fuel development program are described elsewhere (1-3). This paper reviews the fabrication and irradiation testing of three Al-64 wt% U_3Si_2 dispersion fuel rods in the NRU reactor, and presents results from the post-irradiation examinations.

BACKGROUND

In 1993 June, the NRU reactor was completely converted from highly enriched uranium (HEU, 93% U-235 in U) fuel in a U-Al alloy, to LEU fuel. NRU is a heavy-water-moderated and -cooled multipurpose research reactor that operates at 125 MW(th). HEU fuel rods had been used in NRU since 1964, when the reactor was converted from plate-type fuel containing natural uranium metal.

As shown schematically in Figure 1, the NRU driver fuel rod consists of 12 finned fuel elements arranged in two concentric rings. The elements are 2.92 m long but the fuelled portion is 2.74 m. The fuel element core diameter is 5.49 mm and the clad wall thickness is 0.76 mm. Each element has six cooling fins spaced 60° apart around the cladding, the fin width being 0.76 mm and the fin height 1.27 mm.

The 12-element NRU fuel rod has proven to be safe and reliable over the past three decades of operation. Therefore, when the decision was made to convert from HEU to LEU, the rod design was retained. Basically, this meant that a replacement LEU core had to be developed with approximately five times the uranium density (3.15 g/cm^3) of the HEU element core (0.68 g/cm^3). Since the required density was beyond that readily achievable with extrudable U-Al alloys, dispersion fuels containing high-density uranium silicide particles in an aluminum matrix were selected. During the 1980's, LEU fuels were developed and tested at CRL, first in mini-elements (1,2,3), and when these proved successful, in full-length prototype fuel rods (4). As mentioned above, several uranium silicide compounds have been tested in the LEU fuel development program at CRL. These include the binary U-Si alloys, U-3.96Si (U_3Si) and U-7.3Si (U_3Si_2), and the ternary U-Si-Al alloys, U-3.5Si-1.5Al and U-3.2Si-3.0Al. When the decision was made to build a new plant for LEU fuel fabrication, the leading fuel candidate at the time, Al-61 wt% U_3Si, was selected as the reference fuel. Factors that influenced this decision included the safe and predictable behaviour of the fuel under irradiation, and the well-established and successful fabrication process at CRL. However, the development of U_3Si_2 dispersion fuel continued, because it was known that U_3Si_2 was easier to crush into powder than U_3Si and therefore offered fabrication cost savings over the latter. Al-U_3Si_2 had also been tested in plate-type fuel elements in the Oak Ridge Reactor, and its performance was excellent up to high burnups (5).

The Al-64 wt% U_3Si_2 fuel development program followed the plan established for the other uranium silicides previously tested at Chalk River. Mini-elements were fabricated and irradiated to high burnup in NRU (6), and based on their satisfactory results (7), full-length LEU rods were fabricated and irradiated to qualify the fuel. Prototype rods were also used to demonstrate that no problems resulted from scaling-up the fabrication process to manufacture the long NRU rods.

Three full-size LEU fuel rods containing Al-64 wt% U_3Si_2 were fabricated in 1989. By 1990 August, the demonstration/qualification irradiation in NRU had begun. The fabrication and irradiation testing of these prototype rods are described in this report, and results from the post-irradiation examination of the U_3Si_2 fuel are presented.

OBJECTIVE

The objective of the prototype irradiation, experiment Exp-FZZ-924, was to demonstrate the satisfactory irradiation behaviour of full-length Al-64 wt% U_3Si_2 fuel rods to burnups beyond 80 at% U-235 in NRU, and thereby to qualify the fuel and its manufacturing process for use in research reactors with similar driver fuel operating conditions.

FUEL FABRICATION

The fabrication process used to make the Al-64 wt% U_3Si_2 fuel was essentially the same as that used to make Al-61 wt% U_3Si fuel at Chalk River, except for two special processes developed for U_3Si_2. Basically, uranium and silicon were melted in a vacuum induction furnace, cast into billets, then crushed into powders in an inert atmosphere glove box. The uranium silicide powder was

seived into discrete size fractions, mixed with high-purity aluminum powder (Alcan HP52) and blended to homogenize the fuel. The blended powders were loaded directly into the extrusion die cavity under argon gas, then extruded into cores. Except for the U_3Si_2 crushing and Al-U_3Si_2 powder loading processes, all other procedures were based on the standard production flow chart for Al-61 wt% U_3Si fuel. The cores were drawn to size, cut to length and machined to accept end plugs, which were attached to the cores using a rolled joint. The cores and attached end plugs were extrusion clad with aluminum (Alcan 6102). Excess cladding material was machined from the ends of the end plug, and the cladding was welded to the end plugs to hermetically seal the elements. Twelve elements were assembled with flow spacers, welded to a hanger plate, then inserted into an aluminum flow tube. The standard top and bottom sections were attached to the flow tube to complete the assembly (NRU rod).

The U_3Si_2 melt composition was U-7.4% Si. Samples of the U_3Si_2 powder were examined using optical and scanning electron microscopy (SEM) and X-ray diffraction (XRD) analysis. The XRD analysis showed only the characteristic U_3Si_2 peaks, indicating that the powder was nominally pure U_3Si_2, with no detectable secondary phases.

Because U_3Si_2 powders have a lower density (12.2 g/cm^3) than U_3Si (15.4 g/cm^3), they occupy a correspondingly higher volume fraction of the fuel core for a given uranium loading. At the uranium loading required for NRU, 3.15 gU/cm^3, the U_3Si_2 occupies 28 vol% of the core, compared to 21 vol% for U_3Si. The core extrusion process had to be optimized for the higher U_3Si_2 volume fraction, to minimize as-fabricated porosity, which tends to increase as the volume fraction of uranium silicide increases. During extrusion trials, it was also found that U_3Si_2 eroded the extrusion tooling, being much more abrasive than U_3Si. The dies were redesigned and the die material was changed to overcome this problem.

Metallographic examinations of the extruded cores showed that the uranium silicide particles were evenly distributed within the aluminum matrix. Gamma-scanning confirmed that the axial distribution of fuel particles in the cores was reasonably uniform (max/min counts within ± 3.5% of core average) over the ~ 3 m length. Chemical analysis of core samples via controlled-potential coulometry indicated that the uranium content ranged from 58.62 to 59.46 wt% U (an Al-64 wt% U_3Si_2 core should contain 59.3 wt% U). Data for the prototype fuel rods are listed in Table 1.

TABLE 1. Prototype NRU Fuel Rod Data

	FL050	FL051	FL052
Al-64 wt% U_3Si_2 (g)	4004.1	4023.0	4036.0
U_3Si_2 (g)	2562.6	2574.7	2583.6
Enr U (g)	2373.0	2384.2	2392.4
U-235 (g)	467.7	469.9	471.5
Density (g/cm^3)	5.16	5.18	5.20
Porosity (%)	4.1	3.7	3.4

IRRADIATION CONDITIONS

The three prototype 12-element fuel rods were irradiated in NRU from 1990 August to 1992 June. However, the irradiation was interrupted in 1991, due to the year-long shutdown of NRU. The typical NRU driver-fuel operating conditions are summarized in Table 2. During the shutdown,

the fuel rods were removed from the reactor and stored in the light-water bays. The pH of the bay water is typically 7.6-7.7 and conductivity < 30 μS/cm. On restart of the reactor, the fuel rods were loaded in the fuelling machine, drained to remove the light water, and re-installed in the high-purity heavy-water coolant.

The fuel rods were irradiated under the typical fuel management scheme used in NRU: they were first loaded in a relatively low-power site at the periphery of the reactor core, moved to higher power sites near the center of the reactor as burnup increased, and then back to the outside near end of life. Each rod occupies 4-6 lattice positions during its lifetime in-reactor, typically 340 days residence time at 70% efficiency. The axial power profile with burnup for each rod is shown in Figures 2-4. The maximum rod power was 2.1 MW and the maximum element linear power output was approximately 72 kW/m. The irradiation was terminated in 1992 June, when the reactor physics codes showed that the fuel burnup was 87 at% U-235.

TABLE 2 Irradiation Conditions in NRU

Neutron Flux Density	1.1×10^{18} n.m^{-2}s^{-1}
D_2O Coolant:	
Inlet Temperature	37°C
Outlet Temperature	70°C
Inlet Pressure	654 kPa
Velocity	8.8 m/s
pH	5.5-6.5
Conductivity	< 1 μS/cm
Maximum Rod Power	2.1 MW
Element Linear Power	20-72 kW/m

POST-IRRADIATION EXAMINATIONS

Post-irradiation examinations (PIE) included underwater inspections in the bays, and visual and metallographic examinations in the hot cells. The flow tube was cut above and below the fuel, and the 12-element assembly was removed from the flow tube onto a horizontal table in the bay. The assembly was rotated manually for inspection of the outer elements. Following visual inspections, the assemblies were photographed.

Sections were cut from the bottom, middle and top of outer fuel elements for metallographic examinations. The samples were mounted in epoxy, ground and polished, with a final polish of 1/4 μm diamond paste. Photomacrographs and micrographs were taken of the as-polished surface. Samples were also dip-etched in Keller's etch (10 mL Hf/15 mL HCL/25 ml HNO_3/50 mL H_2O) to reveal the aluminum microstructure, and in Murakami's reagent (20 g $K_3Fe(Cn)_6$/20 g KOH/20 mL H_2O) to show the uranium silicide microstructure. Scanning electron microscopy (SEM) examinations were attempted, but the radiation fields from the fuel were too high and swamped the instruments. However, cladding samples were prepared by mounting thin transverse sections at approximately 45° to the normal plane and grinding past the fuel core, leaving only a sliver of the cladding. These were analyzed on the SEM using energy dispersion X-ray (EDX) analysis.

RESULTS AND DISCUSSION

Visual examinations in the water bays showed that the fuel elements were in good condition after irradiation. All end cap welds were intact and there was no evidence of fuel defects. A light-coloured oxide was observed on the cladding over most of the fuelled section of the elements, and a darker oxide covered the unfuelled regions and end plugs. Figure 5 shows the oxide coatings on the fuel elements in FL052. Some crud buildup and slight pitting was observed in the middle portion of the fuel elements, near the mid-length flow spacers (near the 144 cm mark in Figure 5). Wear marks in the fins were also observed under the flow spacers. In rod FL051, four of the five spacers were displaced axially. This was attributed to the fuel handling and flow tube removal process, because the outer fin surfaces appeared shiny between the original and final spacer locations. This is consistent with surface scratches from the spacers as they are pulled over the fin surfaces, due to friction from the flow tube.

An oxide thickness survey was done on each metallographic sample. The results are summarized in Table 3. Figure 6 shows a cross-sectional view of the oxide layer observed on the fuel cladding. The morphology of the oxide varied from sample to sample; some had intact adherent layers while others had circumferential and radial cracks. The literature (8) suggests that the corrosion product formed under experimental conditions similar to those in NRU is boehmite ($Al_2O_3.H_2O$). We were surprised to find layers of boehmite 50-80 μm thick on the cladding of one sample, since previous measurements from fuel rods irradiated to high burnup under similar conditions in NRU typically showed only 20-40 μm thick oxide layers. The only difference between the present and previous prototype rod irradiations (other than the fuel core composition) was the approximately one-year interruption that occurred when NRU was shut down and the rods were removed to the light-water bays. It is known that the pH and impurity levels in the bay water is much greater than that of the heavy-water coolant in NRU, since the bays are used for a variety of tasks, including defective fuel examinations. However, it is not known whether the prolonged interim exposure to contaminated water accelerated subsequent oxidation after irradiation was resumed, or whether the additional oxide built up during storage in the water bay.

TABLE 3. Oxide and Cladding Thickness Measurements

NRU ROD	LOCATION	OXIDE THICKNESS (μm)	CLADDING THICKNESS (mm)
FL050	Top	25-30	0.72 - 0.82
	Middle	50-80	0.67 - 0.74
	Bottom	20-40	0.66 - 0.76
FL 051	Top	20-40	0.70 - 0.79
	Middle	20-60	0.73 - 0.78
	Bottom	15-25	0.70 - 0.81
FL052	Top	50-70	0.73 - 0.78
	Middle	25-60	0.67 - 0.79
	Bottom	25-50	0.70 - 0.82

In preparation for SEM examinations of the fuel and cladding/oxide, a thin sample was sectioned and mounted, but the radiation fields proved to be too high for the instruments. During an attempt to quarter the sample to reduce the fields, the sample broke out of the mount. It was noticed that

some oxide remained on the mount material, so it was examined in the SEM. Figure 7 shows that the oxide that adhered to the mount had radial and circumferential cracks. Detailed examinations of other samples that were ground at an angle (to remove the fuel) revealed cracks adjacent to areas with cutting swarf from the cut off saw, and intact oxide layers remote from those locations. This suggests that the observed oxide fragmentation may be associated with damage from sample preparation. EDX analyses of the oxide layers revealed only Al, with minor traces of Fe (< 0.5%).

Optical metallographic examinations in the hot cells revealed that the fuel behaviour was similar to that of the Al-U_3Si_2 mini-elements previously tested at Chalk River (7). Figure 8 shows the typical microstructure of the fuel from FL050 after 87 at% burnup. As expected, the uranium silicide particles reacted with the aluminum matrix, forming an interfacial layer, UAl_3 with dissolved Si, around each particle. Small uranium silicide particles (less than 20 μm in diameter) completely reacted with the matrix and transformed to the uranium aluminide phase.

Fission-gas bubbles could be seen randomly dispersed in the uranium silicide particles, but few fission-gas bubbles were observed in the interfacial layer. The bubble morphology in the Al-U_3Si_2 rods was generally consistent with that observed in full-size Al-U_3Si_2 plate-type fuel irradiated in ORR (5). Where there was no local restraint, such as at the gap between the end-plug and fuel core, there was evidence of fission-gas bubble coalescence and growth, and plastic deformation of the silicide particles as shown in Figure 9. This behaviour was previously observed in prototype Al-61 wt% U_3Si fuel rods (4), which suggests that both fuels behaved similarly under the conditions tested.

Swelling measurements provide a reliable, quantitative parameter for evaluating and comparing the irradiation behaviour of various fuels under similar irradiation conditions. Immersion density measurements give the most accurate indication of fuel swelling; however, this was not possible with full-length NRU elements. As an alternative, swelling was estimated from fuel core diameter changes, assuming length changes were negligible. The core diameter measurements are shown in Table 4 (as-fabricated core diameter was 5.49 mm). Also included are measurements for similar full-length fuel rods containing Al-61 wt% U_3Si and Al-21 wt% HEU fuel. Note that the diametral increases of the Al-64 wt% U_3Si_2 fuel was consistently smaller, even compared to other fuels with lower burnup.

TABLE 4. Fuel Core Diametral Increases for Various NRU Rods

ROD	FUEL	BURNUP (at%)	DIAMETER (mm) Top	Middle	Bottom	MAXIMUM SWELLING (vol%)
FL-050	Al-64%U_3Si_2	87	5.50	5.56	5.49	2.6
FL-051	Al-64%U_3Si_2	83	5.51	5.60	5.52	4.0
FL-052	Al-64%U_3Si_2	87	5.49	5.60	5.52	4.0
FL-004	Al-61%U_3Si	81	5.60	5.65	5.58	5.9
FL-005	Al-61%U_3Si	87	5.62	5.70	5.62	7.8
FL-006	Al-61%U_3Si	83	5.60	5.69	5.61	7.4
FL-007	Al-61%U_3Si	78	5.56	5.64	5.59	5.5
FE-773	Al-21%HEU	74	5.57	5.62	5.57	4.8

The prototype Al-64 wt% U_3Si_2 fuel swelling measurements are plotted in Figure 10, and are compared with data from mini-elements containing Al-61 wt% U_3Si and mini-elements containing Al-64 wt% U_3Si_2 , irradiated under similar conditions in NRU. The mini-element data is based on accurate immersion density measurements taken after the oxide was stripped from the cladding. At 93 at% burnup, Al-64 wt% U_3Si_2 mini-element core swelling ranged from 4.2 to 4.7 vol%, compared with 5.8 to 6.8 vol% for Al-61 wt% U_3Si. In comparison, the full-length Al-64 wt% U_3Si_2 rods swelled by 2.6 - 4% after 87 at% burnup. It is clear from Figure 10 that the fuel swelling calculated from the present experiment falls within the range measured for other silicide dispersion fuels. This shows that the swelling behaviour of Al-64 wt% U_3Si_2 fuel is good at high burnup, and probably better than that of Al-61 wt% U_3Si or Al-21 wt% HEU.

SUMMARY AND CONCLUSIONS

Al-U_3Si_2 dispersion fuel manufacturing technology has been developed to complement our Al-U_3Si capability at Chalk River. Three prototype NRU rods containing Al-64 wt% U_3Si_2 fuel have been successfully irradiated to 87 at% burnup without incident in NRU, to qualify the fuel and the manufacturing process.

The irradiation behaviour of the three Al-64 wt% U_3Si_2 fuel rods in NRU was satisfactory to burnups of 87 at%. The basic fuel behaviour was similar to that of Al-61 wt% U_3Si irradiated under comparable conditions in NRU; however, diametral increases and the associated fuel swelling were lower. Oxides 50-80 μm thick were observed on the 0.76 mm thick cladding, but this posed no threat to the cladding integrity. It was not determined whether the thick oxide formed due to interim exposure to low-purity water during the approximately one-year interruption of the irradiation.

The Al-64 wt% U_3Si_2 fuel is suitable for use in the NRU reactor, and in other research reactors whose operating conditions are bounded by those tested in NRU.

ACKNOWLEDGEMENTS

The authors would like to thank D. Grice and M. Atfield for reactor physics support, D. Leach and J. Kelm for assistance with the metallographic examinations, and A. Park for assistance with the oxide thickness assessments.

REFERENCES

1. J.C. Wood, M.T. Foo, L.C. Berthiaume, L.N. Herbert and J.D. Schaefer, "Advances in the Manufacturing and Irradiation of Reduced Enrichment Fuels For Canadian Research Reactors", Proceedings of the International Meeting on Reduced Enrichment for Research and Test Reactors, Tokai, Japan, JAERI-M-84-073, 1983 October.

2. J.C. Wood, M.T. Foo and L.C. Berthiaume, "Reduced Enrichment Fuel For Canadian Research Reactors - Fabrication and Performance", Proceedings of the International Meeting on Reduced Enrichment for Research and Test Reactors, ANL, Argonne, Illinois, 1984 October.

3. D.F. Sears, J.C. Wood, L.C. Berthiaume, L.N. Herbert and J.D. Schaefer, "Fabrication and Performance of Canadian Silicide Dispersion Fuel for Test Reactors", Proceedings of

the International Meeting on Reduced Enrichment for Research and Test Reactors, Petten, The Netherlands, 1985 October 14-16.

4. D.F. Sears, L.C. Berthiaume and L.N. Herbert, "Fabrication and Irradiation Testing of Reduced Enrichment Fuels for Canadian Research Reactors", Proceedings of the International Meeting on Reduced Enrichment for Research and Test Reactors, Gatlinburg, Tennessee, 1986 October.

5. J.L. Snelgrove, R.F. Domagala, G.L. Hofman, T.C. Weincek, G.L. Copeland, R.W. Hobbs and R.L. Seun, "The Use of U_3Si_2 Dispersions in Aluminum in Plate-Type Fuel Elements for Research and Test Reactors", Argonne National Laboratory (US) Report, ANL/RERTR/TM-11, 1987 October.

6. D.F. Sears, K.D. Vaillancourt, D.A. Leach, E.L. Plaice, E.J. McKee, R.R. Meadowcroft and W.S. Simmons, "Status of LEU Fuel Development and Irradiation Testing at Chalk River Laboratories", Presented at the International Meeting on Reduced Enrichment for Research and Test Reactors (RERTR), Newport, RI, USA, 1990 September 23-27.

7. D.F. Sears, "Development and Irradiation Testing of Al-U3Si2 Fuel at Chalk River Laboratories", Presented at the International Meeting on Reduced Enrichment for Research and Test Reactors (RERTR), Jakarta, Indonesia, 1991 November 4-7.

8. J.E. Draley, S. Mori and R.E. Loess, "The Corrosion of 1100 Aluminum in Oxygen Saturated Water at 70°C", J. Electrochem. Soc. 110, 6 (1963 June).

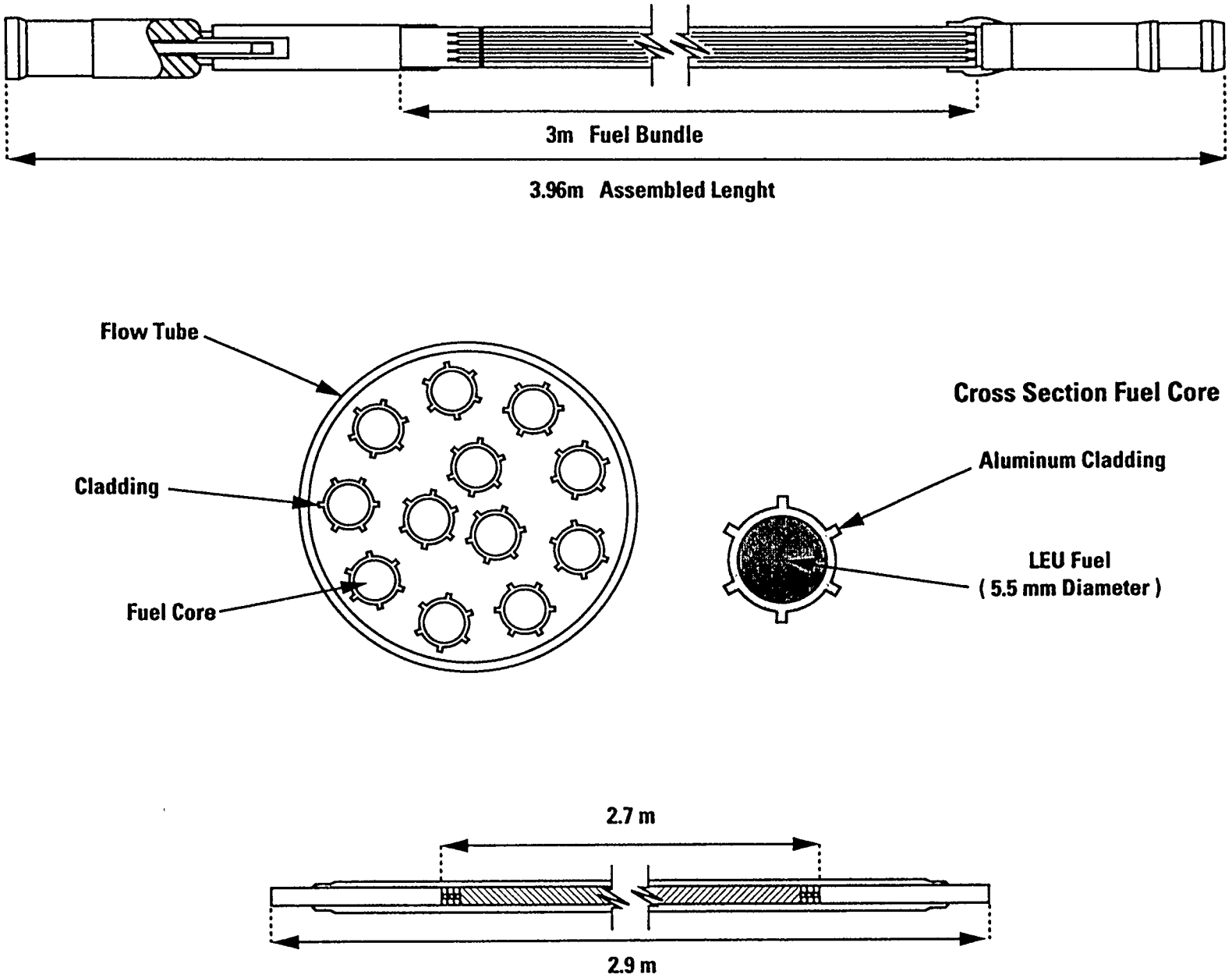

Figure 1. Schematic Diagram of NRU Fuel Rod

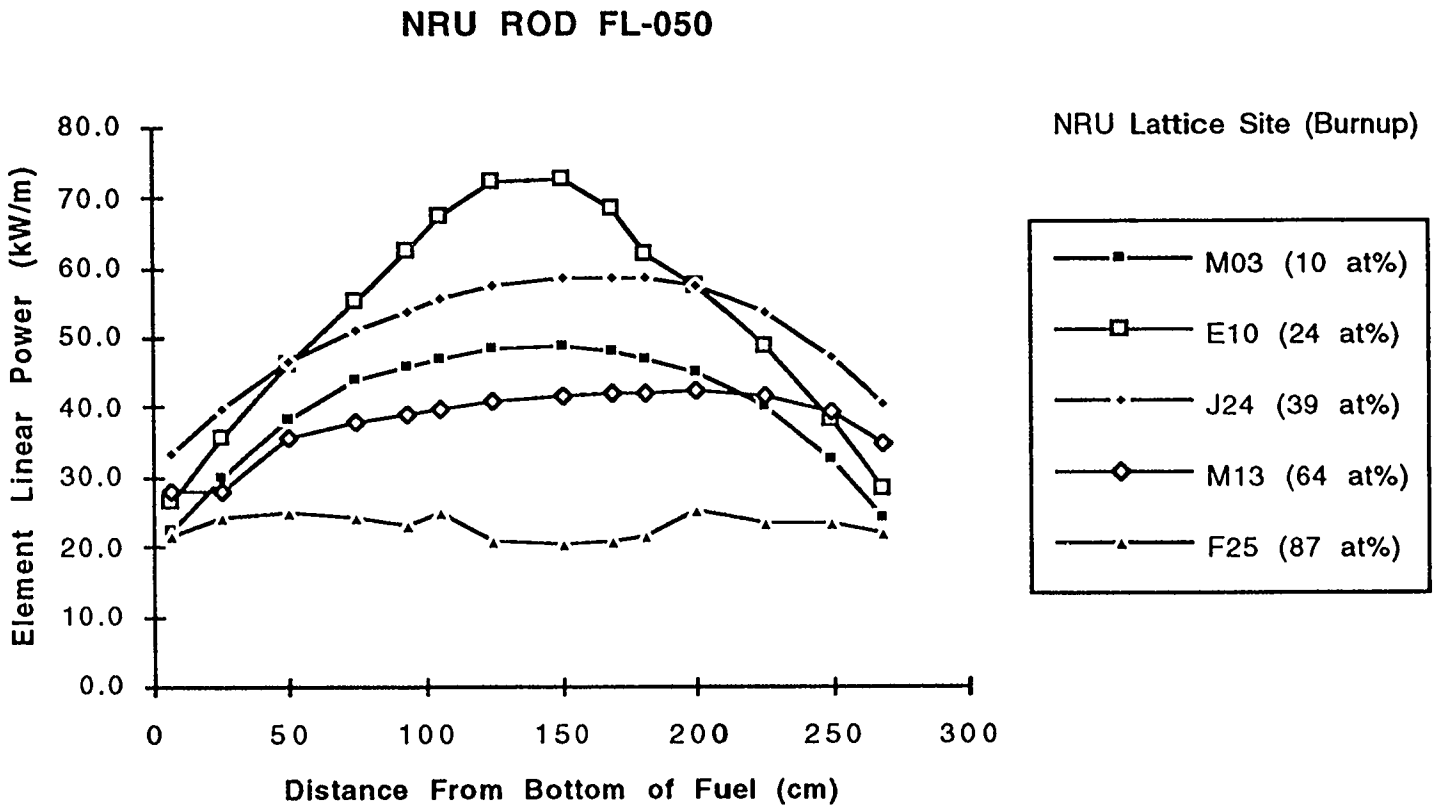

Figure 2. Power History of FL-050 Showing Variation of Element Axial Power Profile with Burnup During Irradiation in NRU Lattice Sites.

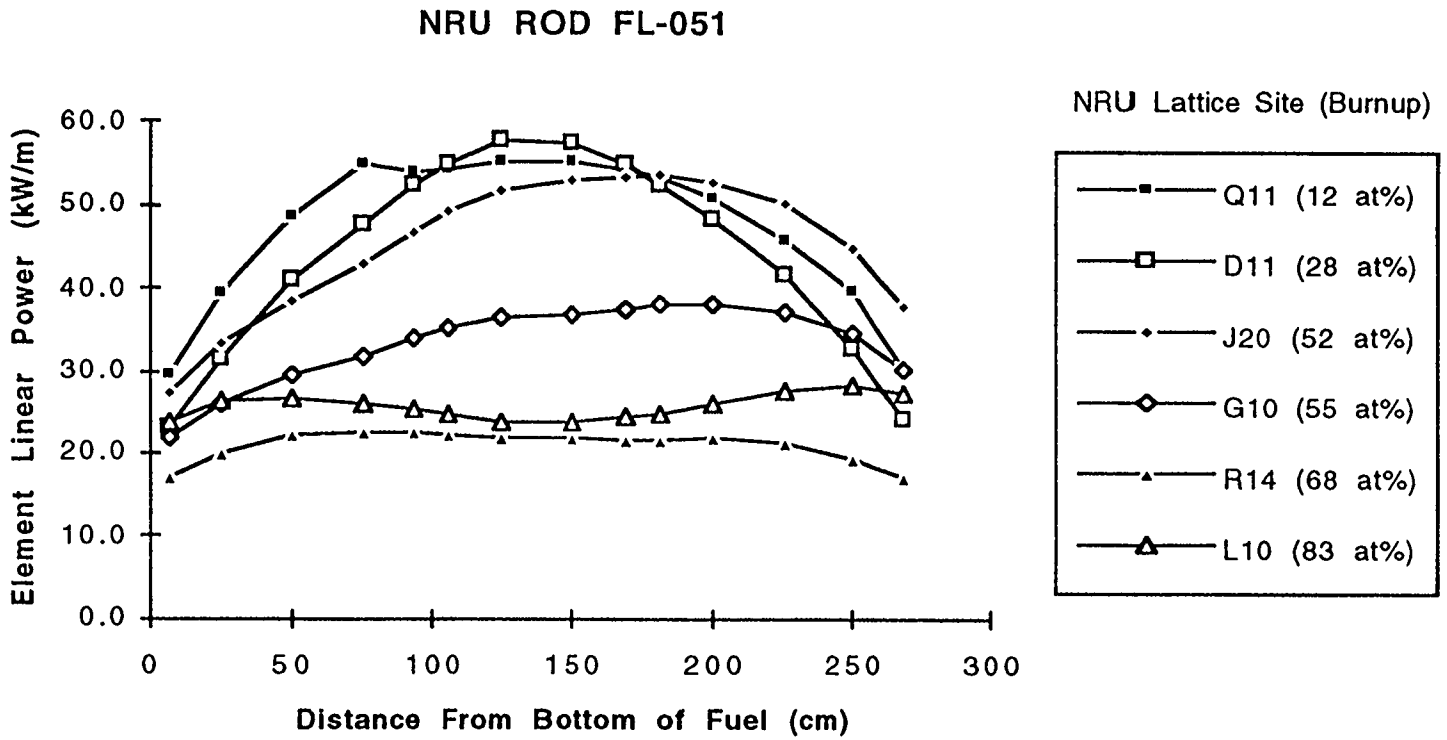

Figure 3. Power History of FL-051 Showing Variation of Element Axial Power Profile with Burnup During Irradiation in NRU Lattice Sites.

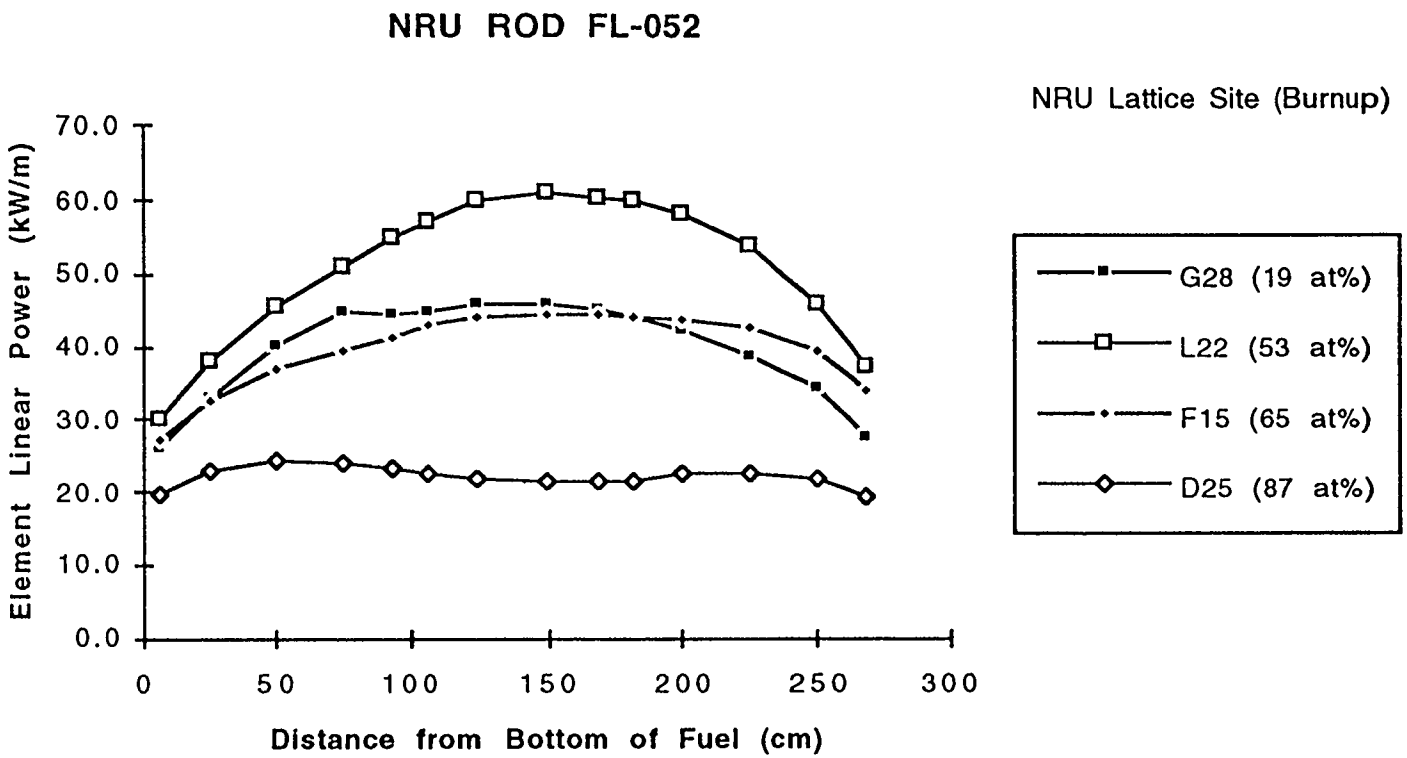

Figure 4. Power History of FL-052 Showing Variation of Element Axial Power Profile with Burnup During Irradiation in NRU Lattice Sites.

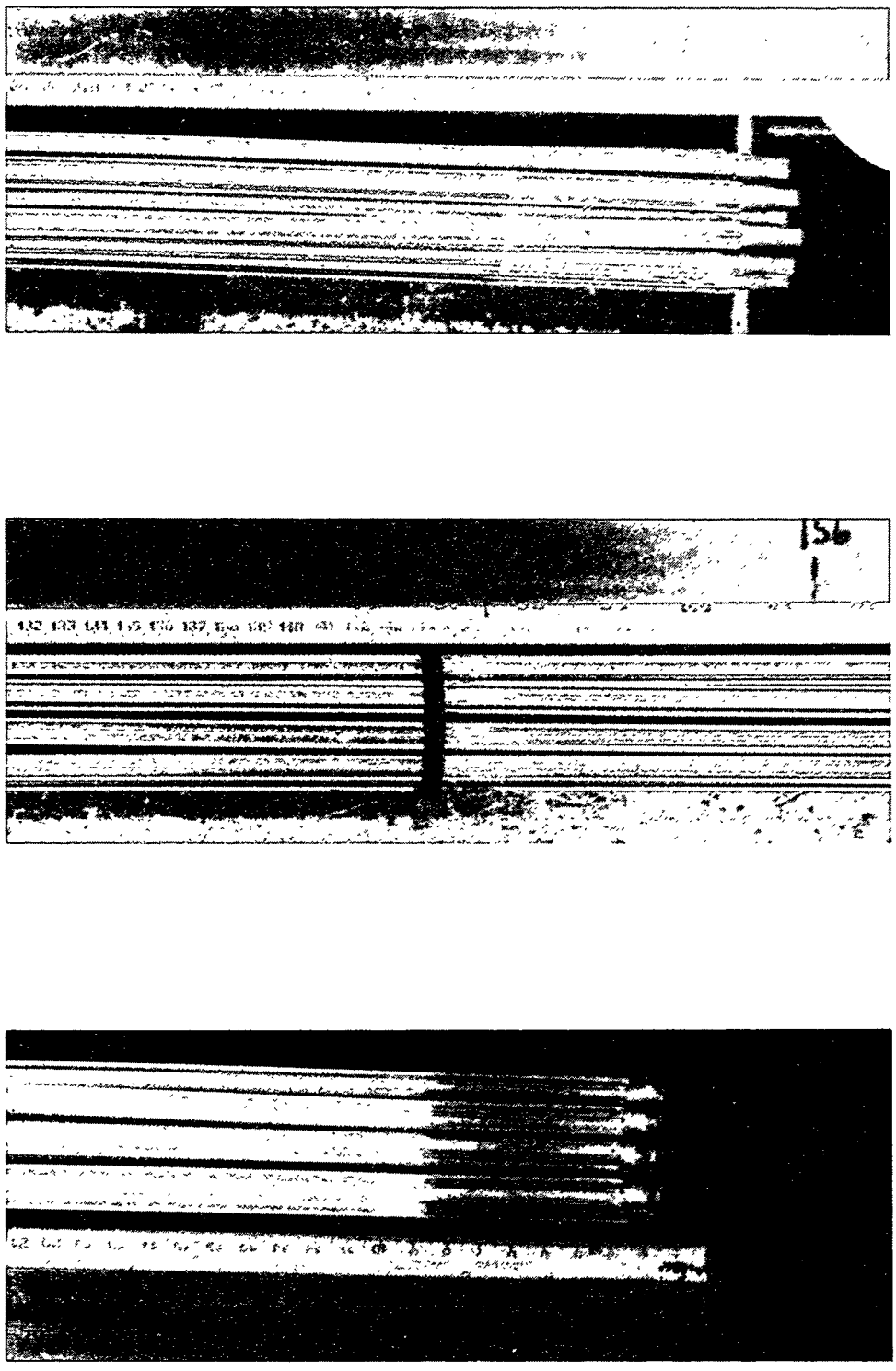

Figure 5 Photograph of Top, Middle and Bottom of Al-64 wt% U_3Si_2 Fuel Rod FL-052 in NRU Bay. Note Difference in Oxide Over Fuel and End Plugs.

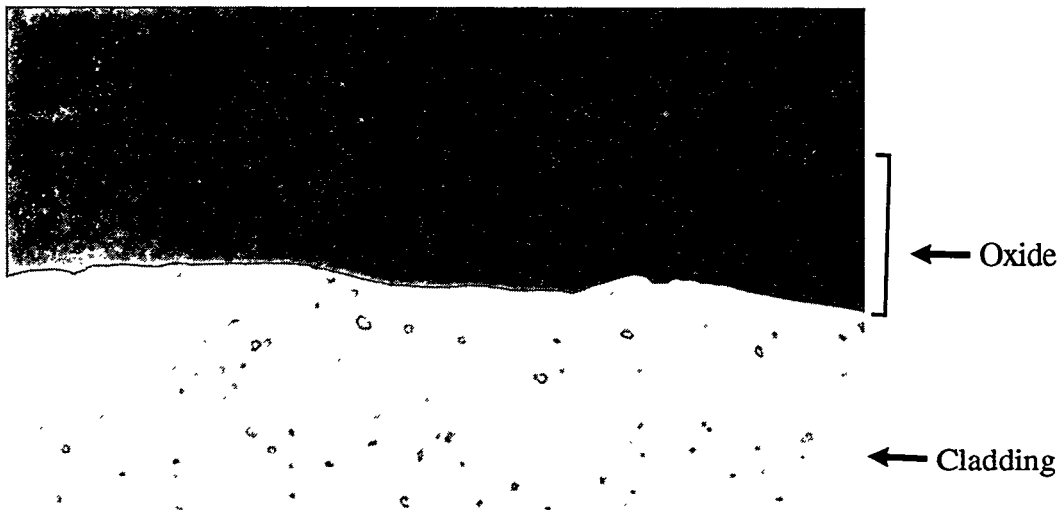

GG15L8 (a) 1000X

GG15P9 (b) 1000X

Figure 6. Micrographs Showing (a) Intact Oxides on FL-051, and (b) Radial and Circumferential Cracks in Oxide on FL-052.

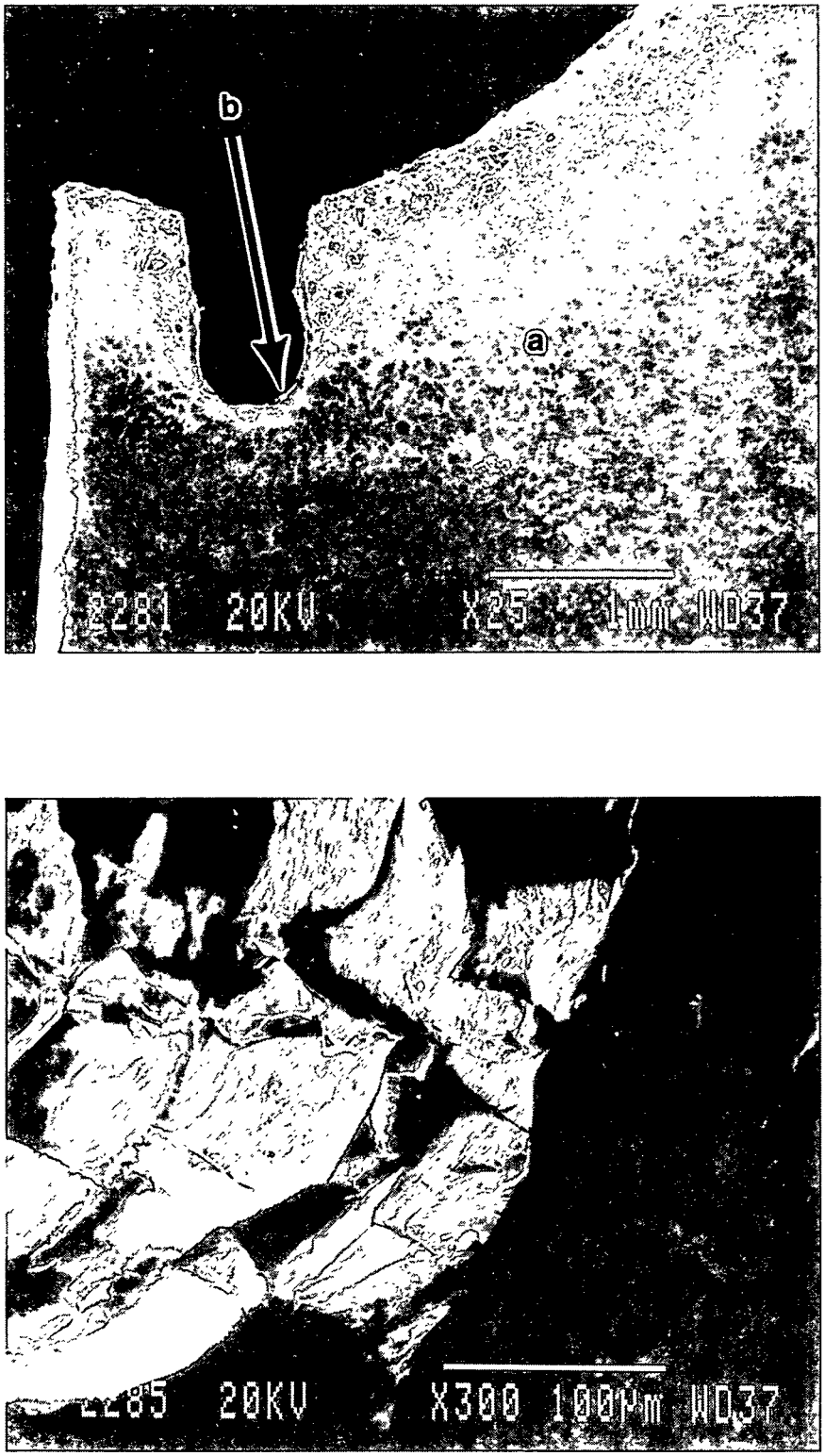

Figure 7. SEM Micrographs Showing (Top) Mount Material (a) with Oxide Layer (b) Adhering to Surface where Fuel Sample was Extracted and (Bottom) Higher Magnification Image of Oxide that Adhered to the Mount Material . WDX Analysis Showed Only Al Present.

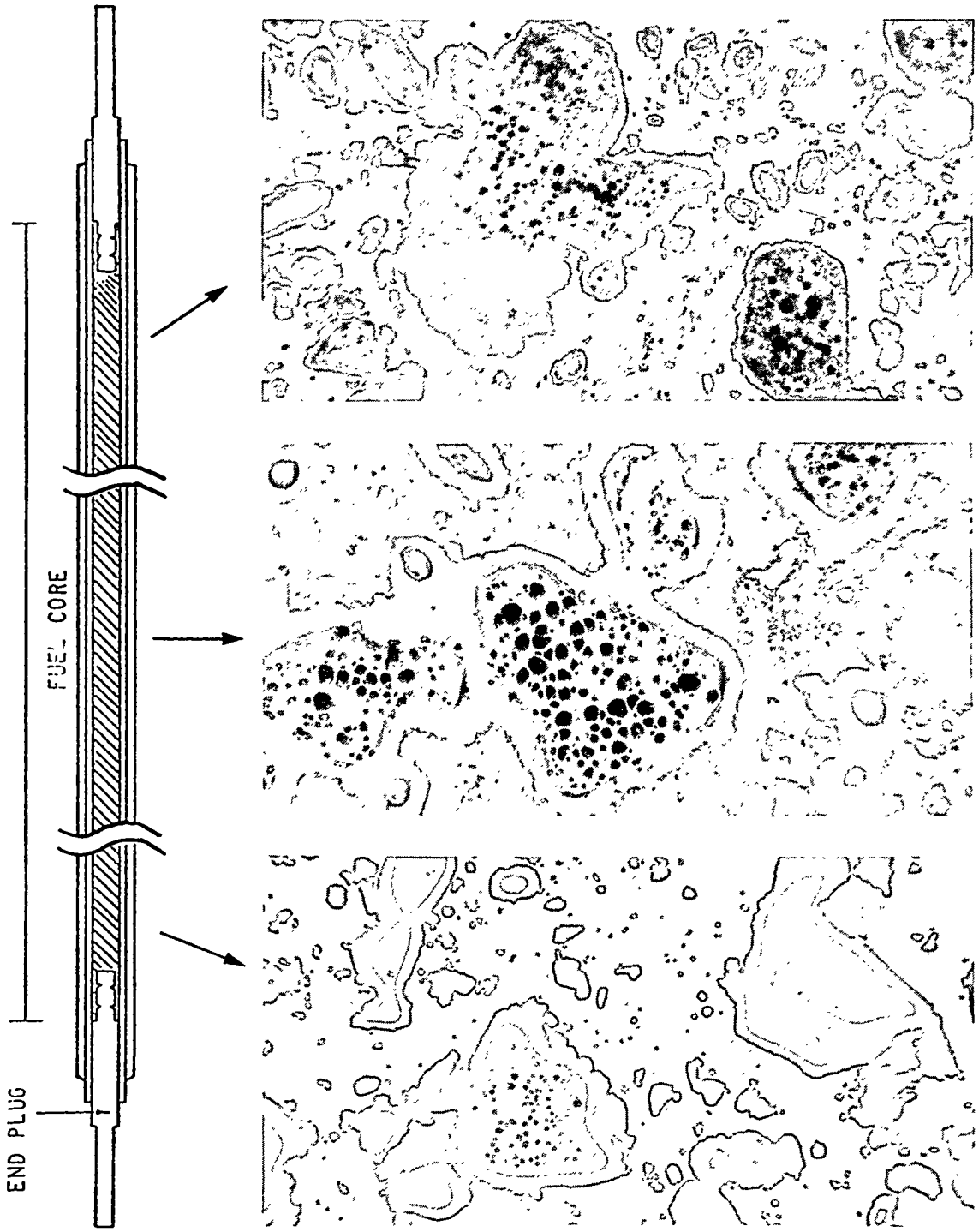

Figure 8. Typical Microstructure at Top, Middle and Bottom of Element from LEU Fuel Rod FL-050 After Irradiation to 87 at% Burnup in NRU. Al-64 wt% U_3Si_2 Fuel (3.15 gU/cm^3). Aluminum matrix (white), uranium aluminide interfacial layer (light grey), uranium silicide particle (dark grey) and fission gas bubbles (black).

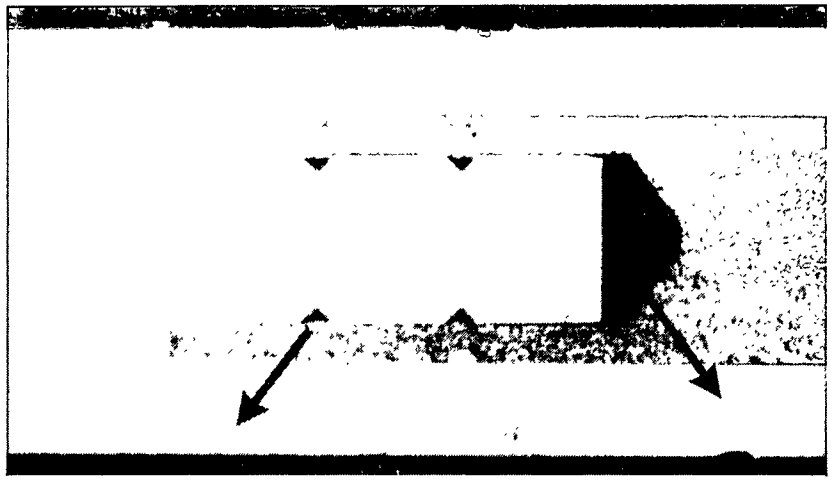

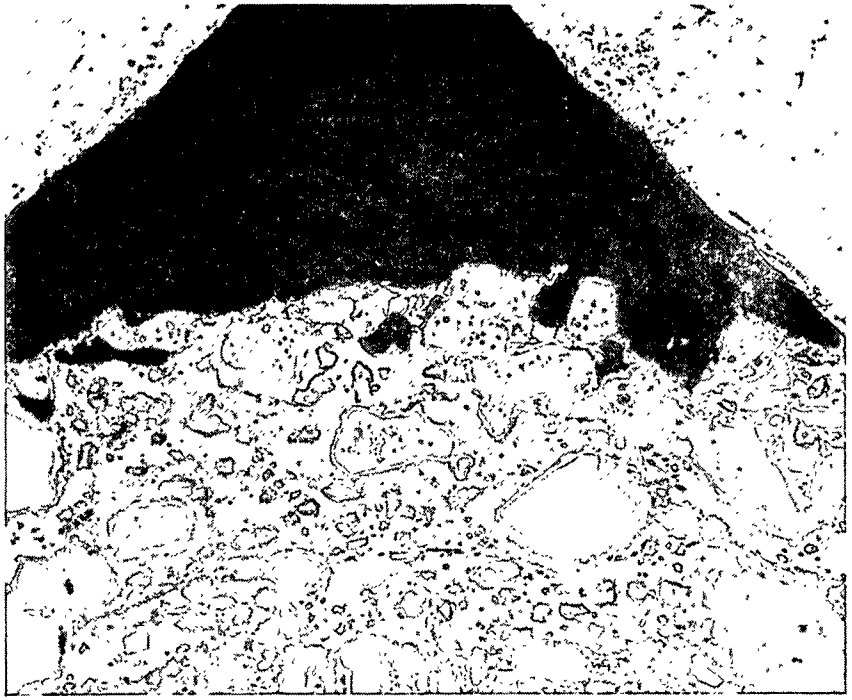

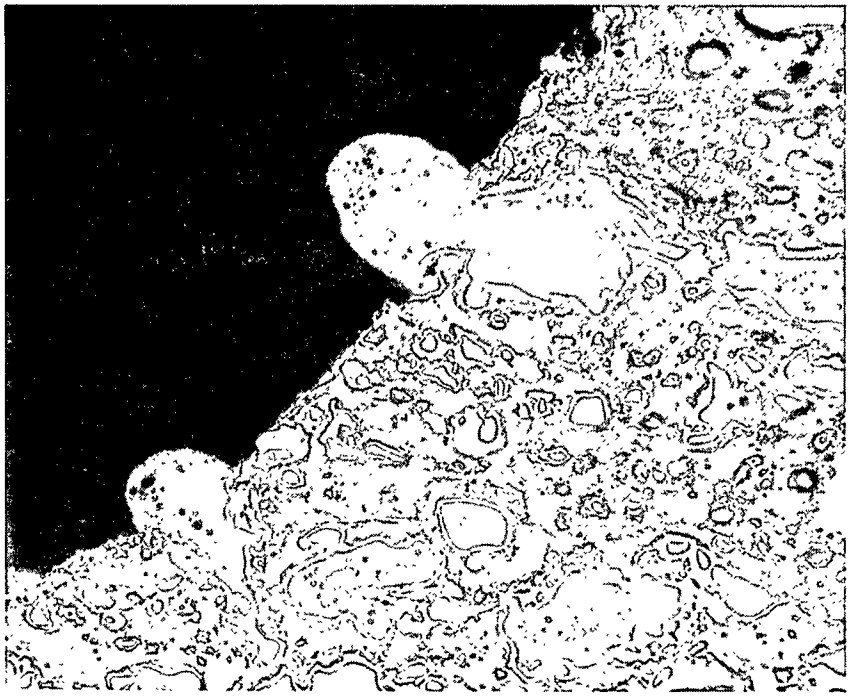

GG15A10 200 X

GG15A13 200X

Figure 9 Microstructure of Al-64 wt% U_3Si_2 Fuel at End-Plug Rolled Joint. U_3Si_2 Particles at Surface of Cavities Swell Under Fission-Gas Pressure and Flow into Void.

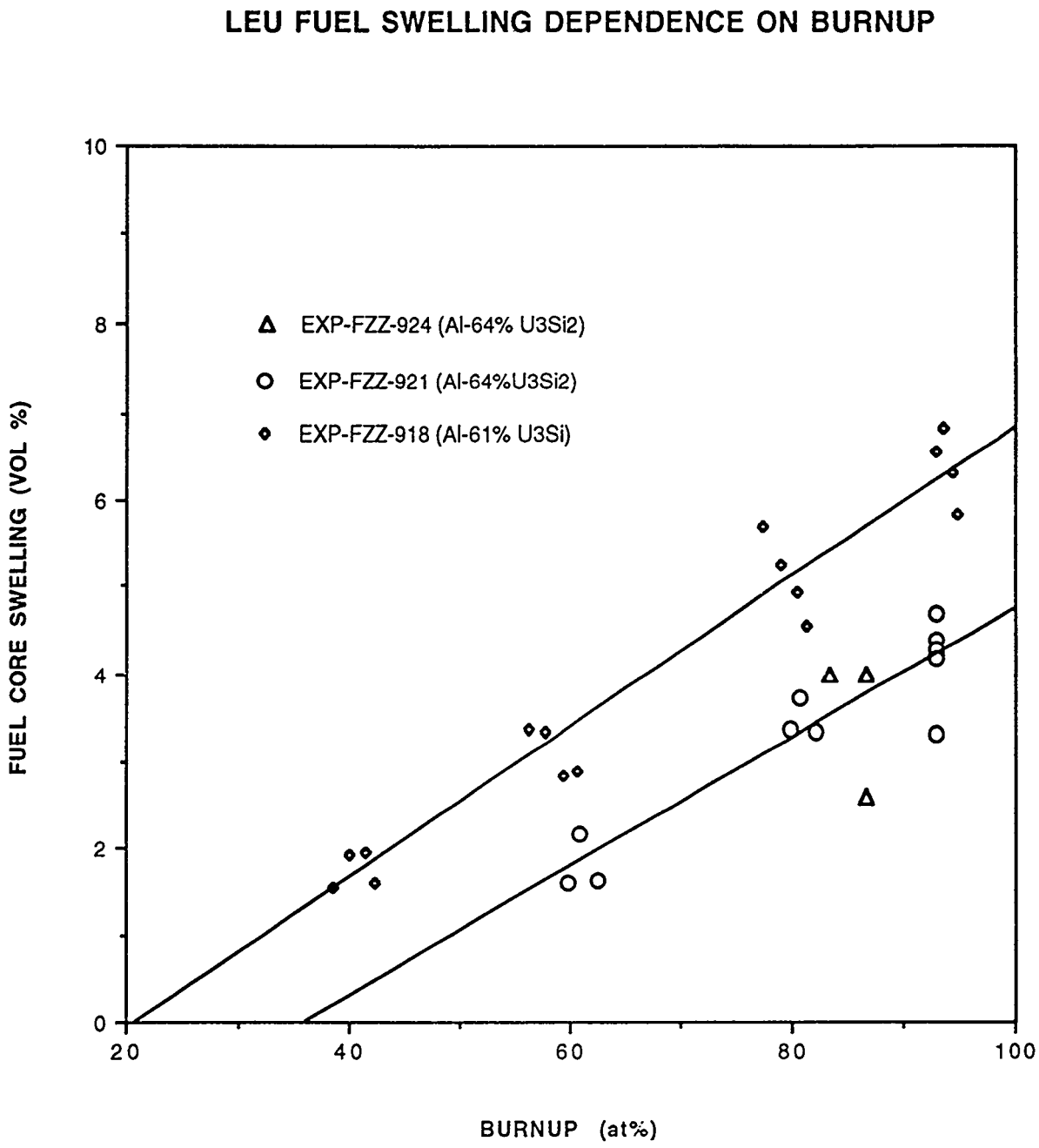

Figure 10. Swelling Dependence on Burnup of LEU Fuels Irradiated in NRU. Full-Length Elements from Exp-FZZ-924 Contained Al-64 wt% U_3Si_2 (U-7.4Si). Mini-Elements from Exp-FZZ-921 Contained Al-64 wt% U_3Si_2 (U-7.0Si). Mini-Elements from Exp-FZZ-918 Contained Al-61 wt% U_3Si (U-3.9Si).

COMPARISON OF IRRADIATION BEHAVIOR OF DIFFERENT URANIUM SILICIDE DISPERSION FUEL ELEMENT DESIGNS

G. L. Hofman, J. Rest,
and J. L. Snelgrove
Argonne National Laboratory
Argonne, Illinois USA

ABSTRACT

Calculations of fuel swelling of U_3SiAl-Al and U_3Si_2 were performed for various dispersion fuel element designs. Breakaway swelling criteria in the form of critical fuel volume fractions were derived with data obtained from U_3SiAl-Al plate irradiations. The results of the analysis show that rod-type elements remain well below the pillowing threshold. However, tubular fuel elements, which behave essentially like plates, will likely develop pillows or blisters at around 90% ^{235}U burnup. The U_3Si_2-Al compounds demonstrate stable swelling behavior throughout the entire burnup range for all fuel element designs.

INTRODUCTION

Uranium silicides have been widely considered as a low-enriched dispersion fuel because of their relatively high density (15.2 g cm^{-3} for U_3Si and 12.2 g cm^{-3} for U_3Si_2). A variation of U_3Si containing from 1 to 2% aluminum, which we call U_3SiAl, has been favored by certain fuel developers because of superior corrosion resistance in water. This aluminum-containing compound is somewhat less dense (14.2 g cm^{-3}) than the pure binary compound.

Irradiation experiments have shown that U_3Si and U_3SiAl are prone to excessive swelling (breakaway swelling) that commences at cumulative fission densities of about 5.5 x 10^{27} fissions m^{-3} and at about 4.5 x 10^{27} fissions m^{-3}, respectively. U_3Si_2 on the other hand has consistently shown very stable swelling behavior[1].

Breakaway swelling leads to blistering or pillowing of fuel elements and therefore appears to render compounds afflicted with this property unsuitable for high-fission-density (high-^{235}U-burnup) applications. However, because breakaway swelling is associated with fission-induced high plasticity of the fuel, it is susceptible to external restraint. The magnitude of mechanical restraint imposed on swelling fuel particles in a dispersion fuel element depends on the fuel element design, i.e., on the amount of matrix aluminum surrounding the fuel particles and on the shape of the element, be it a flat, thin plate, a cylindrical tube, or a solid rod.

This paper examines the swelling behavior of these silicide compounds in various research reactor fuel element designs.

FUEL SWELLING

The swelling data presented here were obtained in experimental irradiations as part of the Reduced Enrichment Research and Test Reactor (RERTR) program. The majority of the data came from so-called "miniplates" that have nominal dimensions of 115 x 50 x 1.3 mm and are fabricated by hot rolling. The fuel core or meat is typically 33-40% of the plate thickness and contains up to 50 vol.% of the fuel particles, up to 20 vol.% voids, and a balance of pure Al powder. The cladding may be made of various Al alloys. These experimental plates were fabricated by NUKEM (Germany), CNEA (Argentina), and ANL (USA).

A separate group of experiments consisted of hot extruded rods of 7-mm diameter with a core of 5.5-mm diameter containing up to 29 vol.% of fuel particles and a small fraction, ~2 vol.%, of voids. These rod-type elements were made and tested by AECL-Chalk River[2]. Finally, recent Russian data from irradiation experiments with extruded tubular fuel elements that contain 34 vol.% U_3SiAl and 3% voids[3] are used in this study.

Fuel core swelling is determined by measuring the volume change of the miniplate or rod after irradiation using the Archimedean immersion method and by subtraction of the cladding volume. The fuel particle swelling $\frac{\Delta V^F}{V_0^F}$ is calculated from the core volume changes $\frac{\Delta V^C}{V_0^C}$ as follows:

$$\frac{\Delta V^F}{V_0^F} = \left[\frac{\Delta V^C}{V_0^C} - \frac{V_0^P - V^P}{V_0^C}\right]\frac{V_0^C}{V_0^F}$$

where ΔV^C is the change in core volume during irradiation, V^P is the amount of as-fabricated porosity remaining in the core after irradiation, and $\frac{V_0^F}{V_0^C}$ is the as-fabricated fuel volume fraction in the core.

Experimental data for both U_3SiAl and U_3Si are shown in Fig. 1. The different swelling behavior of the two compounds and the effect of as-fabricated fuel volume fraction on eventual plate failure by pillowing are apparent.

The particular swelling behavior of the two compounds is due to a somewhat different fission gas bubble development. The bubbles in U_3SiAl are generally larger than those in U_3Si. The bubbles in U_3SiAl eventually interlink across fuel particles, leading to the development of large cavities, enormous (breakaway) swelling, and pillowing of the fuel plate (see Fig. 2). Breakaway swelling and pillowing also occurs in U_3Si at larger as-fabricated fuel loadings, but always at higher fission densities or burnups than in U_3SiAl because of the higher swelling rate of U_3SiAl.

The appearance of the interlinked bubbles suggests a very plastic, viscous behavior of the fuel during irradiation. This behavior has been ascribed to fission-induced amorphization (mictametization) of U_3Si and U_3SiAl.[4]

The effect of fuel loading on breakaway swelling and pillowing is due to the fact that at higher as-fabricated fuel volume fractions the swelling particles contact each other at lower fission density, giving rise to earlier translinkage of gas bubbles.

Since the fuel is evidently very plastic, it should be sensitive to external mechanical restraint. This is clearly demonstrated by the swelling data from rod-type elements, where the swelling fuel particles are under relatively high hydrostatic compression provided by the relatively thick cylindrical cladding.

Swelling of the U_3Si_2 is fundamentally different from that of U_3Si. Fission gas bubbles in the visible range (by SEM) form after a fission density of approximately 3.5 x 10^{27} cm^{-3} causing an increase in swelling rate. The fission gas bubbles, however, remain relatively small and do not interconnect as in the case in U_3Si. The result is the absence of break-away swelling, and of pillowing in highly-loaded dispersion, even at complete ^{235}U burnup. Because of the small bubble size, the affect of external restraint on swelling should be less pronounced in U_3Si_2 than in U_3Si.

IRRADIATION BEHAVIOR MODELING

Our dispersion fuel behavior code DART[4] was used to model the fuel swelling for three different fuel element designs. Modifications to the DART mechanical model were implemented in order to include the constraining effects of the cladding in plate, tube, and rod configurations. The DART mechanical (stress) model consists of a fuel sphere which deforms due to both solid fission product and fission gas-bubble swelling. The fuel sphere is surrounded by an Al matrix shell, which is assumed to behave in a perfectly plastic manner and which deforms (yields) due to fuel particle volume expansion. The effects of the cladding are included by a suitable adjustment of the effective Al volume fraction. Currently, the effects of creep are not included; instead, the stress relaxation is approximated by lowering the Al yield stress to an "effective" value. The deformation of the matrix and cladding material generates stresses within the expanding fuel particles which affect the swelling rate of the fission gas bubbles. Subsequent to the closure of the as-fabricated porosity, the swelling rate is primarily dependent on the plastic yielding of the Al matrix and cladding. At this point, the hydrostatic stress, σ, acting on the gas bubbles is given by

$$\sigma = \frac{2}{3}\left(1 - \ln\left(\frac{V^F \times \Delta V^F}{V_0^C}\right)\right)\beta\sigma_{Al}^Y(T)$$

where $\sigma_{Al}^Y(T)$ is the as-fabricated temperature-dependent yield strength of the Al, and β is a factor which accounts for the effects of irradiation (e.g., irradiation-enhanced creep).

U_3Si, U_3SiAl Fuel

The effective yield stress of irradiated Al matrix material and cladding (i.e., the value of β in the above equation was determined by comparing the results of DART calculations with postirradiation immersion volume measurement of U_3SiAl plates (shown in Fig. 1). This value of the yield stress was then used in all subsequent simulations. Results of the DART calculations are shown in Fig. 3. The lower calculated fuel swelling in the rod-type element is due an assumed biaxial stress state as compared to an assumed uniaxial stress state for the plate and thin-walled tube geometries. Elastic analysis and comparison of plate and tube swelling data[3] support the assumptions. Thermal stress analysis[5] of a thin-walled hollow cylinder shows that the circumferential and axial stresses at the inner surface are only half as great as those in a cylinder with a small bore for the same temperature difference. In addition, the thin-walled hollow cylinder can be treated as a cylindrical shell which can be shown to have a complimentary solution to that obtained for a rectangular beam on an elastic foundation. Fuel swelling in plates results in plate thickness increase only, while plate width and length remain relatively unchanged. Likewise, in tubes, only the wall thickness increases and the overall diameter remains unchanged. There is thus minimal lateral or circumferential strain in the cladding of these element designs and consequently much less restraint compared to the hoop stress state existing in a solid-clad rod.

Results from postirradiation immersion volume measurements at a peak ^{235}U burnup of 70%[3], and a quantitative determination of the fission gas bubble volume fraction obtained by image analysis of fuel meat metallographs compare well with the calculated fuel swelling of the tubular fuel element as shown in Fig. 3. These results are also supported by comparison of calculated bubble-size distributions with the observed bubble morphology in the plate and rod configurations.

Breakaway swelling criteria in the form of critical fuel volume fractions were derived from data obtained from the U_3SiAl plate irradiations. As shown in Fig. 1, all U_3SiAl plates exhibit breakaway swelling and experience pillowing. A pillowing threshold was derived based on the observed effect of loading on pillowing, shown in Fig. 4. When a critical fuel volume fraction in the core is reached, translinkage of gas bubbles becomes prevalent, resulting in large cavity formation, breakaway swelling and pillowing. This situation is shown in Fig. 1 for plates and for the rod- and tube-type fuel elements modeled. Clearly the rod-type element remains well below the pillowing threshold up to complete ^{235}U burnup. However, the tubular fuel element, since it behaves essentially like a plate, will likely develop pillows or blisters at around 90% ^{235}U burnup.

U_3Si_2 Fuel

Figure 5 shows DART-calculated results for fuel-particle swelling of low-enriched (LEU) U_3Si_2-Al fuel plates as a function of fission density for two values of the Al-matrix yield strength (i.e., two values of β), and for U_3Si_2-Al rods for two values of the fission density at which recrystallization is predicted to occur. The calculations shown in Fig. 5 were made in the spirit of the theory presented in references 4 and 6 of irradiation-induced recrystallization in U_3Si_2 and UO_2 fuels. After recrystallization occurs, the gas-atom diffusion to the grain boundaries, bubble nucleation, and accelerated growth (relative to that of bubbles in the bulk material) result in an increased swelling rate, as shown in Fig. 5. The calculations shown in Fig. 5 were made for a homogeneous fuel at a constant temperature. In reality, time-dependent temperature and flux gradients exist across the plate and rod during irradiation. The two curves for the U_3Si_2-Al rod show the effect of such a gradient on the calculated results.

CONCLUSIONS

Irradiation experiments have shown that plate-type dispersion fuel elements can develop blisters or pillows at high ^{235}U burnup when fuel compounds exhibiting breakaway swelling such as U_3SiAl and U_3Si, are used at moderate to high volume fractions. Calculations indicate that tubular fuel elements behave similarly. Rod-type fuel elements, however, are inherently more resistant to pillowing. With a stable swelling compound, such as U_3Si[2], blistering or pillowing is entirely eliminated.

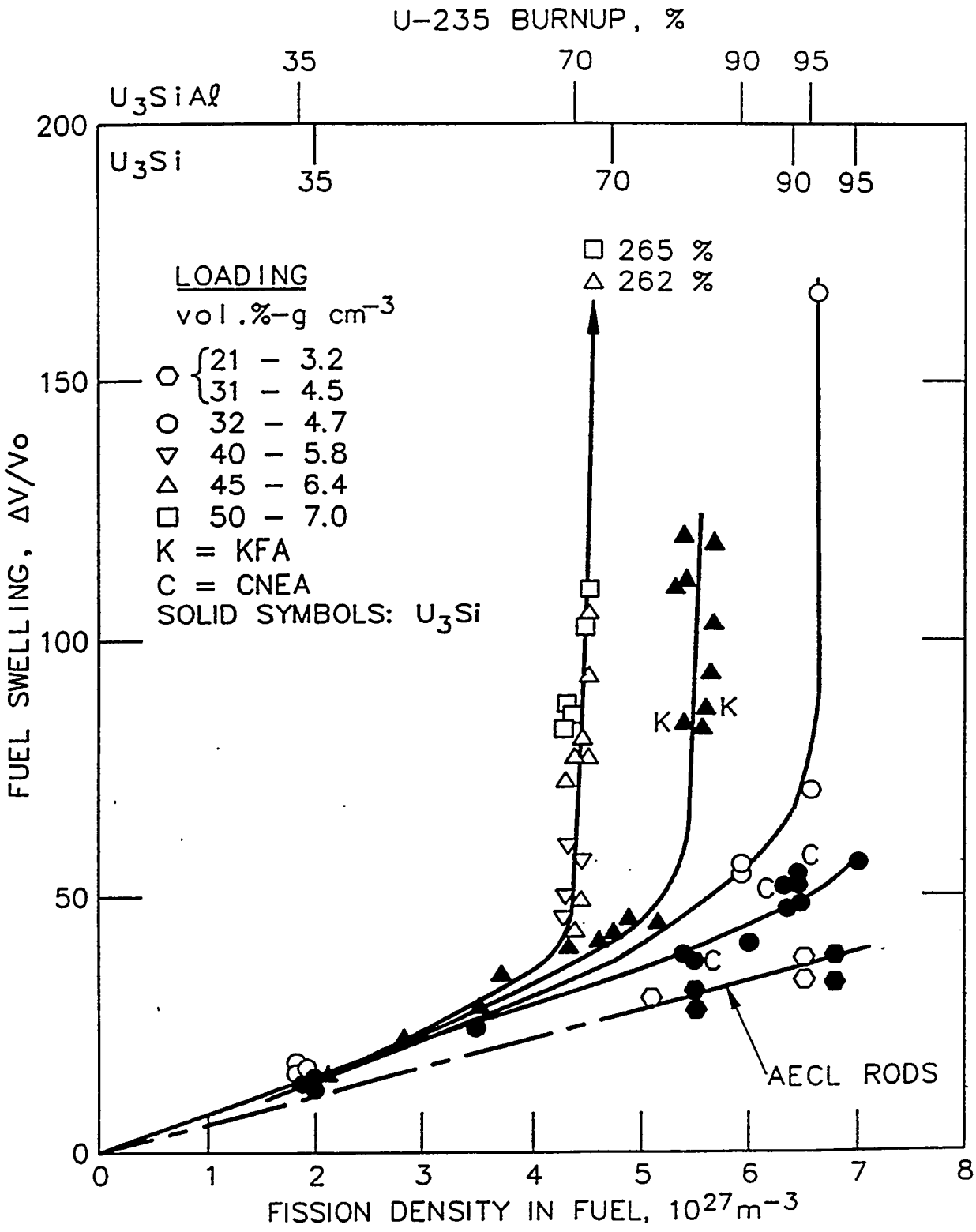

Figure 1. **Fuel Particle Swelling in Experimental U_3Si and U_3SiAl Dispersion Fuel Plates and Rods**

Figure 2. Metallographic Cross-section of High Burnup LEU, U_3Si Dispersion Fuel Plate Showing Breakaway Swelling

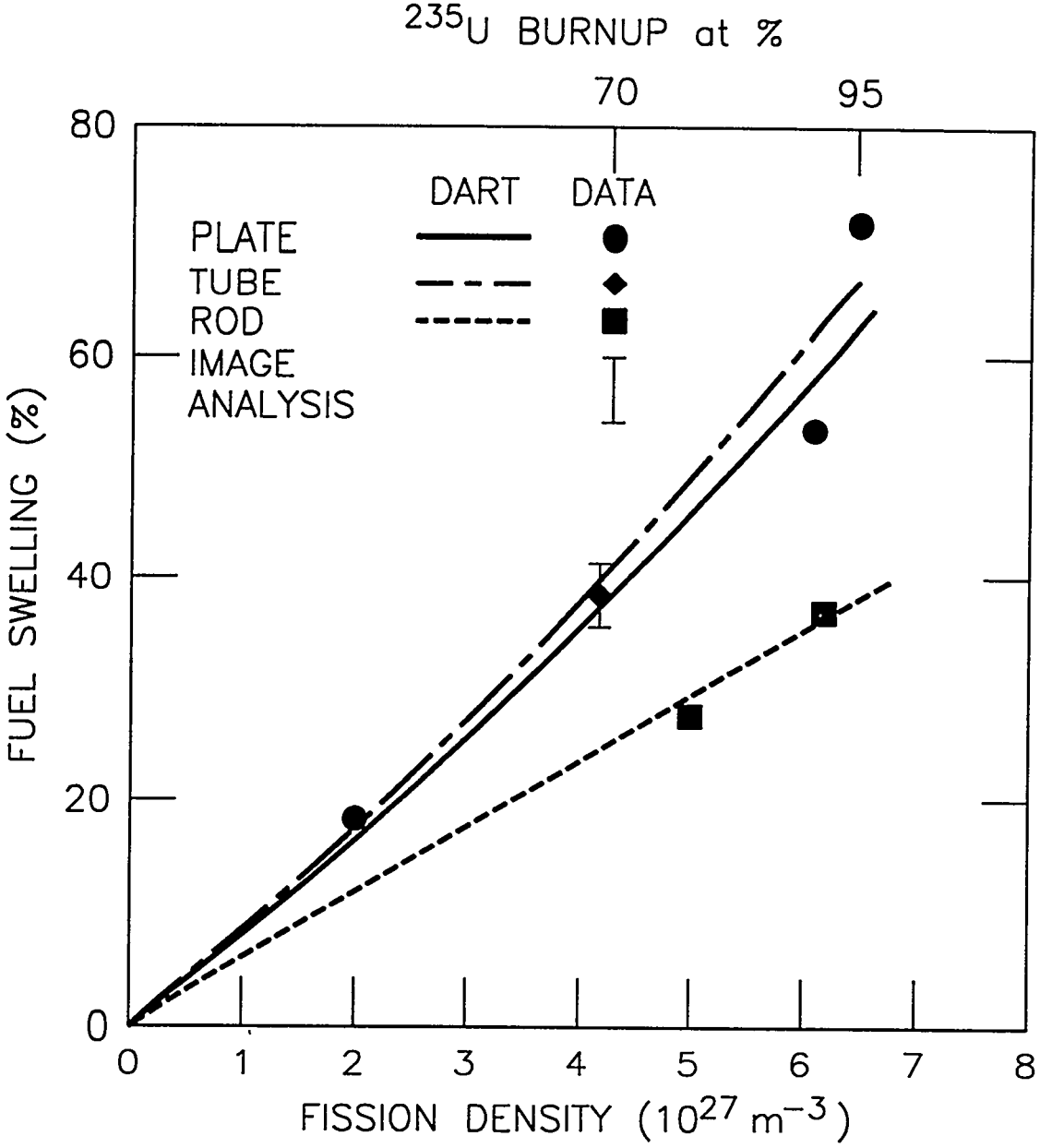

Figure 3. **DART-Calculated Fuel Swelling for U_3SiAl-Al as a Function of Fission Density for Different Fuel Element Designs Compared with Data**

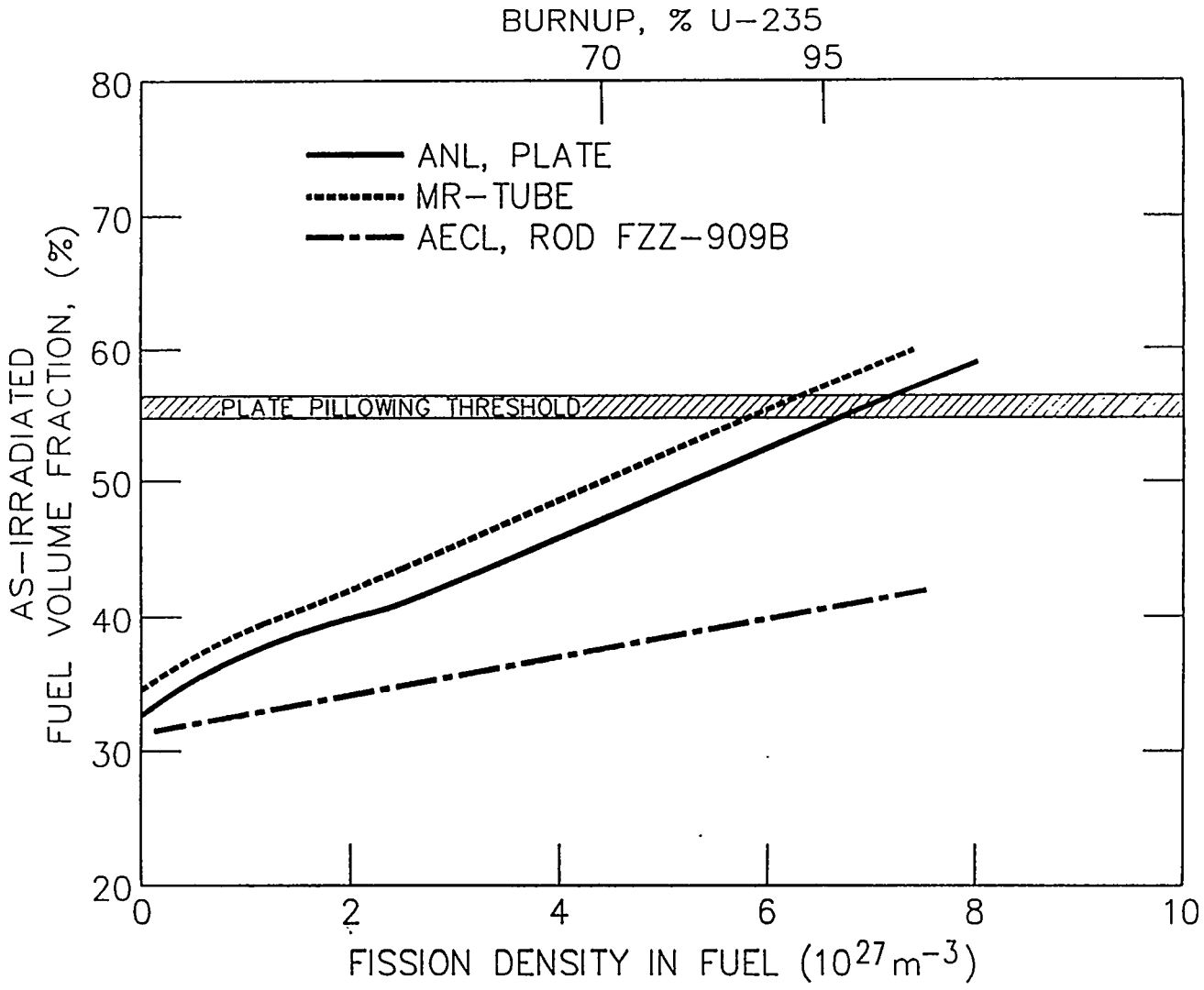

Figure 4. **DART Calculation of U_3SiAl Volume Fraction in Meat of Rod, Tube, and Plate Dispersion Fuel Elements and Pillowing Threshold Derived from Plate Irradiation Experiment**

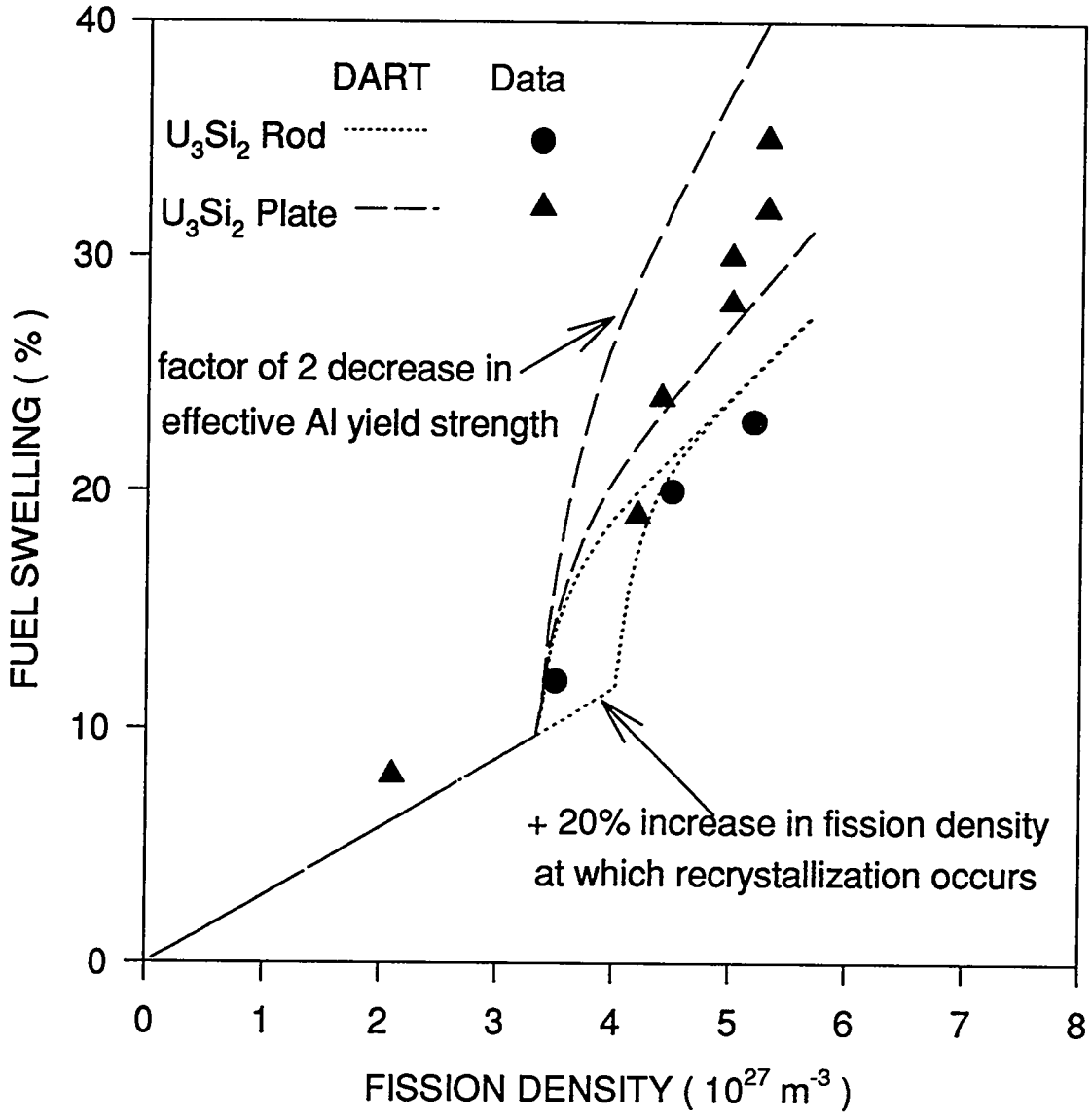

Figure 5. **DART-Calculated Fuel Swelling for U_3Si_2-Al as a Function of Fission Density for Rod and Plate-type Geometries Compared with Data**

REFERENCES

1. G. L. Hofman, "Crystal Structure Stability and Fission Gas Swelling in Intermetallic Uranium Compounds," Journal of Nuclear Materials, Vol 140, pp 256-263 (1986).

2. D. F. Sears, "The Development and Irradiation Testing of Al-U_3Si_2 fuel at Chalk River," Proceedings of the 14th International Meeting on Reduced Enrichment for Research and Test Reactors, Jakarta, Indonesia, November 4-7, 1991,(to be published).

3. G. A. Sarakhova, Y. A. Stetsky, V. D. Zaboikin, and V. B. Suprun, "Development of Fuel Elements for Russian Research Reactors with Fuel of Lower Enrichment," Proceedings of the 16th International Meeting on Reduced Enrichment for Research and Test Reactors, Oarai, Japan, October 4-7, 1993, JAERI-M-94-042 (1994).

4. J. Rest and G. L. Hofman, "Fundamental Aspects of Inert Gasses in Solids," S. E. Donnelly and J. H. Evans, Plenum Press, 443 (1991).

5. Z. Zulows, T. C. Yen, and W. H. Steiselmann, Thermal Stress Techniques in the Nuclear Industry, Chap. 3, American Elsevien Publishing Company, Inc., New York (1965).

6. J. Rest and J. L. Hofman, "Dynamics of Irradiation-induced Grain Subdivision and Swelling in U_3Si_2 and UO_2 Fuels," Journal of Nuclear Materials, pp. 187-202 (1994).

Comparison of Thermal Compatibility between Atomized and Comminuted U_3Si Dispersion Fuels

Woo-Seog Ryu, Jong-Man Park, Chang-Kyu Kim, Il-Hyun Kuk

Korea Atomic Energy Research Institute
P.O. Box 105, Yu-sung, Taejon, 305-600, Korea

ABSTRACT

Thermal compatibility of atomized U_3Si dispersion fuels were evaluated up to 2600 hours in the temperature range from 250 to 500 °C, and compared with that of comminuted U_3Si. Atomized U_3Si showed better performance in terms of volume expansion of fuel meats. The reaction zone of U_3Si and Al occurred along the grain boundaries and deformation bands in U_3Si particles. Pores around fuel particles appeared at high temperature or after long-term annealing tests to remain diffusion paths over the trench of the pores. The constraint effects of cladding on fuel rod suppressed the fuel meat, and reduced the volume expansion.

INTRODUCTION

U_3Si dispersion fuels are composed of two different phases, U_3Si particles dispersed in Al matrix, so long term operation at high temperature occurs in the reaction between two phases. It is well known the reaction of

$$U_3Si + Al \dashrightarrow U(Si,Al)_3. \quad (1)$$

The reaction product of $U(Si,Al)_3$ is a less dense compound than U_3Si, so the difference of density produces the volume expansion of the U_3Si dispersion fuel meats. Al diffuses into U_3Si to react, and the diffusivity of Al in U_3Si is more rapid than the diffusivity of U in Al. This Kirkendall effect makes pores in the side of Al matrix, and the pores are known to be another cause of volume expansion of U_3Si dispersion fuel meats[1,2].

The volume expansion produced by thermal annealing is a reference for thermal stability of fuels, and acts as a factor of swelling performance. In this study, thermal compatibility of atomized U_3Si fuel meats was evaluated, and compared with comminuted U_3Si fuel meats. Effect of cladding of fuel rods on the volume expansion of fuel meat was analyzed in view of constraint stress. Microstructural examination of fuel particles after thermal annealing tests was also carried out to suggest a nature of thermal swelling.

EXPERIMENT

Atomized U_3Si powders were manufactured directly from the melt of U-3.9 wt.% Si using a rotating disk method[3], and fuel rods with and without clad were made using an extrusion technique of 61 wt% U_3Si powders dispersed in Al matrix. All specimens (fuel meat and clad fuel) were made to 25 mm length by cutting the fuel rods. The specimen was cleaned, dried, and vacuum-sealed in a quartz tube. To evaluate the thermal compatibility, volume expansion of fuel meats with and without clad was determined periodically from dimensional changes in diameter and length of fuel rods. The results were compared to the results from the density measurement technique whitin the error range of 3 %. Specimens in vacuum-sealed quartz ampoules were annealed in a furnace. Test temperature was in the range of 250 - 500°C, and test time was up to 2600 hours. Microstructures of the tested specimens were observed using a Scanning Electron Microscope.

RESULTS AND DISCUSSION

Volume Change

Swelling of fuel meats was calculated from dimensional changes in diameter and length, which were measured as a function of temperature and time. Table 1 records a typical result of volume changes of fuel meats with and without clad at 400 °C.

Table 1. Thermal Swelling data of Atomized and Comminuted U_3Si Dispersion fuels with and without clad at 400 ℃.

Time (hr)	Atomized						Comminuted					
	Fuel Meat(%)			Fuel Meat with Clad(%) ※			Fuel Meat(%)			Fuel Meat with clad(%) ※		
	△ℓ	△d	△V	△ℓ	△d	△V	△ℓ	△d	△V	△ℓ	△d	△V
10	0.12	0	0.12				0.16	0.3	0.6			
25	0.16	0.31	0.77				0.45	0.76	1.98			
77	0.3	0.9	2.1	0.51	0.61	1.74	1.2	1.5	4.3	1.78	0.92	3.65
149	0.7	1.5	3.8	0.79	0.61	2.02	2.0	2.4	7.0	4.36	1.07	6.60
221	0.8	1.8	4.5	1.02	0.61	2.26	2.5	3.2	9.1	4.77	1.68	8.32
298	0.96	1.98	5.0	1.15	0.76	2.70	2.9	3.7	10.6	5.04	1.83	8.92
443	1.61	3.05	7.9	1.86	1.68	5.31	3.4	3.97	11.8	5.42	2.90	11.62
661	2.2	3.8	10.1	2.17	1.98	6.27	4.02	4.73	14.1	6.14	3.05	12.72
802	2.5	4.3	11.5	2.41	2.29	7.16	4.56	5.50	16.37	6.52	3.82	14.80
946	2.8	4.7	12.8	2.53	2.60	7.92	4.79	5.65	16.97	6.74	4.58	16.74
1162	2.9	4.9	13.2	2.61	2.90	8.65	5.06	6.26	18.63	6.97	4.73	17.33
1350	3.0	5.0	13.7	2.77	3.36	9.79	5.41	6.56	19.7	7.35	4.89	18.09
2000	3.27	5.64	15.27	2.92	3.51	10.28	5.83	7.02	21.22	7.57	5.34	19.38

※ : the diameter change was obtained from fuel meat section in rod

Irrespective of the difference in U_3Si powder manufacturing process, changes in diameter of fuel meats are somewhat larger than changes in length. Volume changes of fuel meats show a general trend with time, i.e. increasing with time. Volume changes of fuel meats are affected by temperature. Figure 1 shows the dependency of temperature and time on the thermal swelling behaviors of the fuel meats. Volume of the fuel meat increased rapidly and saturated gradually with time. The higher the temperature, the larger the volume change. When compared with comminuted powder-fuel meats, atomized powder-fuel meats showed less volume changes at any test temperature, and their growth values corresponded to about 70% of those of comminuted powder-fuel meats at 350 or 400 °C. The volume changes of comminuted powder-fuel meats were in agreement with AECL's data[1]. At 400 °C, the growth values were about 15 and 21 % after 2000 hours for atomized and comminuted powder-fuel meats, respectively. Below 300 °C, volume of the fuel meat was changed very little with time, but grew gradually after a certain time, indicating that the volume change was a thermally activated process.

The volume expansion during thermal annealing is known to be caused by production of low density-compounds due to the chemical reaction between U_3Si and Al matrix[4]. The chemical reaction involves the diffusion process of Al in fuel

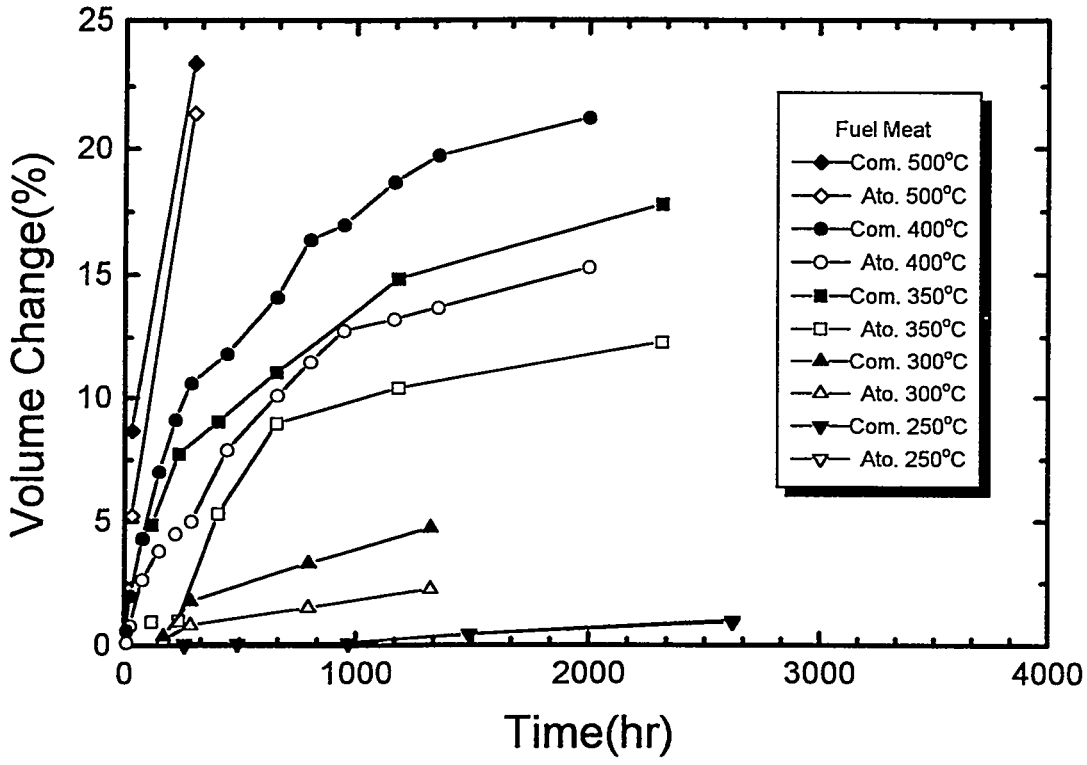

Figure 1. The dependency of temperature and time on the thermal swelling behavior of atomized and comminuted powder fuel meats.

particles. It is supposed that the smaller surface area of atomized powders in comparison to the comminuted powder is attributed to the reduction of volume change of the atomized powder-fuel meat in terms of diffusion.

Constraint Effects of Cladding

Fuel meats with cladding show a different type of dimensional changes as shown in table 1 and figure 2. Changes in length are not affected nearly by constraint effects of cladding, while the changes in diameter of fuel meats with cladding become much lower than those without cladding. Volume changes of both atomized and comminuted powder fuel meats with cladding are reduced, and correspond to 70 - 90% of those without cladding. Atomized powder-fuel meats with cladding showed a better performance with respect to the comminuted fuel rods. Cladding introduced a constraint stress to the fuel meat and suppressed volume expansion in the radial direction significantly. The chemical reaction between fuel particles and matrix is not changed by the constraint stress of cladding. Thus the reduction of volume change due to cladding suggests that some kinds of defects should be attributed to the volume expansion during thermal annealing besides that of the chemical reaction.

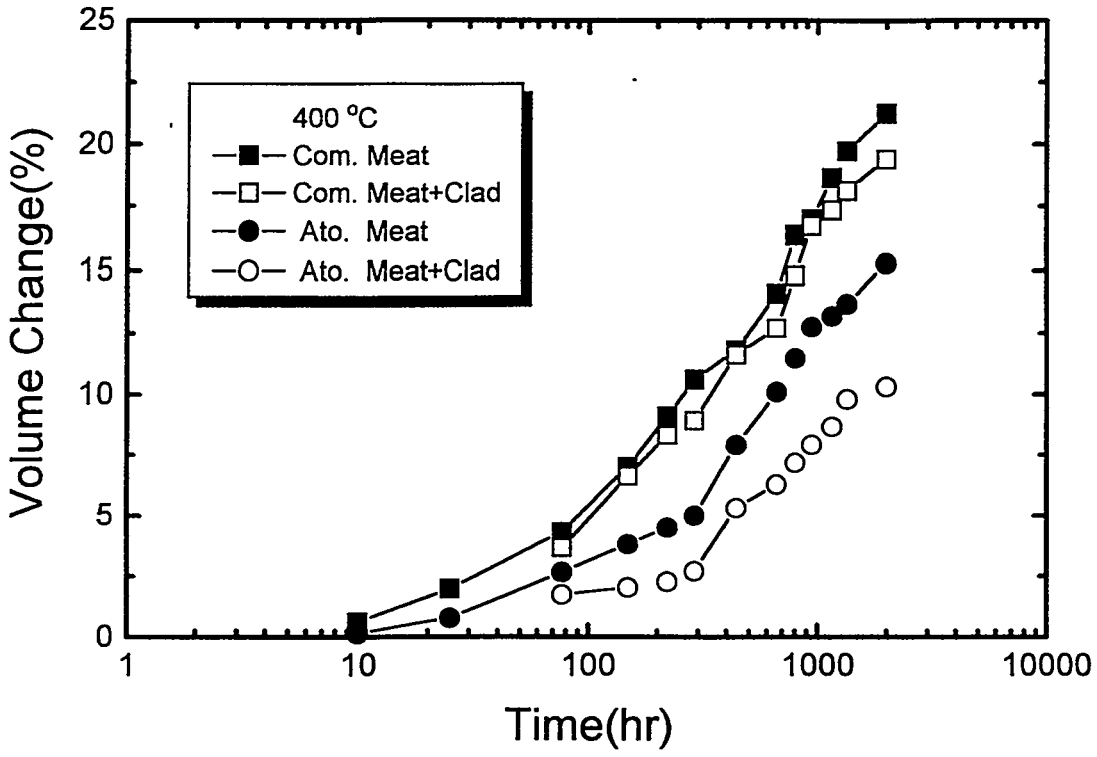

Figure 2. Volume changes of atomized and comminuted powder fuels with and without clad at 400 °C.

Microstructural Observations

Fuel meats were observed after thermal annealing tests, and did not show any distinct appearance in macroscopic observations. Particle morphologies of fuel meats after 2000 hour testing were similar in appearance to initial microstructures. No macrovoid around fuel particles could be apparently found either in comminuted or atomized powder-fuel meats as shown in figure 3. However, reaction zone appeared in fuel particles both of atomized and comminuted powders. The reaction seemed to have occurred along preferred sites. In atomized powder-fuel meats of fine grain structure, the reaction zone corresponded to the grain boundaries of the fuel particles. Inside of each grain, the reaction had not nearly occurred. Comminuted powder-fuel meats also showed similar microstructures as the atomized powder. Compared with atomized powders, comminuted powder-fuel meats had some deformed parts at the edge, and the reaction zone was found at the deformed area as well as the grain boundary. The reaction zone along the grain boundary was observed at the early stage of thermal annealing. After 150 hour testing, the microstructure of the fuel meat showed almost the same morphology as that of the fuel meat after 2000 hours, as shown in figure 4.

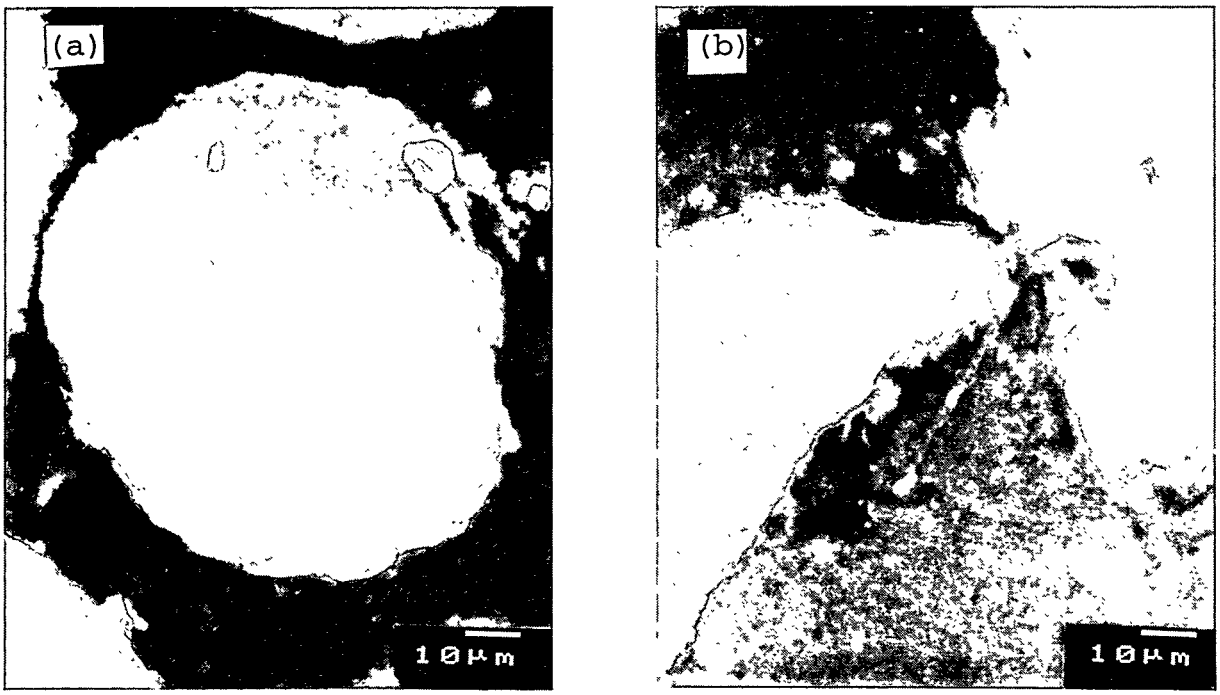

Figure 3. Microstructures of (a) atomized and (b) comminuted powder fuel meats after 2000 hours at 400 °C.

U_3Si reacts with Al to produce a low density-compound of $U(Si,Al)_3$. Grain boundary and deformation band have a path role for diffusion of Al in U_3Si particles. Bulk diffusion rate of Al in U_3Si seems to be very low, so the reaction occurs along the preferred sites at an early stage, and the further growth of the reaction zone into the grain is retarded. Even after 2000 hour testing at 400°C, the microstructure is similar to the microstructure of 150 hour testing. Formation of $U(Si,Al)_3$ produces volume expansion of fuel meat due to low density, but less than 5 % is the maximum volume change. In order to account for 15-20 % of volume expansion of fuel meats after 2000 hour testing, other causes besides that of volume expansion due to the chemical reaction should be attributed. The difference in the diffusivities between U and Al leaves some kinds of defects, such as vacancy clusters, at the side of Al matrix, so called the Kirkendall effect. However in the microstrucure of the atomized and comminuted powder-fuel meats after 2000 hour testing, no distinct macro-defects could be found except for the certain part of edges at the three-point contact area between particles.

A microstructure of the atomized powder fuel meat after 300 hour testing at 500 °C is shown in figure 5. The enforced thermal annealing test, volume expansion of which was 21 %, provided a very interesting and unique morphology. Around the fuel particles, trenchs due to pores were appeared, and paths were connected from Al matrix to fuel particles

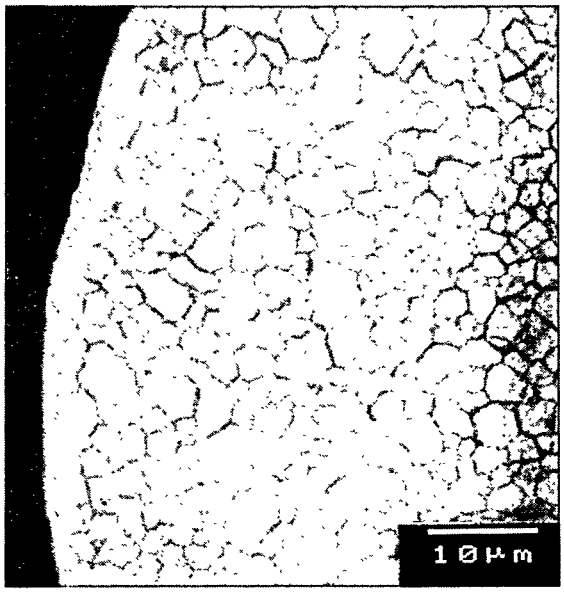

Figure 4. Micostructure of atomized powder fuel meat after 150 hours at 400 °C.

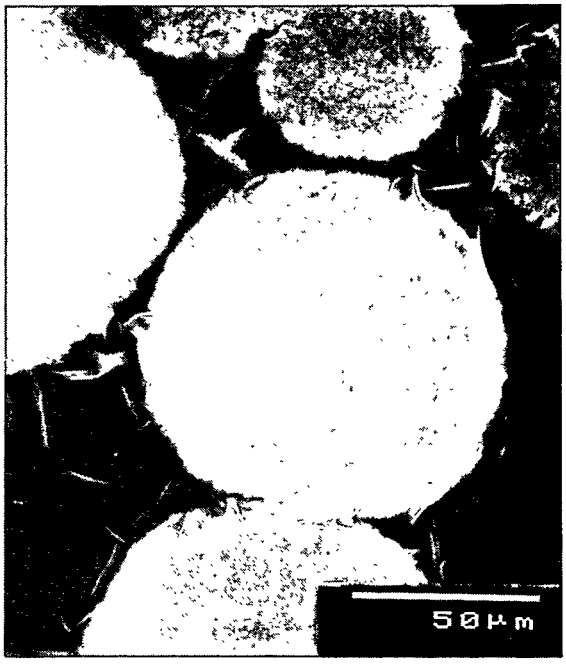

Figure 5. Micostructure of atomized powder fuel meat after 300 hours at 500 °C.

over the trenchs. The trench seemed to be formed due to the Kirkendall effect, and the connecting paths had a role as diffusion pipes of Al. Pores produced by the Kirkendall effect were found to be an important cause of volume expansion during thermal annealing. Moreover, it was suggested that the diffusion of Al between fuel particles and Al matrix should be carried out through a number of paths over pores. These diffusion paths were able to be found at certain defects around fuel particles in the highly magnified microstructures tested at 400 °C, 2000 hours.

Cladding gives constraint stress to fuel particles to suppress the volume expansion of the fuel meat. Figure 6 shows microstructures of fuel meats with Al cladding and end plug after 2160 hour testing at 400 °C. Pores around fuel particles could not be found, but numbers of cracks were developed along the reaction zone inside fuel particles. The volume change of atomized and comminuted powder-fuel meats at 400 °C, after 2000 hours were about 15 and 21%, respectively. The constraint stress of the cladding caused the cracks along the reaction layer in the fuel particle to be very brittle.

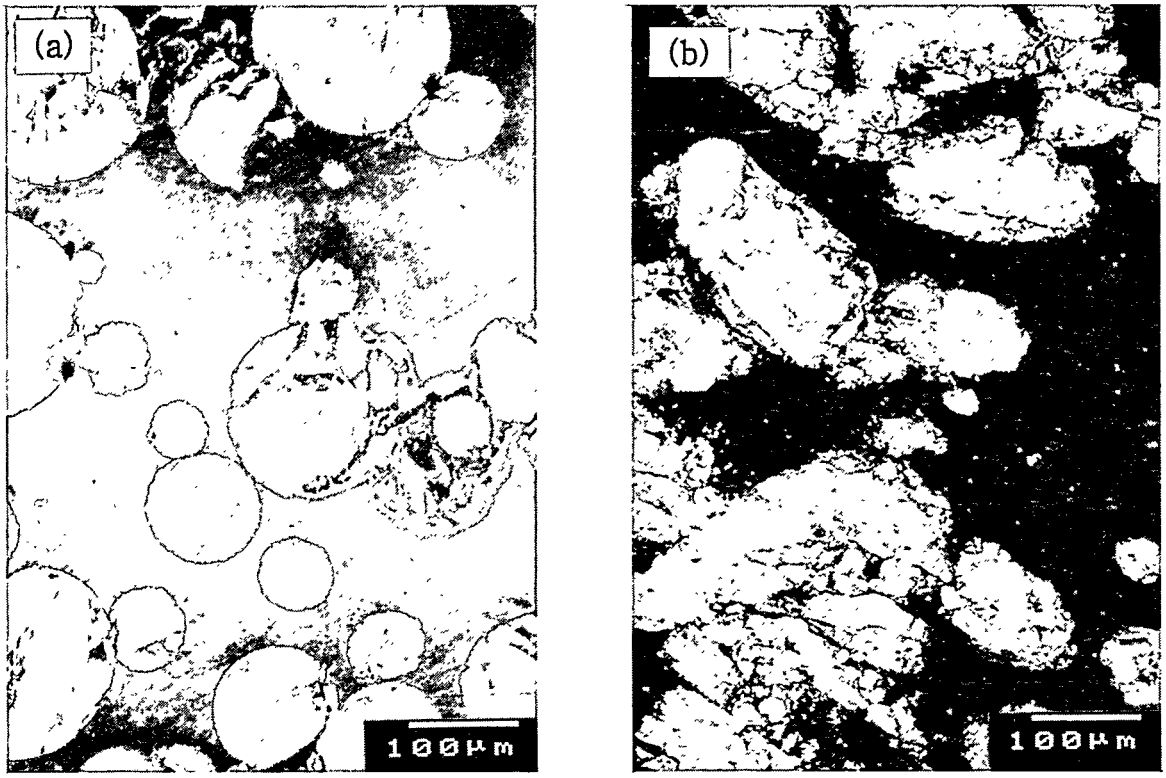

Figure 6. Micostructure of (a) atomized and (b) comminuted powder fuels with clad and end cap after 2160 hours at 400 °C.

SUMMARY

Volume expansion of U_3Si dispersed fuel meats is known to be caused by less dense compounds produced due to the reaction between U_3Si and Al, and by pores leaved around fuel particles. Grain boundaries and deformation bands in U_3Si particles are the fastest diffusion paths of aluminum, and make the reaction zone to occur along such defects. Fast diffusion of Al rather than U brings the Kirkendall effect, and produces pores around fuel particles. Al diffuses into the contact areas with U_3Si particles, and the contact areas are formed diffusion paths over pores after long-time thermal annealing.

Thermal compatibility of atomized U_3Si dispersed fuel meats was characterized, and compared with comminuted U_3Si. Atomized fuel powders had spherical shape, so they had less surface area than comminuted powders. The small surface area of atomized fuel particles retards diffusion of Al into fuel particles, and retards the reaction between U_3Si and Al, which could result in better thermal stability than comminuted powder-fuel meats.

Cladding of the fuel rod gave constraint stress to the fuel meat, thereby suppressing the formation of pores around fuel particles. In an extreme case such as the testing at 2000hours, 400°C, the constraint stress developed cracks along the reaction zone in fuel particles. Volume expansion of the clad samples was reduced by the constraint effect of cladding in the rod-type fuels.

These results of thermal compatibility of atomized U_3Si powder-fuel meats will be used to evaluate the fuel performance in combination with the results of in-pile tests. Tests for irradiation behaviors of atomized U_3Si powder-fuel rods are planned in the KMRR in the near future.

REFERENCES

1. J.C. Wood, M.T. Foo, and L.C. Berthiaume, "The Develpment and Testing of Reduced Enrichment Fuels for Canadian Research Reactors", Proc. of the Int. Meeting on RERTR, Catlinberg, Tennessee, Oct., 1986.
2. T.C. Wiencek, R.F. Domagala and H.R. Thresh, "Thermal Compatibility Studies of Unirradiated Uranium Silicide Dispersed in Aluminum," 7th RERTR Meeting, ANL, USA, Oct., 1984.
3. C.K. Kim, "Atomization of U3Si for Research Reactor Fuel", 13th RERTR Meeting, Jakarta, Indonesia, November, 1991.
4. M.A. Faraday, M.T. Foo, R.D. Davidson, and J.E. Winger, "Thermal Stability of Al-USiAl Dispersion Fuels and Al-U Alloys", Nucl. Technol., 58(1982)233.

POSTIRRADIATION EXAMINATION OF A LOW ENRICHED U_3Si_2-Al FUEL ELEMENT MANUFACTURED AND IRRADIATED AT BATAN, INDONESIA

A. Suripto, S. Sugondo, H. Nasution, and G. L. Hofman*
Nuclear Fuel Element Center
National Atomic Energy Agency (BATAN)
Serpong, Indonesia

ABSTRACT

The first low-enriched U_3Si_2-Al dispersion plate-type fuel element produced at the Nuclear Fuel Element Center, BATAN, Indonesia, was irradiated to a peak ^{235}U burnup of 62%. Postirradiation examinations performed to date shows the irradiation behavior of this element to be similar to that of U_3Si_2-Al plate-type fuel produced and tested at other institutions. The main effect of irradiation on the fuel plates is a thickness increase of 30-40 μm (2.5-3.0%). This thickness increase is almost entirely due to the formation of a corrosion layer (Boehmite). The contribution of fuel swelling to the thickness increase is rather small (less than 10 μm) commensurate with the burnup of the fuel and the relatively moderate as-fabricated fuel volume fraction of 27% in the fuel meat.

INTRODUCTION

Presently, the RSG GAS reactor fuel consists of low enriched (LEU) U_3O_8 dispersed in aluminum in the form of hot-roll-bonded plates with aluminum alloy cladding: This fuel has a maximum loading of 3.2 g cm^{-3} and is fabricated at BATAN.

Several years ago BATAN began a program to acquire the technology to fabricate U_3Si_2 dispersion fuel[1], which would make it possible to increase the uranium loading in the fuel meat to 5 g cm^{-3}.

The fuel element (RI-SIE) was removed from the reactor core when the fuel had reached a ^{235}U depletion of approximately 50%. After an appropriate cooling period the element was γ-scanned at the reactor hot cell, and subsequently shipped to the BATAN RMI hot cell facility for detailed postirradiation examination.

This paper presents results of the non-destructive postirradiation examination of the first U_3Si_2 test element that consisted of 21 fuel plates with an uranium loading of 3.2 g cm^{-3} (equivalent to the current U_3O_8 fuel).

*Argonne National Laboratory, Argonne, IL USA with support from the International Atomic Energy Agency, Expert Section.

Destructive examinations are in progress. Initial results of scanning electron microscopy on a cross-section of the plate shows that the fission gas bubble morphology and fuel-aluminum interaction are consistent with previous observations on U_3Si_2-Al dispersion fuel irradiated at comparable burnup.

EXPERIMENTAL DATA

The as-built data of element RI-SIE-2 as recorded at the BATAN fuel element production installation (FEPI) are given in Table I. Data pertaining to the irradiation in the 30 MWth RSG GAS reactor is given in Table II.

TABLE I
AS-BUILT PARAMETERS FOR PLATE IDA 0036 FROM ELEMENT RI-SIE-2

Fuel Composition	U_3Si_2
Uranium Mass	59.99 g
Fuel Mass Loading	3.2 g U/cm^3
Fuel volume Fraction	27%
As-fabricated Porosity	2%
Meat Matrix	Al
Cladding	Al Mg2
Plate Thickness	1.32 mm
Meat Thickness	0.64 mm
Plate Length	625
Plate Width	70.70 mm
Meat Width	61.4 mm
Meat Length	570 mm

POST IRRADIATION EXAMINATION

Visual Inspection and Plate Removal

The element was visually inspected and photographed with a through-the-hot-cell-wall periscope at a magnification of 12X.

The overall appearance of the aluminum side plates and the two outer fuel plates was as expected. The cladding surfaces had the typical luster of irradiated aluminum having formed a thin layer of hydrated aluminum oxide (Boehmite). No blisters, pits or other evidence of cladding damage was found. A fuel plate from the center position in the element, identified as plate IDA 0036, was removed by milling a slit in the side plate through which the plate could be extracted. Visual inspection showed this plate to be in excellent condition.

TABLE II IRRADIATION FOR ELEMENT RI-SIE-2	
Time at Power	259 days
Total Weight	1259.63 grams
^{235}U	249.54 grams
Enrichment	19.81%
Burnup, ^{235}U Depletion	48.8%
Average Flux	2.0×10^{14} $cm^{-2}S^{-1}$
pH Coolant	6.5-7
Heat Flux	32.3 W cm^{-2}
Power Average	60 KW
Coolant Temperature	(in) 42°C (out) 54°C
Nominal	

γ-Scanning

A Ge-Li detector installed outside the hot cell was used to measure the axial γ activity of plate IDA-0036. The γ radiation is admitted to the detector through the cell wall by means of a 1.1 m long stainless steel collimator.

Complete γ energy spectra were obtained at 5 cm intervals along the length of the plate. The intensity of several characteristic peaks was determined by counting the total pulse height under a Gaussian distribution through the γ energy peaks, and by making the appropriate corrections for dead-time, background and compton scattering contributions. The result for some long half-life nuclide of interest are summarized in Table III.

These nuclides are formed by different reactions ^{134}Cs results from neutron capture in ^{133}Cs which it self is formed by ^{235}U fission. However, ^{137}Cs is a product of ^{235}U fission only, and with its long half-life best reflects the ^{235}U depletion profile in the fuel plate. The different peaking factors for the axial profiles of these nuclides reflect the difference in neutron fluence dependence of their accumulated yields.

As mentioned before, γ-scanning was also performed on the entire element at the reactor facility. A Ge/Li detector was used there as well but with a more rapid scanning method by which simply the pulse height at the γ energy peak of interest is counted in addition to the gross count of the entire γ energy spectrum. Figure 1 shows a comparison of the two methods. The profiles of ^{237}Cs are very similar owing to the fact that this higher energy peak is not much affected by compton contributions. The self shielding effect of the more massive element compared to a single plate results in a flatter distribution for the lower energy peak counts and the gross counts. The similarity in the ^{137}Cs results obtained from either singular plate or whole element indicates that the rapid scanning method of the element also yields a good representation of the burnup or ^{235}U depletion profile.

TABLE III GAMMA SCAN PROFILE PARAMETERS FOR ^{134}Cs AND ^{137}Cs COUNTING TIME 3600 S DETECTOR GeLi				
Nuclide	Energy keV	t 1/2	I Net Count	Peaking Factor Imax./Iave.
^{134}Cs ^{137}Cs	604.7 661.6	2.07 years 30.0 years	90677 260627	1.58 1.26

Plate Thickness Measurements

Plate thickness was measured at 5 cm intervals along 3 axial tracks on the fuel plate with a thickness gauge having an accuracy of 0.005 mm. A "dummy" fuel plate was measured at the fuel manufacturing installation and in the hot cell facility to determine any systematic differences between the as-fabricated and post-irradiation measurement. Statistical evaluation of the comparative measurements indicated a difference of +30 μm between the two instruments. Accordingly, all hot cell measurements were decreased by 30 μm to reflect the true difference between pre- and postirradiation thickness data. The average values of the three axial tracks on plate IDA 0036 is plotted in Fig 2.

In lieu of detailed destructive examination results we have chosen to use previously accumulated data of U_3 Si_2-Al irradiations to analyze the thickness changes measured in the present test.

The maximum burnup in the plate was calculated by multiplying the total element burnup by the ^{137}Cs peaking factor:

$$Bu^{max} = 1.27 \times 49\% = 62\%$$

This burnup corresponds to an accumulative fission density in the U_3Si_2 fuel of 3.3×10^{27} m^{-3}. From fuel swelling data obtained from previous experiments[2] shown in Fig. 3 we obtained an equivalent swelling $\frac{\Delta V^F}{V_0^F} = 12\%$. The fuel swelling is related to the meat swelling as follows.

$$\frac{\Delta V^F}{V_0^F} = \left[\frac{\Delta V^m}{V_0^m} + \frac{V_O^P - V^P}{V_0^m}\right]\frac{V_O^m}{V_0^F}$$

where V_O^P is the as-fabricated porosity in the meat (2% for this plate), V^Pin the residual porosity not consumed by fuel swelling. This yields a value for $\frac{\Delta V^m}{V_0^m}$ of 1.0%. Since meat swelling is completely transferred to meat thickness increase, Δth^m, we obtained

$$\Delta th^m = 0.01 \times 0.64 \text{ mm} = 6 \text{ } \mu m$$

with the customary assumption that the cladding density remains unchanged, we obtained a plate thickness increase due to fuel swelling of 6 μm. This calculation can be performed for the entire axial profile which is indicated in Fig. 3. It appears that the swelling contribution to the plate thickness increase is rather small.

The difference between the total thickness increase and the fraction due to fuel swelling can be attributed to Boehmite formation, amounting to ~30 μm. It has been verified that one half of the Boehmite layer thickness represents aluminum cladding consumed by the oxidation process. Thus the total Boehmite thickness is 2 x 30 μm ≈ 60 μm, that is, ~30 μm on each side of the plate.

By comparison, Boehmite thickness observed on the same cladding alloy (Al Mg2) irradiated in the Oak Ridge Research reactor was ~25 μm. A calculation of the Boehmite thickness using a correlation developed at Oak Ridge National Laboratory[3] yields a value of ~20 μm. Considering the accuracy of the measurements, the difference in operating conditions, and the difference of the coolant chemistry of the different reactors, the value of ~30 μm derived for the present test appears to be very reasonable.

CONCLUSION

The BATAN produced and tested LEU-U_3SI_2-Al dispersion fuel element performed well to a peak ^{235}U depletion of 62%. Non-destructive postirradiation examination revealed no cladding damage or plate distortions and the fuel plate thickness increase was found to be consistent with that measurement in previous irradiation tests on similar fuel. the plate thickness increase is almost entirely due to Boehmite formation.

ACKNOWLEDGEMENTS

We would like to thank Messrs. D. Lufty, G. Antonio, L. Hakim, and Ms. S. Amini for performing various parts of the postirradiation examinations.

REFERENCES

1. A Suripto and S. Soentono, "Progress in the Development of Uranium Silicide (U_3Si_2-Al) Fuel at BATAN," Proc. RERTR meeting, November 3-7, 1994, Jakarta, Indonesia (to be published).

2. G. L. Hofman, J. Rest, R. C. Bircher, and J. L. Snelgrove, "Correlation of Irradiation-Induced Microstructural Changes and Fission Gas Swelling in Uranium Compounds," Proc. of the 1990 International Meeting on Reduced Enrichment for Research and Test Reactors, ANL/RERTR/TM-18, Newport, Rhode Island, September 23-27, 1990.

3. J. C. Griess, et al., "Effect of Heat Flux on the Corrosion of Aluminum by Water, Part IV, ORNL-3514 (February 1964).

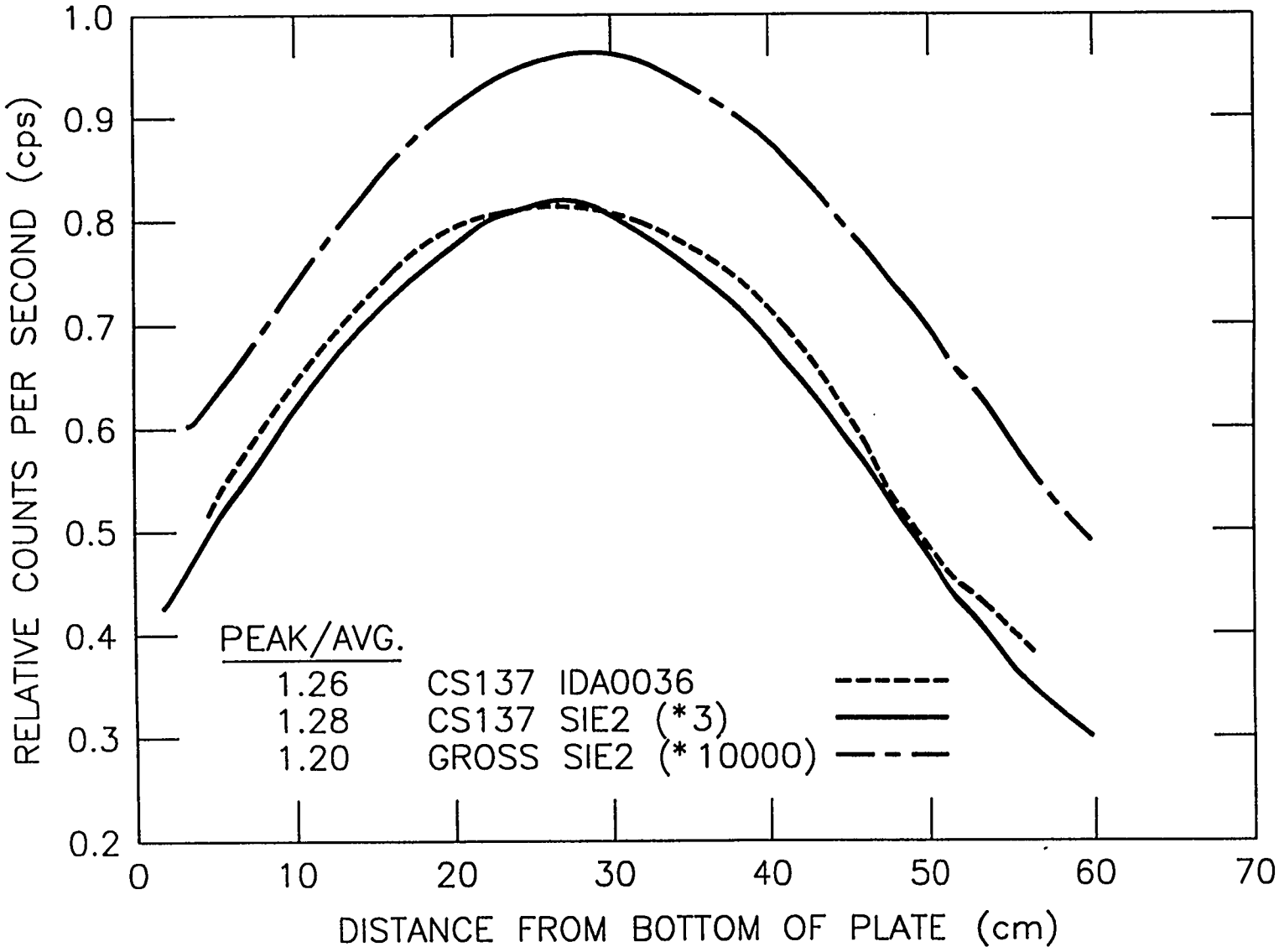
1.0
0.9
0.8
0.7
0.6
0.5
0.4
0.3
0.2
RELATIVE COUNTS PER SECOND (cps)
0
10
20
30
40
50
60
70
DISTANCE FROM BOTTOM OF PLATE (cm)
PEAK/AVG.
1.26 CS137 IDA0036
1.28 CS137 SIE2 (*3)
1.20 GROSS SIE2 (*10000)

Figure 1

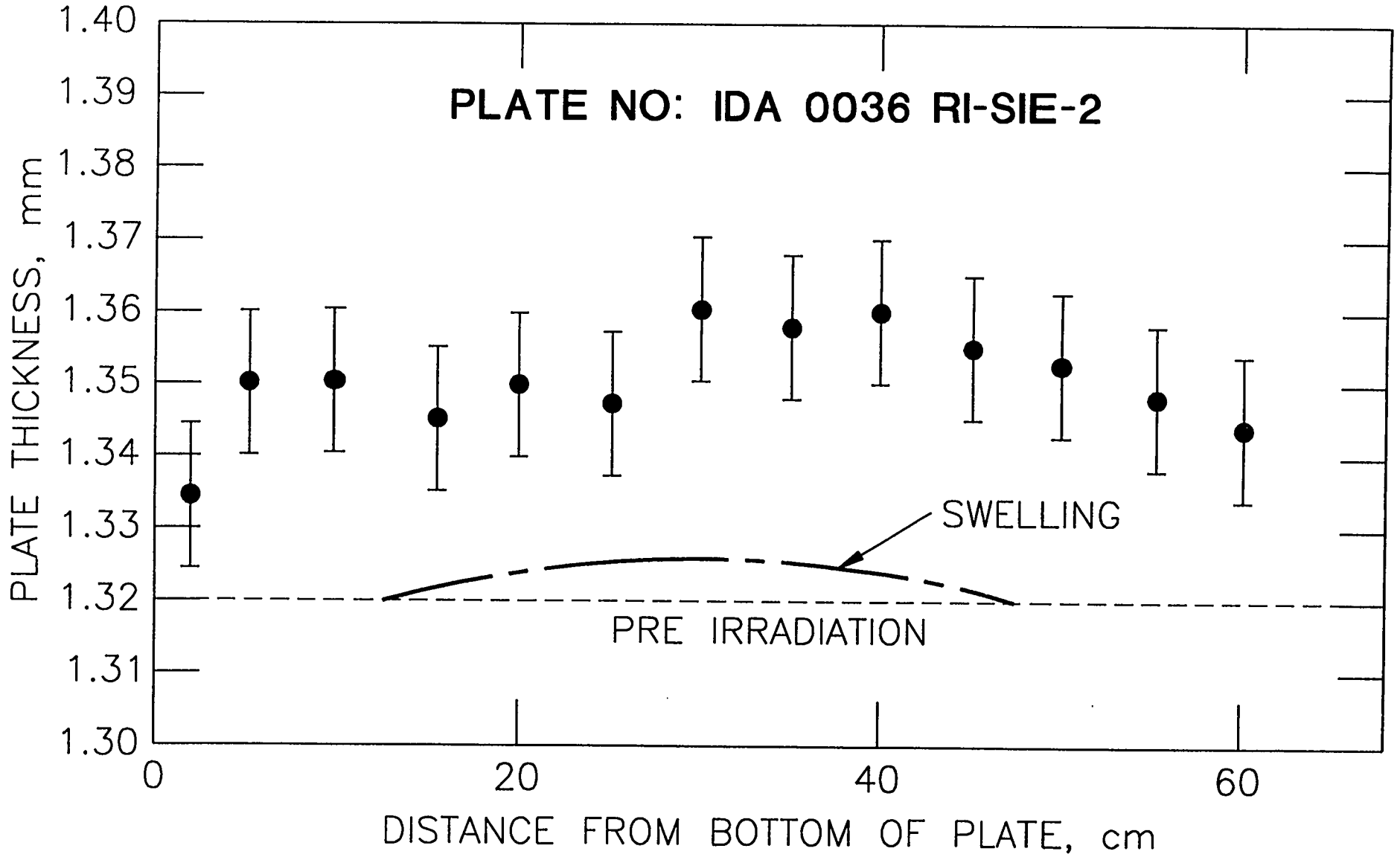
PLATE NO: IDA 0036 RI-SIE-2
PLATE THICKNESS, mm
1.40
1.39
1.38
1.37
1.36
1.35
1.34
1.33
1.32
1.31
1.30
SWELLING
PRE IRRADIATION
0
20
40
60
DISTANCE FROM BOTTOM OF PLATE, cm

Figure 2

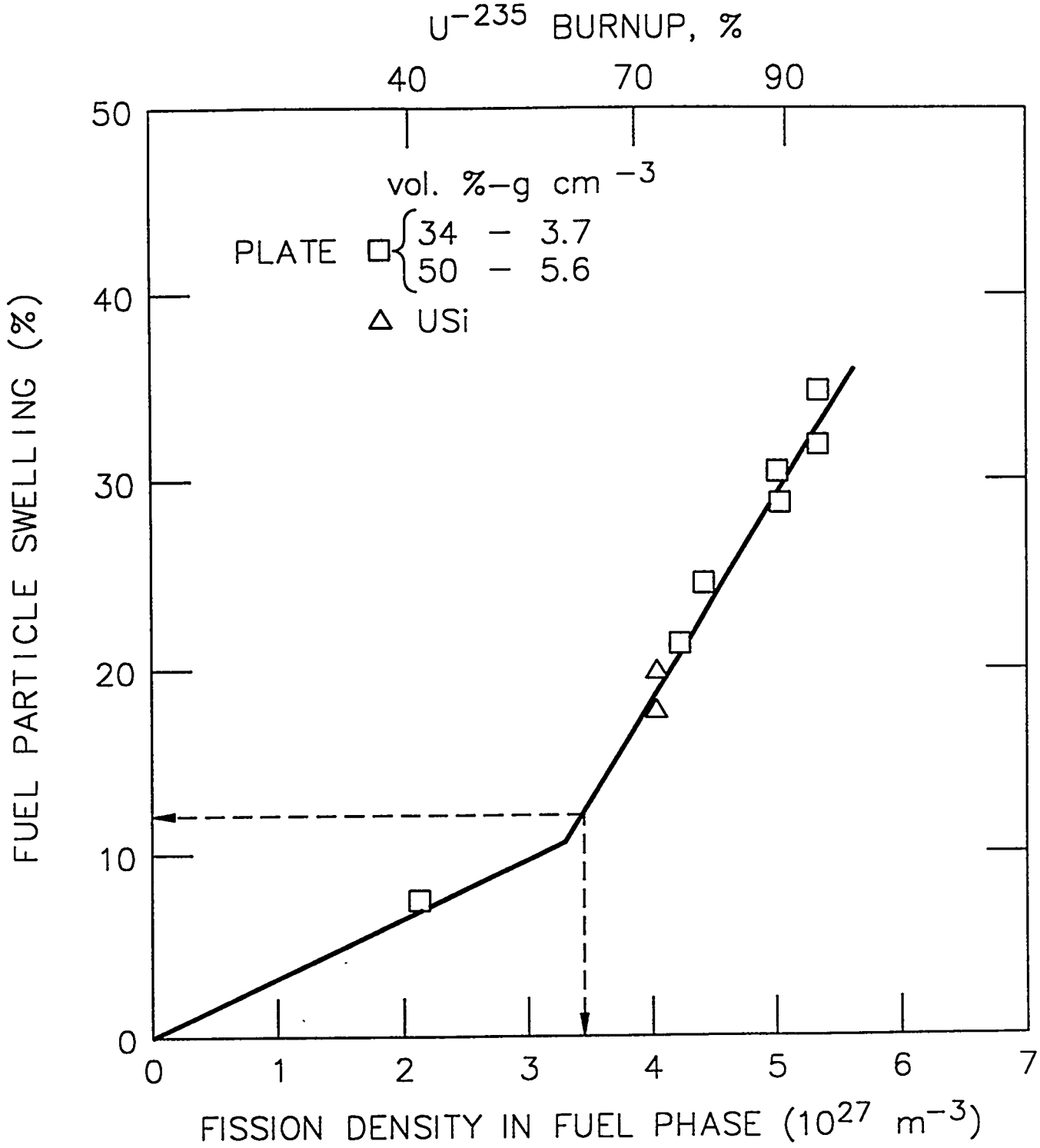
U-235 BURNUP, %
40
70
90
50
vol. %–g cm -3
PLATE
34 – 3.7
50 – 5.6
△ USi
40
30
20
10
0
FUEL PARTICLE SWELLING (%)
0
1
2
3
4
5
6
7
FISSION DENSITY IN FUEL PHASE (10^27 m^-3)

Figure 3

STATUS OF THE ATOMIZED URANIUM SILCIDE FUEL DEVELOPMENT AT KAERI

C.K. Kim, K.H. Kim, H.D. Park, I.H. Kuk

Korea Atomic Energy Reasearch Institute
P.O. Box 105, Yu-sung, Taejon 305-600, Korea

ABSTRACT

While developing KMRR fuel fabrication technology an atomizing technique has been applied in order to eliminate the difficulties relating to the tough property of U_3Si and to take advantage of the rapid solidification effect of atomization. The comparison between the conventionally comminuted powder dispersion fuel and the atomized powder dispersion fuel has been made. As the result, the processes, uranium silicide powdering and heat treatment for U_3Si tranformation, become simplified. The workability, the thermal conductivity and the thermal compatibity of fuel meat have been investigated and found to be improved due to the spherical shape of atomized powder. In this presentation the overall developments of atomized U_3Si dispersion fuel and the planned activities for applying the atomizing technique to the real fuel fabrication are described.

INTRODUCTION

The research reactor has taken an important role in the development of basic and applied science and technology. Many countries have research reactors appropriate for their own circumstances and needs. In Korea, the Korea Multi-purpose Research Reactor (KMRR) with 30 MW is under construction to be used for irradiation tests of nuclear fuel and reactor materials, various studies using neutron beam, radio-isotope production, semiconductor doping, neutron activation analysis, and so on. In conjunction with KMRR construction, research and development for KMRR fuel fabrication technology was launched in 1987. As the first activity two KAERI engineers participated in a three months training course for the

fabrication technology of U_3Si_2 dispersion plate fuel in ANL, which has significantly contributed to our fuel development.

KMRR fuel is a rod type U_3Si fuel. The U_3Si material has relatively high strength and toughness so some difficulties had been experienced in making U_3Si powder from heat treated blank through the machining process. In order to eliminate these difficulties the rotating disk atomization has been applied to the KMRR fuel fabrication process. Accordingly the powder can be produced from the melt without machining and comminuting processes. In addition, this atomizing process has a rapid cooling effect and a tendency to produce spherical shaped particles, which contribute to improved fuel fabrication process and fuel performance properties. These results have been presented four times at the RERTR international meeting.

In Korea there are two TRIGA reactors, which have low neutron flux and are not equiped with an irradiated material examination facility. Therefore it has been difficult to perform the fuel performance test of atomized silicide fuel until now. The construction of KMRR is near its completion and it is expected to start up into operation at the end of 1994 and to reach the normal operating condition in 1996.

In this presentation the developments of atomized uranium silicide dispersion fuel and the planned activities for applying to KMRR fuel fabrication are described.

DEVELOPMENTS OF ATOMIZED U_3Si FUEL

The development of the rotating disk atomization technique for U_3Si powder was initiated in 1989. For the preliminary atomizing experiment the high speed rotating disk driven by a gas turbine motor was installed in the vacuum induction furnace chamber which was used for making uranium alloy ingots. The nozzle device for feeding U-Si alloy melt onto the disk top suface was fixed beneath the tundish. The atomized U_3Si powder showed a spherical shape and its microstructure became much finer due to the rapid solidification effect. The results of this experiment were presented at the 13th RERTR international meeting.

Taking advantage of the above experience, atomizing equipment was designed by our research team and manufactured by a domestic company.

Using this atomizer the U_3Si powder was successfully prepared and analyzed for evaluating the characteristics appropriate for research reactor fuel. The atomized U_3Si powder was found to have spherical shape and fine structure due to the rapid solidification effect, which allowed for a reduction in heat treating time dramatically. The round and smooth surface of the atomized U_3Si powder caused a reduction in extruding pressure and increased elongation in tensile test results. The results were presented at the 14th RERTR international meeting.

The improved workability in forming the blended powder into fuel shape was assumed to have a beneficial effect on fabricating the high loading density fuel such as ANS fuel. ANL requested some atomized U_3Si_2 powder in order to examine the advantages of the spherical powder in ANS fuel fabrication. Accordingly, our research team launched a study for producing spherical U_3Si_2 powder by rotating disk atomization in 1992. U_3Si_2 is melted at much higher temperature, 1665℃, than U_3Si, 1520℃. Therefore, a numerous difficuties had been suffered from developing the U_3Si_2 atomizing technique. However, the spherical U_3Si_2 powder was successfully prepared using a rotating disk atomizer. The investigated characteristics of the atomized U_3Si_2 powder were presented at the 15th RERTR international meeting. Most of the atomized particles appeared to be spherical except for a small number of large size particles, which were found to be of broken and irregular shape with sharp edges due to the collision with the atomizing chamber wall. The controlled powder distribution was analyzed and the mean size was about 90㎛.

The determined results of specific surface area showed that the atomized spherical powder has about 30% smaller area than the comminuted powder. This kind of characteristic was assumed to be responsible for improved fuel performance. So our research team continued to develop the U_3Si_2 atomizing technique.

In order to apply the atomizing technique to the KMRR fuel fabrication some fuel rods were prepared with atomized and comminuted U_3Si powders. A study of thermal conductivity comparision for two kinds of fuel rods was conducted. The examined results showed that the atomized U_3Si fuel has higher thermal and electrical conductivity than the comminuted U_3Si fuel in the radial direction due to different arrangement according to the particle shape. The comminuted powder prepared through a chipping process by machining and a pulverizing process using a shatter box has irregular and longish shape, which induced the particle arrangement to be oriented in the extrusion direction. However, the atomized spherical particles were arranged in the isotropic direction. The results was presented at the 16th

RERTR international meeting.

The compatibility test, one of the important fuel outpile tests, was performed recently with the atomized U_3Si fuel and the conventional comminuted U_3Si fuel. The results showed a tendency that the atomized U_3Si fuel has about 30% lower swelling than the comminuted U_3Si fuel in all temperature range up to 400℃.

Our research team has tried to mainly apply atomizing technique to the KMRR fuel fabrication. We have not investigated the atomized U_3Si_2 dispersion fuel because any fabricating equipments for the plate type fuel is not poccessed at KAERI. However, from above results it is assumed that atomized U_3Si_2 spherical powder would impact a benificial effect upon the U_3Si_2 dispersion plate fuel.

The spherical shaped powder would improve the rolling workability for forming fuel plate and probablely reduce the dog bone problem of fuel meat. Further more, the maximum uranium density of plate type fuel would increase. In addition, the spherical powder may be distributed without preferred orientation and has a tendency for less clustering than the comminuted irregular powder. Accordingly, the atomized U_3Si_2 dispersion fuel ia assumed to improve performance in thermal conductivity and swelling point.

Planned Activities

Until now we have not perfomed any irradiation test of fuel material bacause there is not an irradiation and examination facility. Our research team has carried out the research and development of fuel and its outpile test. KMRR is near the completion of construction and expected to initiate its start-up operation from the end of 1994 and reach the normal condition at the beginning of 1996. An Irradiated Material Examination Facility (IMEF) has been recently built inside KMRR. A Post Irradiation Examination Facility (PIEF) for fuel examination and testing is aleady in operation. Accordingly it is assumed that the irradiation test of fuel materials can be performed from 1996. Our research team intends to prepare two kinds of fuels, the conventionally comminuted U_3Si dispersion fuel and the atomized U_3Si dispersion fuel, and will conduct irradiation tests on them.

The fuels will be fabricated using the laboratory scale fabrication facility. However, in order to have the same quality as a real KMRR fuel, some inspection equipments such as the γ-scanner, X-ray radiograph and so on will be equipped. The rotating disk atomizing equipment was manufactured at the time when we had little experience in U_3Si_2 atomization. Since then many problems have been brought about in atomizing U_3Si and U_3Si_2. Accordingly the atomizing equipment is being modified recently and will resume operation soon. The atomizing efficiency and the powder quality will be further improved.

In order to prepare the irradiation fuels a small amount of low enriched uranium metal will be puchased no later than the middle of 1995 as shown in figure 1. Then the irradiation fuels will be prepared by the end of 1995 in order to meet the normal operation time of KMRR,

Planned Activity	1995		1996		1997	
LEU uranium metal						
Preparation of Fuels						
Irradiation						
Examination of Irradiated Fuels						
Application to KMRR Fuel Fabrication						

Fig. 1. The plan of atomized U_3Si dispersion fuel for KMRR.

when it is available for the iradiation test. About 9 months are needed to burnup fuels fully in KMRR. It is assumed that it takes about 6 months for examining the irradiated fuels and the final results and evaluation are ontained around the spring of 1997. According to these results the atomization technique will actually be implemented to KMRR fuel fabrication.

After the irradiation test of U_3Si dispersion fuels, we are planning to conduct the performance test of the atomized U_3Si_2 dispersion fuel with various uranium loading densities up to the maximun available density.

The performance test results of the atomized spherical U_3Si_2 dispersion fuel is expected to come out in 1997. This kind of test would be more efficient and able to produce the results much sooner when performed in cooperation with an experienced foreign institute or company.

SUMMARY

The U_3Si atomization in dispersion fuel fabrication has been investigated to simplify the process and to improve the properties as well as the outpile performance of fuel. The performance tests of the conventionally comminuted U_3Si dispersion fuel and the atomized U_3Si dispersion fuel are planned to be carried out as KMRR reaches normal operational condition in 1996. According to the results the atomization technique is expected to be applied to KMRR fuel fabrication. From the results of an atomized U_3Si dispersion fuel the fuel is assumed to have some beneficial effects on the uranium loading density and the burnup performance in the reactor. Accordingly, the atomized U_3Si_2 dispersion plate fuel is considered to be in need of irradiation testing. Our research team is open to any cooperation with an irradiation experienced institute and company.

REFERRENCE

1. I.H. Kuk. J.B. Lee, C.T. Lee, S.J. Chang, "Atomization of U_3Si Nuclear Fuel," in Proceedings of International Meeting on Reduced Enrichment for Research and Test Reactors, Rhode Island, USA, Sept. 23-27, 1990

2. C.K. Kim, K.H. Kim, C.T. Lee, I.H. Kuk, "Atomization of U_3Si for Research Reactor", in Proceedings of International Meeting on Reduced Enrichment for Research and Test Reactors, Jakarta, Indonesia, Nov. 3, 1991

3. C.K. Rhee, S.I. Pyun, I.H. Kuk, "The kinetics of the Peritectoid Reaction $3U+U_3Si_2 \rightarrow 2U_3Si$ as a Function of Size of Parent U_3Si_2 Precipate in the Uranium Matrix", Journal of Nuclear Materials, Vol., 184, 1991, 146-149

4. C.K. Kim, K.H. Kim, S.J. Jang, H.D. Jo, I.H. Kuk, "Characterization of Atomized U_3Si_2 Powder for Research Reactor", in Proceedings of

International Meeting on Reduced Enrichment for Research and Test Reactors, Roskilde, Denmark, Sept. 28, 1992

5. C.K. Kim, C.T. Lee, H.D. Park, K.H. Kim, I.H. Kuk, "The Effect of Particle Shape on Thermal and Electrical Conductivities of Uranium Silicide Dispersion Fuel", in Proceedings of International Meeting on Reduced Enrichment for Research and Test Reactors, Oarai, Japan, Oct. 3-7, 1993

6. C.K. Kim, K.H. Kim, I.H. Kuk, and Suk-Joong L. Kang, "Effect of Particle Shape and Distribution on Thermal and Electrical Conductivities in U_3Si-Al Dispersion Fuel", Journal of Nuclear Materials, Vol. 209, 1994, 315-320

NON-DESTRUCTIVE EVALUATION OF THE CLADDING THICKNESS IN LEU FUEL PLATES BY ACCURATE ULTRASONIC SCANNING TECHNIQUE

by

J.Borring, H.E.Gundtoft, K.K.Borum P.Toft.
Risø National Laboratory, Denmark

ABSTRACT

In an effort to improve our ultrasonic scanning technique for accurate determination of the cladding thickness in LEU fuel plates, new equipment and modifications to the existing hardware and software have been tested and evaluated.

We are now able to measure an aluminium thickness down to 0.25 mm instead of the previous 0.35 mm. Furthermore, we have shown how the measuring sensitivity can be improved from 0.03 mm to 0.01 mm.

It has now become possible to check our standard fuel plates for DR3 against the minimum cladding thickness requirements non-destructively. Such measurements open the possibility for the acceptance of a thinner nominal cladding than normally used today.

1. INTRODUCTION

A reliable non-destructive measuring tool for cladding thickness measurements of a dispersion fuel plate has not yet been developed. Instead, a statistical basis has been established for estimating minimum cladding thickness from the distribution of measured minima observed in metallographic cross sections of typical fuel plates. The minimum acceptable cladding thickness has thus been chosen conservatively, knowing that there was a risk that occasionally, fuel plates with partially thinner cladding would be accepted.

At the RERTR meeting in Roskilde in 1992 we presented ultrasonic scanning equipment for non-destructive evaluation of LEU fuel plates including measurement of the cladding thickness (Ref.1). At that time the equipment was able to measure a cladding thickness down to approximately 0.35 mm with a sensitivity of 0.03 mm.

The ultrasonic scanning equipment is an interesting tool for measurement of LEU cladding thicknesses, providing the sensitivity can be improved and the minimum measurable cladding thickness reduced.

Therefore, we have investigated possible improvements of the measurements in these two directions.

This paper presents tests of different new measuring equipment as well as calibration eveluation procedures.

Recently our system has been upgraded, with hardware and software, which enables the measurements to be treated in manv different ways.

2. MEASURING PRINCIPLES AND SPECIFICATIONS

The mechanical part of our ultrasonic scanning equipment is in principle the same as used in 1992 (Figure 1).

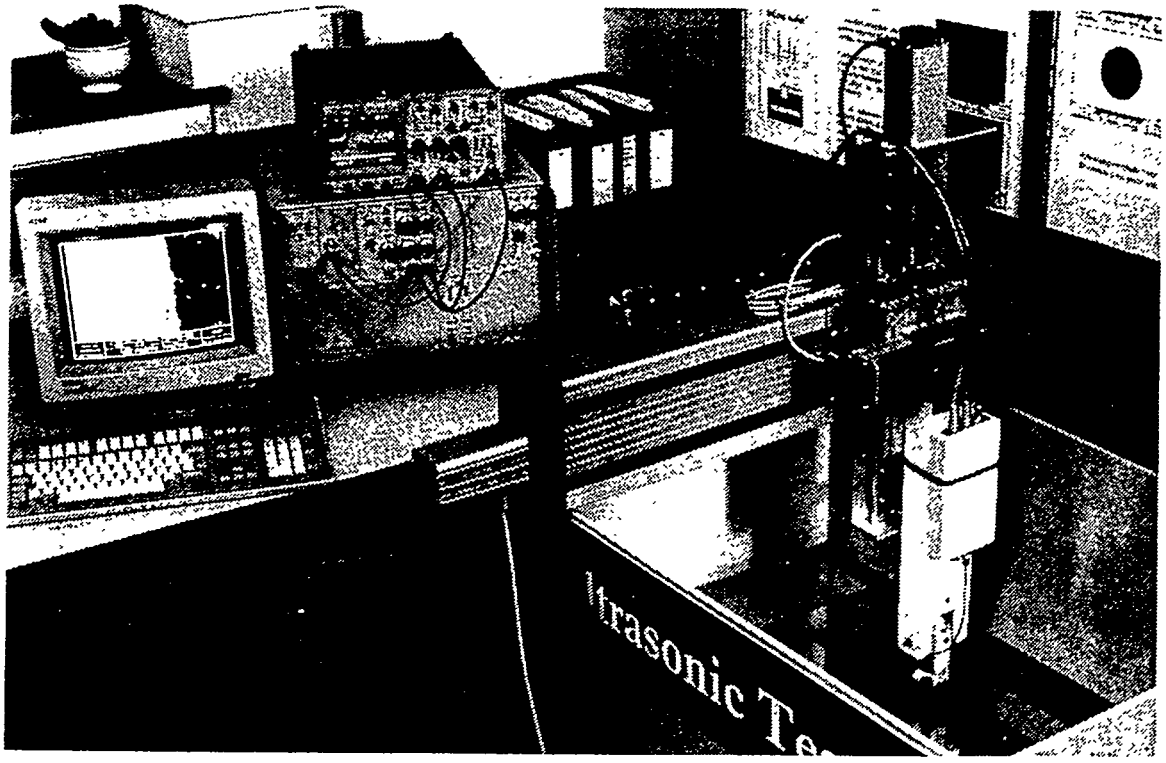

Figure 1. Precision ultrasonic scanning equipment.

The measuring principle is based on ultrasonic echoes. In figure 2 the echo pattern from a fuel plate over the core region is shown schematically. It can be seen that echoes are reflected from the plate surface - interface (IF) and from the core surface (CS). If the echo from the core surface (CS) falls within a set measuring gate, the time of flight from IF to CS can be measured and converted into a distance, knowing the sound velocity in aluminium. The built-in clock in the ultrasonic equipment runs in units of 10 nanosec, and the smallest measurable step for aluminium is equal to approximately 0.03 mm.

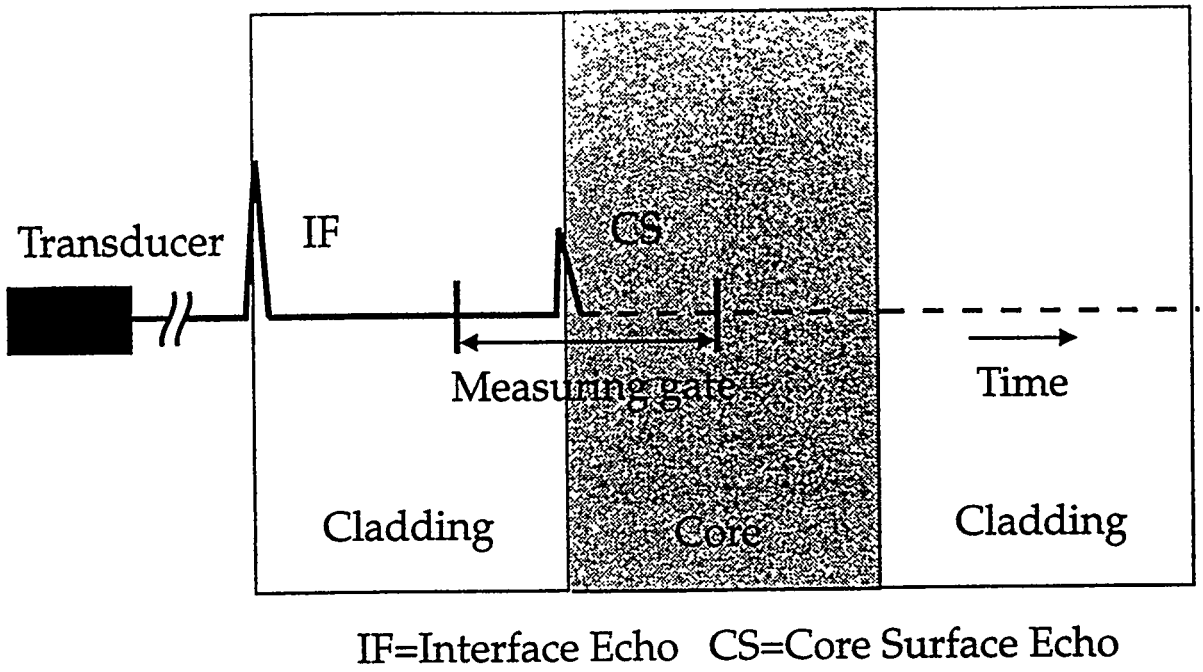

Figure 2. Ultrasonic echo pattern from a fuel plate cross section.

The resolution in the scanning pattern can be varied down to 0.01 mm between the measuring points in both directions.

The maximum scanning speed is 90 mm/sec. Scanning of an area of 1 cm^2 with the optimal resolution (0.01 mm) will then take about 2 min. This time may be decreased if the scanning is made in a more open pattern. If instead the scanning resolution is only 0.1 mm, the area is scanned 10 times faster.

In the scanning direction the system will always make a measurement for each 0.01 mm independent of resolution. However if we scan with 0.1 mm resolution, only the last measured value will be stored. The scanning speed in a scanning line is independent of the resolution.

3. CALIBRATION

When scanning a fuel plate for thickness evaluation it is the time of flight between echoes which is measured and stored. Before these times can be transformed into distances, we need to know exactly how time and distance are related to each other. This is done by making a calibration curve based on scanning of aluminium foils with well-known thicknesses.

The relation has a form as expressed in figure 3, which means that there is not only linearity between the time and the distance (the sound velocity in aluminium) - expressed by A, but also a certain offset - expressed by B.

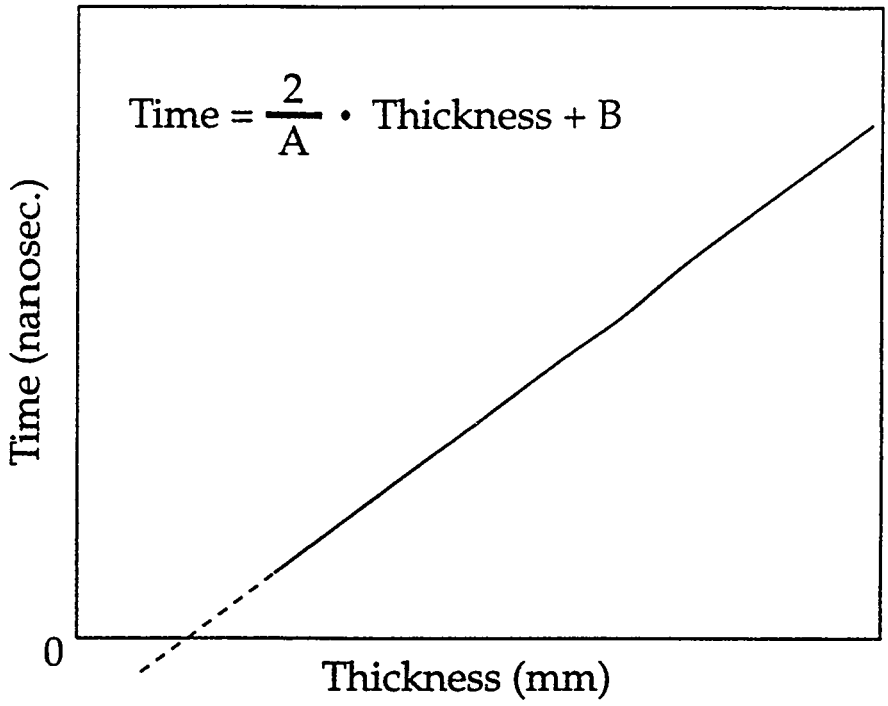

Figure 3. Calibration curve.

4. SENSITIVITY OF THE THICKNESS MEASUREMENTS

As mentioned above, the sensitivity of thickness measurement is normally 0.03 mm and it would be desirable to reduce this to about 0.01 mm. In an effort to fulfil this two approaches have been investigated.

4.1. Panametric 5218.

The ultrasonic part of our equipment -HFUS 2000- is mainly designed for evaluation of composite materials. Therefore it is not optimized for high precision thickness measurements. Special equipment for this purpose can make measurements with a sensitivity of 0.01 mm in metallic materials.

We have tested Panametric 5218, which is equipment especially designed for very accurate measurements of small thicknesses, including the possibility to measure on repetition echoes. In our case it is only possible to measure to the first echo from the core because the repetition echoes from the surface of the porous core are too small and disturbed by other echoes from the core. Our investigation showed that even the first reflection echo was too small and unstable to be used for scanning examination. It was concluded that this type of equipment could not be used for our specific purpose.

4.2. Average Measurements (HFUS 2000).

The time measurement is made with a "flying" digital clock which is started and stopped on echoes from the material. The clock measures in steps of 10 nanosec. This means that repeated measurements taken at the same position will alternate between integer numbers in units of 10 nanosec. For aluminium this time corresponds to a thickness of approximately 0.03 mm. The sensitivity can be improved if the time unit is further reduced. This is not possible for our present equipment, but calculation of an average time (AVG) may improve the sensitivity in the following way.

If optimal resolution during scanning is not required, scans can be made in a more open pattern. If for example a resolution of 0.1 mm is selected, only the last out of 10 measurements taken will be stored.

Some modification in the software made it possible to use all 10 measurements taken for calculation of an average time for each measuring point in the scanning line. This average value is then stored as an integer in units of nanosec, instead of in units of 10 nanosec as in the standard software. The corresponding thickness is thus also calculated with a better sensitivity. This has been proven in practice by scanning foils in aluminium. Figure 4 shows for the same scanning line the calculated average measurement together with single measurements recorded for one of these foils scanned with a resolution of 0.1 mm equal to 10 values for each point. It can be seen that the spread is reduced considerably by using average measurements.

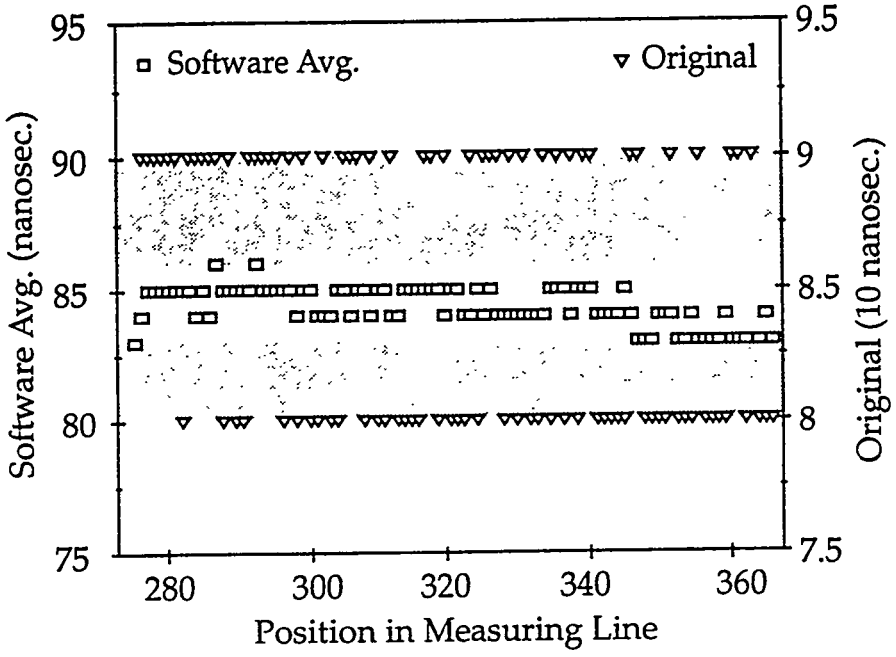

Figure 4. Measurements of 0.35 mm thick Al-foil.

Using the average measurement we are now able to measure the time and calculate the corresponding thickness with a better sensitivity.

5. THE MINIMUM MEASURABLE THICKNESS

When calculating a cladding thickness (or a foil thickness) it is a requirement that a core reflection echo (or back surface echo) falls within a preset measuring gate (a time interval) and the size of the echo has to be higher than a preset threshold.

In figure 5, two different echo patterns from aluminium foils are illustrated. In picture A the back surface echo (BS) falls within the measuring gate (shown at the bottom). In this case, the time of flight between the interface echo (IF) and the BS is recorded and stored. In picture B, the back surface echo occurs to early compared to the measuring gate and no time, or an incorrect time, is measured.

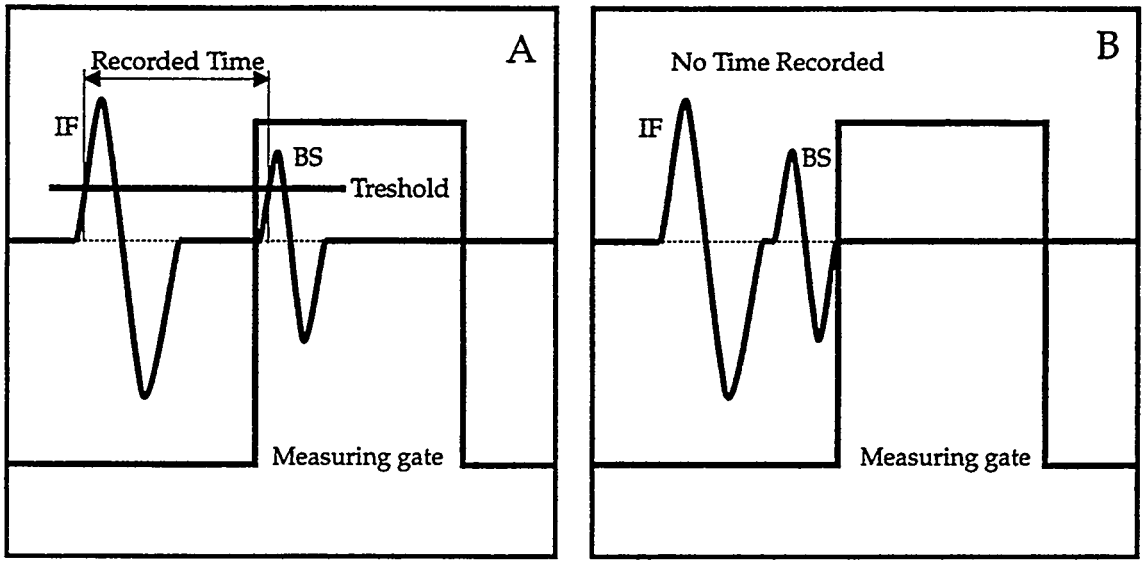

Figure 5. Two different echo patterns.

The starting point and length of the measuring gate can be varied within certain limits. The starting time (delay after the IF echo) has a minimum value due to delays in the electrical circuit. If the time from IF to BS is smaller than this minimum value, it cannot be measured (Figure 5 B) and a corresponding cladding thickness cannot be calculated.

In 1992 the minimum time our equipment was able to measure corresponded to an aluminium thickness of 0.35 mm. To measure smaller thicknesses the starting point of the measuring gate has to be moved closer to the IF.

5.1. Delay Module.

A delay module for our ultrasonic equipment has been tested. With this module the signals are artificially delayed in an electronic circuit and the measuring gate thereby placed closer to the IF (even before the IF). The delay module worked very well but

when tested on fuel plates, oscillations from the IF were increased and extended in time and thereby caused interference with the CS signal.

Thus, the delay module could not be used to reduce the minimum measurable cladding thickness.

5.2. New Digital Gates.

Our scanning system has recently been upgraded with new hardware and software including new digital measuring gates. These gates have made it possible to set the starting point closer to the IF than before.

Installation of the new digital gates has improved the capability of the system and has made it possible to reduce the minimum measurable thickness considerably. This improvement is illustrated in figure 6, which shows calibration curves based on Al-foils measured with old and new measuring gates.

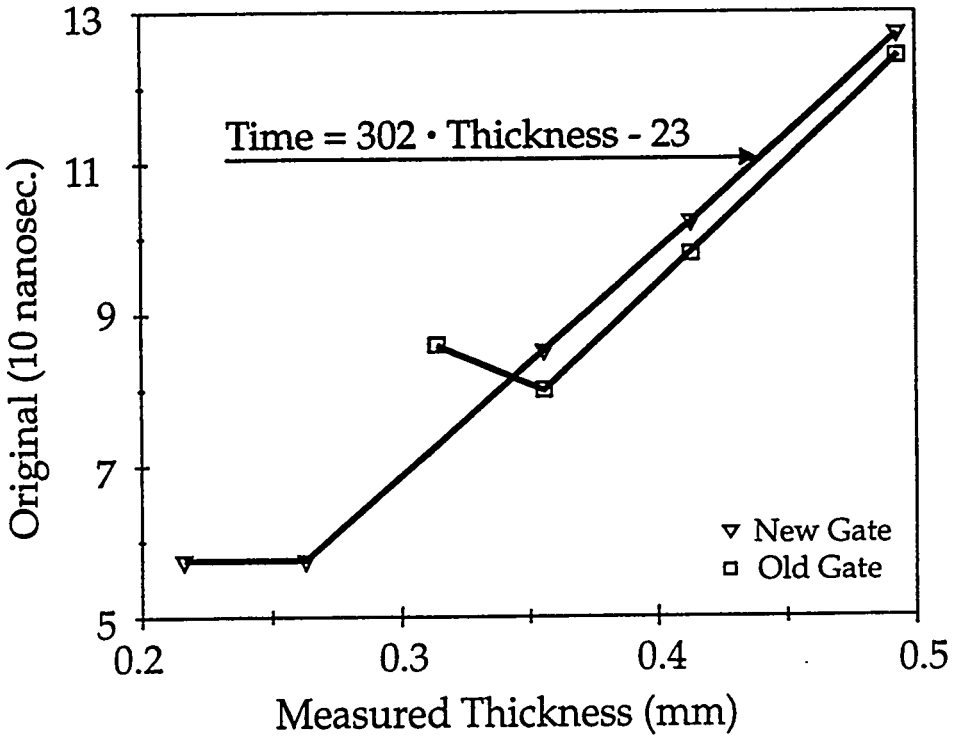

Figure 6. Foil thickness measurements.

The 6 aluminium foils were measured with a micrometer screw gauge to the following thicknesses: 0.493; 0.413; 0.356; 0.314; 0.263 and 0.216 mm.

The time average measurements are extracted from one scanning line crossing all 6 foils. From the figure it can be seen that:

when tested on fuel plates, oscillations from the IF were increased and extended in time and thereby caused interference with the CS signal.

Thus, the delay module could not be used to reduce the minimum measurable cladding thickness.

5.2. New Digital Gates.

Our scanning system has recently been upgraded with new hardware and software including new digital measuring gates. These gates have made it possible to set the starting point closer to the IF than before.

Installation of the new digital gates has improved the capability of the system and has made it possible to reduce the minimum measurable thickness considerably. This improvement is illustrated in figure 6, which shows calibration curves based on Al-foils measured with old and new measuring gates.

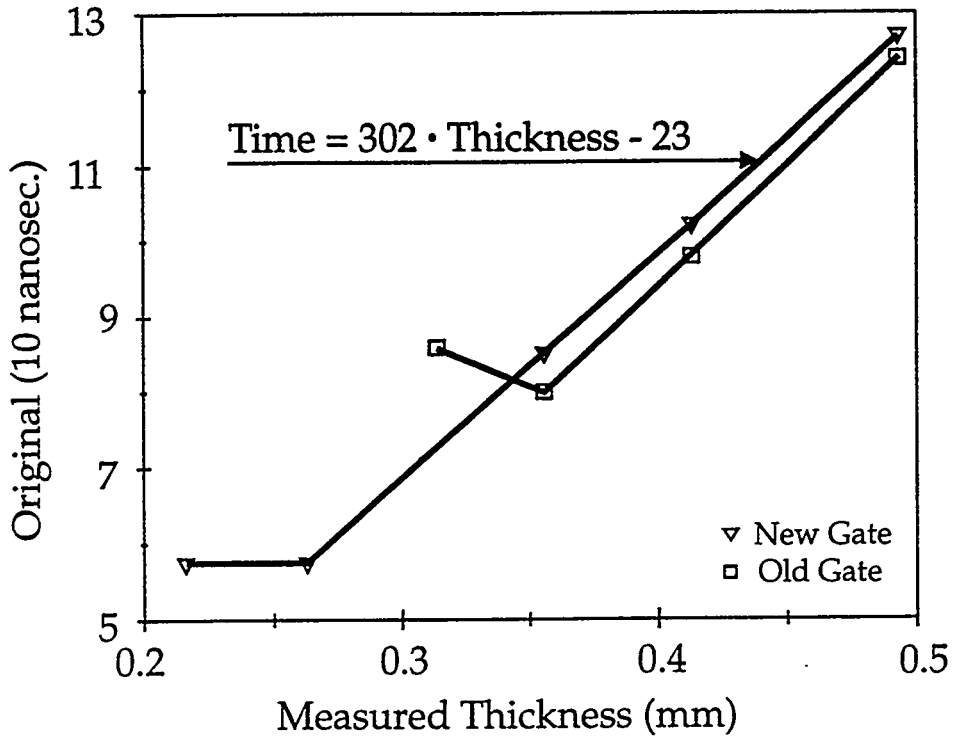

Figure 6. Foil thickness measurements.

The 6 aluminium foils were measured with a micrometer screw gauge to the following thicknesses: 0.493; 0.413; 0.356; 0.314; 0.263 and 0.216 mm.

The time average measurements are extracted from one scanning line crossing all 6 foils. From the figure it can be seen that:

1. With the old gate we almost have linearity for the ultrasonic measurements down to the 0.356 mm foil thickness.

2. For the new gate the linearity in the measurements goes down to the 0.263 mm foil thickness. From this line the following equation can be found between measured foil thickness in mm and measured time in nanosec:

$$TIME = 302 * THICKNESS - 23$$

or the inverse

$$THICKNESS = 0.0033 * TIME + 0.076$$

6. SCANNING OF FUEL PLATES

When scanning a LEU fuel plate the greatest variation in cladding thickness will normally be seen at the core ends where some dogboning is present. Figure 7 shows how the result of scanning of a fuel plate core end can be presented. The scan is made with a resolution of 0.1 mm and the colours represent different thicknesses in steps of approximately 0.03 mm.

Using the calibration found for foils, we have scanned a core area with a resolution of 0.05 mm and made both normal and average measurements (out of 5). This scan is shown in figure 8, and in figure 9 we have, for a single scanning line (see location in figure 8), compared the normal measurement to the average measurement of the thickness. It can be seen that the sensitivity is better for the average measurement, which also tends to reflect a real thickness variation in a better way.

In figure 10, the same average measurement is compared to the thickness of the cladding in a metallographic prepared sample of a cross section in the fuel plate following the scanning line. Although it is difficult to exactly locate the position and prepare a sample without restoring some fuel particles in the boundary area, our thickness measurement, based on the above equation without the offset, looks to represent the cladding thickness very well. The small relative variation between the scanning line and the two adjacent lines (0.05 mm apart), which all are shown at the bottom indicates that the measurements are reproducible and thus reliable, even though at some places they also express local changes in the core surface. The offset found for the foils seems only to be correct at the very first thin core end.

The comparison indicates that even if we are able to measure the time of flights to the core echo very accurate more tuning of the equipment and calibration to well known cladding thicknesses are needed before the measurements can be used for checking fuel plates.

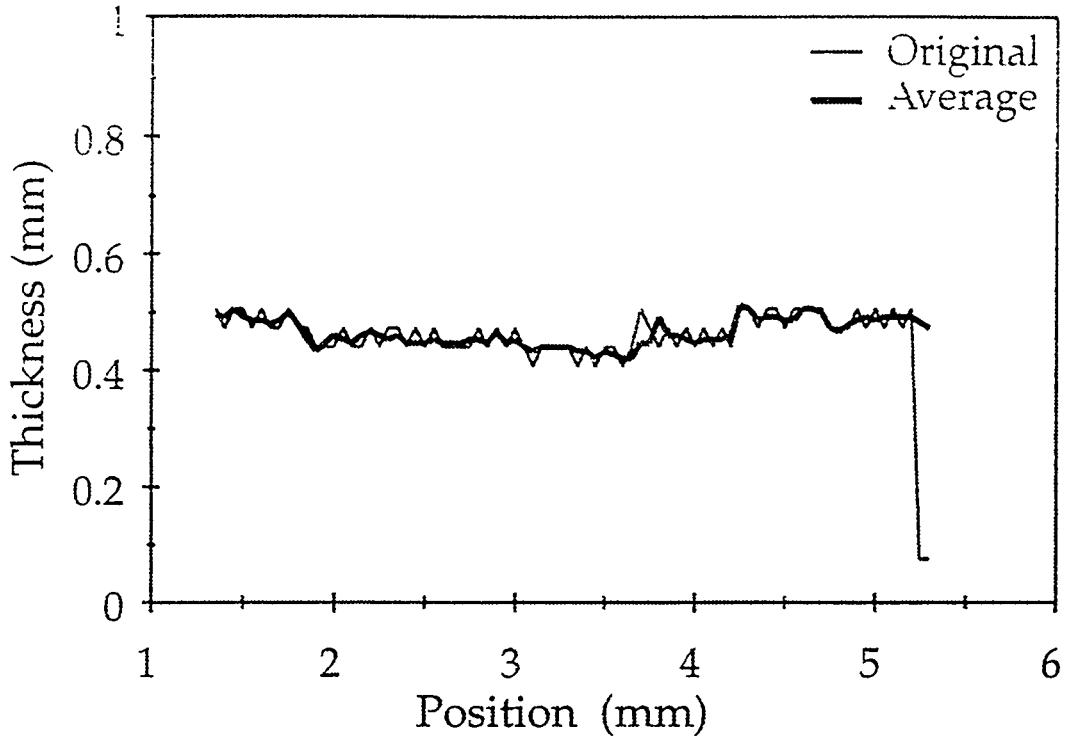

Figure 9. Normal and average measurements in fuel plate.

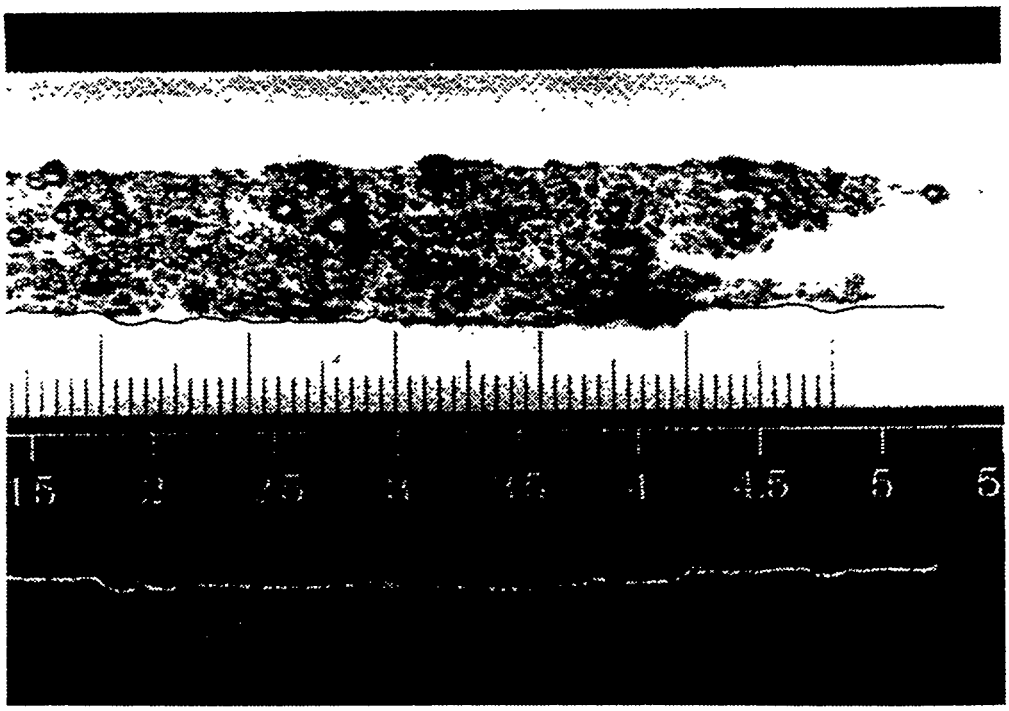

Figure 10. Metallographic prepared cross section in a fuel plate for comparison of cladding thickness with scanned measurements from the same position. At the bottom the scanning line is shown together with the two adjacent lines (0.05 mm apart).

Our new software is more flexible and we can analyze each scan in many new ways. It is possible to scan large areas with high resolution for later examination in details We can make profiles (single scanlines) in both directions and the colour palette can be adjusted so all colours are used for a short distance.

Figures 11 and 12 show a scan made with the new software with maximum resolution and optimal use of the colour palette. Figure 12 shows a partial area of figure 11.

7. CONCLUSION

We have improved our ultrasonic scanning system to measure smaller minimum cladding thicknesses with a better sensitivity. This enables us to use the concept to check, non-destructively, our standard fuel plates for DR3 against the minimum cladding thickness requirement.

With our system we have a tool which improves the statistical background for accepting fuel plates. If the system is further developed it may be posible to measure even thinner claddings, which may be necessary for making fuel plates with high uranium loadings .

ACKNOWLEDGEMENT

The authors wish to thank L.Eschricht and K.L.Jensen for their invaluable contribution to the ultrasonic scanning measurements and evaluations.

REFERENCES

Ref.1: P.Toft, J.Borring, E.Adolph, T.M.Nilsson, Risø National Laboratory, Denmark. " Quality Assurance and Ultrasonic Inspection Studies in LEU Fuel Element Fabrication", presented at the RERTR meeting in Roskilde, Denmark, September 27 - October 1, 1992.

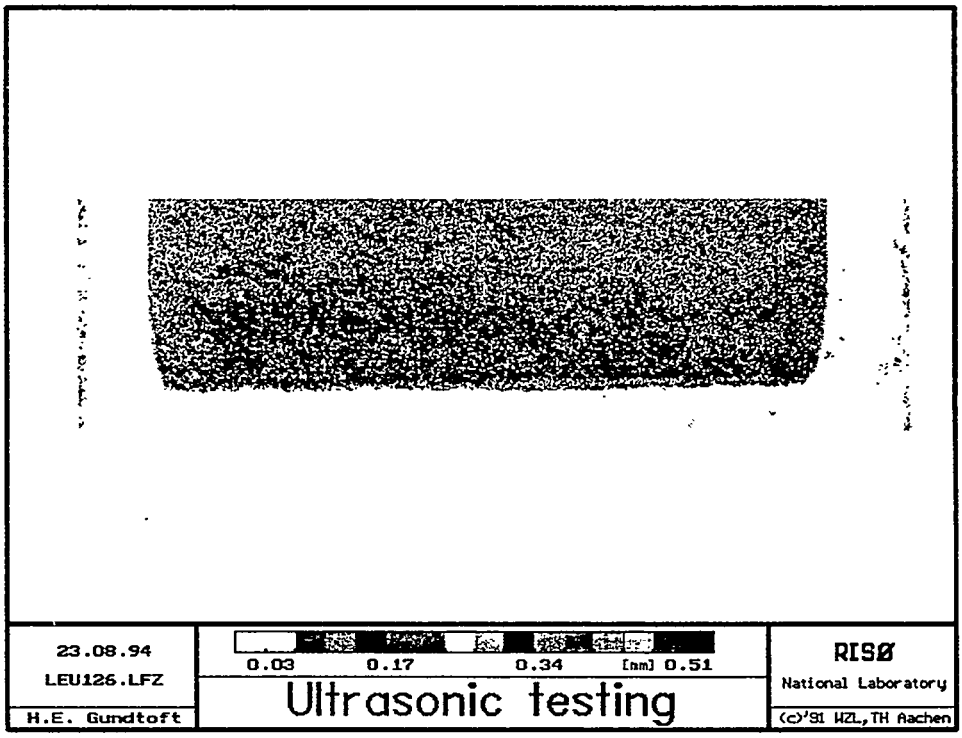

Figure 7. Distance plot of fuel plate end (30 x 110 mm).

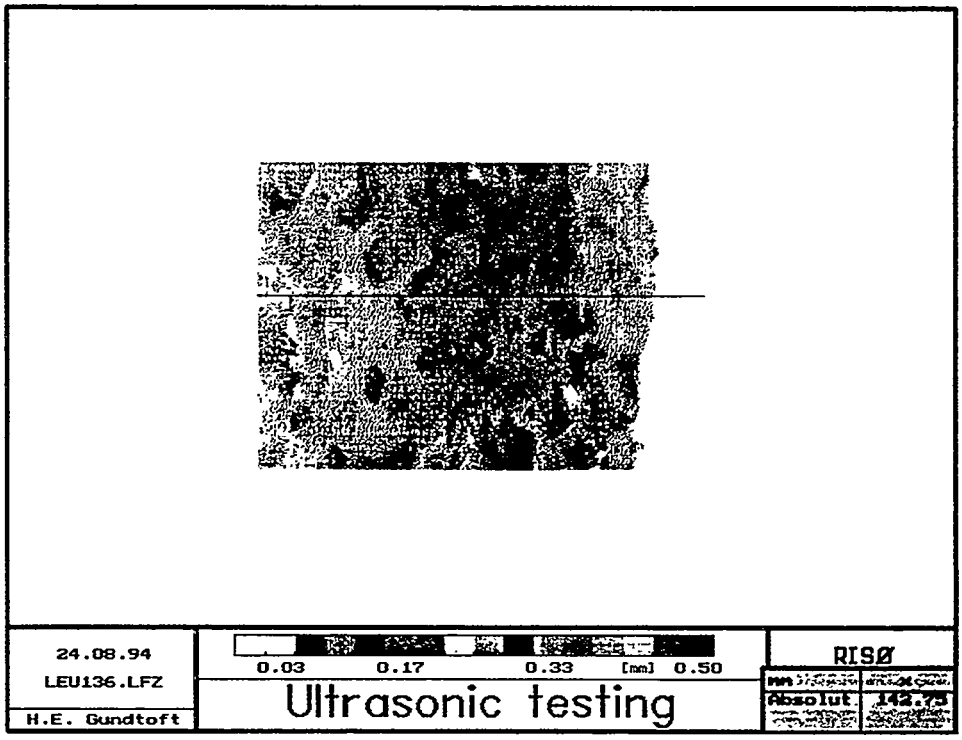

Figure 8. Distance plot of a section (4 x 6 mm) of a fuel plate end. End to the right.

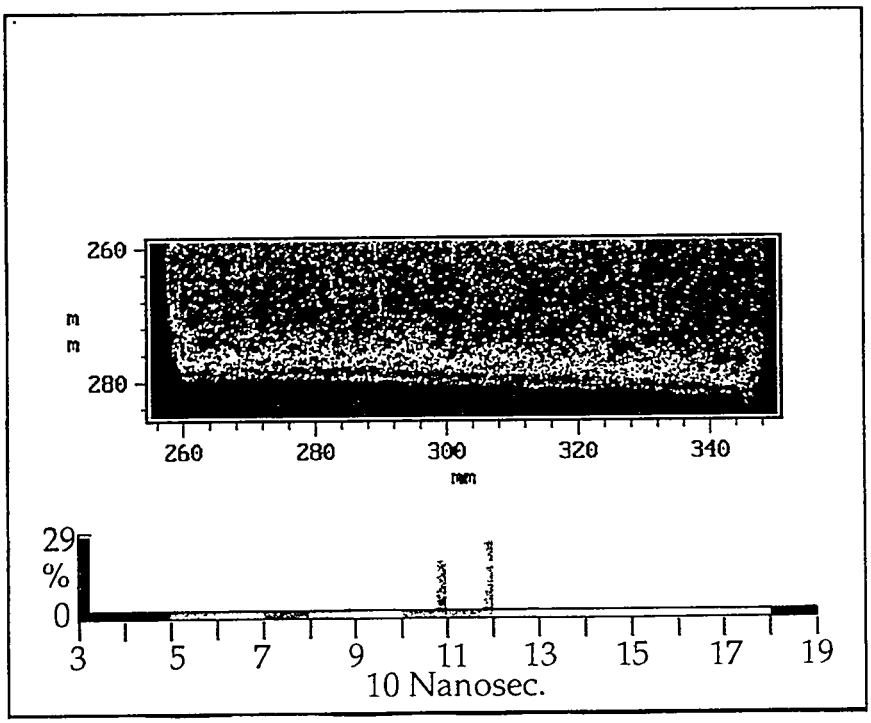

Figure 11. Scan made with new software. At the bottom the distribution on the different colour (time) levels is given in percent.

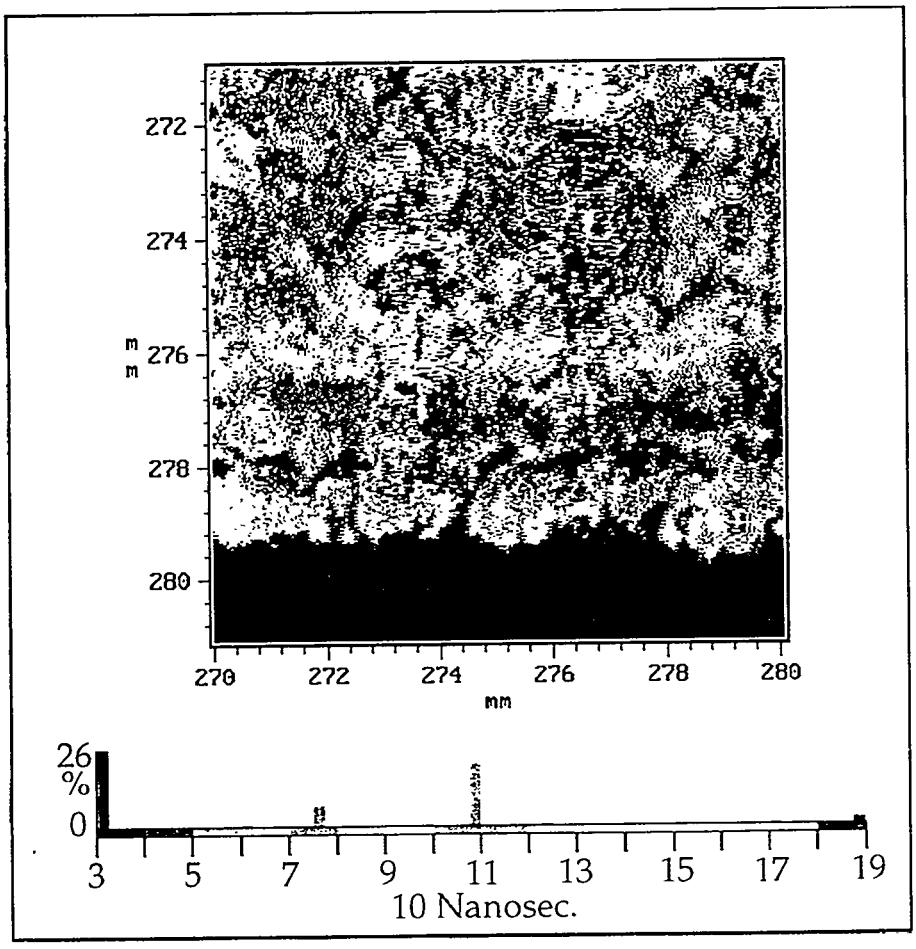

Figure 12. Detail of the scan shown in figure 11.

SESSION III

September 20, 1994

FUELS

Chairman:

G. Copeland
(ORNL, USA)

PRELIMINARY DEVELOPMENTS OF MTR PLATES WITH URANIUM NITRIDE

J.P. Durand - P. Laudamy (CERCA)
K. Richter (European Commission, Joint Research Centre, ITU)

C E R C A
Zone Industrielle "Les Bérauds"
B.P. 1114
26104 ROMANS - FRANCE

I T U
Kommission der Europaischen Gemeinschaften
Institut für Transurane
Postfach 2340
76125 KARLSRUHE - GERMANY

ABSTRACT

In the opinion of CERCA, the total weight of Uranium per MTR plate (without changing the external dimensions) cannot be further increased using U_3Si_2. Limits have been reached on plates with a thicker meat or loaded to 6g Ut/cm^3. The use of a denser fuel like Uranium mononitride could permit an increase in these limits. A collaboration between the Institute for Transuranium Elements (ITU), Joint Research Centre of the European Commission, and CERCA has been set ut. The preliminary studies at the ITU to check compatibility between aluminium and UN proved that there are no metallurgical interactions below 500 °C. Feasibility of the manufacturing, on a laboratory scale at CERCA, of depleted Uranium mononitride plates loaded to 7 g Ut/cm^3 has been demonstrated. The manufacturing process, however, is only one aspect of the development of a new fuel. The experience gained in the case of U_3Si_2 has shown that the development of a new fuel requires considerable time and financial investment. Such a development certainly represents an effort of about 10 years.

INTRODUCTION

Since the very beginning of Material and Test Reactor (MTR) fuel production at CERCA, about 30 years ago, there has been a constant need for an increase in the uranium loading per plate. With the conversion to Low Enriched Uranium in order to assure non-proliferation, the increase in uranium loading has become more important. CERCA has been an active member in this development and has worked on the three following ways to increase the total weight of uranium within a plate without changing the external dimensions:

- Use of denser fuel particles (U_3Si_2 instead of UAl_x)
- Increase in the volume of the meat (reducing the cladding thickness)
- Increase in the volume fraction of fuel particles

As CERCA places the priority on the development of existing manufacturing processes, other ways such as the wire concept or the use of the Hipping developed by ANL, are not mentioned as they require a big change in the manufacturing technology.

The first procedure has been developed since the beginning of the RERTR programme and the uranium loading per cubic centimeter of meat has been increased by 2.5 using U_3Si_2 fuel instead of UAl_x keeping the same volume fraction of fuel particles. For example, in this case, an UAl_x plate loaded to 1.9 g Ut/cm^3 leads to a plate loaded to 4.8 g Ut/cm^3 when U_3Si_2 fuel is used.

The second way has been in development for the French CEA since 1992. U_3Si_2 plates loaded to 4.8 g Ut/cm^3 with a meat thickness of 0.59 mm instead of 0.51 mm (keeping the same plate thickness) were manufactured and are under irradiation tests [1]. The first irradiation cycle has been completed. Other cycles will follow and the results are expected by the end of 1995. However, this method is limited by the fact that the cladding thickness cannot be reduced indefinitely.

In the third method CERCA has developed an advanced process since 1992 [2] which allows the manufacturing problem linked to the high volume fraction of fuel particles (dog bone and homogeneity) to be overcome. The maximum uranium loading attainable with U_3Si_2 fuel is 6 g Ut/cm^3. Above this value, the volume fraction of U_3Si_2 is too high and the meat becomes very difficult to deform homogeneously even with the advanced process [3]. In 1994 the French CEA has ordered 5 enriched plates loaded to 6 g Ut/cm^3 for irradiation tests.

In the meantime, a great deal of development has been carried out in Europe on a dense mixed nitride fuel for power reactors. The INSTITUTE FOR TRANSURANIUM ELEMENTS (ITU) as well as the French CEA have substantial experience both on fuel manufacturing and on behaviour under irradiation at their disposal.

To continue the MTR fuel development program CERCA recently started a collaboration with the ITU, who, for many years, have been developing nitride fuels containing a high weight percentage of uranium for Fast Neutron Reactors. Taking advantage of this experience, the first procedure mentioned above, "the use of a denser fuel", could be developed further .

As an exploratory development program CERCA and the Institute for Transuranium Elements put their knowledge and experience together to test, on a laboratory scale, the manufacture of MTR plates combining the advanced process of CERCA (allowing high volume fraction of fuel within the meat) and the use of uranium nitride fuel (containing a high weight percentage of uranium). Using this method, plates with a very high uranium density around 7 g Ut/cm^3 could be expected.

This paper is divided in two parts. The first part presents the work done at the ITU concerning the uranium nitride compound and its comparison with silicide compound. The second part deals with the results of the manufacturing test of MTR plates at CERCA.

1. THE URANIUM NITRIDE COMPOUND

1.1. Nitride fuel development at ITU

A project "Optimisation of Dense Fuels" was started in 1985 with a programme to fabricate, test and optimise "pure" mixed nitrides, i.e. fuels containing about 500 ppm of both carbon and oxygen for high burn-up in fast reactors.

Development of uranium and uranium-plutonium nitride fabrication processes

The development work was based on previous experience on nitride fuel fabrication within the frame of the ITU - swelling project during the years 1973-76 (irradiation experiments in DFR, RAPSODIE, BR2 and SILOE). Nitride fuels have been fabricated with densities between 90 and 94 % of the theorical density both by the carbothermic reaction of oxide-carbon blends and by the metal-hydride-nitride route with subsequent ball milling, pressing and sintering of the reaction product. Both processes gave similar results with respect to fuel composition and density [5,6].

For the further development of denser fuels, the carbothermic reduction route was chosen, because it has generally been adopted as a technologically acceptable process and avoids handling of fissile material in metal form .

The mixed nitride fuel development programme was started in collaboration with the Département d'Etudes des Combustibles à Base de Plutonium, CEA, Cadarache.

Two special begin of life (BOL) irradiation tests NILOC (NItride Low in Oxygen and Carbon) 1 and 2 were prepared and irradiated in the High Flux Reactor in Petten (irradiation begin Dec. 1986 and Feb. 1987).

For the fuel fabrication for NILOC 1 and 2 , the "green pellets" (before sintering) were prepared at ITU by three different methods, i) by the conventional powder technique, ii) by direct pressing of the clinkers resulting from carbo-reduction and iii) by a modification of this latter method, the direct pressing of granules.

A first fast flux nitride irradiation, NIMPHE 1 (Nitrure Mixte dans Phenix à joint HElium) was started in the Phenix reactor in October 1987. A second irradiation NIMPHE 2 in which the irradiation performance of carbide and nitride is being compared under the same in-pile conditions was started in October 1988. The fuel specifications were the same for the NILOC and NIMPHE experiments. The irradiation conditions for the NILOC experiments were chosen to simulate those of NIMPHE 1 and 2 in the PHENIX reactor. However, the NIMPHE irradiations are scheduled to achieved a high burn up (> 15 $^{a}/_{o}$).

The powder reactivity, agglomerate size as well as the dimensions of the pressed compacts pressed of the oxide-carbon blend are important paramaters wich influence the rate and degree of reaction.

The synthesis of nitrides by carbothermic reaction of an oxide-carbon blend was continuously controlled by monitoring composition of the reaction gas. This proved to be an excellent fabrication control.

Besides the fabrication-oriented process parameters, the kinetics and rate-controlling mechanisms of the PuO_2-UO_2-C-N_2 and H_2 reaction were studied in the temperature range of 1500 to 1700°C by thermogravimetry and X-ray analysis [7].

The fabrication method for nitride fuels, based on a carbothermic process, was developed to a degree which allows the fabrication of mixed mononitride fuel pellets, according to present specifications, with a process applicable under industrial production conditions.

The joint investigations of CEA and ITU in the last years have shown that uranium or uranium - plutonium nitride pellets can be fabricated in conventional mixed oxide installations with an additional step for the carbothermic reduction of the oxides under a nitrogen and a mixed nitrogen- hydrogen atmosphere. The consolidation of the nitrides is performed by either the classical procedure (comminution, cold pressing and sintering) or direct pressing (cold pressing of the nitride reaction product in form of pellets or granulate and then sintering).

The product obtained by these methods meets target specifications. Nitrides with the required characteristics were fabricated with a good reproducibility and in large enough quantities to feed an irradiation program [8, 9, 10, 11].

1.2. Comparison of properties

1.2.1. Uranium silicide and nitride compound :

	U_3Si_2	UN	Delta
- Uranium Content (wt %)	92.7	94.4	+ 1.8 %
- Volume weight (g/cm^3)	12	14.3	+ 19.2 %
- Uranium Density (gU/cm^3)	11.1	13.5	+ 21.6 %

1.2.2. Plate loading

Theoretical loads within the meat of MTR plates as a function of volume fraction of the compound are given below :

Vol %	U_3Si_2	UN
43 %	4.8 g Ut/cm^3	5.8 g Ut/cm^3
54 %	6 g Ut/cm^3	7.3 g Ut/cm^3

1.3. Irradiation behaviour of mixed nitrides and uranium nitride

In a series of fuel performance tests [12, 13, 14, 15], the irradiation potential of mixed uranium-plutonium nitrides has been demonstrated.

Conclusion

Mixed nitrides are strong candidate fuels for advanced liquid metal cooled fast reactors. They possess the merits of oxide fuels with regard to good irradiation behaviour. Besides nitrides have :

- a higher thermal conductivity
- a higher density of fissile atoms with the capability to attain high burn-up
- a straight forward reprocessing, compatible with the established reprocessing method in Europe, the Purex process
- easy handling during fuel fabrication and storage
- and are compatible with the fast reactor coolant sodium.

The above mentioned irradiation experiments were carried out with porous fuels (83 - 88 % TD), He-bonding, high linear ratings and fuel temperatures.

With respect to the irradiation behaviour of MTR fuels, irradiations with Na-bonded fuels, with a high fuel density (> 92 % TD) and low fuel temperature during operation would be more representative. The working conditions can be regarded as constant over a large burn-up range associated with a high fission gas retention and a low fuel swelling rate.

The few data on Na bonded MN are for burnups < 4.5 at % and for nitrides with relatively high level of metallic impurities and oxygen. The temperatures are much lower than in He bonded pins but they are still high compared with MTR fuel [16]. As would be expected from the solid state properties, the nitride shows less restructuring, smaller gas release and less swelling at constant temperature than the carbide for wich much more data exists. With further reduced temperatures one can expected further reductions in gas release and swelling. It is well known and supported by measurements on irradiated nitrides [17] these processes are strongly enhanced with increased temperature. Extensive ion implantation studies performed with fission rare gasses and UN at low temperature [18] have confirmed the beneficial behaviour of UN. Though high fission gas concentrations were used corresponding to those reached at ~ 20 at % burnup, the UN showed some radiation damage but was structuraly stable. Neither break away swelling (known from U metal) nor the large swelling known to occur in U3Si2 [19] were observed .

However, reactors irradiations of UN of low temperatures to very high burn up have not been performed yet. Only such irradiations would give the final answer for the irradiation performance. Beside the temperature, the grain size should be a parameter for such an irradiation since grain boundaries are effective sinks for both fission gas atoms and for point defects thus influencing gas release and swelling also in the athermal range, hence at low temperature.

1.4. The manufacturing of uranium nitride compound at ITU

The uranium nitride was fabricated by carbothermic reduction of a mixture of uranium oxide with carbon powder. After compaction the material was treated under flowing nitrogen and/or a nitrogen-hydrogen mixture in the temperature range of 1100 - 1600 °C. The reaction product was crushed, ballmilled, recompacted and sintered at 1650 °C.

The sintered material was transformed into powder with a specified size distribution.

Figure 1 shows Scanning Electron Micrographs of Uranium powder manufactured at the ITU, which demonstrate that the carboreduction process leads to a powder with an internal porosity of about 10 %. Depending on the carboreduction parameters more or less porosity can be obtained. The porosity level can be optimised with respect to thermal conductivity and fission gas retention.

1.5. Compatibility of UN and aluminium

Before manufacturing plates the metallurgical compatibility of UN and Aluminium was investigated. A dilatometric analysis was carried out on a sandwich made of a pellet of UN between two discs of aluminium. Figure 2 shows the dilatometric graph obtained. A slow expansion of the sample until about 550 °C was observed. Thereafter a fast interaction begins and the sandwich collapses at 620 °C (melting). Similar results were reported in 1966 by D.E. Price [20].

As a metallurgical reaction seems to occur at about 550 °C, compacts made of UN powder mixed with Al powder were heated at 480, 550 and 580 °C for 5, 15 and 20 hour period under argon atmosphere. Optical micrographs, X-ray analysis and Scanning Electron Microscopy gave the following information :

- 480 °C: no diffusion detected
- 550 °C: a slight swelling at the interface between UN and Al but no new phase is detected by X-ray analysis
- 580 °C: a new phase, mainly UAl_3, is detected at the grain boundaries

As a base of comparison U_3Si_2 reacts rather rapidly with aluminium above 600 °C to produce $U(Al,Si)_3$. At 500 °C no reaction zone can be seen in optical micrographs [4].
Uranium nitride does not seem to be more reactive with Aluminium than U_3Si_2 fuel.

2. PRELIMINARY MANUFACTURING TESTS OF MTR PLATES WITH URANIUM NITRIDE

As the studies carried out by the ITU prove that there is no incompatibility between UN and Al below 500 °C, the logical continuation was to set up a preliminary manufacturing test of MTR plates.

ITU manufactured for CERCA depleted uranium mononitride powder and CERCA manufactured a few plates applying the advanced process developed for high uranium densities with U_3Si_2. As the main advantage of the uranium nitride is its high uranium content, the aim of this test was to manufacture plates containing about 7 g Ut/cm^3.

The most interesting results of this manufacturing test on a laboratory scale are given by the Scanning Electron Micrographs. Figure 3 shows a comparison between an uranium nitride and a U_3Si_2 plate. First of all the plates look very similar. On both plates the meat itself has a good metallurgical cohesion. Furthermore the Blister Test did not reveal any lack of bonding between the meat and the cladding.

The overall porosity of the UN plate is about 16 %. Less than an half of this is due to internal porosity of UN particles. This porosity leads to a plate with an uranium density close to 7 g Ut/cm^3.

As can be seen in Figure 4 Scanning Electron Microscopy does not reveal any new phase formed between UN particles and the aluminium matrix with the plate manufactured under CERCA parameters. A new phase (mainly UAl_3) can be seen with a plate which has been overheated at 580 °C.

These results seem to confirm the information given by the studies of ITU wich showed the good compatibility of uranium nitride and aluminium below 500 °C.

CONCLUSION

Even if the market at the moment (on a global point of view) does not express a significant need for densities above 6 g Ut/cm^3,CERCA, as one of the major MTR fuel manufacturers makes a point of exploring all the technological new ways which could be of interest for the reactors of tomorrow.

With this in mind, CERCA has developed in collaboration with ITU new high loaded plates using the denser uranium compound, the mononitride.

The Institute for Transuranium Elements which has a great experience with nitride fuels made the preliminary studies of compatibility between aluminium and UN and proved that there are no metallurgical interactions below 500 °C.

The feasibility manufacturing mononitride plates on a laboratory scale has been demonstrated at CERCA. It was confirmed that no metallurgical reactions occurred. The cohesion of the meat was good and no lack of bonding between the cladding and the meat was detected.

These preliminary investigations show that there are no incompatibilities between uranium nitride fuel and the manufacturing process of MTR plates. The use of mononitride could permit the increase of the maximum uranium loading to 7 g Ut/cm^3. Nevertheless, the metallurgical compatibility of uranium nitride and aluminium during the manufacturing process is only one aspect of the development of a new fuel. Other aspects include :

- A good irradiation behaviour of MonoNitride at high burn-up
- Acceptance of the new fuel by an international consensus
- The necessity of the RERTR program to cover the cost of irradiation and PIE, neutronic calculations and adaptation of computer codes, and the cost of a full core demonstration

Experience gained in the case of the U_3Si_2 has shown that the development of a new fuel requires a lot of time and investments. **Such developments certainly represent an effort of about 10 years.**

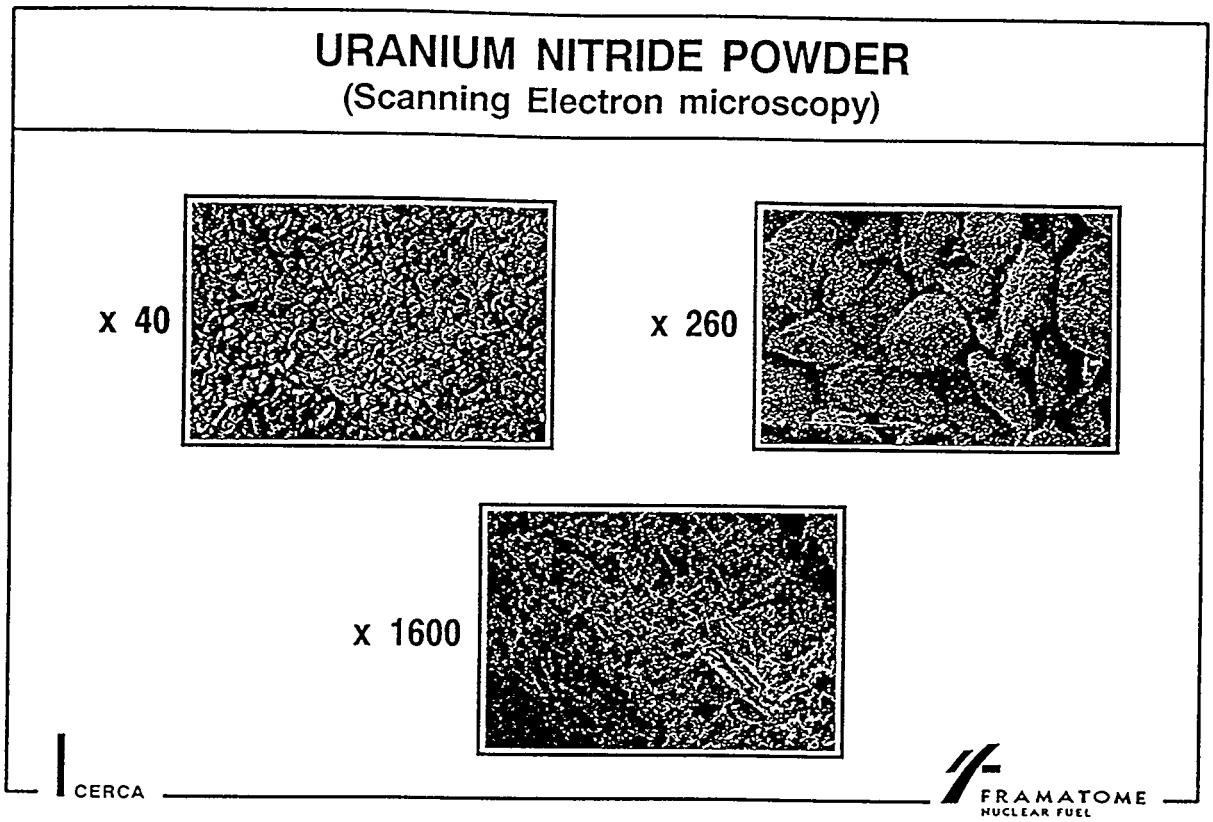

Figure 1

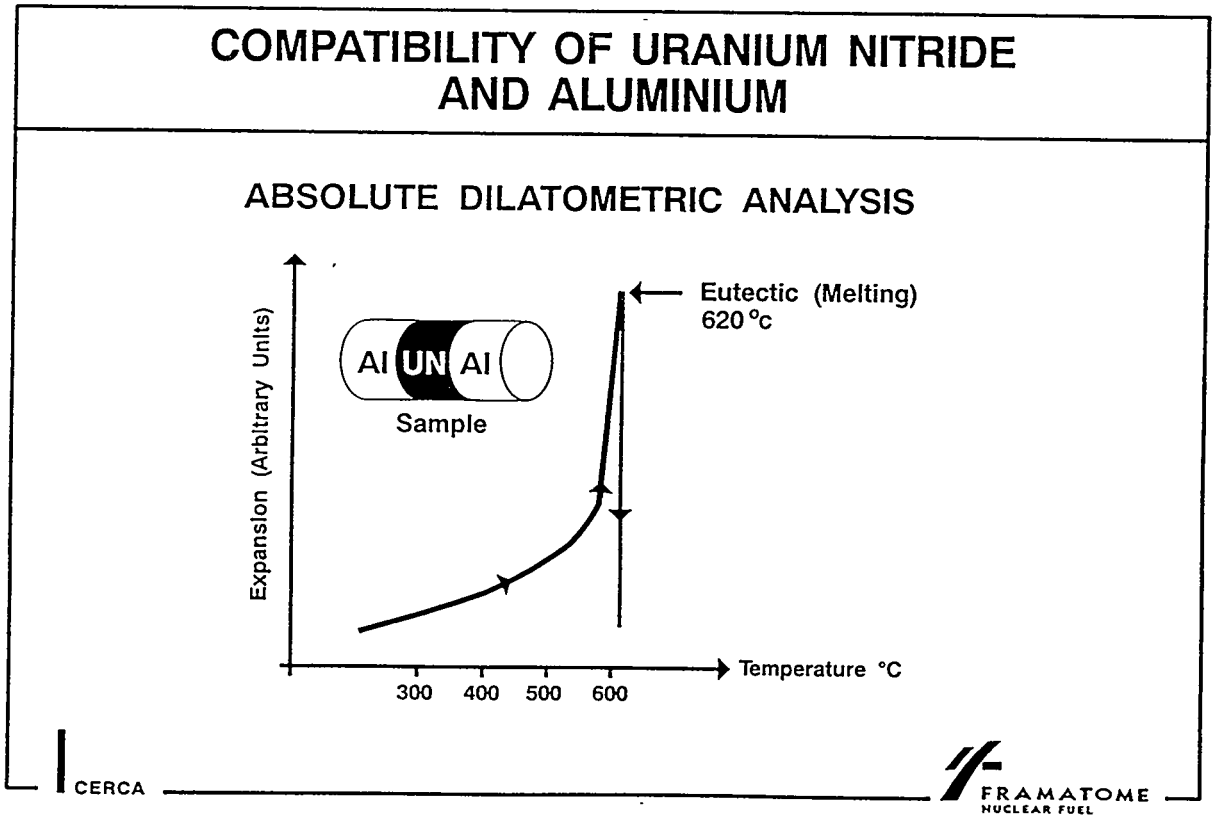

Figure 2

COMPARISON BETWEEN U_3Si_2 AND UN PLATES
(Scanning Electron microscopy)

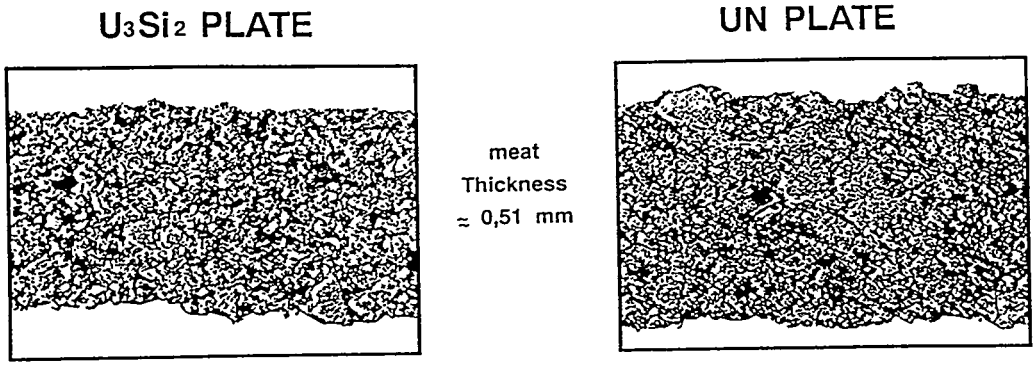

CERCA — FRAMATOME NUCLEAR FUEL

Figure 3

DIFFUSION TEST ON URANIUM NITRIDE PLATES
(Scanning Electron microscopy, Backscatter Electron)

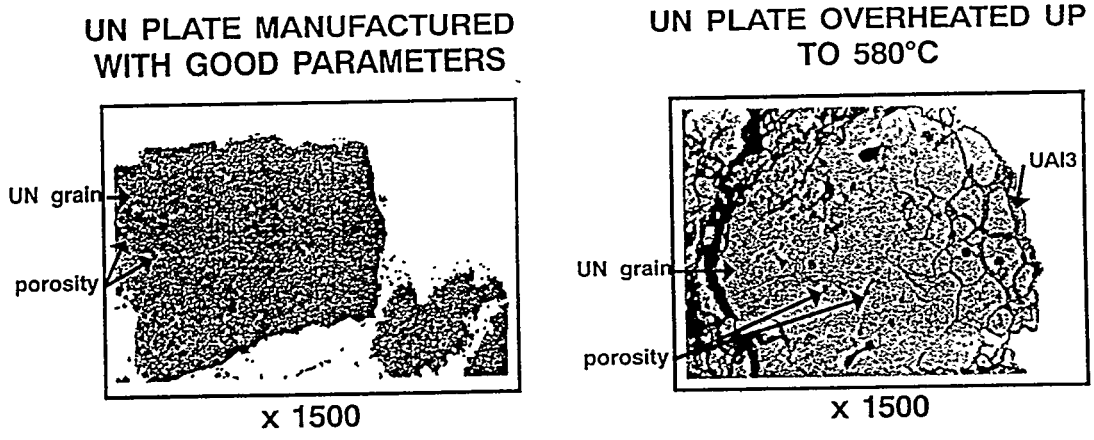

CERCA — FRAMATOME NUCLEAR FUEL

Figure 4

References

(1) Ballagny A., Beylot J.P., Paillere J., Durand J.P., Fanjas Y., and Tissier A., Optimization of silicide fuel elements, RERTR 1992 in Denmark

(2) Durand J.P. and Fanjas Y., LEU Fuel development at CERCA: Status as of October 1992, RERTR 1992 in Denmark

(3) Durand J.P. and Fanjas Y., LEU Fuel development at CERCA: Status as of October 1993, RERTR 1993 in Japan

(4) JL Snelgrove, RF Domagala, GL Hofman, TC Wiencek, GL Copeland, RW hobbs, RL Senn, The use of U3Si2 dispersed in Aluminium in plate type fuel elements for research and test reactors, Argonne National Laboratoty (ANL/RERTR/TM11)

(5) Richter K., Preparation methods for uranium-plutonium non-oxide fuels, Proc. European Nuclear Conf. Progress in Nuclear Energy Series, Paris, April 21-25, 1975, Pergamon Press (1976)

(6) Richter K. et al., Fabrication and characterization of MX-type fuels and fuel pins : Report I on Swelling of MX-type fuels 1973-76, EUR-6154 EN, Commission of the European Communities (1978)

(7) Pautasso G. et al., Investigation of the reaction UO_{2+x} + PuO_2 + C + N_2 by thermogravimetry, J. Nucl. Mat. 158, 1988, 12-18

(8) Muromura T. et al., Formation of uranium mononitride by the reaction of uranium dioxide with carbon in ammonia and a mixture of hydrogen and nitrogen, J. of Nucl. Mat. 80 (1979) 330-338 and 71 (1977) 65-72

(9) Richter K. et al., Direct pressing: a new method of fabricating MX fuel pellets, Nucl. Technology, Vol. 70, 1985, 401-407

(10) Bernard H. et al., Mixed Nitride fuels fabrication in conventional oxide line, Proc. Advanced Fuel for Fast Breeder Reactors: Fabrication and Properties and their Optimization, Vienna, 3-5 November 1987, IAEA-TECDOC-466, Vienna, 1988, 43-51

(11) Richter K. et al., Fabrication processes and characterization of LMFBR carbide and nitride fuels and fuel pins, Proc. Advanced Fuel for Fast Breeder Reactors: Fabrication and Properties and their Optimization, Vienna, 3-5 November 1987, IAEA-TECDOC-466, Vienna, 1988, 61-70

(12) Bauer A.A., Nitride fuels properties and potentials, Reactor Technology, Vol. 15-2 (1972) 87-104

(13) Richter K. et al., Fabrication and in-pile performance of helium-bonded mixed nitride fuel pins at the beginning of life, ANS Winter Meeting, San Francisco, California, November 26-30, 1989, Vol. 60 (1989) 319

(14) Richter K. et al., Investigation of the operational limits of uranium-plutonium nitride fuels, J. Nucl. Mat. 184 (1991) 167-176

(15) Prunier C. et al., European collaboration on mixed nitride fuel, International Conference on Fast Reactors and Related Fuel Cycles (FR '91), October 28 - November 1, 1991 Kyoto (Japan)

(16) Hj Matzke, Science of Advanced LMFBR Fuels, A monograph on Solid State Physics, Chemistry and technology of Carbides, Nitrides and Carbonitrides of Uranium and Plutonium, North Holland, Amsterdam (1986)

(17) C.Ronchi, I.L.F. Ray, H. Thiele and J. van de Laar, J. Nucl. Mater. 74 (1978) 193 , swelling analysis of highly rated MX type LMFBR fuels

(18) A Turos, S Fritf and Hj. Matzke, Phys. Rev. B41 (1990) 187, Defects in ion-implanted Uranium Nitride

(19) J. Rest and G.L. Hofman, J. Nucl. Mater. 210 (1994) 187, Dynamics of irradiation - induced grain subdivision and swelling in U_3Si_2 and UO_2 fuels

(20) Price D.E. et al., Compatibility of uranium nitride with potential cladding metals. Battelle Memorial Inst., Report Nr. BMJ-1760 (EURAEC 1591), Feb. 1966

DUAL FUEL GRADIENTS IN URANIUM SILICIDE PLATES*

Brett W. Pace, Research and Development Engineer
Research and Test Reactor Fuel Elements
Babcock and Wilcox
Lynchburg, Virginia, USA

ABSTRACT

Babcock & Wilcox has been able to achieve dual gradient plates with good repeatability in small lots of U_3Si_2 plates. Improvements in homogeneity and other processing parameters and techniques have allowed the development of contoured fuel within the cladding. The most difficult obstacles to overcome have been the ability to evaluate the bi-directional fuel loadings in comparison to the perfect loading model and the different methods of instilling the gradients in the early compact stage. The overriding conclusion is that to control the contour of the fuel, a known relationship between the compact, the frames and final core gradient must exist. Therefore, further development in the creation and control of dual gradients in fuel plates will involve arriving at a plausible gradient requirement and building the correct model between the compact configuration and the final contoured loading requirements.

INTRODUCTION

Creating a lateral fuel gradient in a fuel plate has been an ongoing production commitment at Babcock & Wilcox with the High Flux Isotope Reactor (HFIR) plates for many years now. The HFIR production process is stable and the production efficiency is good. Instilling lateral and longitudinal gradients in plates which may be required in the proposed Advanced Neutron Source (ANS), however, does not necessarily follow from the same practices as have been used when making HFIR plates. To create the dual fuel gradients, B&W has tested new methods of manufacturing compacts.

The goals of the development effort were threefold. The primary goal was the creation of a fuel gradient which changed the fuel core thickness across the width of the fuel core and down the length of the fuel core. Controlling this gradient in both directions would be the overriding concern of this goal. Complete monitoring of the resulting homogeneity of the fuel would be the second goal, which would require different parameters on the fuel powder used. After establishing the dual gradient the final goal was to ensure that the gradient could be established and controlled using different fuel loadings.

During development of the dual fuel gradient, B&W has manufactured 11 lots of uranium silicide (U_3Si_2) plates using different manufacturing processes on most of the individual lots. A total of 40 plates in all have been made with different degrees of success.

*Research sponsored by the US Dept. of Energy under contract #DE-AC05-84OR21400 through Martin Marietta Energy Systems, Inc.

DUAL GRADIENT FUEL CORES

Contour Design

B&W did not limit the scope of the development strictly to the feasibility of instilling and controlling dual gradients. The fact that a practical manufacturing solution must be found in order to be effectively utilized in a production environment was also considered. During development, feasibility of an idea allows for an almost excessive amount of freedom in the cost of succeeding in the development. Throughout this effort, B&W has maintained that the methods of manufacturing dual fuel gradient plates must be readily transferable to production using existing technology and maintaining reasonable production cost.

The design of the compact to be used in this development was constrained by the need to evaluate the fuel gradient in the final plate stage. Therefore, a significant change in core thickness had to be used to ensure that the differences in core thickness would be measurable and enable a better comparison between plates. The fuel core thickness in the final plate was designated to increase from 0.1mm at the corner of the fuel to 0.73mm in the center. To accomplish this, the fuel thickness portion of the compact respectively changed by 4.88mm. The actual compact design is shown in Figure 1. The fuel core at the final plate phase bulges in the middle and tapers outward toward the corners.

The gradient as described above yields a very thick unfueled layer of as much as 0.56mm on the ends decreasing to 0.25mm in the center of the plate. Using requirements such as these for this development, B&W is able to evaluate numerous possible problems and effects of making dual gradient contours. The thin unfueled layer in the center will be effected mainly when using higher loaded plates where greater concentrations of fuel may cause control problems in the thickness.

The gradient down the length of the plate was instituted on the bottom of the core and the gradient across the width of the plate was instituted on the top of the core. This was done to isolate the two gradients within the fuel to aid in evaluating the results and to make fabrication of the compacts easier. Even though additional sweeping of the fuel into the die cavities was required for the compacts, the isolation of each contour worked well with standard plate processing.

Homogeneity

All plates were monitored for homogeneity by x-ray densitometer measurements and by a digital homogeneity scanning device which measures the attenuation of X-rays passing through the fuel plates. The scanner has been quite useful in the past in evaluating the actual fuel contours on plates, and when combined with good graphics software can provide very helpful visual aides. The scanner readings are compared to standards and are a measure of the average and maximum of local homogeneity readings taken within an area of approximately 0.063 square centimeters.

DEVELOPMENT COMPACT DESIGN

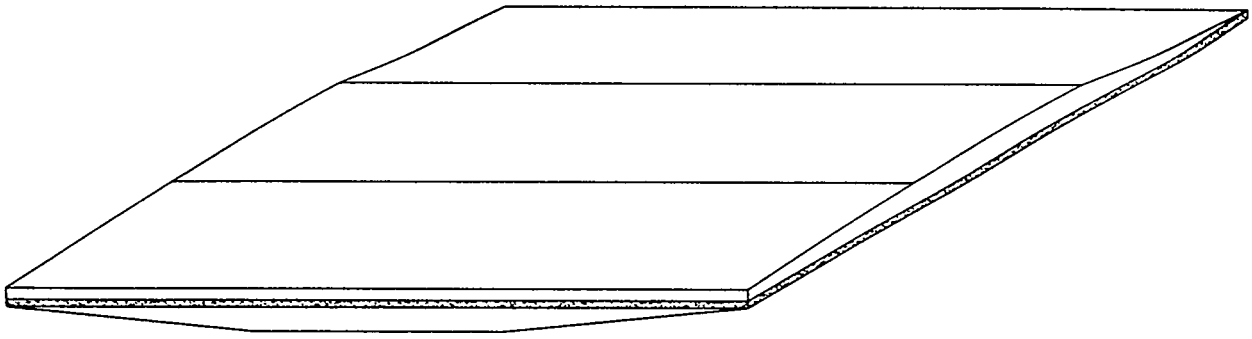

END AND SIDE VIEWS

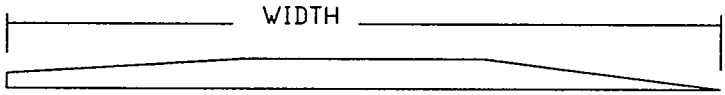

Top portion of compact.

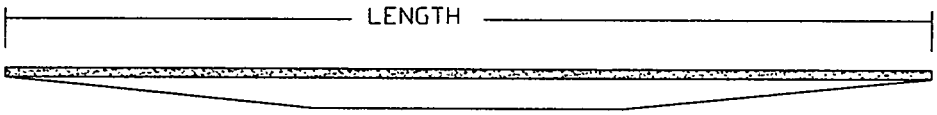

Bottom and lower portion of compact.

Figure 1. Compact configuration

Compaction Differentials

When the actual compaction of the fuel powder and aluminum matrix powder is made, a non linear compaction ratio will be obtained for a given fuel volume differential across a plane perpendicular to the direction of die movement. In other words, the fuel powder in the area which is to be the thinnest will be compacted more than the fuel powder in the area which is the thickest. Figure 2 shows the theoretical relationship that could exist when the gradient condition arises. Note that in the top graph on the left in Figure 2, the ratio of compaction is much greater than to the right where the loading flattens out. The resulting differential may result in some small amount of flow of fuel from the area of greater to the area of lesser density during compaction but this is of very little significance and extremely hard to measure. The best way to adjust for the differential compaction is to adjust the powder distribution to allow for the required final density as shown in the bottom graph in Figure 2.

Fuel Loadings

In addition to the feasibility of dual fuel gradients, the testing of the dual gradient using different fuel loadings is also important. The majority of the tests were performed using the ANS conceptual design fuel loading of 1.3g/cc. Since loading may be increased to accommodate lowered uranium enrichment, four fuel lots of 3 plates each were manufactured using loadings of 1.7, 3.0, 3.5, and 4.8 g/cc. Results from the higher loaded plates are not yet available. EB welding was originally used to seal several of the 1.3 g/cc loaded plates to test the effectiveness and to reduce any chance of oxidation. EB welding was no improvement over traditional welding and was not used further on the 1.3 g/cc loaded plates. However, since higher loading were being tested, the EB weld was used on the plates made with 1.7 g/cc and above. This was done to ensure that all loadings were treated the same and to prevent the loss of the higher loaded plates due to oxidation of U_3Si_2 fuel.

DEVELOPMENT RESULTS

The current method at B&W for evaluating the contoured fuel core is by using the digital homogeneity scanner with a collimated 2 mm diameter x-ray beam. Figure 3 shows the outcome of one of the 1.3 g/cc loaded plates. As can be seen from the figure, the fuel bulges in the middle and slopes off towards the ends as was expected. The gradient across the width is also evident. (Note that the gradient across the width is not symmetric side to side. Refer to the width view on Figure 1.) The digital homogeneity has been analyzed numerous ways and the conclusion is that the data corresponds with the actual fuel thickness tapers which were taken from the destructive evaluation. The digital scanner reads 42 tracks down the length of the plate. These tracks were also analyzed separately. By averaging the homogeneity data across the width and down the length, the overall contour of the fuel core can readily be seen. Figure 4 shows the averages of 4 plates. The top graph shows the contour across the width of the plate and the lower graph shows the contour down the length. Similar analyses were done on all plates and the results varied very little.

TYPICAL FLAT SWEPT COMPACT WITH BOTTOM CONTOUR

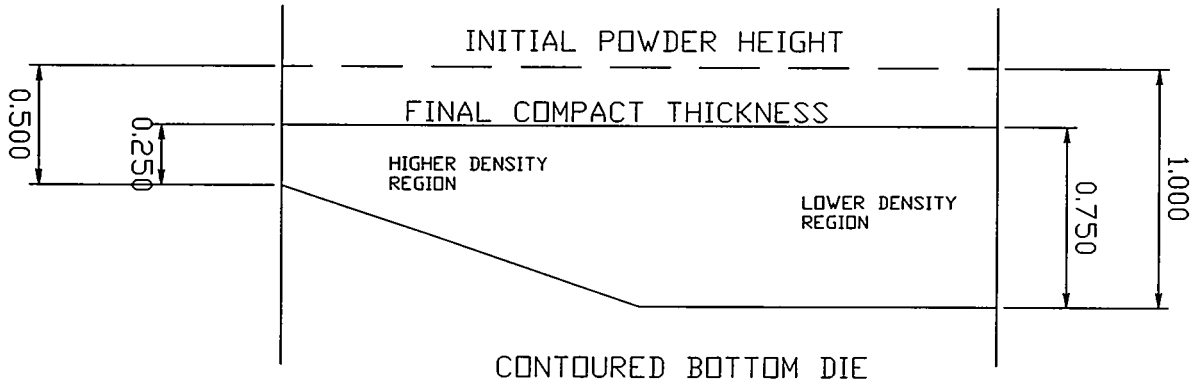

COMPACTION RATIO							
2.0	1.71	1.45	1.38	1.33	1.33	1.33	1.33

All dimensions in inches.

CORRECTIVE SWEPT COMPACT WITH BOTTOM CONTOUR

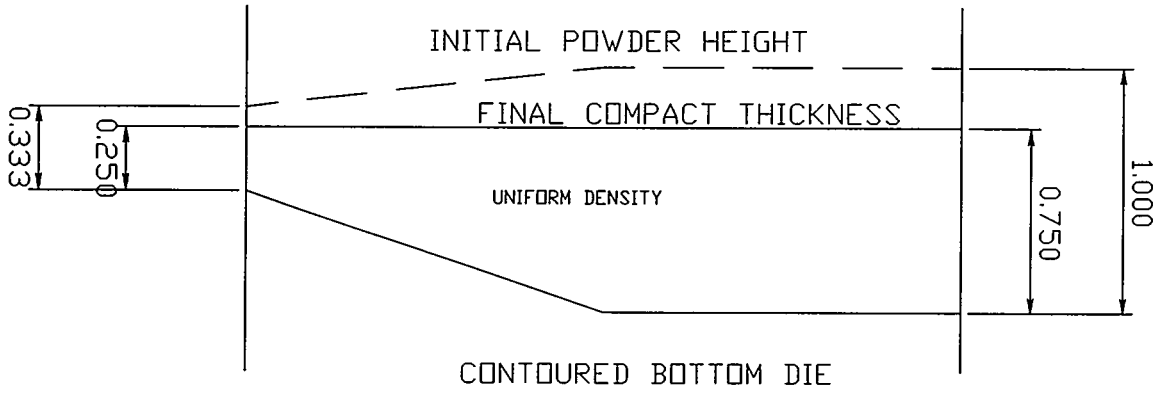

COMPACTION RATIO							
1.33	1.33	1.33	1.33	1.33	1.33	1.33	1.33

Figure 2. Powder Compaction Ratios

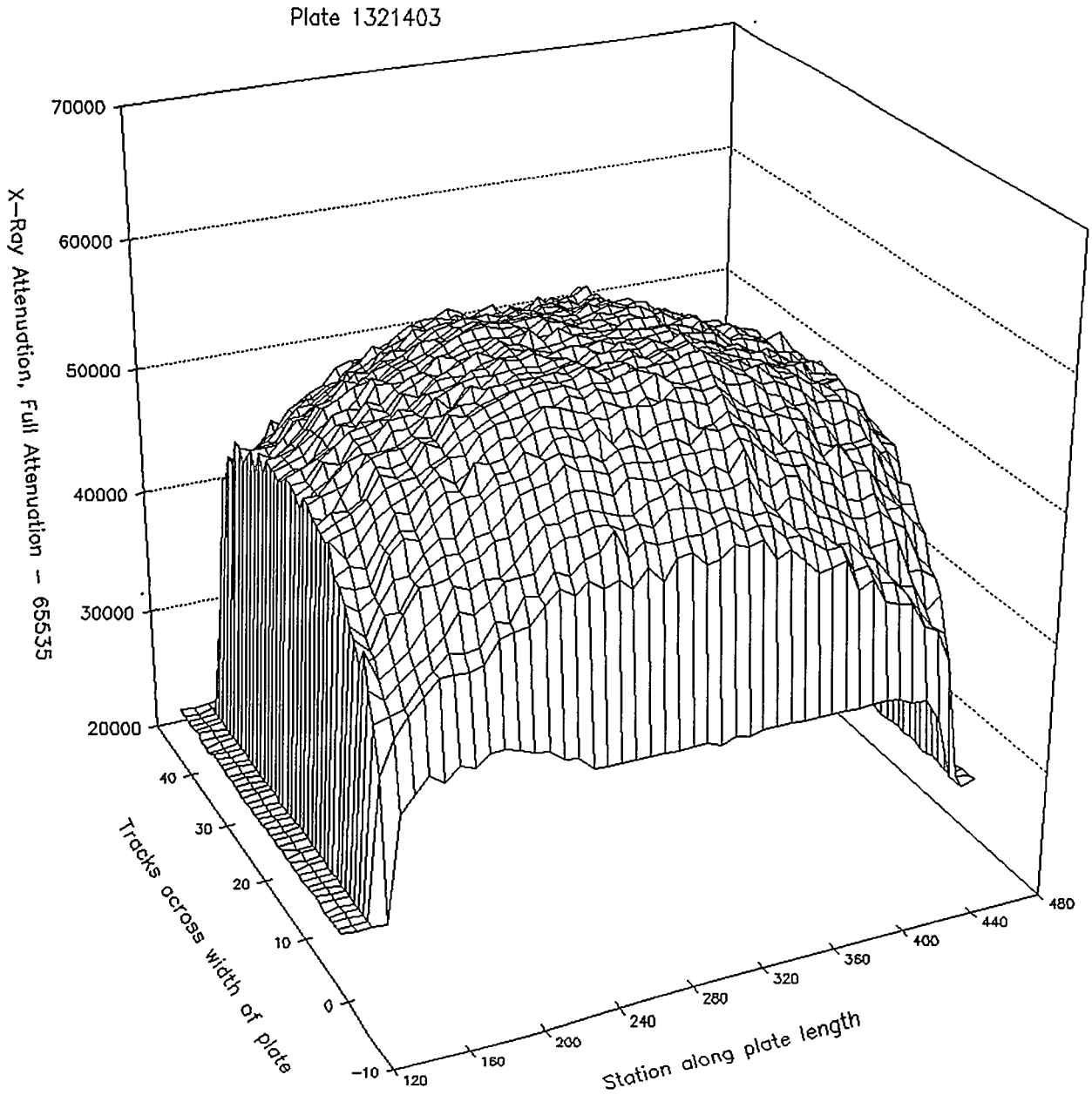

Figure 3. Homogeneity plate data

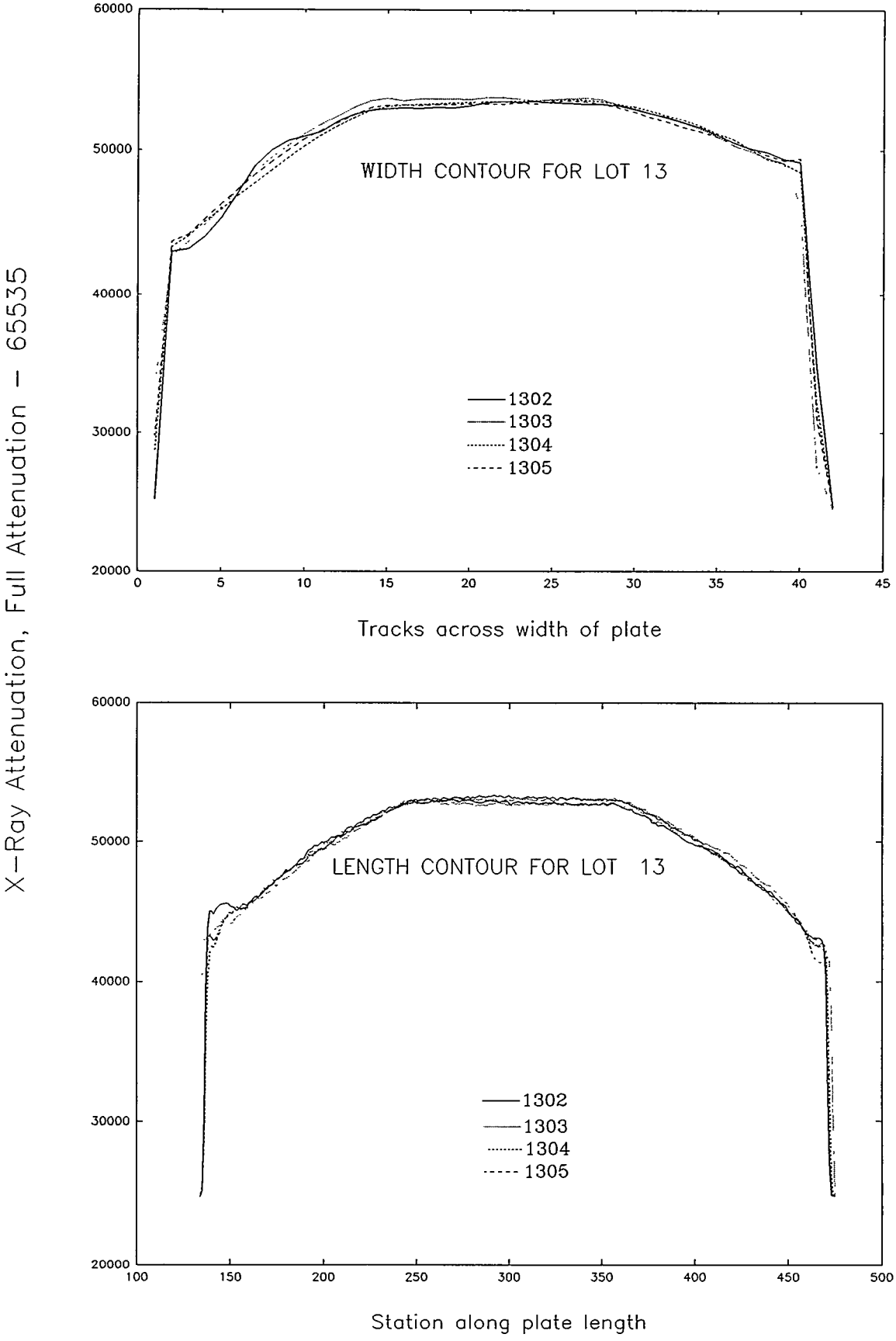

Figure 4. Width and Length Averages

The overall homogeneity of the plates is hard to quantify due to the dual fuel gradient. On a track by track basis however, the estimated homogeneity can be projected for that particular track and contour and a comparison can be made. Figure 5 shows the $\pm$10% lines overlaid on the digital local average readings for track 21 from 4 different plates. All readings fall within the 10% mark. When further work has been done and a larger data base exists, a more exacting measurement for the homogeneity standard will be used. Until then, this method is considered conservative.

The destructive evaluation (DE) results of different plates showed that the minimum cladding thickness in the center of the plate did not go below 0.25mm. The bond evaluation on the mating surfaces showed satisfactory and better bonds and grain growth. The DE results were also used to verify the homogeneity results. The contour is also very evident by looking at the DE data.

CONCLUSION

B&W has developed the ability to reproduce lateral and longitudinal fuel gradients in uranium silicide plates. Numerous methods were used to determine the feasibility and practicality of manufacturing dual gradients some of which were preferred over the others. The gradients appear to be easy to control and the repeatability in these small lots has been better than expected. The fabrication of the dual contour in the compact stage requires a little more effort than the single gradient compacts do today.

To improve the ability to create these fuel gradients, B&W is working to develop a working model of the compact to fuel core relationship so that in the future changing the desired fuel loadings and gradients will require little development work. In addition, the homogeneity improvements and the understanding of the digital homogeneity scanner will allow more in-depth analyses of all fuel plates in the future.

Babcock and Wilcox endeavors to constantly find new and better methods of manufacturing nuclear fuel for test reactors world wide. Each development effort yields knowledge which may be used in many different applications and fuel types. B&W continues to improve the quality of all plates and elements manufactured. In the future B&W intends to develop centered dual gradients within the aluminum cladding, investigate the possibility of using spherical U_3Si_2 fuel, and improve use of reclaimed U_3Si_2 in the present fuel process while keeping production cost at a minimum.

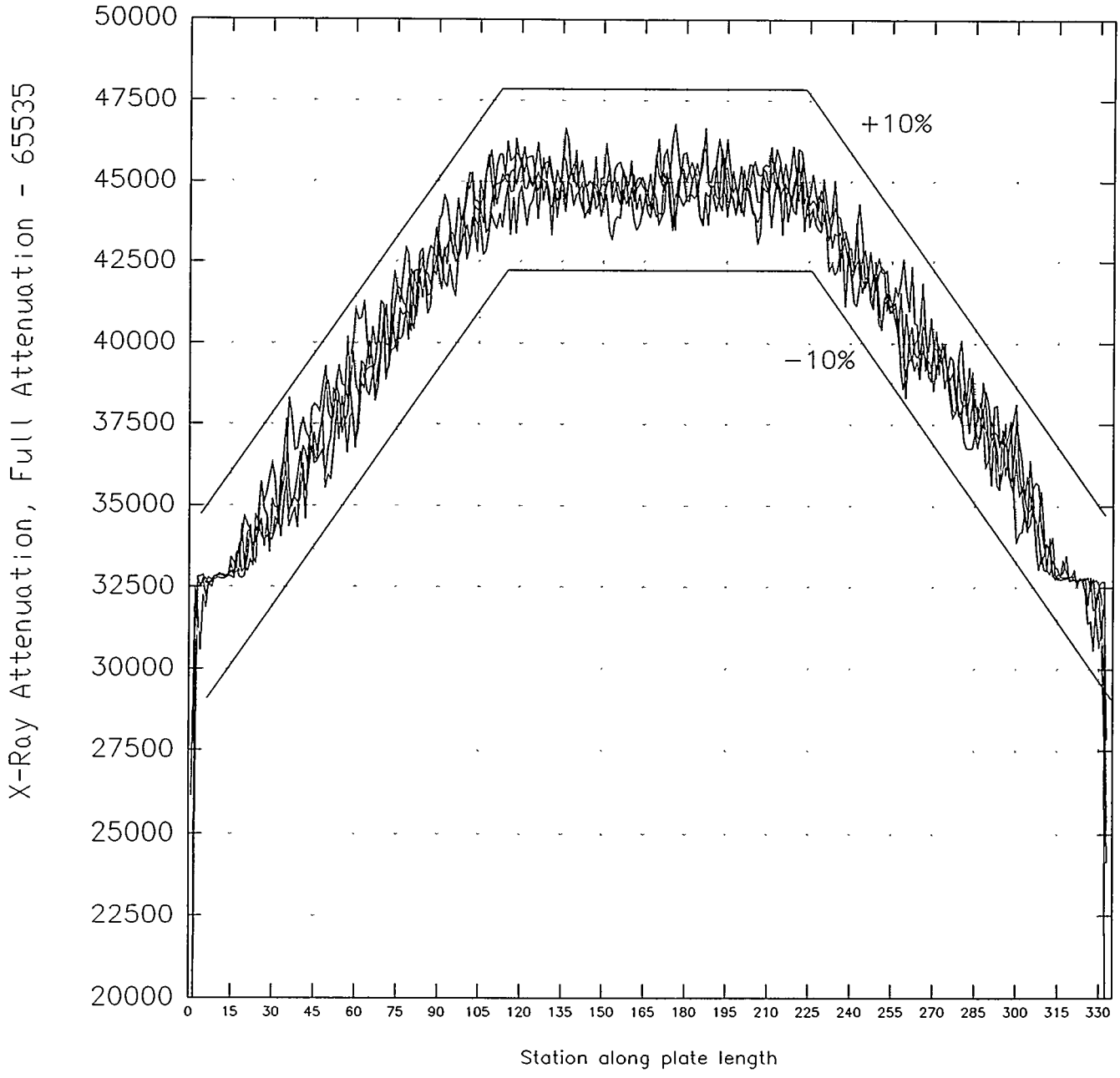

Figure 5. Lot 18, plates 1-4 Homogeneity Track 21, Center of plate

THE MANUFACTURE OF LEU FUEL ELEMENTS AT DOUNREAY

J Gibson

MTR Fuel Fabrication Plant Manager
UKAEA, Dounreay

ABSTRACT

Two LEU test elements are being manufactured at Dounreay for test irradiation in the HFR at Petten, The Netherlands. This paper describes the installation of equipment and the development of the fabrication and inspection techniques necessary for the manufacture of LEU fuel plates. Our experience in overcoming the technical problems of stray fuel particles, dog-boning, uranium homogeneity and the measurement of uranium distribution is also described.

INTRODUCTION

The technical differences between HEU and LEU fuel element production are primarily associated with the manufacture of fuel plates. Only slight changes in our HEU fuel manufacturing procedures have been necessary for the manufacture of LEU fuel. Although the incidence of stray fuel particles has been greater than is our experience with HEU fuel, we have taken measures to reduce this to an acceptable level. The ultrasonic inspection of fuel plates for cladding bond integrity has revealed that the shape of the fuel core around its periphery can result in the unnecessary rejection of fuel plates.

GENERAL DESCRIPTION

The LEU test elements each consist of 18 inner and two outer fuel plates located between two side plates, each containing 20 cadmium wires with an end box casting welded to the lower end of the fuel element. The fuel plates are formed to a curved profile and secured to the side plates by roll swaging. The uranium density in the fuel core is approximately 4.8 g/cm$_3$. The cladding plates and frames were manufactured from type 5251 aluminium. The silicon content of the uranium silicide powder is 7.1% to 7.9% by weight.

MANUFACTURING AND INSPECTION PROCESSES

The manufacturing and inspection processes for LEU fuel are essentially the same as those for HEU fuel plate manufacture and only slight procedural changes have been required.

Silicide Button Production

U_3Si_2 buttons are produced in an arc melting furnace following the same procedures as for HEU button production. Small buttons (eg. 100g or less) were found to break up when they cooled, however, buttons weighing approximately 150g have been found to remain intact.

Button Grinding

Silicide buttons can be readily ground into powder. The grinding of aluminide buttons results in the formation of quite a high proportion of coarse particles which often requires to be re-ground. Silicide buttons, which are harder due to the greater uranium content, can be ground in one operation, ie. re-grinding is not necessary.

Fuel Plate Rolling

Again, no significant problems have been encountered. However, to avoid an unacceptable level of dogboning, the plates are reversed end to end and top to bottom between each rolling pass.

Uranium Distribution

Uranium distribution is determined using a gamma counting technique. This involves checking the fuel plates at seven positions along their longitudinal centre line with a $1cm^2$ collimator. The counting time is sufficient to allow 1×10^4 counts to be taken for production plates and 5×10^4 counts for standard plates. However, due to the greater amount of uranium present in LEU fuel, self shielding prevents the true count rate from being determined. To overcome this problem, standard fuel plates have been produced, one containing uranium at nominal fuel weight, one at nominal less 10%, one at nominal plus 10% and one at nominal plus 20% corresponding to the different fuel zones in a fuel plate. These plates have been gamma counted a number of times and the results plotted on a graph. Figure 1 shows the relationship for count rate against U^{235} loadings for the four standard plates together with the mean values of the LEU fuel plates produced to date. This procedure has been validated by chemically analysing a fuel plate to determine the precise U^{235} loading.

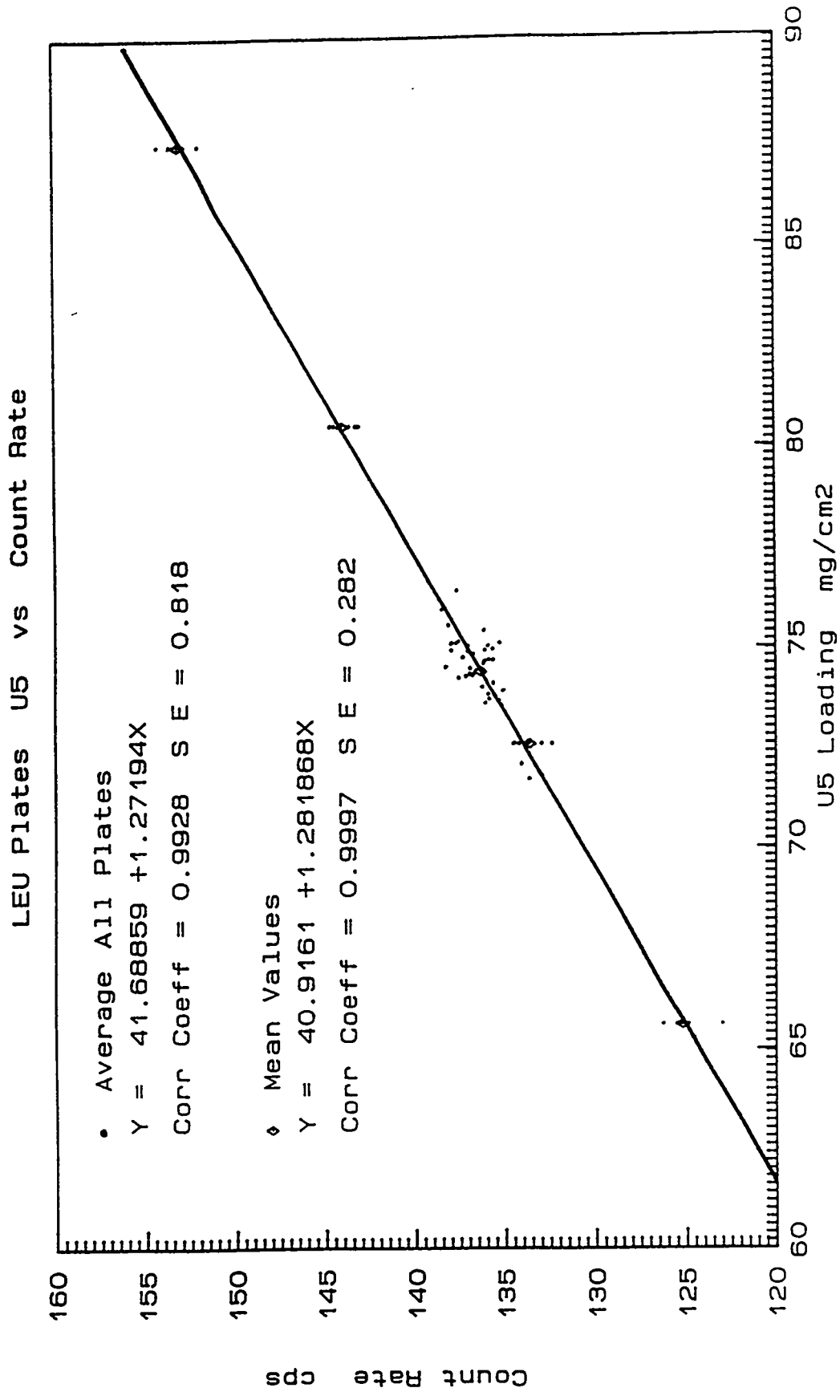

Figure 1 Graph of Count Rate Against U^{235} Content for Uranium Distribution Measurement

Uranium Homogeneity

Uranium homogeneity in the fuel plates is revealed by x-radiography. The fuel plate radiographs to date have shown very little evidence of poor homogeneity. Poor homogeneity results in either uranium or aluminium segregation and can be caused by insufficient blending times or by poor handling procedures from blending up to the compaction stage.

Cladding Bond Integrity

As with HEU fuel plate fabrication, cladding bond integrity is checked initially by a blister test and also by ultrasonic examination. The incidence of blisters has been reduced to an acceptable level by the introduction of vacuum degassing of the fuel compacts and fuel pack assemblies.

The blister test is supported by an ultrasonic examination of the fuel plates. The equipment consists of a water bath inside which is located a perspex jig containing the fuel plate to be examined. The ultrasonic transducer, which both transmits and receives the ultrasonic signal, is driven over the surface of the plate in the x and y directions via computer controlled stepper motors. Ultrasound passes through the fuel plate and is reflected back through the plate to the transducer by a sheet of glass in the base of the tank. The speed of movement along the plate can be infinitely varied and the indexing, or movement of the transducer across the plate after each scan, can be as little as 0.1mm.

The procedure for ultrasonic examination involves scanning a standard plate containing an artificially induced defect of known size. This plate is scanned daily to set the conditions to allow the standard defect to be represented at its true size on a computer screen. With these conditions set, production plates are scanned and any indications discovered can be accurately sized.

The ultrasonic examination of LEU fuel plates is more difficult than that of HEU plates due to the greater significance of fuel core edge effects and the higher uranium content of the fuel core. These edge effects are due to the shape of the fuel core which, if irregular, tends to cause deflection of the ultrasound signal. The effect of this is to reduce the strength of the reflected signal received by the transducer and to leave indications which appear identical to bonding defects possibly resulting in the unnecessary rejection of perfectly good fuel plates.

Figure 2 shows a series of sketches depicting typical fuel core edges. For HEU fuel, the leading and trailing ends tend to taper almost to a point and the longitudinal edges tend to be regular. Ultrasonic scans of these fuel plates indicate core edge effects, but only to a slight extent. For LEU fuel, the leading end tends to exhibit fishtailing and the trailing end tends to be rounded at the very edge whilst the longitudinal edges tend to be regular. Ultrasonic scans of these plates indicate significant edge effects at the leading and trailing ends. For HEU targets, three of the fuel core edges are typically rounded and ultrasonic scans of these plates show indications along the same three edges but the edge effects are less significant than they are in the case of LEU fuel. HEU targets exhibit rounded edges because the aluminium cladding material is softer than that used for HEU or LEU fuel plates.

HEU Fuel Cores

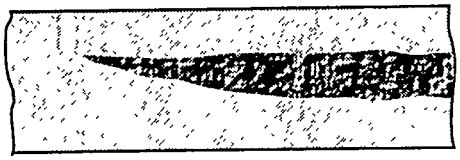

Leading End

Trailing End

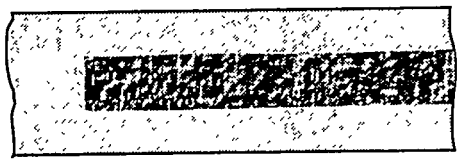

Left Edge

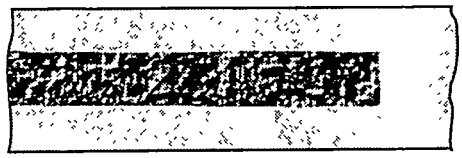

Right Edge

LEU Fuel Cores

Leading End

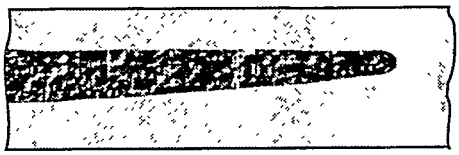

Trailing End

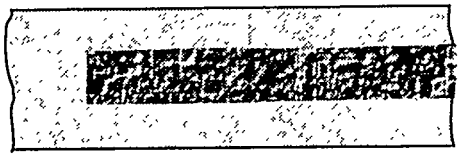

Left Edge

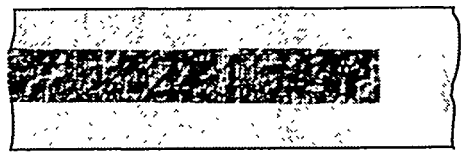

Right Edge

HEU Target Fuel Cores

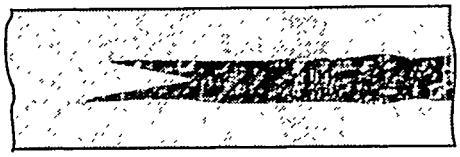

Leading End

Trailing End

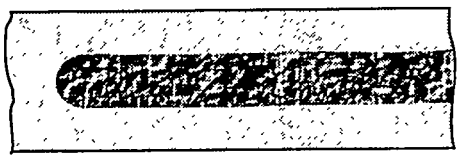

Left Edge

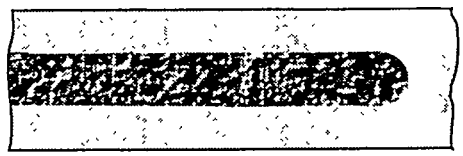

Right Edge

Figure 2

Sketches of Leading End, Trailing End & Transverse Sections of Typical Fuels.

Cladding Thickness

The mean and minimum aluminium cladding thickness requirements, as indicated in the manufacturing specification, have been satisfactorily achieved. Attention to the fuel plate rolling schedule has also ensured that dogboning is minimal in all fuel plates produced.

Stray Particles

In the early stages of LEU fuel plate production, stray particles were a problem. This was overcome by reducing the thickness of the compacts to very slightly less than the cladding frame thickness and by introducing a slight squeeze pass in the first pass of the rolling process. These measures, combined with careful handling of the compacts at the fuel pack assembly stage, have reduced the incidence of stray particles to an acceptable level.

CONCLUSION

Sufficient LEU fuel plates for the assembly of two fuel elements have been successfully produced in the MTR Fuel Element Fabrication Plant at Dounreay. The manufacturing procedures for the production of LEU fuel plates are essentially the same as those for HEU fuel plate production. The main differences between LEU and HEU fuel plate production are associated with the inspection of the fuel plates. These differences are concerned with the determination of uranium distribution in the fuel plates and the confirmation of cladding bond integrity by ultrasonic inspection.

The fuel plates will be formed to the required curved profile in the near future and then roll swaged into side plates and finally attached to the structural components in the next few weeks. A programme of test irradiation, followed by post irradiation examination will then take place.

3. Re-cycled uranium has been used in the manufacture of alloy type MTR fuel elements at Dounreay for many years. Towards the end of the operating life of the DIDO and PLUTO reactors at Harwell, the uranium was on its fourth re-cycle and the ^{236}U content was up to 16% with the estimated ^{232}U content at approximately 15 PPB. The current licence conditions applied to the fuel fabrication plant allow the production of fuel with this amount of ^{232}U.

The average doses to the operators (internal and external) working within the plant over the last six years are shown below:

Year	Average Dose (mSv)
1988	4.22
1989	1.20
1990	1.93
1991	2.27
1992	1.72
1993	1.43

The site imposed limit on total dose is 20 mSv (this compares with the ICRP limit of 50 mSv).

The falling dose rate is attributed to plant refurbishment work, the installation of new plant and improved working practices.

APPENDIX

1. The table below shows the numbers of fuel elements manufactured at Dounreay since 1957.

Hifar (Australia)	866
FRJ-2 (Germany)	1578
Dido/Pluto (UK)	5483
Herald (UK)	344
Herald (Chile)	40
Safari (S Africa)	60
DR-3 (Denmark)	500
Universities (UK)	126
Apsara (India)	40
RV-1 (Venezuela)	20
JRC (Holland)	168

We have manufactured 176 dispersed HEU fuel plates and 40 LEU fuel plates for test irradiation in the HFR at Petten and are currently manufacturing 108 dispersed HEU fuel plates for test irradiation in BR2 Belgium.

2. Below, in diagram form, are the three fuel plate production lines, which can be operated in parallel, in use at Dounreay.

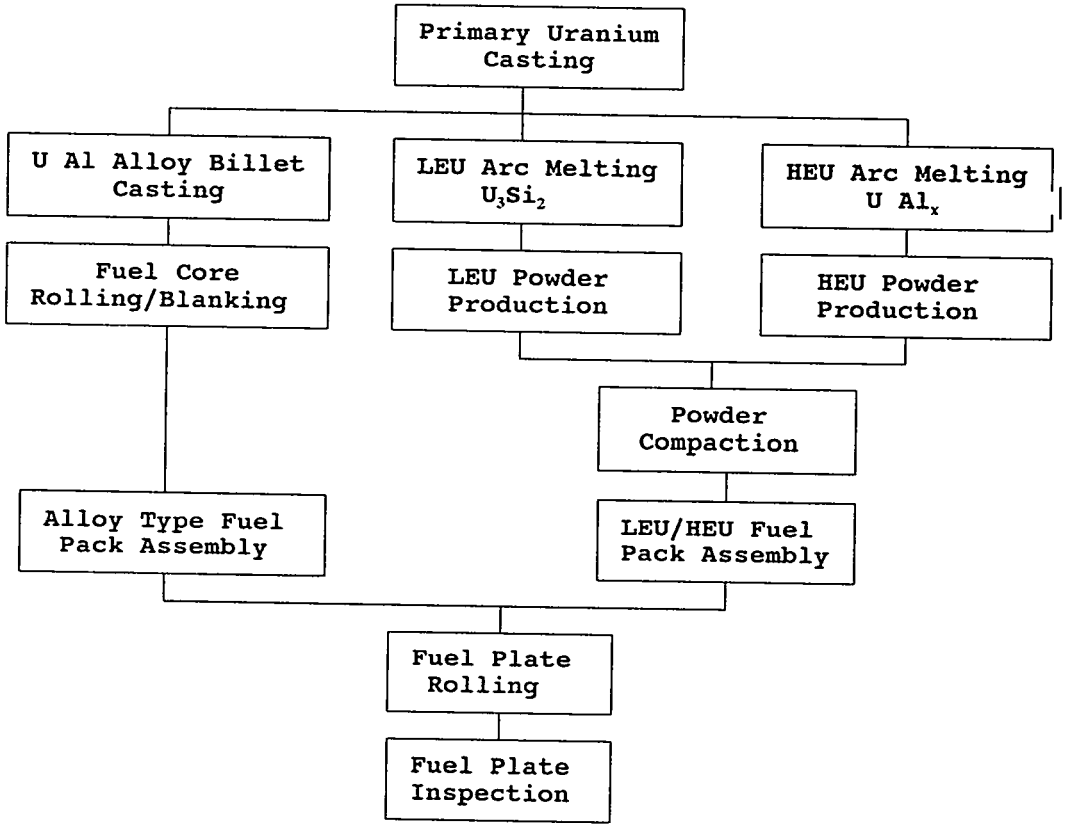

MTR FUEL ELEMENT INSPECTION AT DOUNREAY

J Gibson

MTR Fuel Fabrication Plant Manager
UKAEA, Dounreay

ABSTRACT

To ensure that our production and inspection processes are performed in an acceptable manner, ie. auditable and traceable, the MTR Fuel Element Fabrication Plant at Dounreay operates to a documented quality system. This quality system, together with the fuel element manufacturing and inspection operations, has been independently certified to ISO9002-1987, EN29002-1987 and BS5750:Pt2:1987 by Lloyd's Register Quality Assurance Limited (LRQA). This certification also provides dual accreditation to the relevant German, Dutch and Australian certification bodies. This paper briefly describes the quality system, together with the various inspection stages involved in the manufacture of MTR fuel elements at Dounreay.

INTRODUCTION

Each type of MTR fuel element is produced in accordance with a manufacturing specification and a set of manufacturing drawings agreed between the fabricator and the reactor operator or his representative. The specification sets down the scope and general conditions, the requirements of the manufacturing method, together with the inspection requirements and acceptance criteria. In addition to the specification, an inspection schedule is normally produced which includes all of the supporting documentation such as the inspection and record sheets and certification.

The operation of the fabrication plant and the management of the various contracts passing through it are carried out to a documented quality system which consists of the following:

- Quality Assurance Programme
- System Procedures
- Support Procedures
- Specific Instructions

All personnel working in the fuel fabrication plant are responsible for the quality of the products manufactured. However, to ensure that the decisions of inspection personnel are not influenced by production requirements, the plant is organised such that the inspection department operates independently from the production department.

Inspection operations are carried out on raw materials and bought in components and are performed on the production stages from:

- raw materials to fuel core/compact manufacture
- core/compact to finished fuel plates
- fuel plates to fuel box assembly
- fuel box to fuel element assembly

The inspection department also administers the calibration of all inspection, measuring and test equipment used within the Plant as well as the maintenance of a system to manage Quality Records.

QUALITY ASSURANCE PROGRAMME

The QA Programme is a stand alone document which provides the following:

- a clear statement regarding the quality policy objectives of the Plant
- a description of the organisation and the delegation of responsibility and authority relevant to the operation of the Plant
- a description of the Quality Management system
- a description of the arrangements relating to the management of safety.

SYSTEM PROCEDURES

System procedures have been developed to cover:

- Management Review

  These reviews are carried out to examine management objectives, implementation methods, achieved results and the continuous improvement and development of the applied quality system. They consider the results of QA monitoring, audit reports, non-conformance reports, customer feedback and post job reviews.

- Quality System

  This procedure describes the implementation of the quality system within the Plant to satisfy the requirements of BS 5750:Part 2:1987.

- Control of Non-conforming Product

  This procedure covers the arrangements for the identification, marking, segregation and reporting of non-conforming product. It also covers the requirement for the review of non-conformance reports and the maintenance of an inspection non-conformance register.

- Quality Records

  This procedure sets out the arrangements for the establishment of a records system, the categorisation of records, their storage, preservation and safekeeping.

- Internal Quality Audits

  This procedure describes the arrangements for controlling the management, performance and recording of internal quality audits carried out in compliance with BS 7229: Quality Systems Auditing.

SUPPORT PROCEDURES

A number of support procedures have been developed to cover the following:

- Contract Review
- Document Control
- Inspection, Measuring & Test Equipment
- Training

SPECIFIC INSTRUCTIONS

Specific instructions are prepared to cover production operations, inspection operations and other safety related operations performed in the Plant. To permit audits and inspections to be performed smoothly, a full set of instructions is prepared for each discrete inspection and production operation associated with every manufacturing contract.

INSPECTION OF FUEL ELEMENTS

- Raw Materials

The raw materials, ie. uranium metal, aluminium, silicon and burnable poisons, are analysed for enrichment and impurities and are certified to demonstrate compliance with

the manufacturing specification. The structural materials, clad materials and weld filler materials are also certificated to demonstrate that their mechanical properties comply with the relevant British Standard. For MTR fuel elements, the acceptable levels of impurities in the aluminium are sometimes stricter than is acceptable in commercially available grades of the material. When this is the case, extra material analysis is required to ensure that the cast of material selected meets the required specification.

- Bought-in Components and Assemblies

Bought-in components and assemblies are manufactured by approved vendors following an approved quality plan. Generally, a minimum of ten percent of the bought-in components and assemblies are inspected on receipt by our inspection department and, depending on the results of this inspection, the batch of components and assemblies is either accepted or rejected or a greater level of inspection may be imposed. The level of inspection follows the recommendations given in BS6001, Sampling Procedures and Tables for Inspection by Attributes.

- Inspection From Raw Materials To Fuel Core/compact Stage

Fuel compacts are produced by first arc melting uranium and either silicon for LEU fuel or aluminium for HEU fuel together to form buttons of uranium silicide or aluminide. The buttons are then ground into powder which is sieved to obtain powder of the required range of particle sizes. The required quantities of the different powder size fractions are weighed out to provide the necessary total fuel weight for one compact. The fuel powder is then blended with the required quantity of aluminium powder so that the resultant compact is of the required dimensions. After blending, the composite powder is compressed to form a finished fuel compact.

For each batch of uranium, a data sheet is produced specifying the required weights of uranium and silicon or aluminum to be arc melted into buttons. The data sheet also includes the relevant cast numbers and batch numbers for each type of material used. Prior to arc melting, the materials are weighed out and independently checked by an inspector. The weights of the resultant buttons are also recorded and checked. Strict control of the uranium weight in each compact is achieved by accurately weighing the powders to within 0.01g.

After grinding and sieving, a data sheet is produced for each batch of fuel powder which details the relative weights of the fuel powder size fractions used, together with the necessary weights of aluminium powder required to produce a fuel compact. All of these weights are recorded for each compact produced and are checked by an inspector.

After compaction, each compact is check weighed and dimensionally inspected for compliance with the relevant drawing.

From the inspection of the raw materials to the finished compacts we are able to provide full analysis of the uranium, silicon, aluminium and U_3Si_2 and UAl_x powder as well as enrichment details and isotopic composition of the uranium, together with the compact weight and compact dimensions.

- Inspection From Fuel Compact To Fuel Plate Stage

Prior to assembly, each fuel compact is vacuum degassed to remove any moisture or entrapped gasses and the aluminium components are chemically cleaned to remove the oxide film from the mating surfaces. Each fuel compact is placed in an aluminium picture frame which is then assembled between two aluminium cladding plates. The whole assembly is then argon arc welded around the periphery leaving a gap at the trailing end to allow air to escape during the rolling process. The assembly is then degassed prior to the fuel plate rolling stage.

Each fuel pack is uniquely identified and the identification numbers of the components (clads, frames and fuel compacts) are recorded and checked by an inspector.

- Inspection From Fuel Plate To Fuel Box Stage

Fuel plates are inspected for the following features:

- Cladding Bond Integrity
- Fuel Core Location
- Uranium Distribution
- Uranium Homogeneity
- Dimensional Compliance
- Surface Condition
- Surface Contamination

Cladding Bond Integrity

After rolling, each fuel plate is subjected to a standard blister test to examine the bond between the fuel and the aluminium cladding. This test is supported by an ultrasonic examination, the procedure for which involves scanning a standard fuel plate containing defects of known size; once in the morning before scanning production plates and once at the end of the working day. The amplitude of the ultrasonic signal received by the transducer is displayed on a colour monitor by suitable software to give a plot showing the variation of signal strength over the plate surface. The scanning parameters and software settings are adjusted such that the standard defects appear no smaller than their true size. With these settings, any indications that appear on the scans of the production plates are considered as bonding defects and, if they are larger than the acceptable equivalent diameter quoted in the manufacturing specification, the relevant fuel plate is rejected.

One of the problems with the ultrasonic examination of fuel plates is associated with the existence of core edge effects. These are indications which appear around the periphery of the fuel core at the interface between the fuel core and the aluminium cladding (see Figure 1). These indications have been found to be due to the effect of the shape of the fuel core at the interfaces. At a well defined interface, the amplitude of the ultrasonic signal will be unaffected but, when the edge of the fuel core is rounded or irregular, the signal is deflected such that the amplitude of the reflected signal, expressed as a percentage of the transmitted signal, is significantly reduced. As a result, if the edge of the fuel core is too irregular, it is sometimes not possible to distinguish between bonding defects and core edge effects. This phenomenon is particularly evident with LEU fuel plates and, although this is partly due to the high density of uranium in the fuel, we have found that the most important factor is the shape of the fuel core at the interfaces (see Figure 2).

Fuel Core Location

As-rolled fuel plates are individually placed in a Core Location Unit to precisely locate the fuel core prior to blanking the plates to size. X-rays pass through the plate and impinge on a fluorescent screen giving an image of the fuel core (see Figure 3). The plate can be moved horizontally and vertically such that the fuel core can be located against a graticule. Once the core position is fixed, two locating holes are punched in the excess aluminium at the ends of the plate. These holes allow the plates to be located on dowels on blanking tools enabling the plates to be blanked out to the required size.

Uranium Distribution

Uranium distribution in the fuel plates is determined using a gamma counting technique. Each fuel plate is counted and the results are compared with the results obtained from a standard fuel plate which has been qualified by chemical analysis. The plates are counted at prescribed positions along the centre line.

Uranium Homogeneity

Each fuel plate radiograph is assessed for uranium homogeneity using penetrameters containing known amounts of uranium produced from specially rolled fuel plates. The penetrameters are blanked out from three fuel plates, one containing uranium at nominal fuel weight less 10%, one at nominal plus 10% and one at nominal plus 20%. Three sets of penetrameters are radiographed at the same time as the fuel plates, one set adjacent to the middle of the plate and the other sets adjacent to each end to counter the effects of variations in film exposure along the length of the fuel plates. If there are any areas of aluminium or uranium segregation evident on the radiograph, they can be compared to the penetrameter density reading using a densitometer. The gamma counting equipment, used to determine uranium distribution, can also be used to measure the uanium content in any given area to determine the extent of uranium segregation.

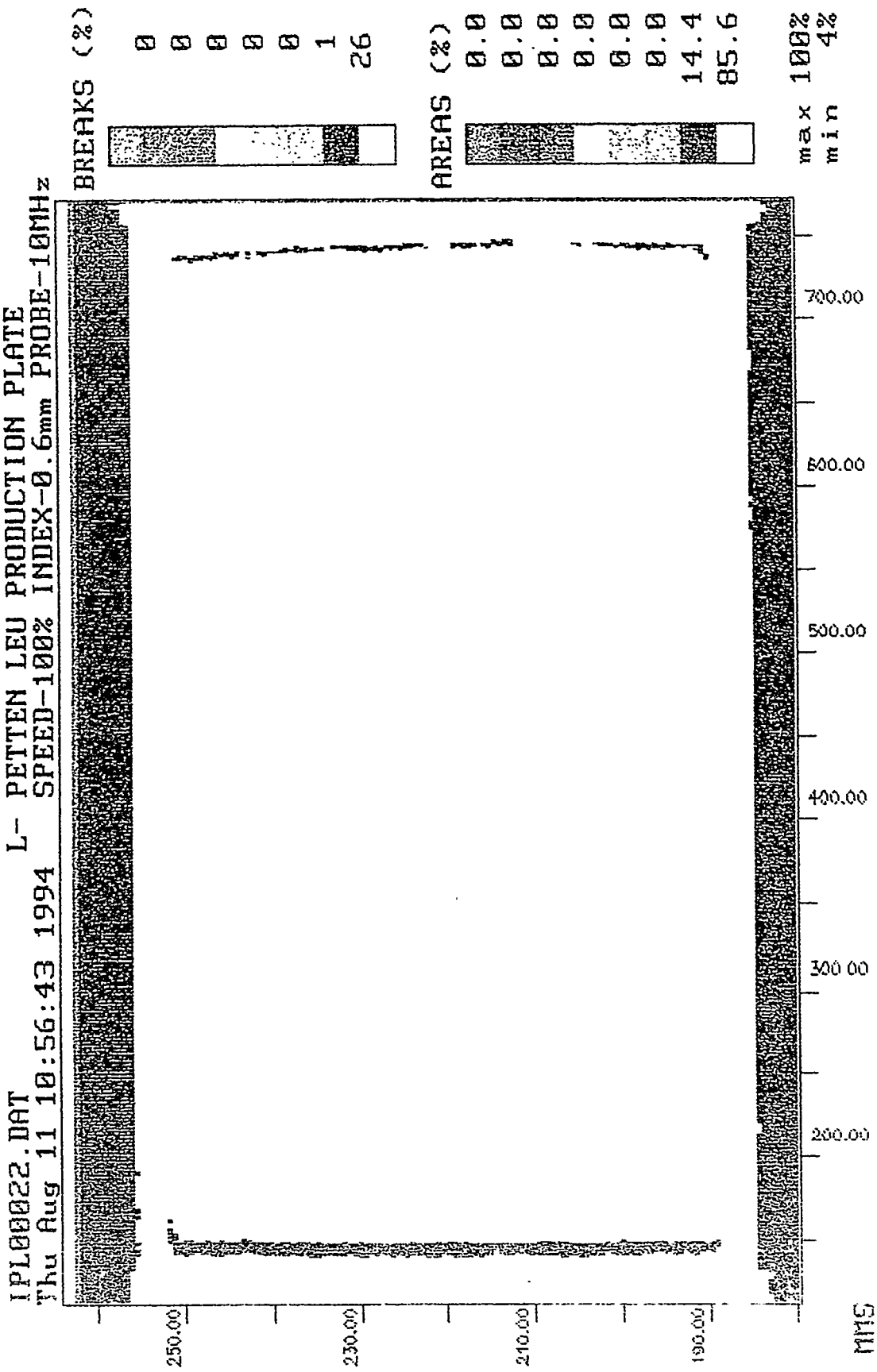

Figure 1 Ultrasonic Scan of LEU Plate Showing Core Edge Effects at Leading and Trailing Ends

HEU Fuel Cores

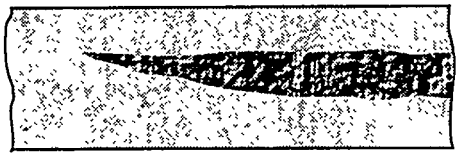

Leading End

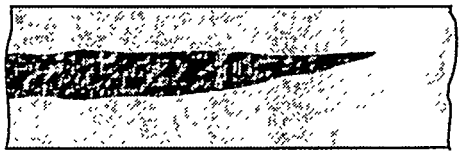

Trailing End

Left Edge

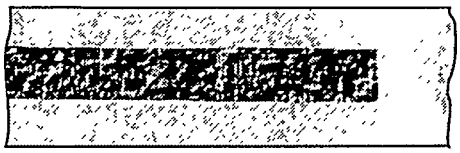

Right Edge

LEU Fuel Cores

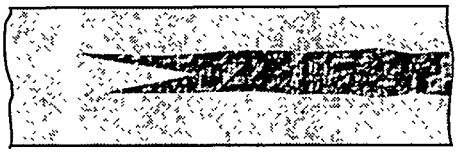

Leading End

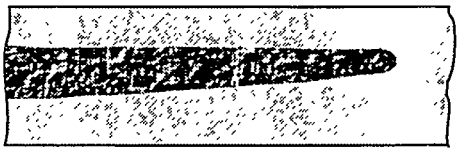

Trailing End

Left Edge

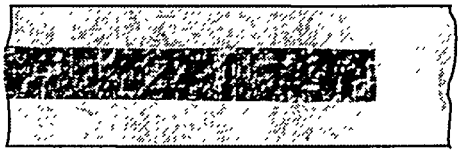

Right Edge

HEU Target Fuel Cores

Leading End

Trailing End

Left Edge

Right Edge

Figure 2

Sketches of Leading End, Trailing End & Transverse Sections of Typical Fuels.

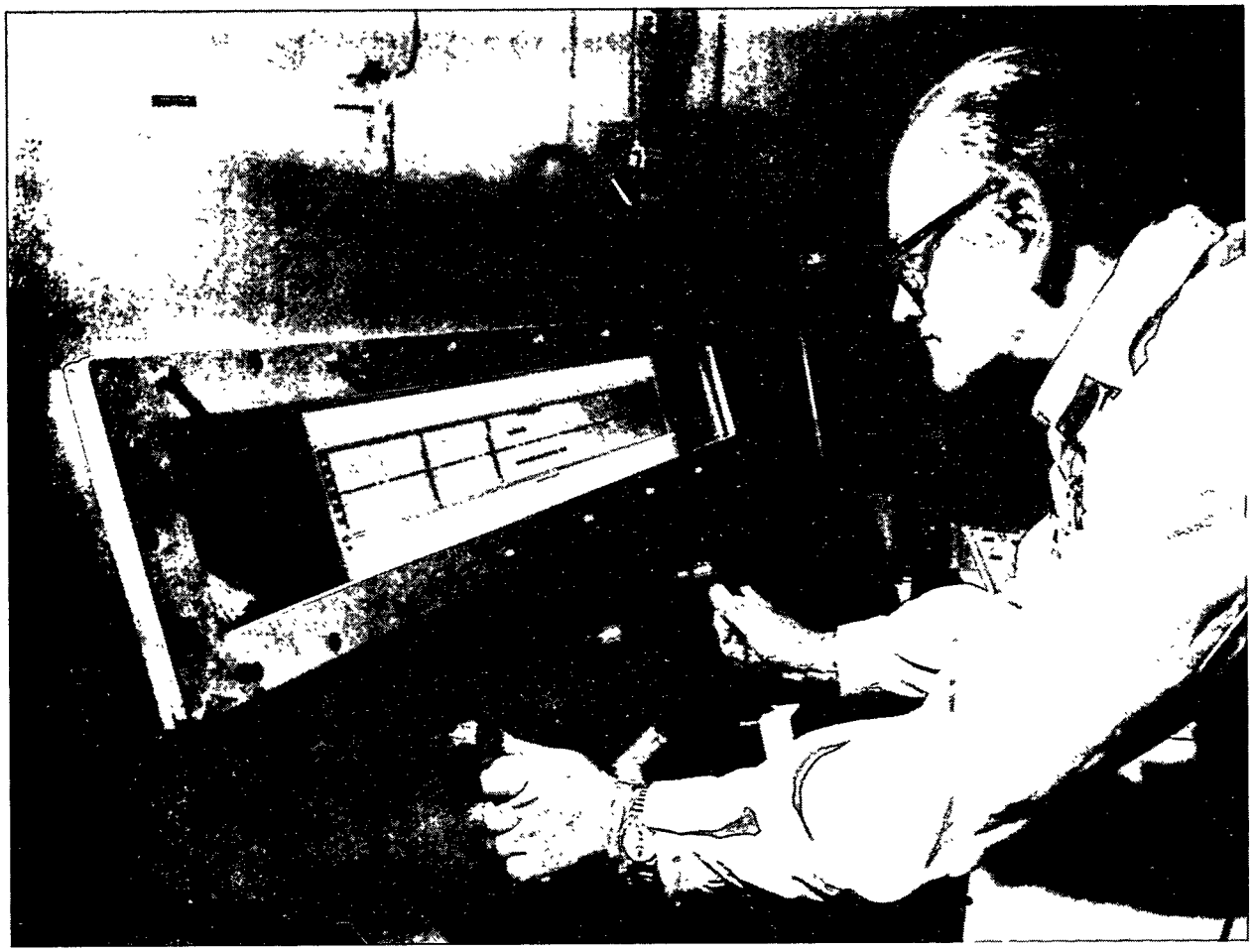

Figure 3 Core Location Unit

Dimensional Compliance

Fuel plates are hot rolled following a rolling schedule that produces a metallurgical bond between the fuel core, the aluminium picture frame and the aluminium cladding plates. The rolling schedule must also produce plates containing fuel cores of the required dimensions, ie. width, length and thickness. One percent of each size of fuel plates produced are destructively examined to check the fuel core and cladding thickness at prescribed positions on the fuel plate (see Figure 4). These samples are also used to determine the extent of dog-boning at the ends of the fuel cores.

Surface Condition

After chemical cleaning, all fuel plates are visually examined for surface defects such as pits and scratches. The position of any such defects is recorded using a grid reference system. Significant defects are examined in detail to determine their depth using a purpose designed instrument (see Figure 5).

Surface Contamination

Fuel plates and tubes are checked for the presence of surface alpha contamination. The items to be checked are placed inside a chamber which is filled with an argon/methane gas mixture and an alpha proportional counter indicates the level of contamination present. This equipment is checked using a standard fuel plate and fuel tube.

The fuel plates which have successfully completed the above inspections are presented to the customer or his representative for acceptance. If they are acceptable, the fuel plates are released for the next stage of manufacture.

Depending on the design of fuel element being produced, the plates are either roll-swaged into fuel boxes or are manufactured into fuel tubes. In both cases, the plates are first formed to the required radius of curvature.

- Inspection From Fuel Box To Finished Fuel Element Stage

For tubular type elements, three curved fuel plates are electron beam welded together to form a fuel tube. After welding, the fuel tubes are compressively sized on a mandrel to ensure that they are of the required dimensions. Four fuel tubes of different diameters are then assembled concentrically to form a fuel box, using combs at each end of the tubes to maintain the coolant channel gaps between the tubes.

For plate type elements, the fuel plates are secured into slotted side plates, or continuous combs depending on the design of fuel element, by roll-swaging. A heavy swaging head carries two hardened steel wheels which cut into the aluminium lands between each slot in the side plates or combs. The fuel plates are successively slipped into the slots and the swaging head is adjusted to the required height. The swaging head is then

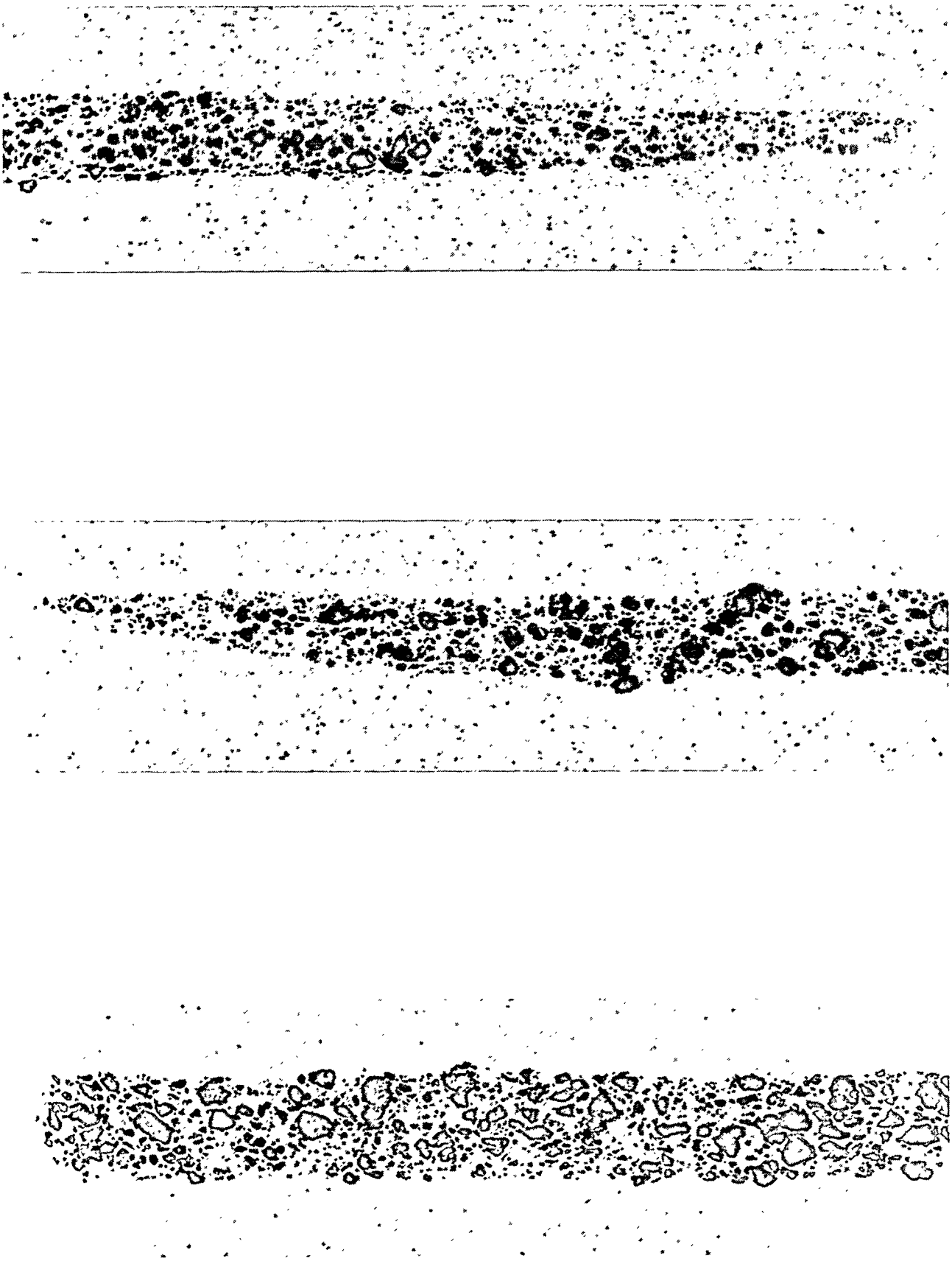

Figure 4 HEU Fuel Plate Micrographs

Figure 5 Surface Defect Depth Measuring Equipment

moved along the fuel plate and, as it moves, the wheels force the edges of the slots into the fuel plate locking it into position. Each fuel plate is assembled in the same way until the fuel box is completed.

After assembly, each fuel box is inspected to ensure that it complies with the manufacturing drawings. The main feature of inspection being the coolant channel gaps which are checked using wire gauges of the required diameter.

To ensure that the strength of the swaged joint is greater than a specified minimum value, it is necessary to carry out pull tests on a dummy fuel box. The swaging settings used for the dummy box are then reproduced for the swaging of fuel boxes containing entiched uranium.

After the fuel box has been assembled, the next stage is to attach the remaining structural components. For tubular type elements, the fuel box is welded inside an unfuelled outer tube and to an upper tube assembly and a lower guide nose. For plate type elements, the fuel box is secured to the structural components either by welding or rivetting. When welding is selected as the securing method, it is often necessary to leave a machining allowance on the components to account for any heat induced distortion that may occur.

Final inspection of the fuel elements involves ensuring that all important dimensions are within the specified limits, the identification numbers are correct and that all the documentation meets the requirements of the manufacturing specification and the inspection schedule.

- Calibration of Inspection, Measuring & Test Equipment

The use of inspection, measuring and test equipment within the fuel fabrication plant is controlled following a procedure which ensures that all such equipment is registered and included on a plant inventory. Every item of equipment has a unique identity number and is calibrated in accordance with its intended use. The calibration system follows the recommendations given in BS5781:Measurement and Calibration systems and ISO10012-1 Quality Assurance Requirements for Measuring Equipment.

- Quality Records

Manufacturing and inspection records, including physical samples, for each fuel element are retained for five years, or until the element is reprocessed, whichever is the shorter period. The documentation requirements of each customer are usually given in the manufacturing specification. A set of blank documents will usually be appended to the specification in the form of an Inspection Schedule which includes all relevant inspection and record sheets, inspection certificates and quality plan.

CONCLUSION

The MTR Fuel Fabrication Plant at Dounreay operates to a quality system that has been independently certified by Lloyds Register Quality Assurance Limited as satisfying the requirements of BS5750, ISO9002 and EN29002. Our objective is to continuously improve our performance with respect to the manufacture and inspection of MTR fuel elements and to refine our quality system to enable us to satisfy this objective.

This paper has briefly described the quality system and some of the equipment and methods used in the inspection of MTR fuel elements at Dounreay.

SESSION IV

September 21, 1994

ANALYSES

Chairman:

A. Lee
(AECL, Canada)

VALIDATION OF THE WIMSD4M CROSS-SECTION GENERATION CODE WITH BENCHMARK RESULTS

J. R. Deen, W. L. Woodruff
Argonne National Laboratory

and

L. C. Leal
Oak Ridge National Laboratory

ABSTRACT

The WIMSD4 code has been adopted for cross-section generation in support of the Reduced Enrichment Research and Test Reactor (RERTR) program at Argonne National Laboratory (ANL). Subsequently, the code has undergone several updates, and significant improvements have been achieved. The capability of generating group-collapsed micro- or macroscopic cross sections from the ENDF/B-V library and the more recent evaluation, ENDF/B-VI, in the ISOTXS format makes the modified version of the WIMSD4 code, WIMSD4M, very attractive, not only for the RERTR program, but also for the reactor physics community.

The intent of the present paper is to validate the WIMSD4M cross-section libraries for reactor modeling of fresh water moderated cores. The results of calculations performed with multigroup cross-section data generated with the WIMSD4M code will be compared against experimental results. These results correspond to calculations carried out with thermal reactor benchmarks of the Oak Ridge National Laboratory (ORNL) unreflected HEU critical spheres, the TRX LEU critical experiments, and calculations of a modified Los Alamos HEU D_2O moderated benchmark critical system. The benchmark calculations were performed with the discrete-ordinates transport code, TWODANT, using WIMSD4M cross-section data. Transport calculations using the XSDRNPM module of the SCALE code system are also included. In addition to transport calculations, diffusion calculations with the DIF3D code were also carried out, since the DIF3D code is used in the RERTR program for reactor analysis and design. For completeness, Monte Carlo results of calculations performed with the VIM and MCNP codes are also presented.

INTRODUCTION

The cross-section generation capability for the RERTR program is based on a modified version of the WIMSD4[1] code, which has been named WIMSD4M[2].

Problem-dependent group-collapsed cross-section libraries generated with the WIMSD4M code are based on a fine-group microscopic cross-section library containing 98 materials in which 69 neutron energy groups are utilized. The basic 69-group cross-section library, presently available at ANL, was created by processing the ENDF/B-V library with the NJOY system[3] with modules RECONR, BROADR, UNRESR, THERMR, GROUPR, and WIMSR. In contrast to other modules of the NJOY system, extensive work was required to make WIMSR produce reliable multigroup cross-section data for the WIMSD4M code.

In addition to the NJOY modules, a utility code, LIBUPD, for adding and replacing isotopes and maintaining the libraries, was also created. This supplementary code makes it possible to edit the WIMSD4M library file into a readable ASCII form.

The NJOY capability of processing the latest version of the ENDF/B file, ENDF/B-VI, has been considered, and in the near future a WIMSD4M fine-group library processed from the ENDF/B-VI file may be added for use by the RERTR program.

CALCULATIONS OF THE ORNL AND TRX THERMAL BENCHMARK WITH WIMSD4M GROUP CROSS SECTIONS

The first series of validation tests of the WIMSD4M cross-section code was carried out with the ORNL homogeneous unreflected critical spheres of ^{235}U and H_2O, ORNL -1, -2, -3, -4, and -10, and the TRX-1 and TRX-2 lattices.[4]

To verify the adequacy of the WIMSD4 generated cross sections, it was decided to rely on the results of transport calculations to avoid possible errors which could be attributed to transport effects. In this regard, the multigroup discrete-ordinates transport codes, TWODANT[5] and XSDRNPM[6], were used in the calculations. In addition to the transport calculations, diffusion calculations have also been performed with the DIF3D code[7].

Fine-group cross sections used in the transport and diffusion calculations with the TWODANT and DIF3D codes were obtained from calculations performed based on the built-in 69 group structure of the WIMSD4M library and subsequently, these fine group cross-section data were collapsed to a 10-group structure used in the benchmark calculations. The collapsed 10-group boundaries are shown in Table 1. The spatial dependence of the neutron spectrum was accounted for in the calculations by using 100 fine spatial intervals. Other parameters which are required in a transport calculation are the angular quadrature and the order of scattering. Calculations performed with 16 quadrature points and the first order scattering ($S_{16}P_1$) proved to be sufficient to reproduce k_{eff} in good agreement with experimental results. The unreflected sphere implies that no particle leaving the system at the sphere surface will return to it, a requirement fulfilled by the vacuum boundary condition option of the TWODANT and DIF3D codes. Prior to the transport calculations with the one dimensional discrete-ordinates transport

code XSDRNPM, the CSASN sequence of the SCALE4.2 code system[8] was used to calculate Bondarenko factors and Nordheim resonance integrals with the codes BONAMI and NITAWL, respectively. The cross-section library used in the calculations is a 238-group library processed from ENDF/B-V.

The continuous-energy Monte Carlo codes VIM[9] and MCNP[10] were also used to calculate the ORNL unreflected spheres and the TRX heterogeneous critical lattices.

The benchmark results of the ORNL HEU critical spheres are very useful to test the performance of the cross-section library as to the neutron scattering in H_2O, the absorption cross section of the fissile material, ^{235}U, and the capture cross section of hydrogen. To assess the performance of the WIMSD4M problem-dependent cross-section library, the infinite and effective multiplication factors for the five spheres were computed. These results are displayed in Table 2. The basic cross-section data used in the calculations are taken from the ENDF/B-V files. The results shown in Table 2 indicate that the infinite multiplication factor calculated by WIMSD4M and VIM codes are in excellent agreement. Likewise, the effective multiplication results computed with the TWODANT code using WIMSD4M 10-group cross-section data are very good. In addition, the fission and capture rates for each isotope were in excellent agreement. These results demonstrate the capacity of the WIMSD4M code for generating problem-dependent group-collapsed cross-section data for applications in H_2O moderated reactor calculations.

In addition to the transport and Monte-Carlo calculations, Table 2 also includes results from the diffusion calculations carried out with the DIF3D code. A homogeneous infinite medium was used in WIMSD4M to obtain broad group cross sections for DIF3D and TWODANT since there is no capability in WIMS to model spherical geometry. TWODANT and VIM reaction rates are in excellent agreement but the fast neutron leakage is slightly different causing eigenvalues about 1% Δk_{eff} larger than VIM for the smaller bare spheres in cases 1-4. The reactivity bias is reduced to 0.45% Δk_{eff} for the largest sphere (#10) in the DIF3D model.

The benchmark results of the ORNL criticals were for a single-region homogeneous HEU sphere. The H_2O moderated uranium experiments, TRX-1 and TRX-2 hexagonal cores,[4] were analyzed to address the heterogeneous effects for a slightly enriched uranium fuel (e = 1.29%) in two different neutron spectra on the WIMSD4M group-collapsed cross sections. The results presented here are calculations of integral properties performed with the WIMSD4M, VIM, and MCNP codes. The calculations performed with both VIM and MCNP codes were performed with 2 million histories in an infinite lattice. The adequacy of the WIMSD4M cross-section data for the very low enriched water-moderated lattices were accounted for with the measured heavy metal reaction rate ratios, ρ^{28}, δ^{25}, δ^{28}, and C*. Measured and calculated integral property values for the TRX-1 and TRX-2 lattices are presented in Tables 3 and 4, respectively. The whole critical core of 764 fuel rods for TRX-1 and 578 fuel rods in TRX-2 lattice were also modeled in VIM, XSDRNPM and DIF3D using WIMSD4M cross sections.

Also included in Tables 3 and 4 are the computed infinite and effective multiplication factors, k_∞ and k_{eff} respectively. As can be seen from a comparison of measured and computed integral parameters, group-collapsed ^{235}U and ^{238}U thermal and epithermal reaction rates are in very good agreement with measured and Monte Carlo Calculations. While the calculated core k_{eff} values are lower than measured using DIF3D and XSDRNPM models, they are in good agreement with the whole core VIM model k_{eff} calculation.

CALCULATIONS OF THE GEOMETRICALLY MODIFIED LOS ALAMOS HIGHLY ENRICHED HEAVY WATER MODERATED BENCHMARKS

Several highly enriched critical assemblies of heavy water moderated core solutions of UO_2-F_2-D_2O were measured at Los Alamos National Laboratory.[11] Six of these spherical critical assemblies were modeled using VIM and found k_{eff}, values of $\approx 1.000 \pm 0.005$ for each measured configuration. These comparisons verified the reliability of VIM to model these D_2O critical systems. Unfortunately, it was not possible to model these measured data in WIMSD4M, since all critical assemblies were in spherical form. Therefore, it was decided to use the uranyl-fluoride heavy water composition in a cylindrical geometry along with the D_2O reflector for a more precise modeling. Each cylinder was assumed to have infinite height. A vacuum boundary condition was used at the outer boundary to specify no return current to the D_2O reflector. Diffusion calculations using DIF3D were performed with cross sections computed with WIMSD4M. Transport calculations were performed with XSDRNPM. The core and reflector dimensions and k_{eff} values for VIM, XSDRNPM and WIMSD4M-DIF3D are presented in Table 5. The core solution was assumed to have a stainless-steel container of 1.0 mm thickness. Each DIF3D calculation was made using 10-broad groups collapsed from a 69-fine group WIMSD4M transport solution. The results for three cases are shown in Table 5. They indicate good agreement between VIM and DIF3D k_{eff} values. The modeling of the smallest core radius sphere of 8.0 cm was performed in the DIF3D calculations with 10- and 18-group cross sections. The addition of eight thermal groups in the DIF3D calculation provided a k_{eff} closer to VIM results.

CONCLUDING REMARKS

The study presented in this paper addressed the adequacy of the WIMSD4M multigroup cross sections in the calculation of experimental and computational benchmark results. Existing light and heavy water homogeneous and infinite lattice benchmark data were modeled to verify the adequacy of the WIMSD4M transport generated group constants. The integral properties of the low enriched TRX criticals and the k_{eff} for the HEU light and heavy water assemblies calculated with broad-group cross sections computed with the WIMSD4M code and subsequently used in the WIMSD4M-DIF3D models showed good agreement with measured, and with Monte Carlo calculations.

REFERENCES

1. "WIMSD4 Winfrith Improved Multigroup Scheme Code System," Radiation Shielding Information Center, CCC-576, Martin Marietta Energy Systems, Inc., Oak Ridge National Laboratory (1990).

2. J. R. Deen, W. L. Woodruff and C. I. Costescu, "New ENDF/B-V Nuclear Data Library for WIMSD4M," Proc. 1993 Int. Mtg. on Reduced enrichment for Research and Test Reactors, October 3-7, 1993, Oarai, Japan (to be published).

3. R. E. MacFarlane, "The NYOY Nuclear Data Processing System, Version 91.0" Documentation for NJOY91.13 code package, Radiation Shielding Information Center, PSR-171, Martin Marietta Energy Systems, Inc., Oak Ridge National Laboratory (1991).

4. "Cross Section Evaluation Working Group Thermal Reactor Benchmark Compilation," CSEWG Data Testing Subcommittee, Thermal Data Testing Group, BNL-19302, Brookhaven National Laboratory (1974).

5. "TWODANT: One- and Two-Dimensional, Multigroup Discrete-Ordinates Transport Code System," Documentation CCC-547, Radiation Shielding Information Center, Martin Marietta Energy Systems, Inc., Oak Ridge National Laboratory (1990).

6. N. M. Greene, W. E. Ford III, L. M. Petrie, and J. W. Arwood, "AMPX-77: A Modular Code System for Generating Couple, Multigroup Neutron-Gamma Cross-Section Libraries from ENDF/B-V," ORNL/CSD-283, Martin Marietta Energy Systems, Inc., Oak Ridge National Laboratory (October 1992).

7. K. L. Derstine, "DIF3D: A Code to Solve One-, Two-, and Three-Dimensional Finite-Difference Diffusion theory Problems," ANL-82-64, Argonne National Laboratory (1982).

8. "SCALE: A Modular Code System for Performing Standardized Computer Analyses for Licensing Evaluation," NUREG/CR-0200, Rev. 4 (ORNL/NUREG/CSD-2/R4), Vols. I, II, and III (draft November 1993). Available from Radiation shielding Information Center at Oak Ridge National Laboratory as CCC-545.

9. R. N. Blomquist, "VIM: A Continuous Energy Neutron and Photon Transport Code," Proc. Topl.Mtg. Advances in Reactor Computations, Salt Lake City, Utah, March 1983, p. 222, American Nuclear Society.

10. J. F. Briemeister, Editor, MCNP - A General Monte Carlo Code for Neutron and Photon Transport," Version 3a, LA-7396-M, Rev. 2, Los Alamos National Laboratory (September 1986).

11. H. Paxton, "Los Alamos Critical Mass Data," LA-3067-MS, Los Alamos National Laboratory (December 1975).

TABLE 1

The 10-Broad-Group Structure Used in the Transport and Diffusion Models

Collapsed 10-Group Structure	
Broad Group	Energy Upper Boundaries (eV)
1	10^7
2	8.221×10^5
3	5.53×10^3
4	4.0
5	2.1
6	1.097
7	0.972
8	0.625
9	0.3
10	0.14[a]

[a]Lower energy boundary is 10^{-5} eV.

TABLE 2
Infinite and Effective Multiplication Factors for the ORNL Critical Spheres

	k_∞		k_{eff}			
	69-group	Continuous	10-group	10-group	238-group	Continuous
ORNL Sphere	WIMSD4M	VIM	TWODANT	DIF3D	XSDRNPM	VIM
1	1.2131	1.2131±0.0005[a]	1.0086	1.0106	0.9987	0.9991±0.0005[a]
2	1.2089	1.2083±0.0005	1.0100	1.0103	0.9985	0.9991±0.0005
3	1.2022	1.2016±0.0005	1.0066	1.0072	0.9955	0.9965±0.0005
4	1.2025	1.2019±0.0005	1.0080	1.0087	0.9969	0.9977±0.0005
10	1.0724	1.0722±0.0005	1.0039	1.0045	0.9980	0.9998±0.0006

[a]Represents 1 σ standard deviation.

Note: The critical spherical radius of cases 1-4 is 34.6 cm and sphere 10 radius is 61.0 cm.

TABLE 3
Integral property values for the TRX-1 Lattice

	k_∞	k_{eff}	ρ^{28}	δ^{25}	δ^{28}	C*
Measured		1.000	1.320±0.021	0.0987±0.0010	0.0946±0.0041	0.797±0.008
WIMSD4M	1.1755	-[b]	1.347	0.097	0.0941	0.797
DIF3D	1.1728	0.9916	-	-	-	-
XSDRNPM	1.1733	0.9902	1.399	0.1010	0.0989	0.813
VIM	1.1814±0.0005[a]	0.9907±0.0006	1.306±0.002	0.09660±0.0001	0.0914±0.0001	0.784±0.0010
MCNP	1.1802±0.0003	-[c]	1.330±0.002	0.0974±0.0001	0.0892±0.0001	0.7880±0.0007

[a]Represents 1 σ standard deviation.
[b]Not possible in WIMSD4M.
[c]The whole core was not modeled in MCNP, only infinite lattice.

Note: Integral parameters correspond to thermal cutoff of 0.625eV. The WIMSD4M ENDF/B-V data uses mod. 2 data for ^{235}U and ^{238}U while VIM and MCNP ENDF/B-V data uses mod. 0 data.

ρ^{28} = ratio of epithermal-to-thermal ^{238}U captures.
δ^{25} = ratio of epithermal-to-thermal ^{235}U captures.
δ^{28} = ratio of ^{238}U fissions to ^{235}U fissions.
C^* = ratio of ^{238}U captures to ^{235}U captures.

TABLE 4
Integral Property Values for the TRX-2 Lattice

	k_∞	k_{eff}	ρ^{28}	δ^{25}	δ^{28}	C^*
Measured		1.000	0.8370±0.016[a]	0.0614±0.008	0.0693±0.0035	0.647±0.006
WIMSD4M	1.1627	-[b]	0.8420	0.0597	0.0675	0.642
DIF3D	1.1594	0.9977	-	-	-	-
XSDRNPM	1.1621	0.9944	0.8710	0.0616	0.0702	0.650
VIM	1.1652±0.0005[a]	0.9938±0.0014	0.8190±0.0014	0.0596±0.0001	0.0661±0.0001	0.6350±0.0008
MCNP	1.1660±0.0003	-[c]	0.8310±0.0013	0.0599±0.0001	0.0643±0.0001	0.6390±0.0005

[a]Represents 1 σ standard deviation.
[b]Not possible in WIMSD4M.
[c]The whole core was not modeled in MCNP, only infinite lattice.

Note: Integral parameters correspond to thermal cutoff of 0.625 eV. The WIMSD4M ENDF/B-V data uses mod. 2 data for ^{235}U and ^{238}U while VIM and MCNP ENDF/B-V data uses mod. 0 data.

ρ^{28} = ratio of epithermal-to-thermal ^{238}U captures.
δ^{25} = ratio of epithermal-to-thermal ^{235}U captures.
δ^{28} = ratio of ^{238}U fissions to ^{235}U fissions.
C^* = ratio of ^{238}U captures to ^{235}U captures.

TABLE 5
UO_2-F_2-D_2O Core Solution with Stainless-Steel Container and D_2O Reflector in Cylindrical Geometry

		k_{eff}			
Inner Core Radius (cm)	Outer Reflector Thickness (cm)	VIM	XSDRNPM	DIF3D	
		Continuous	238-Group	10-Group	18-Group
8.0	71.9	0.9987±0.0007	0.9977	1.0027	1.0009
10.0	39.9	0.9937±0.0007	0.9950	0.9958	0.9937
12.0	27.9	0.9972±0.0007	0.9981	0.9954	0.9943

Methodology and Application of the WIMS-D4m Fission Product Data

S. C. Mo

Argonne National Laboratory
Argonne, IL 60439-4841 USA

ABSTRACT

The WIMS-D4 code has been modified (WIMS-D4m) to generate burn-up dependent microscopic cross sections for use in full core depletion calculations. The calculation of neutron absorption by fission products can be obtained from a reduced fission-product-chain model that includes the ^{135}Xe and ^{149}Sm chains, and a lumped fission product to account for the absorption by fission products not explicitly treated. Burn-up calculations were performed for the ANS MEU core using WIMS and EPRI-CELL cross sections. The calculated eigenvalues and material loadings are in good agreements.

INTRODUCTION

The WIMS-D4 code was originally developed by the UK Atomic Energy Establishment at Winfrith to perform a wide range of reactor lattice cell calculations and to generate few group macroscopic cross sections for neutron diffusion calculations[1-2]. The code has been modified (WIMS-D4m) at ANL to make it more compatible with current computational environment[3]. A new 69-group WIMS library has been created with ENDF/B-V data for use in WIMS-D4m. The cross sections generated from WIMS-D4m and the new library have been tested and good agreements with detailed Monte Carlo results were obtained[3].

The buildups of fission products can be obtained from the WIMS lattice cell depletion calculation or from the REBUS[4] full core calculation by specifying the appropriate fission product chains.This paper presents results of a burn-up study performed for the Advanced Neutron Source reactor (ANS) using the WIMS-D4m fission product data. The buildup behavior, energy dependence of neutron absorption and reactivity worth of major fission products in the ANS reactor will be examined. The result of a reduced fission-product-chain calculation using a lumped fission product and some limitations in the WIMS depletion model in short fuel cycle calculations will be discussed.

GENERATION OF WIMS CROSS SECTIONS

The current ANL WIMS library contains 98 materials of which 35 are fission products[3]. A pseudo fission product is formed to account for the absorption by fission products not explicitly treated by WIMS. The WIMS depletion model has been modified to include ^{135}I and ^{149}Pm in the fission production chains that lead to the productions of ^{135}Xe and ^{149}Sm. Users can specify macroscopic or microscopic cross sections to be generated by WIMS-D4m in the ISOTXS format for use in full core burn-up calculations.

The computational models and compositions for the ANS calculations were provided by the Oak Ridge National Laboratory and the Idaho National Engineering Laboratory. Fifteen-group microscopic cross sections were generated by WIMS-D4m using a 1-dimensional radial model of the MEU core. The model consists of a radial slice through the middle fuel element. The fuel, clad and coolant were homogenized to form a single core composition. An external Dancoff factor was used to account for the spatial shielding of the fuel plates.The core is surrounded on two sides by D_2O reflectors. A schematic diagram of the radial core model is shown in Fig.1.

Burn-up dependent cross sections were generated for the fissile materials and major fission products in the ^{135}Xe and ^{149}Sm chains. The cross sections of the remaining fission products were generated by WIMS-D4m using the material composition and fluxes at mid-cycle. A summary of the fission product data is given in Table 1.

BUILDUPS OF FISSION PRODUCTS IN ANS

The absorption by fission products is a major contribution to the reactivity loss in the ANS reactor[5-6]. It accounts for nearly 9% $\delta k/k$ of reactivity loss in the MEU core. The reactivity worth of fission products in the ANS reactor are compared in Table 2 with data obtained from a DIDO reactor study[7]. The high reactivity worth of the fission products is attributed to the high burn-up, high flux and under-moderated characteristics of the ANS reactor. At the end of the core lifetime (EOL), about 30% of the ^{235}U loading in the fuel elements is burnt and converted into fission products. They account for over 25% of the total neutron absorption in the core.

Strong absorbers or nuclides with short half-lives such as ^{135}Xe and ^{105}Rh, reach their equilibrium concentrations after relatively short irradiations. The equilibrium concentrations depend on the power density and flux level in the fuel element. The concentrations of saturating fission products will gradually decrease due to the depletion of fissile materials at a constant power level. The buildups of ^{135}Xe and ^{105}Rh in the ANS environment are shown in Fig.2. They account for nearly 50% of the fission product absorption at EOL.

Majority of fission products are stable and have relatively small capture cross sections. Their concentrations generally increase linearly with irradiation. Despite their relatively small capture cross sections, the buildups of non-saturating fission products near EOL is

important to the reactivity balance of the reactor. The buildups of fission products ^{133}Cs, ^{131}Xe and ^{152}Sm in the ANS environment are shown in Fig. 3. They account for about 8% of the total fission product absorption at EOL.

FULL CORE BURN-UP CALCULATIONS USING DETAILED FISSION PRODUCT CHAINS

Full core burn-up calculations were performed for the ANS MEU core using the REBUS-3 code and 15-group WIMS cross sections. The REBUS model shown in Fig.4 consists of 3 fuel elements containing 35% enriched U_3Si_2 with a meat density of 3.5 gU/cm^3. The fuel elements are ungraded and the total core volume is 82.6 liter. Each of the fuel elements is divided into 9 regions to account for the spatial buildup of fission products. The reactor operates at 330 MW and has a cycle length of 17 days.

The buildups of fission products in the ANS reactor was calculated by REBUS using a detailed 19 fission-product-chain model. A summary of the 19 fission product chains is given in Fig. 5. The burn-up calculation was performed with five equal time steps. The reflector components were excluded from the diffusion calculation and the control rods were at fully withdrawn positions.

A summary of absorption contributions from major fission products at EOL are given in Table 3. The absorption is dominated by major thermal absorbers such as ^{135}Xe and ^{149}Sm. They account for over 50% of the total fission product absorption. The hard neutron spectrum in the ANS increases the resonance absorption by fission products at epi-thermal energies. Nearly 30% of the fission product absorption occurs above thermal energies ($E > 0.625$ eV). ^{105}Rh which is a less important fission product in thermal reactors, is the third major fission product absorber in the ANS. The energy dependence of the fission product absorption can affect important reactor parameters such as reactivity coefficients.

REDUCED FISSION PRODUCT CHAINS

The buildups of fission products are obtained from the solutions of a large number of isotopic depletion equations. Since the storage requirement in depletion calculations goes up as the square of the number of active nuclides. It is desirable to reduce the number of fission product nuclides in routine full core depletion calculations. In a reduced fission-product-chain model, the buildups of major fission products in the ^{135}Xe and ^{149}Sm chains are treated explicitly in full core depletion calculations. The absorption by other fission products is represented by a single group of lumped fission product. The reduced fission product chains are shown in Fig. 6.

The microscopic cross section of lumped fission product is customarily defined as[8-9]

$$\sigma_g^{lfp}(\beta) = \frac{\sum_i N_i(\beta)\,\sigma_{i,g}}{\int_0^t S(t')\,dt'} \qquad \text{barns/fission,} \qquad (1)$$

where S is the fission source and β is the fractional depletion of ^{235}U given by

$$\beta(t) = \frac{N_{235}(0) - N_{235}(t)}{N_{235}(0)} \quad . \qquad (2)$$

The summation in the numerator of Eq. (1) includes all saturating and non-saturating fissions products not treated explicitly by REBUS. Excluding the contributions from rapidly saturating nuclides such as ^{135}Xe and ^{149}Sm, the asymptotic thermal cross section and resonance integral of the lumped fission product according to the yields for ^{235}U are approximately 44 and 209 barns/fission[8]. The lumped fission product data is treated by REBUS as a polynomial function of ^{235}U burn-up. The total absorption cross section of the lumped fission product is calculated from the cumulative fission source of the fuel element:

$$\Sigma_g^{lfp}(\beta) = \sigma_g^{lfp}(\beta)\int_0^t S(t')\,dt' = \sum_i N_i(\beta)\,\sigma_{i,g} \quad . \qquad (3)$$

Provided the absorption by the lumped fission product is small, the lumped fission product concentration is directly proportional to the cumulative fission source. The fission source integral can be obtained from the calculation of the lumped fission product concentration by assuming a fission yield of unity. The calculation of fission product absorption from Eqs. (1) and (3) is similar to the macroscopic cross sections approach described in reference 5.

The reactivity changes obtained from REBUS calculations using detailed and reduced fission product chains are compared in Fig. 7. The calculated eigenvalues are in very good agreement. The reduced fission-product-chain model over-predicted the total capture rate in the core by about 1%.

The burn-up calculation was repeated with cross sections obtained from the EPRI-CELL code using a ENDF/B-IV based library[9]. The reactivity changes and material loadings obtained from REBUS calculations using reduced fission product chains are compared in Fig. 8 and Table 4. It can be seen that the REBUS/WIMS and the REBUS/EPRI-CELL results are in reasonably good agreement. The consistent 0.6% $\delta k/k$ difference in reactivity is attributed to the different versions of the ENDF data.

WIMS DEPLETION MODEL IN SHORT FUEL CYCLE CALCULATION

The depletion model in WIMS-D4m consists of 26 fission product chains and 36 fission product nuclides. The model neglects the decays of several fission product nuclides which have half- lives comparable with the purposed 17 days cycle length of the ANS reactor. They include the decay of ^{147}Nd (10.98 days half-life) in the secondary ^{149}Sm chain and the decay of ^{143}Pr (13.57 days half-life) in the ^{143}Nd chain. The changes in the core reactivities calculated with and without ^{147}Nd and ^{143}Pr are compared in Fig.9. The neglects of ^{147}Nd and ^{143}Pr in the WIMS fission product chains cause over-predictions in the buildups of ^{147}Pm, ^{148}Pm, ^{149}Sm and ^{143}Nd. The EOL reactivity is under-predicted by about 1.1% δk/k. The discrepancy caused by the neglects of ^{147}Nd and ^{143}Pr in the WIMS depletion model is less important in long fuel cycle calculations.

CONCLUSIONS

The fission product data generated by the WIMS-D4m code using the ANL ENDF/B-V based WIMS library are suitable for most reactor fuel cycle analyses. The code can generate burn-up dependent microscopic or macroscopic cross sections in the ISOTXS format for use in detailed depletion calculations. The results obtained from full core burn-up calculations show good agreements between the WIMS-D4m and EPRI-CELL fission product data.

The calculation of neutron absorption by fission products can be obtained from a reduced fission-product-chain model that includes the ^{135}Xe and ^{149}Sm chains, and a lumped fission product to account for the fission products not explicitly treated. The microscopic cross section of the lumped fission product is given in barn/fission.

Burn-up calculations were performed for the ANS MEU core using the WIMS-D4m fission product data. The reactivity worth of fission products accounts for over 70% of the reactivity loss at EOL. The high absorption by fission products is attributed to the high burn-up, high flux and under-moderated characteristics of the ANS reactor.

REFERENCES

1. J. R. Askew, F. J. Fayers, P. B. Kemshell, "A General Description of the Lattice Code WIMS," J. of Brit. Nucl. Energy Soc., vol. 5, 1966.

2. J. G. Tyror and J.R. Askew, "The United KIngdom Approach to the Calculation of Burn-up in Thermal Reactors," Reactor Burn-up Physics, IAEA, Vienna, 1973.

3. J. R. Deen and W. L. Woodruff, "New ENDF/B-V Nuclear Data Library for WIMS," 16th International RERTR Meeting, Oarai, Ibaraki, Japan, October 1993.

4. B. J. Toppel, "A User's Guide for the REBUS-3 Fuel Cycle Analysis Capability," ANL-83-2 (March 1983).

5. M. M. Bretscher, J. R. Deen, N. A. Hanan, J. E. Matos, S. C. Mo, R. B. Pond, A. Travelli and W. L. Woodrudff, "Relative Performance Properties of the ORNL Advanced Neutron Source Reactor with Reduced Enrichment Fuels", 17th International RERTR Meeting, Williamsburg, Virginia, USA, September 1994.

6. C. A. Wemple, B. G. Schnitzler, A. M. Ougouag, S. C. Mason, R. L. Moore and J. M. Ryskamp, "Advanced Neutron Source Idaho National Engineering Laboratory Monthly Report for April 1994." ANS Monthly Progress Report for April 1994, ORNL/ANS/INT-5/V73.

7. "Research Reactor Core Conversion from the Use of Highly Enriched Uranium to the Use of Low Enriched Uranium Fuels, Guidebook Addendum: Heavy Water Moderated Reactors," IAEA-TECDOC-324, 1985.

8. J. D. Garrison and B. W. Roos, "Fission-Product Capture Cross Sections," Nucl. Sci. Eng Vol 12, 1962.

9. W. R. Cobb, W. J. Eich and D. E. Tivel, "Advanced Recycle Methodology Program System Documentation: EPRI-CELL Code Description", Oct 1975.

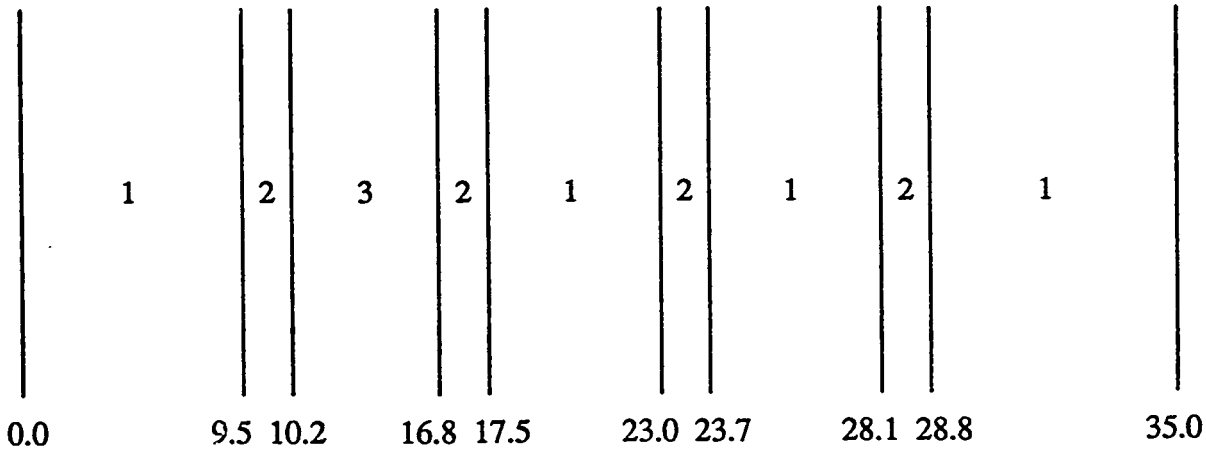

Material compositions

1. D_2O
2. Side Plate
3. Homogenized Fuel

Note: All dimensions in cm

FIGURE 1. One-dimensional model in WIMS depletion calculations

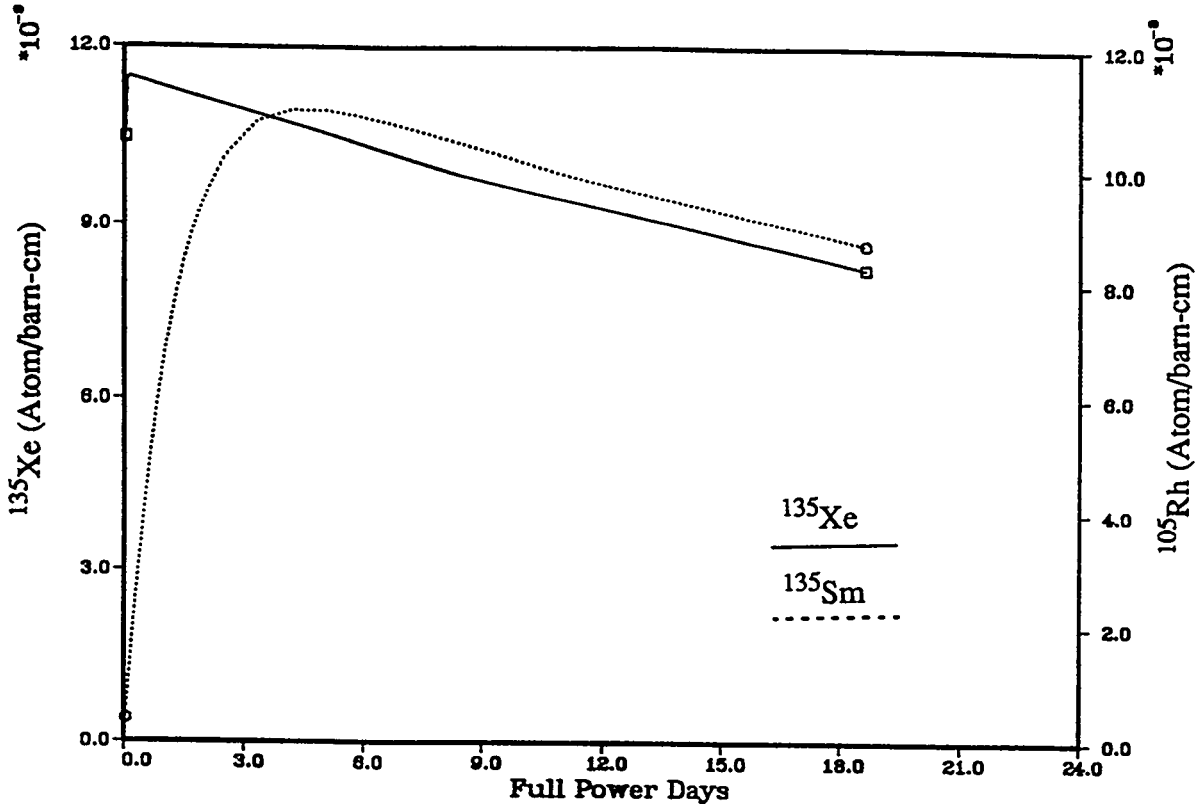

FIGURE 2. Buildups of ^{135}Xe and ^{149}Sm in the ANS environment

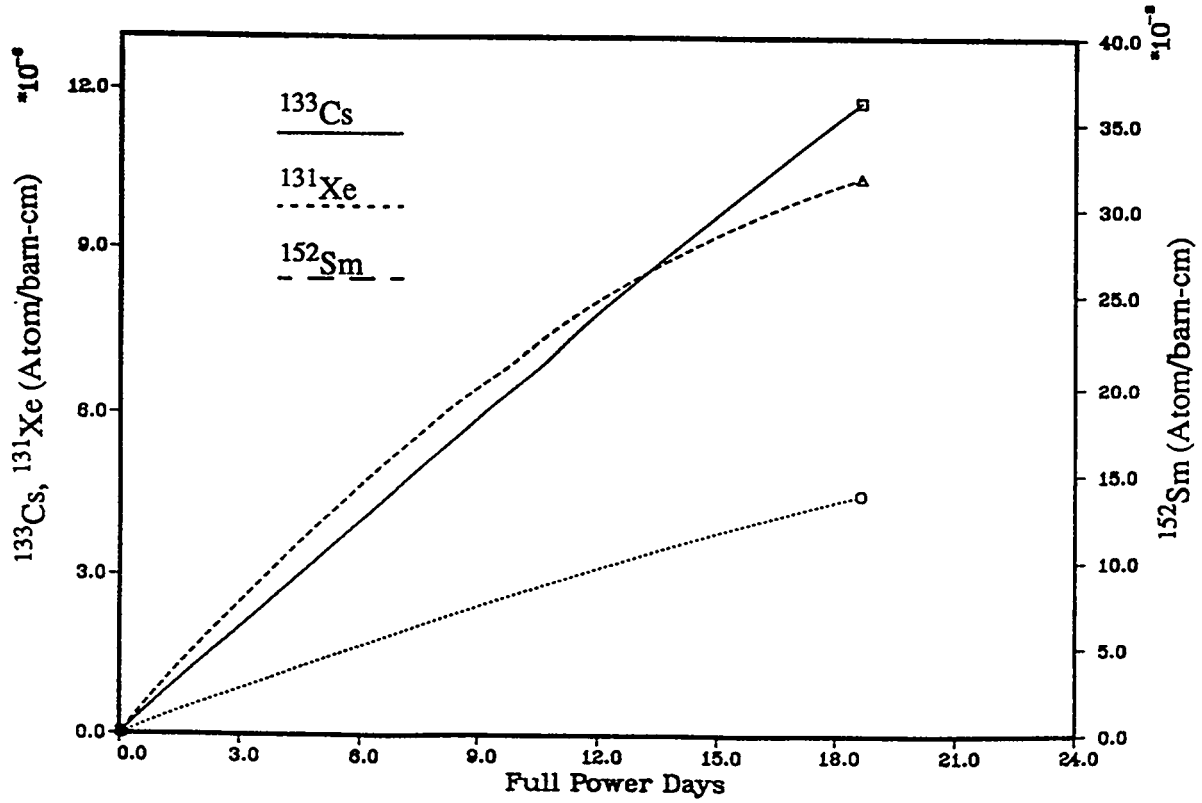

FIGURE 3. Buildups of ^{133}Cs, ^{131}Xe and ^{152}Sm in the ANS environment

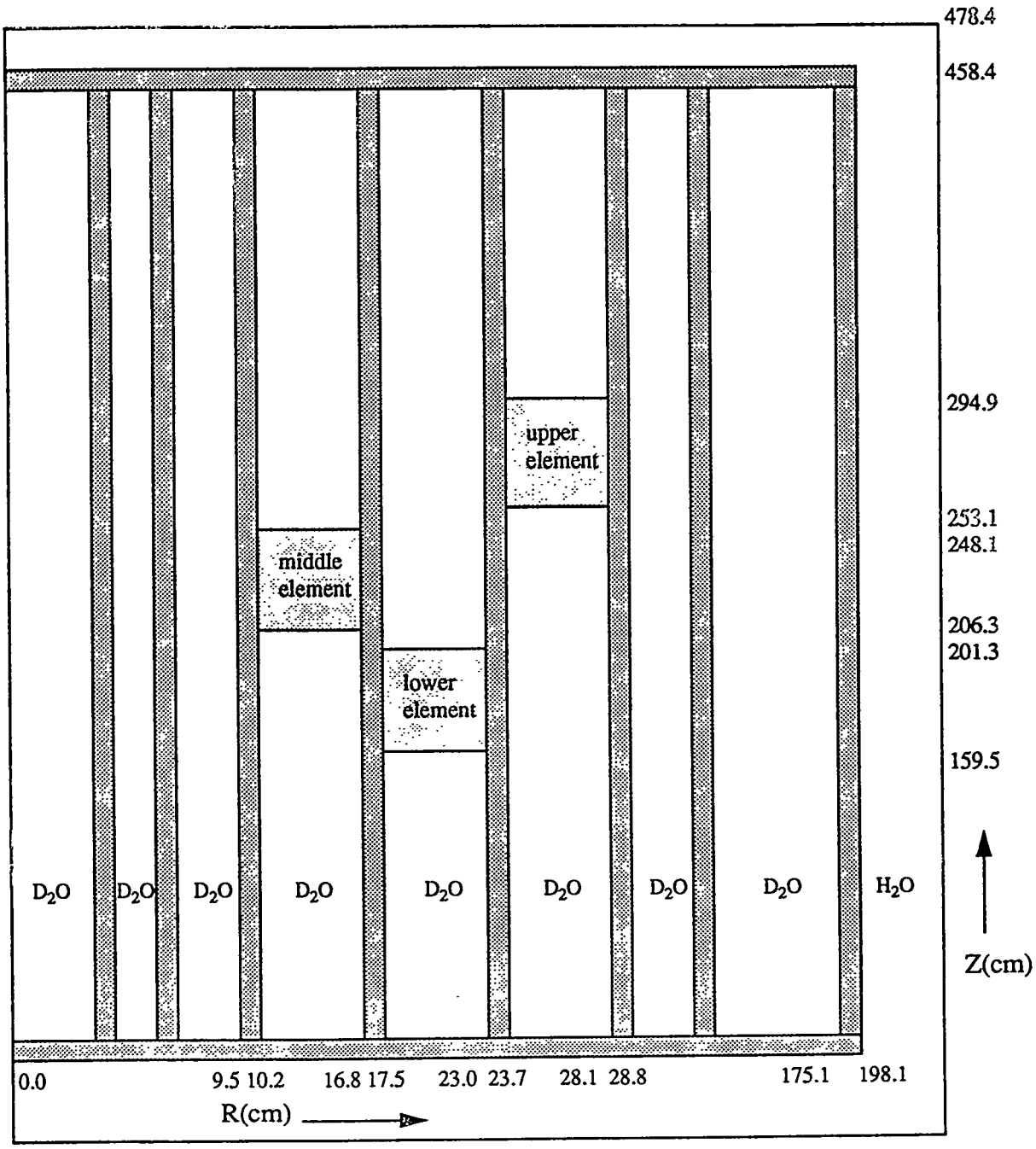

FIGURE 4. Full core model in REBUS depletion calculations

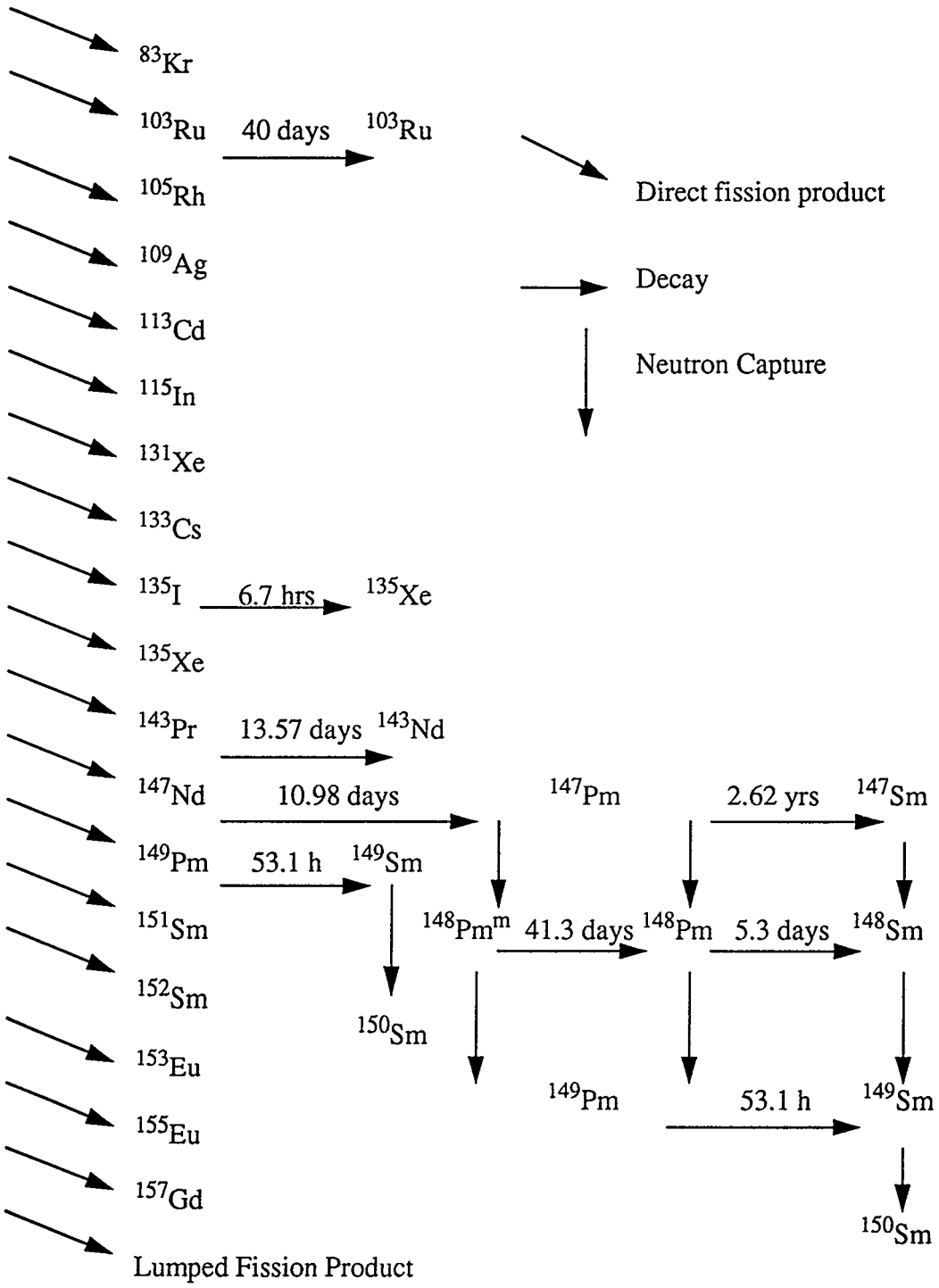

FIGURE 5. Detailed Fission Product Chains in REBUS Depletion Calculation

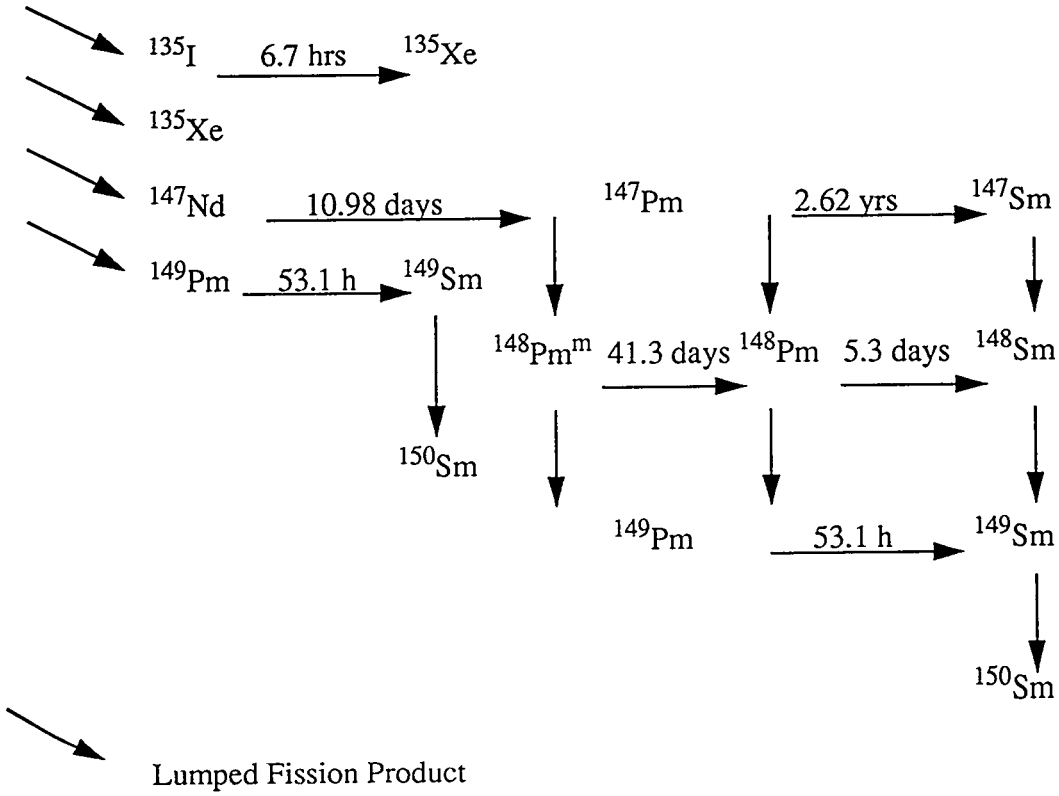

FIGURE 6. Reduced Fission Product Chains in REBUS Depletion Calculation

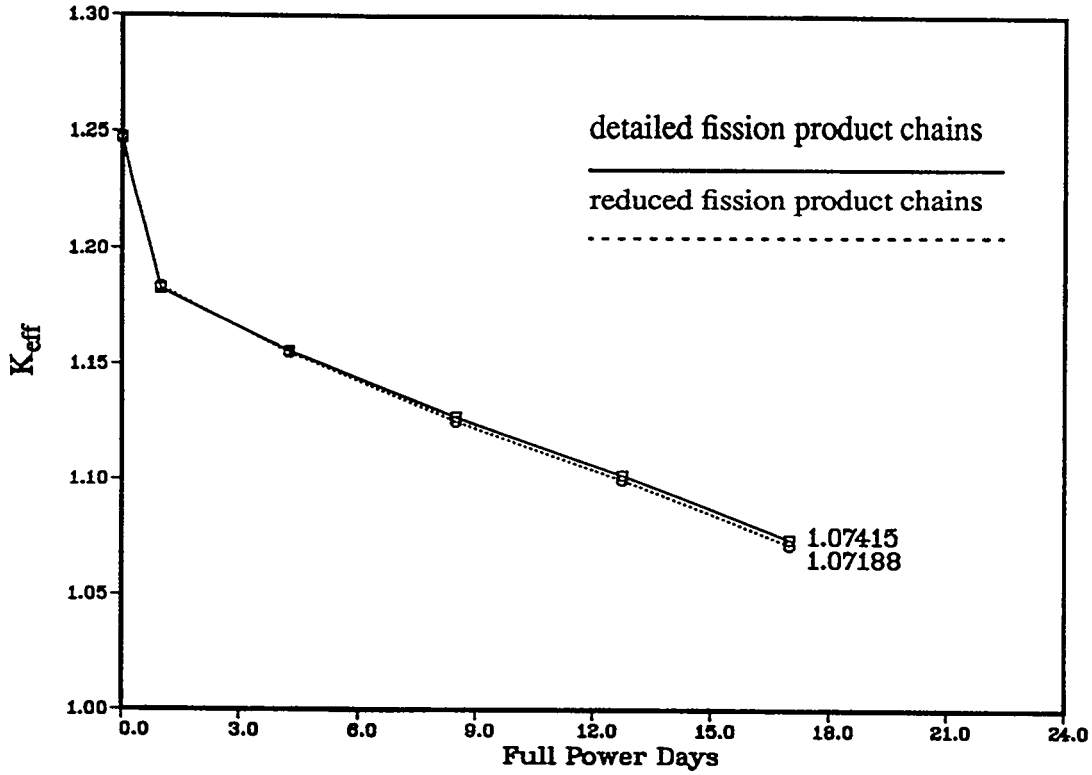

FIGURE 7. K_{eff} changes from detailed and reduced fission product chains calculations

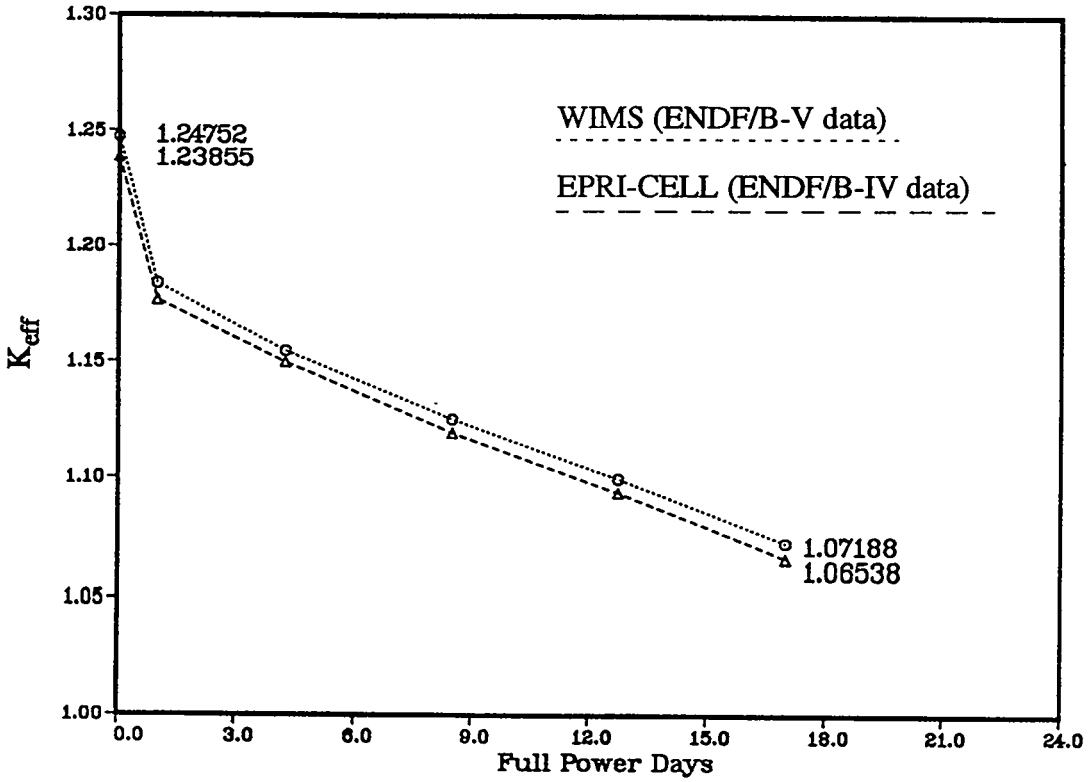

FIGURE 8. K_{eff} changes from reduced fission product chains calculations using WIMS and EPRI-CELL cross sections

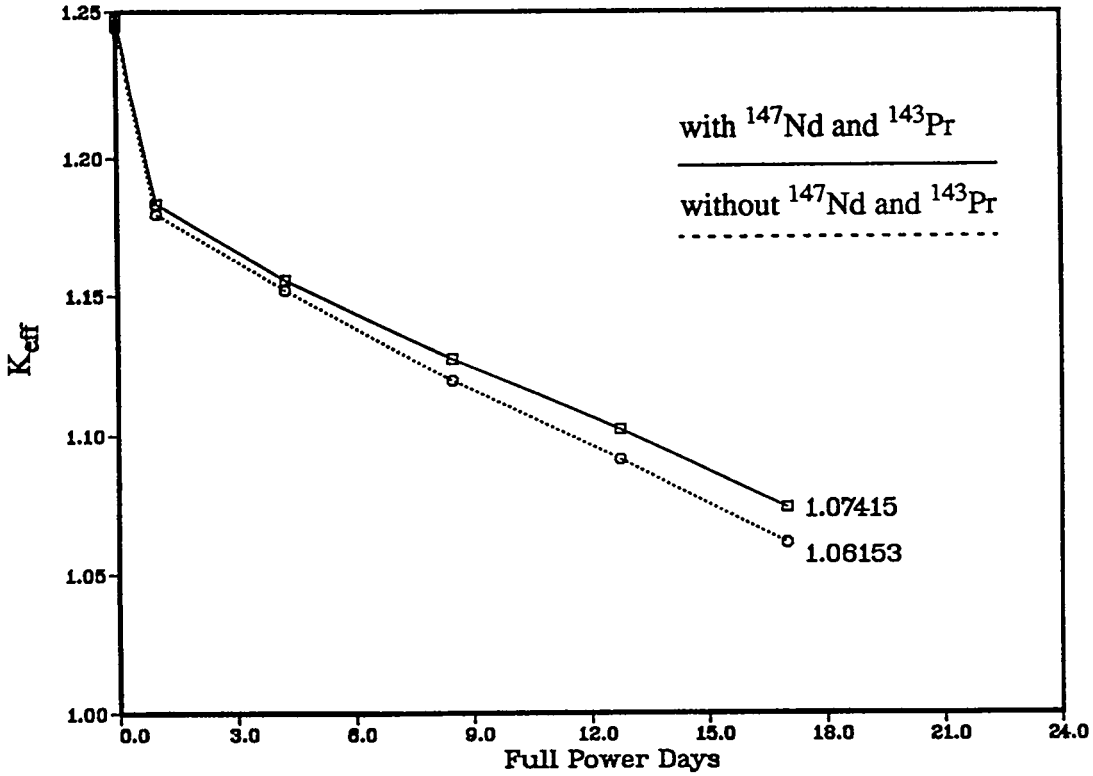

FIGURE 9. K_{eff} changes from detailed fission product chains with and without ^{147}Nd and ^{143}Pr

TABLE 1. Fission Product Data in REBUS Depletion Calculations

Isotope	^{235}U Fission Yield	Half-life	Thermal XS at 2200 m/s (barns)	Resonance Integral above 0.5 eV (barns)
^{83}Kr	0.00536		208	235
^{103}Ru	0.03040	40 days	5	53
^{103}Rh			147	1020
^{105}Rh	0.00967	35 hrs	16000	25300
^{109}Ag	0.00034		89	1390
^{113}Cd	0.00016		20100	360
^{115}In	0.00011		230	3200
^{131}Xe	0.02880		93	879
^{133}Cs	0.06700		29	393
^{135}I	0.06297			
^{135}Xe	0.00242	9.2 hrs	2.67×10^{6}	7520
^{143}Pr	0.05940	13.47 days	90	190
^{143}Nd			330	130
^{147}Nd	0.02252	10.98 days	400	400
^{147}Pm		2.62 yrs	234	3020
^{147}Sm			87	695
$^{148}Pm^{m}$		42 days	27000	32000
^{148}Pm		5.3 days	1500	44000
^{149}Sm			37900	2620
^{150}Sm			102	293
^{151}Sm	0.00418		12400	2340
^{152}Sm	0.00268		208	2990
^{153}Eu	0.00161		390	1583
^{154}Eu			1500	675
^{155}Eu	0.00032		14000	6300
^{157}Gd	0.00006		2.54×10^{5}	520

TABLE 2. Comparison of fission product worth in the ANS and DIDO reactors

	ANS(MEU)	DIDO(MEU)
Reactor Power	330 MW	25.5 MW
Core Volume	82.6 liter	354 liter
Average φ_{th} in core[a]	4.3×10^{14} n/cm^2/s	3.6×10^{14} n/cm^2/s
Average φ_{epi} in core[b]	2.3×10^{15} n/cm^2/s	2.6×10^{14} n/cm^2/s
Cycle Length	17 days	24 days
Average ^{235}U Burn-up	30%	30%
$\delta k/k$ (BOC - EOC)	12.93%	9.69%
$\delta k/k$ (total fission product)	9.22%	6.61%

<u>Major fission product worth at EOL</u>

Fission Product	Reactivity Worth (–% $\delta k/k$)	
	ANS(MEU)	DIDO(MEU)
^{135}Xe	4.34	3.51
^{149}Sm	0.72	0.63
Other fission products	4.16	2.47

a. $E_{th} \leq 0.625$ eV

b. $E_{th} \leq E_{epi} \leq 6$ KeV

TABLE 3. Absorption by Major Fission Products in the ANS MEU Core at EOL

FP Chain Mass Number	Nuclide	% FP Absorption	% thermal
135	^{135}I	0	
	^{135}Xe	45	100
147 & 149	^{147}Nd	1.8	10
	^{147}Pm	2.8	12
	^{148}Pm	1.1	27
	^{148m}Pm	1.2	92
	^{149}Pm	1.2	71
	^{149}Sm	8.2	98
103	^{103}Ru	0.5	11
	^{103}Rh	0.9	22
105	^{105}Rh	3.9	58
143	^{143}Pr	2.5	39
	^{143}Nd	2.2	78

TABLE 4. Comparison of EOL material loadings from REBUS calculations using WIMS and EPRI-CELL data

	REBUS/WIMS	REBUS/EPRI-CELL
^{235}U	16.781 Kg	16.806 Kg
^{239}Pu	0.301 Kg	0.305 Kg
^{135}Xe	0.147 g	0.160 g
^{149}Sm	0.998 g	1.049 g
^{149}Pm	7.651 g	7.377 g

Neutronic Study on Conversion of SAFARI-1 to LEU Silicide Fuel

G. Ball
Atomic Energy Corporation of South Africa Limited
Pretoria, South Africa

R. Pond, N. Hanan and J. Matos
Argonne National Laboratory
Argonne, Illinois 60439-4841, USA

ABSTRACT

This paper marks the initial study into the technical and economic feasibility of converting the SAFARI-1 reactor in South Africa to LEU silicide fuel. Several MTR assembly geometries and LEU uranium densities have been studied and compared with MEU and HEU fuels. Two factors of primary importance for conversion of SAFARI-1 to LEU fuel are the economy of the fuel cycle and the performance of the incore and excore irradiation positions.

INTRODUCTION

The Atomic Energy Corporation of South Africa Ltd (AEC) supports the principles of the Reduced Enrichment for Research and Test Reactor (RERTR) Program and its nonproliferation goal of reducing or eliminating international trade in highly enriched uranium. After exploratory discussions a joint study into the technical and economic feasibility of conversion of the SAFARI-1 Reactor was initiated in September 1993 with the signing of a protocol agreement between the RERTR Program at Argonne National Laboratory (ANL), the United States Department of Energy and the AEC.

This paper presents the results of the first phase of the work, namely the neutronic study. Subsequent phases will include safety studies and economic issues. As the AEC is currently undergoing a transition towards a more commercially oriented organisation the economic impact of any conversion is of primary concern. The fuel cycle and the neutron flux spectrum and the flux level in the incore and excore irradiation positions will feature prominently in the final conversion decision.

In this paper the results of core performance as a function of various enrichments, loadings and assembly geometries are reported. Proven fuel assembly designs and loadings with minimum changes to the current core configuration have been utilised.

SAFARI-1 CHARACTERISTICS AND UTILISATION

The SAFARI-1 reactor is a 20MW pool-type materials testing reactor operated by the AEC at its Pelindaba site near Pretoria, South Africa. Since its commissioning in 1965, the reactor has operated with an exemplary safety record. It is supported by the infrastructure of the AEC which includes a fuel fabrication plant, hot cell facilities, isotope production centre, radioactive waste disposal site and a theoretical reactor physics support group.

The reactor is located in a large pool with easy access to both incore and excore irradiation positions. An 8x9 grid houses 28 fuel assemblies, 5 control rods, 1 regulating rod, the incore irradiation facilities and the reflector elements. The core is fuelled with the 19-plate MTR-type fuel elements shown in Figure 1. The control rods are comprised of a 15 plate fuel follower section (shown in Figure 2) beneath a cadmium absorber section.

The reactor originally was fuelled with 90 wt% enriched uranium-aluminium alloy fuel (HEU) but was converted to a 45 wt% uranium-aluminium alloy (MEU) during the early 1980's. Due to the higher scrap rate in the manufacturing process of our MEU fuel and the availability of HEU in South Africa it was recently decided to return to the manufacture and use of HEU fuel assemblies for economic reasons. The first of the HEU assemblies will be loaded into the core prior to the end of 1994. This decision was made prior to the commencement of this joint study on the feasibility of converting SAFARI-1 to use low enriched uranium silicide fuel.

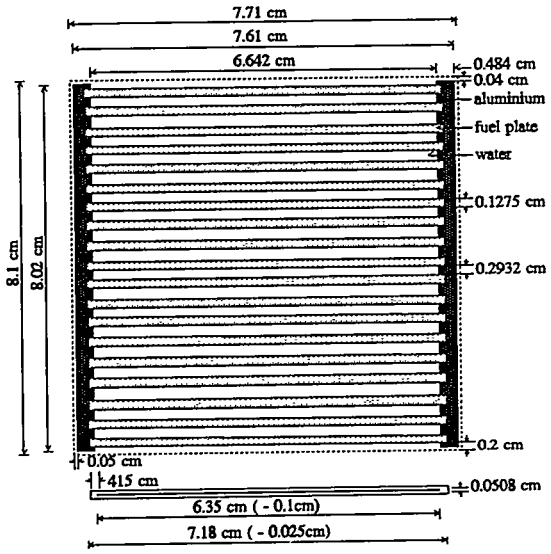

Figure 1: SAFARI-1 Fuel Assembly

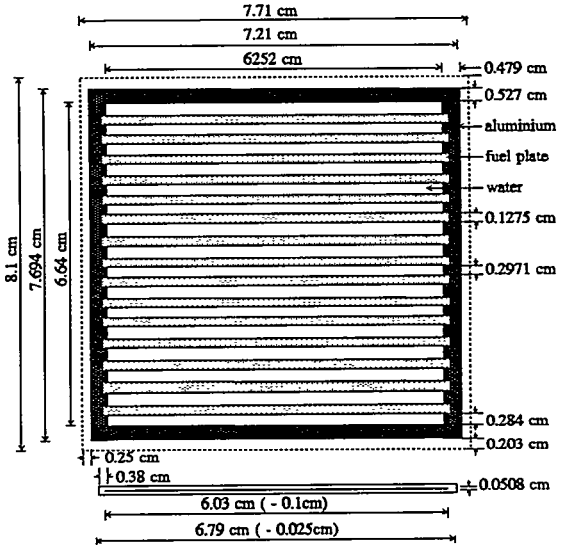

Figure 2: SAFARI-1 Follower Assembly

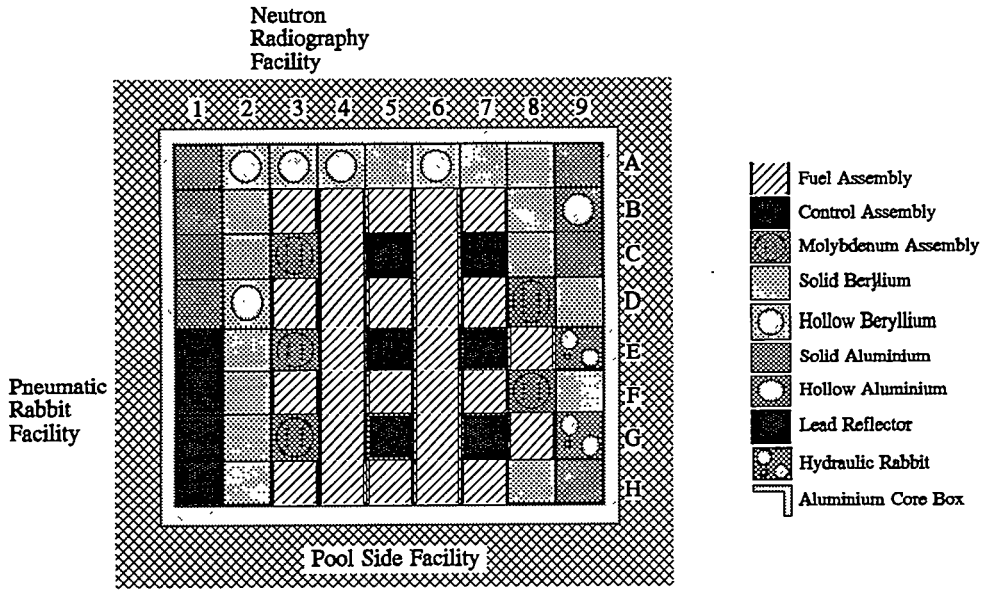

Figure 3: SAFARI-1 Core

SAFARI-1 has several incore irradiation positions, some of which can be loaded while the reactor is at power. Most of these positions are reserved for molybdenum production. All the South African Mo^{99} requirements have been met since June 1993 and a program for the large scale production of molybdenum is in place. Various other radioactive isotopes for medical and industrial applications are also produced.

The reactor vessel is cylindrical in shape except for one flattened side which is also the wall of the rectangular core box adjacent to the pool side facility. This large excore pool side facility allows irradiations to be performed in relatively high neutron fluxes since it is directly adjacent to the fuel elements. Irradiations in the pool side can be performed as close as 3.5cm from the fuel. The pool side houses our automated silicon irradiation facility (SILIRAD)[1] which has a current annual capacity of 5 tons at a reactor power level of 10MW. Gemstone irradiations are also performed in the pool side.

The reactor is also equipped with a number of beam tubes, one of which services our neutron radiography facility, while hydraulic and pneumatic rabbit facilities provide for the irradiation of various material samples.

CALCULATIONAL MODEL

The computer code WIMSD4m[2] was used to generate burnup dependent microscopic cross sections in six energy groups using slab geometry representations for the fuel and control rod follower materials. The fuel cross sections for the standard fuel and follower were generated with

a three-region cell consisting of fuel, clad and moderator while the fuel assembly side plates were modelled by including an extra region containing a volume weighted mixture of water and aluminium. Microscopic cross sections for the irradiation positions and the beryllium, aluminium and lead reflector regions were also generated with WIMSD4m using slab models. The reflector assemblies and irradiation positions have been represented as closely as possible in their true environment (within the limitations of the WIMSD4m one-dimensional model).

The core neutronics and burn-up calculations were performed in three dimensions using the REBUS code system[3] and the DIF3D[4] diffusion theory neutronics code. A detailed Monte Carlo model using the MCNP[5] code was used for benchmarking the accuracy of the diffusion theory model results.

The active fuel and side plate regions have been modelled separately in the diffusion theory calculations. Elements with cylindrical holes were modelled exactly in MCNP and as volume equivalent square holes in DIF3D. A substantial effort was made both in the diffusion theory and Monte Carlo models to accurately represent the key irradiation positions of economic interest. Average thermal fluxes and thermal-to-total ratios have been calculated for each irradiation facility to characterise these positions as a function of the different fuels.

In the pool side, average fluxes and flux-ratios have been calculated in a horizontal region 12 cm from and parallel to the core face at the axial core centre. This position coincides with the centre of the SILIRAD position when it is in operation. The neutron radiography beam tube itself was not modelled but average fluxes and flux ratios calculated in water adjacent to the core box in the vicinity of the beam tube.

The five molybdenum irradiation positions in the core each consist of an aluminium element with a cylindrical hole filled with water into which the target plates are inserted. Fluxes and flux ratios, in water in the positions where the target plates are placed, averaged over all five positions have been calculated. The hydraulic rabbit was modelled homogeneously in both DIF3D and MCNP and the fluxes and flux ratios averaged over the four tubes of the rabbit facility. And lastly, the excore pneumatic rabbits themselves have not been modelled but average fluxes and flux ratios calculated in the water adjacent to the core box in the vicinity of the pneumatic rabbit facility.

MODEL VALIDATION

Initially, comparisons of thermal fluxes and thermal-to-total flux ratios in five irradiation locations were made between DIF3D and MCNP for an all-fresh core with control rods withdrawn. Volume averaged fluxes and flux ratios over each irradiation facility described previously were calculated. Table 1 shows the percentage differences in the flux and flux ratios for each facility.

The smaller differences between the two codes for the hydraulic rabbit is due to its homogeneous treatment by both codes thus eliminating modelling differences with respect to geometrical effects. Notice also that although there is an 8.6% difference in the absolute value of the thermal flux in the pool, side the flux ratio is practically the same.

Table 1: Thermal Flux and Thermal-to-Total Flux Ratios for Fresh Core
(DIF3D percentage differences from MCNP)

Position	Thermal flux (% difference)	Thermal-to-total ratio (% difference)
Pool Side	8.6	0.5
Neutron Radiography Beam Tube	-9.0	-5.9
Molybdenum	-4.8	-6.1
Hydraulic Rabbit	0.5	-1.4
Pneumatic Rabbit Vicinity	-4.9	-7.0

The MCNP results had an uncertainty of ±2%.

Experimentally determined control rod worths were also used to validate the Monte Carlo results. Control rod worths for a fresh and burned core are given in Table 2 below.

Table 2: Control Rod Worths for MEU core

	Fresh Core ($)	Actual Core ($)
Measured	-	32.2
MCNP	31.3 ± 0.3	32.5 ± 0.3
DIF3D	32.8	34.3

The good agreement of the rod worth calculated with diffusion theory is due to the use of internal black absorber boundary conditions in the DIF3D code for the cadmium absorber in the control rods. Without the application of these internal absorber conditions the diffusion calculations underestimate the rod worth by as much as 14%.

BURNUP CHARACTERISTICS FOR EQUILIBRIUM CORES

An equilibrium cycle was defined to represent the current average SAFARI-1 operational procedures as closely as possible. This was achieved by examining the actual reloads performed during the past year and defining an average reload pattern based on these data. The fuel shuffle paths are given in the appendix. The resulting assembly U^{235} mass distribution in the calculated equilibrium core was then compared with the average of the U^{235} masses in each core position estimated from operational data over the past year. The equilibrium core cycle length and discharge burnups of the spent fuel assemblies is in good agreement with operational data.

Equilibrium core studies have been performed for 45 wt% enriched uranium-aluminium alloy fuel (MEU) with a U^{235} loading of 225g per standard fuel assembly (SFE), for 90 wt% enriched uranium-aluminium alloy fuel (HEU) with U^{235} loadings varying from 200g to 300g per SFE and for 19.75 wt% U_3Si_2-Al (LEU) with loadings varying from 225g U^{235} to 485g U^{235} per SFE. HEU

alloy and LEU silicide fuel assemblies that contain less than 340 g of U^{235} have the standard 19-plate fuel geometry with 0.051 cm thick meat. LEU silicide fuel assemblies that contain more than 340g of U^{235} have 18 fuel plates with 0.076 cm thick fuel meat. These 18-plate assemblies allow the same U^{235} loadings per assembly with reduced uranium densities thereby decreasing the possible scrap rate in the manufacturing process and allowing the flexibility of increasing the U^{235} loadings per fuel assembly further.

In all equilibrium core cases the End-of-Cycle (EOC) core excess reactivity has been fixed at the average excess reactivity of several recent cores with control rods fully withdrawn. With the control rods fully withdrawn, the follower fuel coincides exactly with the top and bottom of the active fuel in the core while the bottom of the cadmium is 3.85 cm above the top of the fuel. This being the case and in order to shorten computing times, this model was simplified by neglecting the control rods and assuming symmetry across the axial core centre line. Calculations showed that the effect of neglecting the control rods and modelling the core symmetrically for these cases is minimal and is adequate for these comparative purposes.

The reload pattern described above was applied to equilibrium core calculations with HEU, MEU and LEU fuels. Table 3 summarizes the cycle lengths, percentage burnup of U^{235} in the fuel and followers on discharge and the total number of assemblies (including followers) used per year.

Table 3: Fuel used Annually as Function of Assembly Type

Description	U density ($g.cm^{-3}$)	Cycle Length (fpd)	U^{235} Discharge Burnup (%)		Assemblies used pa[1]
			Fuel	Follower	
MEU 225g, 19 plates	1.35	15.2	48.1	66.6	68
HEU 200g, 19 plates	0.61	12.6	45.4	63.5	82
HEU 250g, 19 plates	0.76	19.2	55.8	74.8	54
HEU 300g, 19 plates	0.92	26.7	65.1	83.8	40
LEU 225g, 19 plates	3.13	13.6	42.0	59.1	76
LEU 285g, 19 plates	3.97	22.3	53.7	72.5	47
LEU 340g, 19 plates	4.73	30.1	60.5	79.1	35
LEU 340g, 18 plates	3.34	28.5	57.4	76.2	37
LEU 400g, 18 plates	3.93	36.7	62.3	80.8	30
LEU 485g, 18 plates	4.76	48.2	67.1	84.9	23

[1] Based on a power level of 20MW and 294 effective full power days per annum.

The cycle lengths of the different fuels as a function of U^{235} content is presented graphically in Figure 4 below. Using the MEU as a basis for comparison it was noted that for the 19 fuel plate assemblies 3% less U^{235} is required to be loaded per HEU fuel assembly while 5% more U^{235} is required per LEU fuel assembly to match the current cycle lengths with MEU. This is due to different quantities of U^{238} in the fuels.

It was also noted that 3% more U^{235} is required in the LEU 18-plate assemblies (thicker fuel meat) than the LEU 19-plate assemblies to match the cycle length of the former fuel assemblies. The advantage however, is that a thicker fuel meat allows more U^{235} to be loaded per assembly.

The increased cycle lengths due to the higher uranium loadings shown in Figure 4 make increased uranium densities an attractive option to cut the fuel operating costs of the reactor. This is an important consideration that will be factored into the economic analysis.

Two additional equilibrium core calculations were performed with 340 grams of LEU loaded per assembly. The fuel assemblies used had 20 fuel plates with meat thicknesses of 0.076 cm and 23 plates with fuel meat thicknesses of 0.051 cm. The resulting cycle lengths, percentage burnup of U^{235} on discharge and total number of assemblies used per year for various assemblies loaded with 340 grams of LEU are given in Table 4 below. Due to the harder spectrum resulting from the use of these LEU 20 and 23 plate assemblies it requires approximately 3 to 4 more fuel assemblies per year to match the cycle length of the 19-plate LEU assemblies.

Table 4: Fuel used Annually for 340 g Loaded LEU Fuel

Description	U density ($g.cm^{-3}$)	Cycle Length (fpd)	U^{235} Discharge Burnup (%)		Assemblies used pa[1]
			Fuel	Follower	
18 plates, 0.076 cm meat	3.34	28.5	57.4	76.2	37
19 plates, 0.051 cm meat	4.73	30.1	60.5	79.1	35
20 plates, 0.076 cm meat	3.00	27.0	54.6	72.7	39
23 plates, 0.051 cm meat	3.91	27.9	56.2	74.0	38

[1] Based on a power level of 20MW and 294 effective full power days per annum.

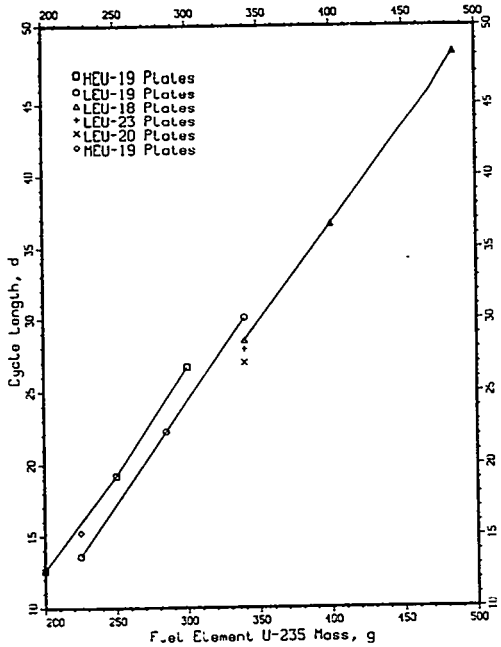

Figure 4: Cycle Length versus Fuel Type and Loading

FLUX AND SPECTRUM COMPARISONS FOR EQUILIBRIUM CORES

As mentioned previously, the neutron flux levels and neutron spectrum in the irradiation positions are of prime importance to the commercial products produced at SAFARI-1.

MEU fuel assemblies with 19 plates and 225 grams U^{235} are currently used in the SAFARI-1 core and as such have been used as the reference in comparing the effects of the other fuels on the flux level and spectrum. Comparisons of the thermal flux and thermal-to-total flux ratios have been made, in each of the irradiation positions mentioned previously, for the different fuels and are given in terms of the percentage differences from the current MEU core operation in the series of figures below.

Figure 5. THERMAL FLUX: POOL SIDE

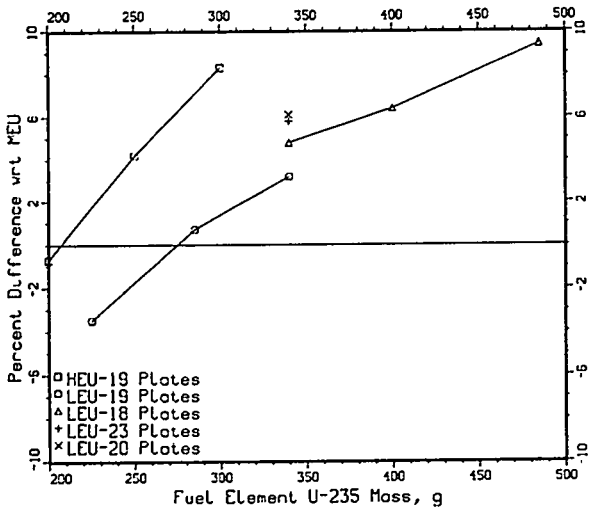

Figure 6. THERMAL-TO-TOTAL FLUX RATIO: POOL SIDE

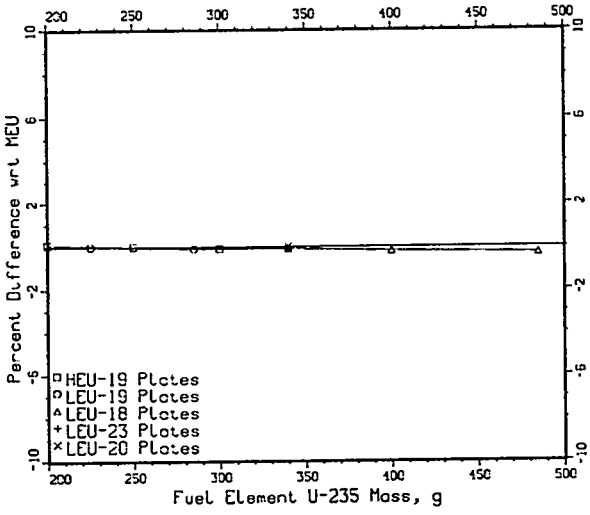

Figure 7. THERMAL FLUX: NEUTRON RADIOGRAPHY BEAM TUBE

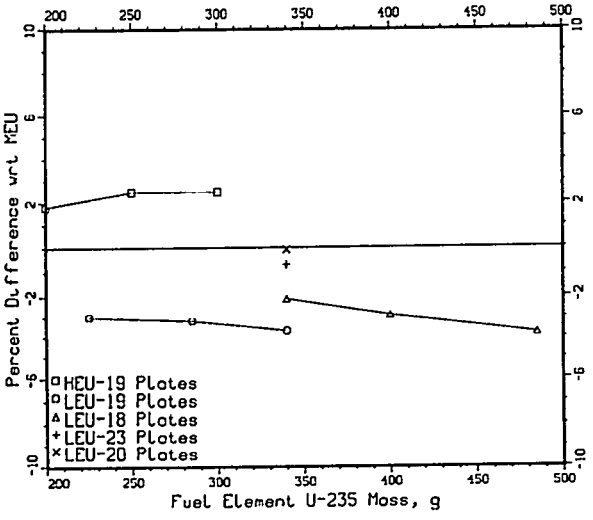

Figure 8. THERMAL-TO-TOTAL FLUX RATIO: NEUTRON RADIOGRAPHY BEAM TUBE

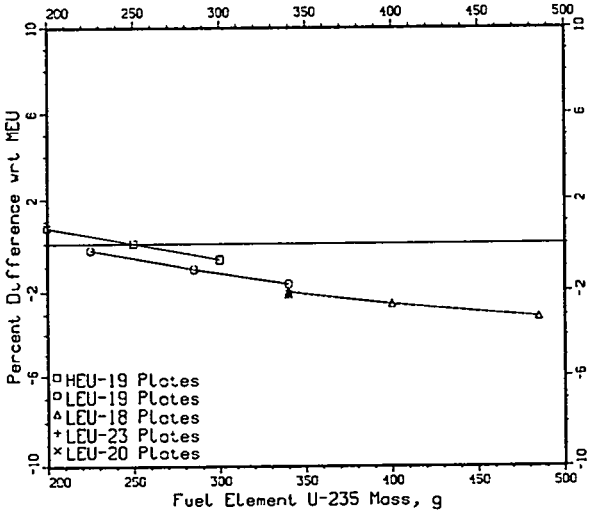

Figure 9. THERMAL FLUX: MOLYBDENUM

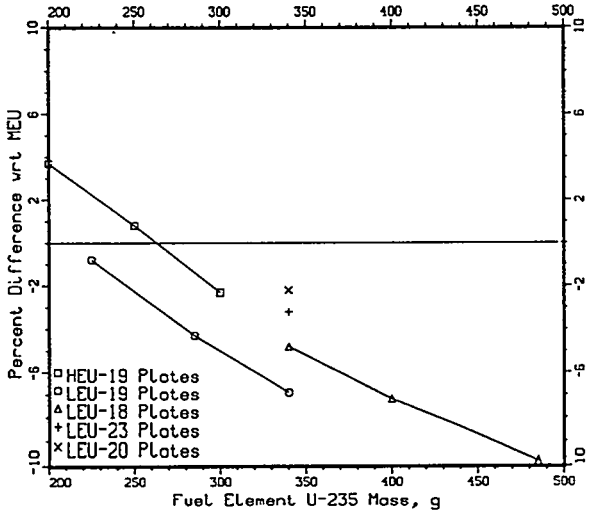

Figure 10. THERMAL-TO-TOTAL FLUX RATIO: MOLYBDENUM

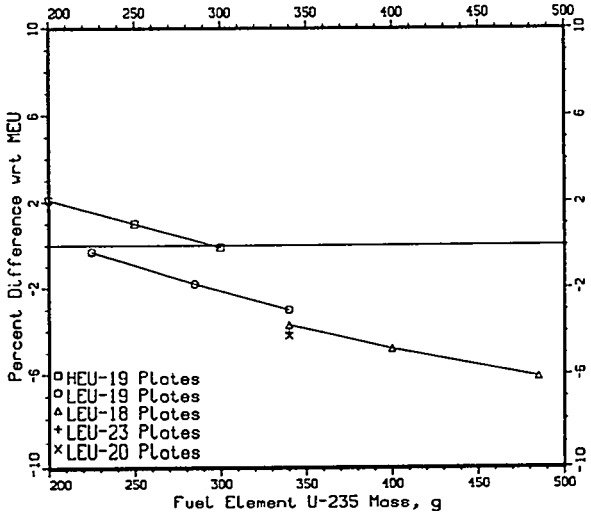

Figure 11. THERMAL FLUX: HYDRAULIC RABBIT

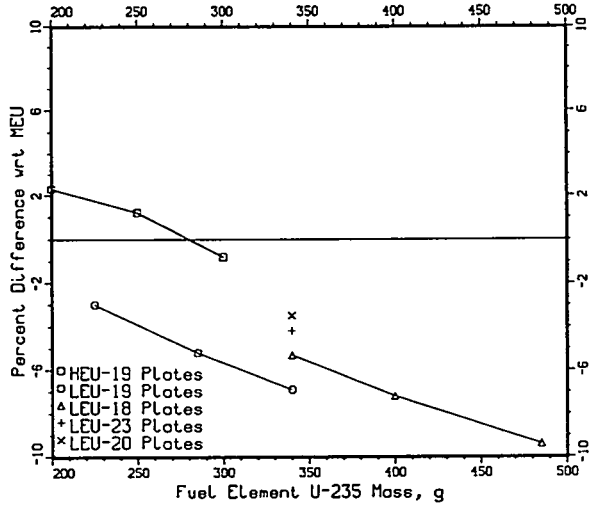

Figure 12. THERMAL-TO-TOTAL FLUX RATIO: HYDRAULIC RABBIT

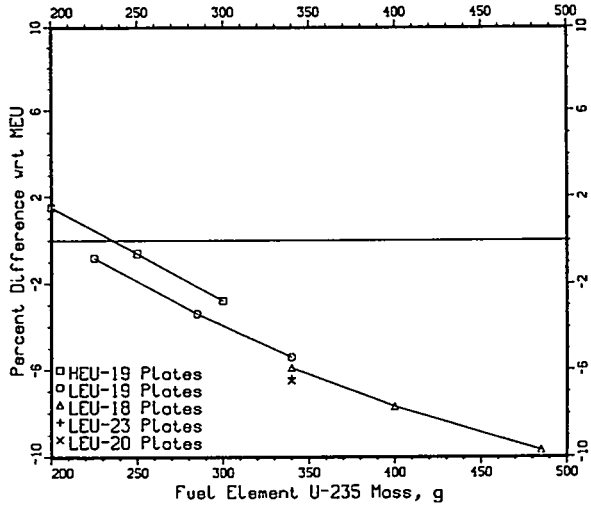

Figure 13. THERMAL FLUX: PNEUMATIC RABBIT

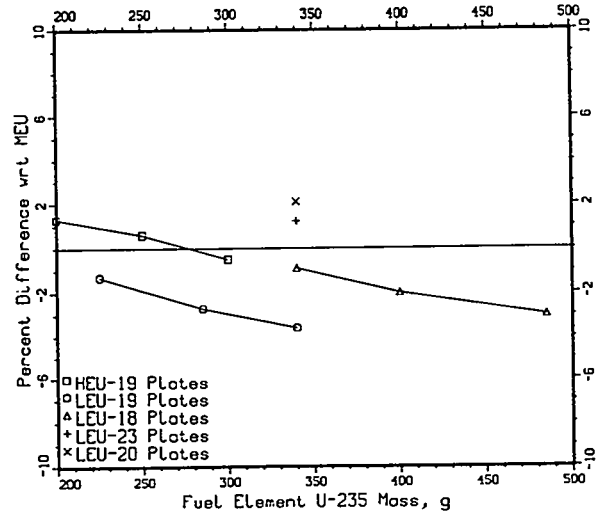

Figure 14. THERMAL-TO-TOTAL FLUX RATIO: PNEUMATIC RABBIT

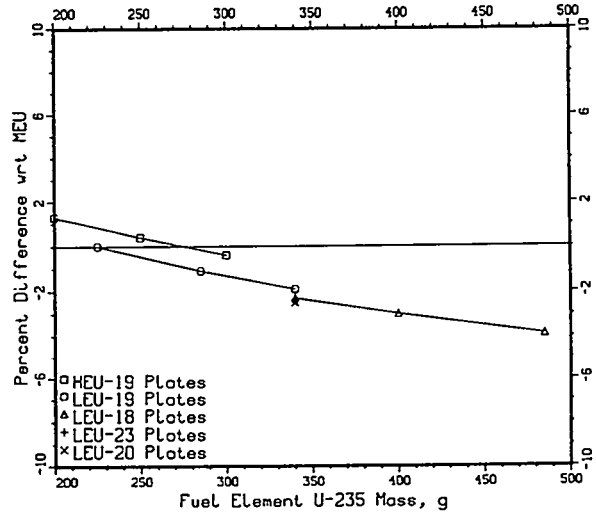

From the results it can be seen that independent of the enrichment of the fuel, increasing the uranium content in the fuel assemblies leads to lower thermal fluxes and a harder spectrum in the core while the fast flux remains relatively constant. Increasing the uranium content also results in an increase in the power densities of the peripheral fuel assemblies thus increasing the leakage from the core. The fluxes at the centre of the SILIRAD facility in the pool side are higher than at present for most of the fuels due to the increased leakage. The fluxes at this position depend solely on the fast neutron leakage while the neutron flux spectrum at this position is practically unchanged for the different fuels. This is important since irradiation damage to the silicon ingots is dependent on the neutron flux spectrum.

Changing the number of fuel plates (and their meat thickness) per assembly also has the effect of changing the spectrum. Since the irradiation positions are located either amongst the peripheral fuel assemblies or outside the core they are all directly influenced by the neutron leakage from the core. Those irradiation positions closer to the core are naturally also effected by the leakage spectrum.

It is generally known that HEU will provide a better core performance than a fuel with lower enrichment. For the sake of comparison, the performance of the irradiation positions have been compared on the basis of equal cycle lengths for two HEU versus LEU cases. The first case is a comparison between the 19-plate assembly for HEU 200 g versus LEU 225 g while the second case compares the 19-plate HEU 300 g assembly versus the 18-plate LEU 340 g assembly. Note that in these comparisons the cycle length in each case is not exactly the same; the LEU cases are some 7% longer than those of the HEU. This is not expected to have an appreciable effect on the comparison which is made in Table 5 below.

Table 5: Comparison Irradiation Facilities for HEU and LEU Fuels with Similar Cycle Lengths (LEU percentage differences from HEU)

Position	Percentage difference in thermal flux		Percentage difference in thermal-to-total ratio	
	200 g HEU vs 225 g LEU	300 g HEU vs 340 g LEU	200 g HEU vs 225 g LEU	300 g HEU vs 340 g LEU
Pool Side	- 3.0	- 3.2	0.0	0.0
Neutron Radiography Beam Tube	- 4.8	- 4.4	- 1.0	- 1.3
Molybdenum	- 4.3	- 2.9	- 2.4	- 3.6
Hydraulic Rabbit	- 5.2	- 4.5	- 2.3	- 3.3
Pneumatic Rabbit Vicinity	- 2.6	- 0.5	- 1.3	- 1.9

The maximum effect on the irradiation positions of the LEU versus HEU fuel in the above comparison is a reduction in the thermal flux of just over 5% and a hardening of the spectrum by just under 4%.

CONCLUSION

A wide range of fuel loadings, uranium enrichments and assembly geometries applicable to SAFARI-1 have been studied. The results provide a neutronic overview of SAFARI-1's current operation as well as its future operation. The impact of fuelling SAFARI-1 with LEU silicide fuel has been shown both from the points of view of the fuel economy and the performance of all major irradiation positions. It is now necessary to perform the safety and overall economic impact studies.

The cycle length and the number of assemblies used annually can be matched with a maximum of just over 5% reduction in the average thermal flux accompanied by a 4% hardening of the average flux spectrum in the irradiation facilities. Although the number of LEU assemblies used will be the same as that of HEU approximately 10% more uranium-235 would be required for the manufacture of the LEU fuel assemblies due to their larger loading.

The following example defines an envelope into which all the calculational results presented in this paper fall. If, for example, the U^{235} content per assembly is increased to 485 g with LEU silicide fuel, it is possible to reduce the current number of MEU fuel assemblies used per year by a factor of almost three. Performance in the irradiation facilities shows a maximum 10% reduction in the thermal flux and 10% hardening of the spectrum; the performance in the pool side shows a 10% increase in the thermal flux with no change in the thermal-to-total flux ratio.

ACKNOWLEDGEMENT

The authors wish to thank the staff of the RERTR Program at ANL and the Applied Radiation Technology Program at the AEC for their invaluable advice and assistance.

REFERENCES

[1] P.A. Louw, D.G. Robertson, W.J. Strydom, "Neutron Transmutation Doping in the SAFARI-1 Research Reactor", Proceedings of the 9th Pacific Basin Nuclear Conference, Sidney, Australia, 1-6 May 1994.

[2] M.M. Bretscher, "Testing WIMSD4m Cross Sections and the ANL ENDF/B-V 69-Group Library: Results from Global Diffusion and Monte Carlo Calculations Compared with Measurements in the Romanian 14-MW TRIGA Reactor", JAERI-M 94-042, (March 1994)

[3] B.J. Toppel, "User's Guide for the REBUS-3 Fuel Cycle Analysis Capability", ANL-83-2 (March 1983)

[4] K.L. Derstine, "DIF3D: A Code to Solve One-, Two-, and Three-dimensional Finite-Difference Diffusion Theory Problems", ANL-82-64, (April 1984)

[5] "MCNP4A: Monte Carlo N-Particle Transport Code System", Los Alamos National Laboratory, CCC-200, (March 1994)

APPENDIX

Fuel Shuffle Scheme for Equilibrium Cycles

Cycle	Fuel Path 1	Fuel Path 2	Fuel Path 3	Control Path 1	Control Path 2
1	H3	H7	B3	G7	C7
2	H6	G8	H4	G7	C7
3	B7	B4	H5	G7	C7
4	D3	G4	E8	G7	C7
5	F3	B5	B6	C5	E7
6	D7	F7	G6	C5	E7
7	C4	D4	C6	C5	E7
8	F4	F6	F5	C5	E7
9	E6	D5	E4	E5	G5
10		D6		E5	G5
11				E5	G5
12				E5	G5

EVALUATION OF THE USE OF NODAL METHODS FOR MTR NEUTRONIC ANALYSIS

F Reitsma and E Z Müller
Atomic Energy Corporation of South Africa Limited

ABSTRACT

Although modern nodal methods are used extensively in the nuclear power industry, their use for research reactor analysis has been very limited. The suitability of nodal methods for material testing reactor analysis is investigated with the emphasis on the modelling of the core region (fuel assemblies). The nodal approach's performance is compared with that of the traditional finite-difference fine mesh approach. The advantages of using nodal methods coupled with integrated cross section generation systems are highlighted, especially with respect to data preparation, simplicity of use and the possibility of performing a great variety of reactor calculations subject to strict time limitations such as are required for the RERTR program.

INTRODUCTION

Modern nodal methods [1] have found wide use in the nuclear power reactor industry [2] but has as yet not achieved acceptance by the research reactor community. Most research reactor core calculations are still performed with traditional finite-difference (FD) diffusion codes which generally require excessive manpower and computational resources. It is perhaps for this reason that reactor calculations are not performed on a routine basis at many research reactor establishments. Despite this, there appears [3] to be a growing interest among research reactor operators in acquiring practical and efficient core analysis capabilities. The need to satisfy ever stricter licensing and safety requirements makes accessibility to a reliable neutronics code essential. Nodal methods offer many advantages in both manpower efficiency and computational requirements which could make routine core analysis for research reactors a reality.

This paper attempts to address some of the issues related to the suitability of nodal methods for research reactor core analysis. The possible advantages of the nodal approach with regard to the data management and manpower requirements associated with a routine core analysis capability are briefly discussed with the focus placed on Cartesian-geometry, light-water-moderated materials testing reactors (MTRs). By utilizing the recently developed OSCAR-3 [4] reactor calculational system which has both FD and nodal options, a comparison is drawn between the performance of a "standard" calculational approach and the nodal approach for a somewhat simplified two-dimensional (2-D) MTR problem.

Because of the limited scope of this particular study, several outstanding problems are identified for further investigation in order to obtain an overall view of the potential of the nodal approach for MTR analysis.

METHODOLOGY

The "standard" approach to MTR core analysis is here defined as that one which is often perceived to be the most correct way of modelling the core, namely with each fuel assembly modelled as a fuel zone sandwiched between two side plate zones. In the nodal approach, a fuel assembly is represented as a single homogeneous channel (fuel and side plates homogenized together) and it clearly has an advantage over the standard approach in that considerably fewer material regions need to be modelled. The nodal approach thus minimizes computer memory requirements to such an extent that it becomes possible to perform three-dimensional core depletion calculations on modern PC platforms. The speed of nodal methods further enables such calculations to be done on a regular daily basis, a feat which is probably impractical with FD methods. This, combined with the much simplified input data preparation and data handling requirements associated with nodal methods, enhances manpower efficiency considerably. However, nodal methods have the potential disadvantage that the preparation of few-group nodal cross sections might require much more complex lattice depletion calculational procedures (e.g. 2-D transport calculations) than those needed in the standard approach (cell and/or super-cell calculations). This aspect is considered as of primary importance for establishing the suitability of the nodal approach to MTR analysis and is therefore the subject of study in the following.

For purposes of comparison, a 2-D MTR core modelled according to the standard approach is considered as the reference core. This core is loaded with medium-enriched (45wt% U^{235}) uranium-aluminium alloy assemblies and is totally surrounded by a water reflector (see Figure 1). The BOC (beginning-of-cycle) status of this core is defined to consist of three fuel zones corresponding to fuel depleted to 5%, 25% and 45% by mass of U^{235}. The assembly design used for this problem (see Figure 2) represents a slight simplification of the actual physical design of the assemblies used in the South African SAFARI-1 reactor.

For this unrodded model problem static BOC (xenon-free) as well as cycle depletion core calculations are performed at a thermal power level of 10 MW and a cycle length of 25 days. Burnup steps of 2.5 days at constant power are used with xenon concentrations determined by depletion. These reactor calculations are performed in 6 energy groups using the MGRAC code [4]. The reference calculations are performed on a relatively fine mesh with an analytic nodal method instead of a FD method (the spatial truncation errors for the nodal method are considerably smaller than for the FD method). Note that this is still defined as the "standard" approach because of the explicit material representation in the core.

The side plate and exposure-dependent fuel cross sections (microscopic data for the most important actinides) for the standard approach are prepared with the CROGEN package

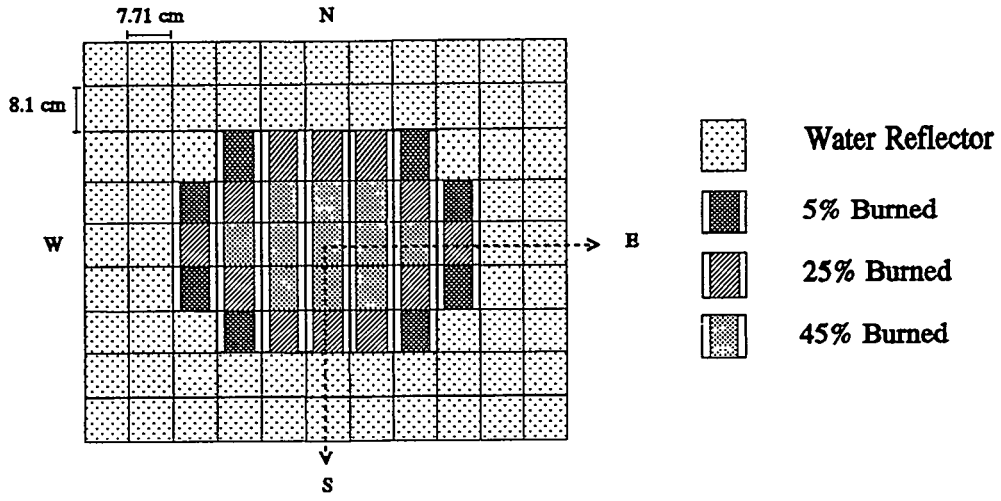

Figure 1. MTR Model Problem Description

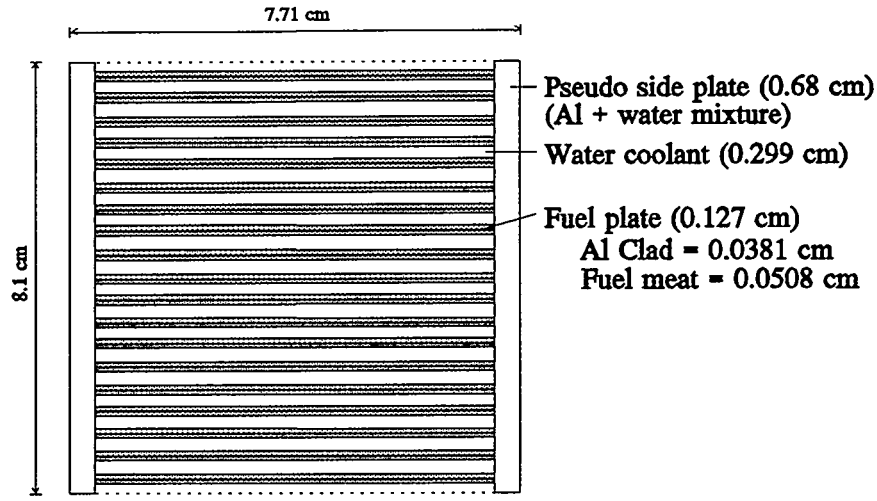

Figure 2. Fuel Assembly Description

of the OSCAR-3 code system (see Ref. 4) using the one-dimensional (1-D) plate super-cell model of Figure 3. The fuel region 6-group cross sections of each assembly in Figure 1 are prepared by group collapsing and spatial smearing of the fuel, clad and coolant cross sections. The side plate cross sections are obtained from group collapsing the cross sections of the corresponding region in Figure 3. For simplicity, the water reflector cross sections are determined by flux-collapsing the cross sections of the coolant water in Figure 3; this is not important for the present study which focuses on cross sections for the core region.

For the nodal approach, two different methods are used for preparing the 6-group nodal data. In the first method, flux-volume-weighted (FVW) homogenized cross sections as well as discontinuity factors (DFs) are determined from static 6-group single-assembly MGRAC calculations utilizing the side plate and fuel cross sections as prepared for the standard case.

This step is often referred to as a second homogenization stage and it presents a very simple but effective means by which to evaluate the significance of DFs for MTR fuel assemblies. Although MGRAC can perform depletion calculations, it does not have the mechanism for parametrizing exposure-dependent nodal cross sections and DFs in the format required by the cross section handling routines of OSCAR-3. Therefore, only BOC calculations were performed with these 6-group nodal data.

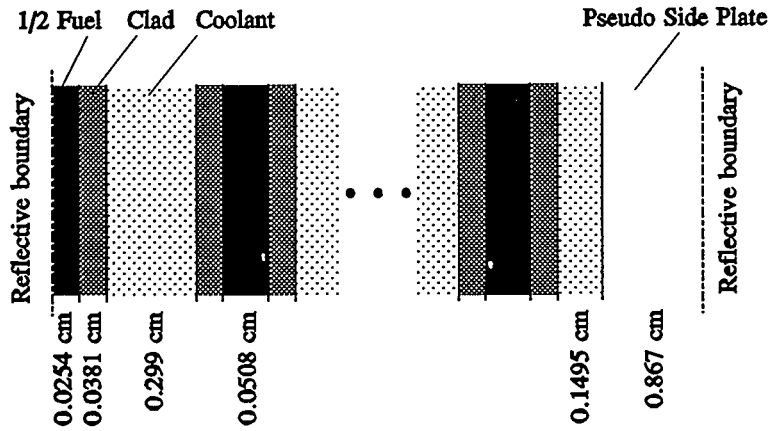

Figure 3. Fuel Assembly Super-Cell Model (9½ fuel plates)

The second method determines exposure-dependent FVW homogenized (microscopic) cross sections directly from the 1-D super-cell calculations mentioned above. In fact, this is currently the production method used in OSCAR-3 and the procedure has been highly automated within the CROGEN package. The approximate nature of this method naturally casts some doubt on its suitability for generating nodal cross section data. However, it is one of the objectives of this paper to evaluate the performance of this simple approach in relation to that of the widely accepted standard approach to MTR analysis. With these FVW cross sections, cycle depletion calculations become possible in the nodal approach.

NUMERICAL ANALYSIS

As a first step in the numerical comparisons of the different approaches mentioned above, a series of BOC test calculations were performed to determine an appropriate reference solution for the standard core representation. Here the multigroup analytic nodal model available in MGRAC was selected as the reference solution method and mesh sizes were progressively reduced until the results appeared to converge. The results of this exercise are summarized in Table 1 with the selected reference calculation indicated by an asterisk. The K-eff of the chosen reference is within 2 pcm and the relative assembly powers within 0.1% of that of subsequent finer mesh calculations.

Also included are the CPU times and results obtained with the FD option of MGRAC. It is of particular interest to compare a FD calculation using a mesh structure typical of that employed in practical MTR analysis with the selected reference results to obtain some estimate of the accuracy of such FD calculations. Such a calculation, roughly using a 1 cm mesh structure, is represented by the FD results in the fourth row of Table 1. In comparison to the reference, this typical FD calculation produced a -146 pcm error in K-eff and a

maximum relative assembly power error of 1%. However, these errors are still very small and unimportant in normal reactor calculations. The rapid increase in CPU-time and memory requirements (8 Mb for the 1 cm 2-D FD calculation) with mesh refinement, makes detailed full core three-dimensional FD calculations virtually impossible on PC platforms.

Table 1. BOC Standard Core Mesh Refinement Analysis

Meshes in quarter core	Approx mesh size	Analytic Nodal Method		Finite-difference Method	
		K-eff	CPU time	K-eff	CPU time
65	6-8 cm	1.027087	53	-	-
162	3-4 cm	1.026792	104	-	-
* 468	2 cm	1.026696	299	1.022290	150
1584	1 cm	1.026683	2151	1.025237	976
2790	0.7 cm	-	-	1.025817	3171
3564	0.65 cm	1.026680	9180	1.025975	3710
4851	0.6 cm	-	-	1.026176	5790

Having selected a reference solution to the test problem, the next step was to evaluate the nodal approach to solving this problem. First, it was deemed necessary to determine the significance of assembly DFs as computed from 2-D MGRAC assembly calculations. For this purpose the DFs on the east face (identical to west face) for the 5%, 25% and 45% depleted assemblies at BOC are tabulated in Table 2. The north face (identical to south face) DFs are not given here since they are equal to unity, i.e. there is no material heterogeneity in the north-to-south direction within an assembly as represented in the MGRAC calculations.

Table 2. East Face Assembly Discontinuity Factors

Energy group	Energy range	5% depleted BOC	25% depleted BOC	45% depleted BOC
1	10.0 - 0.821 MeV	0.987233	0.987041	0.986803
2	821.0 - 5.53 keV	0.997745	0.997581	0.997380
3	5.53 keV - 4.00 eV	1.003003	1.002865	1.002736
4	4.00 - 0.625 eV	1.003867	1.003599	1.003418
5	0.625 - 0.140 eV	1.018598	1.018238	1.024628
6	0.140 - 0.00 eV	1.080988	1.065513	1.046861

It appears from the values of the DFs that they might not be very important since the maximum ratio between DFs for any two fuel nodes at their interface is only 1.018, while at the core-reflector interface, this maximum ratio is 1.081. This suspicion is supported by BOC nodal (one node per assembly) calculations for the model reactor problem. The relative assembly power errors for several BOC calculations are given in Figure 4, where the cases with and without DFs are indicated as 2-D FVW XS + DFs and 2-D FVW XS, respectively (XS stands for cross sections).

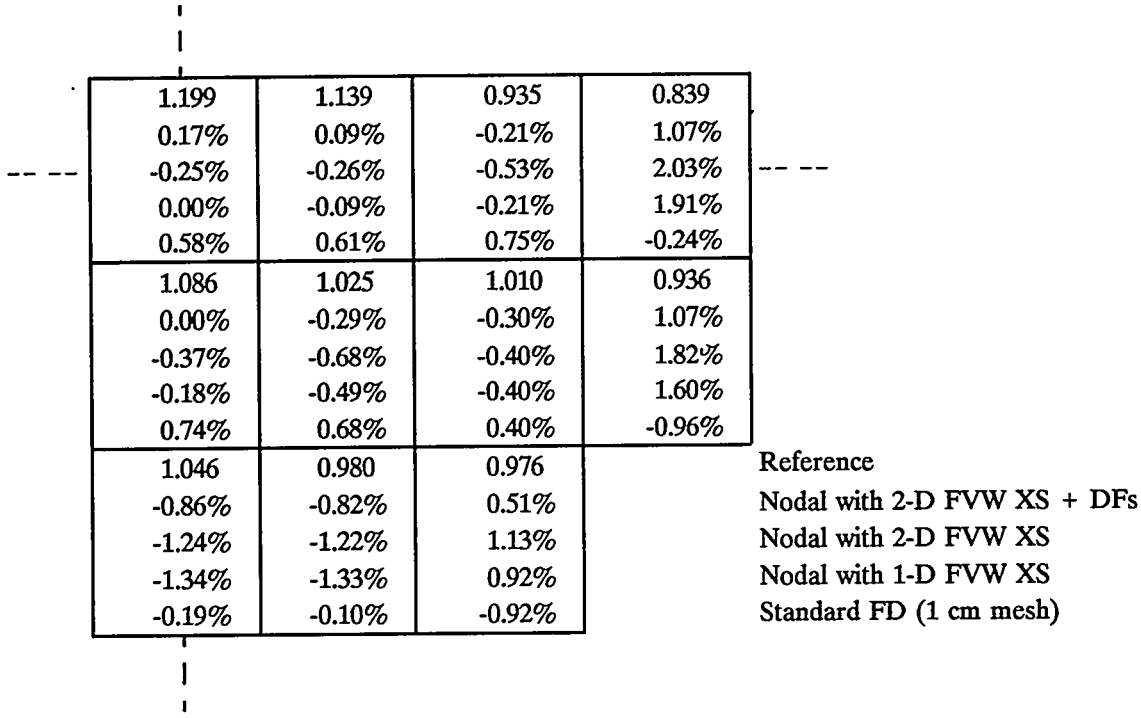

Figure 4. BOC Core Power Distribution Comparison (% errors)

These results indicate that DFs affect the assembly powers for this problem by less than 1%, which is practically insignificant. The K-eff for these two cases (see Table 3) also differ by an insignificant 70 pcm (or < 0.1%). Hence one might conclude that fuel assembly DFs may not be essential for the application of a nodal approach in MTR analysis. However, the use of the DFs halves the maximum power error relative to the reference results and may therefore be useful for high quality calculations.

Although the DFs include all heterogeneity effects it is still assumed that the equivalent nodal parameters (XS + DFs) are environment insensitive. The remaining errors in the relative powers (1%) and the K-eff (272 pcm) can therefore only be due to the neglect of the environment dependence of the equivalent nodal parameters or to the spatial truncation errors of the nodal method. From auxiliary mesh refinement calculations it was found that the spatial truncation errors are negligible (14 pcm in K-eff and 0.4% in nodal powers), and that the greater part of the errors can be attributed to the noted environmental effects. Although colorset calculations can be performed to approximately include the effects of different environments, this is impractical because the possible combinations of environments of an assembly throughout its residence in the core is immense. Moreover, the assembly power errors of these nodal calculations (with and without DFs) relative to the reference calculation are smaller than 2.1% and should be acceptable from a practical point of view. As far as the core multiplication factor is concerned, the above nodal calculations are in error by 270 to 340 pcm relative to the reference. This is about a 0.3% overestimate in K-eff, which should also be acceptable from a practical point of view.

The impression that assembly DFs may not be too important leads one to suspect that the simple FVW homogenized cross sections obtained via the 1-D procedure described at the end of the previous section might be quite adequate for the nodal approach. Results for nodal calculations with these 1-D cross sections are also given in Figure 4 and in Table 3. Indeed, these 1-D cross sections yield results which are at least as good as those obtained with the 2-D FVW cross sections.

Table 3. Summary of BOC Core Results

Case	K-eff	Error	Maximum Power Error	Average Power Error
Reference	1.026696	-	-	-
Nodal with 2-D FVW XS + DFs	1.029413	271.7 pcm	1.07%	0.53%
Nodal with 2-D FVW XS	1.030068	337.2 pcm	2.03%	0.97%
Nodal with 1-D FVW XS	1.028515	181.9 pcm	1.91%	0.85%
Standard FD (1 cm mesh)	1.025237	-145.9 pcm	0.96%	0.58%

To gain some perspective, the results for a standard FD calculation (using a 1 cm mesh structure and the standard core representation) have also been included in Figure 4 and Table 3. It is seen that the relative power and K-eff errors of the simplified (1-D FVW XS) nodal approach are somewhat larger than that of the standard FD approach. However, it should be noted that a FD calculation with a 2 cm mesh, which might also be considered as a "practical" calculation, would in turn yield larger errors than the nodal calculation. For such a 2 cm mesh FD calculation a maximum power error of 3.3%, an average power error of 1.9% and a 441 pcm underestimation of the K-eff are obtained. Based on this, one could conclude that the accuracy of the simplified (i.e. with the 1-D XS) nodal approach is similar to that of the FD approach. To determine if this deduction remains true with core depletion, a cycle depletion calculation with each of these two approaches has been compared with the equivalent reference depletion calculation. The EOC (end-of-cycle) results are summarized in Table 4 and Figures 5 and 6.

It is important to note that during depletion the error in K-eff only changed by +27 pcm for the nodal calculation (-6 pcm for FD calculation), while the maximum and average power errors remained virtually unchanged. This consistency with cycle depletion shows that there is no depletion induced errors and hence that depletion itself is correctly modelled in the nodal calculation. This is confirmed by the EOC U^{235} mass distribution comparison given in Figure 6. The EOC mass distributions show no significant errors in any of the two approaches used. This confirms that the power errors are acceptable from a practical point of view. Furthermore, the consistency of the K-eff error with depletion makes a constant fix-up possible if the 0.2% error is considered unacceptable.

The small CPU times for the nodal calculations clearly make routine reload and fuel optimization studies possible. Note that the nodal calculations are in the order of 40 times faster than the FD calculations. The FD calculation also requires 12 times more memory than the nodal calculation. These ratios would be much larger for full-core 3-D calculations.

Table 4. Summary of Cycle Depletion Results

Burnup step	Reference K-eff	Nodal with 1-D FVW XS					Standard FD (1 cm)				
		K-eff	Error	Maximum Power Error	Average Power Error	CPU time (sec)	K-eff	Error	Maximum Power Error	Average Power Error	CPU time (sec)
0	1.026696	1.028515	182 pcm	1.9%	0.9%	15.5	1.025237	-146 pcm	1.0%	0.6%	976
1	1.024495	1.026338	184 pcm	1.9%	0.9%	9.1	1.023030	-146 pcm	1.0%	0.6%	380
2	1.022281	1.024151	187 pcm	1.9%	0.8%	9.0	1.020811	-147 pcm	1.0%	0.6%	380
3	1.020057	1.021954	190 pcm	1.8%	0.8%	9.1	1.018581	-148 pcm	1.0%	0.6%	380
4	1.017822	1.019747	193 pcm	1.8%	0.8%	9.0	1.016341	-148 pcm	1.1%	0.6%	380
5	1.015578	1.017530	195 pcm	1.8%	0.8%	9.1	1.014091	-149 pcm	1.0%	0.6%	380
6	1.013323	1.015303	198 pcm	1.8%	0.8%	9.0	1.011830	-149 pcm	1.0%	0.6%	380
7	1.011058	1.013066	201 pcm	1.8%	0.8%	9.0	1.009558	-150 pcm	1.0%	0.6%	380
8	1.008782	1.010818	204 pcm	1.9%	0.8%	9.1	1.007275	-151 pcm	1.0%	0.6%	380
9	1.006495	1.008560	206 pcm	1.8%	0.8%	9.1	1.004981	-151 pcm	1.1%	0.6%	380
10	1.004197	1.006291	209 pcm	1.8%	0.8%	9.1	1.002677	-152 pcm	0.9%	0.5%	380

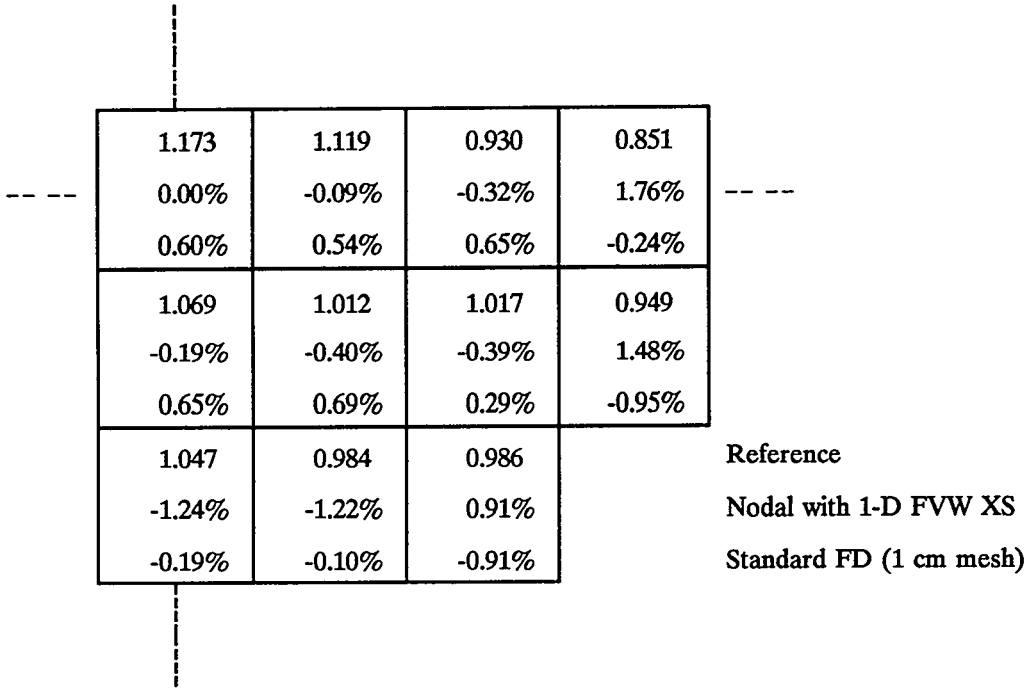

Figure 5. EOC Core Power Distribution Comparison (% errors)

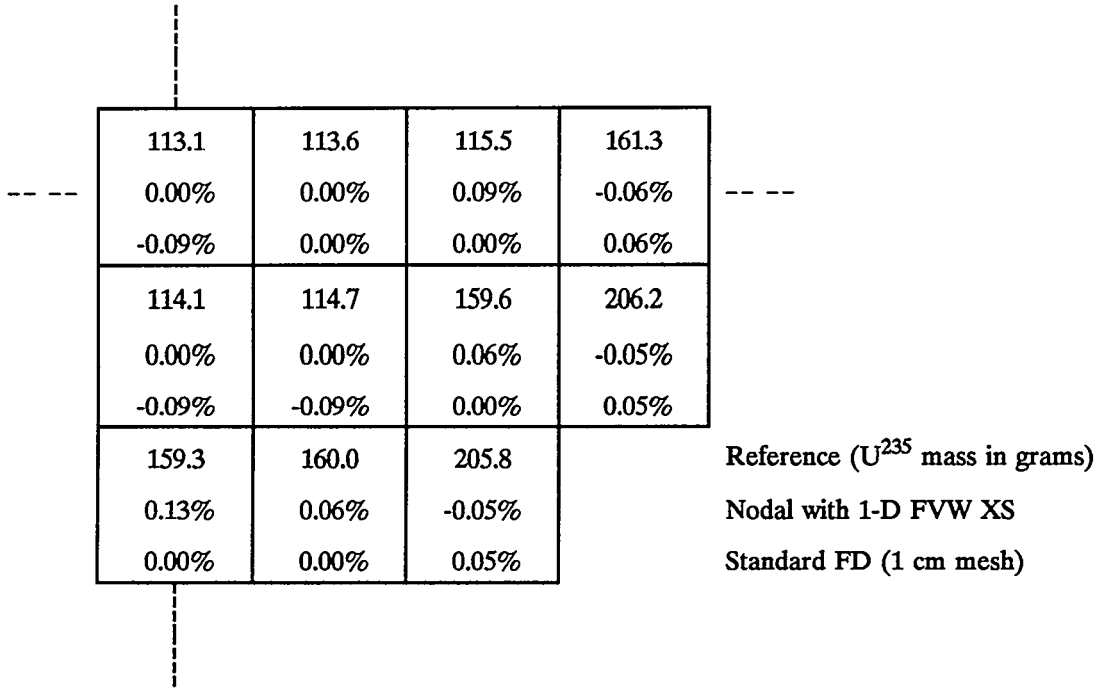

Figure 6. EOC U^{235} Mass Distribution Comparison (% errors)

CONCLUDING REMARKS

In this paper the suitability of nodal methods for application to MTR core analysis was addressed. As a first step in this direction, the adequacy of simple plate-type super-cell models for generating the nodal cross sections for fuel assemblies was investigated. The numerical results for a simplified but realistic 2-D MTR model problem suggested that such an approach would yield accuracies in unrodded core power distribution and reactivity as well as assembly exposures which could roughly match those obtained with a standard fine-mesh finite-difference approach utilizing an explicit representation of assembly side-plate regions. Thus, one is tempted to conclude that if the standard finite-different approach is considered adequate for MTR core analysis, then so would the simplified (1-D XS) nodal approach. However, such a conclusion would be somewhat premature in that the modelling of rodded assemblies and of heterogeneous reflector regions which would require suitable homogenization schemes in nodal calculations have not been studied.

Fortunately, nodal equivalence theory [5] offers a suitable solution to the homogenization problem for rodded fuel assemblies and while this option would require 2-D transport theory assembly or colorset calculations for generating the nodal parameters, it should be seriously considered. Based on theoretical considerations, it is suggested that even for standard finite-difference calculations the equivalence theory homogenization approach might be superior to the "blackness theory" approach [6] currently being used.

As far as the homogenization problem posed by reflector regions is concerned, it is hoped that this issue would be successfully resolved through the use of certain equivalent nodal reflector models which were developed for PWR radial reflectors [7]. Several such reflector models are available in the OSCAR-3 calculational system [4] which was used in this investigation. Preliminary nodal studies with some of these reflector models have already shown promising results. In fact, it is the opinion of the authors that the use of such equivalent reflector models is required even in standard finite-difference analysis of MTR cores in order to account for energy condensation and transport effects which are so dominant in high leakage cores. This, and the need to use high-order transport calculations utilizing at least P_3 scattering matrices for generating reflector data has long been recognized by some reactor analysts [8]. Likewise, it may be prudent to investigate the use of discontinuity factors to account for energy condensation and transport effects for fuel regions since it may then become feasible to significantly reduce the number of few groups used in global core analysis.

In conclusion, it can be stated that preliminary indications are that the nodal approach to MTR core analysis should be capable of meeting normal accuracy requirements. Moreover, the nodal approach offers considerable advantages over the standard finite-difference approach in so far as computational resources and manpower efficiency is concerned. The use of nodal methods within a highly automated system such as OSCAR-3 should make it possible to perform routine (daily or even more frequent) core follow and core reload calculations for MTRs. The benefits that such a calculational system offers for survey type and core design calculations such as those undertaken within the RERTR program is also quite obvious and participants in this program are therefore encouraged to evaluate the merits of the nodal approach in this regard.

ACKNOWLEDGEMENTS

The efforts of Michael Scott in determining optimum iteration parameters for the methods used in this paper are greatly appreciated.

REFERENCES

1. R.D. Lawrence, "Progress in Nodal Methods for the Solution of the Neutron Diffusion and Transport Equations," Progress in Nuclear Energy, Vol 17, No 3, p271-301, 1986.

2. K.S. Smith, "Modern Reactor Core Design Codes and Comparison to Measured Data," Proceedings of the International Conference on Mathematical Methods and Supercomputing in Nuclear Applications, Karlsruhe, Germany, 19-23 April 1993.

3. M. Ravnik, "Reactor Calculations as Part of Research Reactor Operation and Safety Assessment," Paper presented at the Interregional Seminar on Research Reactor Centres - Future Prospects, Budapest, Hungary, 22-26 November 1993, IAEA-SR-183/43.

4. E.Z. Müller, G. Ball, W.R. Joubert, H.C. Schutte, C.C. Stoker and F. Reitsma, "Development of a Core Follow Calculational System for Research Reactors," Proceedings of the 9th Pacific Basin Nuclear Conference, Sydney, Australia, 1-6 May 1994.

5. K.S. Smith, "Assembly Homogenization Techniques for Light Water Reactor Analysis," Progress in Nuclear Energy, Vol 17, No 3, p303-335, 1986.

6. M.M. Bretscher, "Blackness Coefficients, Effective Diffusion Parameters, and Control Rod Worths for Thermal Reactors - Methods," Proceedings of the 1984 International Meeting on Reduced Enrichment for Research and Test Reactors, ANL/RERTR/TM-6, Argonne, Illinois.

7. E.Z. Müller, "Reflector Modeling in Advanced Nodal Analysis of Pressurized Water Reactors," Proceedings of the IAEA Specialist Meeting on Advanced Calculational Methods for Power Reactors, Cadarache, France, 10-14 September 1990, IAEA-TECDOC-678.

8. J. Mondot, CEA, France, Private communication to E.Z. Müller, 1990.

The Effect of Core Configuration on Temperature Coefficient of Reactivity in IRR-1

M. Bettan, I. Silverman, M. Shapira and A. Nagler

Soreq Nuclear Research Center, Yavne 81800, Israel

ABSTRACT

Experiments designed to measure the effect of coolant moderator temperature on core reactivity in an HEU swimming pool type reactor were performed. The moderator temperature coefficient of reactivity (α_w) was obtained and found to be different in two core loadings. The measured α_w of one core loading was -13 pcm/°C at the temperature range of 23-30°C. This value of α_w is comparable to the data published by the IAEA. The α_w measured in the second core loading was found to be -8 pcm/°C at the same temperature range. Another phenomenon considered in this study is core behavior during reactivity insertion transient. The results were compared to a core simulation using the Dynamic Simulator for Nuclear Power Plants. It was found that in the second core loading factors other than the moderator temperature influence the core reactivity more than expected. These effects proved to be extremely dependent on core configuration and may in certain core loadings render the reactor's reactivity coefficient undesirable.

Introduction

The temperature coefficient of reactivity (α) plays a significant role in the determination of the steady state and transient properties of the reactor. One of the major sections of the core Safety Analysis Report (SAR), which must be updated when core parameters are significantly changed, concerns the determination of that coefficient.

The Israel Research Reactor No. 1 (IRR-1), a 5 MW swimming pool type reactor, was originally fueled by 90% enriched uranium in MTR-type fuel elements with curved plates. Recently the replacement of the core fuel by fuel elements containing 93% enriched uranium in flat plates was completed. In addition the boron carbide centralized control blade was replaced by a fork type In-Cd-Ag control blade.

In many practical cases the temperature coefficient of reactivity can be estimated on the basis of data found in the literature. A comprehensive summary of benchmark calculations is included in the summary volume (Vol. 1) of the Research Reactor Core Conversion Guidebook (IAEA-TECDOC-643) [1]. The temperature coefficient of reactivity has several components which may be characterized by the main components of the core: moderator, structure materials and fuel. During operation the core average moderator temperature at IRR-1 ranges up to 38°C. The values of the moderator temperature coefficient of reactivity ($\alpha_{Tw} + \alpha_{Dw}$) published in the guidebook for this range are 15.3 to 21 -$\Delta\rho$/°C x 10^5 (α_{Tw} is the water temperature coefficient and α_{Dw} is the water

density coefficient). The IRR-1 SAR states a value of 15 $-\Delta\rho/°C \times 10^5$. Since α_w is dependent on the reactor loading specifications [2], measurement is recommended following a major change in the core.

This paper describes measurements of the effect of coolant-moderator temperature on reactivity of a core located in a large water reservoir. These measurements were performed as part of a series of experiments designed to determine specified reactor physics characteristics of the IRR-1 core in order to update the values reported in the IRR-1 Safety Analysis Report.

Numerical simulation of the core behavior following a reactivity step was performed using the Dynamic Simulator for Nuclear Power Plants (DSNP), which was adapted to the IRR-1. The measured and published values of the moderator coefficient of reactivity were used in the simulation.

Moderator Temperature Coefficient of Reactivity (α_w) Measurements

The IRR-1 core is located in a 10 meter deep pool filled with 400 m^3 of demineralized water. The holdup tank contains an additional 180 m^3. A schematic diagram of the primary and secondary loops is shown in fig. 1.

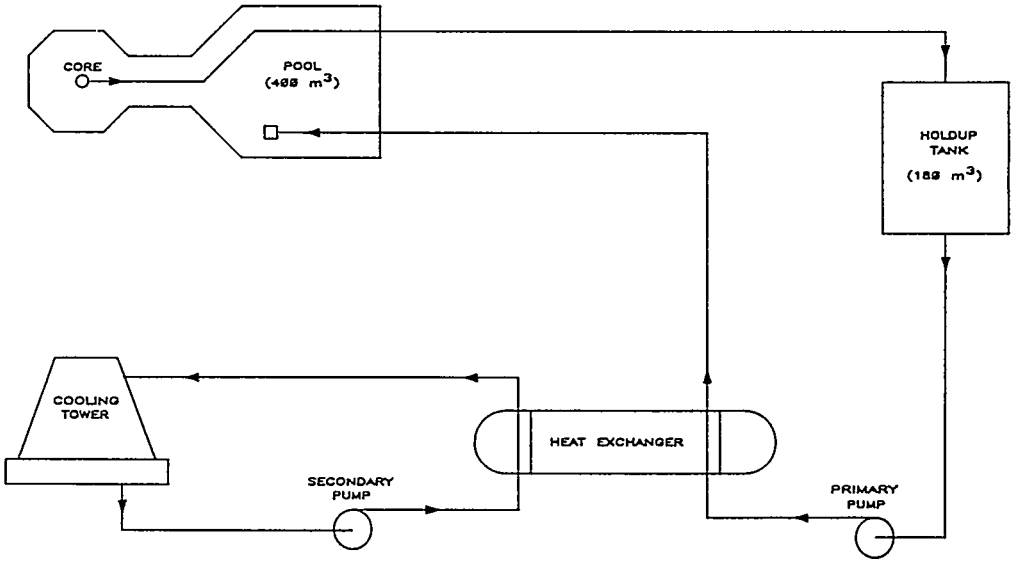

Figure 1: A schematic diagram of the primary and secondary loops.

The experiments were performed on two core loading patterns (shown in fig. 2). Core loading A includes 4 irradiation positions containing boron. Core loading B has no boron irradiation positions but one flux trap. This core loading was constructed in order to measure the effect of a flux trap as used in the RERTR benchmark problem. The difference between the two core loadings lies primarily in the power distribution in the core. In core loading B the power peaks in the vicinity of the flux trap, whereas in core loading A the radial flux is more uniform.

The water temperatures at the inlet and outlet of the core were measured by two resistance thermometers and two thermocouples. The accuracy of the resistance thermometers and the thermocouples used in the experiments was $\pm 0.1°C$. The data was recorded by a PC-oriented data acquisition system.

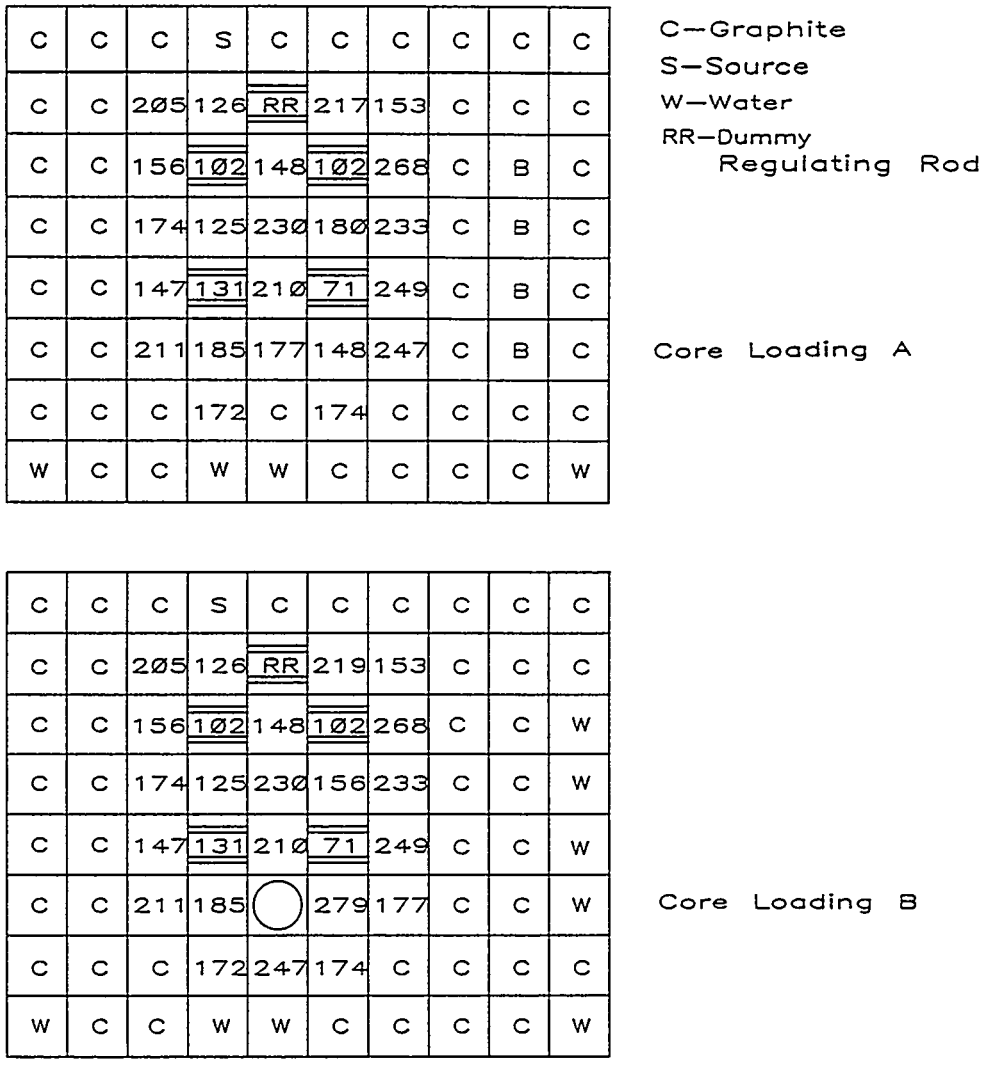

Figure 2: The two core loading patterns with U-235 content in grams.

In order to measure the moderator temperature coefficient it is necessary to control the moderator temperature inside the core and measure the change in core reactivity as a result of moderator temperature change. Changes in the reactivity of the core can be determined by monitoring the regulating rod position when in automatic mode and using its calibration table to calculate the reactivity worth of the change in rod position. The difficulty lies in controlling and measuring the moderator temperature distribution in the core.

The ideal way to simulate the total effect of moderator temperature on core reactivity during operation would have been by gradually increasing reactor power, monitoring the core average coolant temperature and monitoring the change in the regulating rod position. The problem is that as the power increases other reactivity feedback mechanisms, such as poison buildup or burnup and other reactivity coefficients related to reactor power, affect core reactivity. An alternative method would be to change the pool water temperature while the reactor is operating at low power.

A common practice used in changing the moderator temperature is to heat the coolant [2, 3].

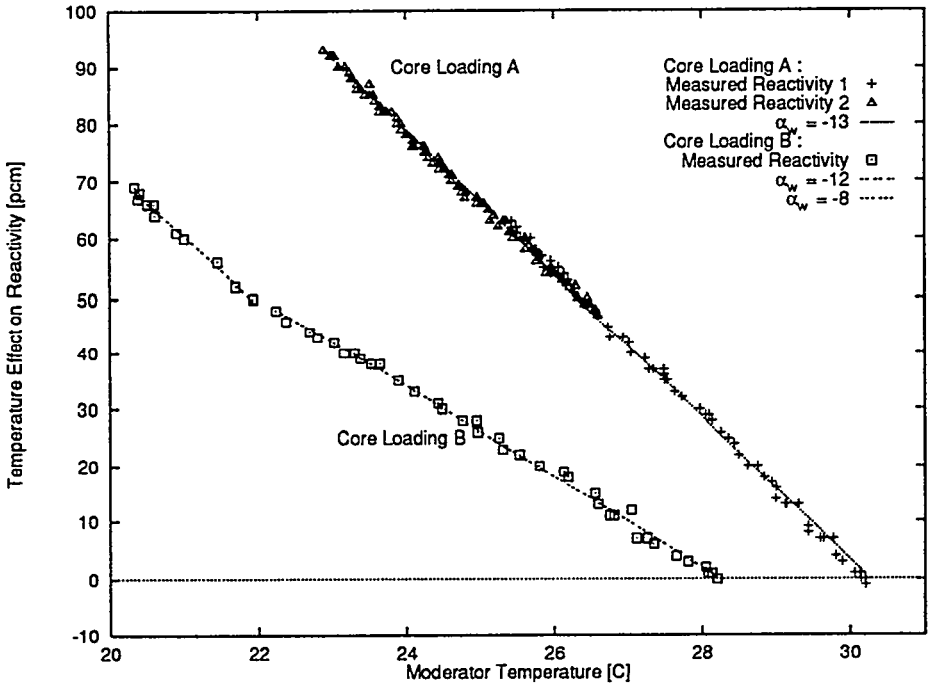

Figure 3: Moderator temperature effect on reactivity.

This method is practical for tank and small pool reactors. Due to the large bulk of coolant in IRR-1, the only available means of heating the water is nuclear power. On the other hand, the large quantity of water contained in the system enabled us to heat the water using reactor power, then shut down the reactor for a week to allow for xenon decay and still sustain pool water at a temperature of 30°C at the start of the experiment. Thus the change in pool water temperature during low power operation can be achieved by cooling the water as opposed to heating it. This method measures the reactivity effect of uniform temperature changes in the core and surrounding water, which is not necessarily the moderator temperature coefficient of reactivity experienced during normal operation. During power operation a substantial temperature distribution exists along the core length and across construction materials. Furthermore, when the reactor is at power, the reflector temperature is much lower than the core temperature.

The reactor was operated at a power level of 1 kW, the lowest power level the regulating system is able to stabilize. The primary water pump was operated until the point at which a thermal equilibrium was achieved in the primary loop. The secondary loop then was put into operation and the moderator temperature was reduced while the regulating rod position was recorded. The positive reactivity resulting from the reduction in the moderator temperature was calculated using the calibration table of the regulating rod.

In the moderator temperature coefficient measurements the moderator temperature was varied within the range of 30.1°C to 20.2°C during three runs. In the first and second runs performed on core loading A the pool water was cooled from 30.1°C to 25.2°C and from 26.6°C to 22.8°C, respectively. The total changes in reactivity were 67 and 46 pcm, respectively. In the third run performed on core loading B the pool water was cooled from an initial temperature of 28.2°C to 20.2°C. The total changes in reactivity was 69 pcm. The results of the experiment are shown in fig. 3.

As can be seen from these curves the reactivity change as a function of water temperature in core

loading A is quite linear. The moderator temperature coefficient calculated from the curves of both runs is -13 pcm/°C, which is comparable to the values stated in the IRR-1 SAR and calculated by JAERI [1]. In core loading B α_w calculated over the temperature range 22.1-32.5°C is -8 pcm/°C, which is significantly less than the published values. In the range 20.2-21.9°C, α_w calculated from the curve is -11 pcm/°C. It should be noted that the lower temperature range was not achieved in the experiment performed on core loading A as it was for core loading B.

Core Behavior Following Positive Reactivity Insertion

The insertion of a positive reactivity step in a reactor is expected to increase the reactor power with a stable period (after decay of transients) causing the core temperature to increase. As the temperature rises, the reactivity of a core which has a negative temperature coefficient should decrease. If the reactivity step is small enough, reactor power should stabilize after the negative temperature coefficient negates the positive reactivity step.

In this experiment, after establishing a stable low power, the regulating rod was withdrawn to a position corresponding to a small positive reactivity insertion. The reactor power and water temperature at the core inlet were monitored at less than 1 minute intervals.

The behavior of the core following a positive reactivity step is shown in figs. 4 and 5. After a reactivity insertion of 9 pcm in core loading A the power increases in a manner suggesting a zero reactivity coefficient. Core reactivity then declines to zero reactivity and the power stabilizes at 3300 kW. The core excess reactivity at a low power level reached after terminating the experiment was found to be 90 pcm less than at the beginning of the experiment. This lesser amount of excess reactivity may be explained by xenon buildup which introduced negative reactivity and counterbalanced the positive reactivity step.

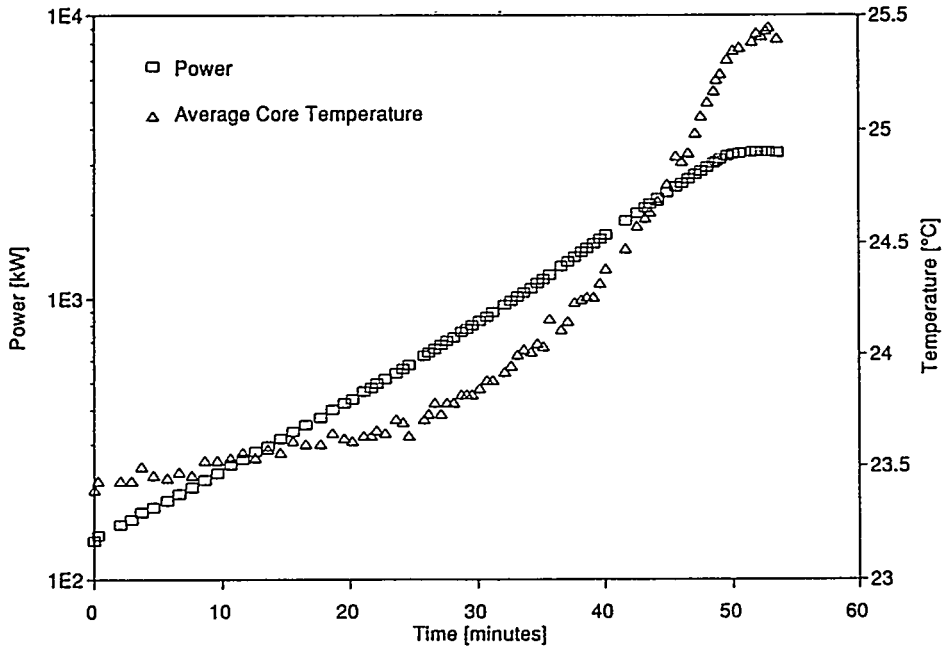

Figure 4: Core loading A response to a reactivity step of 9 pcm.

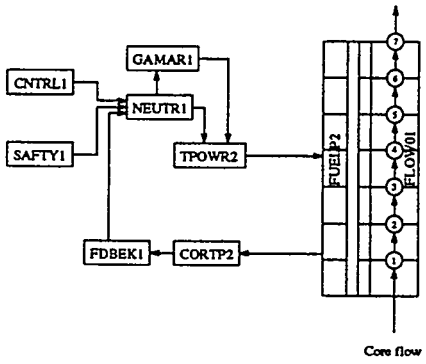

Figure 6: DSNP flow chart of IRR-1.

a clean core and does not consider xenon buildup and other power-related effects. These differences point out the fact that reactivity coefficient components other than moderator temperature affect core reactivity during a reactivity step transient. In order to simulate this type of transient these reactivity coefficient components should be identified, measured and then included in a DSNP simulation.

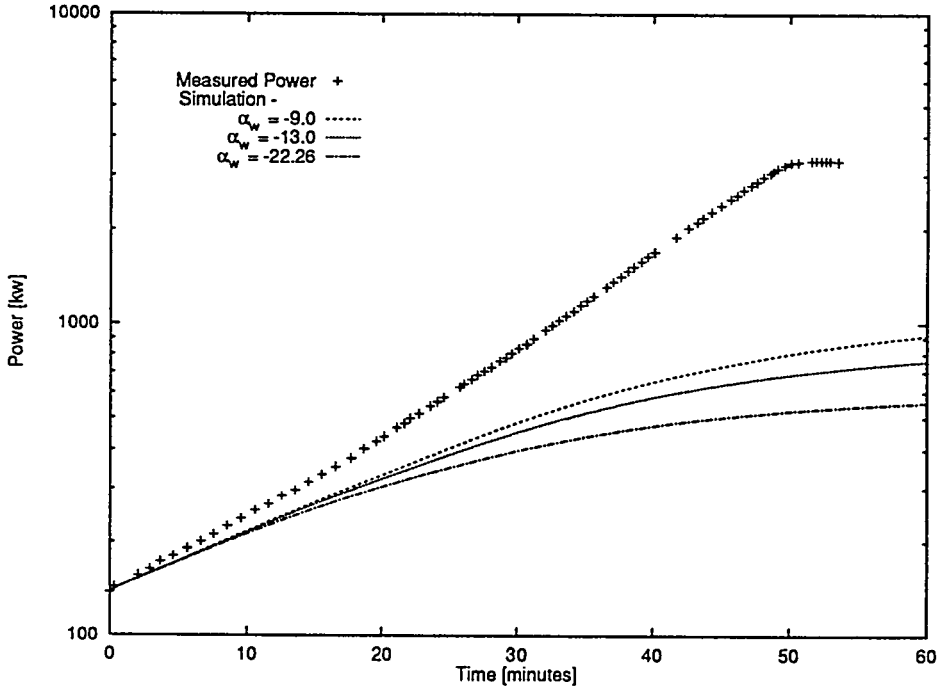

Figure 7: DSNP simulation of the reactivity step experiment performed on core loading A.

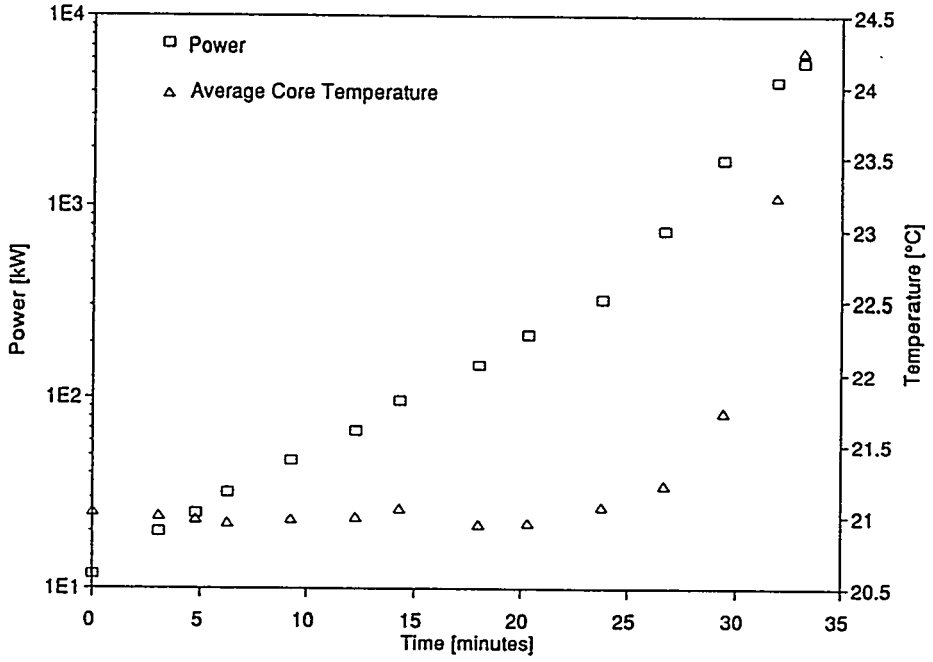

Figure 5: Core loading B response to a reactivity step of 24 pcm.

Core loading B exhibits a different behavior. After insertion of 24 pcm there is a sharp change in the power increase rate at a power level of approximately 300 kW. This type of reactor behavior could suggest the presence of a positive coefficient of reactivity which overrides the negative α_w previously measured.

Numerical Simulation

The Dynamic Simulator for Nuclear Power Plants (DSNP) [4] is a special purpose block-oriented simulation language by which a large variety of nuclear reactors can be simulated. The dominant feature of DSNP is the ability to transform a flowchart or block diagram of a reactor's primary and secondary loops directly into a simulation program.

In this study the simulation of the core alone is analyzed. Hence, it employs an open-loop primary coolant flow model. The core flow rate, its inlet temperature and pressure are assumed to be constant during the simulation. The DSNP flowchart is given in fig. 6. The DSNP modules are designed to account for the lengthwise distribution of power and to give detailed profiles of temperature, coolant velocity and density along the core. Core neutronics is modeled by the following modules: CNTRL1 simulates control rods reactivity, FDBEK1 simulates feedback reactivity, SAFTY1 simulates scram reactivity, and NEUTR1 calculates normalized neutronic power by solving the reactor kinetic equations. GAMAR1 calculates fission products decay normalized power. The output of NEUTR1 and GAMAR1 are used for the calculation of the reactor thermal power by TPOWR2 which is used as input for FUELP2.

Using the measured and published coolant temperature feedback coefficients, core response was simulated. The results are superimposed on the recorded power history in fig. 7. As can be seen, the recorded power does not correspond to any of the simulations. The analysis was performed on

Conclusion

This study demonstrates the significance that core configuration has on the value of reactivity coefficients of the core. The measured effect of a uniform increase in moderator temperature on core reactivity varied from -8 pcm/°C to -13 pcm/°C, depending on the core loading.

In spite of the negative effect the moderator temperature had on core reactivity, the core behavior observed following an insertion of a 9 pcm positive reactivity step revealed a zero reactivity coefficient for core loading A.

Core loading B experienced an additional change in core reactivity following an insertion of 24 pcm. The change took place at a power level of approximately 300 kW. It is suspected that a positive reactivity effect influenced core reactivity in this manner.

In light of the results of these experiments verification of the reactivity coefficient of a core following any new critical core loading is recommended. Due to the startup procedure at IRR-1, this phenomenon can not be observed during startup, and a method such as the one described in this paper should be performed in order to verify that the reactivity coefficient of the new core loading falls within acceptable limits.

Further investigation of possible factors causing the above-described behaviors of the core is being considered at IRR-1.

Acknowledgment

The authors wish to express their thanks to the operational team at IRR-1 for smooth operation of the reactor and their support of the experimental activities reported in this paper. Special thanks are due to Mr. T. Arbel for his valuble assistance.

References

[1] "Research Reactor Core Conversion Guidebook, Volume 1: Summary", IAEA-TECDOC-643, IAEA Vienna (1992).

[2] K. Kanda, S. Shiroya, M. Mori, M. Hayashi, T. Shibata, "Study on Temperature Coefficients of MEU and HEU Cores in the KUCA", "Research Reactor Core Conversion Guidebook, Volume 3: Analytical Verification", IAEA-TECDOC-643, IAEA Vienna (1992).

[3] "IRL Research Reactor Start-up Test Program Report", AMF Atomics (1959).

[4] D. Saphier, "The DSNP Users Manual, Dynamic Simulation for Nuclear Power Plants", Vol. II, rev. 4.4, RASG-115-85 (1992).

Studies of mixed HEU-LEU-MTR cores using 3D models

Ph. Hänggi, E. Lehmann, J. Hammer, R. Christen

Paul Scherrer Institute

5232 Villigen PSI, Switzerland

ABSTRACT

Several different core loadings were assembled at the SAPHIR research reactor in Switzerland combining the available types of MTR-type fuel elements, consisting mainly of both HEU and LEU fuel. Bearing in mind the well known problems which can occur in such configurations (especially power peaking), investigations have been carried out for each new loading with a 2D neutron transport code (BOXER). The axial effects were approximated by a global buckling value and therefore the radial effects could be studied in considerably detail. Some of the results were reported at earlier RERTR meetings and were compared to those obtained by other methods [1] and with experimental values.
For the explicit study of the third dimension of the core, another code (SILWER), which has been developed in PSI for LWR power plant cores, has been selected. With the help of an adapted model for the MTR-core of SAPHIR, several important questions have been adressed.
Amoung other aspects, the estimation of the axial contribution to the hot channel factors, the influence of the control rod position and of the Xe-poisoning on the power distribution were studied.
Special attention was given to a core position where a new element was assumed placed near a empty, water filled position. The comparison of elements of low and high enrichments at this position was made in terms of the induced power peaks, with explicit consideration of axial effects.
The program SILWER has proven to be applicable to MTR-cores for the investigation of axial effects. For routine use as for the support of reactor operation, this 3D code is a good supplement to the standard 2D model.

1. Introduction

The MTR type swimming pool reactor SAPHIR was in operation since 1957. Starting on a power level of 1 MW it was upgraded up to 10 MW_{th} in 1984. The reactor was intensively used for beam tube experiments with neutron scattering, isotope production, irradiation tests of reactor materials, silicon doping, neutron activation analysis, neutron radiography and last but not least for the education of nuclear power plant operators.

Within the RERTR program the EIR (now PSI) played an active role over many years (see e.g. [1,2]). The new fuel was used starting with medium enriched uranium (45%). LEU fuel elements were in use since 1986. Because of the satisfactory performance of mixed cores and a relatively large stock of unirradiated HEU elements the full conversion to pure LEU cores was never been completed.
On the other hand critical loadings containing different types of MTR fuel had to be assembled very carefully. This was especially important because the relatively high amount of fissible material inside the SAPHIR elements (410 g U235 per element) could cause problems with power peaking effects.

Beside a prescribed but more or less empiric procedure for the assembling of the loadings, core calculations were performed for each new loading since 1990. In this manner hot core positions could be avoided and a better feeling of the properties in the core could be achieved. These calculations were done by means of a twodimensional transport code (BOXER) [3] in orthogonal coordinates. Whereas the radial effects could be analysed in good detail axial effects were taken into account by a global buckling value only

Because of the relatively small cores size of research reactors the control rods can cause large local perturbations. This might significantly influence the power distribution over the core. Such axial effects can be studied among others by three-dimensional calculations with the nodal program (SILWER) [4] developed in PSI. In this paper results are described for a standard mixed core configuration as well as a special LEU core containing a fresh element near a water hole.

Although the research reactor SAPHIR was shut down at the end of 1993 and prepared for decommisioning since May 1994, the investigations reported here should be of general interest for all other operators of MTR reactors.

2. A typical composition of the SAPHIR core

The SAPHIR reactor was operated at the maximal power level of about 10 MW during 3 to 4 weeks, followed by a low power period of one week which was used for reloading, maintenance and training activities.

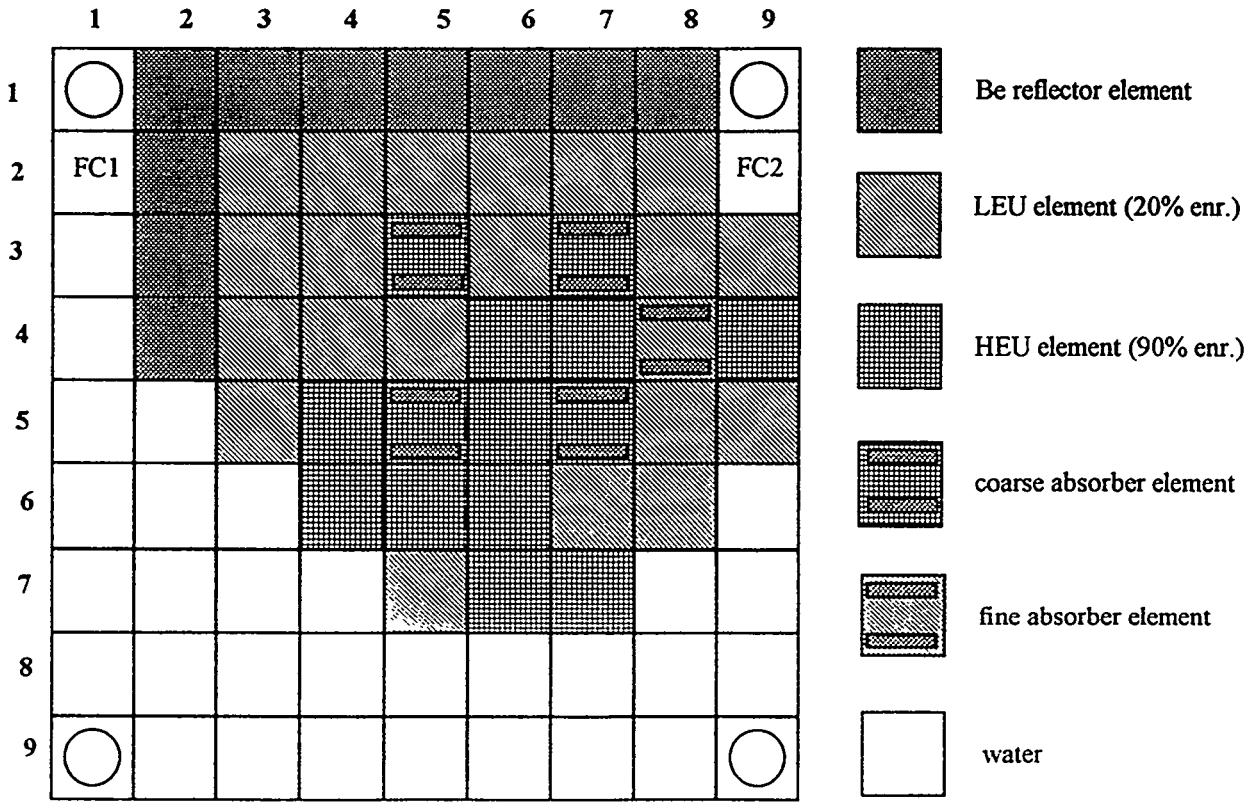

Fig.1: Core composition of loading 622 (the last one of SAPHIR)

The standard core loading has to guarantee an excess reactivity for the envisisaged operation period, the required worthes of the control rods, sufficient distance to boiling limits for each core position and best neutronic conditions for all users of the facility.

A typical core composition as result of the optimisation of the conditions as described above is shown in figure 1. The 10 beryllium reflector elements are aranged between the fuel elements and the beam tube heads in direction of the upper part of figure 1. The nonreflected core positions were used for irradiation experiments (isotope production, silicon doping, irradiations for activation analysis, material tests).

The averaged burnup of a core loading was between 30 and 35%. New elements were inserted at first in a peripheral position. After some runs they were moved step by step towards the core centre and reached a final burnup of about 65 %. The more or less empirical loading strategy devided up the core into 3 concentric areas which should not contain more than a prescribed amount of U-235. A visual inspection of the emmited light at full power was used as indicator of the power distribution. Shadows were interpreted as distortions or signs of starting boiling effects.

Since 1990 systematic investigations of the core behaviour of mixed loadings were performed. For each new loading a two-dimensional calculation with the transport option QP1 of the code BOXER [3] (part of the code system ELCOS) was done before fuel elements were shuffled.

As a consequence of these investigations empty incore positions filled with water were avoided, because in the vicinity of such places very high power peaks can occur (see section 3.3). Furthermore, reactor operation with nonsymmetric control rod positions was forbidden, as this can cause the power density to rise locally above a secure level.

A value of 200 $W \cdot cm^{-3}$, corresponding to a heat current of 43.2 $W \cdot cm^{-2}$ was fixed as the permitted upper limit of the local power density (axial mean). This was in good agreement with the results of thermohydraulic studies which were performed in parallel [5].

3. Three-dimensional investigations

The two-dimensional core calculations could be performed with a good geometric resolution (1 cm in the standard case down to 0.2 cm for special purposes). In some cases the maximum achievable power density value could only be determinated with the best resolution.

The disadvantages of an only two-dimensional core description are the neglection and simplification of axial effects which are caused by the control rods and the different boundary conditions. With the help of a three-dimensional program the following questions should be answered:

- How is the power peaking influenced by the control rod position ? What are the maximal achievable hot channel values ?
- What is the influence of the axial distribution of the burnup ?
- How large is the effect of the Xe-poisonning on the properties of the core ?
- Are the calculated reactivity values of the control rods in agreement with the experiments ?

Most of the answers will be presented in the next parts of this paper.

3.1. The program SILWER for three-dimensional core calculation

As shown in figure 2 the program SILWER is a part of the code system ELCOS which was developed for steady state calculation of light water reactors as well as for the production of input

parameters for dynamic simulation of nuclear power plants. ELCOS consists of the following components (see fig. 2):

1 **ETOBOX** for the generation of group cross sections from data libraries in the ENDF/B-format

2. **BOXER** for cell calculations and two-dimensional diffusion or transport description of the core

3. **CORCOD** for the derivation of interpolation coefficients of group constants suited for the three-dimensional calculations

4. **SILWER** for three-dimensional neutronic and thermohydraulic calculations

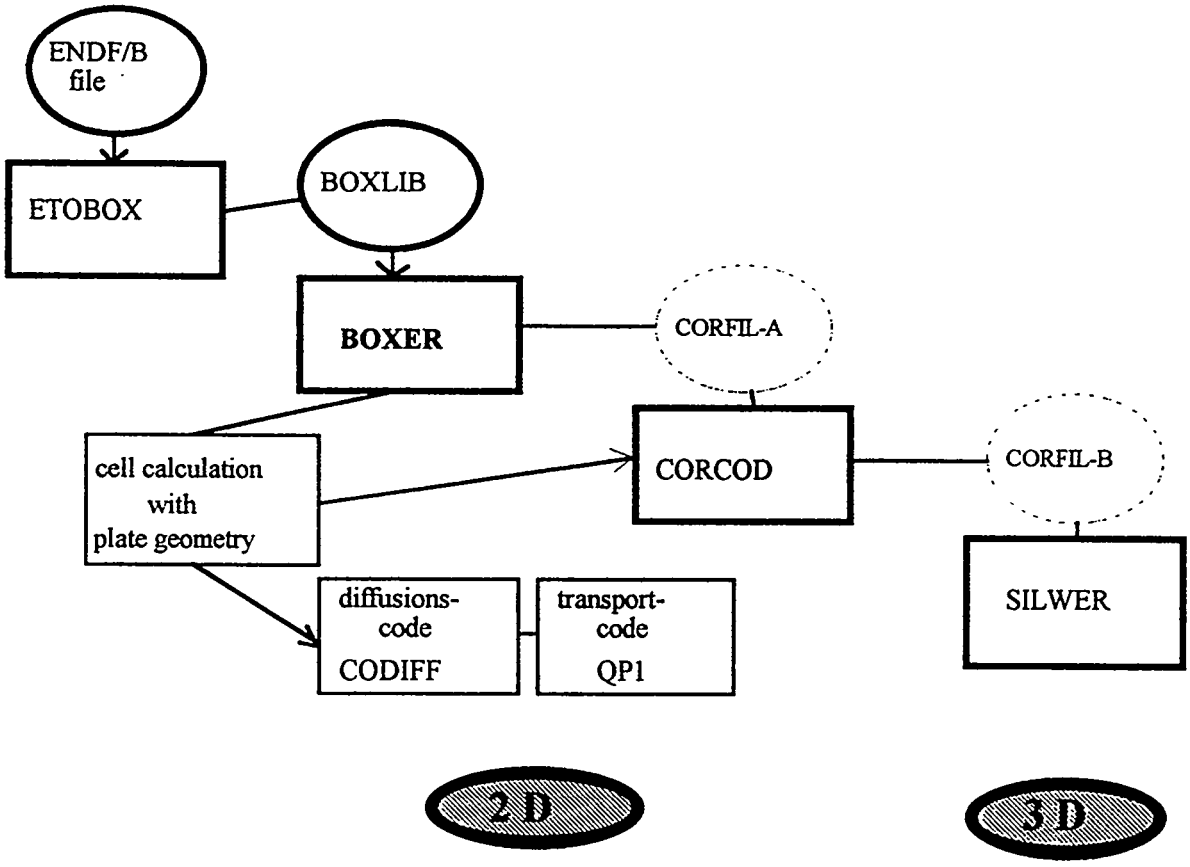

Fig. 2: The components of the code system ELCOS and their connections

Starting with a 70 group cross-section library produced with ETOBOX from ENDF/B formated data, cell calculations were performed in BOXER in real plate geometry with periodic boundary conditions. The number of the resulting flux weighted macroscopic cross sections is usually reduced to 6. Either the full core calculations in 2D or the preparation of cross sections for use in SILWER were done with BOXER. The latter ones were generated in dependency on the burn up of the fuel element type considered. At discret burn up steps the BOXER results were compiled and transfered to a data file CORFIL-A. This data are the reference coordinates for the interpolation which will be done in CORCOD. In this manner the data can be produced for all arbitrary burn up states of the fuel elements in the core. These data are stored in CORFIL-B. The fuel elements containing control rods cannot modellize the absorber plates in detail. Controlled or uncontrolled fuel element zones are

distinguished in SILWER to describe the effect of the absorption in the control rods. For the outer zones (Be and water reflectors) in the radial and axial directions special data sets were prepared.

The core configuration to be investigated is described by three-dimensional orthogonal gridmeshes. The spatial resolution can be raised from one mesh point per element (about 8 cm) to 1 cm for calculations of the whole core. The group number was usually 2 or 6 respectively. For the case with the highest resolution in space and energy the cpu-time is in the order of 100.000 seconds on a SUN-workstation. For most of the investigations of SAPHIR cores two groups and a 4 cm grid width turned out to be a good compromise.

The burn up of the fuel elements is known from the operation history for each individual element with an accuracy of 2 to 5% [2]. This information was used in the core model together with an axial distribution derived from gamma spectroscopy investigations. The ^{137}Cs activity distribution of a spent fuel element was taken as measure of the burn up along the fuel element.

3.2. The estimation of the power distribution

As results of a SILWER calculation the eigenvalue of the configuration, the group fluxes and also the power distribution were estimated. The power density P(x,y,z) (usually in W/cm³) represents an array of 100 to 200000 values, depending on the spatial resolution of the used reactor model. This relatively large amount of data is not easy to handle for the description of the core behaviour with regard in relation to possible boiling processes. Therefore, averaging procedures were applied to determine the core positions with the highest heat loading and to evaluate their security against boiling phenomena.

3.2.1. Hot channel factor vs. hot element factor

For the cores of nuclear power plants (NPP) **the hot channel factors (HCF)** are defined. The largest power density values of the pins, the elements and those in the axial direction are independently been connected. To guarantee a sufficient distance to boiling behaviour the HCF values should not exceed a prescribed upper limit.

The definition of the hot channel factor is:

$$HCF = \left(\frac{P_{plate}^{max}}{P_{element}^{mean}}\right)^{max} * \left(\frac{P_{element}^{mean}}{P_{core}^{mean}}\right)^{max} * \left(\frac{P_{axial}^{max}}{P_{axial}^{mean}}\right)^{max} \qquad (1)$$

The cores of the MTR research reactors are small (less than 1 m³) compared to those of NPP (about 25 m³). Therefore, local effects like control rod movements or poisonning can have more influence on the HCF value. This overestimation of HCF is mainly caused by the axial contribution.

A better possibility to describe the core with regard to safety against boiling is the definition of a **hot element factor (HEF)**. It looks in the data array P(x,y,z) for the absolute hottest position and compares this point with the averaged behaviour of the core.

$$HEF = \left[\left(\frac{P_{plate}^{max}}{P_{element}^{mean}}\right)_{element}^{max} * \left(\frac{P_{element}^{mean}}{P_{core}^{mean}}\right)_{element}^{max} * \left(\frac{P_{axial}^{max}}{P_{axial}^{mean}}\right)_{element}^{max}\right]^{max} \qquad (2)$$

The figure 3 gives a comparison of both factors for a standard core loading when the control rods are moved into the core from the upper to the lower position. The reactor power was held on the same level of 10 MW during the rod insertion.

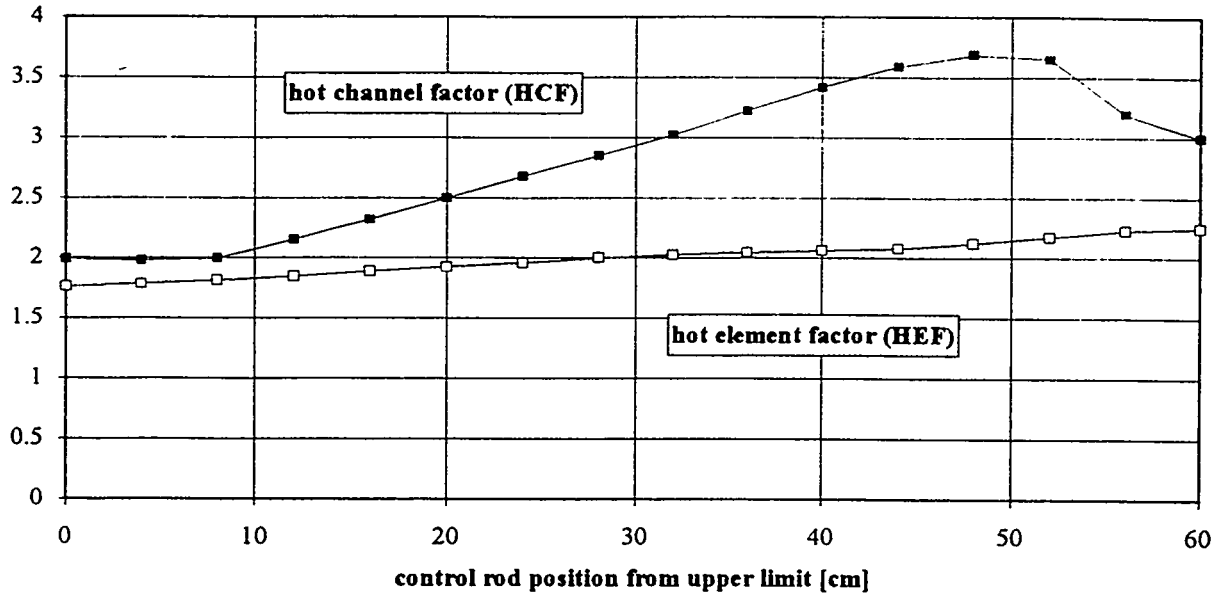

Fig. 3: Hot channel factor and hot element factor respectively for a standard core configuration in dependency on the control rod position (power level constant)

The HEF value is not influenced strongly by the insertion of the control rods while the HEF value does increase substantially. This behaviour is caused mainly by the axial distortion of the flux distribution. In the HCF calculation the axial effects are considered independently and the global reduction of the power density inside the control elements is neglected. The high HCF values represent a strong overestimation of the core behaviour against boiling tendencies. For an adequate description of the operation properties the HEF model is preferable. Nevertheless, the situation with full withdrawn control rods (end of run) is those one with the largest margin against boiling in both models. The "start of cycle" configuration (cold, unpoisoned, small burn up) is the most difficult configuration with regard to boiling.

3.2.2. Influence of the burnup on the power density distribution

In the three dimensional model the axial burn up is described by a distribution based on gamma spectroscopic investigations [7]. Depending on the resolution, 8 to 60 zones with different burn up values are defined. In the radial direction a space independent distribution is assumed. Therefore, the core properties, especially the power distribution, are strongly determined by axial effects. Thus the advantage of the code SILWER is the possibility of investigations under the explicit consideration of unequal burn up over the core height.

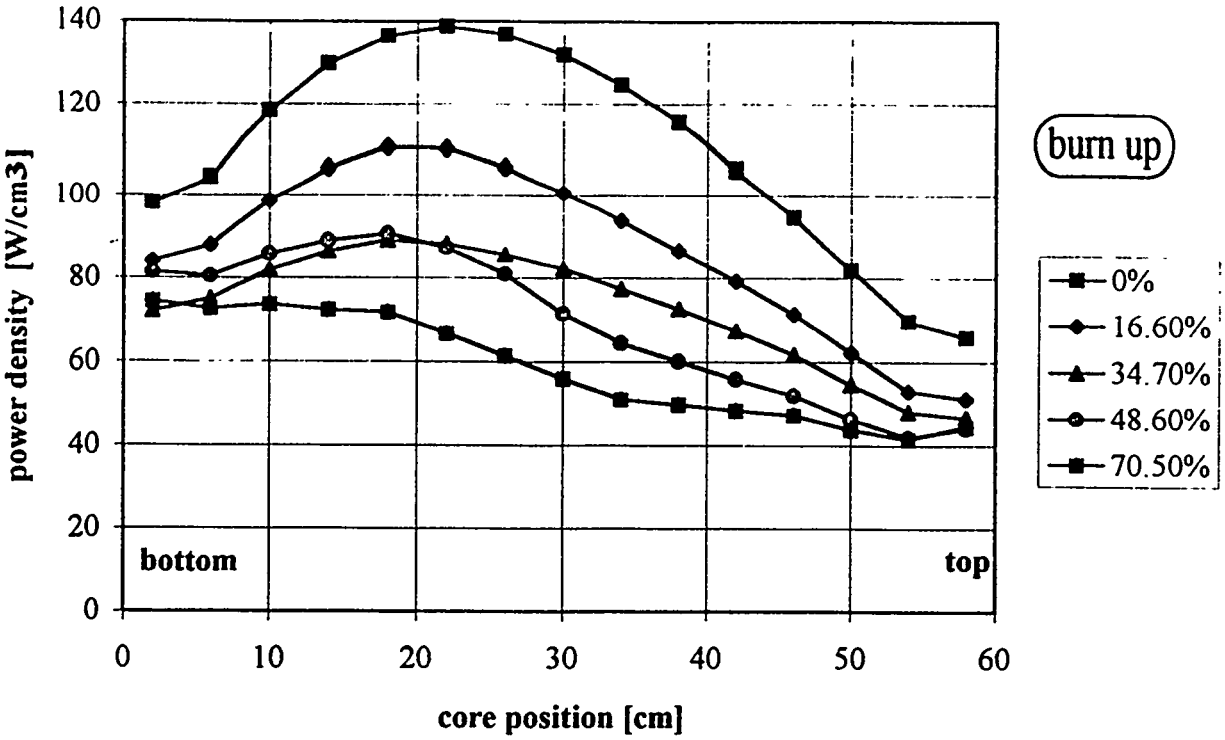

Fig. 4: Axial power distribution in dependency on the burn up of the LEU elements (control rods (plates) half inserted from top)

Figure 4 represents a comparison between the power density distributions over the height of LEU elements with different burn up. The strong rise in direction of the core centre in the case of a fresh LEU element is flattend more and more with growing burn up.

3.2.3. Xe-poisoning of the core

The cross section data for the calculations of the SAPHIR core with SILWER are normally prepared for the state of a saturated poisoning . This standard case can be modified into the Xe-free status by setting the nuclear densities of ^{135}Xe to zero. In this manner the influence of the poisoning on the power distribution can be studied by comparing both of the cases described before.

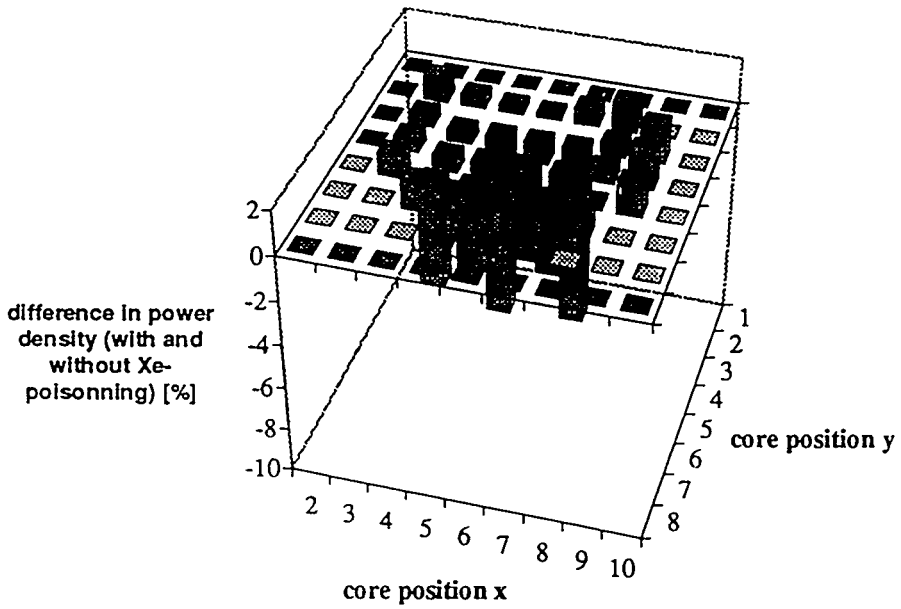

Fig. 5: Effect of the Xe-poisoning on the axial averaged power distribution in a standard core (comparison of the states with and without Xe)

The difference between the two cases concerning the axial averaged power density is in the order of some per cent only. This is a low effect compared to the change in the reactivity which is in the range of 5$. Figure 5 shows that the power density will be reduced in the core centre but increased in the outer elements due to the effect of Xe-poisoning. This means a flattening of the radial power distribution during the reactor operation. The HCF and HEF values became a little smaller in the poisoned case.

Because the compensation of the reactivity loss by poisoning is usually done by removing the control rods, the power distribution is smoothed in axial direction as well.

From this study it can be concluded that the risk of power peaking is lower for the poisoned MTR reactor as the unpoissoned one. But this effect is less important than the influence of the axial burn up described before.

3.4. Special case: a fresh LEU element near an empty core position

Fresh LEU elements contain about one third more fissile uranium than the HEU ones. This is necessarry to obtain a comparable flux level and to reach an reasonable final burn up. The relatively high amount of U-235 can lead to power peak values if the element is driven by high thermal neutron

fluxes. This can occur if a new MTR-LEU element is placed in the core centre (56) near an empty, water filled position (66).

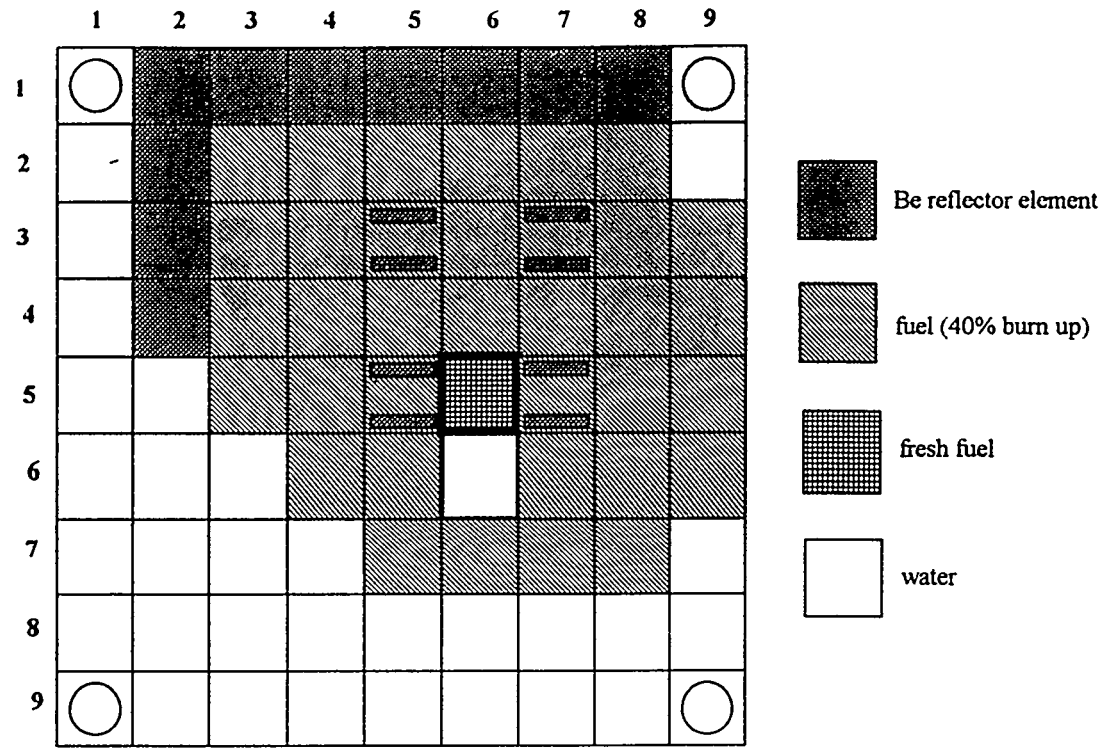

Fig. 6: Core configuration with a fresh fuel element near an empty, water filled position

This behaviour of this special loading was investigated by means of 2D and 3D calculations. An image of the core configuration is given in figure 6. All standard elements were assumed to have a burn up of 40%. The water hole was at the grid position 55. The elements to investigate were placed at position 56.

Using the 2D (x,y) model it was possible to calculate the radial power density distribution very detailed. The resolution was raised from about 1 cm to 0.25 cm. As shown in figure 7 this high resolution have to apply if the real maximum of the peaking should be found.

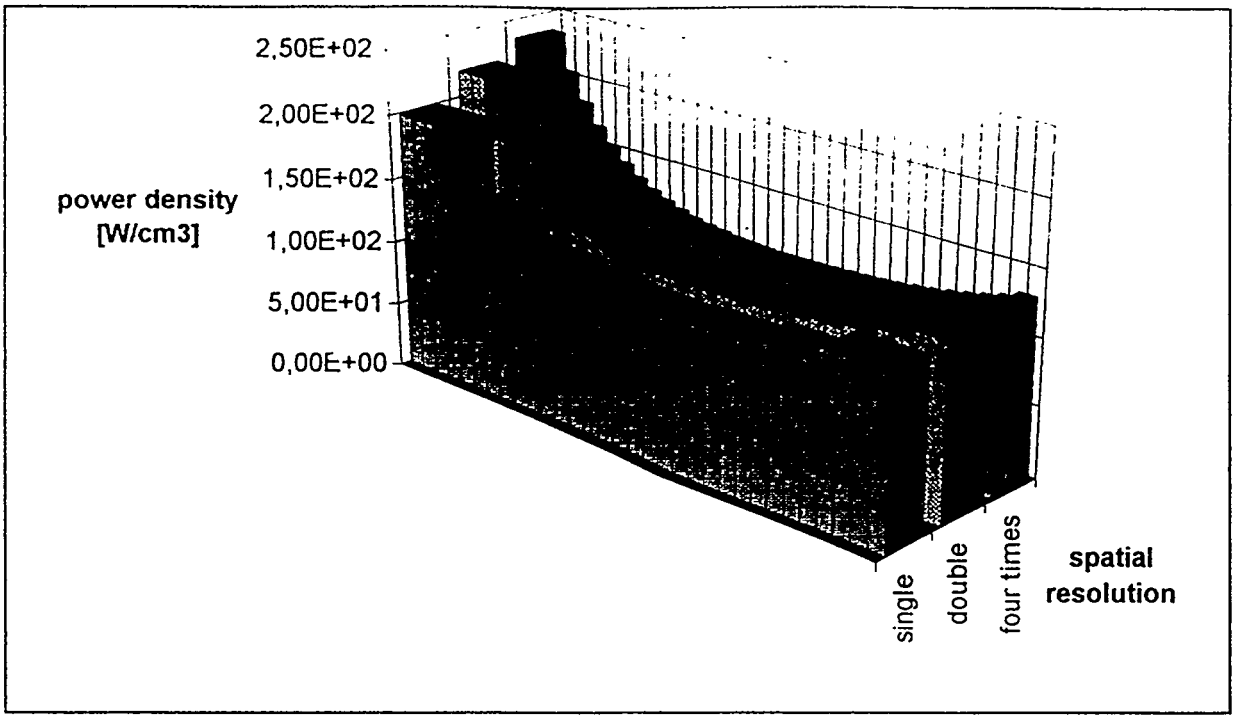

Fig. 7: Power density in a fresh LEU element into the direction to the water hole

The large value of the power density (higher than 200 W/cm^3) at the surface of the fuel element might be difficult for the reactor operation on high power level because the cooling conditions at the outer plate are reduced by the empty grid position.

Taking the third direction into account the calculations with SILWER cannot be performed with the same high spatial resolution as in the case of the 2D model. Nevertheless, a comparison of the behaviour of HEU and LEU elements at this difficult position can be given. Furthermore, the influence of the control rod position on the values of HEF (relevant for thermohydraulic considerations) can be investigated. This data are given in figure 8. For both the types of fresh fuel the largest HEF value can be found at half inserted control rods. This is mainly caused by the two control elements in the direct neighbourhood of the test position 56 (see figure 6).

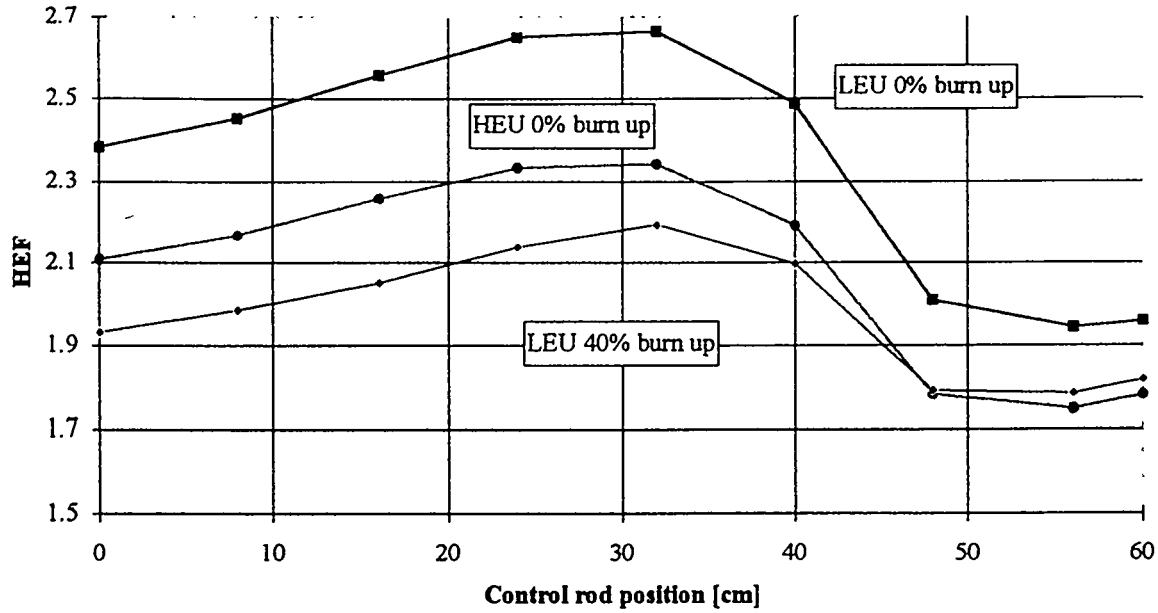

Fig. 8: Hot element factors for the core configurations with different fuel elements (fresh LEU, fresh HEU, burned LEU) at core position 56 near a water hole in dependence on the control rod position

The Hot element factors are in the case of the new LEU higher than for HEU by more than 0.3. Compared with a standard core loading (see 3.2.1. and figure 3) the HEF are higher by 0.7. This indicates an unacceptable high value for a reactor operation on high power level.

3.4 Control rod worthes

By means of the 2D core model regarding the effect of the control rods the two reactor states (full inserted, full withdrawn) can be described only. Therefore it is difficult or unpossible to investigate the operation state with half inserted rods.

	experiments	**calculations**	
beta = 0.0085	rod drop	transport 2D	diffusion 3D
coarse rod 1	1.74 $	1.82 $	1.71 $
coarse rod 2	1.56 $	1.49 $	1.46 $
coarse rod 3	2.35 $	1.67 $	1.95 $
coarse rod 4	1.87 $	1.38 $	1.62 $
all rods together	5.83 $	7.62 $	6.69 $
sum of all single rods	7.67 $	6.36 $	6.90 $
all rods/sum of single	**0.76**	**1.2**	**0.97**

Table: Comparison of measured and calculated reactivity values of the coarse control rods indicating their interaction in the core

The advantage of the 3D calculations is the adequate analysis of axial effects. The partly inserted rods can be simulated by zones which contain the real amount of absorbing material. From the calculated eigenvalues in relation to those of the unperturbed case the reactivity values can be estimated for each rod position. The control rod worth curve for the fine control rod is shown in figure 9 and compared to the experimental data.

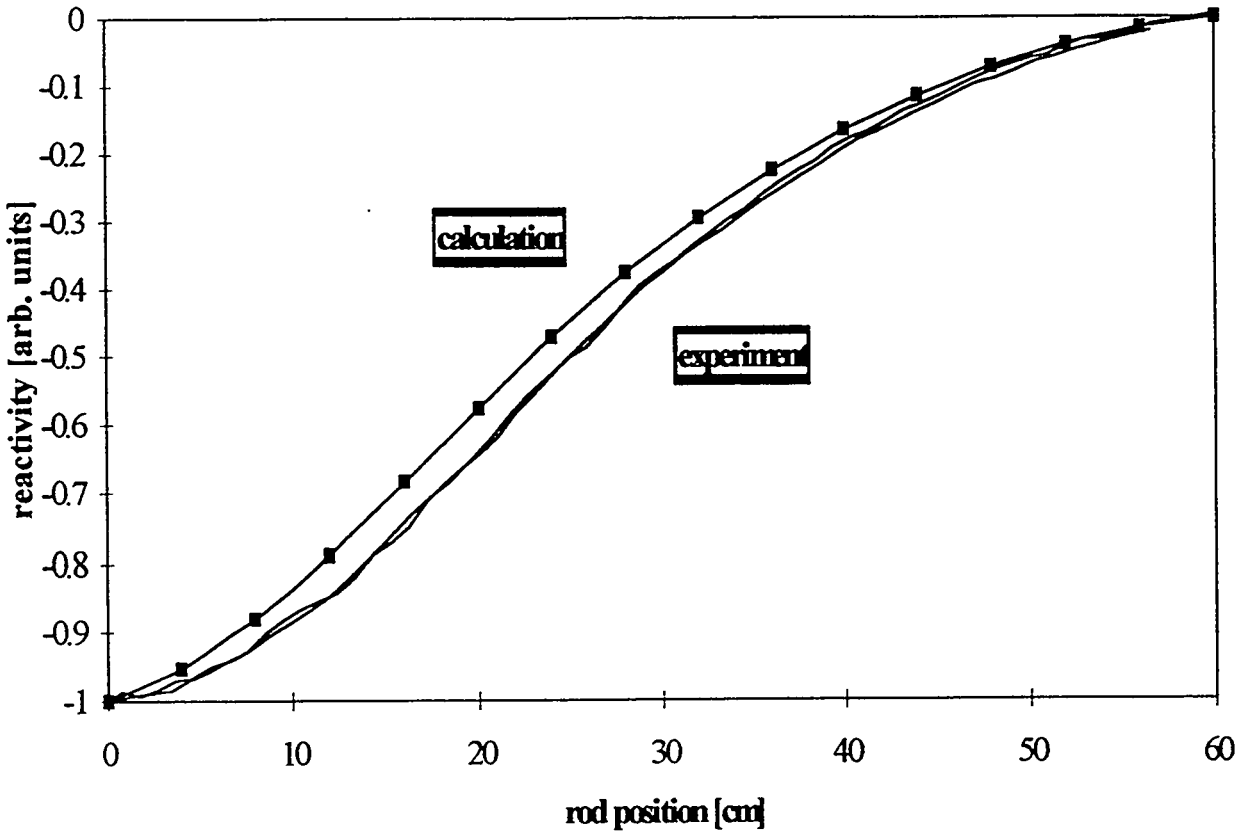

Fig. 9: Comparison of the measured and calculated fine control rod worth in dependence of the rod position

The agreement between the two curves is quite satisfactory. The total reactivity value (in the order of 50 Cents) of this fine control rod can be described with an accuracy of about 10%, depending on the energetic and spatial resolution in the calculations. It should be noted that the measurements have several errors and methodical uncertainties also.

In the case of the four coarse control rods the situation is more difficult. Because of the high worthes (several Dollars) of each rod the total curve as seen in figure 9 could not be measured directly. Usually the rod drop value starting from the critical state was measured for each rod intependently and for all rods simultanuosly. These experimental values could not compared with results from 2D calculations because only the rod positions "full inserted" or "full withdrawn" can be analysed. The estimation of the total rod worth was done by means of a calibration curve.

In the table a comparison is given between the measured and calculated rod worthes. In the experiments the sum of the individual worthes of the four rods is larger than the value of the

reactivity when all rods were inserted simultanously The 2D calculations could not support this result. The ratio is here smaller than 1.

The 3D model was able to overcome the methodical error which are mainly caused by the simplification of axial effect. As shown in the table, the 3D reactivity values of all rods together show a shadowing effect as seen in the experiments. The measured reactivity worthes are influenced by the position of the detector position and by the time resolution of the counter. The accuracy of the 3D calculations depends on the number of grid meshes and of energy groups. They are limited by the computer capabilities.

4. Summary

The program SILWER as component of the code system ELCOS has proven to be able to describe axial effects of a MTR core very well. Some limitations regarding the spatial resolution can be overcome by additional detailed calculations with the 2D modul BOXER.

Some interesting conclusions could be drawn from the performed calculations concerning the use of LEU and HEU in mixed cores. It is regarded to do calculations for each new core loading before the operation at power in order to indentify and to avoid hot core positions.

The most dangerous status in respect of the core cooling is the begin of the run when the control rods are half inserted. Effects like poisoning, burn up and rod withdrawal induce a flattening in the power distribution, mainly in axial direction.

Core configurations with water holes surrounded by fuel should be handled with care. The placement of fresh LEU in the vicinity can cause large power peak values.

The code system should be made available on request for other users, especially for the operators of research reactors with MTR fuel.

Acknowledgement

The authors express their thanks to P. Grimm and J.M.Paratte for making available the code system ELCOS and for their numerous hints.

Reference:

[1] H. Winkler, J. Zeis, Benchmark-Calculations for MTR-Reactors, Research Reactor Core Conversion from the Use of Highly Enriched Uranium to the Use of Low Enriched Uranium - Guidebook, IAEA-TECDOC-233, p.485

[2] J. Hammer, R. Christen, R. Chawla, Burnup Determination of LEU fuel at the SAPHIR Reactor, Proc. of the 1990 Int. Meeting on Reduced Enrichment for Research and Test Reactors, Newport, Rhode Island

[3] J. M. Paratte et al., BOXER User's Manual, Internal Report PSI-TM-41-90-38

[4] P. Grimm et al., User Instructions for SILWER, Internal Report PSI-TM-45-82-55

[5] L. Nechvatal, Thermohydraulic operation limits of the research reactor SAPHIR (in German), internal report PSI-AN-41-94-02

SESSION V

September 21, 1994

ADVANCED REACTORS

Chairman:

P. Robinson
(DOE, USA)

ADVANCED NEUTRON SOURCE ENRICHMENT STUDY*

R.A. Bari, H. Ludewig, and J.R. Weeks
Brookhaven National Laboratory
P.O. Box 5000
Upton, New York 11973-5000

ABSTRACT

A study has been performed of the impact on performance of using low enriched uranium (20% ^{235}U) or medium enriched uranium (35% ^{235}U) as an alternative fuel for the Advanced Neutron Source, which is currently designed to use uranium enriched to 93% ^{235}U. Higher fuel densities and larger volume cores were evaluated at the lower enrichments in terms of impact on neutron flux, safety, safeguards, technical feasibility, and cost. The feasibility of fabricating uranium silicide fuel at increasing material density was specifically addressed by a panel of international experts on research reactor fuels. The most viable alternative designs for the reactor at lower enrichments were identified and discussed. Several sensitivity analyses were performed to gain an understanding of the performance of the reactor at parametric values of power, fuel density, core volume, and enrichment that were interpolations between the boundary values imposed on the study or extrapolations from known technology.

INTRODUCTION

The Advanced Neutron Source is a nuclear reactor that is being designed by Oak Ridge National Laboratory under the sponsorship of the U.S. Department of Energy. Its purpose is to produce intense quantities of neutrons for use in fundamental and applied research in physics, chemistry, biology, medicine, and materials technology. The performance goal is to build a machine with a neutron beam intensity, or flux, that is at least five times higher than existing facilities. The Advanced Neutron Source will be a more powerful research tool than existing facilities and will replace some facilities after their useful lifetime is reached.

As with all other research reactors that have been operated for the purpose of producing a very high flux of neutrons, the Advanced Neutron Source is designed to burn highly enriched uranium (HEU) fuel. This means that the fuel is comprised of 93% of the isotope ^{235}U and 7% of the isotope ^{238}U. With this isotopic mix, the design meets the performance goal, has acceptable safety characteristics, and is feasible to build within state-of-the-art engineering practices and cost envelopes.

Considerable effort has gone into the design of the reactor over the past several years and the design has evolved as new information became available or requirements were imposed. The budget guidance for fiscal 1994 for the Advanced Neutron Source included the directive that a study be

*This work was performed under the auspices of the U.S. Department of Energy.

conducted of the impact on performance of using medium enriched uranium (MEU) fuel or of using low enriched (LEU) fuel. LEU contains a mix of 20%/80% of $^{235}U/^{238}U$, and MEU contains ratios greater than that of LEU but less than that of HEU. For the purposes of this paper, MEU is defined as uranium containing 35% ^{235}U. The Department of Energy requested that Brookhaven National Laboratory lead this Enrichment Study.

Because of concerns about HEU fuel being diverted for non-peaceful purposes, both in the USA and elsewhere, this study was performed. The logic was that, if the USA forgoes the use of HEU in its plans for the Advanced Neutron Source, other countries might be persuaded to do likewise in their plans for new high-performance research reactors. Compared to LEU or MEU, HEU is much more attractive to those who would seek to divert uranium fuel for non-peaceful purposes. For perspective, a prompt critical system (consisting of an unmoderated, unreflected sphere of uranium metal) based on HEU involves approximately 50 kilograms, and one based on MEU and LEU involves one tonne and six tonnes, respectively. The total uranium content for a core of the existing HEU design of the Advanced Neutron Source is approximately 25 kilograms.

APPROACH

The Brookhaven Study involved the participation of three other national laboratories with special expertise in fuel enrichment studies of research reactors. These are Argonne National Laboratory, which has conducted extensive evaluations of HEU to LEU conversion of research reactors worldwide, Oak Ridge National Laboratory, which is responsible for the design of the Advanced Neutron Source, and Idaho National Engineering Laboratory, which contributes technically to the design and has much experience in the design of research and test reactors. The study was conducted in a collegial manner; the laboratory participants agreed upon a mode of technical inquiry and on work assignments for each laboratory. A set of calculations were agreed upon for various enrichments, core volumes, and fuel densities. Technical criteria for the acceptability of results were defined. In order to perform the analysis within the confines of the schedule, it was decided that Oak Ridge National Laboratory and Idaho National Engineering Laboratory run the computer cases that the four laboratories determined should be run. Argonne National Laboratory and Brookhaven National Laboratory provided quality assurance checks of the calculations by running selected cases at their own organizations and with their codes. Interim study results were evaluated jointly, and areas for further investigation were defined, and tentative conclusions were identified. All of the laboratories performed careful and critical reviews of key assumptions and results. Argonne and Brookhaven requested additional calculations which became available to all participants. Between meetings of the Study Group, the participants performed analysis at their respective institutions.

During the course of the study, a special expert panel on fuels was convened to assess the feasibility of developing and manufacturing a postulated fuel form that would be needed in the reactor at lower enrichments. The panel was comprised of international experts in fuel design, manufacture, and performance. The conclusions of this panel are also included in this study.

The scope of the Enrichment Study, as defined by the Department of Energy, was to work within the existing design of the reactor, not produce a much higher power reactor that would greatly

increase the capital costs, and to investigate the implications of using a hypothetical fuel with material density approximately five times greater than the fuel specified for the existing design.

The impact of using either low or medium enrichment fuel in the ANS was measured by considering the change in the following four parameters.

1. Neutron Flux - As a representative parameter the maximum unperturbed thermal neutron flux in the reflector was used as a measure of performance. The value of this flux was compared to the baseline design goal, which in turn has been fixed at 7.0×10^{19} n/m^2-s.

2. Cost - The cost of the ANS is composed primarily of two components: construction and operating costs. Changes in the construction costs are a function of the reactor power and significant deviations from the currently chosen operating power (330 MW) have an impact on the plant cost. Changes in the operating cost are dominated by the number of fuel elements fabricated and burned per year.

3. Safety - The safety impact of using lower enrichment uranium is composed of several elements and some of these are given here. First, the higher fertile content of the fuel enhances the Doppler coefficient, reducing the demand on the control system. Second, the higher fuel density required with lower enrichments reduces the fuel thermal conductivity, and hence increase the fuel centerline temperature and reduce the safety margin. Lower enrichment cores may require larger volumes with radially longer fuel plates of lower curvature, which would be mechanically less stable at high coolant velocities. The power density in alternative core configurations must be kept within acceptable safety margins. There would be increased plutonium build-up with irradiation and this would impact the cleanup following a severe accident.

4. Safeguards - The safeguards dimensions are measured in terms of the requirements of implementing safeguards programs in the U. S. as a function of enrichment, the potential for diversion of fuel elements, the production of plutonium, and the implications for international policy. While this study was motivated by international policy concerns, its objective was to focus on the technical impacts of using alternative enrichments for the fuel of the Advanced Neutron Source. The study does determine the implications of potential alternative designs on the DOE domestic safeguards program, on the number of cores that would be required for non-peaceful purposes, and on the amount of plutonium produced. These parameters provide a measure of the significance of designs with various enrichments and this may be useful in determining the implications for international policy.

The Study Group determined that two parameters should independently be varied to assess the impact of using either MEU or LEU in the reactor. One parameter is the uranium fuel density which would be increased to compensate for decreased ^{235}U content in the lower-enriched fuels. The other parameter is the reactor core volume, which would be increased to compensate for reactivity losses that would result from lowering the enrichment. Thus the fuel density was varied from the existing design value of 1.7 gU/cc to values in excess (in response to the directive of the Department of Energy) of 6 gU/cc. Three core volumes were studied: the existing core volume of 67.6ℓ, and two larger cores of 82.6ℓ and 108ℓ. The existing core is comprised of two cylindrical shell fuel elements,

and the two larger cores each contain three cylindrical shell fuel elements. The 108ℓ core is a hypothetical example that was constructed to study the physics behavior of a large core. In practice, this core design may suffer from large and unsafe deflections of the fuel plates due to forces acting on the wide relatively flat, and, therefore, flexible plate span. Thus, an additional research and development program would be required to investigate the mechanical fluid dynamic, heat transfer, and safety implications of the 108ℓ core, were it to be selected for the ANS.

RESULTS

Many potential configurations of fuel density, enrichment, and core volume were analyzed and only those that met criteria for sufficient initial reactivity, acceptably safe power density and fuel temperature, and the capability of sustaining an acceptable (at least 17 days) core life were retained for further consideration. A wider range of configurations was considered than are feasible or desirable in order to enhance intuition with regard to the impact of parametric variations. Table 1 is a summary of nineteen cases that were considered.

Case 1 was the reference design of the ANS when this study was performed. Based on the many configurations evaluated, the following main conclusions are drawn.

1. HEU is better than lower enriched uranium fuels for the flux performance of the Advanced Neutron Source. In particular, configurations with enrichments of 35% or less consistently led to flux performance that is inferior to the HEU design.

2. If the enrichment were to be reduced to 35% (which we now define as reference MEU), then a reactor configuration was identified (case 6) which meets the above criteria. In this reactor, the core volume would be increased to 82.6ℓ, the fuel density would be increased to 3 gU/cc, the power would remain at 330 megawatts, but the resulting neutron flux would be approximately 20% below the reference design. The additional cost of the project, above the current cost of the existing design, would be approximately $0.4 billion. This cost increase is mostly due to an increase in operating costs over the lifetime of the plant. Only $5M additional would be needed for total project costs including an increased fuel development program. The uranium mass of the core would be approximately 60 kg, and from a safeguards perspective, 17 full cores would be required to achieve a prompt critical system. For the reference case, two full cores would be required for a prompt critical system.

3. If the enrichment were to be reduced to 20%, then a reactor (case 9) could be designed within the confines of the technology which would be utilized for the reference plant. The core volume would be increased to 82.6ℓ, the fuel density would be increased to 3.5 gU/cc (the practical upper limit), the power would have to be decreased to 125 megawatts, and the resulting neutron flux would be approximately 70% below the reference design. The additional cost of the project would be approximately $70 million. This cost increase results from a $160M increase in operating costs over the plant's lifetime relative to the reference plant and approximately $90M decrease in total project costs because this reactor would operate at a much lower power. At this enrichment, more than 88 full cores would be needed to achieve a prompt critical system.

Table 1 - Performance Comparisons for Various Cores

Case	Element Number	Power (MW)	Enrichment (%)	Fuel Density (gU/cc)	Relative Flux	TPC* Penalty	OC* Penalty	Pu Prod.# (kg/yr)	DOE Safeguards Category+
1	2	330	93	1.7	1.0	0	0	0.95	I
2	2	330	80	2.1	0.99	0	0	1.92	I
3	3	330	50	2.0	0.80	+5	+400	3.22	II/III
4	3	400	50	2.2	0.96	+29	+480	3.95	I/III
5	3	405	35	3.5	0.93	+20	+480	7.24	III
6	3	330	35	3.0	0.78	+5	+400	5.53	III
7	3L**	530	20	7.2	0.97	>202	>520	23.74	III/IV
8	3L	449	20	6.0	0.82	+202	+520	18.10	III/IV
9	3	125	20	3.5	0.3	-86	+160	3.6	III/IV
10	3L	330	20	4.8	0.65	+135	+360	12.07	III/IV
11	2	330	35	6.5	0.91	+132	0	9.21	III
12	3	340	50	2.0	0.82	+8	+360	3.28	II/III
13	3	370	35	3.3	0.85	+19	+440	6.62	III
14	3L	430	20	5.8	0.82	+171	+480	17.18	III/IV
15	3	330	93	1.0	0.83	+5	+400	0.53	II
16	2	200	45	3.5	0.59	-54	-200	4.06	III
17	3	250	45	1.8	0.64	-27	+280	2.66	III
18	3	200	35	2.1	0.52	-48	+240	2.80	III
19	3L	260	35	1.8	0.54	-21	+280	3.64	III

* $M, TPC = Total Plant Cost, and OC = Operating Cost Over 40 Years
# 14 cycles per year are assumed
**3L = 108ℓ 3 element core; all other 3 element cores are 82.6ℓ
+Determined by DOE Order 5633.3A

These main conclusions are given for design configurations that would have the best technical chance of succeeding for the stated enrichments and with the derived flux and cost penalties. For MEU fuel, it is possible to design other reactors (case 5) for which the flux penalty relative to the existing design would be approximately 10%. This can be achieved by increasing the power to 405 megawatts, the maximum permissible based on heat removal considerations, and increasing the fuel density to 3.5 gU/cc. The additional cost of this design, relative to the reference design, is $0.5B. A high flux can also be achieved with MEU by increasing (case 11) the fuel density to 6.5 gU/cc in the reference core volume with power at 330 megawatts. However, it was the conclusion of the Fuel Experts Panel that a program to develop fuel with the required heat transfer properties and dimensional tolerances at a uranium density 6.5 gU/cc has more than 90% chance of failure.

For LEU fuel, it is also possible to design reactors with a less severe flux penalty than described in item 3. A reactor can be designed (case 10) with LEU that has a 35 % flux penalty relative to the reference design, would operate at 330 megawatts in the largest core volume, 108ℓ, and requires a fuel density of 4.8 gU/cc. Again, the Fuel Experts Panel have judged that development of fuel for the Advanced Neutron Source at this density has a significant chance of failure. Higher fluxes can be achieved (case 8) by increasing the power in this core to 449 megawatts and increasing the fuel density to 6.0 gU/cc. This implies a flux penalty of 18%. In addition, a research and development program would be needed to assess the technical feasibility of the 108ℓ core.

The Study Group also evaluated the impact of reducing the enrichment of the fuel to 80%, 50%, and to 45%. For 80% enrichment (case 2), no significant differences were found in performance, cost, technical feasibility, or safety. Three full cores (6 elements) would be needed to achieve a prompt critical system. For the case of 50% enrichment, the flux penalty could be limited to 10% provided that the power is increased to 400 megawatts in the 82.6ℓ core. The fuel density would be increased to the reasonably achievable value of 2.2 gU/cc, but the additional operating costs would be $0.5 billion over the life of the facility. On the order of eight cores would be needed to achieve a prompt critical system. The 45% enrichment cases were lower power density studies in the 67.6ℓ and 82.6ℓ core volumes. Both led to approximately 40% flux penalties with fuel densities that do not exceed 3.5 gU/cc.

Safeguards requirements are determined by Category as shown in Table 1. Requirements for Categories I and II include material control and accountability planning and management, threat considerations, performance criteria, accounting systems, physical inventories, measurement control, control limits, loss detection elements, training, access controls, containment, surveillance, etc. For Categories III and IV, requirements are determined by the local DOE Field Office and are less stringent. The differences between Categories I and II are small (with respect to the effort and cost of following requirements). The requirements for Categories III and IV are significantly less obtrusive, but the cost of following the requirements may not be significantly less than meeting the requirement for Categories I or II.

FUEL EXPERTS PANEL EVALUATION

The ANS-LEU Fuel Panel was convened as part of this project to assess the feasibility of achieving higher density LEU fuels for the ANS. This Panel consisted of five international experts on aluminum-based fuels for research and test reactors (see Acknowledgement Section).

They noted that there is no fuel in commercial production that can be compared with the ANS proposed designs: the gradients of the meat (lateral and longitudinal), power densities, heat flux, temperatures, dimensional tolerances, and percent burn-up each require extrapolations of known technology in fabrication, inspection, and irradiation performance, even for the HEU 1.7 gU/cc fuel currently being considered.

The Panel attempted collectively to quantify its conclusions, based on past experience with other fuel types and on the intuitive judgment of each individual member, with the results given in Reference 1. Heat transfer properties, which are essential in a high performance reactor, degrade

significantly at densities greater than 3.5 gU/cc. Panelist Yves Fanjas noted that, with techniques that are still proprietary, CERCA has successfully rolled flat plates, with no gradient or high heat transfer requirements, at meat concentrations of 4.8 and 6.0 gU/cc. However, 6.0 gU/cc must be counted as the maximum density achievable using conventional plate fabrication technology. Densities greater than 6.0 will certainly require development of new fuel plate fabrication technologies.

The Panel concluded that increasing the fuel density up to 3.5 gU/cc, using the current fabrication technology and U_3Si_2 fuel particles, will stretch current technology, but probably will not add greatly to the costs or decrease significantly the probability of success. Going to fuel loadings of 4.8 gU/cc and higher will introduce larger costs and uncertainties and require considerable development effort. Fuel loadings greater than 6.0 gU/cc will require a major development program, including development and testing of new fabrication technologies, which has a low likelihood of success.

QUALITY ASSURANCE

The quality assurance process forms an integral aspect of the analysis work performed in the project. A two pronged approach was taken in this effort. First, the numerical techniques were validated against all relevant critical experiments. The Monte Carlo physics methods are judged by their ability to reproduce the measured results of the FOEHN experiments (see Reference 1). All other physics methods, diffusion theory, and deterministic transport theory are judged by their ability to reproduce the Monte Carlo results. Second, independent calculational efforts were carried out by ANL and BNL staff, to check selected core analyses. In the case of the Monte Carlo calculations this consists primarily of checking the input parameters for consistency, and executing a selection of problems. In the case of the burn-up calculations, the ANL team started with a description of the core and created an independent input file which was executed on their software package for representative range in core volumes, enrichments and fuel densities (see Reference 2 for details). In this manner both the Monte Carlo and burn-up steps of the analysis are checked.

Quality assurance discussions from ANL and BNL are included in Reference 1. Monte Carlo calculations carried out at BNL agreed very closely with those carried out at INEL using different versions of the MCNP code.

In general, ANL results for the 93% enrichment core agree with ORNL results. There is also good agreement on fluxes and initial reactivities for the reduced enrichment cores, but the lifetimes calculated by ANL for the cores with 35% and 20% enrichment are significantly shorter than those reported by ORNL. However, there are sufficient differences in the methods employed by ANL and ORNL to account for the differences observed in the calculated results. Additionally, the results are, in general, consistent with previously reported comparisons of deterministic and stochastic methods used on the ANS design project [3]. Nevertheless, an additional set of calculations are currently being done to identify and resolve the causes of these differences. Finally, it should be pointed out, that regardless of the outcome of these calculations and the resolution of the differences, all study participants agree that the main results of this paper (and Reference 1) do not change.

SUMMARY

In summary, it was the finding of the Enrichment Study Group that although it would be feasible to redesign the Advanced Neutron Source to operate with MEU or LEU fuels, such designs would significantly reduce performance and increase cost. Other designs, which have the potential to maintain performance, would incur significant additional costs, and moreover would have a high probability of technical failure.

ACKNOWLEDGEMENTS

We hereby acknowledge the multilaboratory participants, without whom, this study would not have been possible. They are: Argonne National Laboratory: A. Travelli, J. Matos, J. Snelgrove, and G. Hofman; Brookhaven National Laboratory: L. Forman, B. Keisch, and M.Todosow; Idaho National Engineering Laboratory: A. Ougouag, J. Ryskamp, and C. Wemple; Oak Ridge National Laboratory: G. Copeland, J. Gehin, F. Peretz, D. Selby, P. Thompson, and C. West. We also are grateful to the external members of the Expert Panel on Fuels: Y. Fanjas, R. Hobbins, H. Kalish, J. Marks, and H. Peacock. We have benefitted from helpful guidance from the BNL Steering Group for this project: S. Baron, M. Blume, and M. Brooks. Finally we appreciate the encouragement and support from R. Hunter, J. Mulkey, and R. Awan of the U.S. Department of Energy.

REFERENCES

1. R. A. Bari, H. Ludewig, and J. R. Weeks, "Advanced Neutron Source Enrichment Study," Brookhaven National Laboratory, Draft Final Report, BNL-52433, January 1994.

2. M. M. Bretscher, et al., "Reduced Enrichment Study for the ORNL Advanced Neutron Source Reactor," Argonne National Laboratory, June 1994.

3. L. A. Smith, et al., "Validation of Collapsed Zone Weighted Neutron Cross-Sections for the Advanced Neutron Source," 1994 Topical Meeting on Advances in Reactor Physics, Vol. III, p. 262, Knoxville, TN, April 11-15, 1994.

STUDIES OF THE IMPACT OF FUEL ENRICHMENT ON THE PERFORMANCE OF THE ADVANCED NEUTRON SOURCE REACTOR

Colin D. West
Oak Ridge National Laboratory
P.O. Box 2009
Building FEDC
Oak Ridge, Tennessee, 37831-8218, USA

ABSTRACT

As part of a larger study involving several organizations, the Advanced Neutron Source (ANS) Project made performance calculations for 19 different combinations of reactor core volume, fuel density and enrichment, power level, and other relevant parameters. These calculations were performed by Idaho National Engineering Laboratory (INEL) and Oak Ridge National Laboratory (ORNL). Subsequently, ORNL analyzed 14 other cases.

With the aid of data from these 33 cases, we have been able to correlate the most important performance characteristics (peak thermal flux in the reflector and core life) with fuel enrichment, fuel density, and power. The correlations permit us to investigate additional cases without going to the expense of doing completely new neutronics calculations for each new one and can be used to prepare curves showing the effects of different enrichments and of different fuel densities within the entire range from existing technology to the very advanced, as yet undeveloped fuels that have been proposed from time to time.

INTRODUCTION

The Advanced Neutron Source is a new laboratory for neutron research proposed for construction at Oak Ridge. The neutron source is a 330 MW(f) heavy water-cooled and reflected research reactor. As designed, the entire facility[1] occupies about 40 acres and includes (1) a guide hall/research support area containing most of the neutron beam experiment systems, shops, and support facilities; (2) a reactor containment building housing a neutron source (330 MW(f) heavy-water research reactor) and selected scientific research facilities; (3) an operations support building with the majority of the plant systems; (4) an office/interface complex providing a focused entry point for access control, offices, and administrative support facilities; and (5) other site facilities, including an electrical substation, a cryogenic compressor building, heavy-water cleanup and upgrade equipment, a diesel generator building, and user housing. The technical objectives of the project are shown in Table 1 and are realized in the baseline design by a 330 MW(f) reactor cooled, moderated, and reflected by heavy water.[2] The design is constrained by the requirement that technical risks should be minimized by basing the reactor on known technology. Specifically, the design should not rely on the development of new technology to meet the minimum design criteria.

Table 1. Project technical objectives

•	To design and construct the world's highest flux research reactor for neutron scattering
—	5—10 times the flux of the best existing facilities
•	To provide isotope production facilities that are as good as, or better than, the High Flux Isotope Reactor (HFIR)
•	To provide materials irradiation facilities that are as good as, or better than, HFIR

The overall reactor system concept involves many passive safety features designed to reduce risk. The baseline core consists of annular elements similar to the elements of the Institut Laue-Langevin reactor and the Oak Ridge High Flux Isotope Reactor. However, the two elements in the ANS baseline core are of different diameters, and they are arranged coaxially but not concentrically (see the left sketch in Fig. 1). In the baseline design, the fuel is a mixture of aluminum powder and U_3Si_2 at a density of 1.7 g U/mL with 93% enriched uranium.

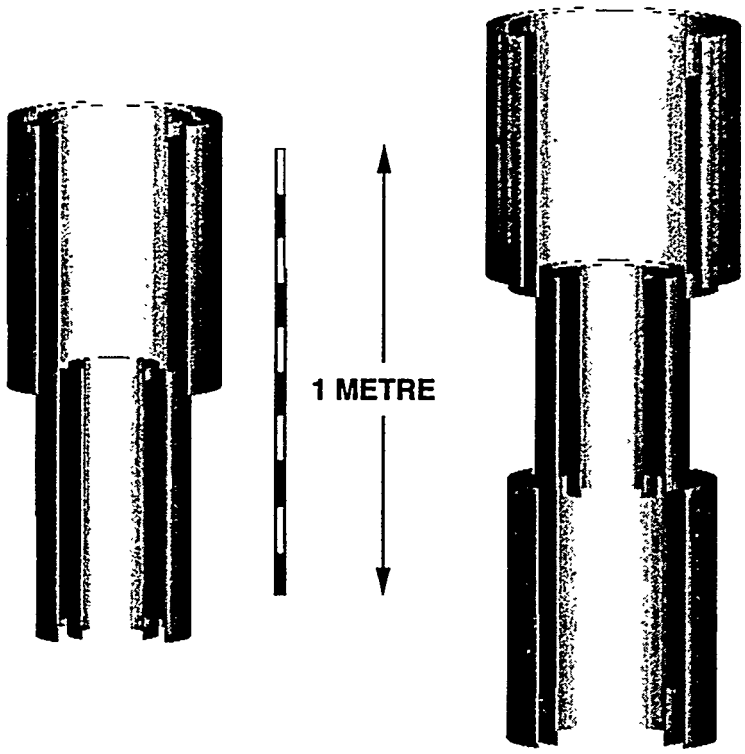

Fig. 1. Baseline two-element core and 82.6-L, three-element core.

These studies[3,4] confirmed earlier calculations which had shown that the baseline core is very highly optimized for maximum performance under safe operating conditions and that departures from the specifications (e.g., a reduction in enrichment) bring severe penalties. Figure 2 illustrates that with a fuel density of 2.2 g U/mL, which is the maximum that all the fuel experts involved in these studies considered to be free of development risk for use in a high flux reactor of this kind (see Table 2), the neutron flux falls off rapidly at enrichments below 70%, and the core will not even go critical for any enrichment below about 45%. Accordingly, we also studied the three-element configuration, which has greater volume available for fuel, shown on the right-hand side of Fig. 1.

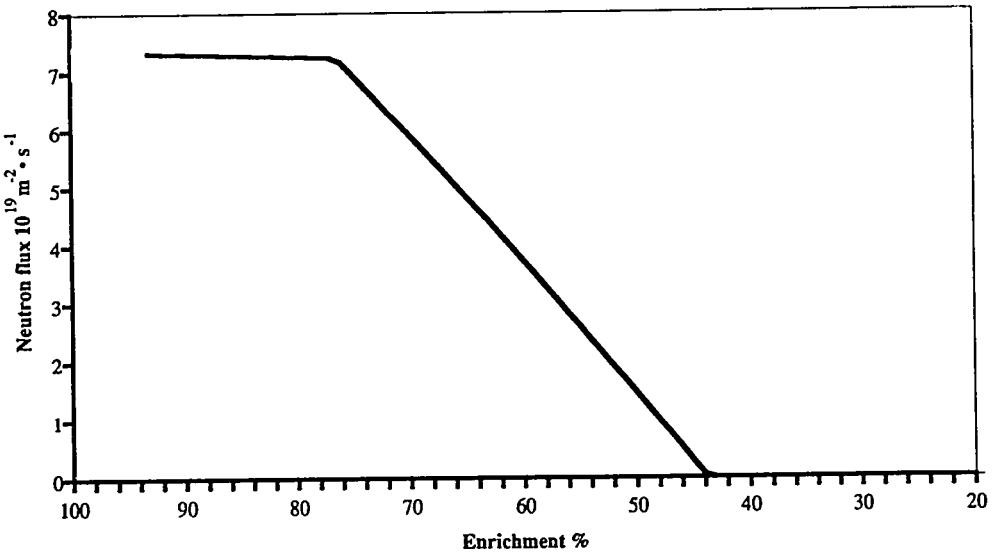

Fig. 2. Neutron flux vs enrichment for the baseline core design with 2.2 g U/mL fuel density.

RESULTS

The baseline two-element core and a three-element design were both optimized in the sense that they maximize the peak thermal neutron flux available for a given safety margin between the operating power and the incipient boiling limit; these cores are shown in Fig. 3. Reference 5 describes the way in which these optimized dimensions were derived. During the enrichment study, some calculations were also performed on a larger three-element design "...a hypothetical example that was constructed to study the physics behavior of a large core. In practice, the design would suffer from large and unsafe deflection of the fuel plates due to forces acting on the wide, relatively flat, and therefore, flexible plate span."[3] The 108-L results are listed in ref. 3 but are not discussed here.

Our data show a good, linear correlation among the product of core life and power, total uranium mass at the beginning-of-cycle, and uranium enrichment. This correlation is well illustrated in Fig. 4. There is also a reasonably good linear correlation among the rendement (or ratio of peak thermal neutron flux to reactor power) the fuel enrichment, and the product of reactor power and core life, as illustrated in Fig.5.

Table 3 summarizes the correlations for the two cores shown in Fig. 3. Note that other dimensions or configurations would generally have different (perhaps very different) correlations.

Table 2. Advanced Neutron Source fuel development: uranium density, technical risk, and reactor safety

Uranium density (g/mL)	BNL[a] study expert evaluation	DOE[b] review of ANS[c] fuel development program	Notes
>6.0	<10% probability of success in development program		
>4.8			ANS Project calculations show that the low thermal conductivity of such fuels would necessitate a reduced reactor power for safe operation
6.0–3.5	50–95% probability of success in development programs		BNL Panel also found "going to fuel loadings of 4.8 g U/mL and higher will introduce larger costs and uncertainties and require considerable development effort"
<3.5		Four (of five) panel members believe this fuel could be qualified with minimal cost and schedule impact	
3.5–1.3	95–100% probability of success in development programs		
<2.2		The fifth panel member believes that this fuel could be qualified with minimal cost and schedule impact	
1.7			Baseline ANS design

[a]BNL = Brookhaven National Laboratory.
[b]DOE = U.S. Department of Energy.
[c]ANS = Advanced Neutron Source.

Table 3. Summary of correlations

Core	MWd vs density and enrichment	Rendement vs MWd and enrichment
67.6-L, two-element	(7822E - 1103) x rhoU - 5100	$2.588 - 4.301 \times 10^{-5} \times MWd - \frac{0.1180}{E}$
82.6-L, three-element	(9564E - 931) x rho U - 1780	$2.128 - 3.497 \times 10^{-5} \times MWd - \frac{0.070085}{E}$

In order to maintain the availability required by the scientific users, a minimum core life of about 17 days is needed. In order to minimize technical risks by staying within the safe operating region defined by the project's conceptual design, and to avoid potentially large cost increases above the present estimate, our studies concentrated on designs with the baseline power level of 330 MW or below. A few cases with higher power were studied for completeness rather than as practical alternatives.

The minimum acceptable core life, 17 days, results in a "cliff" in the relationship between thermal neutron flux and enrichment that is easily seen in Fig. 2. This cliff arises because as enrichment is reduced, there comes a point, for any given fuel density, at which the amount of ^{235}U in the core can no longer sustain the full power of 330 MW(f) for 17 days. At any lower enrichment, the power level, and, therefore, the neutron flux, must be reduced to keep the core

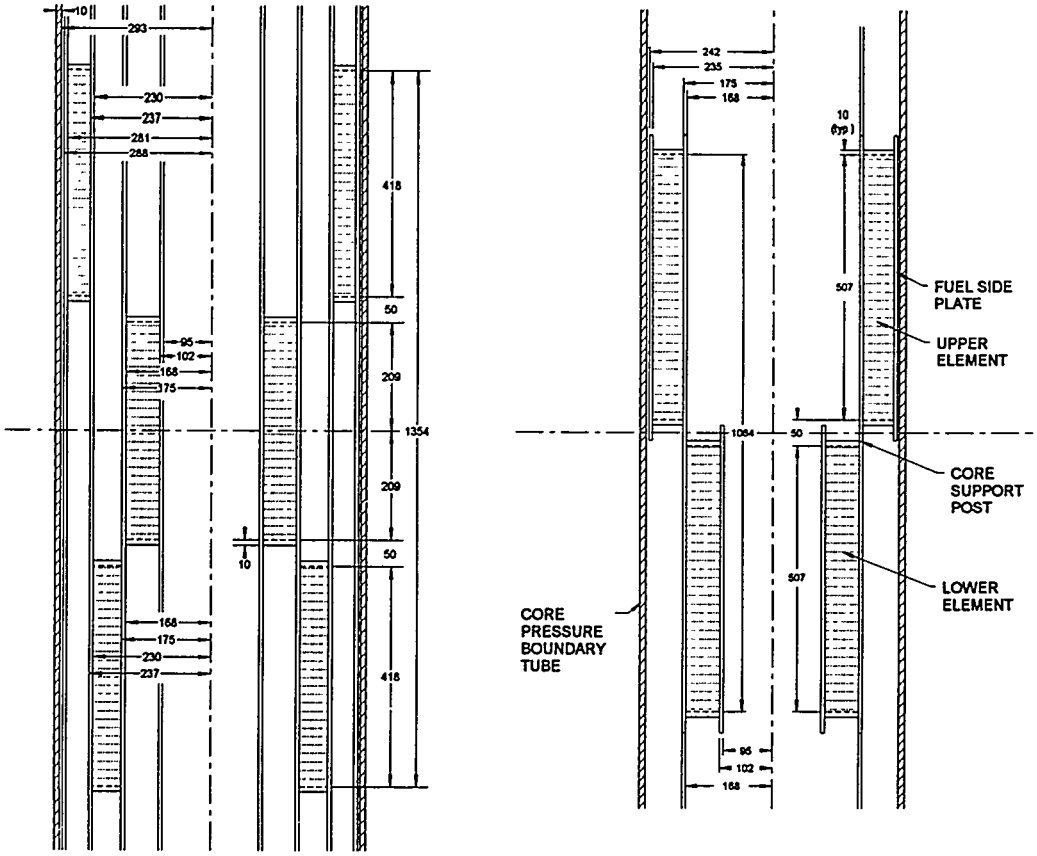

Fig. 3. Optimal three-and two-element cores.

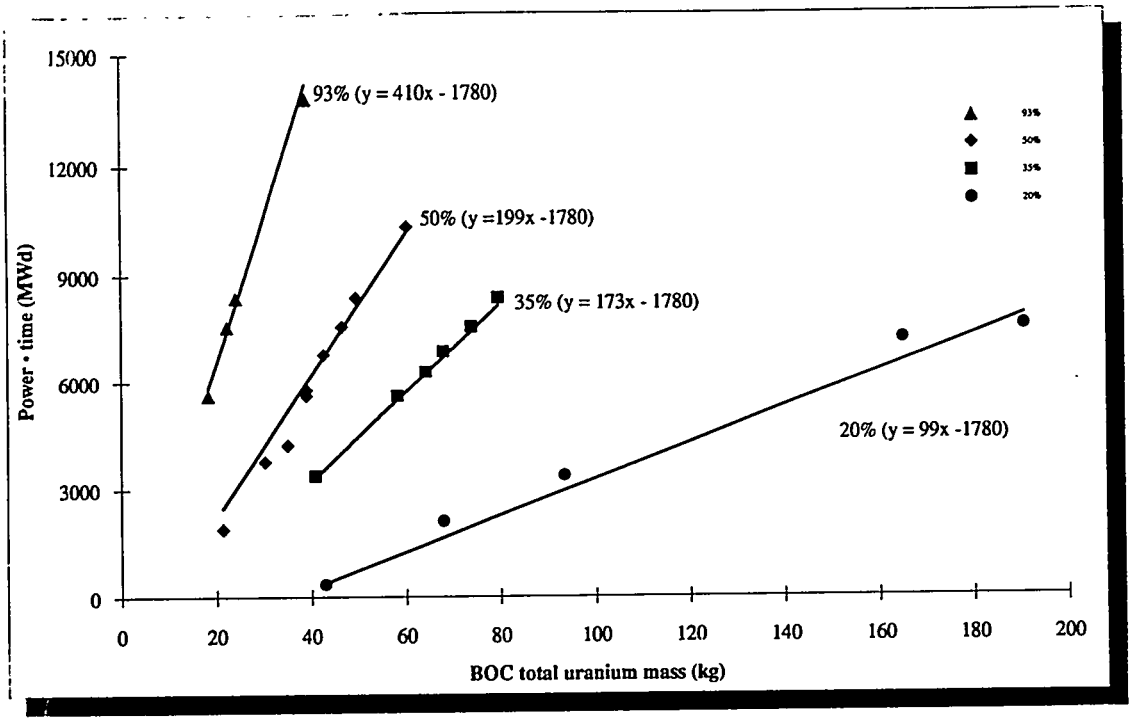

Fig. 4. Correlations for MWd, enrichment, and beginning-of-cycle uranium mass for 82.6-L, three-element cores.

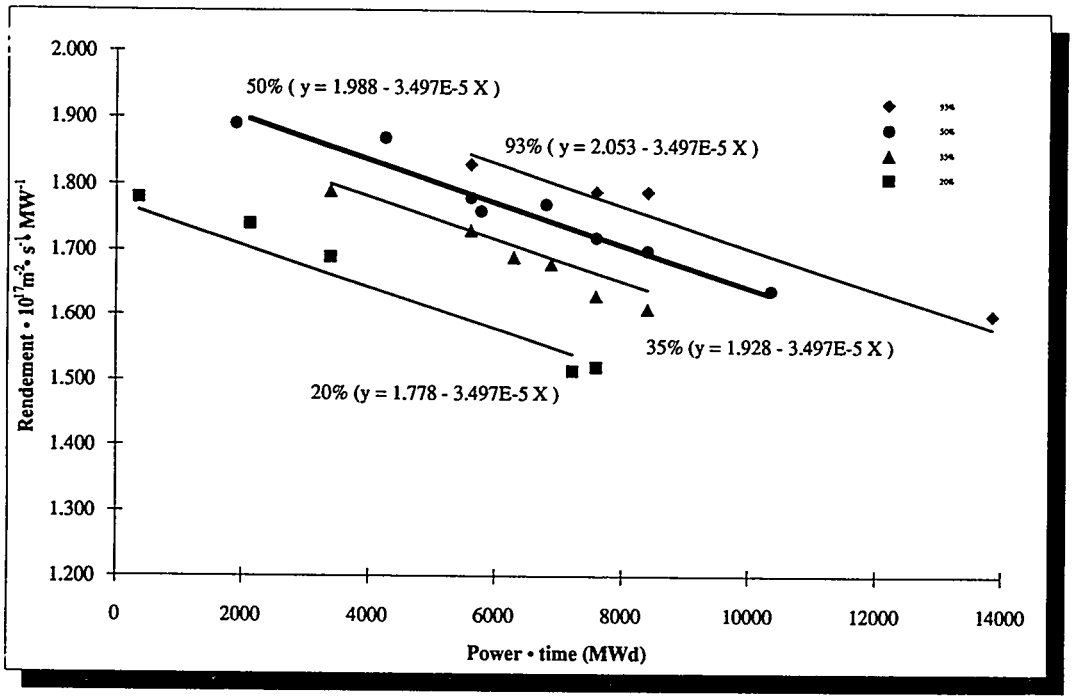

Fig. 5. Correlations for rendement, MWd, and enrichment for 82.6-L three-element cores.

operating for the full 17 days. Because of the larger volume available and the greater surface area, which reduces self-shielding, the three-element core can operate at full power with lower enrichment. However, its rendement is necessarily lower, and so the neutron flux, our main performance indicator, is poorer. This finding is illustrated in Fig. 6, which compares the baseline and the modified (three-element, 83-L) designs.

CONCLUSION

The correlations show that to avoid falling off the enrichment cliff (i.e., to be able to maintain full power for at least 17 days) the baseline core with 20% enriched uranium would need a fuel density of about 23 g U/mL, an impossibility because the density of pure uranium is less than 20 g/mL. On the other hand, the three-element, 83-L core can use medium enriched uranium with existing fuel technology, albeit with a major performance penalty (15–20% less neutron flux). Furthermore, as Fig. 7 shows, development of a high, but perhaps still physically realizable, density fuel form would permit further reduction in enrichment while still meeting the minimum design goals. It is very important to note that, because of the high core power density that is inseparable from a high flux beam reactor, whatever fuel is used must be of high thermal conductivity, even after burnup, and capable of fabrication with a graded thickness of fuel meat to provide power shaping and to avoid unacceptable hot spots or regions. If such a fuel was qualified and fabricable, it could be used with the modified core design when it became available.

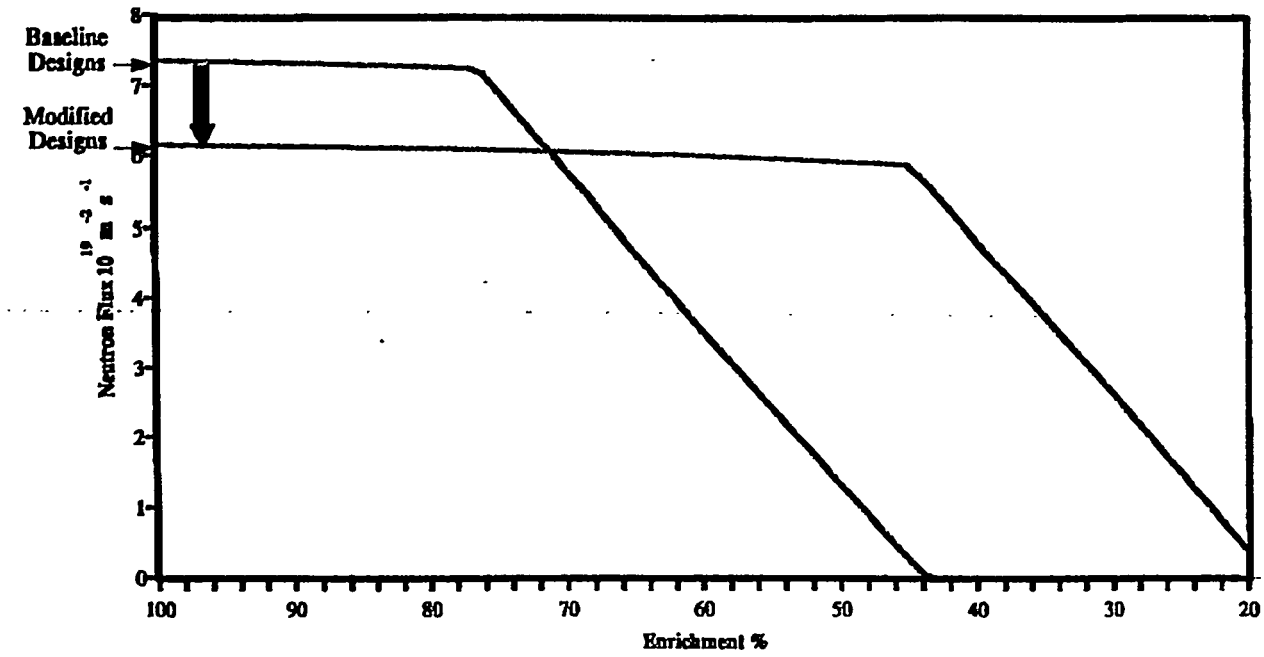

Fig. 6. Compared with the baseline, the modified design has better performance below 70% enrichment, because the "enrichment cliff" is postponed, but it has about 17% less flux with high enriched uranium (330 MW maximum power, 2.2 g U/mL).

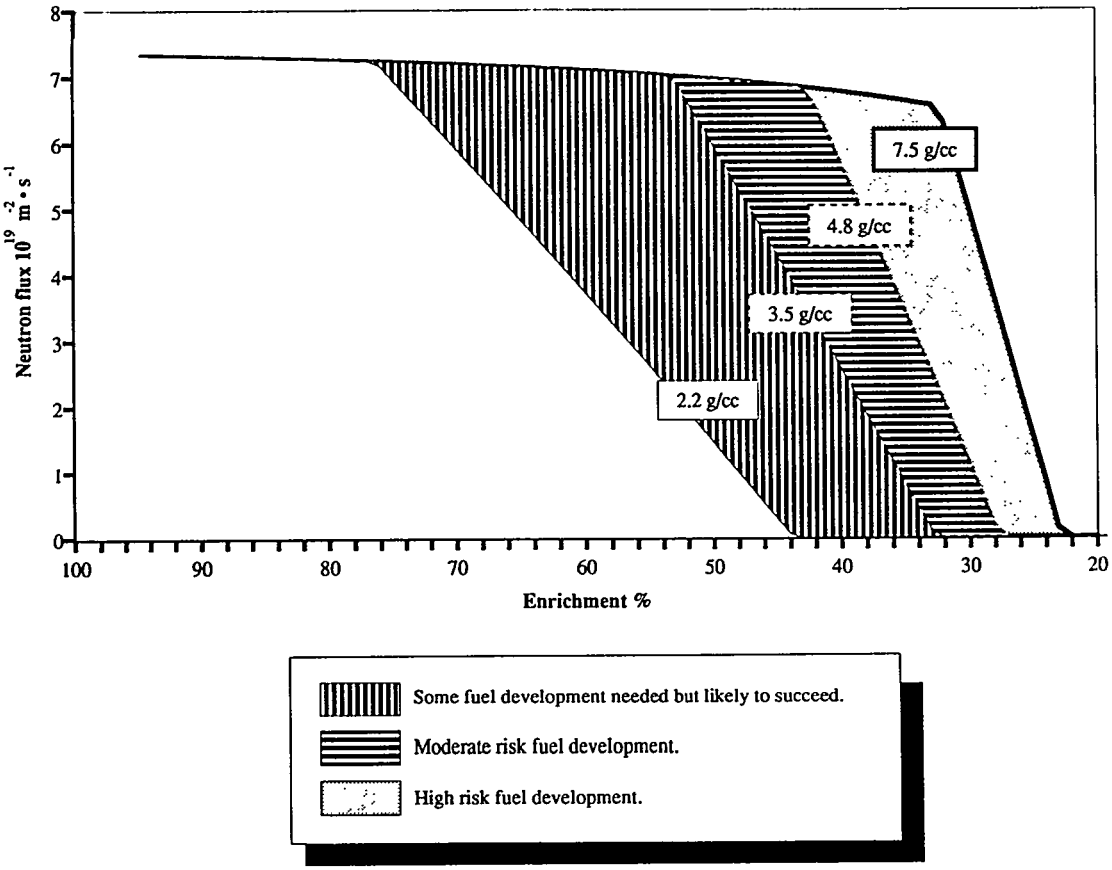

Fig. 7. Neutron flux for different fuel densities and enrichments; baseline core design; 17-d life; 330-MW maximum power level.

ACKNOWLEDGMENTS

The ANS fuel program is carried out at Argonne National Laboratory, Babcock & Wilcox, and ORNL. The neutronics work is mostly carried out at INEL and ORNL. I should like to thank my colleagues at those and many other places for their conduct of the work described here.

REFERENCES

1. C. D. West, "An Overview of the Planned Advanced Neutron-Source Facility," *Physica B* **174**, 430–437, 1991.

2. F. J. Peretz, *ANS Conceptual Design Report Summary*, ORNL/TM-12184, Martin Marietta Energy Systems, Inc., Oak Ridge National Laboratory, Oak Ridge, Tennessee, June 1992.

3. E. E. Alston, J. C. Gehin, C. D. West, *Fuel Density, Uranium Enrichment, and Performance Studies for the Advanced Neutron Source Reactor*, ORNL/TM-12775, Martin Marietta Energy Systems, Inc., Oak Ridge National Laboratory, Oak Ridge, Tennessee, June 1994.

4. R. A. Bari, H. Ludewig, *Advanced Neutron Source Enrichment Study*, Vols. 1 and 2, BNL-52433, Brookhaven National Laboratory, Brookhaven, New York, to be published.

5. G. L. Copeland, et al., *Advanced Neutron Source Final Preconceptual Reference Core Design*, ORNL/TM-11234, Martin Marietta Energy Systems, Inc., Oak Ridge National Laboratory, Oak Ridge, Tennessee, August 1989.

RELATIVE PERFORMANCE PROPERTIES OF THE ORNL ADVANCED NEUTRON SOURCE REACTOR WITH REDUCED ENRICHMENT FUELS

M. M. Bretscher, J. R. Deen, N. A. Hanan, J. E. Matos, S. C. Mo,
R. B. Pond, A. Travelli, and W. L. Woodruff

Argonne National Laboratory
Argonne, Illinois 60439 USA

ABSTRACT

Three cores for the Advanced Neutron Source reactor, differing in size, enrichment, and uranium density in the fuel meat, have been analyzed. Performance properties of the reduced enrichment cores are compared with those of the HEU reference configuration. Core lifetime estimates suggest that none of these configurations will operate for the design goal of 17 days at 330 MW. With modest increases in fuel density and/or enrichment, however, the operating lifetimes of the HEU and MEU designs can be extended to the desired length. Achieving this lifetime with LEU fuel in any of the three studied cores, however, will require the successful development of denser fuels and/or structural materials with thermal neutron absorption cross sections substantially less than that of Al-6061. Relative to the HEU reference case, the peak thermal neutron flux in cores with reduced enrichment will be diminished by about 25-30%.

INTRODUCTION

The Advanced Neutron Source (ANS) is a very high performance nuclear research reactor being designed at the Oak Ridge National Laboratory (ORNL). Operating under steady state conditions, the ANS reactor is intended to provide a neutron flux at experiment locations which is at least five times higher than that available at any existing facility.

The ANL RERTR Program was commissioned[1] to evaluate performance characteristics of ANS cores with fuel of reduced enrichment. This study focuses on the neutronic properties of three cores differing in size, enrichment, and uranium density in the fuel meat. Performance properties of a 108.2 liter LEU core (20.0 wt % ^{235}U, 4.8 g U/cm^3) and a 82.6 liter MEU core (35.0 wt % ^{235}U, 3.5 g U/cm^3) are compared with those of the 67.6 liter HEU reference core (93.2 wt % ^{235}U, 1.7 g U/cm^3). To meet desired operational requirements, the reference core is designed to operate for 17 full power days (FPD) at a fission power of 330 MW. Larger core volumes and higher fuel densities are needed in the MEU and LEU designs to match this reference cycle length and power level. Consequently, cores with fuel of reduced enrichment will have lower thermal neutron fluxes at the experiment locations.

GEOMETRIC MODELS OF THE ANS REACTOR

Geometric models and material compositions used in this study were supplied by ANS personnel[2] at both ORNL and the Idaho National Engineering Laboratory (INEL). Alternate core designs, significantly different from those proposed by ORNL, were not evaluated in this study.

Figures 1-3 show RZ models (not to scale) of the heavy water-moderated and -reflected ANS reactor. The HEU 67.6 liter core uses two fuel elements while the lower enrichment cores need three fuel elements. Natural hafnium rods control the reactor. These figures do not show the hafnium shutdown

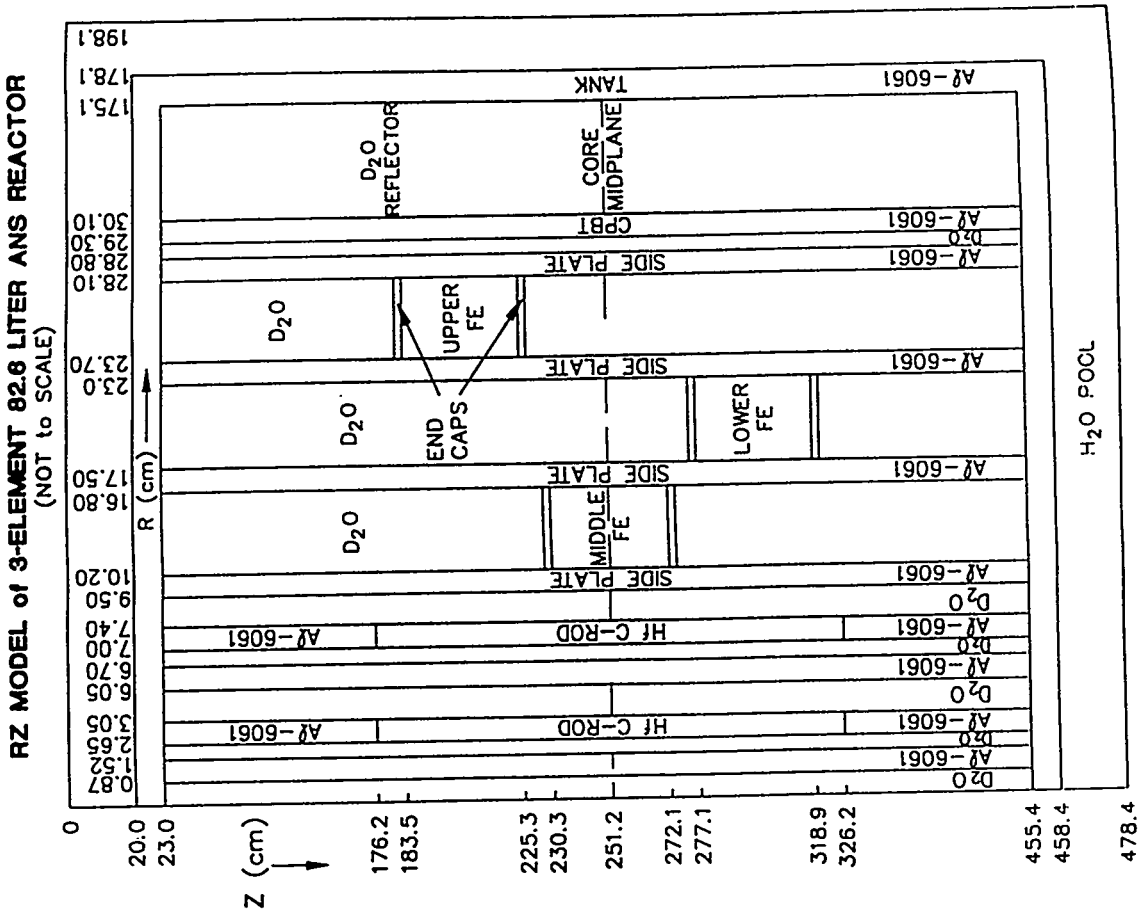

Figure 2

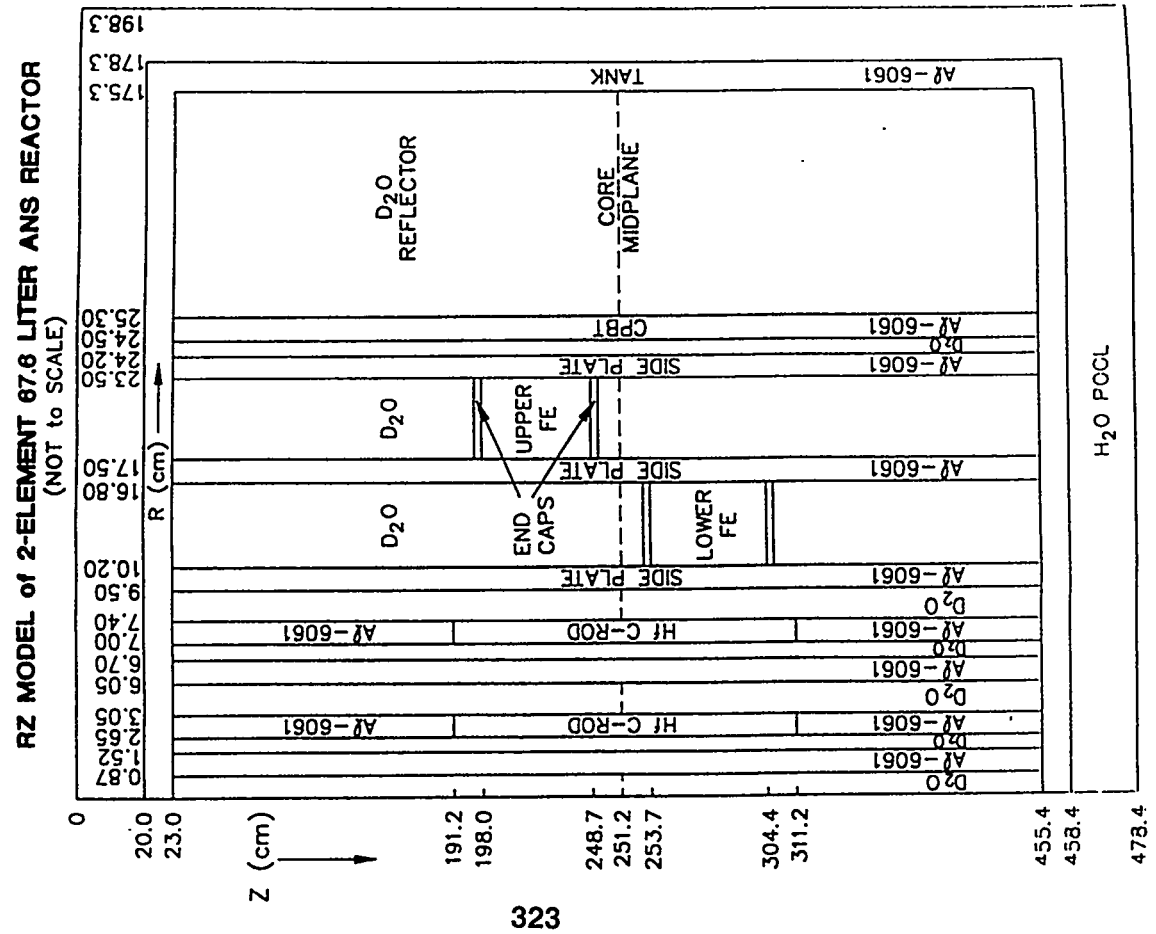

Figure 1

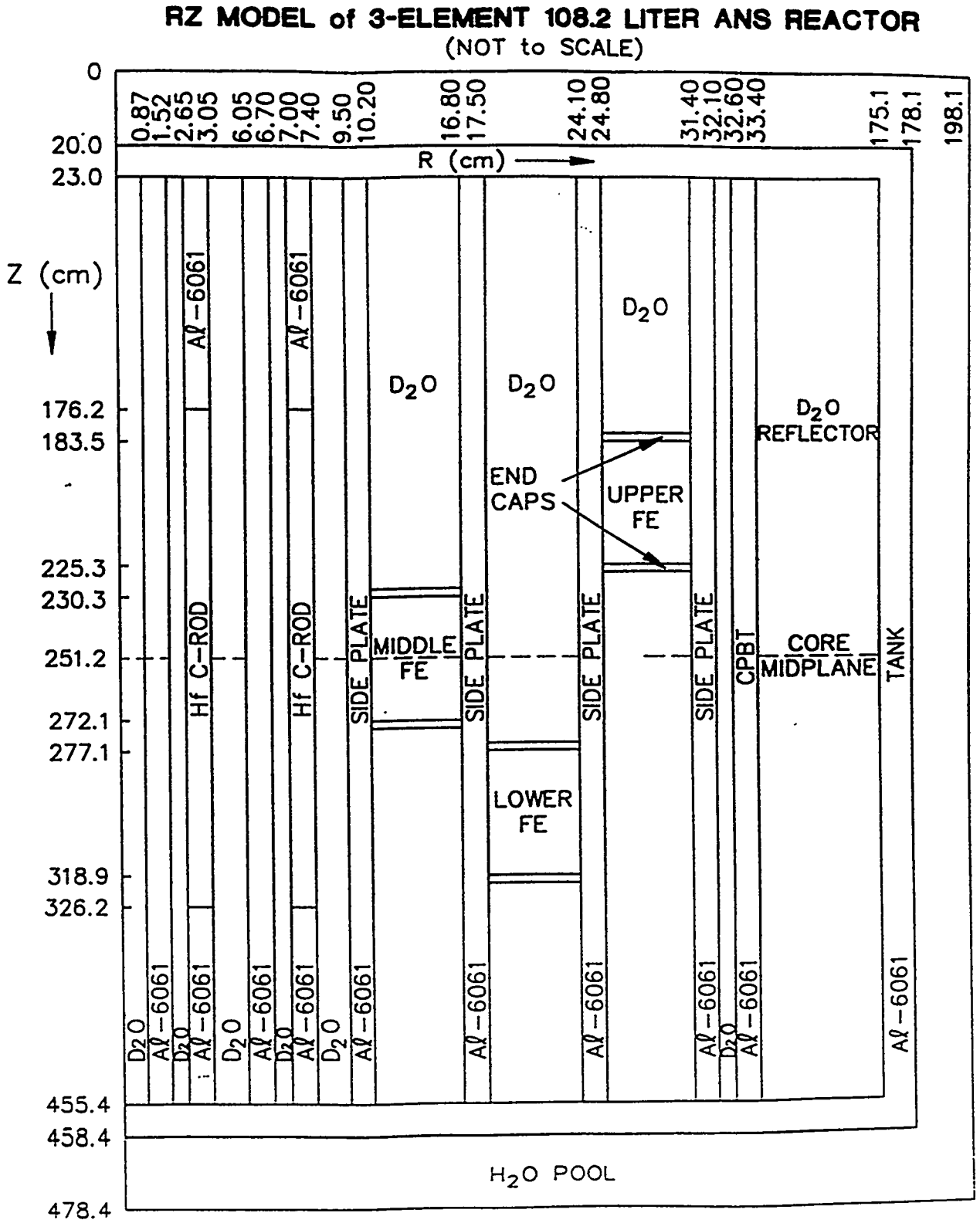
RZ MODEL of 3-ELEMENT 108.2 LITER ANS REACTOR
(NOT to SCALE)
R (cm)
Z (cm)
0
20.0
23.0
176.2
183.5
225.3
230.3
251.2
272.1
277.1
318.9
326.2
455.4
458.4
478.4
0.87
1.52
2.65
3.05
6.05
6.70
7.00
7.40
9.50
10.20
16.80
17.50
24.10
24.80
31.40
32.10
32.60
33.40
175.1
178.1
198.1
Al-6061
Hf C-ROD
SIDE PLATE
D2O
MIDDLE FE
LOWER FE
END CAPS
UPPER FE
D2O REFLECTOR
CPBT
CORE MIDPLANE
TANK
H2O POOL

Figure 3

rods, the internal irradiation targets, nor the components (beam tubes, targets, hot and cold sources, etc.) in the D_2O radial reflector.

Fuel plates and coolant channels are of equal thickness (0.127 cm) and follow the path of an involute from the inner to the outer circular side plate of the fuel element. The fuel meat consists of U_3Si_2 particles dispersed in aluminum. For the HEU reference design, the meat thickness varies in both the axial and radial directions. This fuel "grading" is designed to minimize power peaking effects. A filler of 1100 aluminum powder is used to maintain a constant plate thickness. The meat-filler combination is clad with Al-6061 plates 0.0254 cm thick.

If the total ^{235}U content in the core is fixed, the neutron multiplication factor and the neutron flux at experiment positions are quite insensitive to meat thickness variations. For these neutronic calculations, therefore, the meat thickness was assumed to be uniform for the MEU and LEU fuel elements. In an actual core design, fuel grading probably would be necessary and so a uniform aluminum filler of the same volume used in the HEU plates was added to the fuel plates of reduced enrichment. However, this filler volume has not been optimized.

Figure 4 shows a sketch of the reflector components in the axial midplane of an ANS 3-element core. This complicated geometry can only be roughly approximated in an RZ model. Monte Carlo methods with generalized 3D geometry descriptions are best suited to describe the effects of the reflector components.

Figure 4 also shows the cluster of three hafnium control rods at the center of the reactor. For 2-dimensional RZ calculations these rods are replaced with two concentric rods (see Figs. 1-3) whose radii and spacing were carefully chosen so as to match the reactivity worth of the actual 3-rod cluster and not distort the power shape.

Table 1 provides a summary of the fuel element properties for the three ANS cores analyzed in this study. Some characteristics of the involute-shaped fuel plates are given in Table 2. Region-dependent atom densities are shown in Table 3. Note that the heavy water is assumed to contain a light water impurity of 0.25 atom %.

The composition of the end cap regions above and below the fuel (see Figs. 1-3) was assumed to be a 50/50 volume percent mixture of Al-6061 and heavy water. In an actual fuel element design, it may be necessary to assign a burnable poison to this region to hold down the initial reactivity and to reduce power peaking. For these analyses, however, the burnable poison was omitted.

COMPUTATIONAL METHODS

Our neutronic analyses of the ANS cores depend on a combination of continuous energy Monte Carlo and finite difference multigroup diffusion theory calculations. Because of its very generalized three-dimensional capability, the Monte Carlo neutron/photon-coupled MCNP code[3] can best describe the complicated geometries of the reflector components (see Fig. 4). For fuel cycle analyses, however, the REBUS code[4], with DIF3D[5] fluxes, was used for fuel depletion studies. This code package uses burnup-dependent multigroup cross sections correlated with ^{235}U depletion.

Multigroup Cross Sections

Multigroup cross sections were generated with the WIMS-D4M code[6] together with a new 69-group library[7]. As for MCNP, the cross section library is based on ENDF/B-V data. In the ANS fuel regions the neutron spectrum is strongly influenced by neutrons scattered back into the fuel by the surrounding heavy water. Therefore, a large cylindrical cell duplicating a radial slice through the ANS reactor in the horizontal plane of one of the fuel elements was used in WIMS. By flux-weighting cross

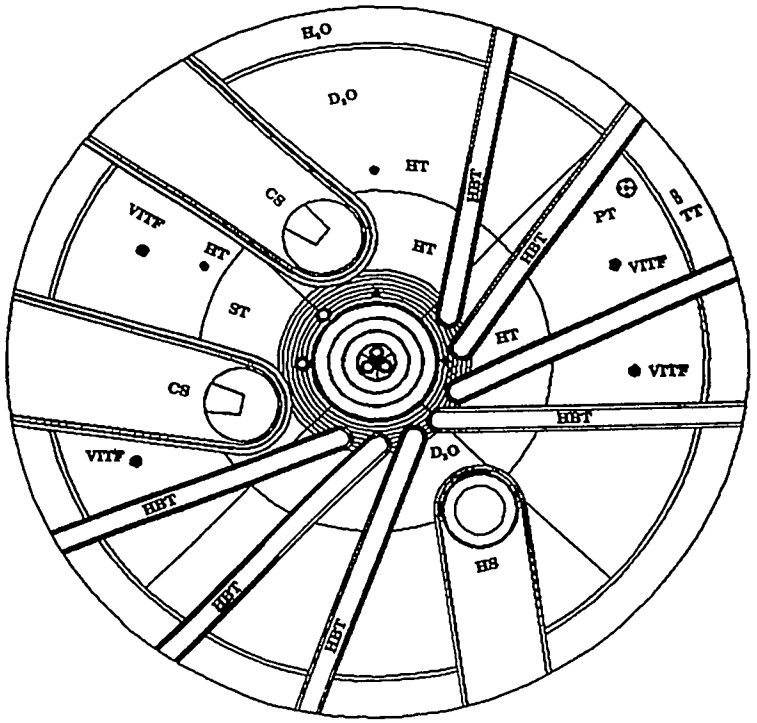

Figure 4
Reflector Components in the Horizontal Midplane of the ANS 3-Element Core

Definitions
CS ≡ cold source
HBT ≡ horizontal beam tube
HS ≡ hot source
HT ≡ hydraulic tube
PT ≡ pneumatic tube
ST ≡ slant tube
TT ≡ transfer tube
VITF ≡ vertical isotope target facility

TABLE 1
ANS FUEL ELEMENT PROPERTIES

Property	HEU Core	MEU Core	LEU Core
Isotopic Enrichment (wt. %)			
^{234}U	1.053	0.364	0.199
^{235}U	93.200	35.000	20.000
^{236}U	0.429	0.161	0.092
^{238}U	5.318	64.475	79.709
U Density in Fuel Meat (g/cm^3)	1.7	3.5	4.8
Fuel Plate Thickness (cm)	0.127	0.127	0.127
Coolant Channel Thickness (cm)	0.127	0.127	0.127
Thickness of Side Plates (cm)	0.70	0.70	0.70
Active Height of Fuel (cm)	50.7	41.8	41.8
Number of Fuel Elements	2	3	3
Inner/Outer Radii of Fuel Zones (cm)			
Upper Fuel Element	17.5/23.5	23.7/28.1	24.8/31.4
Middle Fuel Element	--	10.2/16.8	10.2/16.8
Lower Fuel Element	10.2/16.8	17.5/23.0	17.5/24.1
Core Volume (liters)			
Upper Fuel Element	39.2	29.9	48.7
Middle Fuel Element	--	23.4	23.4
Lower Fuel Element	28.4	29.3	36.1
Total	67.6	82.6	108.2
Fuel Plates Per Element			
Upper Fuel Element	433	586	613
Middle Fuel Element	--	252	252
Lower Fuel Element	252	433	433
Initial ^{235}U Mass (kg)			
Upper Fuel Element	14.78	8.64	11.62
Middle Fuel Element	--	6.76	5.59
Lower Fuel Element	8.93	8.45	8.60
Total	23.71	23.85	25.81
Average Fuel Meat Thickness (cm)	0.0563	0.0599	0.0632

TABLE 2
PROPERTIES OF INVOLUTE-SHAPED FUEL PLATES
(DISTANCES IN CM AND ANGLES IN RADIANS)

Core Volume (liters)	Parameter*	Upper Fuel Element	Middle Fuel Element	Lower Fuel Element
67.6	s	7.029	--	8.735
	θ	0.896	--	1.309
	dθ/ds	0.064	--	0.075
82.6	s	4.808	8.735	6.364
	θ	0.637	1.309	0.853
	dθ/ds	0.066	0.075	0.067
108.2	s	7.478	8.735	7.845
	θ	0.603	1.309	0.947
	dθ/ds	0.052	0.075	0.060

*s is the length of the involute path from the inner to the outer side plate and θ is the angle subtended by s with respect to the radial center of the circular side plates. dθ/ds is a rough index of the stiffness of the fuel plates and increases with increasing rigidity.

From the parametric equations for the involute of a circle, it follows that

$$s = \frac{a}{2}\left[\frac{b^2}{a^2} - 1\right], \quad \theta = \left[\frac{b^2}{a^2} - 1\right]^{1/2}, \text{ and } \quad d\theta/ds = (b^2 - a^2)^{-1/2}$$

where a and b are the inner and outer radii of the annular fuel zone, respectively.

TABLE 3
REGION-DEPENDENT ATOM DENSITIES
(in units of atoms/barn-cm)

Element or Isotope	Control Rods	Al-6061 Alloy	Homogenized Fuel		
			HEU 1.7 gU/cm^3[b]	MEU 3.5 gU/cm^3	LEU 4.8 gU/cm^3
H			8.1622-5	8.1622-5	8.1622-5
D			3.2567-2	3.2567-2	3.2567-2
O-16			1.6324-2	1.6324-2	1.6324-2
Mg		6.6871-4	1.3374-4	1.3374-4	1.3374-4
Al		5.8220-2	2.7101-2	2.5045-2	2.0360-2
Si		3.4722-4	8.9510-4	1.5261-3	2.1371-3
Cr		6.2517-5	1.2504-5	1.2504-5	1.2504-5
Mn		4.4377-5	1.2717-5	1.2206-5	1.1713-5
Fe[a]		3.5352-4	1.1132-4	1.0590-4	1.0069-4
Cu		7.6072-5	2.1803-5	2.0924-5	2.0078-5
Hf	4.4773-2				
^{234}U			1.2034-5	7.7368-6	6.1004-6
^{235}U			1.0604-3	7.4000-4	6.1146-4
^{236}U			4.8572-6	3.3896-6	2.8008-6
^{238}U			5.9744-5	1.3460-3	2.4062-3
Isotope	Light and Heavy Water				
	H_2O		D_2O Near C-Rods	D_2O Near FE's	D_2O Radial Refl.
H	6.6633-2		1.6618-4	1.6236-4	1.6604-4
D			6.6310-2	6.4784-2	6.6236-2
O-16	3.3316-2		3.3236-2	3.2482-2	3.3199-2

[a] Scaled to account for neutron absorption in the trace quantities of Ti and Zn present in Al-6061.

[b] Atom densities correspond to the maximum meat thickness in the graded HEU fuel.

sections over distinct annular regions, multigroup cross sections were obtained not only for the homogenized fuel ring, but also for each H_2O, D_2O, Al-6061, and Hf region. In order to make the cross sections less dependent on neutron spectrum changes, a structure of 15 energy groups was adopted. Burnup-dependent cross sections were generated for the fuel region and complete cross section sets were prepared for each fuel enrichment. Explicit fission product cross sections were generated for ^{135}Xe and ^{149}Sm together with their precursors ^{135}I and ^{149}Pm. A lumped fission product cross section was created to represent the combined effect of all the remaining fission products. The burnup behavior of the lumped fission products is discussed in a separate paper[8] at this conference. At the beginning-of-cycle (BOC) the WIMS-generated cross sections were found to compare very favorably with those calculated by the MCNP and VIM[9] Monte Carlo codes. Table 4 illustrates this comparison for some uranium cross sections. WIMS and VIM results are for identical cells, but MCNP is for a 3D model of the reactor with cross sections collapsed over a single fuel element.

Fuel cross sections were generated using a homogenized mixture of fuel meat (including the aluminum filler), cladding material, and heavy water in the annular fuel ring of the WIMS cylindrical cell model. In reality, however, the fuel element region is a heterogeneous succession of involute-shaped fuel meat, clad, and heavy water channels. Monte Carlo calculations were performed to estimate the importance of these heterogeneous effects. Table 5 illustrates some of these results for the case of ^{238}U capture in the LEU fuel elements. The general conclusion is that the hard spectrum in the fuel region makes heterogeniety effects unimportant.

Hafnium Control Rods

Natural hafnium is a strong neutron absorber with large capture resonances in the 1-12 eV energy range. Because of the large absorption cross sections in groups 9-15, steep flux gradients occur near the hafnium surfaces. These steep gradients violate the conditions under which diffusion theory is valid. Therefore, special methods are needed for treating hafnium control rods in diffusion theory calculations. For groups 1-8 the hafnium capture cross sections are small enough so that normal diffusion theory can be applied.

The method used in this study treats hafnium as a non-diffusing medium for groups 9-15 by applying a group-dependent internal boundary condition at the hafnium surfaces. This internal boundary condition is the neutron current-to-flux ratio. Beginning with the same cylindrical model used to generate the WIMS cross sections, but with a much finer mesh within and about the hafnium rods, P_1S_{16} transport calculations were used to determine numerical values for the internal boundary conditions. For a few groups, these values were too large and thus were replaced by values corresponding to the limiting case of a "black" rod of the same radius. Figure 5, derived from data in Ref. 10, is a plot of the radius-dependent black boundary condition.

Table 6 compares BOC MCNP integral rod worths for the 2-ring model with corresponding REBUS/DIF3D values based on the use of internal boundary conditions. Within 1σ statistics both methods give the same values for the Hf control rod worths. For the purpose of these calculations, the "rods out" condition was taken to be that with the hafnium (Figs. 1-3) replaced by Al-6061.

Reflector Component Worths

The reactivity worth of the reflector components severely limits the cycle lengths of the ANS cores. Because of the complicated geometry of these components (Fig. 4), they are best described by the generalized 3D treatment in MCNP. However, approximate RZ models of the reflector components have been developed by the ORNL group[2] for use in their VENTURE-diffusion code. We have used MCNP as well as REBUS/DIF3D (with ORNL's RZ models) to calculate the worth of the reflector components at both beginning-of-cycle (BOC) and at end-of-cycle (EOC). With the control rods withdrawn and parked in the upper reflector at EOC, REBUS EOC atom densities were used in the MCNP Monte Carlo

TABLE 4
MICROSCOPIC CROSS SECTION RATIOS FOR LEU FUEL Hf CONTROL RODS WITHDRAWN (LOWER FUEL ELEMENT)

Group	E_L - eV	$^{235}U(n,f)$		$^{238}U(n,\gamma)$	
		WIMS/VIM[a]	WIMS/MCNP[b]	WIMS/VIM[a]	WIMS/MCNP[c]
1	8.21+5	1.000	1.012	1.004	0.996
2	6.73+4	1.000	1.001	1.000	1.000
3	1.50+4	0.995	0.996	1.014	1.002
4	5.53+3	1.001	0.998	1.009	0.958
5	1.43+3	1.002	0.997	0.964	0.929
6	3.67+2	1.003	0.978	0.930	0.937
7	2.77+1	0.981	0.945	0.895	0.881
8	9.88	0.999	1.003	0.976	0.969
9	4.00	0.931	0.945	0.939	0.979
10	1.04	0.974	0.996	0.996	0.996
11	0.625	1.002	1.001	1.000	0.998
12	0.300	1.014	1.018	1.003	1.003
13	0.180	0.998	0.999	1.006	1.006
14	0.042	1.023	1.014	1.018	1.008
15	1.0-5	0.998	0.999	1.002	0.997

[a] The 1σ statistics are <<1% for all groups.
[b] The 1σ statistics are <2% for all groups.
[c] The 1σ statistics are <3.2% for all groups.

TABLE 5
$^{238}U(n,\gamma)$ HOMOGENEOUS/HETEROGENEOUS CROSS SECTION RATIOS IN THE ANS LEU CORE

Group	E_L - eV	Homogeneous/Heterogeneous Ratio	
		VIM (Cell)[a]	MCNP (Middle FE)[b]
1	8.21+5	0.977	0.974
2	6.73+4	0.993	0.993
3	1.50+4	1.002	1.000
4	5.53+3	1.032	1.000
5	1.43+3	1.004	1.014
6	3.67+2	1.010	1.031
7	2.77+1	1.028	1.016
8	9.88	1.031	1.071
9	4.00	1.034	1.044
10	1.04	1.002	1.004
11	0.625	1.005	1.004
12	0.300	1.012	1.009
13	0.180	1.015	1.017
14	0.042	1.019	1.022
15	1.0-5	1.037	1.033

[a] Statistical error of 1σ <1.4% for all groups.
[b] Statistical error of 1σ <5.8% for all groups.

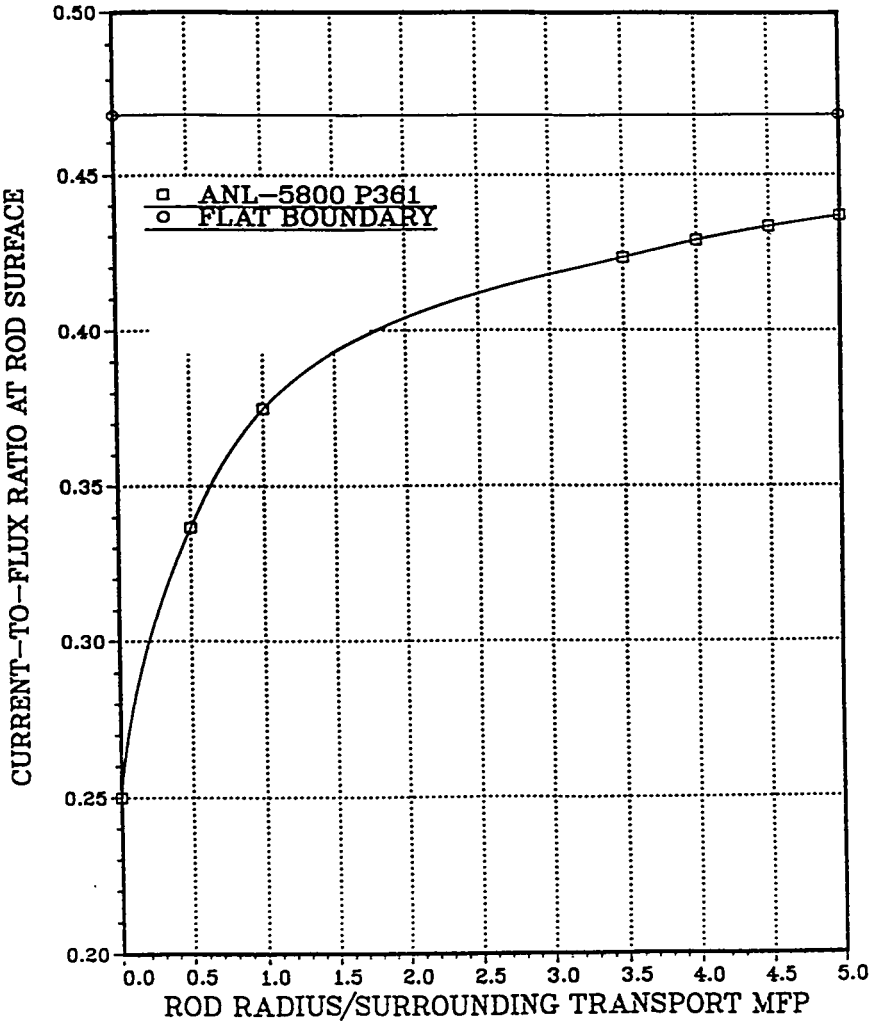

Figure 5

TABLE 6
INTEGRAL WORTHS IN % $\delta k/k^2$ OF THE ANS HAFNIUM CONTROL RODS AT BOC

Core	With Refl. Components ?	DIF3D Diffusion	MCNP Monte Carlo
67.6L HEU	No	-14.01	-14.27±0.20
1.7 gU/cm^3	Yes	-17.58[a]	-17.01±0.23
82.6L MEU	No	-14.15	-14.16±0.23
3.5 gU/cm^3	Yes		-16.35±0.27
108.2L LEU	No	-12.88	-13.03±0.26
4.8 gU/cm^3	Yes		-14.75±0.29

[a] This calculation uses the ORNL-VENTURE RZ model of the reflector components.

calculation. The neutron absorption effect of all the fission products not present in the ANL MCNP library was represented in terms of equivalent, region-dependent, ^{10}B concentrations. Each fuel element was divided into a 3x3 array of equal-volume regions. As a first approximation, the ^{10}B concentrations were chosen to match the combined thermal neutron absorption rates of ^{135}I, ^{135}Xe, ^{149}Pm, and the lumped fission products. These region-dependent ^{10}B concentrations were scaled until a diffusion calculation gave the same eigenvalue as the original EOC REBUS calculation. The EOC MCNP Monte Carlo calculation used these equivalent ^{10}B number densities together with the other EOC atom densities from REBUS.

Table 7 summarizes the results for the reactivity worths of the ANS reflector components. Note that relative to the 3D MCNP calculations, the RZ diffusion model for the HEU reference case overpredicts the worth of the reflector components by nearly 3% $\delta k/k^2$. It appears that the ORNL VENTURE model for the reflectror components is incorrect for the HEU case. The MCNP calculations show that the worth of the reflector components at EOC with the control rods withdrawn is smaller but nearly equal to the BOC value with the control rods fully inserted. This useful result allows the extrapolation of MCNP BOC reflector component worth calculations to EOC conditions.

ANALYTICAL RESULTS

This section presents the results obtained from REBUS/DIF3D diffusion and MCNP Monte Carlo calculations for the three ANS cores studied. Emphasis is placed on eigenvalues, peak thermal neutron fluxes, and core lifetime comparisons.

BOC DIF3D/MCNP Comparisons

Table 8 compares diffusion theory and Monte Carlo results for BOC eigenvalues and peak thermal neutron fluxes for each of the ANS models analyzed in this study. The reflector components are included in some of the MCNP models, but not in the DIF3D calculations. For the purpose of these comparisons, the control rod "out" configuration corresponds to the inserted Hf rods (Figs. 1-3) replaced with Al-6061. In reality, however, the fully withdrawn control rods are parked in the upper reflector with the bottom of the hafnium located on the plane where the top of the hafnium would be for a fully inserted rod. Figures 1-3 show the control rods in the fully inserted position. Table 8 shows that the BOC DIF3D eigenvalues are consistently larger than the corresponding MCNP values by an amount of the order of 1% $\delta k/k^2$.

The peak thermal neutron flux is a function of control rod elevation and is largest for fully inserted rods. However, the product of the flux and the eigenvalue is rather insensitive to control rod elevation and fuel burnup. Since the reactor would operate at an effective multiplication factor of unity, this product is a realistic estimate of the peak thermal neutron flux. Table 8 shows that these products for the MCNP calculations are about 1% higher than the corresponding DIF3D values. Relative to the HEU reference core, the Monte Carlo "rods in" unperturbed peak fluxes (i.e. those without the reflector components modeled) for the MEU and LEU cores are reduced by factors of 0.74 and 0.69, respectively. The reflector components perturb the BOC fluxes and lower them by about 20% relative to the corresponding unperturbed values. Figure 6 is a plot of the BOC unperturbed DIF3D thermal neutron flux distributions on the axial midplane of the three cores in the radial reflector outside the core pressure boundary tube (CPBT).

EOC Properties of the Three ANS Cores

A design objective for the ANS is that it operate for 17 days at 330 MW before refueling. Some calculated characteristics at the end of 17 FPD for the ANS cores analyzed in this study are summarized in Table 9. For the REBUS depletion calculations, the reflector components were not modeled and the

TABLE 7
REACTIVITY WORTHS OF THE ANS REFLECTOR COMPONENTS

Core	FPD[a]	Control Rod Position	Worth of Reflector Components in % $\delta k/k^2$	
			REBUS/DIF3D[b]	MCNP
67.6 Liter HEU	0.0	Fully Out	-8.30	-5.13±0.18
1.7g U/cm^3	0.0	Fully In		-7.86±0.25
	17.0	Fully Out	-10.28	-7.50±0.27
82.6 Liter MEU	0.0	Fully Out	-4.74	-4.45±0.20
3.5 g U/cm^3	0.0	Fully In		-6.65±0.30
	17.0	Fully Out	-5.56	
108.2 Liter LEU	0.0	Fully Out	-4.44	-4.92±0.22
4.8g U/cm^3	0.0	Fully In		-6.64±0.32
	17.0	Fully Out	-5.15	-6.38±0.31

[a] All cores were assumed to operate for 17.0 full power days (FPD) at 330 MW.

[b] Based on ORNL RZ models of the reflector components used in their VENTURE diffusion code.

TABLE 8
BOC DIF3D/MCNP EIGENVALUE AND PEAK THERMAL NEUTRON FLUX COMPARISONS

Core	C-Rods	Code	With Refl. Comp.'s ?	Eigenvalue k_{eff}	Peak Flux[a] E+15 n/cm^2-s	Product k_{eff}*Flux
67.6L HEU	Out	DIF3D	No	1.2927	5.16	6.67
1.7 gU/cm^3	Out	MCNP	No	1.2800±0.0020	5.29±0.06	6.77±0.08
	Out	MCNP	Yes	1.2012±0.0019	4.50±0.09	5.41±0.10
	In	DIF3D	No	1.0945	6.18	6.77
	In	MCNP	No	1.0823±0.0019	6.29±0.08	6.81±0.08
	In	MCNP	Yes	0.9974±0.0019	5.55±0.11	5.53±0.11
82.6L MEU	Out	DIF3D	No	1.2438	4.02	5.00
3.5 gU/cm^3	Out	MCNP	No	1.2234±0.0020	4.13±0.05	5.06±0.06
	Out	MCNP	Yes	1.1602±0.0020	3.32±0.08	3.85±0.09
	In	DIF3D	No	1.0577	4.82	5.10
	In	MCNP	No	1.0428±0.0020	4.86±0.05	5.07±0.06
	In	MCNP	Yes	0.9752±0.0022	4.23±0.10	4.12±0.10
108.2L LEU	Out	DIF3D	No	1.2204	3.65	4.45
4.8 gU/cm^3	Out	MCNP	No	1.2056±0.0023	3.71±0.05	4.48±0.06
	Out	MCNP	Yes	1.1381±0.0021	3.23±0.08	3.67±0.09
	In	DIF3D	No	1.0546	4.46	4.70
	In	MCNP	No	1.0419±0.0022	4.53±0.06	4.72±0.06
	In	MCNP	Yes	0.9745±0.0023	4.35±0.09	4.24±0.09

[a] The peak flux is for neutrons with energies below 0.625 eV and for a power of 330 MW. MCNP statistics are the 1σ values.

ANS UNPERTURBED MIDPLANE THERMAL NEUTRON FLUX DIST.

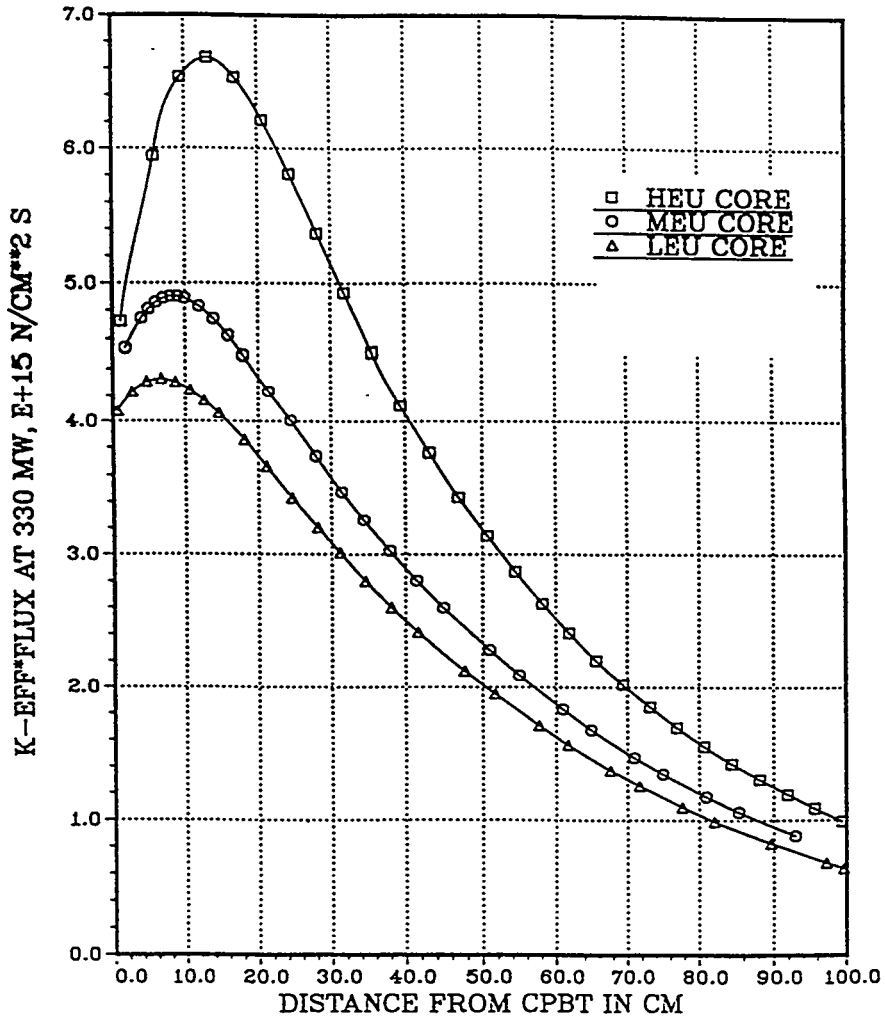

Figure 6

TABLE 9
PROPERTIES OF ANS CORES AT THE END OF 17 FULL POWER DAYS
(CONTROL RODS WITHDRAWN, P = 330 MW)

Core	Code	With Refl. Comp's ?	Eigenvalue k_{eff}	Peak Flux E+15n/cm²-s	Product k_{eff}*Flux	% ^{235}U Burnup	Pu Mass g
67.6L HEU 1.7 gU/cm³	REBUS	No	1.0981	6.18	6.79	30.9	46.9
	MCNP	No	1.0945±0.0025	6.62±0.13	7.25±0.14		
	MCNP	Yes	1.0115±0.0018	5.56±0.11	5.62±0.11		
82.6L MEU 3.5 gU/cm³	REBUS	No	1.0620	4.70	5.03	29.7	369.6
108.2L LEU 4.8 gU/cm³	REBUS	No	1.0570	4.21	4.44	27.0	644.1
	MCNP	No	1.0492±0.0021	4.83±0.11	5.07±0.12		
	MCNP	Yes	0.9834±0.0024	3.73±0.08	3.67±0.08		

reactor was allowed to operate for 17 days at 330 MW with the control rods fully withdrawn. Like the results given earlier at BOC, Table 9 shows that after 17 FPD the peak unperturbed flux is significantly degraded for the MEU and LEU cores relative to the HEU reference and that the reflector components further reduce the peak flux compared with the unperturbed values. The EOC flux ratios are comparable to the BOC values discussed earlier.

Maximum core lifetime estimates have been made using the EOC reactivity balance table shown in Table 10. This table was constructed from data given in Tables 7-9. Normally, a reactivity reserve would be included in this table. This reserve is needed to overcome the buildup of ^{135}Xe and restart the reactor within a short time after an unanticipated shutdown. This balance table determines the minimum unperturbed multiplication factor needed at EOC from which the maximum core lifetime can be found. Figure 7 shows how these lifetime estimates were obtained. The estimated maximum core life for the 67.2 liter HEU, the 82.6 liter MEU, and the 108.2 liter LEU core is 17.0, 15.4, and 12.3 days, respectively, at 330 MW.

Three-Element 108.2 Liter LEU Overlap Core

In recent ANS internal progress reports[11] it was stated that increased peak thermal neutron fluxes and core reactivities would result if the upper fuel element were lowered to be even with the middle fuel element (see Fig. 3). We have analyzed this "overlapping" core configuration for the 108.2 liter LEU case.

With the control rods fully inserted, BOC MCNP Monte Carlo calculations showed that the peak unperturbed thermal neutron flux for this overlap core increased by a factor of 1.052 relative to the normal configuration. The corresponding flux ratio from REBUS/DIF3D calculations was 1.055. For the MCNP perturbed calculations the peak flux for the overlap core decreased by a factor of 0.968 relative to the non-overlap configuration. An estimate of the lifetime of this overlap core was determined, as described earlier, on the basis of an EOC reactivity balance table. The MCNP-calculated worth of the reflector components at BOC is 8.42 ± 0.19 % $\delta k/k^2$. Using results in Table 7 as a guide for extrapolation, the EOC worth of the reflector components for this overlap configuration was estimated to be 8.09% $\delta k/k^2$. Including an EOC REBUS bias factor of 0.68% $\delta k/k^2$, the required excess reactivity at EOC for the unperturbed REBUS calculation is 8.77% $\delta k/k^2$. This translates into a required EOC eigenvalue of 1.0961. Figure 8 shows the unperturbed eigenvalues as a function of exposure in FPD as well as core lifetime estimates for the normal and overlap configurations for the 108.2 liter LEU core. This figure indicates that no significant improvement in core life results from the overlap configuration. The increased worth of the reflector components offsets the advantages of larger eigenvalues for the overlap core.

Sensitivity of Lifetime and Performance to the Choice of Structural Material

For the ANS cores a significant reactivity loss is associated with parasitic neutron capture in the Al-6061 structural materials. Sizeable reactivity gains would be achieved if some or all of the Al-6061 could be replaced with a material significantly less absorbing to neutrons. To investigate the potential effects of this type of substitution, some calculations were performed with magnesium replacing Al-6061 in some or all of the structures of selected ANS cores.

The results show that dramatic improvements would result if substitutions of this type were feasible. For example, substitution of all structural materials (excluding fuel plates) in the LEU 108.2 liter core with 4.8 g U/cm^3 would increase the reactivity available after 17 days at 330 MW by approximately 12% $\delta k/k^2$, which could be used to increase the core lifetime from 12.3 to 36.2 days. The peak thermal neutron flux would also increase 15%, from 4.4 to 5.1 x 10^{15} n/cm^2 s. Similar results were obtained for other ANS cores. In particular, for the 82.6 liter core, substitution of magnesium for Al-6061 in all structural materials yielded a 13% $\delta k/k^2$ increase in reactivity at EOC. Substitution for individual

TABLE 10
REACTIVITY BALANCE TABLE AT THE END OF 17 FPD[a]
(CONTROL RODS WITHDRAWN)

Reactivity Component	Reactivity Worth (% $\delta k/k^2$)		
	67.6 Liter HEU 1.7g U/cm^3	82.6 Liter MEU 3.5g U/cm^3	108.2 Liter LEU 4.8g U/cm^3
Reflector Components	7.50	6.34	6.38
DIF3D Bias (Relative to MCNP)	0.30	0.50	0.70
Total, ρ	7.80	6.84	7.08
Required EOC k-eff = $(1-\rho)^{-1}$	1.0846	1.0734	1.0762

[a] This balance table assumes:

1. The control rods are parked in the upper reflector.
2. The H_2O contamination in D_2O is 0.25 atom %.
3. The worth of the reflector components is based on MCNP Monte Carlo calculations.
4. DIF3D bias factors (relative to MCNP) are included.

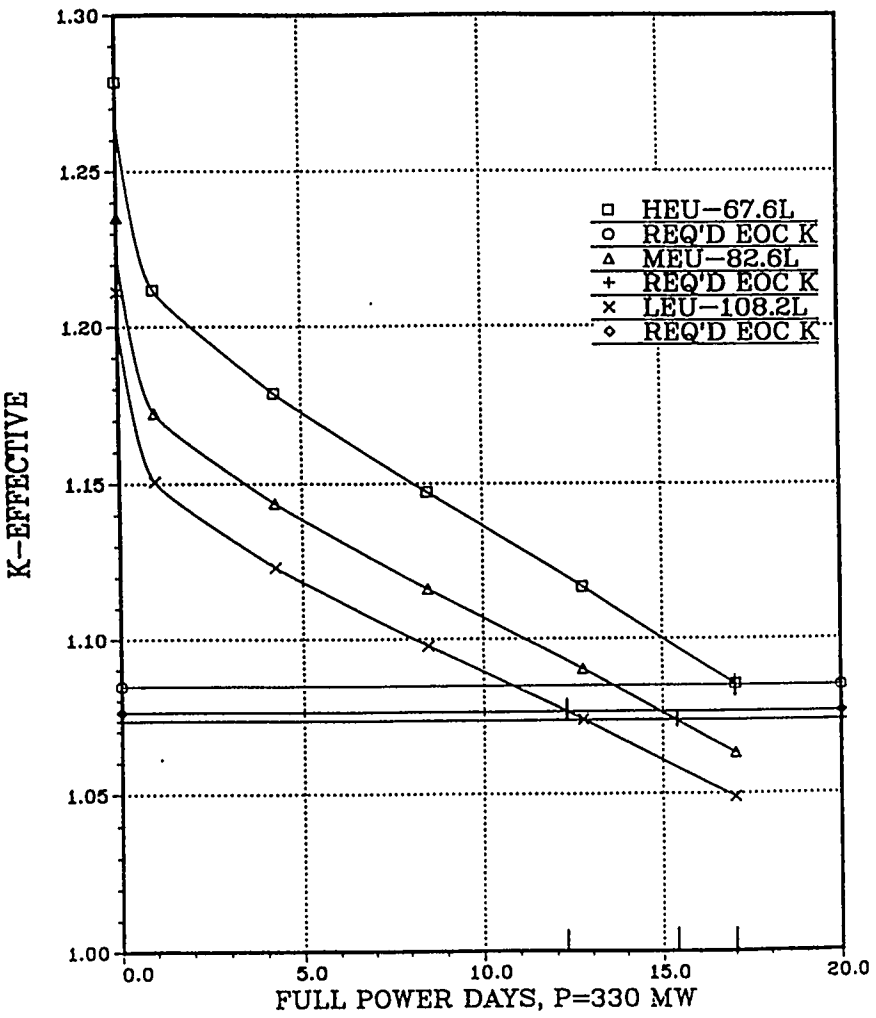

Figure 7

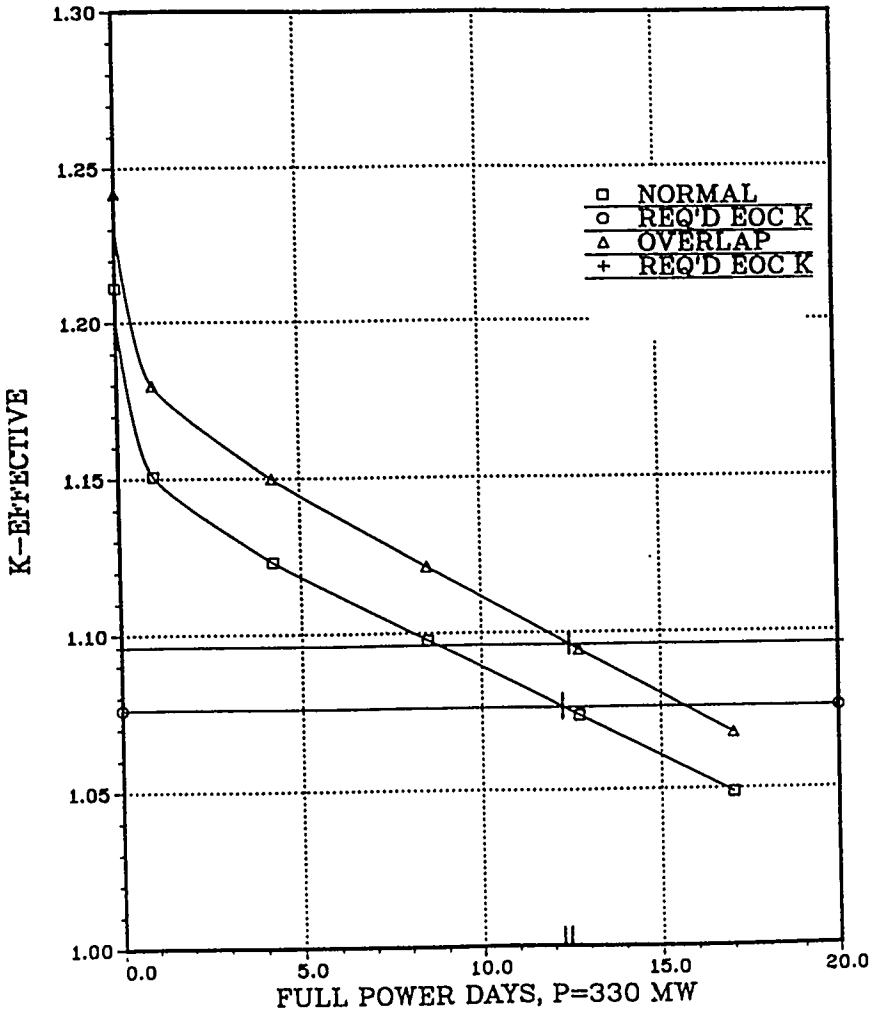

Figure 8

TABLE 11
CORE LIFETIME ESTIMATES AND BOC MCNP PEAK THERMAL NEUTRON FLUKES RELATIVE TO THE UNPERTURBED HEU REFERENCE CORE FOR FULLY INSERTED CONTROL RODS

Core	Lifetime	Relative Peak Thermal Neutron Flux	
	FPD[a]	No Reflector Comp's	With Reflector Comp's
67.6 Liter HEU 1.7g U/cm^3	17.05	1.00[b]	0.81
82.6 Liter MEU 3.5g U/cm^3	15.35	0.74	0.60
108.2 Liter LEU 4.8g U/cm^3	12.30	0.69	0.62
108.2 Liter LEU 4.8g U/cm^3 (overlay case)	12.48	0.75	0.61

[a] FPD ≡ Days at 330 MW.

[b] The peak thermal neutron flux for the unperturbed HEU reference core was 6.81E+15 n/cm^2-sec.

structural components contribute to this total in the following percentages: fuel element side plates (50%), core pressure boundary tube (27%), reflector components (13%), and control rod followers and tubes (10%). Thus, the effect of using structural materials other than Al-6061 even in structures which will be present in the ANS core for only short periods of time, like the fuel element side plates, would be very significant.

These considerations address only the neutronic effects of the substitution. Whether high magnesium content alloys are available or can be developed to withstand the harsh environment of an ANS core is of fundamental importance, but is an issue not addressed in this study.

CONCLUSIONS

Peak thermal neutron fluxes relative to the unperturbed HEU reference core, as well as lifetime estimates for the three ANS cores analyzed in this study, are summarized in Table 11. This table illustrates the size of neutron flux penalties associated with the use of larger volume cores required by fuels of reduced enrichment and also flux reductions caused by the reflector components. Since the reactivity balance tables, upon which the core lifetime estimates are based, do not include allowances for in-core target facilities nor for any operational reserves, it is unlikely that any of these cores will operate for 17 days at 330 MW of fission power. However, the uranium density for the HEU core could be increased to offset these additional reactivity requirements. Similarly, the 82.6 liter MEU core design could be modified by increasing the enrichment and/or the fuel density so that it too could operate for 17 full power days.

However, design improvements will be needed for obtaining substantial reactivity additions before the 108.2 liter LEU core could operate for the desired cycle length at 330 MW. Our calculations indicate that the maximum power density in the LEU core is about one half that in the HEU reference. This suggests that perhaps some of the aluminum filler assigned to the LEU fuel plates is not needed and could be replaced with additional fuel meat. Carefully placed burnable poisons will help limit initial power peaking values. But it seems likely that this LEU core design will require the development and certification of higher density fuels with improved thermal conductivities. Large reactivity additions are also possible if structural materials with significantly less parasitic absorption for thermal neutrons than Al-6061 can be developed for use in the fuel side plates and/or other ANS structures. Otherwise, the LEU core will have to operate for a shorter cycle and/or a lower power level.

Several important issues have not been addressed by this study. Table 2 shows that for these three core designs the fuel plates in the upper element of the LEU core are the least stable. Whether these plates are mechanically stable under the high coolant flow rates required to maintain centerline meat temperatures at acceptable levels for the high density, low thermal conductivity, LEU fuel is of central importance but beyond the scope of this study. To reduce power peaking effects it is assumed that, like the HEU reference core, the LEU fuel will need to be graded in both the axial and radial directions. Whether the high density LEU fuel can be graded and fabricated with acceptable yields is another important issue outside the scope of this study.

REFERENCES

1. Communication from Edward Fei, Director, International and Regional Security Division, Office of Nonproliferation and National Security, U.S. Department of Energy and Robert A. Bari, Department of Nuclear Energy, Brookhaven National Laboratory, September 1993.

2. J. P. Renier and J. C. Gehin of the ORNL Reactor Physics Analysis Group provided input streams for their VENTURE depletion code used to analyze several ANS configurations. C. A. Wemple from INEL gave similar information for use with the MCNP Monte Carlo code. This information allowed us to carry out this study using ANS models consistent with theirs.

3. "Documentation for CCC-200/MCNP 4.2 Code Package", RSIC Computer Code Collection, Oak Ridge National Laboratory, September 1993.

4. B. J. Toppel, "A User's Guide for the REBUS-3 Fuel Cycle Analysis Capability", ANL-83-2, March 1983.

5. K. L. Derstine, "DIF3D: A Code to Solve One-, Two-, and Three-Dimensional Finite-Difference Diffusion Theory Problems," Argonne National Laboratory Report ANL-82-64, April 1984.

6. C. I. Costescu, D. G. Cacuci, J. R. Deen, and W. L. Woodruff, "Microscopic Cross Sections for and from the WIMS-D4 Cell Code," Trans. Amer. Nucl. Soc. 68, 471 (1993).

7. J. R. Deen, W. L. Woodruff, and C. I. Costescu, "New ENDF/B-V Nuclear Data Library for WIMS-D4M," 16th International RERTR Meeting, Oarai, Ibaraki, Japan, October 3-7, 1993.

8. S. C. Mo, "Methodology and Application of the WIMS-D4M Fission Product Data," 17th International RERTR Meeting, Williamsburg, Virginia, USA, September 18-23, 1994.

9. R. Blomquist, "VIM-A Continuous Energy Neutronics and Photon Transport Code," ANS Proceedings of the Topical Meeting on Advances in Reactor Computations, Salt Lake City, Utah, pp. 222-224, March 1983.

10. L. J. Templin, Ed., "Reactor Physics Constants", 2nd edition, pp. 361-363, ANL-5800, July 1963.

11. F. Gallmeier, et al., Oak Ridge National Laboratory, unpublished information (June 1994).

SESSION VI

September 21, 1994

REACTOR CONVERSIONS

Chairman:

K. Kanda
(KURRI, Japan)

THE WHOLE-CORE LEU SILICIDE FUEL DEMONSTRATION IN THE JMTR

Tomokazu ASO, Kazutomo AKASHI, Yoshiharu NAGAO, Yoshihiro KOMORI
Katsumune YAMAMOTO, Toshisada NIIHO, Rokuro OYAMADA

Oarai Research Establishment
Japan Atomic Energy Research Institute
Narita-cho, Higashiibaraki-gun, Ibaraki-ken 311-13 Japan

ABSTRACT

The JMTR was fully converted to LEU silicide (U_3Si_2) fuel with cadmium wires as burnable absorber in January, 1994. The reduced enrichment program for the JMTR was initiated in 1979, and the conversion to MEU(enrichment ; 45%) aluminide fuel was carried out in 1986 as the first step of the program. The final goal of the program was terminated by the present LEU conversion.

This paper describes the results of core physics measurement through the conversion phase from MEU fuel core to LEU fuel core. Measured excess reactivities of the LEU fuel cores are mostly in good agreement with predicted values. Reactivity effect and burnup of cadmium wires, therefore, were proved to be well predicted. Control rod worth in the LEU fuel core is mostly less than that in the MEU fuel core. Shutdown margin was verified to be within the safety limit. There is no significant difference in temperature coefficient of reactivity between the MEU and LEU fuel cores. These results verified that the JMTR was successfully and safely converted to LEU fuel. Extension of the operating cycle period was achieved and reduction of spend fuel elements is expected by using the silicide fuel with high uranium density.

INTRODUCTION

The JMTR is a 50MW tank type reactor, moderated and cooled by light water, and achieved the first criticality with HEU U-Al alloy fuel in 1968. Along with international cooperation on reduced enrichment for research and test reactors, efforts had been continued on LEU conversion for the JMTR since 1979 and the conversion was completed in January, 1994. The LEU fuel is silicide fuel (U_3Si_2) with 4.8gU/cc, and cadmium wires are placed in each side plate as burnable absorber. After the conversion, three operation cycles with whole LEU fuel core were experienced and core physics measurement was carried out. This paper briefly looks back on the LEU conversion program history and describes the core physics parameters of the LEU fuel cores.

HISTORY OF LEU CONVERSION PROGRAM FOR THE JMTR

Reduced enrichment program for research and test reactors in JAERI was started in 1979. Conversion efforts have been continued since then and the JMTR was fully converted to LEU silicide fuel in 1994. The reduced enrichment program history for the JMTR during the fifteen years are summarized as follows.

Table 1 History of Reduced Enrichment Program for the JMTR

Year	*Major Steps*
1979	JAERI started reduced enrichment program.
1980	ANL-JAERI joint study on reduced enrichment of JAERI research reactors was started.
1983	MEU aluminide fuel core experiment was started in the JMTRC.
1985	Irradiation test of MEU aluminide fuel elements was conducted. Irradiation test of LEU silicide fuel miniplates was conducted.
1986	The JMTR was fully converted to MEU aluminide fuel. (U density ; 1.6g/cc)
1992	The license for use of LEU silicide fuel in the JMTR was obtained.
1993	Upgradings of safety systems and replacement of diesel engine generators associated with the LEU conversion were completed.
1994	The JMTR was fully converted to LEU silicide fuel. (U density ; 4.8g/cc)

Feasibility study for LEU conversion of JAERI research reactors was carried out in the early and middle 1980s in close collaboration with ANL. Since aluminide fuel with uranium density up to 2.2g/cc became available by international efforts on LEU fuel development, the JMTR was converted to the MEU (45%) aluminide fuel as the first step to LEU conversion in 1986. After the MEU conversion, neutronic analysis was continued for LEU conversion with developed high uranium density silicide fuel with 4.8 gU/cc. Analytical results showed that LEU conversion is feasible using the high uranium density silicide fuel without any disadvantage in reactor safety and it gives an advantage of eliminating middle shutdown for refueling which was carried out for HEU and MEU fuel core operations. Cadmium wires were introduced to suppress excess reactivity at BOC(beginning of cycle) below the safety limit. Specifications of HEU, MEU and LEU fuels used in the JMTR were shown in Table 2.

Table 2 Specifications of the JMTR Fuel

	HEU	MEU	LEU
Fuel Meat	U-Al Alloy	UAl_x-Al Dispersion Alloy	U_3Si_2-Al Dispersion Alloy
Enrichment (%)	93	45	20(19.75)
Uranium Density (g/cc)	0.7	1.6	4.8
Uranium Content (g/element)	279	310	410
Burnable absorber	—	—	Cadmium wires
Conversion Year	(1968)	1986	1994

Since the new DNB(departure from nucleate boiling) correlation was employed in the safety analysis, upgradings of safety systems became necessary to ensure safety in the postulated piping failure accident. The flow rate of the emergency cooling system was increased by operating a main circulating pump as the emergency cooling system. Associated with this upgrading, diesel engine generators were replaced new ones with higher capacity. The new channel was also provided in the safety protection system to scram the reactor faster than the present system.

TRANSITION FROM MEU FUEL CORE TO LEU FUEL CORE

For core conversion, the transition core operation was carried out from November 24 to December 20, 1993. Two LEU test fuel elements were loaded with 20 MEU fuel elements in the transition core. The two LEU test fuel elements were subjected to visual inspection and sipping test after the operation, and they were verified to perform well. Whole core conversion to LEU fuel was made in January, 1994. The LEU initial fuel core operation (#108cycle) was carried out with 20 fresh LEU fuel elements and the two LEU test fuel elements loaded from the transition core (January 27 to February 21, 1994).

After the LEU initial fuel core operation ended, two LEU equilibrium core operations(LEU core A[#109cycle] and LEU core B[#110cycle]) were carried out in the period March through July, 1994. Fuel loading patterns during the conversion phase and core configurations are shown in Table 3 and Fig.1, respectively.

Table 3 Fuel Elements Loading Pattern

cycle	Core	Standard Fuel Element				Fuel Follower	
		MEU Fuel	LEU Fuel			MEU Fuel	LEU Fuel
			Fresh	1 cycle used	2 cycle used		
#106	MEU Core	22				5	
#107	Transition Core	20	2			5	
#108	LEU initial Core		20	2			5
#109	LEU core A		10	10	2		5
#110	LEU core B		12	10			5

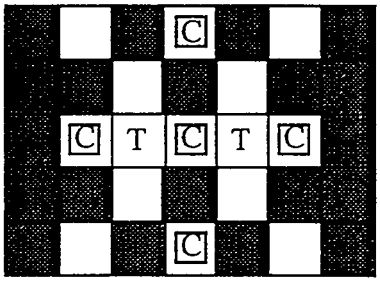

Transition Core
(#107cycle)

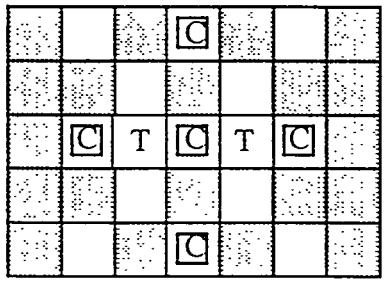

LEU initial Core
(#108cycle)

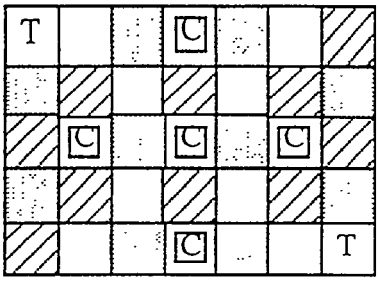

LEU Core A
(#109cycle)

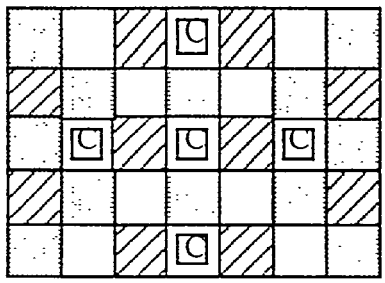

LEU Core B
(#110cycle)

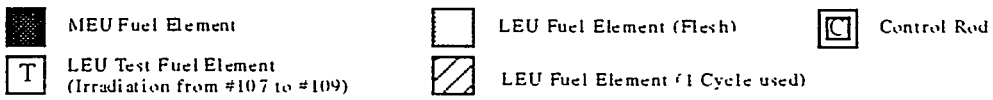

Fig. 1 Core Configurations

PHYSICAL PROPERTY OF THE LEU CORE

Core physics measurement was conducted through the conversion phase in order to ensure operability and safety of the LEU fuel cores, and control rod worth, excess reactivity, shutdown margin, temperature coefficient of reactivity were measured.

Cold Clean Excess Reactivity at the beginning of an operation cycle

Excess reactivities at BOC were measured by the positive period method in the fuel addition process for MEU core, LEU initial core and LEU core A. The excess reactivity for LEU core B was measured by comparing control rods positions with those in LEU core A. The measured results are shown in Table 4 with calculated values. Calculation was carried out by diffusion theory code CITATION. There has been several discussion in how to obtain excess reactivity from reactivities of each fuel element measured by the fuel addition method. Measured reactivities of each fuel element were directly summed here based on the calculated result simulating the fuel addition process.

Measured excess reactivity of the LEU initial core, which is 10.0%Δk/k, is kept at relatively low due to reactivity effect of cadmium though the mass of U-235 loading increased by about 3kg compared with that of the average of the MEU cores. Calculated cold clean excess reactivity at BOC is 1.2%Δk/k larger than measured value for LEU initial core but about 1%Δk/k less than the measured value for the LEU core A and B. No systematic difference was found between measured and calculated value. Excess reactivities of these cores are less than the safety limit of 15%Δk/k.

Table 4 Excess Reactivity at the Beginning of an Operating Cycle

(%Δk/k)

Core	Measured	Calculated	C/E
MEU core (#103)	11.4	11.6	1.02
Initial LEU core	10.0	11.2	1.12
LEU core A	11.9	10.9	0.92
LEU core B	12.0	11.3	0.94

Measured values were obtained by direct summation of reactivities of each fuel element.

It was found by calculational study simulating the fuel addition process that calculated excess reactivity is also larger than the measured for the minimum core (consisted of 17 fuel elements) with the LEU fresh core. This suggests that the calculation overepredicts the excess reactivity, and input data such as group constants of the fuel element should be reconsidered. It is also needed to review estimation of poison reactivity for the LEU equilibrium cores.

Excess Reactivity Change during Operation

Excess reactivity change during operation was measured by control rods positions with their differential reactivity curve. Measured excess reactivity changes are shown in Fig.2. The excess reactivity curve for the transition core was typical one for MEU core operations, and excess reactivities decreased as burnup of the fuel. For the initial LEU core, excess reactivity change after Xe saturation was very small and the increase in excess reactivity was observed between about 300MWd and 700MWd due to balance between burnup of uranium and cadmium. For LEU cores, almost identical pattern is seen for both core A and core B and excess reactivity were almost constant from about 200MWd to 700MWd.

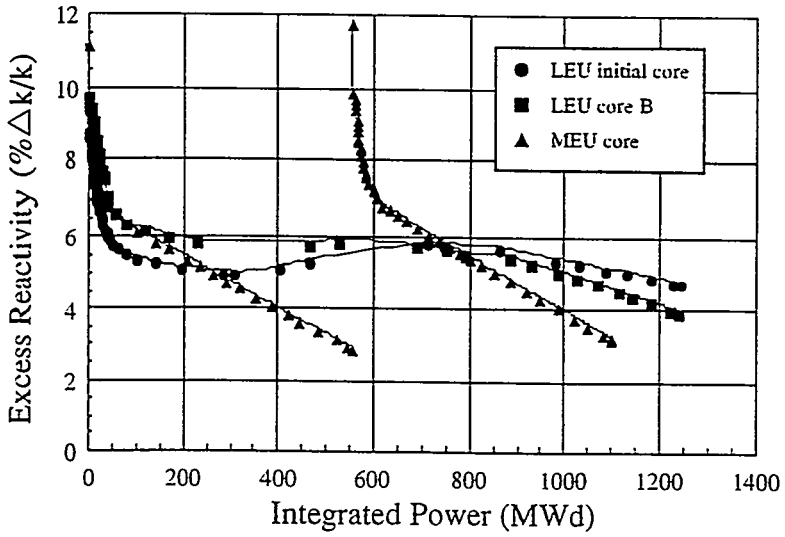

Fig.2 Excess Reactivity Change during Operation

These measured excess reactivity changes were compared with calculated results by diffusion theory burnup calculation code COREBN as shown in Fig.3. Calculated excess reactivity change agrees fairly well with the measured value for the initial LEU core, and increase of the excess reactivity around middle of the operation cycle is well predicted by calculation. This indicates that burnup of cadmium wires is calculated well. Considering that calculated cold clean excess reactivity of the LEU first core is larger than the measured value, reactivity of xenon may be overpredicted. Calculated excess reactivity is about 1%Δk/k less than the measured value throughout the operation for LEU core A. The same tendency was found also for the LEU core B.

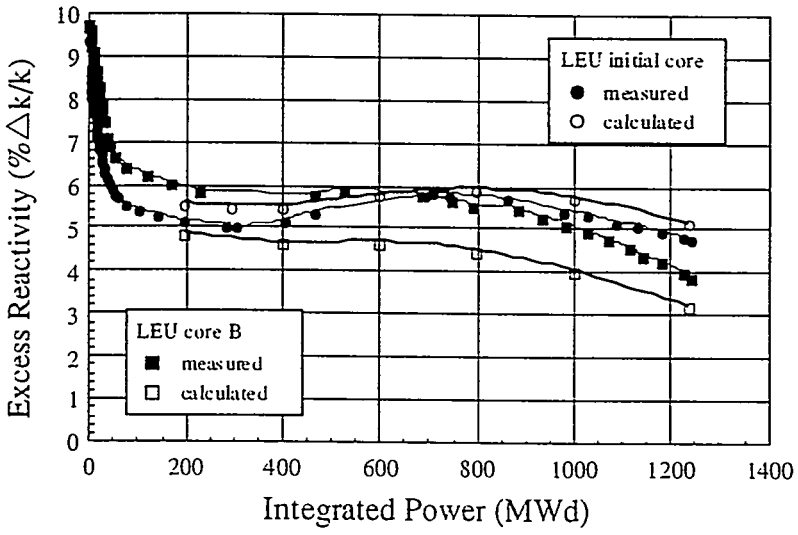

Fig.3 Measured and Calculated Excess Reactivity Change during Operation

Control Rod Calibration

The control rods were calibrated by positive period method. There are five control rods in the core. Three rods of these are shim rods (SH-1, SH-2, and SH-3), the others are regulation rods (SR-1 and SR-2). SH-1 and SH-3 are used for startup by gang withdrawn. During reactor operation, SH-2 is used for compensating burnup. Either SR-1 or SR-2 is used as the automatic control rod, and the rest one is used as the safety rod. The calibration of control rods was carried out as simulating control rod position changes during operation.

Obtained calibration curve for SH-2 is shown in Fig.4. The peak value of differential reactivity for LEU core A is about 11% less than that for the MEU core.

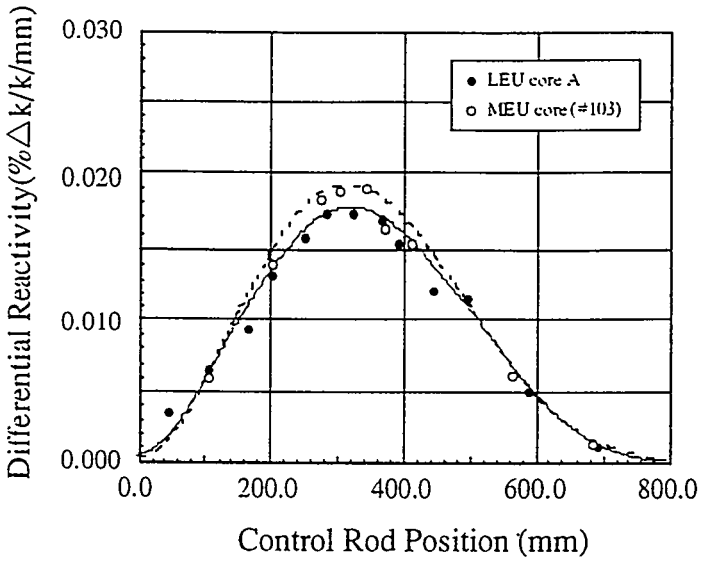

Fig. 4 Differential Reactivity Curve for SH-2

The control rod worth was obtained by integrating the differential reactivity curves. Those are shown in Table 5(a). In the LEU core A, the gang rod worth of SH-1,3 is about 28% less, and the worth of SH-2 is about 4% less than that in the MEU core. Although worth of SR-1 is also about 24% less, there is no difference in worth of SR-2 between the MEU and LEU fuel cores. Thus the control rod worth in the LEU core is mostly less than in the MEU core. Thermal neutron flux decrease in the LEU core due to using high uranium density fuel is mainly responsible for this.

The comparison of measured and calculated worth is shown in Table 5(b). The calculation is in good agreement with the measurement.

Table 5 Control Rod Worth

(a) Comparison of LEU core and MEU core (%Δk/k)

Control Rod	LEU Core	MEU Core	LEU/MEU
SH-1,3 (550mm~800mm)	1.34	1.86	0.72
SH-2 (0mm~800mm : Full range)	6.80	7.11	0.96
SR-1 (550mm~650mm)	0.26	0.34	0.76
SR-2 (550mm~650mm)	0.24	0.24	1.00

(b) Comparison of Measured and Calculated worth (%Δk/k)

Control Rod	Measured	Calculated	C/E
SH-1,3 (550mm~800mm)	1.34	1.50	1.12
SH-2 (0mm~800mm : Full range)	6.80	5.53	0.81
SR-1 (550mm~650mm)	0.26	0.26	1.00
SR-2 (550mm~650mm)	0.24	0.23	0.96

Control rod strokes are 0 to 800 mm.

Shutdown Margin

Shutdown margin was measured by rod drop method. The measured results are shown in Table 6 with the calculated values.

Shutdown margin was verified to be within the safety limit (keff<0.9). Although Calculated shutdown margins are more than measured values, calculations are on the conservative side. It was confirmed that sufficient shutdown capability is assured in the LEU core.

Table 6 Shutdown Margin in each core (keff)

Core	MEU core	LEU initial core	LEU core A	LEU core B
Measurement	0.79	0.82	0.74	0.80
Calculation	0.82	0.88	0.87	0.88

One rod stuck margin was also measured and it was confirmed that the core was kept subcritical.

Temperature Coefficient of Reactivity

The temperature coefficient of reactivity was measured for the MEU core , LEU initial core and the LEU core A. The primary coolant system was operated at 20kW reactor power, and the coolant temperature was raised by heat of main pumps in the measurement. The temperature coefficient was obtained by control rod position with variation of the coolant temperature.

The measured results is shown in Fig.5. The measured result for MEU initial core (#75cycle) is also shown together. There is no significant difference in the temperature coefficient between the MEU and LEU fuel cores. Absolute values of temperature coefficient tended to increase with temperature raise for all cores. It was verified that reactivity feedback effect for LEU core is equivalent to that for the MEU core.

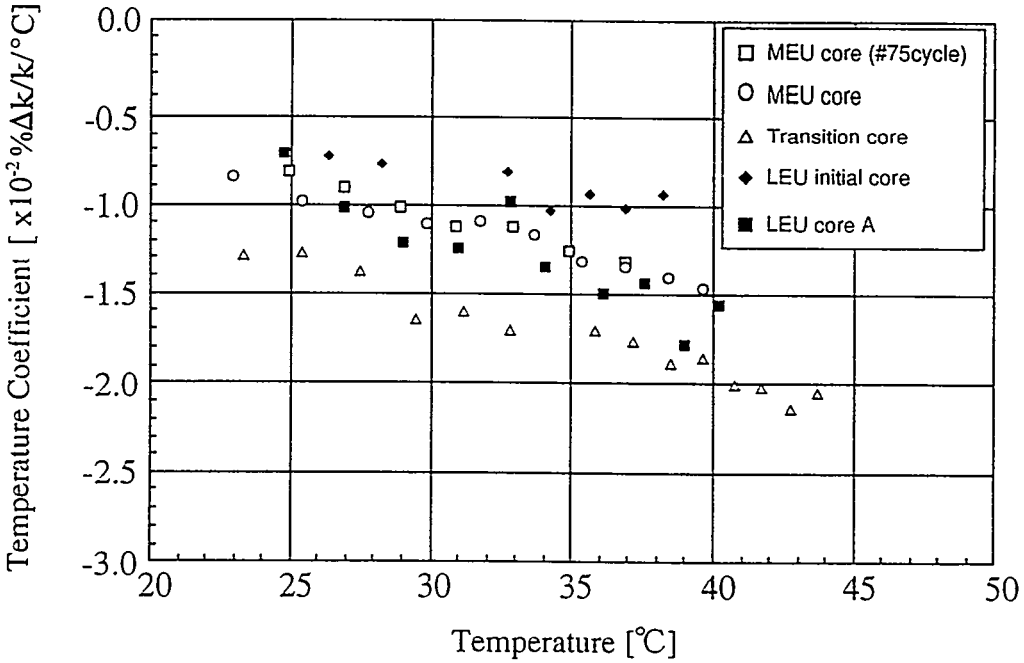

Fig.5 Temperature Coefficient of Reactivity

OPERATIONAL ADVANTAGES WITH LEU FUEL CORES

On the reactor operation and management, use of high density fuel resulted in the following advantages.

Extension of the Operating Cycle Period

The JMTR had been operated for 24days with two days middle shutdown for refueling with the MEU fuel cores, and normal integrated power per operation cycle was 1050MWd. With the LEU fuel cores, consecutive 26days operation became possible due to high uranium density of the silicide fuel, and normal integrated power per operation cycle was extended to 1240MWd.

Further extension is now being discussed.

Spent Fuel Elements

It is expected that about eighty spent fuel elements come from the reactor for five cycle operations with the LEU fuel cores per year, which is less than those from the MEU fuel operation by about forty-five.

Neutron Flux and Fluence

The neutron flux was calculated for LEU and MEU cores. The comparison of the neutron flux and fluence is shown in Table 7. The fast neutron flux of LEU core is almost the same as MEU core in the fuel region. Therefore the fast neutron fluence becomes about 17% larger than MEU core due to extension of the operating cycle period. In the beryllium reflector 1st region, which is first layer of the beryllium reflector around the fuel region, the thermal neutron flux of LEU core is about 7% less than MEU core. However the thermal neutron fluence per cycle is about 6% larger than MEU core .

Table 7 Comparison of the Neutron Flux & Fluence for LEU core and MEU core (%)

	Fast Neutron		Thermal Neutron	
	Flux	Fluence/cycle	Flux	Fluence/cycle
Fuel Region	+2.9	+16.9	-13.8	-2.0
Be 1st Region	+0.4	+14.1	-7.1	+5.6

Flux (%) = [{flux(LEU) / flux(MEU)} - 1] x 100

Fluence/cycle (%) = [{flux(LEU) / flux(MEU)} x 25/22 - 1] x 100

SUMMARY

The JMTR was fully converted to LEU silicide (U_3Si_2) fuel with cadmium wires as burnable absorber in January, 1994. Core physics measurement was carried out through the conversion phase, and it was confirmed that the JMTR was successfully and safely operated with the LEU fuel. Several operational advantages were obtained by using high uranium density fuel.

EXPERIMENTAL EVALUATION OF NEW LEU CORES IN THE UVAR

P. Farrar, B. Hosticka, D. Krause,
R. Mulder and R. Rydin
Department of Mechanical, Aerospace and Nuclear Engineering
University of Virginia
Charlottesville, Virginia, USA

ABSTRACT

The University of Virginia began working on converting the UVAR reactor to LEU fuel in the Spring of 1986. The Safety Analysis Report was completed and submitted to the NRC in late 1989. After review, the DOE order to manufacture LEU fuel was placed at B&W in March 1992, and the new fuel was received in January 1994. The 4-by-4 fully-graphite-reflected LEU-1 core went critical on April 20, 1994, and the 4-by-5 partially-graphite-reflected operational LEU-2 core went critical on April 29. Full power was achieved on May 12, 1994. Both cores behaved very much as originally predicted. All of the old HEU fuel has been shipped to Savannah River.

DESCRIPTION OF THE UVAR FACILITY

The UVAR is a 2 MWT pool-type research reactor. It is made up of plate-type MTR fuel elements mounted on an 8-by-8 grid plate that is suspended from a movable bridge above a large, open pool of water. The reactor can be moved to either end of the pool while the other pool half is drained for maintenance purposes. However, the core can only be operated at full power when it is mounted at the South end of the pool, directly above a coolant funnel that provides forced down-flow circulation. This position is shown in Figure 1, which also shows the location of the experimental beam ports.

The original UVAR design was done by J.L. Meem [1] et al., circa 1960, using analytical two-group theory. The Technical Specifications (TS) require maintenance of a minimum shut-down margin of -0.4% $\Delta k/k$, not counting the regulating rod, with the largest worth shim rod fully withdrawn. They permit a maximum excess reactivity of 5% $\Delta k/k$. Any core arrangement that will fit on the grid plate and that meets these TS can be used, providing that the control rods are experimentally recalibrated each time a new core arrangement, not previously tried, is assembled. The UVAR has been operated for more than thirty years using experimental techniques to determine TS compliance. During this time, both 12-flat-plate fuel elements and 18-curved-plate HEU fuel elements have been used in separate cores, and arrangements having anywhere from 16 to 27 fuel elements have been operated. Some cores have been entirely water reflected, and others graphite reflected, while most cores have had water on some sides and graphite on the others.

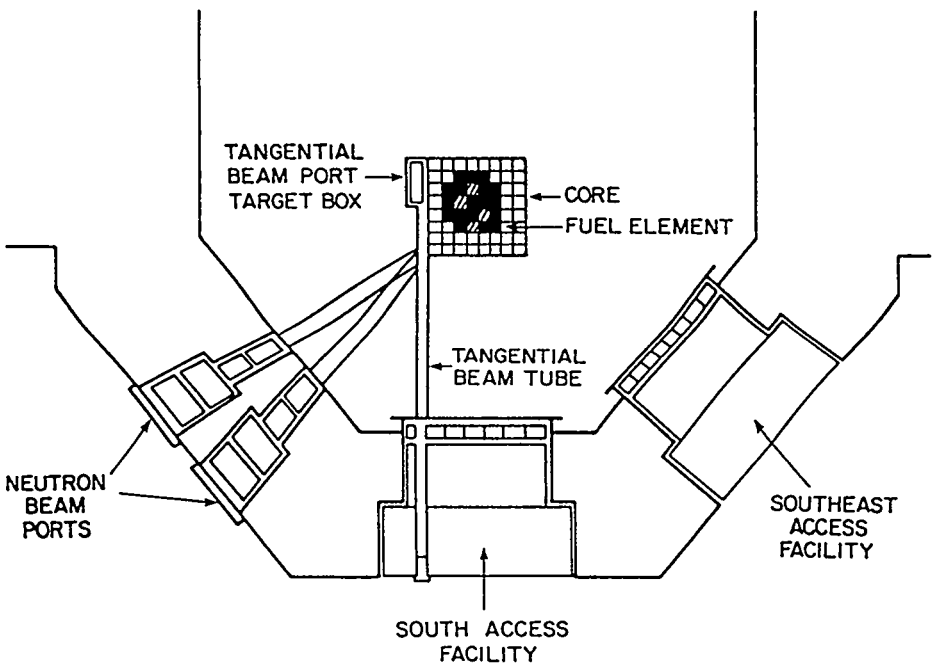

Figure 1. Sketch of UVAR Pool Showing 8-by-8 Grid Plate

LEU DESIGN STUDIES

The LEU design studies were performed on ideal, fully-graphite-reflected cores having 4-by-4, 4-by-5 and 5-by-5 fuel elements. The results have been reported in References 2-5. Although the original HEU fuel used 18 plates/element, it was decided to upgrade the LEU design to use 22 plates/element, which should produce an approximately 50% longer core life for a 20% increase in uranium loading. We furthermore concluded that we should try to keep a fixed 4-by-5 core array and not allow the core to become as large as has been used in the past. A qualitative conclusion from the design studies was that LEU-22-plate cores should be slightly more reactive than the HEU-18-plate cores that they were replacing.

LEU-1 CORE EXPERIMENTS

The 4-by-4 LEU-1 core went critical on April 20, 1994. The final core configuration is shown in Figure 2, and contains two partial fuel elements. The corresponding HEU core from 1975 went critical with only one partial element, i.e., the LEU fuel was indeed slightly more reactive than the HEU fuel it replaced. The approach to critical plot for the LEU-1 is given in Figure 3 for alternate positions of the control rods. The excess reactivity of the LEU-1 core is 4.66% $\Delta k/k$, and the shutdown margin is -1.21% $\Delta k/k$. Both are well within TS limits.

G 11	G 12	G 13	S 14	G 15	G 16	G 17	G 18
G 21	G 22	PF VP-002 23	F VS-002 24	F- REG VC-001 25	PF VP-001 26	G 27	G 28
G 31	G 32	F VS-004 33	F-CR1 VC-002 34	F VS-005 35	F VS-003 36	G 37	G 38
G 41	G 42	F VS-007 43	F VS-008 44	F-CR2 VC-003 45	F VS-009 46	G 47	G 48
G 51	G 52	F VS-010 53	F-CR3 VC-004 54	F VS-011 55	F VS-012 56	G 57	G 58
G 61	G 62	G 63	G 64	G 65	G 66	G 67	G 68
G 71	G 72	G 73	G 74	G 75	G 76	G 77	G 78
G 81	G 82	G 83	G 84	G 85	G 86	G 87	G 88

CORE LOADING LEU-1 SHUTDOWN MARGIN 1.21 % delta k/k

Date April 21, 1994 EXCESS REACTIVITY 4.66 % delta k/k

U-235 3571 GRAMS EXPERIMENT WORTH ____ % delta k/k

F - Normal Fuel Element
PF - Partial Fuel Element
CR - Control Rod Fuel Element
G - Graphite Element
S - Graphite Source Element
REG - Control Rod Fuel Element with Regulating Rod
P - Grid Plate Plug
HYD RAB - Hydraulic Rabbit
THER RAB - Thermal Pneumatic Rabbit
EPI RAB - Epithermal Pneumatic Rabbit
RB - Radiation Basket

Rod Worths #1 - 3.46 % #2 - 3.86 % #3 - 2.41 % Reg - 0.375 %

Figure 2. LEU-1 Core Loading Diagram

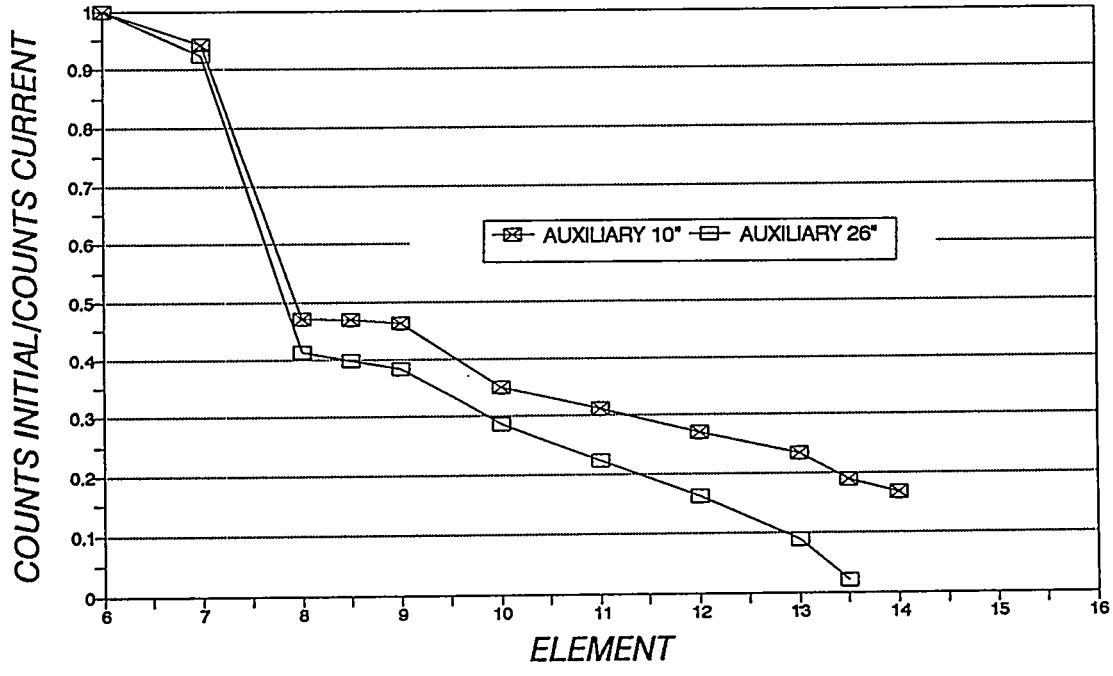

Figure 3. LEU-1 Approach to Critical

Effective control rod cross sections for the UVAR had been generated using transport theory codes, as described in Reference 6. A comparison of the experimental and calculated control rod worths for the old HEU and new LEU-1 cores is given in Table 1.

A value of β_{eff}=0.0074 [5] was used to convert the calculated data to $. The LEU-1 calculation is the original prediction and does not include the two partial elements. The steel regulating-rod effective cross sections were not as reliably predicted by the methodology as were the control rod cross sections. Considering ±10% uncertainties, the agreement between experiment and calculation is quite good. In any event, the original prediction was that the worths of the control rods would not be very different for HEU and LEU cores, and this has been adequately demonstrated.

Table 1. Control Rod Worths for 4-by-4 Cores

Case	Rod 1 $	Rod 2 $	Rod 3 $	Reg Rod $
HEU Expt	4.75	5.00	3.06	0.57
HEU Calc	4.71	4.96	2.86	0.73
LEU-1 Expt	4.68	5.22	3.26	0.51
LEU-1 Calc	4.69	4.91	2.90	0.84

LEU-1 VOID COEFFICIENTS AND FLOW COASTDOWN

A series of 2D void coefficient calculations were made using the LEOPARD/2DBUM codes for 4-by-5 unrodded, fully-graphite-reflected UVAR core models[4]. The calculations considered the case of uniformly distributed voids as a function of the percentage of the moderator in the core that was voided. The reactivity effect is nominally proportional to the amount of voiding, with a spectral shift superimposed as the net voiding becomes significant. A few local center-core calculations were also made which showed the flux-importance effect of voiding. The results are reproduced in Figure 4. For LEU fuel, the void coefficient was predicted to be in the range of -0.2 to -0.6% Δk/k per% void.

Void coefficient measurements were made for the LEU-1 core by inserting voided plastic swords in the eighth fuel channel from the east side of the core in the following fuel elements: Element VS-007 in grid position 43, Element VS-008 in grid position 44, and Element VS-010 in grid position 53 (See Figure 2). Two types of swords were used, one that could be flooded and one that was voided. The sword design is shown in Figure 5. The voided volume of the swords was measured under pressure by displacement methods. The total core water volume with and without rod channels and the water volume within one fuel element was calculated.

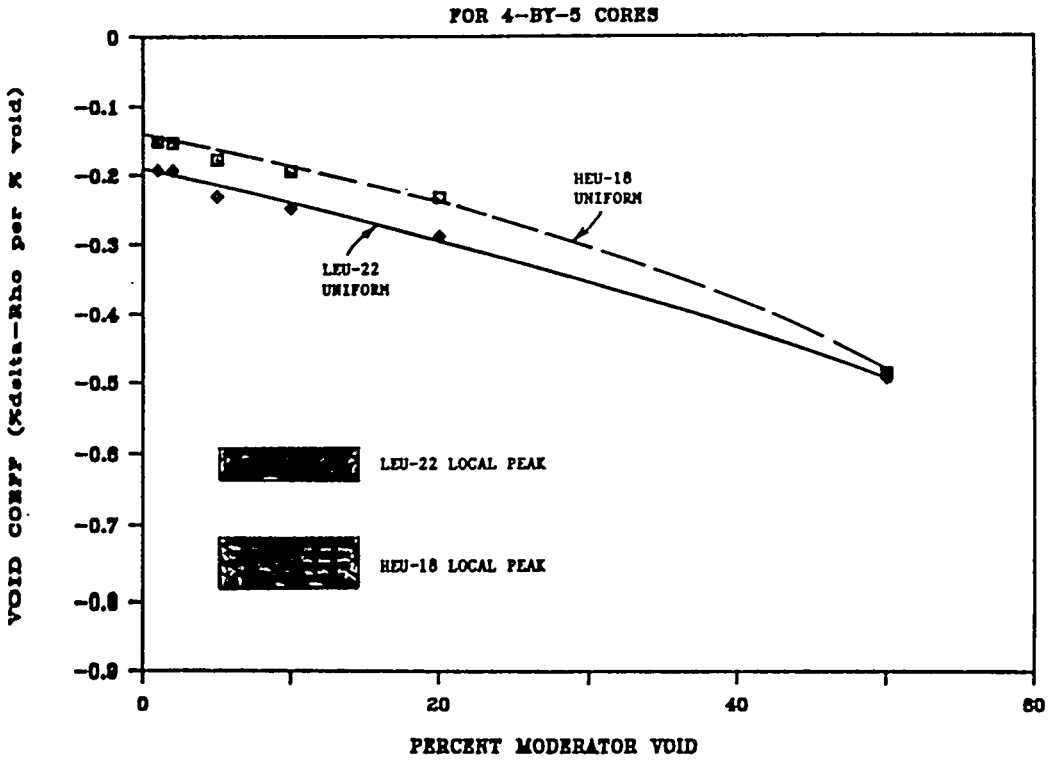

Figure 4. Uniform and Local Void Coefficients for 4-by-5 UVAR Cores.

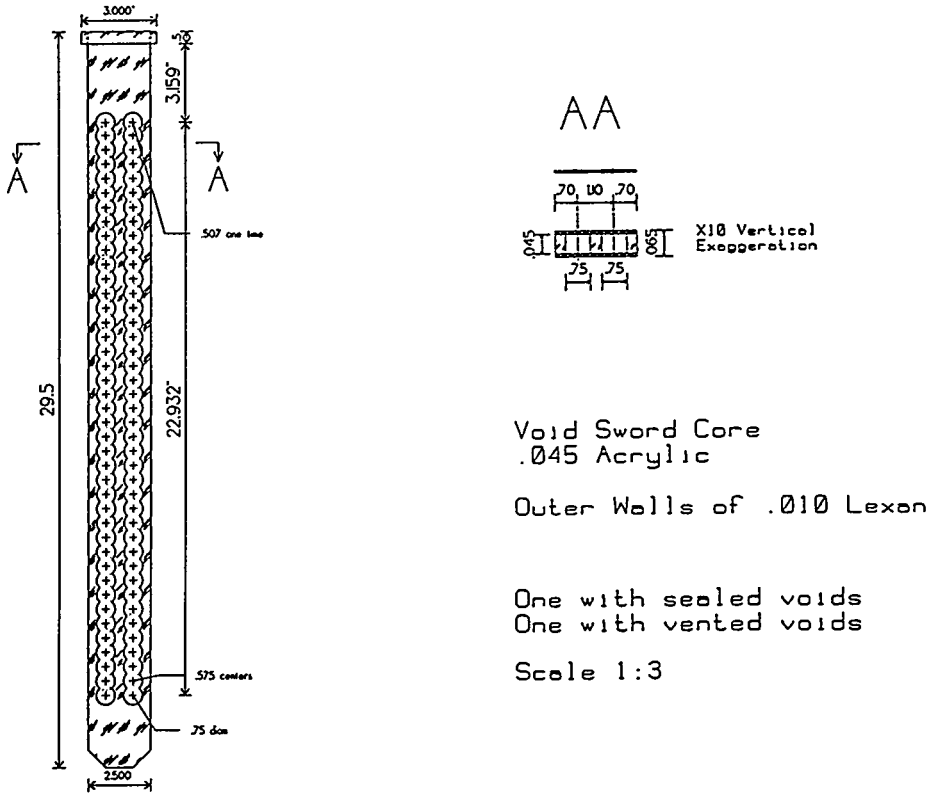

Figure 5. UVAR LEU 22-Plate Void Swords

The results of the measurements are given in Table 2. The experimental results lie on the lower edge of the earlier predictions and verify that the void coefficient for LEU-1 is indeed negative and of the correct order of magnitude. Looking at the core arrangement in Figure 2, it is intuitive to expect that the void coefficient should be smaller in the corner element VS-010 than in the edge element VS-007. However, the smaller 4-by-4 LEU-1 core has control rods inserted at about half depth near the fuel elements under study. A 3D analysis would be needed to resolve these subtle differences.

Table 2. Measured Void Coefficients for LEU-1

Element	Location	Worth,%Δk/k per % Void
VS-008	Central	-0.190
VS-007	Edge	-0.125
VS-010	Corner	-0.181

Extensive thermal-hydraulic predictions for LEU cores were reported in Reference 7. It was determined that the 4-by-4 core array would be more limiting than the 4-by-5 and larger core arrays due to the higher power density and larger pressure drop in the smaller core. A flow coastdown measurement was made for the LEU-1 core, as shown in Figure 6. The slope of the measured coastdown curve matches very closely with that predicted and reported in the Safety Analysis Report (SAR). In all cases, the flow exceeds the limiting flow needed to keep the core safe.

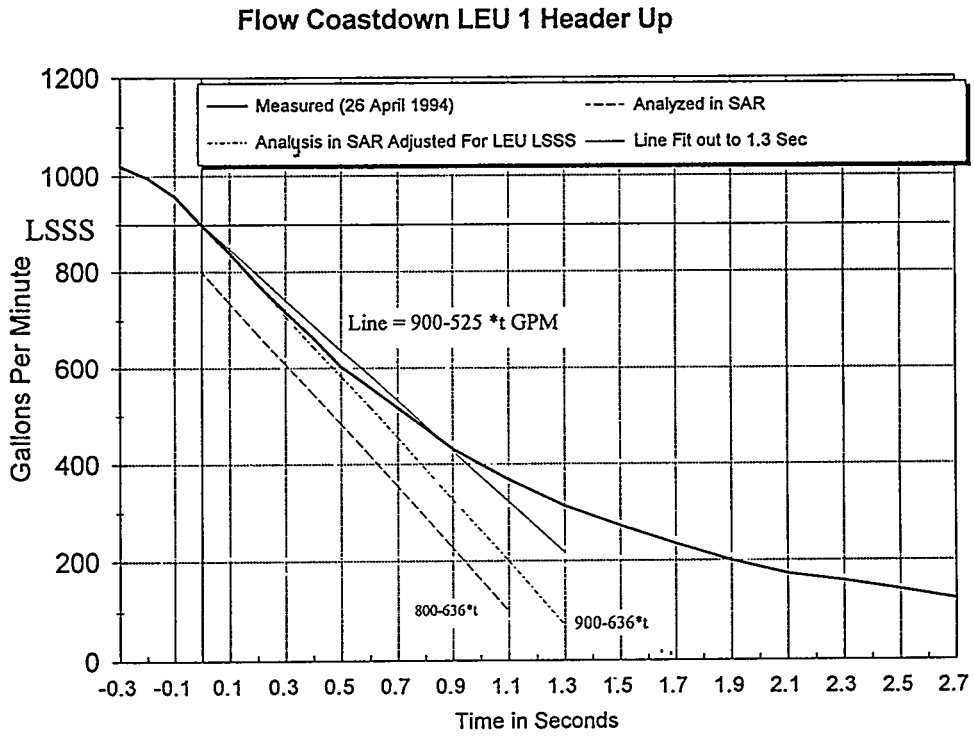

Figure 6. Flow Coastdown for LEU-1

LEU-2 CORE EXPERIMENTS

Because of our desire to quickly return the UVAR to full power operation for the benefit of experimental programs, the LEU-2 Core configuration contains all of the normally used experimental facilities that were available in the HEU configuration. As shown in Figure 7, these facilities include a Mineral Irradiation Facility (MIF), placed on the North (pool) face of the core directly adjacent to fuel, used for color enhancement of Topaz. We have plans to eventually mount a submersed Boron Neutron Capture Therapy (BNCT) epithermal neutron filter and small animal irradiation chamber on the MIF supports; this will be used to verify the design of a proposed BNCT facility that will penetrate the South pool wall. The East face of the core is available for the Canister Irradiation Facility (CIF), used for activating Iridium seeds for brachytherapy and oil-well logging. The South face is used for irradiating steel samples in boron-filtered hot thimbles (HT) to assess radiation damage. The Southwest face contains a graphite nosepiece used to thermalize neutrons and extract them through a beam tube for Neutron Radiography.

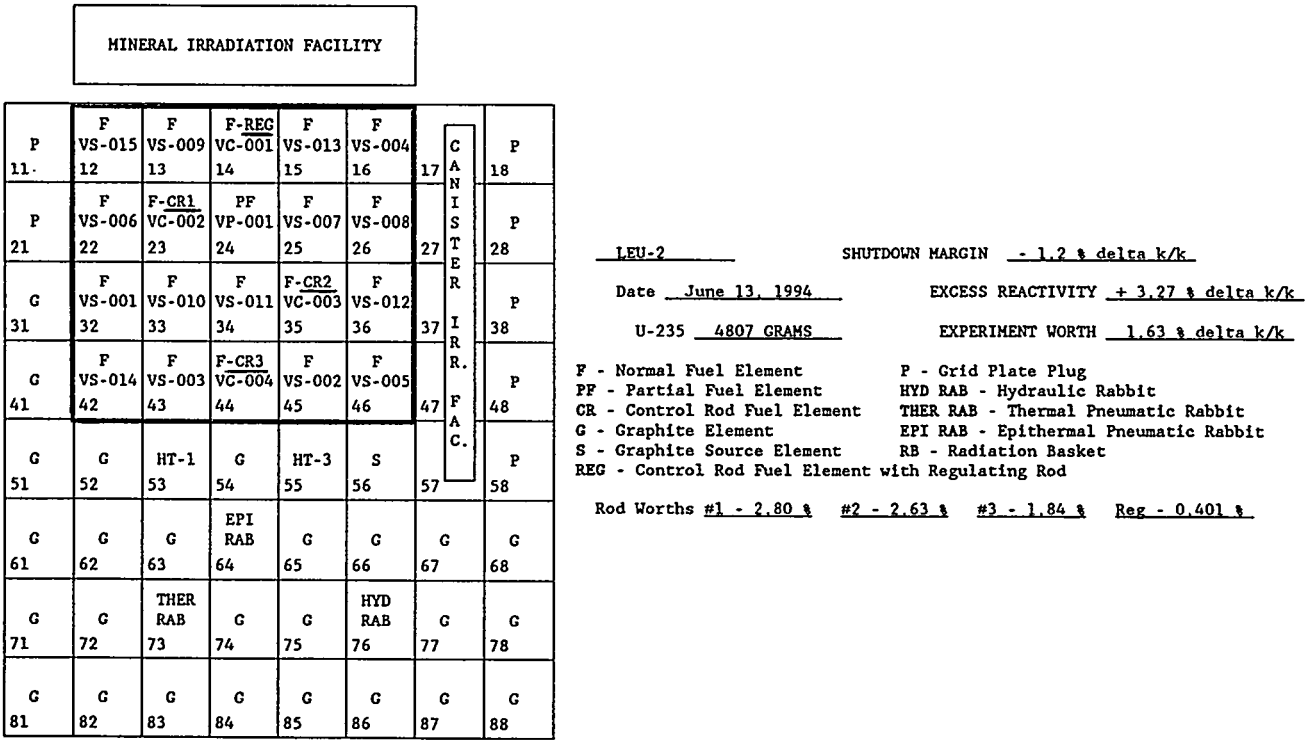

Figure 7. LEU-2 Core Loading Diagram

Fuel was added to the LEU-2 core, one element at a time, in a manner similar to that used for the LEU-1 core. The original prediction was that the 4-by-5 core would approximately meet TS limits with water on two faces and graphite on the other two. In fact, the final configuration contains one partial element in a central location and graphite on somewhat less than two faces. The excess reactivity is 3.27% Δk/k, and the shutdown margin is -1.2% Δk/k, meeting TS. Note that in the 4-by-5 configuration, the control rods are only worth 70-80% of their values in the smaller core.

LEU-2 TEMPERATURE COEFFICIENTS

Previous temperature coefficient measurements on HEU cores are more properly described as "power coefficient" measurements, since they were determined during a core heat-up experiment. The values quoted in Reference 2 were obtained by taking the net core $\Delta k/k$ and dividing by the average coolant temperature rise. This ignores the fact that the temperature rises more in the hot central fuel channels where the reactivity worth is highest. The experimental values, thus determined, are approximately three times the values calculated by assuming a uniform temperature change.

For the LEU-2 core, the temperature coefficient was determined at low power by doing a pool-cooldown experiment. The reactor was operated all day at full power on May 13, 1994, and the pool temperature was 97.9 °F when the reactor was shut down. The cooling systems were secured and the reactor remained shut down for three days to allow Xenon to decay. The reactor was taken critical at low power on May 16, 1994. The pool temperature then was 86.9 °F and the ΔT was 0.0 °F. The secondary cooling system was energized and the pool was allowed to cool down. The power level was maintained by adjusting Rod #2. The pool was cooled for 1.5 hours. The core outlet temperature changed by 11.24 °F. Rod #2 moved from 14.39 inches at the beginning of the test to a final position of 14.16 inches. The reactivity associated with this change was obtained from the rod worth curves and determined to be 0.05 % $\Delta k/k$. Rod #2 was then moved back to it's original position of 14.39 and doubling times were taken to determine the reactivity associated with the rod movement as a check against the rod curves. The reactivity associated with the doubling times was 0.039 % $\Delta k/k$, and the temperature change during this measurement was 9.18 °F. An average of these measurements yielded a value for the moderator temperature coefficient.

A "power coefficient" measurement was also performed. The reactor was taken critical at low power in a xenon-free condition and the critical rod positions were noted. Rod #2 was withdrawn 0.5 inch to put the reactor on a positive period. Doubling times were measured with a stop watch using the linear instrument. The power was allowed to rise until it leveled off at 870 kW due to negative temperature effects. The average temperature rise across the core was noted. The doubling times were converted to reactivity, and matched almost exactly with the reactivity worth of rod #2 when it was withdrawn as determined from the rod worth curve. It is noted that this measurement includes both the fuel doppler and moderator temperature effects.

All previous data refer to 4-by-4 cores. Hence, at this time, only a qualitative comparison can be made between cores, as shown in Table 3. We see that the experimentally determined "power coefficients" for the 4-by-4 HEU and the 4-by-5 LEU-2 are quite comparable, whereas the experimental LEU-2 moderator coefficient is approximately half as big as the previously calculated HEU and LEU moderator coefficients for 4-by-4 cores. The experiments ($\pm 25\%$) are not very precise for such small reactivity changes, so it is difficult to judge the significance of the difference. Nonetheless, the results point out the desirability of doing an LEU-2 core-specific moderator coefficient calculation, which will possibly have to be done in 3D to include the control rod position effects.

It is clear that the moderator coefficient for a uniform core temperature change is not the same as the "power coefficient" for a reactivity-worth-weighted core temperature-distribution change. We should not expect to compare these numbers directly.

Table 3. Feedback Coefficient Comparison

Case	Moderator Coefficient $\Delta k/k/\Delta T(°C)$ $(x\ 10^4)$	"Power Coefficient" $\Delta k/k/\Delta T(°C)$ $(x\ 10^4)$
HEU Calc 4-by-4	-1.9	-
HEU Expt 4-by-4	-	-5.2
LEU Calc 4-by-4	-1.7	-
LEU-2 Expt 4-by-5	-0.78	-4.9

CONCLUSIONS

The primary conclusion is that the UVAR has been successfully converted from HEU to LEU fuel. The initial criticality predictions for 4-by-4 and 4-by-5 LEU core arrays were qualitatively correct, leading to a practical LEU-2 core configuration that meets all TS. The prediction that control rods worths would not be very different between HEU and LEU cores was borne out. Void coefficient measurements agree reasonably well with prior predictions. Temperature coefficient measurements are fairly comparable between HEU and LEU cores. And finally, flow coastdown measurements confirm that adequate cooling is available.

Additional core-specific computational work is in progress to resolve minor uncertainties. Otherwise, the experimental verification experiments are essentially finished and the UVAR is back in routine full-time operation.

REFERENCES

1. J.L. Meem, Two Group Reactor Theory, Appendix A, Gordon and Breach Science Publishers, New York, N.Y., 1964.

2. R.A. Rydin, M. Fehr, S. Wasserman, D. Freeman and B. Hosticka, "Status of the University of Virginia Reactor Conversion to LEU Fuel," Proceedings of the XIth International Meeting, Reduced Enrichment for Research and Test Reactors, San Diego, Ca, September 19-22, 1988, pp. 346-357.

3. M.K. Fehr, "Design Optimization of a Low Enrichment University of Virginia Nuclear Reactor," M.S. Thesis, University of Virginia, January 1989.

4. R.A. Rydin, D.W. Freeman, B. Hosticka and R.U. Mulder, "Safety Analysis for the University of Virginia Reactor LEU Conversion," Proceedings of the XIIth International Meeting, Reduced Enrichment for Research and Test Reactors, Berlin, FRG, 10-14 September 1989, pp 211-226.

5. D.W. Freeman, "Neutronic Analysis for the UVAR Reactor HEU to LEU Conversion Project," M.S. Thesis, University of Virginia, January 1990.

6. S. Wasserman, "Effective Diffusion Theory Cross Sections for UVAR Control Rods," M.S. Thesis, University of Virginia, January 1990.

7. B. Hosticka, C. Mora and R.A. Rydin, "State of the LEU Conversion Effort at the University of Virginia Reactor," Proceedings of the XIIIth International Meeting, Reduced Enrichment for Research and Test Reactors, Newport, RI, 23-27 September 1990, pp. 360-367.

ACKNOWLEDGEMENT

This research was supported under DOE grant No. DEFG0588ER75388.

CONVERSION PROGRAM IN SWEDEN

Erik B Jonsson

Studsvik Nuclear AB, Nyköping, Sweden

ABSTRACT

The conversion of the Swedish 50 MW R2 reactor from HEU to LEU fuel has been successfully accomplished over a 16 cycles long process. The conversion started in January 1991 with the introduction of 6 LEU assemblies in the 8*8 core. The first all LEU core was loaded in March 1993 and physics measurements were performed for the final licensing reports. A total of 142 LEU fuel assemblies have been irradiated up until September 1994 without any fuel incident.

The operating licence for the R2 reactor was renewed in mid 1994 taking into account the new fuel type. The Swedish Nuclear Inspectorate (SKI) pointed out one crucial problem with the LEU operation, that the back end of the LEU fuel cycle has not yet been solved. For the HEU fuel we had the reprocessing alternative. We are now relying heavily on the success of the USDOEs Off Site Fuels Policy to take back the spent fuel from the research reactors. We have in the meantime increased our intermediate storage facilities. There is, however, a limit both in time and space for storage of MTR-type of assemblies in water.

The penalty of the lower thermal neutron flux in LEU cores has been reduced by improvements of the new irradiation rigs and by fine tuning the core calculations. The Studsvik code package, CASMO-SIMULATE, widely used for ICFM in LWRs has been modified to suit the compact MTR type of core.

Paper to be presented at the 17th International Meeting on Reduced Enrichment for Research and Test Reactors (RERTR) 1994 Williamsburg, USA, September 1994.

BACKGROUND

The Swedish R2 reactor is a 50 MWth materials testing reactor of pool type. It has been in operation since 1960. The reactor is used for material testing, fuel testing, isotope production and silicon doping. It has 9 horizontal beam tubes giving thermal neutrons for research work. The reactor and the Hot Cell Laboratory are since 1992 operated by a private company Studsvik Nuclear AB, which is a subsidiary of the largest utility in Sweden, Vattenfall AB.

TRANSITION TO LEU FUEL CYCLE

The R2 reactor has now since the introduction of LEU in January 1991 operated with 58 different high power cores. There has been good agreement between the calculated flux and power distributions and the measured ones after the conversion was completed in March 1993. The calculated k_{eff} has during the transition period slowly but steadily become closer to 1.0 indicating improved agreement on the power and depletion with an increasing number of LEU fuel elements. No fresh HEU fuel has been added during the conversion period.

During this period the number of fuel elements in the core has varied between 47 and 49 plus 6 control rod follower. These cores have had 9 to 11 irradiation positions in the 8x8 core matrix. Compare Figure 1.

The loading principles for the cores have changed in a rather pragmatic way with the requirements of the different experimental positions guiding the loading. This means that the radial power peaking has decreased, as the irradiation facilities moved to the periphery of the cores.

THE BACK END OF THE LEU FUEL CYCLE

The possibility to send back the used high enriched fuel to US was suddenly stopped in 1988. At first this was just an annoyance for the research reactor operators, which we thought would be solved rather expedite. After a couple of years we had learnt better. US DOE has together with the research reactor operators in the Edlow group put much effort into reopening the Off-Sites Fuel Policy. We have expectations that it will be solved with the EIS (Environmental Impact Statement) in the end of 1995.

In the meantime many operators have problem with the storage capacity for their spent fuel. Studsvik solved the storage problem by converting one pool in an on-site storage facility for spent LWR fuel, for the R2 fuel. The construction of storage racks was rather simple and the new storage racks were in use from 1991. Already after two years it was realised that the pool capacity had to be increased and a second layer of storage racks were constructed. The two-story racks will be totally filled by the end of 1994.

This storage facility was originally equipped with cooling and cleaning systems, but we constructed a simple submersible pump- ion-exchanger system (Figure 2). This system works without daily supervision and the water is kept sufficiently clean with a six month interval between changes of the ion-exchanger cartridge.

CASMO -SIMULATE AS CALCULATIONAL TOOLS

The reduction in the thermal neutron flux with the LEU fuel necessitated improvements in the core calculations. The Studsvik code package, CASMO-SIMULATE, which is widely used for ICFM in LWRs has been modified to suit the compact MTR type of core and the special control rod follower concept.

CASMO is a two-dimensional, multigroup transport code for the calculation of the eigenvalue, flux and power distribution as a function of depletion in pin cells and on LWR fuel assemblies. The code is capable of handling fuel rods, absorbing rods and absorbing slabs. The feature of the code is the ability to perform detailed transport theory calculations in 70 groups with a standard cross section library based on ENDF/B IV and VI libraries. The code has no option for plate type fuel, but the LEU (or HEU) assemblies are easily modelled as a 18x18 rod assembly with equivalent fuel rod geometry. The flux and power mismatch between HEU and LEU fuel assemblies has earlier been studied with the CASMO-3 code

The CASMO code is normally used to produce burnup dependent, homogenized, two group cross sections for the 3-D nodal code SIMULATE or diffusion core analysis codes for PWR and BWR cores. Each of the R2 fuel types has thus been modelled and depleted to give the burnup dependent cross sections and isotopic compositions. Cross sections for the reflectors, isotope rigs and absorbers have also been determined with the CASMO code.

The SIMULATE code is an advanced 2-group nodal code for reactor analysis. It provides two or three dimensional calculations of the neutronic parameters needed for in-core fuel management and reaction rate determination. The code has several advanced features as automated expansion or contraction of the core in radial and/or axial directions. It gives reactivity coefficients for parameters such as moderator and fuel temperature and also control rod reactivity worth including shut down margin. There is explicit representation of transient Xe/I and Sm/Pm number densities and thus cross sections during varying power conditions. Local power and flux distributions within a node can be reconstructed for all nodes within 1 % RMS of a transport fine mesh solution.

We are still in the phase of testing the code system on different reference cores, but the results hitherto seem to confirm our confidence in the system.

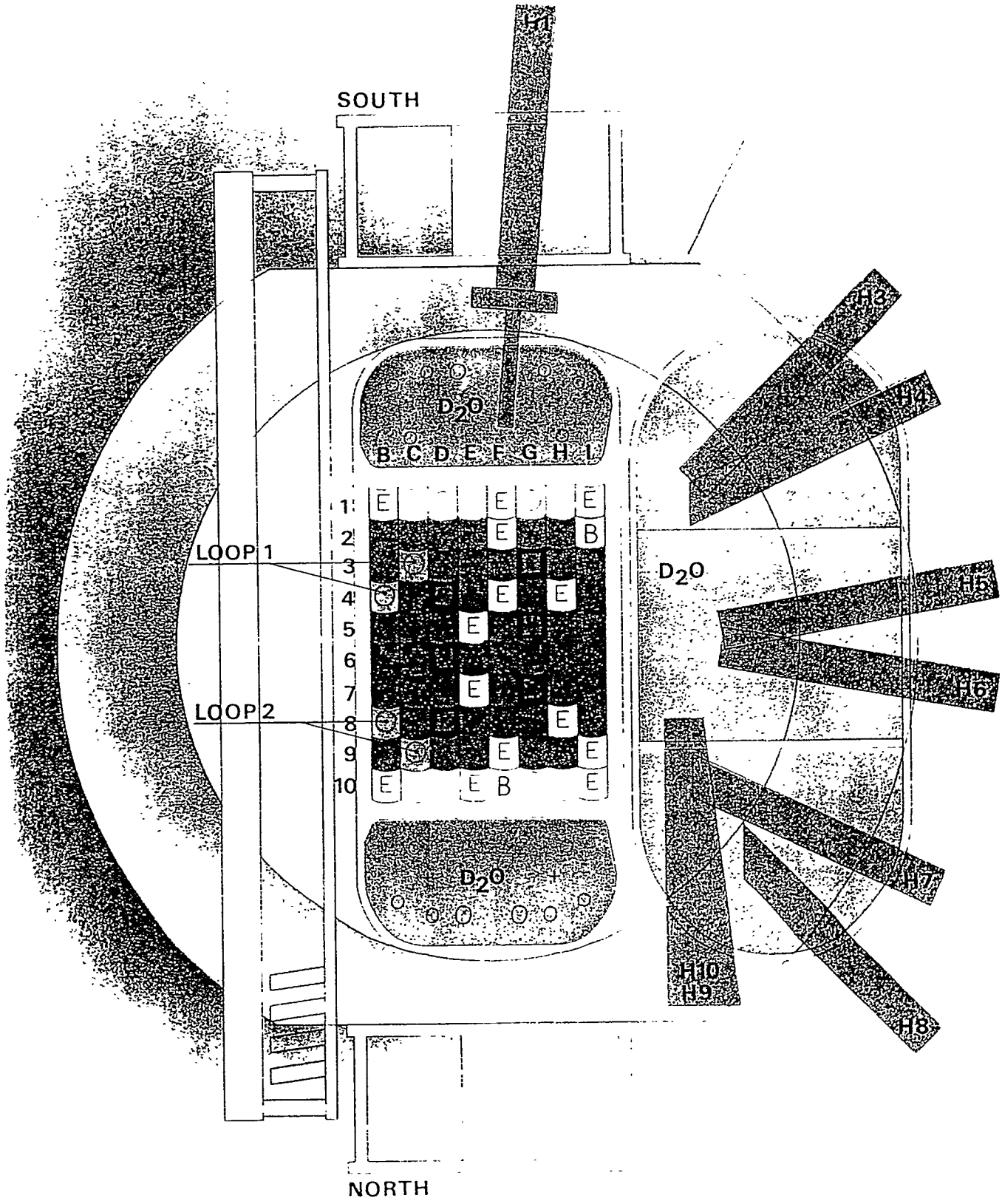

Figure 1. Schematic Layout of the R2 Core with Experimental Positions.

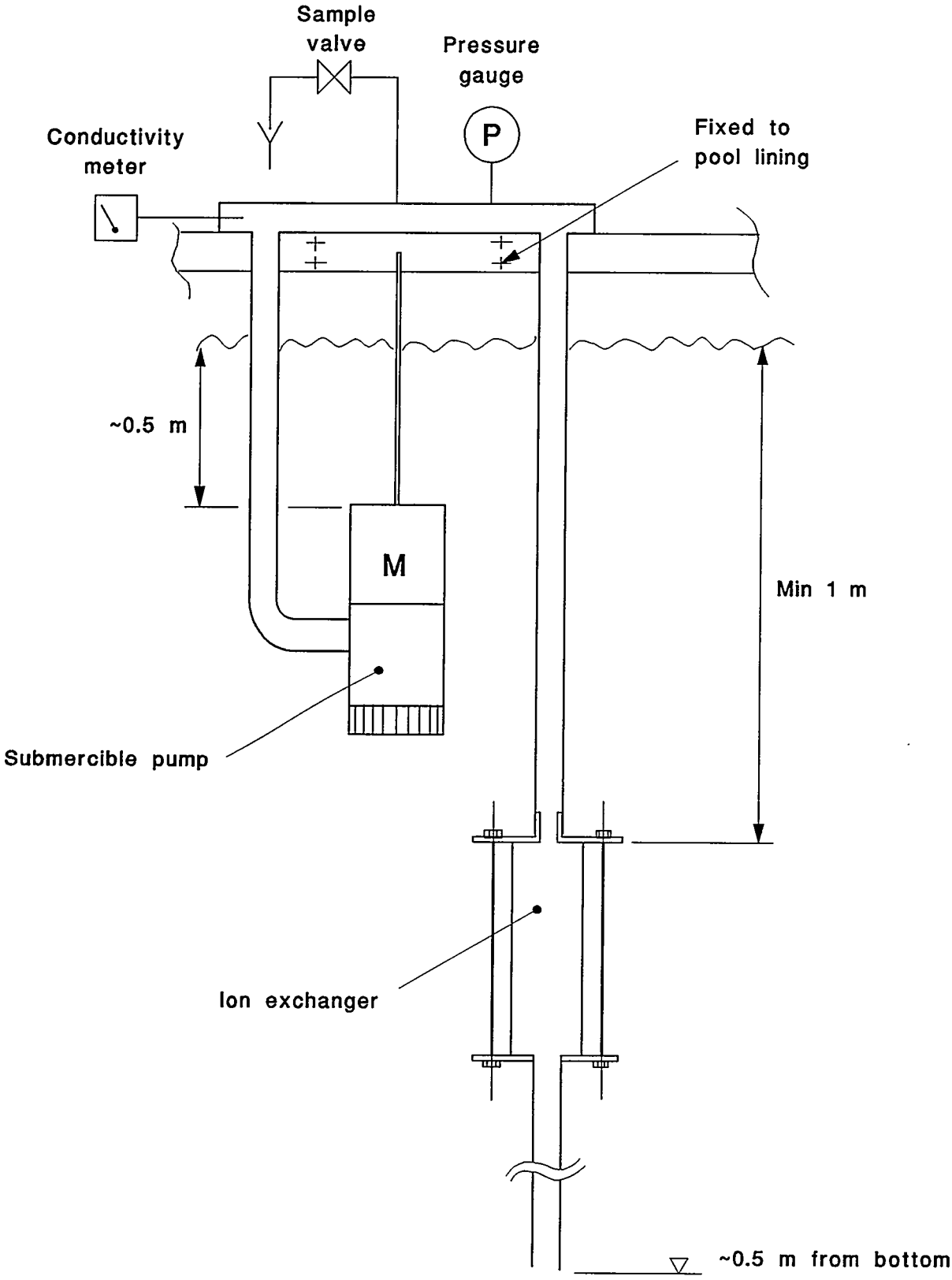

Figure 2. Layout of the Submersible Pump and Ion-exchanger System.

STATUS OF CORE CONVERSION WITH LEU SILICIDE FUEL IN JRR-4

TERUO NAKAJIMA, NOBUAKI OHNISHI and EIJI SHIRAI

Department of Research Reactor,
Tokai Research Establishment,
Japan Atomic Energy Research Institute
Tokai-mura, Naka-gun,Ibaraki-ken, JAPAN

ABSTRACT

Japan Research Reactor No.4(JRR-4) is a light water moderated and cooled, 93% enriched uranium ETR-type fuel used and swimming pool type reactor with thermal output of 3.5MW. Since the first criticality was achieved on January 28, 1965, JRR-4 has been used for shielding experiments, radioisotope production, neutron activation analyses, training for reactor engineers and so on for about 30 years. Within the framework of the RERTR Program, the works for conversion to LEU fuel are now under way, and neutronic and thermal-hydraulic calculations emphasizing on safety and performance aspects are being carried out. The design and evaluation for the core conversion are based on the Guides for Safety Design and Evaluation of research and testing reactor facilities in Japan.

These results show that the JRR-4 will be able to convert to use LEU fuel without any major design change of core and size of fuel element. LEU silicide fuel (19.75%) will be used and maximum neutron flux in irradiation hole would be slightly decreased from present neutron flux value of 7×10^{13}(n/cm^2/s). The conversion works are scheduled to complete in 1998, including with upgrade of the reactor building and utilization facilities.

This paper describes the current status of the core conversion program from HEU fuel to LEU silicide fuel in JRR-4.

INTRODUCTION (Outline of JRR-4)

JRR-4 was constructed in 1965 as a radiation shielding research reactor for research and development of the first nuclear ship "MUTSU" in Japan. After that, the reactor has been mainly utilized for shielding experiments during about 10 years on the maximum thermal power with 2,500kW. Since the maximum thermal power increased up to 3,500kW in 1976 as a multi-purpose

reactor with middle power level, JRR-4 has been utilized for radioisotope production, neutron activation analyses, training for reactor engineers, silicon semiconductor production, shielding experiments and so on.

The reactor facility includes No.1 and No.2 pools, thermal column, scattering experimental room, irradiation equipments, cooling facility, reactor building and others. The reactor core is housed in the lower part of the aluminum cylindrical core tank (1.5m dia.) which is suspended from the reactor core bridge on the rails of pool side.

The standard core is composed of 20 fuel elements, seven control rods, five irradiation pipes, one neutron source and graphite reflectors. The core is arranged with lattice of 8x8.

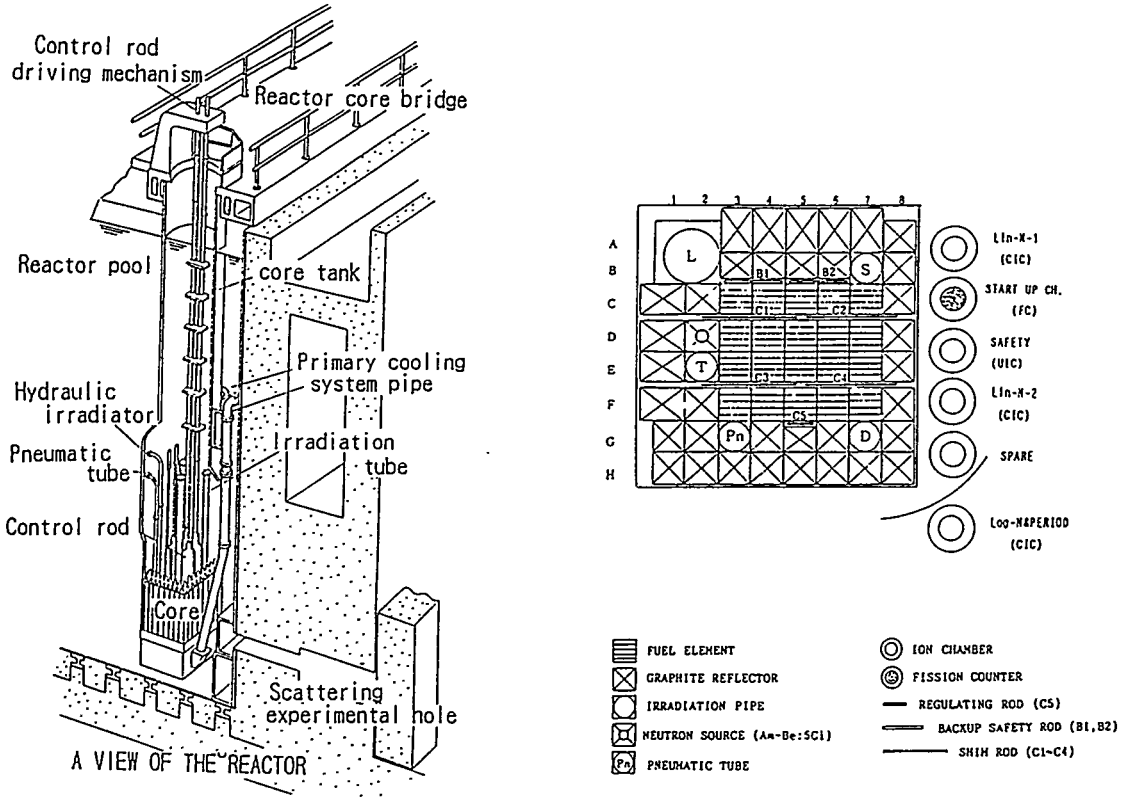

Fig.-1 JRR-4 core arrangement

One fuel element is composed of 15 fuel plates, two side plates, handle and guide plug. The fuel meat of 93% highly enriched uranium-aluminum alloy is 0.5mm thick and cladded with aluminum plate of 0.38mm thick. The outside dimension of a fuel element is 80mm square and 1025mm in total length, the active length (core height) is 600mm and the weight of U-235 per element is about 166g. About five fuel elements are used every year in normal operation schedule.

The three pumps and two heat exchangers are used in the primary cooling system. At high power operation (>200kW), the flow rate of the primary coolant is about 7 m^3/min. The maximum thermal neutron flux in the irradiation holes are $7x10^{13}$ n/cm^2/s.

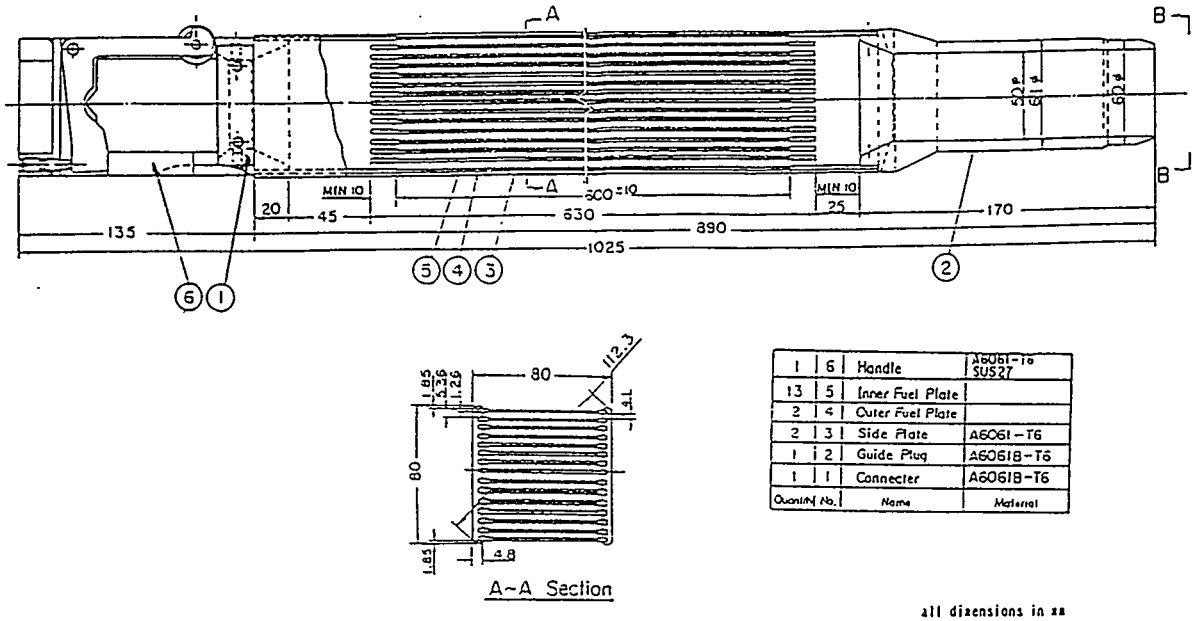

1	6	Handle	A6061-T6 SUS27
13	5	Inner Fuel Plate	
2	4	Outer Fuel Plate	
2	3	Side Plate	A6061-T6
1	2	Guide Plug	A60618-T6
1	1	Connecter	A60618-T6
Quantity No.		Name	Material

Fig.–2 JRR–4 fuel element

JRR-4 REDUCED ENRICHMENT PROGRAM

Core conversion activities at JAERI were begun in 1980's. At first, a design and safety evaluation for the core conversion with low enriched uranium aluminide fuel was carried out in the JAERI's RERTR program. The two full size fuel elements for the demonstration of safety review were manufactured in 1984 and irradiated in the two reactors, respectively. These fuel elements were 16 plates with about 224g/U–235. One was irradiated until 50% burn up in JRR–2 and confirmed to be no problem by post irradiation experiments at Tokai Hot Laboratory, and another one was irradiated up to 20% burn up in order to investigate neutronic performance in JRR–4.

In 1991, since it was expected to have enough stock of the highly enriched uranium fuels for only five years operation, new design and evaluation for core conversion with LEU silicide fuel were started in Japan. These evaluation were based on the examination guide of water cooled reaserch and testing reactors. As the results of evaluation, it was expected that the conversion was able to keep current performance without changing size of fuels and core. Furthermore a feasibility study was carried out concerning the design and evaluation for the conversion with TRIGA LEU fuel to compare with silicide fuel.

In order to submit the JRR–4 safety analysis report for the licensing review by Japanese authority, final neutronic and thermal–hydraulic design and evaluation, and utilization system design (for example; boron neutron capture therapy facility) are now under way.

This safety review will be examined by Japanese government in 1995, and then the core conversion and some modification works will be started. These works will be completed in 1998 and the JRR–4 will be re–utilized widely.

SILICIDE FUEL FOR JRR-4

The LEU silicide fuel for JRR-4 is just the same as HEU aluminide fuel except fuel meat material. From the result of parameter calculation for core performance evaluation, the uranium density is decided as 3.8 g/cm^3 for inner fuel plate (13 plates) and 1.9 g/cm^3 for outer fuel plate (2 plates). The comparison of LEU fuel with HEU fuel is showed table-1.

Table-1 Comparison of LEU fuel with HEU fuel

Item	LEU fuel	HEU fuel
Enrichment, %	19.75	93
Uranium density, g/cm^3(outer plate)	3.8(1.9)	0.66(0.33)
Specific content of U-235per element,g	204	166
Number of fuel plate per element	15	
Fuel meat material	U_3Si_2-Al	UAl
Cladding material	Aluminum-alloy	
Maximum Burn-up, %	50	20
Size of fuel element, mm	80x80x1025	

NEUTRONIC DESIGN

(1) Design scope

* The excess reactivity and shutdown margin are designed to keep subcriticalities of 0.01 dk/k when a control rod with the largest reactivity worth was stuck.
* Moderator temperature coefficient, moderator void coefficient and doppler coefficient are negative value, respectively, and the total reactivity coefficient is always effectual for power down.
* Thermal neutron flux is kept current level.
* The average burn-up of a fuel element is not exceeded 50%.

(2) Calculation method

* The design analyses calculated by SRAC code system in JAERI.
* The code was verified by the comparison of measured value with calculated one of HEU fuel core.

(3) Results of calculation

* The excess reactivity of core with fresh 20 LEU fuel elements is 11.7%dk/k, and the one rod stuck margin value is about -1.3%dk/k(Table-2).
* The power distribution is good as the maximum peaking factor is 2.7.
* The reactivity coefficient is negative in the calculated range.
* The maximum average burn-up of fuel element is about 40% in 5 batch refueling system.

* The maximum thermal flux in irradiation area is about 6 x 10^{13} n/cm²/s.

Table–2 Excess reactivity and one rod stuck margin of LEU core

	Initial core	Equilibrium Core	15% burn–up
Excess reactivity, %Δk/k	11.7	6.5	5.3
One rod stuck margin, %Δk/k	–1.34	–5.9	–7.2

THERMAL-HYDRAULIC DESIGN

(1) Design scope

* On the normal operation, the reactor coolant is not boiling(it means that the coolant temperature under the ONB(onset of nucleate boiling) temperature.
* On the abnormal transient condition, minimum DNBR(departure from nucleate boiling ratio) should be more than 1.5.
* And, on the abnormal transient conditions, the fuel meat temperature should be under 400°C.

(2) Calculation method

* The ONB temperature calculated by COOLOD code in JAERI.
* The minimum DNBR is evaluated by relative equation of primary coolant temperature, flow rate, coolant pressure, power level and power distribution. These calculations used COOLOD code on the normal operation, and EUREKA–2 code and THYDE–P code on the abnormal transient conditions.
* The main parameter of thermal–hydraulic design is shown in Table–3.

(3) Results of evaluation

* The fuel surface temperature is about 109 °C which value is not exceeded 126 °C as ONB temperature.
* The minimum DNBR on the normal operation and transient condition are about 3.2 and 2.6 respectively, and those are not below 1.5 as safety limit.
* The fuel meat temperature is about 111°C at rated power operation and 117°C in over power condition(110%), respectively. For the abnormal transient event [reactivity insertion by experimental facility], that value is about 124°C which is enough low from 400 °C.

OTHERS

(1) Revised study for site evaluation

The safety evaluation showed that the fuel should not failed at any events in both abnormal transient conditions and accidents. As the hypothetical events, two cases which are one fuel element failure and all fission product release from core were evaluated. The results showed that JRR–4 site evaluation satisfied the judgment criteria of safety evaluation guide of Japan.

(2) Modification of utilization facility

According the shutdown of JRR-2in 1996, BNCT (Boron Neutron Capture Therapy) irradiation facility will be installed in a modified thermal column of JRR-4.

Table-3 Characteristics of thermal-hydraulic design at normal operation

Item	LEU core
Rated thermal Power, MW	3.5
Coolant flow rate, m^3/min	8
Inlet coolant temperature, °C	40
Average heat flux, W/cm^2	15
Maximum temperature at hottest cannel, °C	109
Maximum temperature at fuel meat, °C	111
ONB temperature at hot spot, °C	126
Minimum DNBR	3.2

CONCLUDING REMARKS

In the RERTR program for JRR-4, a silicide fuel is chosen to convert from HEU uranium-aluminum alloy fuel. From the results of neutronic and thermal-hydraulic design calculations for new core, it is shown that thermal neutron flux is slightly decreased compared with HEU fuel core, and excess reactivity and safety shutdown margin is kept within safety limit. In addition, it is clarified that fuel temperature is below of safety limit and minimum DNBR of more than 2.6 is safety kept in the any abnormal transient conditions. These evaluation is carried out based on the safety evaluation guide for light water moderated and cooled research and testing reactor of Japan.

We hope that the safety review will be held by Japanese regulatory authority in 1995, and then the core conversion work including modification for BNCT facility will be started, and the JRR-4will achieve the criticality in 1998 again.

ACKNOWLEDGMENT

The authors wish to thank all members of the JRR-4 LEU Project for their energetic help and cooperation in the present work.

REFERENCES

1) K.Koba, et.al., "Construction of JRR-4",JAERI-1141(1967)

2) M.Saito, et.al., "Status of Reduced Enrichment Program for Research Reactors in Japan", Proceedings of the 16th International Meeting on RERTR, Oarai, Japan, JAERI-M 94-042(March 1994)

3) S.Watanabe, et.al., "Neutronic and Flow Analysis of LEU Core in JRR-4", Proceedings of the International Meeting on RERTR, Tokai, Japan, JAERI-M84-073(1984)

4) M.Morozumi, et.al., "Irradiation and Nuclear Characteristics Measurements of JRR-4 LEU Fuel Elements", Proceedings of the International Meeting on RERTR, Petten, The Netherlands, October 14-16,1985

5) K.Arigane, "Neutronic and Thermo-hydraulic Design of LEU Core for Japan Research Reactor No.4", JAERI-M88-078(1988)

6) M.Takayanagi, "The Reduced Enrichment Program for JRR-4",Proceedings of the Asian Symposium on Research Reactor,November 11-14,1991Sunpia Hitachi, Japan, JAERI-M92-028(1992)

7) Y.Nakano, "Neutronic Analysis on JRR-4Core by the Use of Low Enriched Uranium Silicide Fuels with Several Uranium Densities", JAERI-M92-103(1992)

8) Y.Nakano, H.Ichikawa, T.Nakajima, "Comparison of JRR-4 core Neutronic Performance between Silicide Fuel and TRIGA Fuel", Proceedings of the 16th International Meeting on RERTR, Oarai, Japan, JAERI-M94-042(March 1994)

Transient Analyses and Thermal-hydraulic Safety Margins for the Greek Research Reactor (GRR1)

W. L. Woodruff, J. R. Deen
Argonne National Laboratory
Argonne, Illinois 60439, USA
and
C. Papastergiou
National Centre for Scientific Research "Demokritos"
Institute of Nuclear Technology-Radiation Protection
Athens, Greece

ABSTRACT

Various core configurations for the Greek research reactor (GRR1) have been considered in assessing the safety issues of adding a beryllium reflector to the existing water reflected HEU core and the transition from HEU to an all LEU core. The assessment has included both steady-state and transient analyses of safety margins and limits. A small all fresh Be reflected HEU core with a rather large nuclear peaking factor can still be operated safely, and thus adding a Be reflector to the larger depleted HEU core should not pose a problem. The transition mixed core with 50% LEU elements has larger void and Doppler coefficients than the HEU reference core and gives a lower peak clad temperature under transient conditions. The transition cores should give ever increasing margins to plate melting and fission product release as LEU elements are added to the core.

Introduction

The 5 MW Greek research reactor, GRR1, is light water cooled and moderated with MTR type HEU fuel. The current plan is to first add a beryllium reflector to two faces of the HEU core and to then convert to LEU fuel by adding one or more fresh LEU element at the beginning of each fuel cycle. Thus, the core will be run in various configurations. Most of the extreme conditions are covered by these analyses. In addition to a reference water reflected HEU core, a small HEU core with a Be reflector is considered, and a mixed core of 50% HEU and 50% LEU fuel is considered. The mixed core with the more heavily loaded LEU elements next to HEU elements is expected to be more limiting than the all LEU core. These analyses include assess-

ments of safety margins with nuclear and engineering peaking factors applied and various limiting conditions for both steady-state and transients.

Codes and Methods

The collection of codes used for these analyses are all codes routinely used at ANL for neutronics and thermal-hydraulics analysis. The nuclear peaking factors were extracted from REBUS[1] computations for all fresh fuel. The steady-state thermal-hydraulics computations use the PLTEMP code[2] for forced convection cases, and the NATCON code[3] for natural convection cases. The steady-state cases include engineering peaking factors as determined from uncertainties allowed in the LEU fuel element specifications and the Technical Specifications[4]. Since peaking factors for the original HEU fuel are not available, the peaking factors for the LEU fuel were used throughout (f_q = 1.21, f_b = 1.20 and f_h = 1.30, see Table 1)[5]. The LEU fuel elements, except for the meat content, are identical to the current HEU fuel elements. The PARET code[6] was used for all of the transient cases.

Table 1: LEU Peaking Factor Components

Uncertainties	Peaking Factors		
	f_q	f_b	f_h
Mass Loading	1.02	1.02	--
Meat Thickness	1.05	--	--
Channel Thickness	--	1.16	1.03
Fuel Homogeneity	1.20	1.05	--
Flow	--	1.10	1.08
Power	1.05	1.05	--
Heat Transfer Coeff.	--	--	1.20
Statistical Combination	1.21	1.20	1.30

The cores considered in this study include a 35 element HEU water reflected core as the reference core, a 30 element Be reflected core, and a HEU and LEU mixed core with a Be reflector. The fuel elements and core models are described in detail in Refs. 7 and 8. Table 2 provides some of the relevant characteristics of the three cores. In each of the cores the maximum nuclear peaking was found to occur in a control element adjacent to the water channel for the control blade. The smaller

HEU core has the largest nuclear peaking and at the same time the largest flow velocity. The smaller Be reflected HEU core is representative of a start-up core with the Be reflector installed, and the mixed core is representative of a transition core in the conversion to all LEU fuel.

Table 2: Core Characteristics

Parameter	Core[a]		
	HEU Ref.	HEU with Be	Mixed with Be
18 Plate Standard Elements	30	25	28
10 Plate Control Elements	5	5	5
Total Nuclear Peaking	2.161	2.360	2.109
Uranium Density, g/cm^3	0.569	0.569	3.29
HEU Elements, %	100	100	50
Flow Velocity, m/s	1.036	1.221	1.103

[a] All HEU and LEU plates and elements have identical dimensions.

Steady-state Analyses

The steady-state analyses include some of the limits set in the original Technical Specifications[4], while including an analyses of Departure from Nucleate Boiling (DNB) and Flow Instability (FI) margins as typically included in most safety documents. The original Technical Specifications provide an operating envelope of limiting inlet temperatures as a function of flow rate with the reactor operating at the upper limit of 6.5 MW and with the coolant outlet temperature at the limit of 56 °C. Table 3 provides a comparison of the three cores with the original data at four values of the flow rate. The first and last values in the table represent the lower and upper limits for the flow rate. The PLTEMP code is predicting values that are in very good agreement with the original data. These analyses do not include peaking factors. The almost identical results for all of the cores show that the power to flow ratio is relatively constant as the number of elements in the core changes.

The DNB and FI ratios for the three cores are given in Table 4 along with the peak surface temperature for the clad. The PLTEMP model represents the hottest channel with peaking factors included. The flow and inlet temperatures are at nominal values. All of the cores have substantial margins to FI. The smallest core with the largest nuclear peaking factor has the lowest margin to FI, but even this core

would have to reach a power of 10.1 MW before the onset of FI is predicted.

Table 3: Operating Envelope of Limiting Inlet Temperatures at 6.5 MW and 56 °C Outlet

Flow Rate, m^3/hr	Inlet Temperature Limit, °C			
	Original Tech. Specs.	HEU Ref.	HEU with Be	Mixed with Be
160[a]	16.0	18.0	18.5	18.5
250	30.0	32.0	32.0	32.0
350	39.5	39.0	39.0	39.0
450[b]	43.0	42.5	42.5	42.5
[a] Lower limit of flow				
[b] Maximum flow rate				

Table 4: DNB and FI Margins for Forced Convection Cooling

Core	DNB Ratio[a]	FI Ratio[b]	Peak T_s, °C
HEU Ref.	7.77	2.21	101.6
HEU with Be	6.14	2.02	107.8
Mixed with Be	7.51	2.26	101.0
[a] DNB using the Mirshak correlation.			
[b] FI using the Whittle and Forgan correlation.			

For the natural convection mode of operation, the Technical Specifications limit the clad temperature to not reach the "boiling point of the water coolant." This limit is taken to mean the Onset of Nucleate Boiling (ONB) rather than the bulk boiling point of the coolant. The ONB limit is more restrictive. The margin to ONB and the peak surface temperature of the clad is given in Table 5 for the hottest channel. The margin is smallest for the Be reflected HEU core with the largest nuclear peaking factor. None of the cores considered, however, exceed the ONB limit.

Table 5: ONB Margins for Natural Convection at 400 kW and a 56 °C Inlet Temperature

Core	ONB Margin, °C	Peak T_s, °C
HEU Ref.	39.4	78.4
HEU with Be	8.6	109.9
Mixed with Be	16.7	101.6

Transient Analyses

Transient analyses are presented for two reactivity insertion cases based on a postulated maximum start-up accident and the maximum allowed worth of all experiments (1.6%Δk/k) as described in the safety documents.[4] A loss-of-flow transient with the trip point set at the low flow limit is also included. In each case control insertion includes a delay time of 0.020s following the trip. The kinetics parameters, feedback coefficients and control worths are provided in Table 6. The feedback coefficients have been found to be relatively unchanged by the addition of a Be reflector,[8] and the same coefficients are used for both HEU cases. The void coefficient for the mixed core is somewhat larger, while the coolant temperature coefficient is slightly smaller. A significant Doppler contribution is now seen from the LEU elements in the mixed core. The control worths for the smaller Be reflected HEU core would be significantly higher than for the reference core, but this difference was not accounted for in these analyses.

Table 6: Kinetics Parameters, Feedback Coefficients and Control Worths

	HEU Ref.	HEU with Be	Mixed with Be
β_{eff}	0.007611	0.007612	0.007559
Λ, μs	50.33	53.47	51.66
Void Coeff., $/% void	-0.1937	--	-0.2264
Coolant Temp. Coeff., $/°C	-1.171E-02	--	-1.032E-02
Doppler Coeff., $/°C	~0.0	--	-6.47E-04
Control			
Full Worth, $	-14.04	--	-13.70
With Stuck Blade, $	-9.59	--	-9.37
Insertion Delay, s	0.020	--	0.020

A maximum start-up accident is described and accompanied with estimates of the consequences in the Safety Analysis Report. In this accident at start-up all period trips are assumed to fail, and the trip is on the maximum power limit of 6.5 MW (130%). An estimated step reactivity insertion of 7.84E-03 Δk/k was used based on the start-up source strength and the subcritical multiplication, and this value was also used in the PARET analyses. The PARET analyses also assumes that at scram the most reactive blade is stuck in the withdrawn position, and the control worth is reduced as shown in Table 6. The current analyses gives the results shown in Table 7 with feedback included (the results without feedback are only slightly higher, e.g. for the HEU Ref. P_m = 8.12 MW). The estimate in the Safety Analysis Report for that HEU case is considerably higher at 20.3 MW. In all of the cases the accident is of little consequence and the peak clad temperatures in the hot channel are quite low.

Table 7: Start-up Accident with One Stuck Blade

	HEU Ref.	HEU with Be	Mixed with Be
7.84E-03Δk/k, $	1.030	1.030	1.037
P_m, MW	7.68	8.56	8.87
t_m, s	1.36	1.45	1.33
E_{tm}, MWs	0.873	1.13	1.10
Peak T_s, °C	56.0	74.8	70.1

A step insertion equivalent to the allowed worth of all experiments of 1.6%Δk/k corresponds to more than a $2 insertion in all cases. The period trip is assumed to fail, and the reactor scrams on an over power trip at 6.5 MW. The PARET results for each core are provided in Table 8, where the peak power, the time of peak power, the energy deposition to the time of peak power, and the peak surface temperature of the clad may be compared. Again the small Be reflected HEU core with the highest nuclear peaking gives the highest clad surface temperature for the hot channel. The response for this case is quite different largely due the different prompt neutron generation time, where the power increases more slowly with the peak at a later time. The mixed core gives a lower peak power and energy compared to the reference HEU core primarily due to increase feedback from voiding and Doppler. The void coefficient is larger for the mixed core due to the presents of the LEU elements, and there is a substantial amount of voiding in each core. More importantly the peak surface temperature of the clad for the mixed core is significantly lower than the HEU cases. In each case the clad temperature is well below the solidus temperature of the AG3NE clad.

Table 8: Step Insertion of Allowed Worth of All Experiments (1.6%Δk/k)

	HEU Ref.	HEU with Be	Mixed with Be
Step, $	2.102	2.102	2.117
P_m, MW	1267	986	1078
t_m, s	0.130	0.137	0.132
E_{tm}, MWs	11.5	9.66	10.3
Peak T_s, °C	537	548	455

Although the original safety documents do not specify a loss-of-flow accident, a generic 25s exponential loss-of-flow transient was specified for each core with the trip on low flow set at the low flow limit of 160 m^3/hr (35.6%). This trip setting is very low compared to more conventional settings of about 80%. Again a delay time of 0.020s is included. The transients are followed through flow reversal and the establishment of natural convection cooling. The results of these transients are shown in Table 9. In each case two peak surface temperatures are observed, one before flow reversal and another as natural convection cooling is established. The conditions for the two HEU cores are very similar, and again the mixed core gives slightly lower temperatures for the clad. None of the cases raise any new safety issues.

Table 9: Loss-of-flow Accidents

	HEU Ref.	HEU with Be	Mixed with Be
Time of Low-flow Trip, s	21.5	21.5	23.0
Peak T_s, °C	121	121	114
Time of Flow Reversal, s	56.5	56.5	57.5
Peak T_s with Natural Convection, °C	78.7	78.6	76.8

Conclusions

An HEU Be reflected core with a reduced number of elements was used to assess safety issues for the addition of a Be reflector to the current water reflected core, and a mixed core was used to assess the transition phase of the conversion from HEU to all LEU. These cores have been compared to a water reflected HEU

reference core for some of the various steady-state margins and transient limits addressed in the original safety documents. Margins to DNB and FI and loss-of-flow accidents were also considered. These analyses indicate that a small, all fresh, HEU core with a Be reflector can be operated safely, and thus a Be reflector can be safely added to the existing depleted core. The mixed core with 50% LEU elements has larger void and Doppler coefficients than the HEU reference core. The transient response of the mixed core gives lower peak clad temperatures and a greater margin to plate melting and fission product release than the all HEU core. The transition from an HEU core to an all LEU core can be done safely. Since the power peaking is most limiting for the control elements, care should be taken in the loading of the fresh LEU control elements.

References

1. B. J. Toppel, "A User's Guide for the REBUS-3 Fuel Cycle Analysis Capability," ANL-83-2 (1983).

2. K. Mishima, K. Kanda and T. Shibata, "Thermal-hydraulic Analysis for Core Conversion to the Use of Low-enriched Uranium Fuels in the KUR," KURRI-TR-258, Kyoto University Research Reactor Institute (1984).

3. R. S. Smith and W. L. Woodruff, "A Computer Code, NATCON, for the Analyses of Steady-state Thermal-hydraulics and Safety Margins in Plate-type Research Reactors Cooled by Natural Convection," ANL/RERTR/TM-12, Argonne National Laboratory (1988).

4. C. Papastergiou, Ed., "Safety Analysis Report of the Greek Research Reactor-1, Vol. I and II (Annex 2 - Technical Specifications)," National Centre for Scientific Research "DEMOKRITOS', Institute of Nuclear Technology-Radiation Protection (1985).

5. W. L. Woodruff, "Evaluation and Selection of Hot Channel (Peaking) Factors for Research Reactor Applications," Proc. 1987 Int. Mtg. on Reduced Enrichment for Research and Test Reactors, Sept. 28 - Oct. 2, 1987, Buenos Aires, Argentina (to be published).

6. W. L. Woodruff, "A Kinetics and Thermal-hydraulics Capability for the Analysis of Research Reactors," Nucl. Technol., 64, 196 (1984).

7. J. R. Deen, James L. Snelgrove and C. Papastergiou, "Greek Research Reactor Performance Characteristics After Addition of Beryllium Reflector and LEU

Fuel," Proc. 1992 Int. Mtg. on Reduced Enrichment for Research and Test Reactors, Sept. 27 - Oct. 1, 1992, Roskilde, Denmark, ANL/RERTR/TM-19, Argonne National Laboratory (1993).

8. J. R. Deen, J. L. Snelgrove and K. Papastergiou, "Analyses of Greek Research Reactor with Mixed HEU-LEU Be Reflected Core," Proc. 1993 Int. Mtg. on Reduced Enrichment for Research and Test Reactors, October 4 - 7, 1993, Oarai, Japan, JAERI-M 94-042, Japan Atomic Energy Research Institute (1994).

COMMENTS ON THE FUTURE ACTIVITIES OF THE RERTR PROGRAM - PART II*

W. Krull
GKSS research centre Geesthacht GmbH
Max-Planck-Straße
D-21502 Geesthacht

1. Introduction

At the last (16) RERTR meeting an historical overview was given and the status and consequences of enrichment reduction were discussed. At that time and some what more today many doubts are raised that enrichment reduction, as a tool for reducing the proliferation risk, is being done in the most efficient and convincing manner.

The informations presented in this report were taken from IAEA, US-DOE, US-GAO publications and from proceedings of the RERTR meetings. The data presented should be compared only on a relative basis. It was not the intention for many reasons to present quantitative exact values as some figures used for developing the conclusions are being confidential. Others are available in the above mentioned publications and proceedings. But nevertheless conclusions drawn and recommendations developed are believed to be worth to be taken into account by research reactor operators, their funding organizations and administrators when they are faced with decisions about the future of their facilities.

All of the internationally effort on reducing the enrichment on research and test reactors has their only justification from the INFCE (International Nuclear Fuel Cycle Evaluation) conclusions to reduce the proliferation risk worldwide to a large extent. Worldwide is important. IAEA and others have to convince operators and organizations upon the necessity in doing so. One of the best way convincing people is giving convincing examples. At present none of the nations having a military nuclear weapons program is giving such a convincing example. Even in cases where the qualified fuel and all other necessary tools for converting specific research reactors are existing only small or no progress can be seen. Only non-weapon states are being pressed today.

2. Conclusions drawn at the 1993 RERTR meeting

At the 16. RERTR meeting [1] the comments on the RERTR activities were summarized and concluded in details. It should be mentioned that part I of this report was written more or less from the standpoint of a medium power research reactor operator. Below only a few of these conclusion are being repeated:

a) Conversion of a research reactor from HEU to LEU leads to severe difficulties for all parties involved:
   - the operator has to accept many penalties, licensing problems and increasing operation cost
   - the licensing authority must deal with new problems and consider increasing physical protection demands
   - the IAEA has to prepare for an increased frequency of safeguard inspections
   - the public internationally should feel deeply concerned about the increasing proliferation risk.

*) paper presented at the 17. RERTR Meeting, September 19-22, 1994, Williamsburg, USA

No one has any advantage from converting a specific reactor now.

b) If there is no conversion there is an increasing proliferation risk with the HEU spread wordwide

c) If there is no shipment of spent HEU fuel elements to a central storage (the country of origin of the U) there is an increasing proliferation risk with the HEU spread world-wide.

d) The countries of origin of the enriched U have to take back the spent fuel elements for a given time to allow the research reactor operator

- to look at other solutions for e.g. an interim storage or final disposal in the home country
- to shutdown the reactor and without having remaining spent fuel elements during the decommissioning period.

Countries of origin are US, Russia (USSR), China, UK and others?

e) To reduce the proliferation risk the ideal situation would be to have no research reactor in operation worldwide with HEU. Therefore, all research reactors should be converted from HEU to LEU including e.g. the unique purpose reactors, the reactors build by the USSR and operated in many countries (36 %, 80 %, 90 %), the reactors in China and others. Otherwise conversion makes little sense.

3. Spent fuel is fresh fuel

The proliferation risk is coming up from the theft and/or diversion of materials usable for the production of atomic weapons. There are many different issues of importance when considering the proliferation risk e.g. the different kind, chemical composition and enrichment of materials, different radiation level, different safeguarding efforts and different physical protection efforts. Especially it has been recognized that the involved efforts for the theft of irradiated material is depending sensitively on the radiation level or radiation dose which is depending on the irradiation history of that material. Two IAEA definitions are existing at present when irradiated fuel should be considered as fresh fuel for the discussion of proliferation risk*. Unfortunately these two different definitions can be found in use in Member States of the IAEA.

IAEA safeguard definition [3]: Spent fuel has to be considered as fresh fuel if the radiation dose at 1 m distance in air unshielded per kg U_{eff} is below 1 Gy/h (1 eff kg is the weight of U in kg multiplied by the square of its enrichment).

IAEA physical protection definition [2]: Spent fuel has to be considered as fresh fuel if the radiation level is below 1 Gy/h at one meter in air unshielded.

The significant difference between the two definitions is that within the INFCIRC definition any relation to an amount of material and weighing this amount in eff kg is missing. Such a relation as it is being used in the safeguard definition takes into account the purpose for such a definition as the proliferation resistance is depending on the amount of eff kg. It is open to what the INFCIRC definition refers to: fuel rod, fuel element, fuel plate, reactor core, 1 g U, 1 kg U, 1 t U, U at the site or what? Such an open definition is really difficult to rationalize.

Similar the quantity of uranium is being considered as category I material (highest physical protection demands) if the amount is ≥ 5 kg U [2] resp. 5 kg eff U [3] for enrichments ≥ 20 %. This quantity differs significantly. For 20 % enrichment by a factor of 25!

There are severe difficulties in understanding the logic of the latest IAEA-INFCIRC definition when irradiated fuel should be treated as fresh fuel from the point of view of physical protection. But as it is the latest definition it should be used. Nevertheless for most of

*) Remember: One of the founding reasons for the IAEA was to avoid the further spread of atomic weapons.

the conclusions drawn when looking at the consequences in considering spent fuel as fresh fuel the conclusions are equally valid for the older definition [3], too, as it has been used in [1]. This is true as for HEU with 90 % and 93 % enrichments as it is normally being used in many research reactors, the difference is small (up to 19 %). But it should be noted that these two definitions used for the same purpose having no relation to each other. Consequently under certain circumstances conclusions drawn using one definition contradict conclusions drawn using the other definition. This is really a confusing situation.

3.1 Safeguards

Safeguarding efforts are described in the nuclear non proliferation treaty. They are depending on the amount of strategic material as a function of its enrichment (≥ 20 %). The actual control effort is depending on the status fresh or spent fuel, too. In practice it is assumed - no other example is being known - that fuel is being considered as spent if it is irradiated. No discussion on the radiation level. But if the radiation level is taken into account, too, and the existing definition is being used for fresh fuel for the different reactor categories (see chapter 4) the safeguarding efforts is as follows:

Reactor type	A (50 MW)	B (10 MW)	C (< 1 MW)
Operation + storage < 2 years	adequate	adequate	inadequate
Storage of spent fuel > 2 years	adequate	inadequate	-
Storage of spent fuel > 6 years	inadequate	inadequate	-

3.2 Physical protection

Physical protection demands having two sources

- the total amount of fission product inventory in the facility (reactor core* and spent fuel storage)
- the amount of fresh strategic material with enrichment ≥ 20 %.

Both lead to similar requirements. Therefore, the physical protection demands can be categorized. Reactors belonging to category I (nuclear power plants, too) have to fulfill the highest demands. Category III gives the lowest level of demands - normally very close to nothing.

category	proliferation resistance amount of U	fission product inventory reactor power
I	> 5 kg, > 20 %, fresh	Q ≥ 20 MW
II	> 1 kg, > 20 %, fresh or > 10 kg, 10 % - 20 %, fresh or > 5 kg, > 20 %, spent**	1 MW ≤ Q < 20 MW
III	below category II	Q < 1 MW

As the fuel in low power (< 1 MW) research reactors has to be taken as fresh fuel by the existing definition, if operators are not able to demonstrate the opposite, these reactors are not belonging to physical protection category III as this is international practice (they are at present open to the public like a department store. In the US, too). These reactors have to be secured in accordance to physical protection category II (in some cases category I!) with by far more stringent physical protection demands due to their inventory of HEU.

Example: It is more than surprising to restrict the amount of fresh fuel for operating university reactors of category II to only a few fresh fuel elements when on the other hand large amounts of not sufficient protected material is distributed over the country in open

*) Normally greater by orders of magnitudes than within the spent fuel storage.

**) radiation beyond the level defined above.

houses (in low power research reactors which are not sufficiently physical protected).

3.3 Solutions?

There are three possible ways in solving this problem

a. As in any case the definitions relating to 1 Gy/h are in some way arbitrary one can reduce the radiation level e.g. 1 Gy/h –> to 1 r/h = 10 mGy/h. But even in this case it will not solve the problems for the large number of critical facilities.

b. Increasing the physical protection to category II or I. This costs an extremely large amount of money and will be for many facilities out of practical feasibility.

c. Reducing the enrichment to < 20 % is the cheapest and most logical way. It solves all the problems.

4. What research reactors are believed to be a significant or a marginal proliferation risk?*

Considerations and evaluations being made for estimating the proliferation risk from the operation of research reactors** should include all kinds of research reactors and the complete fuel cycle of that research reactor. To underline the conclusions more clearly the discussion is restricted and simplified in looking at only three groups of research reactors.

A. Power Q ≥ 20 MW, average 50 MW
These reactors normally have a high utilization (250 d). The average annual consumption is > 30 kg U (93 %) per reactor, ca. 4 times of the core loading

B. Power Q with 1 MW ≤ Q < 20 MW, average 10 MW
These reactors have a relatively high utilization (200 d). The average annual consumption is ca. 5 kg U (93 %), ca. 80 % of a core loading

C. Power Q < 1 MW
These reactors have normally a very low utilization, a life time core and a core loading of 4 kg U (90 %).

The following steps have to be considered for the evaluation of the proliferation resistance (or risk) in the fuel cycle of a research reactor:

1. shipping enriched material from the enrichment plant to the fabricator
2. storing the material at the fabricators site
3. fabricating fuel elements
4. storing the fabricated fuel elements at the fabrication plant
5. shipping to reactor site
6. storing at reactor site
7. fuel elements in the research reactor
8. storing spent fuel at the research reactor site while the fuel is self protecting
9. storing spent fuel at the research reactor site after the fuel is no longer self protecting
10. shipping spent fuel to a central storage, final storage or reprocessing plant.

Assuming that for reactor types A and B the U-cycle takes
3 years for steps 1 - 6
1 year for step 7
2 years*** for step 8 (for B type reactors) or 6 years*** (for A type reactors)

Shipment (10) is being made after two years storage at the facility.

---

*) all figures should be taken only qualitatively

**) other reactors should be considered similarly including reactors used for production of fissile materials, too, as it is recommended in INFCE conclusions.

***) very approximate estimates.

For an operating reactor it is very clear that the main proliferation risk results from the total amount of material involved in the fuel cycle. Looking at the different fuel cycle steps it is easy to determine the total amount of HEU (93 %) in kg for the reactor type. This total amount of U has to be considered as the overall proliferation risk coming up from the operation of the research reactor

Reactor type	A	B	C
continuously in cycle	134	24	4
20 a operation	630	100	4
safeguard, adequate	yes?	mostly	no
physical protection, adequate	yes?	mostly	no

For non-proliferation discussions one has to distinguish between theft and diversion:

For easy diversion the amount of fresh sensitive, strategic material is important. Physical protection aspects are relatively unimportant for this discussion.

1. For this reason category A reactors - including as the most important reactors in this category the US unique purpose reactors, too - are of by far greatest importance. Every efforts should be made to reduce their enrichment to less than 20 %. These are the real dangerous reactors from the aspect of diversion of strategic material.

2. For diversion purposes category B reactors should be converted, too, but they are of some what lesser importance than the category A reactors.

3. Depending on the amount of material on hand diversion from a category C research reactor will cause enough international trouble.

Summarizing diversion:

Reactor type	A	B	C
Proliferation risk	extreme	great	small

In the discussion of theft of fresh sensitive strategic material one has to take into account mainly the existing safeguard and especially the physical protection efforts. The situation is completely different from the diversion situation.

Summarizing theft:

Reactor type	A	B	C
Operation	negligible	negligible	extreme
Storage of spent fuel > 2 years	negligible	small	extreme
Storage of spent fuel > 5 years	great	great	extreme

Large proliferation risk considering theft of strategic material is coming from two sources

- category C reactors which are not sufficiently physical protected and
- from the long term storage of spent fuel at the reactor site.

As category C reactors have a lifetime core only limited technical pressure can be applied to reduce the enrichment of these reactors. Operators and organizations have to be convinced. This can be done in the best and most excellent way in giving good examples. Is the US willing to lead the way to a larger extent.

In conclusion to reduce the proliferation risk effectively and quickly the optimal procedure is:

First:	reducing the enrichment of category A and C reactors
Second:	taking spent fuel away from the reactor site
Third:	reducing the enrichment of category B reactors.

At present and within the last decade both the international practice and the US pressure in converting reactors and reducing the proliferation risk has been acting in the opposite way: looking mainly at category B reactors and some category A reactors outside the US.

5. Criticism of the present RERTR activities

In the following some actions taking place within the last decade and at present which are directed pro and against enrichment reduction are being discussed and criticized.

5.1 Secretary O'Leary's letter of July 13, 1993.

The announcement being made by the Secretary of US-DOE is a very important milestone in reestablishing DOE as a reliable partner for non US research operators enabling a trustful international cooperation. The leading ideas behind this announcement are being appreciated to a very high degree, e.g. it is very clear, that at the end of the 20th century people must take into account conditions of the changing world in international safety, in physical protection and in environmental protection to mention a few important points. Fruitful cooperation can take place only if all parties involved have mutual confidence and trust in each other. For example it is understandable that the US can not be the designated waste repository for all research reactor spent fuel elements forever even if it has been implicitly promised in the past. But on the other hand partners must have the required necessary informations, the needed assistance and time to develop acceptable solutions for their own needs. The announcement of the Secretary is on the right way. But does it includes reasonable conditions and schedules to support the plans?

The Secretary of US-DOE proposed a policy in a three-tiered approach to fulfill the remaining commitments in the RERTR program. As an old friend and a sponsor of the RERTR activities and one who is convinced in the necessity in having such activities as an important part in reducing the proliferation risk the author would prefer making the announcement for a policy to assist the RERTR program in the following way:

1. Operators, who are cooperating intensively with the RERTR program and having already performed or started conversion of their research reactors, should get a bonus to encourage their continued cooperation.

2. Operators who express their willingness to cooperate and convert their research reactors should be given all necessary assistance and encouragement to help them to achieve the goal in a manner acceptable to all involved parties.

3. Operators who are not willing to cooperate or not willing to convert should get clear indications to allow them to rethink their position.

The Secretary of US-DOE announces the following to encourage the conversion of foreign research reactors:

1. Reactors having converted
   Receipt of spent LEU fuel for a ten year period following implementation of this policy.

2. Reactors convert within 5 years of the effective date of this policy.
   (Convert = start conversion or finished conversion? What means start or finished?)
   Spent LEU fuel will be accepted for a ten year period following the initial order (?) for low enriched uranium fuel.

3. Reactors not willing to convert
   Their HEU fuel will be accepted by US-DOE forever.

What is the situation?

	Author proposed policy	US-DOE proposed policy
Reactors having cooperated with RERTR	bonus	penalty
Reactors willing to cooperate	acceptable conditions	acceptable conditions
Reactors not willing to cooperate	penalty	super bonus

Is there any one able to explain this situation and these conditions? Nevertheless hope-

fully there will be a big difference between the proposed and effective policy later on.

5.2 The kind, friendly and very polite US-GAO [4] report

On page 5 of that report there is written the following:

- DOE officials acknowledge that this situation (research reactors already converted) is **unfair to the foreign operators** that have converted their reactors under the reduced enrichment program. [Nothing more! especially no hint to deal fair with the foreign research reactor operators.]

- Despite US pressure on the foreign research reactors to participate in the reduced enrichment program, the four DOE-operated research reactors also (like US university reactors) continue to use HEU fuel.

The situation is very clear: Non US research reactors using HEU of US origin are being forced to convert and to accept technical, safety, licensing and commercial penalties. It is obvious that one has to distinguish between announcements and declarations on the one side and the actions of departments and commissions on the other side. Announcements are being made to promote and to accelerate the reduction of proliferation risk worldwide (in and outside US). Actions are being made primarily only for foreign research reactor operators. Therefore many times at RERTR meetings non US participants have pointed out the necessity that US reactors must convert at least in the same way under the same conditions and with the same time schedule as none US research reactors. GAO expressed the situation clearly that US reactors are far behind these goals and promises.

The lack of promotion of RERTR activities within the US

- in acting against the conversion of 6 major research reactors
- in slowing down activities in the conversion of research reactors with power levels ≥ 1 MW (converting only 3 of 19 research reactors) and
- converting only 2 of 18 low power research reactor

will be taken by others as an example how to deal with actions in converting their own research reactors.

The resulting situation can be summarized in another way: The international competition of research reactors is depending on their technical and scientific possibilities, their economical operation and their licensing difficulties. Research reactors having converted are being penalized in international competition in all these areas i.e. they are discriminated to a large extent since their competitors are neither being forced to convert soon nor to shutdown until they do convert.

5.3 Unique purpose reactors

In 1984 and 1988 Fed. Reg. Notes were published in the US to have as many US research reactors as possible excluded from the present need to convert following the INFCE demands. For this reason the definition of so called Unique Purpose Reactors was created. Besides six US (ATR, HFIR, HBWR, Missouri, NIST, MIT) research reactors there are 3 other research reactors in Europe accepted to be excluded from conversion at present.

As explained last year:

- the definition of unique purpose reactors is special made for excluding some research reactors from the need for conversion

- the definition discriminates and penalizes other reactors in an unacceptable way as the unique purpose reactors are normally rich and the others are in general poorer

- if a definition of unique purpose is necessary at all the existing definition is by far too simple

Within the Fed. Reg. Note Vol. 47 No. 131, July 8, 1984, there is the stringent demand: "the licensee must use HEU fuel as close to 20 % as is available and acceptable to the Commission (NRC)". In addition: "Each licensee shall develop and submit a proposed schedule for meeting the requirements".

Since U_3Si_2 with 4,8 g U/cc is being qualified for a decade where are the unique purpose reactors within the US going down with their enrichments? It is possible for all of them.

In early discussions at the IAEA and at the RERTR meetings there has been seen the necessity for the development of higher density fuel for the conversion of all research reactors to below 20 % enrichment with marginal (?) penalties. From the US status reports presented annually at the RERTR meetings over the years (see table 1) the US policy can be easily determined:

middle of the 80´s - high density fuel will be qualified 1989/90.
end 80´s, beginning 90´s - offset of the conversion of own "unique purpose reactors" and in the development of high density fuel
present - looking for funding for the development of high density fuel.

This policy is a hugh discrimination to all international competitors of US research reactors. Is such a position in agreement with the INFCE conclusions?

5.4 Progress in enrichment reduction

At the RERTR meetings over the last decade only the progress in non US research reactor ($Q \geq 1$ MW) core conversion has been presented in figures and tables. US research reactors, research reactors with low power and research reactors using HEU from other sources were never included. But if one is looking at the reduction of proliferation risk worldwide, such reactors are of equal importance. Excluding these research reactors makes only little sense and gives the wrong impression.

Table 2 contains an overview taken from IAEA database information upon all research reactors using HEU: Comparing this information with the above mentioned presentation it can be seen that:

- The number of the research reactors within the US (not counted!) is of the same order as the counted non US research reactors
- In total 75 % of the research reactors are missing.
- No fuel has been qualified at the moment for a large number of these reactors.
- Many research reactors now under pressure to convert have shipped their fuel to reprocessing over years, so that the operators were willing to reduce the proliferation risk associated with storage of the spent fuel (see chapter 3).
- Many other research reactors in operation over years, never shipped fuel to reprocessing, storing large amounts of spent fuel over the years. Most of it must be considered as fresh fuel now. These reactors must be included in the counting with their real proliferation danger.
- Only a global view which includes all research reactors with enrichments ≥ 20 %, the amount of spent fuel at the facility, the present safeguarding and physical protection levels can give a realistic impression on the existing proliferation risk worldwide.
- A revised action plan which must be internationally agreed upon and administrated by the IAEA will lead to a successful achievement of the nonproliferation goals.

Conclusion: A progress report makes sense only if it includes all relevant informations of importance for the reduction of proliferation risk. If too many facts are not included the information is of questionable use only and may give the wrong impression.

5.5 New research reactors

May be the following is not absolutely correct, but it looks not wrong: A newspaper reported, that only new research reactors being built within the US (e.g. the ANS) may get

*) INFCE = International Fuel Cycle Evaluation

HEU in the future. Non US research reactors will not get HEU under any circumstances - no technical, scientific (unique purpose), commercial, licensing, survival justification will be taken into account. This is a very clear and convincing statement acting directly against the spirit and activities of the RERTR program.

5.6 The role of the IAEA

The very substantial effort at the end of the 70th in evaluating the nuclear fuel cycle to reduce the proliferation risk was very impressive. The IAEA was playing an active part within the INFCE* process as it can be read in the communique of the final INFCE conference 25-27 February 1980: "The delegates recognized the central role that the IAEA has played in the past and must continue to play in the future in meeting the problems that were the focus of the INFCE study".

It is stated there:

1. That the IAEA has played a central role in the past. This is gratefully acknowledged.

2. That the IAEA has to play in the future (after 1980) a central role in meeting the problems that were the focus of the INFCE study!

But what was the role of the IAEA after INFCE?

- initiating (?) the first of the 17th RERTR conferences.

No further meeting was initiated or organized by the IAEA. None of these proceedings were published in any conjunction with the IAEA. One or more participants of the IAEA were normally present at these meeting, but the IAEA has not played an important role in these meeting as it is the case when organizing e.g. symposia, seminars in member states

- preparing a serious of important TEC DOC´s

The publication of the most important one has been delayed for eight years

- organizing training courses on reduced enrichment

These training courses giving a broad spectrum of informations are believed to be helpful for many participants.

But is this really a central role? Are there not many things missing?

The reduction of proliferation risk through RERTR activities does not appear - if looking to the visible actions of the IAEA - to be of major importance to the IAEA. The IAEA never coordinated, administered, reviewed, controlled, accelerated or major influenced the RERTR activities to a great extent which is believed to be necessary if the IAEA intends to play the necessary central role. It is strongly recommended the IAEA should rethink its position to become the central active and the leading partner. Such a role of the IAEA would have a positive impact on the present RERTR activities in developing new high density fuel, converting research reactors and reducing the proliferation risk worldwide.

6. Summary and conclusions

All of the conclusions drawn in part I [1] of this report are still valid so no repetition will be made. From part II the following summary and conclusions can be drawn:

- Two definitions are existing under what conditions spent fuel has to be considered as fresh fuel which are not totally in agreement. The latest (INFCIRC) one is believed to be not the best one.

- As irradiated fuel is normally taken to be spent fuel there are two fuel conditions for which this is not true if using one of the IAEA definitions
  - low power research reactor fuel in general, and
  - spent fuel after some decay time

- Safeguarding is insufficient for these two fuel conditions

- Low power research reactors should be classified in the physical protection category I or II. In almost all cases they are at present in category III with very limited physical protection efforts.

- The fuel cycle of high power research reactors ($Q \geq 20$ MW) can be used most effectively for easy diversion. Therefore these reactors must convert as soon as possible.

- The threatening of theft from the research reactor fuel cycle is highest for low power research reactors ($Q < 1$ MW).

- For low power research reactors with lifetime cores the most effective way in converting these reactors is by example and afterwards demanding it.

- To reduce the proliferation risk most effectively high and low power research reactors should be converted first, spent fuel stockpiles should be reduced as a second step and of third importance is the conversion of medium power research reactors.

- Within the important announcement of the Secretary of DOE on July 13, 1993, there is a not understandable promotion of research reactors with no intention to convert (acting against RERTR) and at the same time the most worst conditions made available for research reactors intensively cooperating with RERTR programs.

- The US-GAO concluded that DOE should acknowledge its effective discrimination against non US research reactors already converted. But that´s it.

- The US-GAO concluded that within the US conversion activities have been slowed down.

- Reactors converted are being discriminated in loosing international competition. Competitors in some countries (particular the US) have an unfair advantage.

- Unique purpose reactors never followed the command given in Fed. Reg. Note 47 to reduce their enrichment to close to 20 % as possible.

- After supporting the development of higher density fuel middle of the 80´s US-DOE has offset all these activities. This is a clear indication

- Progress in enrichment reduction has only been counted at non US facilities and for 25 % of the research reactors using HEU worldwide.

- Only a global overview which includes all research reactors with enrichments ≥ 20 %, the amount of spent fuel at the facility, the present safeguarding and physical protection efforts can give a realistic impression on the existing proliferation risk worldwide.

- RERTR activities should be internationally coordinated and administered by the IAEA. This has been missing over years, but should be seen as a direct outcome of INFCE conclusions.

- It is clear that new non US research reactors will not have access to US origin HEU. In contrast, the new US research reactors (e.g. ANS) will probably burn HEU.

- The present situation, especially the hardware activities has some similarity with George Orwell´s "Animal Farm"
  - all are equal (have to convert)
  - some (the weapon states) are more equal (may be excluded)

Is this the reasonable and equitable policy to achieve the nonproliferation goal?

Literature:

[1] W. Krull: Comments on the future activities of the RERTR program
The 16th International Meeting on Reduced Enrichment for Research and Test Reactors (RERTR), October 3-7, 1993, Oarai, Ibaraki, Japan

[2] The physical protection of nuclear material, INFCIRC/225/Rev., 3, IAEA, September 1993

[3] a) Draft of IAEA TEC-DOC 643

b) Application in Nuclear Data and Reactro Physics, IAEA, February 17 - March 21, 1986, in Triest, pages 922 - 930

[4] Concerns with US Delays in Accepting Foreign Research Reactors´ Spent Fuel, GAO/RCED-94-119, March 1994

Table 1:

DOE promises for U densities > 4,8 g U/cc as reported

1982 - RERTR	A long term plan will be made
1983 - RERTR	7 g U/cc available in 1988
1984 - RERTR	7 g U/cc qualified (!) beginning of 1989
1985 - RERTR	7 g U/cc qualified in 1989
1986 - RERTR	7 g U/cc qualified now in 1990
1987 - RERTR	7 g U/cc is included in plans for the future
1988 - RERTR	Fabrication of up to 8,6 g U/cc appear feasible, preparation of fabrication will be made
1989 - RERTR	Along the lines planned in 1988
1990 - RERTR	Hold on any further development of high density fuel
1991 - RERTR	Beginning of 1990 new guidance from DOE had redirected the efforts away from the development of new and better fuels
1992 - RERTR	A plan to resume the development of higher density fuel was submitted to DOE
1993 - RERTR	Make plans and general preparation to resume high density fuel develpoment for DOE
1994 - February	At present no money, but looking for funds
1994 - RERTR	When discrimination of medium power reactors is coming to an end?

Country	number Q ≥ 1 MW ( ) converted	number Q < 1 MW () converted	reprocessing	US counting	Missing in US counting
Argentina	(1)	1	no	1	1
Australia	1	1	no	1	1
Austria	(1)	2	1 yes	1	2
Belarus	1	0	no	0	1
Belgium	1	1	1 yes	1	1
Brazil	1	0	no	1	0
Canada	1 + (2)	6	3 yes	3	6
Chile	2	0	no	1	1
China	2	5	7 yes	0	7
Columbia	0	1	no	0	1
Czech. Republic	1	2	no	0	3
Denmark	(1)	0	1 yes	1	0
France	4 + (1)	7	5 yes	5	7
Germany	6 + (1)	0	6 yes, 1 no*	6	1*
Greece	1	0	1 yes	1	0
Hungary	1	0	no	0	1
Indien	1	0	1 yes	0	1
Iran	(1)	0	open	1	0
Israel	1	1	open	1	1
Italy	0	1	no	0	1
Jamaika	0	1	no	0	1
Japan	3 + (1)	5	3 yes	4	5
Kazakhstan	3	0	no	0	3
Korea DPR	1	0	no	0	1
Korea RP	1	0	no	1	0
Latvia	0	1	no	0	1
Lybia	1	1	no	0	2
Mexico	1	1	no	1	1
Netherlands	2	1	2 yes	2	1
Pakistan	(1)	1	no	1	1
Peru	0	1	no	0	1
Philippines	(1)	0	no	1	0
Poland	2	1	no	0	3
Portugal	1	0	no	1	0
Russia	12	4	16 yes	0	16
South Africa	1	0	no	1	0
Sweden	(1)	1	1 yes	1	1
Switzerland	1	1	1 yes	1	1
Taiwan	(1)	1	no	1	1
Turkey	1	0	no	1	0
Ukraine	1	0	no	1	0
United Kingdom	0	6	no	0	6
USA	19 (3)	18 (2)	37 yes	0	37
Uzbekistan	1	0	no	0	1
Vietnam	0	1	no	0	1
Yugoslavia	1	1	no	0	2
	77 + (13) 54,9 % = 47,0 % +7,9 %	74 45,1 %	88 yes, 76 no 29 ≥ 1 MW 47 < 1 MW	42 25,6 %	122 74,4 %

*) Rossendorf

Leaving Chicago, from left to right Marti Travelli, Loyeen Woodruff, Sharon Richmond, (ANL, USA) Gavin Ball (AEC, South Africa), Armando Travelli, and Helen Weber, (ANL, USA)

Sunday Breakfast at the Williamsburg Woodlands, from left to right Vasily Lukichev, Evegny Kartashov, RDIPE, Russia, and Galena Sarikovha (NVVIINM, Russia)

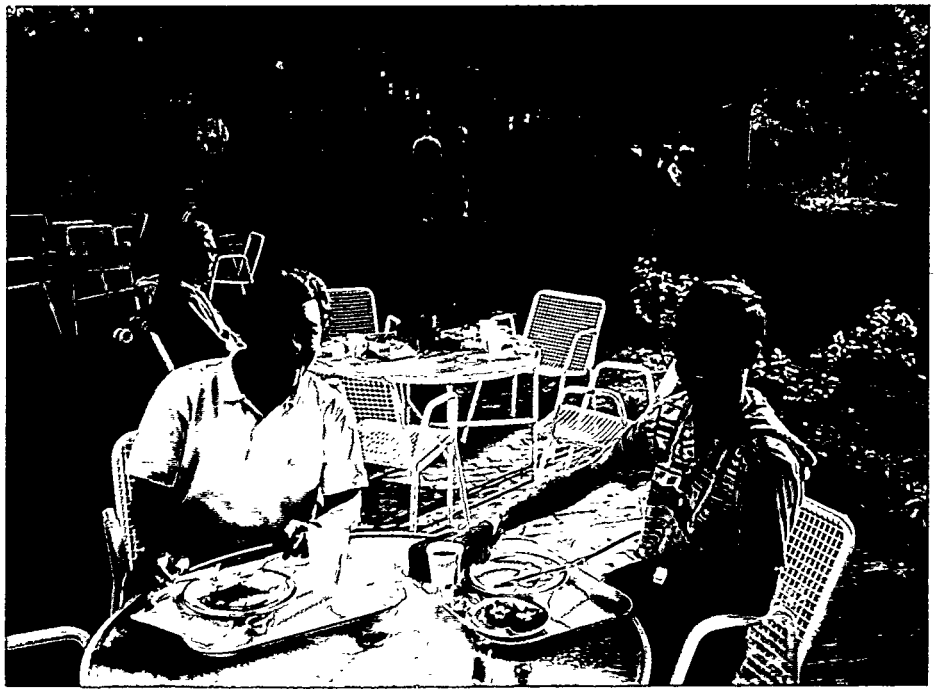

Also enjoying breakfast were Sugundo, (BATAN, Indonesia) and Gavin Ball (AEC, South Africa)

Visiting the Revolutionary War Museum in Yorktown were Fred Reitsma (AEC, South Africa), Ray Pond, Sharon Richmond, Chino Srinivasan, Helen Weber (ANL, USA), Gavin Ball (AEC, South Africa, and Sugundo (BATAN, Indonesia)

Lunch on Sunday at the Newport Pub was being enjoyed by Ray Pond, Nelson Hanan, Helen Weber, Sharon Richmond, Chino Srinivasan (ANL, USA), and Fred Reitsma (AEC, South Africa)

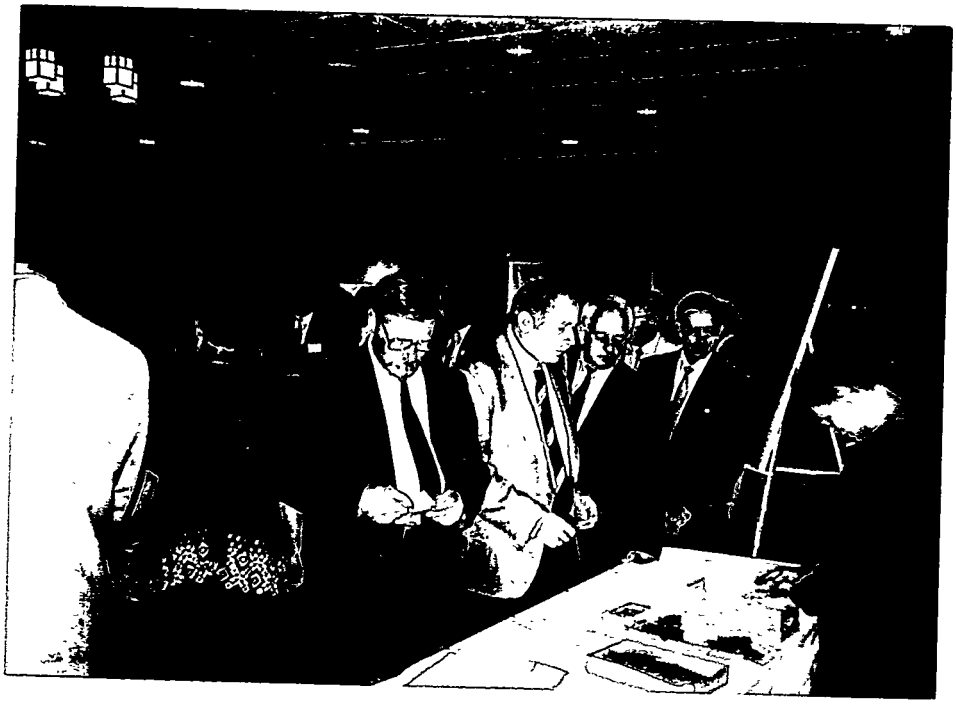

Picking up agendas and badges on Sunday were E. Kartashow, V. Stetsky, V. Aden, (RDIPE, Russia), N. Arkhangelsky (MINATOM, Russia), and H. Weber (ANL, USA)

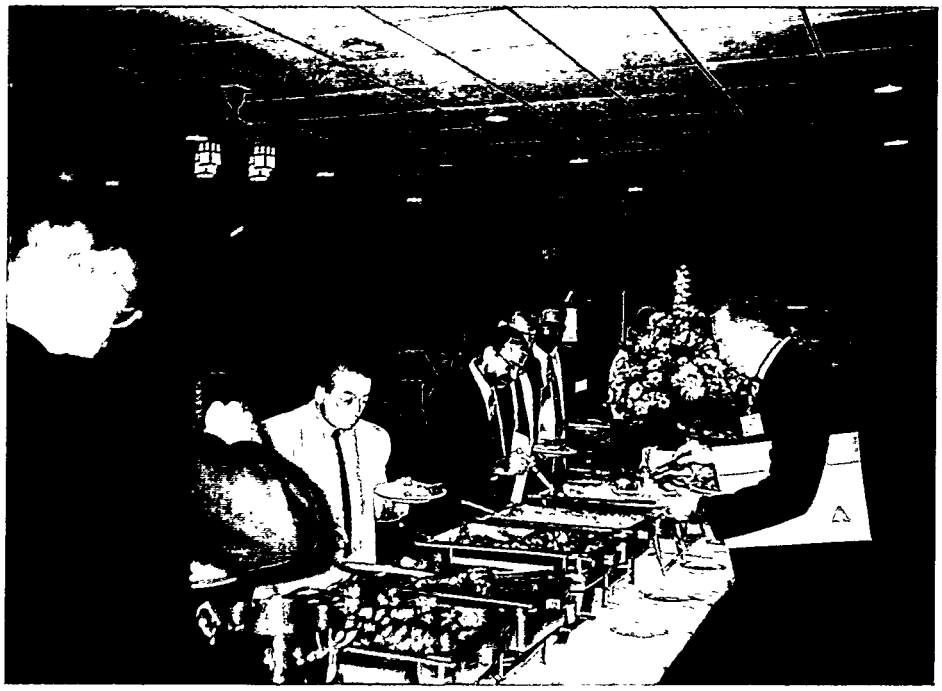

Our participants enjoying morning breakfast brunch

Also enjoying the breakfast brunch were Sai-Chi Mo, Inessa Minkov, and Vladimir Minkov (ANL, USA)

Having a discussion during the morning break were N. Ermakov (MINATOM, Russia) and R. Olsson (SKI, Sweden)

Having a discussion with Vladimir Minkov (ANL, USA) was Marilena Conde (Edlow, USA) with Phil Robinson looking on in the background

W. Krull (GKSS, Germany) was checking the news of the day with R. Olsson (SKI, Sweden and R. Ball (B&W, USA) in the background

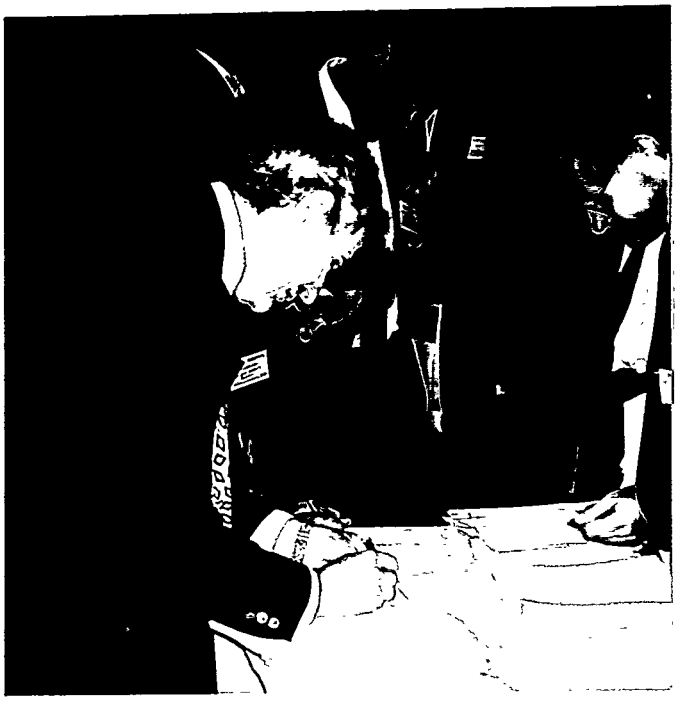

Personnally autographing a copy of his presentation for Michael Bettan (SOREQ, Israel) is Marvin Mendoka (NRC, USA) with Moshe Shapira (SOREQ, Israel) looking on

Vadim Artamkin (RDIPE, Russia) enjoying the balladeer entertainment at the RERTR banquet

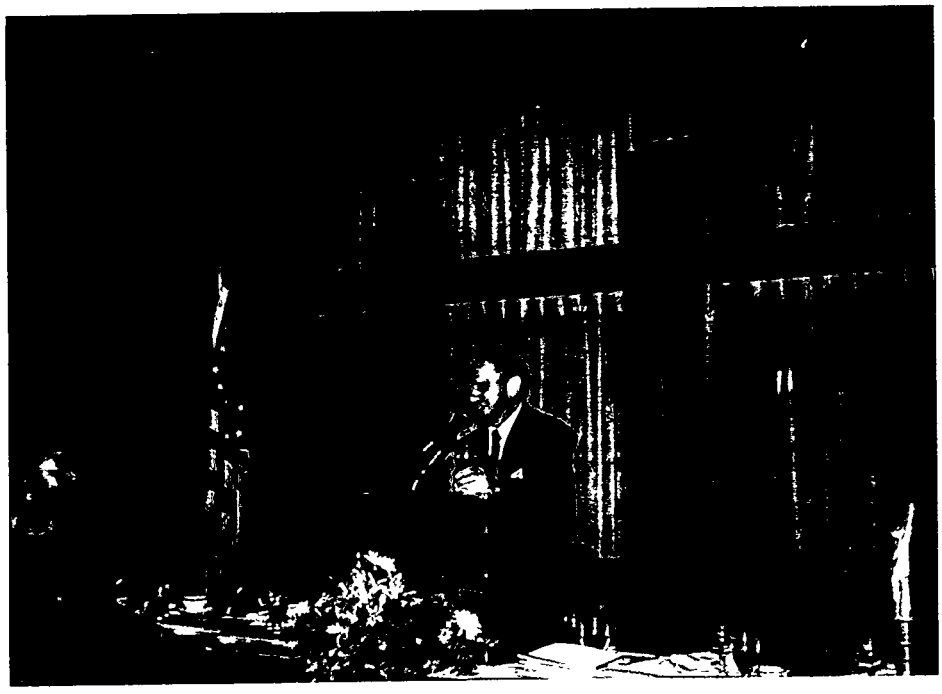

Armando Travelli, our host, at the podium

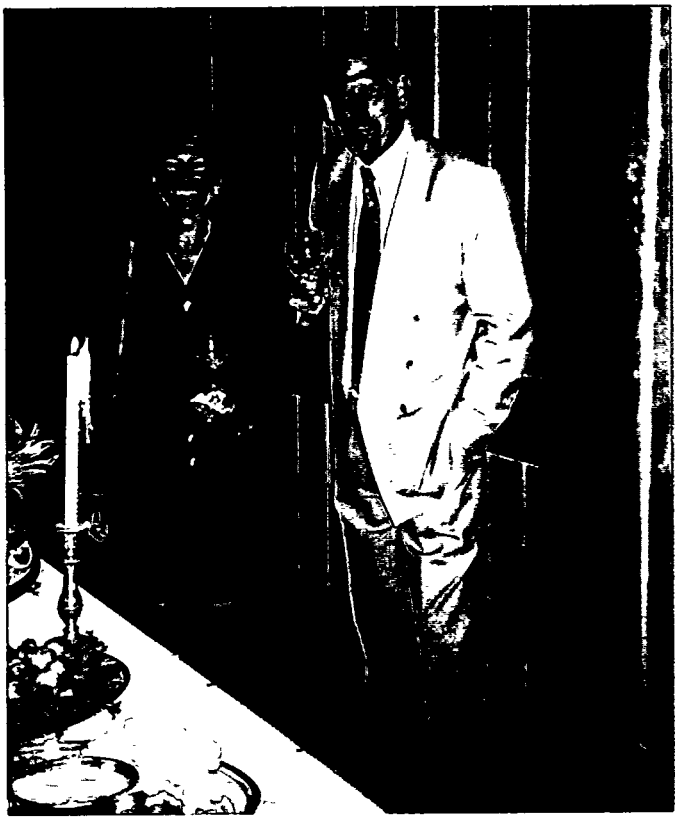

Jan Borring and his lovely wife Marit (Risø, Denmark) enjoying refreshments at the RERTR banquet

The ladies of the program enjoying some refreshments at the banquet, Rachael DiMeglio (University of Rhode Island, USA), Janet Matos, Marti Travelli and Helen Weber with Armando Travelli (ANL, USA)

David Sears (Chalk River, Canada) Marti Travelli (ANL, USA) W. Ryu, C. Kim (KAERI, Korea) and J. Rest (ANL, USA) enjoying some interesting discussions

V. Minkov (ANL, USA), N. Ermakov (MINATOM, Russia), J. Rest, G. Hofman (ANL, USA) Y. Stetsky, and V. Aden (RDIPE, Russia) enjoying the entertainment at the banquet

The University of Virginia tour group listening to the history of the University for which Thomas Jefferson was the architect

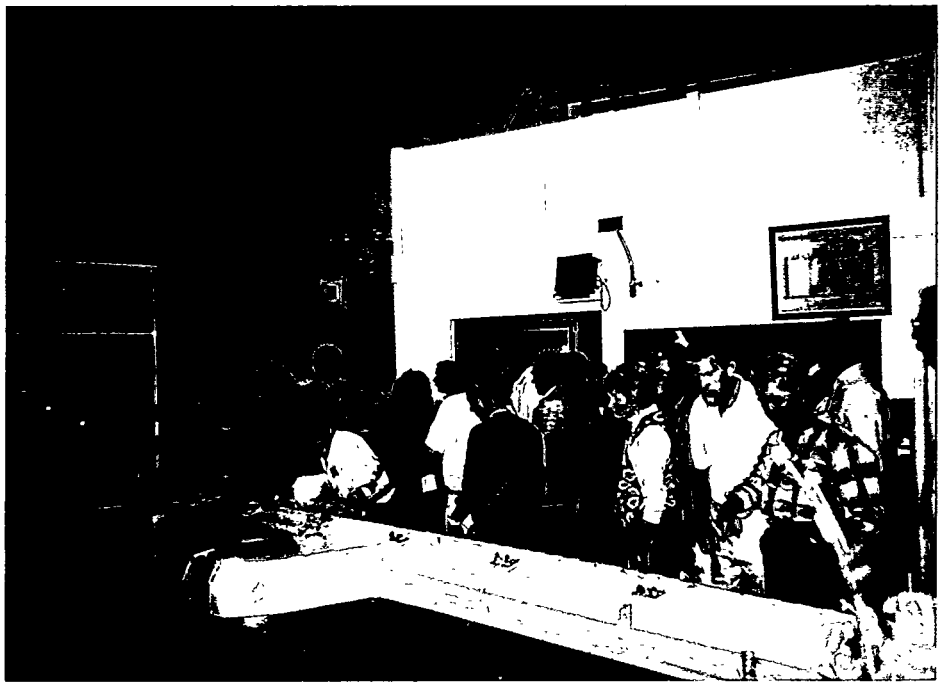

The tour group viewing the core of the UVAR reactor

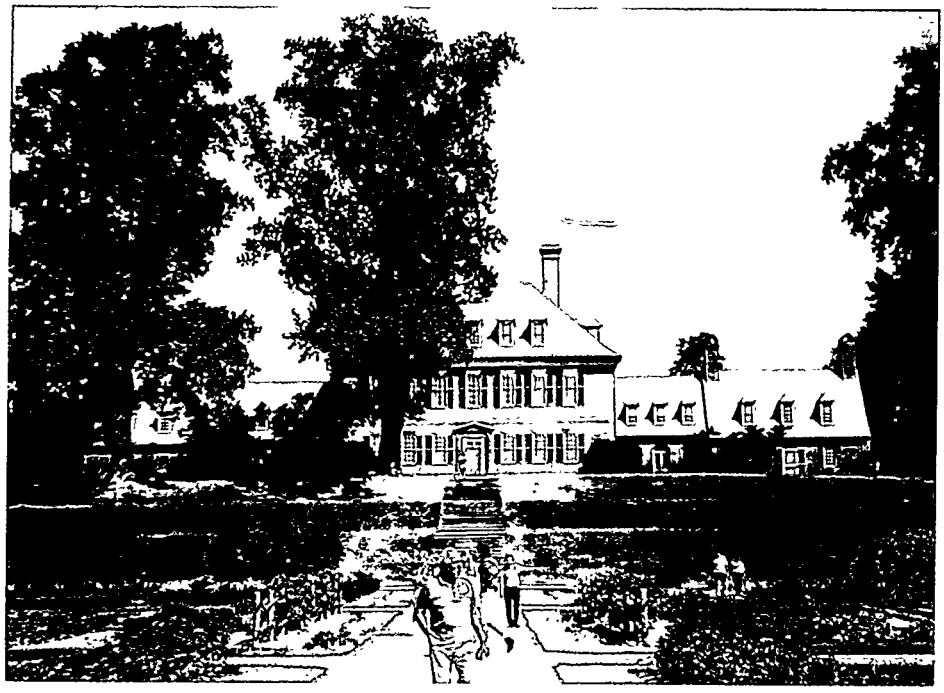

The Governor's Mansion in Collonial Williamsburg

We bid a fond farewell to Williamsburg

ATTENDEES 1994 INTERNATIONAL MEETING
ON REDUCED ENRICHMENT FOR RESEARCH AND TEST REACTORS
September 18-23, 1994
Williamsbug, Virginia

Vladimir G. Aden
RDIPE
PO Box 788
Moscow 101000, Russia

Phone: 7 (095) 264-9478
Fax: 7 (095) 975-2019
E-Mail: pol@energy.nikiet.msk.su

Eivind Adolph
Fuel Element Manufacture Plant
Risø National Laboratory
PO Box 49, DK-4000
Roskilde, Denmark

Phone: 45 (46) 77-5702
Fax: 45 (4) 35-1173

J. Arends
Radiochemical Center
MALLINGkRODT Medical B.V.
PO Box 3, NL-1755 ZG Petten
The Netherlands

Gunes Argon
Naval Nuclear Fuel Division
Babcock and Wilcox
PO Box 785
Lynchburg, VA 24505-0785 USA

Phone: (804) 522-6458
Fax: (804) 522-5922

Nikolai Arkhangelsky
MINATOM
Department of Nuclear Reactors
Staromonetny 26
109180 Moscow, Russia

Phone: 7 (095) 239-4144
Fax: 7 (095) 230-2420

Vadim N. Artamkin
RDIPE
PO Box 788
Moscow 101000, Russia

Phone: 7 (095) 268-9316
Fax: 7 (095) 975-2019
E-Mail: pol@ebergy,nikiet,msk.su

Tomokazu Aso
Japan Atomic Energy Research Institute
3607 Narita-cho, Oarai-machi
Higashi-ibaraki-gun
Ibaraki-ken, Japan 311-13

Phone: 81 (29) 264-8335
Fax: 81 (29) 264-8480

Anton Axmann
Research Reactor BER II
Hahn-Meiter-Institut Berlin GmbH
Glienicker Strasse 100
D-14109 Berlin, Germany

Phone: 49 (30) 8062-2740
Fax: 49 (30) 8062-2082

Gavin Ball
Reactor Theory, Energy Systems
Atomic Energy Corporation
of South Africa, Ltd.
PO Box 582 Pretoria 0001
South Africa

Phone: 27 (012) 316-6040
Fax: 27 (012) 316-5925
E-Mail: 100075.777@compuserve.com

Russell M. Ball
Babcock and Wilcox
Advanced Systems Division
2220 Longhorne Road
PO Box 10548
Lynchburg, VA 24506-0548 USA

Phone: (604) 948-4728
Fax: 804-948-4846

Alain Ballagny
DRE/DIR, Bat. 530
CEN/SACLAY
91191 Gif Sur Yvette Cedex
France

Phone: 33 (16) 908-4195
Fax: 11 (16) 908-8015

Robert Bari
Brookhaven National Laboratory
PO Box 5000
Upton, NY 11973-5000 USA

Phone: (516) 282-2629
Fax: (516) 282-5266

Michael Bettan
Israel Atomic Energy Commission
SOREQ Nuclear Research Center
Yavne 81800, Israel

Phone: 97 (28) 43-4719
Fax: 97 (28) 43-4133

Ira Bornstein
Building 201
Argonne National Laboratory
9700 South Cass Avenue
Argonne, IL 60439 USA

Phone: (708) 252-4673
Fax: (708) 252-5149

Jan Borring
Fuel Element Manufacture Plant
Risø National Laboratory
PO Box 49, DK-4000
Roskilde, Denmark

Phone: 45 (46) 75-738
Fax: 45 (42) 351-173

Manuel Bretscher
TD Division-RERTR Program - 207
Argonne National Laboratory
9700 South Cass Avenue
Argonne, IL 60439-4841 USA

Phone: (708) 252-8616
Fax: (708) 252-5161

Eleanor R. Busick
Department of State
2201 C Street, NW
Washington, DC 20520 USA

Phone: (202) 647-4812
Fax: (202) 647-0775

Phil J. Cartwright
UKEA Government Division
Nuclear Site Operations
D6000 Dounreay
Thurso Caithness KW147TZ
United Kingdom

Phone: 44 (84) 780-3036
Fax: 44 (84) 780-3049

Kenneth R. Catlett
Naval Nuclear Fuel Division
Babcock and Wilcox Company
PO Box 785
Lynchburg, VA 24505-0785 USA

Phone: (804) 522-5985
Fax: (804) 522-5922

Dennis Charuau
COGEMA, Inc.
7401 Wisconsin Avenue
Bethesda, MD 20814-3426 USA

Phone: (301) 986-8585
Fax: (301) 652-5690

Alexander G. Chernov
GNSS
1001 G Street NW
Suite 425 NW
Washington, DC 20001 USA

Phone: (202) 628-3028
Fax: (202) 628-3020
E-Mail: 49611769 (GNSSDC)

Marilena Conde
Edlow International Company
1666 Connecticut Avenue, NW, Suite 500
Washington, DC 20009 USA

Phone: (202) 483-4959
Fax: (202) 483-4840

George L. Copeland
Oak Ridge National Laboratory
Bldg. 4508, MS-609089
PO Box 2008
Oak Ridge, TN 37831-6089 USA

Phone: (615) 574-3909
Fax: (615) 576-3894
E-Mail: GLC@ORNL.GOV

James R. Deen
RERTR Program-207
Argonne National Laboratory
9700 South Cass Avenue
Argonne, IL 60439-4841 USA

Phone: (708) 252-4853
Fax: (708) 252-5161
E-Mail: b19281@sol14.ep.anl.gov

Paul Dejonghe
Centre d'Etude de l'Energie Nucleaire
SCK/CEN, Boeretang 200
B-2400 Mol, Belgium

Phone: 32 (14) 33-2111
Fax: 32 (14) 31-8936

Jacob W. DeVries
HOR/IRI, Delft University of Technology
Melekweg 15 (PO Box 5042)
NL 2629 JB Delft
The Netherlands

Phone: 31 (15) 78-1402
Fax: 31 (15) 78-6422

A. Francis DiMeglio
1207 Chalkstone Avenue
Providence, RI 02908 USA

Phone: (401) 272-4740
Fax: (401) 354-5551

Dana Dixon
Subcontract Administrator - 201
Argonne National Laboratory
9700 South Cass Avenue
Argonne, IL 60439 USA

Phone: (708) 252-3080
Fax: (708) 252-4517

Jean-Pierre Durand
CERCA
Zone Industrielle "Les Berauds" BP-1114
26104 Romans Sur Isere
France

Phone: 33 (75) 05-6143
Fax: 33 (75) 05-3968

Jack Edlow
Edlow International Company
1666 Connecticut Avenue, NW, Suite 500
Washington, DC 20009 USA

Phone: (202) 483-4959
Fax: (202) 483-4840

Nikolai I. Ermakov
Head of Main Department
MINATOM
Garibaldi Street
Moscow, Russia

Phone: 7 (095) 233-1826
Fax: 7 (095) 230-2420
E-Mail: VPK@mape.msk.su

Peter Ernst
McMaster University
1280 Main Street, West
Hamilton, Ontario L8S 4KI, Canada

Phone: 905-525-9140
Fax: (905) 546-1252

Peter Faulhaber
Kernforschungszentrum Karlsruhe Gmbh
D-76021 Karlsruhe
Postfach 3640, Germany

Phone: 49 (72) 478-5325
Fax: 49 (72) 478-5982

Toyoshi Fuketa
Japan Atomic Energy Research Institute
Department of Reactor Safety Research
Tokai, Ibaraki 31911, Japan

Phone: 81 (292) 82-6386
Fax: 81 (292) 82-6160

Peter-Michael Fuse
NUKEM GmbH
D-63754 Alzenau, Germany

Phone: 49 (6023) 91-1604
Fax: 49 (6023) 91-1600

Glen R. Gale
Babcock and Wilcox
PO Box 785
Lynchburg, VA 20545 USA

Phone: (804) 522-5494
Fax: (804) 522-5922

John Gibson
UKAEA Government Division
D-1202 Dounreay
Thurso Caithness KW147TZ
United Kingdom

Phone: 44 (847) 80-3275
Fax: 44 (847) 80-3284

Michael Goppel
Euratom Supply Agency
200 Rue de la Loi
1049 Brussels, Belgium

Phone: 32 (2) 295-5586
Fax: 32 (2) 295-0527

Jean-Jacques Graf
CERCA
Tour Fiat, Cedex 16
92084 Paris La Defense
France

Phone: 33 (1) 4796-5880
Fax: 33 (1) 4796-5892

Gerhard Gruber
NUKEM GmbH, Postfach 1313
Industriestr. 13
63755 Alzenau, Germany

Phone: 49 (6023) 91-1609
Fax: 49 (6023) 91-1600

Joel Guidez
CEA
CE Saclay, 91191 Gif/Yvette
Cedex, France

Phone: 33 (69) 08-8676
Fax: 33 (69) 08-6511

Karsten Haack
DR 3 Reactor
Risø National Laboratory
PO Box 49, DK-4000
Roskilde, Denmark

Phone: 45 (46) 77-4302
Fax: 45 (46) 75-5052

Walter Hajek
Physikalisch-Technische Bundesanstalt
Bundesallee 100
D-38116 Braunschweig, Germany

Phone: 49 (531) 592-7110
Fax: 49 (531) 592-7015

Nelson Hanan
TD Division-RERTR Program - 207
Argonne National Laboratory
9700 South Cass Avenue
Argonne, IL 60439-4841 USA

Phone: (708) 252-6627
Fax: (708) 252-5161

Richard J. Harrison
Chalk River Laboratories
Chalk River, Ontario
K0J IJ0, Canada

Phone: (613) 584-3311
Fax: (613) 584-1825

Takao Hashimoto
Nissho Iwai Corporation
4-5 Akasaka, 2-chmo
Minato-ku, Tokyo 107, Japan

Phone: 81 (3) 34588-2787
Fax: 81 (3) 3588-4924

Horst W. Hassel
JECTA Consulting Gmbh
Postfach 35 26
63747 Alzenau, Germany

Phone: 49 (0) 6023-9724-0
Fax: 49 (0) 6023-9724-24

Mary Alice Hayward
General Accounting Office
111 Massachusetts Avenue, NW
Suite 201
Washington, DC 20001 USA

Phone: (202) 512-6896
Fax: (202) 512-6880

Charles Head
Office of Spent Fuel Management
U.S. Department of Energy, EM-37
1000 Independence Avenue, SW
Washington, DC 20585 USA

Phone: (202) 586-0200
Fax: (202) 586-5256

Gerard Hofman
Fuels and Engineering Division
Argonne National Laboratory-207
9700 South Cass Avenue
Argonne, IL 60439-4841 USA

Phone: (708) 252-6683
Fax: (708) 252-5161

Joseph Hutter
Chemical Technology Division - 205
Argonne National Laboratory
9700 South Cass Avenue-Bldg. 205
Argonne, IL 60439 USA

Phone: (708) 252-6497
Fax: (708) 252-5246

Wolfgang Jager
Deputy Director General
GKSS-Forschungszentrum
D-214944 Geesthacht
Postfache 1160, Germany

Phone: 49 (415) 287-1670
Fax: 49 (415) 287-1618

Reed Johnson
Dept. of Nuclear Eng. & Eng. Physics
University of Virginia Reactor Facility
Charlottesville, VA 22903-2442 USA

Phone: (804) 982-5440
Fax: (904) 982-5473

Erik B. Jonsson
STUDSVIK Nuclear
S-61182 NYKÖPING
Sweden

Phone: 46 (155) 22-1000
Fax: 46 (155) 26-3070

Keiji Kanda
Research Reactor Institute
Kyoto University
Kamatori-cho, Sennan-gun
Osaka 590-04, Japan

Phone: (81) 724-52-0901 (Ext. 2614)
Fax: (81) 724-53-2145

Evegny Kartashev
Russian Development Institute of Power Eng.
PO Box 788
Moscow 101000, Russia

Phone: 7 (095) 263-0991
Fax: 7 (095) 975-2019
E-Mail: pol@energy.nikiet.msk.su

Frank Keeling
AECL Research
Chalk River Laboratories
Chalk River, Ontario
KOJ1JO, Canada

Phone: (613) 584-3311
Fax: (613) 584-1825
E-Mail: LEEDERD@CRL.AECL.Ca

Chung Kyu Kim
Korea Atomic Energy Research Institute
PO Box 105, Yusung
Taejon 305-600, Republic of Korea

Phone: 82 (42) 868-2309
Fax: 82 (42) 868-5496

Rodney W. Knight
Research Reactor Div., Bldg. 7910
Oak Ridge National Laboratory
PO Box 2008
Oak Ridge, TN 37831 USA

Phone: (615) 574-5713
Fax: (615) 574-0967

Masaru Kobayashi
PECHINEY, Japan
43rd Floor, Shinjuku Bldg.
No. 2-1-1 Nishi-Shinjuku
Shinjuku-ku Tokyo 163-04, Japan

Phone: 81 (3) 3349-6660
Fax: 81 (3) 3349-6670

Donald R. Krause
Dept. of Mechanical Aerospace
and Nuclear Eng.
University of Virginia Reactor Facility
Charlottesville, VA 22902 USA

Phone: (804) 982-5440
Fax: (804) 982-5473

Wilfried Krull
GKSS Research Centre Geesthact
Postfach 1160
D-21494 Geestacht, Germany

Phone: 49 (4152) 87-1200
Fax: 49 (4152) 87-1338

Albert Lee
AECL Research
Whiteshell Laboratories
Pinawa, Manitoba
Canada R0E IL0

Phone: (204) 753-2311
Fax: (204) 753-2248
E-Mail: LEEA@WL.AECL.CA

Eberhard Lehmann
Paul Scherrer Institute
Würenlingen and Villigen
CH-5232 Villigen PSI
Switzerland

Phone: 41 (56) 99-2311
Fax: 41 (56) 99-2327

Robert C. Liimatainen
Office of the Nuclear Waste Negotiator
1823 Jefferson Place, NW
Washington, DC 20036 USA

Phone: (202) 634-6244
Fax: (202) 634-6251

Vasily Lukichev
Russian Development Instute of Power Eng.
PO Box 788
Moscow 101000, Russia

Phone: 7 (095) 268-9316
Fax: 7 (095) 975-2019
E-Mail: pol@energy.nikiet.msk.su

John Mangusi
Transnuclear, Inc.
Two Skyline Drive
Hawthorne, NY 10532-2120 USA

Phone: (914) 347-2345
Fax: (914) 347-2346

James E. Matos
TD Division-RERTR Program - 207
Argonne National Laboratory
9700 South Cass Avenue
Argonne, IL 60439-4841 USA

Phone: (708) 252-6758
Fax: (708) 252-5161
E-Mail: JMATOS@ANL.GOV

James E. Mays
Naval Nuclear Fuel Division
Babcock and Wilcox Company
PO Box 785
Lynchburg, VA 24505-0785 USA

Phone: (804) 522-5722
Fax: (804) 522-5922

Michael B. McDonough
1451 Brookgreen Drive
Myrtle Beach, SC 29577 USA

Phone: (803) 448-4705
Fax: (803) 448-4838

Marvin Mendonca
U.S. Nuclear Regulatory Commission
11H3 NRR
Washington, DC 20555 USA

Phone: (301) 504-2170
Fax: (301) 504-2260

Franklin H. Metz
Naval Nuclear Fuel Division
Babcock and Wilcox Company
PO Box 785
Lynchburg, VA 24505-0785 USA

Phone: (804) 522-5873
Fax: (804) 522-5922

Vladimir E. Minkov
TD Division-RERTR Program - 207
Argonne National Laboratory
9700 South Cass Avenue
Argonne, IL 60439-4841 USA

Phone: (708) 252-4515
Fax: (708) 252-5161

Sai-Chi Mo
TD Division-RERTR Program - 207
Argonne National Laboratory
9700 South Cass Avenue
Argonne, IL 60439-4841 USA

Phone: (708) 252-6054
Fax: (708) 252-5161

Josè Mota
Commission of the European Communities
Euratom Supply Agency
Rue de la Loi, 200
B-1049 Brussels, Belgium

Phone: 32 (2) 295-2399
Fax: 32 (2) 295-0527

Hans Mueller
NUKEM GmbH
Postfach 1313, Industriestr. 13
D-63754 Alzenau, Germany

Phone: 49 (6023) 91-1608
Fax: 49 (6023) 91-1600

Yoji Murayama
Oarai Establishment
Japan Atomic Energy Research Institute
Oarai-machi
Ibaraki-ken, Japan 311-13

Phone: 81 (292) 64-8300
Fax: 81 (292) 64-8480

Alan Murray
Office of the Counsellor (Nuclear)
Embassy of Australia
1601 Massachusetts Avenue, NW
Washington, DC 20007 USA

Phone: (202) 797-3042
Fax: (202) 483-5156
E-Mail: amurry@capcon.net

Samir Naccache
CERCA
Tour Fiat Cedex 16
92084 Paris La Defense
France

Phone: 33 (1) 4796-5880
Fax: 33 (1) 4796-5892

Ami Nagler
SOREQ Nuclear Research Center
Yavne 81800, Israel

Phone: 972 (8) 43-4615
Fax: 972 (8) 43-4133

Teruo Nakajima
Japan Atomic Energy Research Institute
2-4 Shirakata-Shirane
Tokai-mura, Naka-gun
Ibaraki-ken, Japan 319-13

Phone: 81 (0292) 82-5613
Fax: 81 (0292) 82-5636

Richard Olsson
Swedish Nuclear Power Inspectorate
PO Box 27106
S-102 52 Stockholm
Sweden

Phone: 46 (8) 665-4400
Fax: 46 (8) 661-9086

Rokuro Oyamada
Oarai Establishment
Japan Atomic Energy Research Institute
Oarai-machi, Higashi-Ibaraki-gun
Ibaraki-ken, Japan 311-13

Phone: 81 (292) 64-8300
Fax: 81 (292) 64-8480

Brett W. Pace
Babcock and Wilcox
PO Box 785
Lynchburg, VA 20545 USA

Phone: (804) 522-6866
Fax: (804) 522-5922

Constantinos Papastergiou
National Center for Scientific Research
"Demokritos"
PO Box 60228, GR-15310 Aghia Paraskevi
Aghia Paraskeri, Attiki 15310, Greece

Phone: 30 (1) 651-4118
Fax: 30 (1) 653-3431

John-Man Park
Korea Atomic Energy Research Institute
PO Box 7, Daeduk-Danji
PO Box 105
Taejon 305-600
Republic of Korea

Fax: 82 (42) 886-2549

Harold B. Peacock
E. I. duPont de Nemours & Co.
Savannah River Laboratory
Building 773-A
Aiken, SC 29801 USA

Phone: (803) 725-1277
Fax: (803) 725-1660

Raymond B. Pond
RA Division-RERTR Program - 207
Argonne National Laboratory
9700 South Cass Avenue
Argonne, IL 60439-4841 USA

Phone: (708) 252-7090
Fax: (708) 252-5161

Ian Porter
British Nuclear Fuels
Risley Warrington Ceshire WA3 6AS
United Kingdom

Phone: 44 (925) 83-3633
Fax: 44 (925) 83-2833

Daniele Raisonnier
Transnucleaire, SA
9-11 Rue Christope Colomb
75008 Paris, France

Phone: 33 (1) 4069-7700
Fax: 33 (1) 4069-7701

Norman Ravenscroft
Edlow International Company
1666 Connecticut Avenue, NW, Suite 500
Washington, DC 20009 USA

Phone: (202) 483-4959
Fax: (202) 483-4840

Nat H. Reasor
Babcock and Wilcox
Nuclear Fuel Division
PO Box 10548
Lynchburg, VA 24506-0548 USA

Phone: (804) 522-62239
Fax: (804) 522-5922

Fredrick Reitsma
Atomic Energy Corporation of South Africa, Ltd.
PO Box 582 Pretoria 0001
South Africa

Phone: 27 (12) 316-6279
Fax: 27 (12) 316-5295

Jeffrey Rest
ET Division, Building 212
Argonne National Laboratory
9700 South Cass Avenue
Argonne, IL 60439 USA

Phone: (708) 252-5026
Fax: (708) 252-4798

Sharon Richmond
TD Division-RERTR Program - 207
Argonne National Laboratory
9700 South Cass Avenue
Argonne, IL 60439-4841 USA

Phone: (708) 252-7657
Fax: (708) 252-6757

M. Karl Richter
European Institute for Transuranium Elements
PO Box 2340
76125 Karlsruhe, Germany

Phone: 72 (47) 95-567
Fax: 72 (47) 95-1599

Iain Ritchie
International Atomic Energy Agency
PO Box 100, Wagramerstrasse 5
A-1140 Vienna, Austria

Phone: 43 (1) 2360-2759
Fax: 43 (1) 23-4564

Philip Robinson
Office of Nonproliferation Policy
NN-40, U.S. Department of Energy
Washington, DC 20585 USA

Phone: (202) 586-6184
Fax: (202) 586-6789

Hans-Joachim Roegler
Siemens AG
Postfach 100100
D51425 Bergisch Gladbach, Germany

Phone: 49 (2204) 84-4681
Fax: 49 (2204) 84-2207

Roger A. Rydin
Dept. of Mechanical, Aerospace & Nuclear Eng.
University of Virginia Reactor Facility
Charlottesville, VA 22903-2442 USA

Phone: (804) 982-5468
Fax: (804) 982-5473
E-Mail: RAR@VIRGINIA.EDU

Woo-Seog Ryu
Korea Atomic Energy Research Institute
PO Box 105, Yu-sung
Taejon, 305-600
Republic of Korea

Phone: 82 (42) 868-2441
Fax: 82 (42) 862-5496

A. Ali Sameh
Mallinckrodt Medical B.V.
PO Box 3, 1755 ZG Petten
The Netherlands

Phone: 31 (0) 2246-7123
Fax: 31 (0) 2246-3700

Galina A. Sarakhova
VNIINM
Moscow 123160, Rogova
Russia

Phone: 7 (095) 190-8149
Fax: 7 (095) 975-2019
E-Mail: pol@energy.nikiet.msk.su

Jack Schreader
Chalk River Laboratories
Chalk River, Ontario, K0J IJ0
Canada

Phone: (613) 584-3311
Fax: (613) 584-1825

Thomas Schmidt
Nuclear Cargo and Service GmbH
Rodenbacher Chaussee 6
Postfach 11 00 30
D-63434 Hanau, Germany

Phone: 49 (6181) 50-1254
Fax: 49 (6181) 57-3692

David Sears
AECL Research
Chalk River Laboratories
Chalk River, Ontario, Canada, KOJ1J0

Phone: (613) 584-3311
Fax: (613) 584-3250
E-Mail: SEARSD@AECL.CRL2.CRL.CA

John D. Sease
Research Reactor Div., Bldg. 7910
Oak Ridge National Laboratory
PO Box 2008
Oak Ridge, TN 37831-6392 USA

Phone: (615) 576-7622
Fax: (615) 574-0967

Moshe Shapira
SOREQ Nuclear Research Center
Yavne 81800, Israel

Phone: 972 (8) 43-4285
Fax: 972 (8) 43-4227

Klaus Singer
Risø National Laboratory
PO Box 49, DK-4000
Roskilde, Denmark

Phone: 45 (46) 77-4607
Fax: 45 (42) 36-8531

Barry Smith
Manager, Regulatory Development
Science Applications International Corp.
20202 Century Boulevard
Germantown, MD 20874 USA

Phone: (301) 353-8338
Fax: (301) 428-3482

Mike Smith
NAC SERVICES, Inc.
655 Engineering Drive, Suite 200
Norcross, GA 30092 USA

Phone: (404) 447-1144
Fax: (404) 447-1797

James L. Snelgrove
Engineering Physics Division
RERTR Program-207
Argonne National Laboratory
9700 South Cass Avenue
Argonne, IL 60439-4841 USA

Phone: (708) 252-6369
Fax: (708) 252-5161

Yo Song
Office of Nonproliferation Policy, NN-40
U. S. Department of Energy
Washington, DC 20585 USA

Phone: (202) 586-2611
Fax: (202) 586-2323

B. Chino Srinvasan
Chemical Technology Division - 205
Argonne National Laboratory
Argonne, IL 60439-4841 USA

Phone: (708) 252-9829
Fax: (708) 252-5246
E-Mail: chino_srinvasan@gmgate.anl.gov

Yuri Stetsky
VNIINM
PO Box 788
Moscow 123160, Rogova, Russia

Phone: 7 (095) 190-8186
Fax: 7 (095) 975-2019
E-Mail: pol@energy.nikiet,msk.su

Sugundo
National Atomic Energy Agency (BATAN)
Kawasan Puspiptek
Serpong 15310, Indonesia

Phone: 62 (021) 7560-915
Fax: 62 (021) 7560-895

Janine M. Sweeney
Attorney Advisor
U.S. Department of Energy
GC-53, Room 6A-113
Washington, DC 20585 USA

Phone: (202) 586-6947
Fax: (202) 586-7373

Aristidis Terzis
National Centre for Scientific Research
"Demokritos"
153 10 AG, Paraskevi Attikis
PO Box 60228
Athens, Greece

Phone: 30 (1) 651-4118
Fax: 30 (1) 653-3431

David Thom
AEA Technology
AEA Fuel Services Dounreay Product Services
Thurso Caithness KW147TZ
Scotland

Phone: 44 847 803006
Fax: 44 847 803053

Horst Walter Tiffe
Med. Hochschule Hannover
Kodysny-Gutschow-Str. 8
30623 Hannover
Germany

Phone: 49 511 532 3762
Fax: 49 517 532 2315

Larry Todd
Naval Nuclear Fuel Division
Babcock and Wilcox
PO Box 785
Lynchburg, VA 24505-0785 USA

Phone: (804) 522-6876
Fax: (804) 522-5922

Armando Travelli
Manager, RERTR Program-207
Argonne National Laboratory
9700 South Cass Avenue
Argonne, IL 60439-4841 USA

Phone: (708) 252-6363
Fax: (708) 252-5161
E-mail: b13808@anlvm.ctd.anl.gov

Horst Tschiesche
Nuclear Cargo & Service GmbH
Rodenbacher Chaussee 6
Postfach 11 00 30
D-6450 Hanau 11, Germany

Phone: 0049 6181-501216
Fax: 0049 6181-573692

George Vandegrift
Chemical Technology Division - 205
Argonne National Laboratory
9700 South Cass Avenue-Bldg. 205
Argonne, IL 60439 USA

Phone: (708) 252-4513
Fax: (708) 252-5246
E-mail: george_vandegrift@qmgate.anl.gov

James M. Viebrock
NAC Services, Inc.
655 Engineering Drive, Suite 200
Norcross, GA 30092 USA

Phone: (404) 447-1144
Fax: (404) 447-1797

Peter Watkins
Joint Research Centre
Commission of the European Communities
PO Box 2
1755 ZG Petten, The Netherlands

Phone: 31 2246 5120
Fax: 31 2246 1449

Helen Weber
RERTR Program-207
Argonne National Laboratory
9700 South Cass Avenue
Argonne, IL 60439-4841 USA

Phone: (708) 252-5240
Fax: (708) 252-5161

Thomas Wiencek
ET Division, Building 212
Argonne National Laboratory
9700 South Cass Avenue
Argonne, IL 60439 USA

Phone: (708) 252-5020
Fax: (708) 252-4798
E-mail: t_wiencek@qmgate.anl.gov

Colin West
Oak Ridge National Laboratory
Bldg. FEDC
PO Box 2009
Oak Ridge, TN 37831-8218 USA

Phone: (615) 574-0370
Fax: (615) 576-3041

Daniel Westall
Australian Nuclear Safety Bureau
US Nuclear Regulatory Commission
MS 0-11-B-20
Washington, DC 20555 USA

Phone: (US) (301) 504-1079
Fax: (US) (301) 504-2260

Fred J. Wijtsma
Joint Research Centre
Commission of the European Communities
PO Box 1, 1755 ZG
Petten, The Netherlands

Phone: 31 2246 5009 and 5013
Fax: 31 2246 1612

Walter H. Wolf
President
Wolfco, Inc.
19516 Burlingame Way
Montgomery Village, MD 20879 USA

Phone: (301) 840-0016
Fax: (301) 840-0017

William Woodruff
TD Division-RERTR Program - 207
Argonne National Laboratory
9700 South Cass Avenue
Argonne, IL 60439-4841 USA

Phone: (708) 252-8634
Fax: (708) 252-5161
E-mail: wwoodruff@anl.gov

Chi-Tse (Steve) Wu
ET Division, Building 212
Argonne National Laboratory
9700 South Cass Avenue
Argonne, IL 60439-4841 USA

Phone: (708) 252-9967
Fax: (708) 252-4798
E-mail: steven_wu@qmgate.anl.gov

William Zagotta
5155 Lillian Court
Livermore, CA 94550 USA

Phone: (510) 443-0451
Fax: (510) 423-6978

Abe Zeitoun
Assistant Vice President
Science Applications International Corp.
20201 Century Boulevard
Germantown, MD 20874 USA

Phone: (301) 353-8327
Fax: (301) 428-0145

DISTRIBUTION FOR ANL/RERTR/TM-20 (CONF-9409107)

Internal:

TIS Files (1)

All ANL Attendees (14)

A Travelli (50)

External:

ANL East Library

ANL West Library

DOE-OSTI, for distribution per UC-940 (80)

Manager, Chicago Operations Office, DOE

Director, Technology Management Div., DOE-CH

Technology Development Division Review Committee:

Robert J. Bunditz, Future Resources Associates, Inc.
W. Reed Johnson (Chairman) University of Virginia
Marvin M. Miller, Massachusetts Institute of Technology
Billy D. Shipp, Battelle Pacific Northwest National Laboratory
William G. Sutcliffe, Lawrence Livermore National Laboratory

All Non-ANL Attendees and Participants (133)